

|  |  |  |  |  |           |
|--|--|--|--|--|-----------|
| 1. Report No.<br>FHWA/TX-14/0-6716-1   |  | 2. Government Accession No.                          |  | 3. Recipient's Catalog No.   |           |
| 4. Title and Subtitle<br>DESIGN PARAMETERS AND METHODOLOGY FOR MECHANICALLY STABILIZED EARTH (MSE) WALLS   |  |  |  | 5. Report Date<br>December 2013<br>Published: October 2014                               |           |
|  |  |  |  | 6. Performing Organization Code  |           |
| 7. Author(s)<br>Charles P. Aubeny, Giovanna Biscontin, Jie Huang, Vishal S. Dantal, Rafat Sadat, and Sazzad Bin-Shafique   |  |  |  | 8. Performing Organization Report No.<br>Report 0-6716-1                                 |           |
| 9. Performing Organization Name and Address<br>Texas A&M Transportation Institute<br>College Station, Texas 77843-3135   |  |  |  | 10. Work Unit No. (TRAIS)  |           |
|  |  |  |  | 11. Contract or Grant No.<br>Project 0-6716  |           |
| 12. Sponsoring Agency Name and Address<br>Texas Department of Transportation<br>Research and Technology Implementation Office<br>125 East 11th Street<br>Austin, Texas 78701-2483  |  |  |  | 13. Type of Report and Period Covered<br>Technical Report:<br>September 2011–August 2013 |           |
|  |  |  |  | 14. Sponsoring Agency Code   |           |
| 15. Supplementary Notes<br>Project performed in cooperation with the Texas Department of Transportation and the Federal Highway Administration.<br>Project Title: Validation and Justification of Design Parameters for Mechanically Stabilized Earth (MSE) Walls<br>URL: <a href="http://tti.tamu.edu/documents/0-6716-1.pdf">http://tti.tamu.edu/documents/0-6716-1.pdf</a>  |  |  |  |  |           |
| 16. Abstract<br>Since its appearance in 1970s, mechanically stabilized earth (MSE) walls have become a majority among all types of retaining walls due to their economics and satisfactory performance. The Texas Department of Transportation (TxDOT) has primarily adopted the Federal Highway Administration (FHWA) and American Association of State Highway and Transportation Officials (AASHTO) guidelines for the design of MSE walls. Researchers (1) conducted laboratory tests on backfill materials and the statistical analysis to determine variability of soil properties (such as friction angle and unit weight) for soils meeting the TxDOT specifications, (2) performed Monte Carlo simulation using the determined soil property variation to assess the effect of spatial variability of material properties on the calculated factor of safety on sliding and overturning, (3) carried out numerical analysis using a Fast Lagrangian Analysis of Continua (FLAC) program to investigate possible failure modes under conditions of complicated geometries and rapid drawdown, and (4) evaluated the effect of precast panel on the compound failure analysis. Researchers evaluated design parameters for sliding analysis recommended by AASHTO and recommended modified design parameters calculated from FLAC simulations for different geometries and for different soil parameters. Similarly, a parametric study was performed to address issues related to bearing capacity for MSE walls and justify AASHTO recommendation with German code (EBGEO) for MSE walls. |  |  |  |  |           |
| 17. Key Words<br>MSE Walls, Large Scale Triaxial Testing, Unconsolidated Triaxial Testing, Statistical Analysis, Monte Carlo Simulation, FLAC Simulations, Minimum Reinforcement Length, Bearing Capacity Analysis   |  |  | 18. Distribution Statement<br>No restrictions. This document is available to the public through NTIS:<br>National Technical Information Service<br>Alexandria, Virginia<br><a href="http://www.ntis.gov">http://www.ntis.gov</a> |  |           |
| 19. Security Classif. (of this report)<br>Unclassified   |  | 20. Security Classif. (of this page)<br>Unclassified |  | 21. No. of Pages<br>356  | 22. Price |



# **DESIGN PARAMETERS AND METHODOLOGY FOR MECHANICALLY STABILIZED EARTH (MSE) WALLS**

by

Charles P. Aubeny  
Professor  
Texas A&M University

Giovanna Biscontin  
Associate Professor  
Texas A&M University

Jie Huang  
Assistant Professor  
The University of Texas at San Antonio

Sazzad Bin-Shafique  
Associate Professor  
The University of Texas at San Antonio

Vishal S. Dantal  
Ph.D. Candidate  
Texas A&M University

and

Rafat Sadat  
Graduate Student  
The University of Texas at San Antonio

Report 0-6716-1

Project 0-6716

Project Title: Validation and Justification of Design Parameters for Mechanically Stabilized Earth (MSE) Walls

Performed in cooperation with the  
Texas Department of Transportation  
and the  
Federal Highway Administration

December 2013

Published: October 2014

TEXAS A&M TRANSPORTATION INSTITUTE  
College Station, Texas 77843-3135



## **DISCLAIMER**

This research was performed in cooperation with the Texas Department of Transportation (TxDOT) and the Federal Highway Administration (FHWA). The contents of this report reflect the views of the authors, who are responsible for the facts and the accuracy of the data presented herein. The contents do not necessarily reflect the official view or policies of the FHWA or TxDOT. This report does not constitute a standard, specification, or regulation.

## **ACKNOWLEDGMENTS**

This project was conducted in cooperation with TxDOT and FHWA. The authors of this project thank the Project Director Mr. Sean Yoon for his encouragement and valuable guidance throughout this project. The authors also thank Project Advisors Mr. John Delphia, Ms. Dina Dewane, Mr. Marcus Galvan, Mr. Kevin Pete, and Mr. Jon Kilgore for their valuable suggestions and technical inputs toward this project. The contributions from Mr. Frank Espinosa and Mr. Wade Odell toward this project are greatly appreciated. The technical advice from Dr. Dov Leshchinsky on certain parts of project was insightful and helpful on finishing this project, and the authors are much obliged for that. Finally, the authors acknowledge the contributions from geotechnical engineering graduate students who showed interest and collaborated on this project.

# TABLE OF CONTENTS

|  | Page      |
|--|-----------|
| <b>List of Figures</b> .....                             | <b>ix</b> |
| <b>List of Tables</b> .....                              | <b>xx</b> |
| <b>Chapter 1: Introduction</b> .....                     | <b>1</b>  |
| <b>Chapter 2: Literature Review</b> .....                | <b>3</b>  |
| Overview of Backfill Material Used in MSE Walls .....    | 3         |
| Types A, B, and D.....                                   | 3         |
| Type C.....  | 5         |
| Internal Stability Design .....                          | 10        |
| Minimum Reinforcement Length .....                       | 12        |
| External Stability .....                                 | 14        |
| Bearing Capacity.....                                    | 14        |
| Sliding and Overturning.....                             | 16        |
| Compound Failure .....                                   | 17        |
| Overview of MSE Wall Performance .....                   | 19        |
| Summary of Survey Outcome.....                           | 19        |
| <b>Chapter 3: Case Histories</b> .....                   | <b>23</b> |
| Case Histories of Not-Well Performing MSE Walls .....    | 23        |
| IH 10 at Beaumont District.....                          | 23        |
| US 281 at FM 162 in Pharr District.....                  | 32        |
| Bridge Approaches IH 410 in San Antonio District .....   | 36        |
| IH 35 and FM 310 at Hillsboro, TX .....                  | 40        |
| US 281 at Brook Hollow Blvd, San Antonio.....            | 43        |
| IH 35 at Walnut Street, Comal County, TX.....            | 46        |
| Summary of the Identified Failure/Distress Modes .....   | 47        |
| Summary of the Possible Causes .....                     | 47        |
| Literature Review of TxDOT 0-5506 .....                  | 48        |
| <b>Chapter 4: Validation of Design Assumptions</b> ..... | <b>53</b> |
| Lab Testing and Test Data .....                          | 53        |
| Overview of Testing Procedure .....                      | 57        |
| Material Classification .....                            | 59        |
| Sample Preparation .....                                 | 63        |
| Testing.....   | 67        |
| Consolidated Undrained Triaxial Testing.....             | 68        |
| Calculations and Corrections .....                       | 73        |
| Overview of Data Interpretation.....                     | 74        |
| Overview of Testing Results.....                         | 76        |
| Statistical Analyses .....                               | 79        |
| Statistical Analysis of Test Data.....                   | 79        |
| Monte Carlo Analysis on FOS.....                         | 86        |
| Monte Carlo Method.....                                  | 86        |
| FOSs for Sliding and Overturning.....                    | 87        |
| FLAC Analysis for Minimum Length .....                   | 95        |

|  |            |
|--|------------|
| <b>Chapter 5: Justification of Design Methodology.....</b>           | <b>99</b>  |
| Bearing Capacity.....  | 102        |
| Numerical Analysis.....  | 102        |
| Results and Discussion .....   | 107        |
| Conclusion .....   | 110        |
| Global Stability.....  | 110        |
| Material Properties Used for Backfill and Foundation Soil.....       | 110        |
| Reinforcement Property .....   | 111        |
| Concrete Panel Property .....  | 111        |
| Horizontal Back Slope .....  | 112        |
| 3H:1V Back Slope .....   | 121        |
| 2H:1V Back Slope .....   | 128        |
| 3H:1V Fore Slope .....   | 132        |
| 2H:1V Fore Slope .....   | 137        |
| Rapid Drawdown in Front of the MSE Wall .....                        | 141        |
| Compound Failure Analysis .....                                      | 146        |
| MSE Walls with Backslopes.....                                       | 146        |
| MSE Walls with Foreslopes and with/without Shallow Water Table ..... | 146        |
| Two-Tiered MSE Wall .....  | 146        |
| FLAC Model.....  | 147        |
| Analysis in FLAC .....   | 147        |
| Analysis Cases for Series 4.....                                     | 148        |
| <b>Chapter 6: Parametric Study.....</b>                              | <b>153</b> |
| Parametric Study for Sliding and Overturning Analysis .....          | 153        |
| Horizontal Back Slope .....  | 153        |
| 3H:1V Back Slope .....   | 160        |
| Conclusion .....   | 165        |
| Parametric Study Using FLAC Simulations.....                         | 166        |
| Analysis for Cohesionless Soils.....                                 | 166        |
| Parametric Study for Bearing Capacity Analysis .....                 | 188        |
| Bearing Capacity Analysis for Cohesionless Soils.....                | 188        |
| Bearing Capacity Analysis for Undrained Cohesive Soils .....         | 195        |
| Bearing Capacity Analysis for $c$ - $\phi$ Foundation Soils.....     | 199        |
| <b>Chapter 7: Conclusions and Recommendations .....</b>              | <b>203</b> |
| Conclusions.....   | 203        |
| Laboratory Results for Backfill Materials .....                      | 203        |
| FLAC Analysis for Minimum Length .....                               | 204        |
| Bearing Capacity.....  | 204        |
| Global Stability .....   | 205        |
| Compound Failure Analysis .....                                      | 206        |
| Conclusions from Parametric Studies.....                             | 206        |
| Recommendations.....   | 208        |
| <b>References .....</b>  | <b>211</b> |
| <b>Appendix A: Survey on MSE Wall Practice.....</b>                  | <b>215</b> |
| <b>Appendix B: Laboratory Test Results .....</b>                     | <b>275</b> |
| <b>Appendix C: Results from FLAC Simulations.....</b>                | <b>301</b> |



## LIST OF FIGURES

|   | <b>Page</b> |
|---|-------------|
| Figure 1. TxDOT MSE Wall Backfill Material Gradation (Developed from TxDOT Standard Specifications 2004 and FHWA 2009). .....   | 4           |
| Figure 2. Calculation of Vertical Stress for Horizontal Back Slope Condition, including Live Load and Dead Load Surcharges for Internal Stability Design (AASHTO 2002). ..... | 12          |
| Figure 3. Ultimate Bearing Capacity of Rigid Footing. ....  | 15          |
| Figure 4. Bearing Capacity of Retaining Walls. ....   | 16          |
| Figure 5. Compound Failure (Berg et al. 2009). ....   | 18          |
| Figure 6. Example of MSE Wall Failure along the Slope. ....   | 19          |
| Figure 7. Locations of the MSE Walls. ....  | 24          |
| Figure 8. Recurring of Cracks on the Pavement. ....   | 25          |
| Figure 9. Field Observations. ....  | 25          |
| Figure 10. Boring Location Plan. ....   | 26          |
| Figure 11. SPT Corrected N and Friction Angle along the Depth. ....   | 27          |
| Figure 12. MSE Retaining Wall Movements Measured by Inclinator. ....  | 28          |
| Figure 13. Cross-Section and Material Properties of Back Analysis. ....   | 29          |
| Figure 14. Global Stability Analysis. ....  | 31          |
| Figure 15. Location of the Distressed MSE Wall. ....  | 33          |
| Figure 16. Distress at Various Locations. ....  | 34          |
| Figure 17. Outward Movement of Corner Panel at the Departure. ....  | 34          |
| Figure 18. Particle Size Distribution. ....   | 35          |
| Figure 19. Geographic Location of the MSE Wall of EB IH 410 On ramp at Blanco Road. ....  | 36          |
| Figure 20. Distress at Pavement, Approach Slab, and Barriers. ....  | 37          |
| Figure 21. The Outward Movement of MSE Wall. ....   | 37          |
| Figure 22. GPR, Coring, and DCP Locations (McDaniel 2011). ....   | 39          |
| Figure 23. DCP Penetration Data for Both Approach and Departure (McDaniel 2011). ....   | 39          |
| Figure 24. Fill Material underneath the Pavement. ....  | 40          |
| Figure 25. Geographic Location of the MSE Wall at IH 35 and FM 310. ....  | 41          |
| Figure 26. Distress at Various Locations. ....  | 42          |
| Figure 27. Dislocation of the MSE Wall Panels. ....   | 42          |
| Figure 28. Clay Layer underneath BAS. ....  | 43          |
| Figure 29. Water Drainage through Panel Joints. ....  | 43          |
| Figure 30. Geographic Location of the MSE Wall at US 281 and Brook Hollow Blvd. ....  | 44          |
| Figure 31. Distress Modes. ....   | 45          |
| Figure 32. Geographic Locations. ....   | 46          |
| Figure 33. Distress Modes. ....   | 47          |
| Figure 34. Illustration of Proposed Narrow MSE Wall in Front of an Existing Stable Face (after Kniss et al. 2007). ....   | 48          |
| Figure 35. Proposed Design Chart for Nondeformable Walls Placed in Front of an Existing Stable Face from Plaxis Simulations (after Kniss et al. 2007). ....                   | 50          |
| Figure 36. Values of the Vertical Stress Influence Factor at the Top and Bottom of the Wall (after Kniss et al. 2007). ....   | 51          |

|  |    |
|--|----|
| Figure 37. Large Diameter Triaxial Schematic.....  | 54 |
| Figure 38. Large-Scale Triaxial Chamber.....   | 55 |
| Figure 39. Trautwein Pressure Panel (Left) and Volume Change Device (Right) Used in Testing.....       | 56 |
| Figure 40. Data Acquisition Program.....   | 57 |
| Figure 41. Type A Borrow Gradation.....  | 60 |
| Figure 42. Type B Borrow Gradation.....  | 60 |
| Figure 43. Type C Borrow Gradation.....  | 61 |
| Figure 44. Type D Borrow Gradation.....  | 61 |
| Figure 45. Sorted Particle Sizes of Type B Material.....   | 64 |
| Figure 46. Sample Mixing of Passing #200 for Type D Material.....                                      | 65 |
| Figure 47. Compaction of Specimen.....   | 66 |
| Figure 48. Leveling Top Cap of Specimen and Final Prepared Specimen.....                               | 67 |
| Figure 49. Sample Placed on the Bottom Cap of Triaxial Chamber.....                                    | 69 |
| Figure 50. Stretching Membrane on Spreader and Placing Membrane on Sample.....                         | 70 |
| Figure 51. Geotac Loading Frame and Geotac Sigma-CU Program Used to Perform Triaxial CU Test.....      | 71 |
| Figure 52. Sample during Consolidation.....  | 72 |
| Figure 53. Stress-Strain Curve on Sigma-CU Program and Deformed Sample at 20 percent Axial Strain..... | 72 |
| Figure 54. Parabolic Deformation of Test Specimen.....   | 76 |
| Figure 55. Stress-Strain for a Gradation Type A1.....  | 78 |
| Figure 56. Volumetric Strain Curves for a Gradation Type A1.....                                       | 78 |
| Figure 57. Type A Material p-q Diagram.....  | 79 |
| Figure 58. Statistical Control Limits (www.3sigma.com).....  | 80 |
| Figure 59. Normal Distribution of Friction Angle of Type A.....  | 81 |
| Figure 60. Normal Distribution of Unit Weight of Type A.....   | 82 |
| Figure 61. Normal Distribution of Friction Angle of Type B.....  | 82 |
| Figure 62. Normal Distribution of Unit Weight of Type B.....   | 83 |
| Figure 63. Normal Distribution of Friction Angle of Type D.....  | 83 |
| Figure 64. Normal Distribution of Unit Weight of Type D.....   | 84 |
| Figure 65. Friction Angle vs. Confidence Level.....  | 84 |
| Figure 66. Unit Weight vs. Confidence Level.....   | 85 |
| Figure 67. Dry Unit Weight vs. Relative Compaction.....  | 85 |
| Figure 68. Monte Carlo Analysis Example.....   | 87 |
| Figure 69. Monte Carlo Model for Sliding and Overturning FOS Analysis.....                             | 88 |
| Figure 70. Overturning FOS of Type A ( $\phi_f=26^\circ$ ).....  | 89 |
| Figure 71. Sliding FOS of Type A ( $\phi_f=26^\circ$ ).....  | 89 |
| Figure 72. Overturning FOS of Type A ( $\phi_f=30^\circ$ ).....  | 90 |
| Figure 73. Sliding FOS of Type A ( $\phi_f=30^\circ$ ).....  | 90 |
| Figure 74. Overturning FOS of Type B ( $\phi_f=26^\circ$ ).....  | 91 |
| Figure 75. Sliding FOS of Type B ( $\phi_f=26^\circ$ ).....  | 91 |
| Figure 76. Overturning FOS of Type B ( $\phi_f=30^\circ$ ).....  | 92 |
| Figure 77. Sliding FOS of Type B ( $\phi_f=30^\circ$ ).....  | 92 |
| Figure 78. Overturning FOS of Type D ( $\phi_f=26^\circ$ ).....  | 93 |

|  |     |
|--|-----|
| Figure 79. Sliding FOS of Type D ( $\phi_r=26^\circ$ ).  | 93  |
| Figure 80. Overturning FOS of Type D ( $\phi_r=30^\circ$ ).  | 94  |
| Figure 81. Sliding FOS of Type D ( $\phi_r=30^\circ$ ).  | 94  |
| Figure 82. MSE Prototype of Minimum Reinforcement Length Analysis.   | 95  |
| Figure 83. FLAC Model for Minimum Length Analysis.   | 97  |
| Figure 84. Reinforcement Length vs. Deflection.  | 97  |
| Figure 85. Effect of Non-Horizontal Back Slope.  | 100 |
| Figure 86. Effect of Non-Horizontal Fore Slope.  | 100 |
| Figure 87. Effect of Groundwater and Rapid Drawdown.   | 101 |
| Figure 88. Stability of Two-Tiered Walls.  | 101 |
| Figure 89. Model of 10 ft Wide Strip Footing in FLAC.  | 103 |
| Figure 90. Displacement Vectors at Failure in FLAC Model.  | 105 |
| Figure 91. Load vs. Displacement from FLAC Model ( $\phi = 30^\circ$ , $c = 1000$ psf, 600 psf Surcharge on Both Sides).   | 105 |
| Figure 92. Numerical Model in FLAC Simulating the Bearing Capacity of MSE Wall (Surcharge Load on One Side Only).  | 106 |
| Figure 93. Typical Load vs. Displacement Curve for Footing Loaded under Uniform Pressure and Surcharged from One Side Only ( $\phi = 35^\circ$ , $c = 0$ , $\gamma = 120$ pcf, Cohesion =0, Surcharge Height = 15 ft). | 107 |
| Figure 94. Comparison between FLAC Results and Terzaghi's Equation Excluding Surcharge Term.   | 109 |
| Figure 95. Comparison between $q_{ult}$ (FLAC) vs. Terzaghi's Bearing Capacity Including Surcharge Term.   | 109 |
| Figure 96. Dimensions and Properties Used for Series 1 Case 1.   | 112 |
| Figure 97. Concrete Panels and Strips Length Used for Series 1 Case 1.   | 113 |
| Figure 98. Series 1 Case 1 Foundation Angle $\phi=26^\circ$ , Backfill Angle $\phi=34^\circ$ , and $\gamma_{back}=105$ pcf $\gamma_{retain}=125$ pcf Maximum Shear Strain Rate.  | 117 |
| Figure 99. Series 1 Case 1 Foundation Angle $\phi=26^\circ$ , Backfill Angle $\phi=34^\circ$ , and $\gamma=105$ pcf Maximum Shear Strain Rate.   | 118 |
| Figure 100. Series 1 Case 1 Foundation $c_u=500$ psf, Backfill Angle $\phi=34^\circ$ , and $\gamma=105$ pcf Maximum Shear Strain Rate.   | 119 |
| Figure 101. Series 1 Case 1 Foundation $c_u=2000$ psf, Backfill Angle $\phi=34^\circ$ , and $\gamma=125$ pcf Maximum Shear Strain Rate.  | 119 |
| Figure 102. Series 1 Case 1 Foundation $c_u=2000$ psf, Backfill Angle $\phi=34^\circ$ , and $\gamma=105$ pcf Maximum Shear Strain Rate. Foundation Depth Equals to Wall Height.  | 120 |
| Figure 103. Dimensions and Properties Used for Series 1 Case 2.  | 121 |
| Figure 104. Series 1 Case 2 Foundation Angle $\phi=26^\circ$ , Backfill Angle $\phi=34^\circ$ , and $\gamma=105$ pcf Maximum Shear Strain Rate.  | 123 |
| Figure 105. Series 1 Case 2 Foundation Angle $\phi=35^\circ$ , Backfill Angle $\phi=34^\circ$ , and $\gamma=125$ pcf Maximum Shear Strain Rate.  | 124 |
| Figure 106. Series 1 Case 2 Foundation $c_u=500$ psf, Backfill Angle $\phi=34^\circ$ , and $\gamma=105$ pcf Maximum Shear Strain Rate.   | 124 |
| Figure 107. Series 1 Case 2 Foundation $c_u=2000$ psf, Backfill Angle $\phi=34^\circ$ , and $\gamma=105$ pcf Maximum Shear Strain Rate.  | 125 |

|  |     |
|--|-----|
| Figure 108. Series 1 Case 2 Foundation $c_u=2000$ psf, Backfill Angle $\phi=34^\circ$ , and $\gamma=105$ pcf Maximum Shear Strain Rate. Foundation Depth Equals to Wall Height. .... | 125 |
| Figure 109. Circular Failure Surface. ....   | 126 |
| Figure 110. Circular + Plane Failure Surface. ....   | 126 |
| Figure 111. Vertical Failure Surface. ....   | 127 |
| Figure 112. Wedge Failure Surface. ....  | 127 |
| Figure 113. Wedge + Vertical Failure Surface. ....   | 128 |
| Figure 114. Dimensions and Properties Used for Series 1 Case 3. ....   | 129 |
| Figure 115. Series 1 Case 3 Foundation Angle $\phi=30^\circ$ , Backfill Angle $\phi=34^\circ$ , and $\gamma=105$ pcf Maximum Shear Strain Rate. ....                                 | 130 |
| Figure 116. Series 1 Case 3 Foundation Angle $\phi=26^\circ$ , Backfill Angle $\phi=34^\circ$ , and $\gamma=125$ pcf Maximum Shear Strain Rate. ....                                 | 131 |
| Figure 117. Series 1 Case 3 Foundation $c_u=500$ psf, Backfill Angle $\phi=34^\circ$ , and $\gamma=105$ pcf Maximum Shear Strain Rate. ....  | 131 |
| Figure 118. Series 1 Case 3 Foundation $c_u=2000$ psf, Backfill Angle $\phi=34^\circ$ , and $\gamma=105$ pc Maximum Shear Strain Rate. ....  | 132 |
| Figure 119. Dimensions and Properties Used for Series 2 Case 2. ....   | 133 |
| Figure 120. Series 2 Case 2 Foundation Angle $\phi=26^\circ$ , Backfill Angle $\phi=34^\circ$ , and $\gamma=105$ pcf Maximum Shear Strain Rate. ....                                 | 134 |
| Figure 121. Series 2 Case 2 Foundation Angle $\phi=35^\circ$ , Backfill Angle $\phi=34^\circ$ , and $\gamma=105$ pcf Maximum Shear Strain Rate. ....                                 | 135 |
| Figure 122. Series 2 Case 2 Foundation Angle $\phi=30^\circ$ , Backfill Angle $\phi=34^\circ$ , and $\gamma=125$ pcf Maximum Shear Strain Rate. ....                                 | 135 |
| Figure 123. Series 2 Case 2 Foundation $c_u=500$ psf, Backfill Angle $\phi=34^\circ$ , and $\gamma=105$ pcf Maximum Shear Strain Rate. ....  | 136 |
| Figure 124. Series 2 Case 2 Foundation $c_u=2000$ psf, Backfill Angle $\phi=34^\circ$ , and $\gamma=125$ pcf Maximum Shear Strain Rate. ....   | 136 |
| Figure 125. Dimensions and Properties Used for Series 2 Case 3. ....   | 137 |
| Figure 126. Series 2 Case 3 Foundation Angle $\phi=26^\circ$ , Backfill Angle $\phi=34^\circ$ , and $\gamma=125$ pcf Maximum Shear Strain Rate. ....                                 | 138 |
| Figure 127. Series 2 Case 3 Foundation Angle $\phi=30^\circ$ , Backfill Angle $\phi=34^\circ$ , and $\gamma=125$ pcf Maximum Shear Strain Rate. ....                                 | 139 |
| Figure 128. Series 2 Case 3 Foundation Angle $\phi=35^\circ$ , Backfill Angle $\phi=34^\circ$ , and $\gamma=125$ pcf Maximum Shear Strain Rate. ....                                 | 139 |
| Figure 129. Series 2 Case 3 Foundation $c_u=500$ psf, Backfill Angle $\phi=34^\circ$ , and $\gamma=105$ pcf Maximum Shear Strain Rate. ....  | 140 |
| Figure 130. Series 2 Case 3 Foundation $c_u=2000$ psf, Backfill Angle $\phi=34^\circ$ , and $\gamma=105$ pcf Maximum Shear Strain Rate. ....   | 140 |
| Figure 131. Analysis Cases for Rapid Drawdown. ....  | 141 |
| Figure 132. Failure Plane for MSE Wall Subjected to Rapid Drawdown with Horizontal Fore Slope. ....  | 143 |
| Figure 133. Global Failure Pattern for MSE Wall with Fore Slope Subjected to Rapid Drawdown. ....  | 143 |

|   |     |
|---|-----|
| Figure 134. Maximum Shear Strain for Case 1, Horizontal Fore Slope, Foundation Friction Angle = 30. ....  | 144 |
| Figure 135. Max Shear Strain Rate for Case 1, 3:1 Fore Slope, Foundation Friction Angle = 30. ....  | 144 |
| Figure 136. Maximum Shear Strain for Case 2, Horizontal Fore Slope, Foundation Friction Angle = 30. ....  | 145 |
| Figure 137. Max Shear Strain Rate for Case 2, 3:1 Fore Slope, Foundation Friction Angle = 30. ....  | 145 |
| Figure 138. Analysis of Compound Failure. ....  | 147 |
| Figure 139. General Failure Mode of a Two-Tier MSE Wall. ....   | 149 |
| Figure 140. Maximum Shear Strain for Setback of 10 ft and Second Wall Height of 20 ft with $\phi=30^\circ$ . ....   | 149 |
| Figure 141. Maximum Shear Strain for Setback of 10 ft and Second Wall Height of 20 ft with $\phi=40^\circ$ . ....   | 150 |
| Figure 142. Maximum Shear Strain for Setback of 20 ft and Second Wall Height of 20 ft with $\phi=30^\circ$ . ....   | 150 |
| Figure 143. Maximum Shear Strain for Setback of 20 ft and Second Wall Height of 10 ft with $\phi=30^\circ$ . ....   | 151 |
| Figure 144. MSE Wall with 20 ft Wall Height and Horizontal Back Slope. ....   | 153 |
| Figure 145. Factor of Safety against Sliding for a 20-ft Wall Height with No Back Slope for Different $\phi_{\text{retaining}}$ at a Constant $\phi_{\text{found}}=26^\circ$ . ....                   | 155 |
| Figure 146. Factor of Safety against Sliding for a 20-ft Wall Height with No Back Slope for Different $\phi_{\text{retaining}}$ at a Constant $\phi_{\text{found}}=30^\circ$ . ....                   | 155 |
| Figure 147. Factor of Safety against Sliding for 2a 0-ft Wall Height with No Back Slope for Different $\phi_{\text{retaining}}$ at a Constant $\phi_{\text{found}}=35^\circ$ . ....                   | 156 |
| Figure 148. Factor of Safety against Overturning for a 20-ft Wall Height with No Back Slope for Different $\phi_{\text{retaining}}$ . ....  | 156 |
| Figure 149. Factor of Safety against Sliding for a 20-ft Wall Height with No Back Slope with $\gamma_{\text{ret}}=105$ pcf and $\gamma_{\text{back}}=105$ pcf for Different Friction Angles. ....     | 157 |
| Figure 150. Factor of Safety against Sliding for a 20-ft Wall Height with No Back Slope with $\gamma_{\text{ret}}=105$ pcf and $\gamma_{\text{back}}=125$ pcf for Different Friction Angles. ....     | 157 |
| Figure 151. Factor of Safety against Sliding for a 20-ft Wall Height with No Back Slope with $\gamma_{\text{ret}}=125$ pcf and $\gamma_{\text{back}}=105$ pcf for Different Friction Angles. ....     | 158 |
| Figure 152. Factor of Safety against Overturning for a 20-ft Wall Height with No Back Slope with $\gamma_{\text{ret}}=105$ pcf and $\gamma_{\text{back}}=105$ pcf for Different Friction Angles. .... | 158 |
| Figure 153. Factor of Safety against Overturning for a 20-ft Wall Height with No Back Slope with $\gamma_{\text{ret}}=105$ pcf and $\gamma_{\text{back}}=125$ pcf for Different Friction Angles. .... | 159 |
| Figure 154. Factor of Safety against Overturning for a 20-ft Wall Height with No Back Slope with $\gamma_{\text{ret}}=125$ pcf and $\gamma_{\text{back}}=105$ pcf for Different Friction Angles. .... | 159 |
| Figure 155. MSE Wall with 20-ft Wall and 3H:1V Back Slope. ....   | 160 |
| Figure 156. Factor of Safety against Sliding for a 20-ft Wall Height with 3H:1V Back Slope for Different $\phi_{\text{retaining}}$ at a Constant $\phi_{\text{found}}=26^\circ$ . ....                | 160 |
| Figure 157. Factor of Safety against Sliding for a 20-ft Wall Height with 3H:1V Back Slope for Different $\phi_{\text{retaining}}$ at a Constant $\phi_{\text{found}}=30^\circ$ . ....                | 161 |

|  |     |
|--|-----|
| Figure 158. Factor of Safety against Sliding for a 20-ft Wall Height with 3H:1V Back Slope for Different $\phi_{\text{retaining}}$ at a Constant $\phi_{\text{found}}=35^\circ$ .....                    | 161 |
| Figure 159. Factor of Safety against Overturning for a 20-ft Wall Height with 3H:1V Back Slope for Different $\phi_{\text{retaining}}$ .....   | 162 |
| Figure 160. Factor of Safety against Sliding for a 20-ft Wall Height with 3H:1V Back Slope with $\gamma_{\text{ret}}=105$ pcf and $\gamma_{\text{back}}=105$ pcf for Different Friction Angles.....      | 162 |
| Figure 161. Factor of Safety against Sliding for a 20-ft Wall Height with 3H:1V Back Slope with $\gamma_{\text{ret}}=105$ pcf and $\gamma_{\text{back}}=125$ pcf for Different Friction Angles.....      | 163 |
| Figure 162. Factor of Safety against Sliding for a 20-ft Wall Height with 3H:1V Back Slope with $\gamma_{\text{ret}}=125$ pcf and $\gamma_{\text{back}}=105$ pcf for Different Friction Angles.....      | 163 |
| Figure 163. Factor of Safety against Overturning for a 20-ft Wall Height with 3H:1V Back Slope with $\gamma_{\text{ret}}=105$ pcf and $\gamma_{\text{back}}=105$ pcf for Different Friction Angles. .... | 164 |
| Figure 164. Factor of Safety against Overturning for a 20-ft Wall Height with 3H:1V Back Slope with $\gamma_{\text{ret}}=105$ pcf and $\gamma_{\text{back}}=125$ pcf for Different Friction Angles. .... | 164 |
| Figure 165. Factor of Safety against Overturning for a 20-ft Wall Height with 3H:1V Back Slope with $\gamma_{\text{ret}}=125$ pcf and $\gamma_{\text{back}}=105$ pcf for Different Friction Angles. .... | 165 |
| Figure 166. MSE Wall with 20 ft Wall Height and No Back Slope Model Geometry for FLAC.....   | 166 |
| Figure 167. MSE Wall with 10 ft Wall Height and No Back Slope.....   | 167 |
| Figure 168. MSE Wall with 20-ft Wall and 3H:1V Back Slope. ....  | 167 |
| Figure 169. Strips Spacing for Each Panel of MSE Wall. ....  | 169 |
| Figure 170. FLAC FOS with Respect to $\phi$ (Retain) for a 10-ft Wall Height with No Dilation Angle. ....  | 171 |
| Figure 171. FLAC FOS with Respect to $\phi$ (Retain) for a 10-ft Wall Height with Dilation Angle. ....   | 171 |
| Figure 172. FLAC FOS with Respect to $\phi$ (Retain) for a 20-ft Wall Height with No Dilation Angle.....   | 172 |
| Figure 173. FLAC FOS with Respect to $\phi$ (Retain) for a 20-ft Wall Height with Dilation Angle. ....   | 172 |
| Figure 174. FLAC FOS with Respect to $\phi$ (Retain) for a 20-ft Wall Height with 3H:1V Back Slope with No Dilation Angle.....   | 173 |
| Figure 175. FLAC FOS with Respect to $\phi$ (Retain) for a 20-ft Wall Height with 3H:1V Back Slope with Dilation Angle.....  | 173 |
| Figure 176. Free Body Diagram of Forces Acting on MSE Wall. ....   | 174 |
| Figure 177. $K_a$ _FLAC Comparison with $K_a$ _Rankine for Different $\phi$ (Retain) for a 10-ft Wall Height with No Dilation Angle. ....  | 175 |
| Figure 178. $K_a$ _FLAC Comparison with $K_a$ _Rankine for Different $\phi$ (Retain) for a 10-ft Wall Height with Dilation Angle. ....   | 176 |
| Figure 179. $K_a$ _FLAC Comparison with $K_a$ _Rankine for Different $\phi$ (Retain) for a 20-ft Wall Height with No Dilation Angle. ....  | 176 |
| Figure 180. $K_a$ _FLAC Comparison with $K_a$ _Rankine for Different $\phi$ (Retain) for a 20-ft Wall Height with Dilation Angle. ....   | 177 |
| Figure 181. $K_a$ _FLAC Comparison with $K_a$ _Rankine for Different $\phi$ (Retain) for a 20-ft Wall Height with 3H:1V Back Slope with No Dilation Angle. ....  | 177 |

|   |     |
|---|-----|
| Figure 182. $K_a$ _FLAC Comparison with $K_a$ _Rankine for Different $\phi$ (Retain) for a 20-ft Wall Height with 3H:1V Back Slope with Dilation Angle.....                           | 178 |
| Figure 183. $\delta_w$ for Different $\phi$ (Retain) for a 10-ft Wall Height with No Dilation Angle.....  | 178 |
| Figure 184. $\delta_w$ for Different $\phi$ (Retain) for a 10-ft Wall Height with Dilation Angle.....   | 179 |
| Figure 185. $\delta_w$ for Different $\phi$ (Retain) for a 20-ft Wall Height with No Dilation Angle.....  | 179 |
| Figure 186. $\delta_w$ for Different $\phi$ (Retain) for a 20-ft Wall Height with Dilation Angle.....   | 180 |
| Figure 187. $\delta_w$ for Different $\phi$ (Retain) for a 20-ft Wall Height with 3H:1V Back Slope with No Dilation Angle.....  | 180 |
| Figure 188. $\delta_w$ for Different $\phi$ (Retain) for a 20-ft Wall Height with 3H:1V Back Slope with Dilation Angle.....   | 181 |
| Figure 189. $\delta_b/\phi$ (Found) for Different $\phi$ (Found) for a 10-ft Wall Height with No Dilation Angle.....  | 181 |
| Figure 190. $\delta_b/\phi$ (Found) for Different $\phi$ (Found) for a 10-ft Wall Height with Dilation Angle.....   | 182 |
| Figure 191. $\delta_b/\phi$ (Found) for Different $\phi$ (Found) for a 20-ft Wall Height with No Dilation Angle.....  | 182 |
| Figure 192. $\delta_b/\phi$ (Found) for Different $\phi$ (Found) for a 20-ft Wall Height with Dilation Angle.....   | 183 |
| Figure 193. $\delta_b/\phi$ (Found) for Different $\phi$ (Found) for a 20-ft Wall Height with 3H:1V Back Slope with No Dilation Angle.....  | 183 |
| Figure 194. $\delta_b/\phi$ (Found) for Different $\phi$ (Found) for a 20-ft Wall Height with 3H:1V Back Slope with No Dilation Angle.....  | 184 |
| Figure 195. FOS Calculated with $\delta_b$ from FLAC for Different $\phi$ (Found) for a 10-ft Wall Height with No Dilation Angle.....   | 185 |
| Figure 196. FOS Calculated with $\delta_b$ from FLAC for Different $\phi$ (Found) for a 10-ft Wall Height with Dilation Angle.....  | 185 |
| Figure 197. FOS Calculated with $\delta_b$ from FLAC for Different $\phi$ (Found) for a 20-ft Wall Height with No Dilation Angle.....   | 186 |
| Figure 198. FOS Calculated with $\delta_b$ from FLAC for Different $\phi$ (Found) for a 20-ft Wall Height with Dilation Angle.....  | 186 |
| Figure 199. FOS Calculated with $\delta_b$ from FLAC for Different $\phi$ (Found) for a 20-ft Wall Height with 3H:1V Back Slope with No Dilation Angle.....                           | 187 |
| Figure 200. FOS Calculated with $\delta_b$ from FLAC for Different $\phi$ (Found) for a 20-ft Wall Height with 3H:1V Back Slope with No Dilation Angle.....                           | 187 |
| Figure 201. Loads Acting on the Base of Wall.....   | 189 |
| Figure 202. Factor of Safety for Bearing Using Different Equations for Different $\phi$ (Found) for a $\phi_{\text{retain}}=26^\circ$ and Loads Calculated from FLAC Simulation.....  | 192 |
| Figure 203. Factor of Safety for Bearing Using Different Equations for Different $\phi$ (Found) for a $\phi_{\text{retain}}=30^\circ$ and Loads Calculated from FLAC Simulation.....  | 192 |
| Figure 204. Factor of Safety for Bearing Using Different Equations for Different $\phi$ (Found) for a $\phi_{\text{retain}}=40^\circ$ and Loads Calculated from FLAC Simulation.....  | 193 |
| Figure 205. Factor of Safety for Bearing Using Different Equations for Different $\phi$ (Found) for a $\phi_{\text{retain}}=26^\circ$ and Loads Calculated from Rankine's $K_a$ ..... | 193 |

|   |     |
|---|-----|
| Figure 206. Factor of Safety for Bearing Using Different Equations for Different $\phi$ (Found) for a $\phi_{\text{retain}}=30^\circ$ and Loads Calculated from Rankine's $K_a$ ..... | 194 |
| Figure 207. Factor of Safety for Bearing Using Different Equations for Different $\phi$ (Found) for a $\phi_{\text{retain}}=40^\circ$ and Loads Calculated from Rankine's $K_a$ ..... | 194 |
| Figure 208. Factor of Safety for Bearing Using Different Equations for Different Cohesion (Found) for a cohesion <sub>retain</sub> =500 psf and Loads Calculated from FLAC.....       | 197 |
| Figure 209. Factor of Safety for Bearing Using Different Equations for Different Cohesion (Found) for a cohesion <sub>retain</sub> =1000 psf and Loads Calculated from FLAC.....      | 197 |
| Figure 210. Factor of Safety for Bearing Using Different Equations for Different Cohesion (Found) for a cohesion <sub>retain</sub> =2000 psf and Loads Calculated from FLAC.....      | 198 |
| Figure 211. Factor of Safety Values for Bearing Analysis, Sliding Analysis, and from FLAC Simulation for Different Cohesion (Found) for a Retaining $\phi=26^\circ$ .....             | 200 |
| Figure 212. Factor of Safety Values for Bearing Analysis, Sliding Analysis and from FLAC Simulation for Different Cohesion (Found) for a Retaining $\phi=30^\circ$ .....              | 200 |
| Figure 213. Factor of Safety Values for Bearing Analysis, Sliding Analysis and from FLAC Simulation for Different Cohesion (Found) for a Retaining $\phi=40^\circ$ .....              | 201 |
| Figure B. 1. Gradation A1 Stress-Strain and Volumetric Strain Curves.....   | 277 |
| Figure B. 2. Gradation A2 Stress-Strain and Volumetric Strain Curves.....   | 278 |
| Figure B. 3. Gradation A3 Stress-Strain and Volumetric Strain Curves.....   | 279 |
| Figure B. 4. Gradation A4 Stress-Strain and Volumetric Strain Curves.....   | 280 |
| Figure B. 5. Type A Material p-q Diagram.....   | 281 |
| Figure B. 6. Gradation B1 Stress-Strain and Volumetric Strain Curves.....   | 283 |
| Figure B. 7. Gradation B2 Stress-Strain and Volumetric Strain Curves.....   | 284 |
| Figure B. 8. Gradation B3 Stress-Strain and Volumetric Strain Curves.....   | 285 |
| Figure B. 9. Gradation B4 Stress-Strain and Volumetric Strain Curves.....   | 286 |
| Figure B. 10. Type B Material p-q Diagram.....  | 287 |
| Figure B. 11. Gradation C1 Stress-Strain and Pore Pressure-Strain Curves.....   | 289 |
| Figure B. 12. Gradation C2 Stress-Strain and Pore Pressure-Strain Curves.....   | 290 |
| Figure B. 13. Gradation C3 Stress-Strain and Pore Pressure-Strain Curves.....   | 291 |
| Figure B. 14. Gradation C4 Stress-Strain and Pore Pressure-Strain Curves.....   | 292 |
| Figure B. 15. Type C-1 and C-2 p-q Plots.....   | 293 |
| Figure B. 16. Type C-3 and C-4 p-q Plots.....   | 294 |
| Figure B. 17. Gradation D1 Stress-Strain and Volumetric Strain Curves.....  | 296 |
| Figure B. 18. Gradation D2 Stress-Strain and Volumetric Strain Curves.....  | 297 |
| Figure B. 19. Gradation D3 Stress-Strain and Volumetric Strain Curves.....  | 298 |
| Figure B. 20. Gradation D4 Stress-Strain and Volumetric Strain Curves.....  | 299 |
| Figure B. 21. Type D Material p-q Diagram.....  | 300 |
| Figure C. 1. Dimensions and Properties Used for Series 1 Case 1.....  | 301 |
| Figure C. 2. Series 1 Case 1 Foundation Angle $\phi=26^\circ$ , Backfill Angle $\phi=34^\circ$ , and $\gamma=105$ pcf Maximum Shear Strain Rate.....                                  | 301 |
| Figure C. 3. Series 1 Case 1 Foundation Angle $\phi=30^\circ$ , Backfill Angle $\phi=34^\circ$ , and $\gamma=105$ pcf Maximum Shear Strain Rate.....                                  | 302 |



|  |     |
|--|-----|
| Figure C. 4. Series 1 Case 1 Foundation Angle $\phi=35^\circ$ , Backfill Angle $\phi=34^\circ$ , and $\gamma=105$ pcf Maximum Shear Strain Rate. ....  | 302 |
| Figure C. 5. Series 1 Case 1 Foundation Angle $\phi=26^\circ$ , Backfill Angle $\phi=34^\circ$ , and $\gamma=125$ pcf Maximum Shear Strain Rate. ....  | 303 |
| Figure C. 6. Series 1 Case 1 Foundation Angle $\phi=30^\circ$ , Backfill Angle $\phi=34^\circ$ , and $\gamma=125$ pcf Maximum Shear Strain Rate. ....  | 303 |
| Figure C. 7. Series 1 Case 1 Foundation Angle $\phi=35^\circ$ , Backfill Angle $\phi=34^\circ$ , and $\gamma=125$ pcf Maximum Shear Strain Rate. ....  | 304 |
| Figure C. 8. Series 1 Case 1 Foundation $c_u=500$ psf, Backfill Angle $\phi=34^\circ$ , and $\gamma=105$ pcf Maximum Shear Strain Rate. ....           | 304 |
| Figure C. 9. Series 1 Case 1 Foundation $c_u=1000$ psf, Backfill Angle $\phi=34^\circ$ , and $\gamma=105$ pcf Maximum Shear Strain Rate. ....          | 305 |
| Figure C. 10. Series 1 Case 1 Foundation $c_u=2000$ psf, Backfill Angle $\phi=34^\circ$ , and $\gamma=105$ pcf Maximum Shear Strain Rate. ....         | 305 |
| Figure C. 11. Series 1 Case 1 Foundation $c_u=500$ psf, Backfill Angle $\phi=34^\circ$ , and $\gamma=125$ pcf Maximum Shear Strain Rate. ....          | 306 |
| Figure C. 12. Series 1 Case 1 Foundation $c_u=1000$ psf, Backfill Angle $\phi=34^\circ$ , and $\gamma=125$ pcf Maximum Shear Strain Rate. ....         | 306 |
| Figure C. 13. Series 1 Case 1 Foundation $c_u=2000$ psf, Backfill Angle $\phi=34^\circ$ , and $\gamma=125$ pcf Maximum Shear Strain Rate. ....         | 307 |
| Figure C. 14. Dimensions and Properties Used for Series 1 Case 2. ....   | 307 |
| Figure C. 15. Series 1 Case 2 Foundation Angle $\phi=26^\circ$ , Backfill Angle $\phi=34^\circ$ , and $\gamma=105$ pcf Maximum Shear Strain Rate. .... | 308 |
| Figure C. 16. Series 1 Case 2 Foundation Angle $\phi=30^\circ$ , Backfill Angle $\phi=34^\circ$ , and $\gamma=105$ pcf Maximum Shear Strain Rate. .... | 308 |
| Figure C. 17. Series 1 Case 2 Foundation Angle $\phi=35^\circ$ , Backfill Angle $\phi=34^\circ$ , and $\gamma=105$ pcf Maximum Shear Strain Rate. .... | 309 |
| Figure C. 18. Series 1 Case 2 Foundation Angle $\phi=26^\circ$ , Backfill Angle $\phi=34^\circ$ , and $\gamma=125$ pcf Maximum Shear Strain Rate. .... | 309 |
| Figure C. 19. Series 1 Case 2 Foundation Angle $\phi=30^\circ$ , Backfill Angle $\phi=34^\circ$ , and $\gamma=125$ pcf Maximum Shear Strain Rate. .... | 310 |
| Figure C. 20. Series 1 Case 2 Foundation Angle $\phi=35^\circ$ , Backfill Angle $\phi=34^\circ$ , and $\gamma=125$ pcf Maximum Shear Strain Rate. .... | 310 |
| Figure C. 21. Series 1 Case 2 Foundation $c_u=500$ psf, Backfill Angle $\phi=34^\circ$ , and $\gamma=105$ pcf Maximum Shear Strain Rate. ....          | 311 |
| Figure C. 22. Series 1 Case 2 Foundation $c_u=1000$ psf, Backfill Angle $\phi=34^\circ$ , and $\gamma=105$ pcf Maximum Shear Strain Rate. ....         | 311 |
| Figure C. 23. Series 1 Case 2 Foundation $c_u=2000$ psf, Backfill Angle $\phi=34^\circ$ , and $\gamma=105$ pcf Maximum Shear Strain Rate. ....         | 312 |
| Figure C. 24. Series 1 Case 2 Foundation $c_u=500$ psf, Backfill Angle $\phi=34^\circ$ , and $\gamma=125$ pcf Maximum Shear Strain Rate. ....          | 312 |
| Figure C. 25. Series 1 Case 2 Foundation $c_u=1000$ psf, Backfill Angle $\phi=34^\circ$ , and $\gamma=125$ pcf Maximum Shear Strain Rate. ....         | 313 |

|  |     |
|--|-----|
| Figure C. 26. Series 1 Case 2 Foundation $c_u=2000$ psf, Backfill Angle $\phi=34^\circ$ , and $\gamma=125$ pcf Maximum Shear Strain Rate. ....         | 313 |
| Figure C. 27. Dimensions and Properties Used for Series 1 Case 3. ....   | 314 |
| Figure C. 28. Series 1 Case 3 Foundation Angle $\phi=26^\circ$ , Backfill Angle $\phi=34^\circ$ , and $\gamma=105$ pcf Maximum Shear Strain Rate. .... | 314 |
| Figure C. 29. Series 1 Case 3 Foundation Angle $\phi=30^\circ$ , Backfill Angle $\phi=34^\circ$ , and $\gamma=105$ pcf Maximum Shear Strain Rate. .... | 315 |
| Figure C. 30. Series 1 Case 3 Foundation Angle $\phi=35^\circ$ , Backfill Angle $\phi=34^\circ$ , and $\gamma=105$ pcf Maximum Shear Strain Rate. .... | 315 |
| Figure C. 31. Series 1 Case 3 Foundation Angle $\phi=26^\circ$ , Backfill Angle $\phi=34^\circ$ , and $\gamma=125$ pcf Maximum Shear Strain Rate. .... | 316 |
| Figure C. 32. Series 1 Case 3 Foundation Angle $\phi=30^\circ$ , Backfill Angle $\phi=34^\circ$ , and $\gamma=125$ pcf Maximum Shear Strain Rate. .... | 316 |
| Figure C. 33. Series 1 Case 3 Foundation Angle $\phi=35^\circ$ , Backfill Angle $\phi=34^\circ$ , and $\gamma=125$ pcf Maximum Shear Strain Rate. .... | 317 |
| Figure C. 34. Series 1 Case 3 Foundation $c_u=500$ psf, Backfill Angle $\phi=34^\circ$ , and $\gamma=105$ pcf Maximum Shear Strain Rate. ....          | 317 |
| Figure C. 35. Series 1 Case 3 Foundation $c_u=1000$ psf, Backfill Angle $\phi=34^\circ$ , and $\gamma=105$ pcf Maximum Shear Strain Rate. ....         | 318 |
| Figure C. 36. Series 1 Case 3 Foundation $c_u=2000$ psf, Backfill Angle $\phi=34^\circ$ , and $\gamma=105$ pcf Maximum Shear Strain Rate. ....         | 318 |
| Figure C. 37. Series 1 Case 3 Foundation $c_u=500$ psf, Backfill Angle $\phi=34^\circ$ , and $\gamma=125$ pcf Maximum Shear Strain Rate. ....          | 319 |
| Figure C. 38. Series 1 Case 3 Foundation $c_u=1000$ psf, Backfill Angle $\phi=34^\circ$ , and $\gamma=125$ pcf Maximum Shear Strain Rate. ....         | 319 |
| Figure C. 39. Series 1 Case 3 Foundation $c_u=2000$ psf, Backfill Angle $\phi=34^\circ$ , and $\gamma=125$ pcf Maximum Shear Strain Rate. ....         | 320 |
| Figure C. 40. Dimensions and Properties Used for Series 2 Case 2. ....   | 320 |
| Figure C. 41. Series 2 Case 2 Foundation Angle $\phi=26^\circ$ , Backfill Angle $\phi=34^\circ$ , and $\gamma=105$ pcf Maximum Shear Strain Rate. .... | 321 |
| Figure C. 42. Series 2 Case 2 Foundation Angle $\phi=30^\circ$ , Backfill Angle $\phi=34^\circ$ , and $\gamma=105$ pcf Maximum Shear Strain Rate. .... | 321 |
| Figure C. 43. Series 2 Case 2 Foundation Angle $\phi=35^\circ$ , Backfill Angle $\phi=34^\circ$ , and $\gamma=105$ pcf Maximum Shear Strain Rate. .... | 322 |
| Figure C. 44. Series 2 Case 2 Foundation Angle $\phi=26^\circ$ , Backfill Angle $\phi=34^\circ$ , and $\gamma=125$ pcf Maximum Shear Strain Rate. .... | 322 |
| Figure C. 45. Series 2 Case 2 Foundation Angle $\phi=30^\circ$ , Backfill Angle $\phi=34^\circ$ , and $\gamma=125$ pcf Maximum Shear Strain Rate. .... | 323 |
| Figure C. 46. Series 2 Case 2 Foundation Angle $\phi=35^\circ$ , Backfill Angle $\phi=34^\circ$ , and $\gamma=125$ pcf Maximum Shear Strain Rate. .... | 323 |
| Figure C. 47. Series 2 Case 2 Foundation $c_u=500$ psf, Backfill Angle $\phi=34^\circ$ , and $\gamma=105$ pcf Maximum Shear Strain Rate. ....          | 324 |
| Figure C. 48. Series 2 Case 2 Foundation $c_u=1000$ psf, Backfill Angle $\phi=34^\circ$ , and $\gamma=105$ pcf Maximum Shear Strain Rate. ....         | 324 |

|  |     |
|--|-----|
| Figure C. 49. Series 2 Case 2 Foundation $c_u=2000$ psf, Backfill Angle $\phi=34^\circ$ , and $\gamma=105$ pcf Maximum Shear Strain Rate. ....         | 325 |
| Figure C. 50. Series 2 Case 2 Foundation $c_u=500$ psf, Backfill Angle $\phi=34^\circ$ , and $\gamma=125$ pcf Maximum Shear Strain Rate. ....          | 325 |
| Figure C. 51. Series 2 Case 2 Foundation $c_u=1000$ psf, Backfill Angle $\phi=34^\circ$ , and $\gamma=125$ pcf Maximum Shear Strain Rate. ....         | 326 |
| Figure C. 52. Series 2 Case 2 Foundation $c_u=2000$ psf, Backfill Angle $\phi=34^\circ$ , and $\gamma=125$ pcf Maximum Shear Strain Rate. ....         | 326 |
| Figure C. 53. Dimensions and Properties Used for Series 2 Case 3. ....   | 327 |
| Figure C. 54. Series 2 Case 3 Foundation Angle $\phi=26^\circ$ , Backfill Angle $\phi=34^\circ$ , and $\gamma=105$ pcf Maximum Shear Strain Rate. .... | 327 |
| Figure C. 55. Series 2 Case 3 Foundation Angle $\phi=30^\circ$ , Backfill Angle $\phi=34^\circ$ , and $\gamma=105$ pcf Maximum Shear Strain Rate. .... | 328 |
| Figure C. 56. Series 2 Case 3 Foundation Angle $\phi=35^\circ$ , Backfill Angle $\phi=34^\circ$ , and $\gamma=105$ pcf Maximum Shear Strain Rate. .... | 328 |
| Figure C. 57. Series 2 Case 3 Foundation Angle $\phi=26^\circ$ , Backfill Angle $\phi=34^\circ$ , and $\gamma=125$ pcf Maximum Shear Strain Rate. .... | 329 |
| Figure C. 58. Series 2 Case 3 Foundation Angle $\phi=30^\circ$ , Backfill Angle $\phi=34^\circ$ , and $\gamma=125$ pcf Maximum Shear Strain Rate. .... | 329 |
| Figure C. 59. Series 2 Case 3 Foundation Angle $\phi=35^\circ$ , Backfill Angle $\phi=34^\circ$ , and $\gamma=125$ pcf Maximum Shear Strain Rate. .... | 330 |
| Figure C. 60. Series 2 Case 3 Foundation $c_u=500$ psf, Backfill Angle $\phi=34^\circ$ , and $\gamma=105$ pcf Maximum Shear Strain Rate. ....          | 330 |
| Figure C. 61. Series 2 Case 3 Foundation $c_u=1000$ psf, Backfill Angle $\phi=34^\circ$ , and $\gamma=105$ pcf Maximum Shear Strain Rate. ....         | 331 |
| Figure C. 62. Series 2 Case 3 Foundation $c_u=2000$ psf, Backfill Angle $\phi=34^\circ$ , and $\gamma=105$ pcf Maximum Shear Strain Rate. ....         | 331 |
| Figure C. 63. Series 2 Case 3 Foundation $c_u=500$ psf, Backfill Angle $\phi=34^\circ$ , and $\gamma=125$ pcf Maximum Shear Strain Rate. ....          | 332 |
| Figure C. 64. Series 2 Case 3 Foundation $c_u=1000$ psf, Backfill Angle $\phi=34^\circ$ , and $\gamma=125$ pcf Maximum Shear Strain Rate. ....         | 332 |
| Figure C. 65. Series 2 Case 3 Foundation $c_u=2000$ psf, Backfill Angle $\phi=34^\circ$ , and $\gamma=125$ pcf Maximum Shear Strain Rate. ....         | 333 |

## LIST OF TABLES

|   | <b>Page</b> |
|---|-------------|
| Table 1. Material Parameters Used by TxDOT (Yoon 2011).....   | 4           |
| Table 2. Unit Weights for Select Backfill (TxDOT 2011). ....  | 4           |
| Table 3. Local Marginal Materials Used in Forest Service Structures<br>(after Keller 1995).....         | 7           |
| Table 4. Property Requirements for MSE Walls with Extensible Soil Reinforcement<br>(CalTrans 2004)..... | 9           |
| Table 5. Aggressive Soil Environments (Elias et al. 2009).....  | 9           |
| Table 6. Summary of Factor of Safety Used in MSE Design Check.....                                      | 17          |
| Table 7. Generalized Soil Properties. ....  | 27          |
| Table 8. Summary of FOSs from Back Analysis.....  | 30          |
| Table 9. Parametric Analysis of Sliding. ....   | 30          |
| Table 10. Select Backfill Gradation Limits (TxDOT 2004).....  | 58          |
| Table 11. Tested Backfill Gradations. ....  | 59          |
| Table 12. Specific Gravity Test Results. ....   | 62          |
| Table 13. Specific Gravity Test Results for Type C.....   | 62          |
| Table 14. Atterberg Limits of Passing the #200 Sieve .....  | 62          |
| Table 15. Maximum Density Test Results.....   | 63          |
| Table 16. Friction Angles for Types A, B, and D Backfill Tested. ....                                   | 77          |
| Table 17. Friction angles for Type C Backfill Material.....   | 77          |
| Table 18. Specific Gravity of Types A, B, and D.....  | 86          |
| Table 19. Unit Weight at Different Compaction. ....   | 86          |
| Table 20. FOSs for Different Reinforcement Length. ....   | 95          |
| Table 21. k and n Values.....   | 96          |
| Table 22. Material Properties for Bearing Capacity Calculation Model. ....                              | 104         |
| Table 23. Summary of FLAC Analysis and Manual Calculation.....  | 108         |
| Table 24. Material Properties for Frictional Backfill and Frictional Foundation Material. ....          | 110         |
| Table 25. Material Properties for Cohesive Foundation Material. ....                                    | 111         |
| Table 26. Series 1 Case 1: Horizontal Back Slope with Frictional Foundation Soil.....                   | 115         |
| Table 27. Series 1 Case 1: Cohesive Foundation Soils.....   | 118         |
| Table 28. Factor of Safety Comparison for Series 1 Case 1 with Different Depth. ....                    | 120         |
| Table 29. Series 1 Case 2: Back Slope 3:1 with Frictional Foundation Soil.....                          | 121         |
| Table 30. Series 1 Case 2: Cohesive Foundation Soils.....   | 122         |
| Table 31. Factor of Safety Comparison for Series 1 Case 2 with Different Depths.....                    | 123         |
| Table 32. Series 1 Case 3: Back Slope 2:1 with Frictional Foundation Soil.....                          | 130         |
| Table 33. Series 1 Case 3: Cohesive Foundation Soils.....   | 130         |
| Table 34. Series 2 Case 2: Fore Slope 3:1 with Frictional Foundation Soil.....                          | 133         |
| Table 35. Series 2 Case 2: Cohesive Foundation Soils.....   | 134         |
| Table 36. Series 2 Case 3: Fore Slope 2:1 with Frictional Foundation Soil.....                          | 138         |
| Table 37. Series 2 Case 3: Fore Slope 2:1 with Cohesive Foundation Soils.....                           | 138         |
| Table 38. Factor of Safety Analysis Results for Case 1. ....  | 142         |
| Table 39. Factor of Safety Analysis Results for Case 2. ....  | 142         |
| Table 40. Analyzed Cases for Series 4. ....   | 148         |

|   |     |
|---|-----|
| Table 41. Material Properties for Frictional Backfill, Retaining Materials and Frictional Foundation Material. .... | 168 |
| Table 42. Matrix of Properties Changed in FLAC Simulation for Three Different Wall Types. ....                      | 169 |
| Table 43. Factors for Bearing Capacity Equations Used from Different Codes and Authors. ....                        | 190 |
| Table 44. Material Properties Used for Pure Cohesive Soils for FLAC Simulations. ....                               | 196 |
| Table 45. Material Properties for FLAC Simulations $c$ - $\phi$ Foundations. ....                                   | 199 |
| Table 46. Laboratory Results for Types A, B, and D. ....  | 203 |
| Table 47. Laboratory Test Results for Type C Material. ....   | 204 |
| Table B. 1. Friction Angles for Type A, B, and D Backfill Tested. ....  | 275 |
| Table B. 2. Laboratory Test Results for Type C Material. ....   | 275 |
| Table B. 3. Type A Test Results. ....   | 276 |
| Table B. 4. Type B Test Results. ....   | 282 |
| Table B. 5. Type C Test Results. ....   | 288 |
| Table B. 6. Type D Test Results. ....   | 295 |



## **CHAPTER 1: INTRODUCTION**

Mechanically stabilized earth (MSE) walls have been used for many different purposes such as supporting bridges, residential/commercial buildings, sound walls, roadways, and railroads. Invented by the French architect and engineer, Henri Vidal, in the 1960s, MSE walls have gradually become a widely accepted retaining wall type. The MSE wall was introduced to the United States in the 1970s, and the first MSE wall was built in the state of California in 1972. So far, over 60,000 MSE walls higher than 35 ft are in service at the U.S. highway system (Alzamora and Barrows 2007). Approximately 9,000,000 ft<sup>2</sup> (850,000 m<sup>2</sup>) were added into the U.S. transportation system annually, which accounted for more than half of all types of retaining wall usage (Berg et al. 2009). The Texas Department of Transportation (TxDOT) is one of the leading transportation organizations in the application of MSE walls in the United States. MSE walls accounted for more than 80 percent of TxDOT retaining walls according to statistical data collected between August 1, 2006, and June 20, 2007 (Galvan 2007). The MSE walls constructed by TxDOT comprised more than 20 percent of the MSE walls constructed annually in the U.S. transportation system.

The MSE walls have become the preferred retaining wall type because they are less expensive, easier to construct, more tolerable to differential settlement, and perform better under seismic loading compared with other types of retaining walls (Christopher et al. 2005). Besides retaining soil/rock mass, MSE walls have been built to support various heavily loaded superstructures, such as bridges and towers (Adams et al. 2011).

This project addresses several aspects of the MSE wall design, including material parameter selections and design assumptions. Chapter 2 includes a literature review on materials used by TxDOT and other transportation governing agencies, followed by an overview on current design assumptions and procedures for MSE walls adopted by TxDOT. Chapter 3 documents the case histories of poorly performing MSE walls in Texas. This chapter also discusses a TxDOT project on MSE walls in front of stable faces (Kniss et al. 2007). Chapter 4 assesses the design assumptions by testing backfill materials used by TxDOT, conducting statistical analysis of these backfill materials, and investigating the effects of variability of the backfill properties on sliding and overturning analyses of MSE walls. It also includes validating the minimum reinforcement length required for MSE walls. Chapter 5 focuses on numerical

simulation to justify the design methodology. It assesses the validity of the currently used bearing capacity equation and analyzes the MSE wall for global stability using the finite difference code—Fast Lagrangian Analysis of Continua (FLAC©). In this chapter, a global stability analysis is performed on different geometries with different material properties. In addition to global stability, this chapter also investigates compound failures of MSE walls of complicated geometries and/or groundwater conditions. A parametric study is performed in this project to better understand the effect of different geometries, different material properties of retained and foundation soils on sliding analysis, and bearing capacity analysis of MSE walls. This parametric study is documented in Chapter 6 for sliding and bearing capacity analysis using the American Association of State Highway and Transportation Officials (AASHTO) (2002) guidelines for forces acting on the wall and as well as forces calculated from FLAC simulations. Finally, Chapter 7 draws conclusions from all the above chapters on MSE walls for testing backfill materials, performing numerical simulations, and conducting statistical analysis on backfill materials. This chapter also provides recommendations for design assumptions in terms of material properties and on design methodology to be used for MSE walls.

The focus of this study is the MSE wall with precast panel and metallic reinforcement, but not the MSE wall with modular blocks and geosynthetic reinforcement. Therefore, the contents of Chapters 3–7 are for MSE walls using precast panel and metallic reinforcement.



## **CHAPTER 2: LITERATURE REVIEW**

The research team conducted a literature search to synthesize the state-of-the art practice of MSE walls. The literature review covers the following aspects of the MSE wall design:

- Materials: backfill material types, material properties, and related standard specifications.
- Design: required minimum factors of safety, bearing capacity, and minimum reinforcement length.
- Performance: failure modes, causes of failure, and performance data.
- Modeling: numerical modeling

Along with the literature review, the research team conducted a survey to gather information on current design methodologies and assumptions that have been employed by other state transportation agencies. The received survey replies are in Appendix A, and the major conclusions of this survey are summarized in this chapter.

### **OVERVIEW OF BACKFILL MATERIAL USED IN MSE WALLS**

#### **Types A, B, and D**

Various types of backfill materials have been applied to MSE wall construction. Existing AASHTO specifications for construction of MSE walls call for the use of high quality, free-draining granular material (AASHTO 2002). TxDOT allows three types (A, B and D) of backfill materials in permanent MSE walls as listed in Table 1 (TxDOT 2004). According to Item 423 of TxDOT material specifications, the percent passing a #200 sieve ranges from 0 to 15 percent, and there is no plasticity index (PI) requirement listed, which are slightly different from FHWA requirements for fine contents (<15 percent) and PI value (<6), especially, the gradation of each type of backfills deviates from FHWA specifications in terms of amount of fine content allowed as shown in Figure 1. However, the friction angle is directly adopted from FHWA guidelines without any modifications. FHWA does not specify the unit weight of backfill materials to be used, but TxDOT uses two sets of aggregate unit weight value for select backfill in current practice as presented in Table 2.

**Table 1. Material Parameters Used by TxDOT (Yoon 2011).**

| Type of Fill           | Material               | Short-term |              | Long-term |                      |
|------------------------|------------------------|------------|--------------|-----------|----------------------|
|                        |                        | c (psf)    | $\phi$ (deg) | c (psf)   | $\phi$ (deg)         |
| Reinforced fill        | Types A, B, and D      | 0          | 34           | 0         | 34                   |
|                        | Type C                 | 0          | 30           | 0         | 30                   |
| Retained fill          | Controlled fill, PI<30 | 750        | 0            | 0         | 30 or PI correlation |
| Foundation soil (fill) | Controlled fill, PI<30 | 750        | 0            | 0         | 30 or PI correlation |

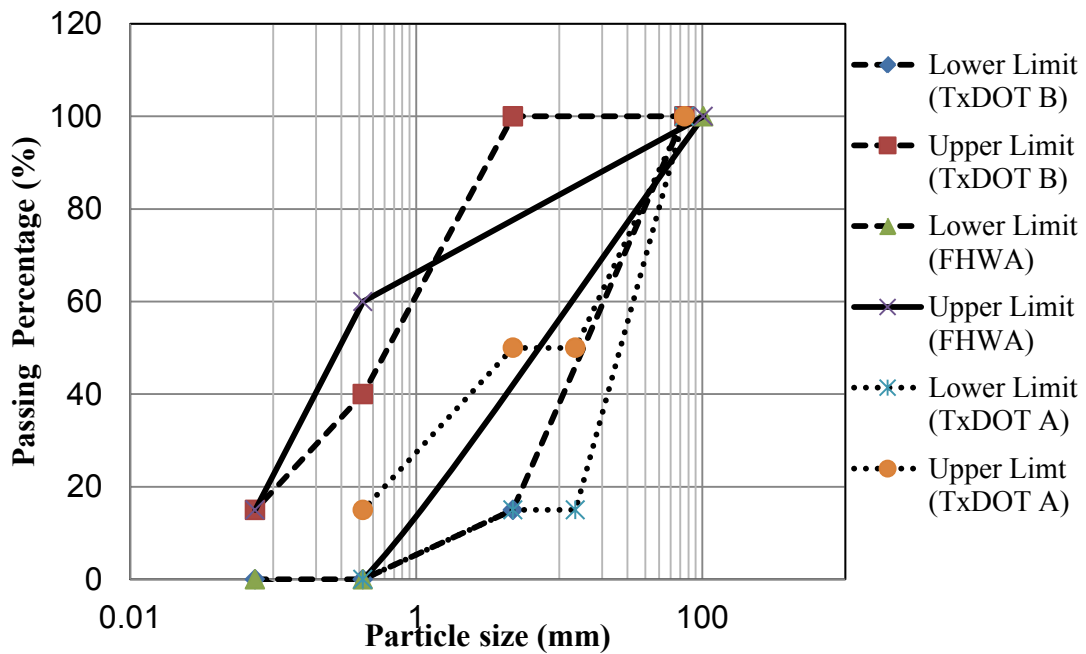


**Figure 1. TxDOT MSE Wall Backfill Material Gradation (Developed from TxDOT Standard Specifications 2004 and FHWA 2009).**

**Table 2. Unit Weights for Select Backfill (TxDOT 2011).**

| Type A, B, and D | Unit Weight (pcf) | Internal Stability | External Stability                 |
|------------------|-------------------|--------------------|------------------------------------|
|                  | 105               | Pullout            | Sliding, Overturning, Eccentricity |
|                  | 125               | Rupture            | Bearing capacity                   |

Both the friction angle and the unit weight of backfill materials have significant influence on the calculated factor of safety (FOS). Duncan (2000) completed a study on the variation of parameters for the calculation of FOS, which indicated that a variation of friction angle between

34° and 28° could influence the calculated FOS against sliding by up to 25 percent, and the variation of unit weight between 127 lb/ft<sup>3</sup> and 113 lb/ft<sup>3</sup> could influence the calculated FOS by approximately 10 percent. Harr (1984) and Kulhawy (1992) indicate that the variation of the friction angle of the foundation soil can lead to 13 percent variation of the calculated FOS. The material properties are influenced by the material type as well as the construction quality. Mooney et al.(2008) indicated that the inadequate compaction often occurred at the zones within 3–4 ft of the wall facing.

### **Type C**

TxDOT Type C material specifications permit a fines content of more than 15 percent, which is an unsuitable backfill material according to FHWA specifications (Berg et al. 2009). Note that TxDOT allows the use of Type C only for temporary walls. It is also usually considered a marginal fill-in practice. There is an argument that the FHWA specification is too conservative in its limitation on the fines content, since the National Concrete Masonry Association (NCMA) adopted a 35 percent fines content criterion (NCMA 2002). It was claimed that the marginal backfill material, if appropriately used, could lead to a well-performing MSE wall with 20–30 percent cost saving compared with the MSE walls using AASHTO/FHWA specified backfill material (Christopher et al. 2005). FHWA (2001) presented cases of MSE walls and reinforced slopes design and construction, and presented several case histories on utilizing various backfill materials such as glacial till, decomposed granite, and sandy clay soils with geo-reinforcement. Overall, the performance of structures has been satisfactory with no major problems observed.

However, studies also showed that inappropriate usage of the marginal fill can cause excessive lateral deformation of walls, vertical settlement of reinforced fill, and movement, cracking of the facing. Once the above-mentioned problem occurred, the repair/remedy cost would make the total cost of repair much higher than the construction cost of the MSE walls using AASHTO/FHWA specified backfill materials (Dodson 2010). The usage of marginal backfill material has been in a debate for long time. NCHRP has sponsored a seven-year project (Project 24-11) titled “Selecting Reinforced Fill Materials for Mechanically Stabilized Earth (MSE) Retaining Walls.” The project was extended for another year and thus the final report is not publicly available. The investigators have surveyed 35 departments of transportations (DOTs) in their practice on using marginal fill in MSE walls. In addition to TxDOT, the survey has

identified other two DOTs allowing backfill material with more than 15 percent fine contents. Most of the DOTs surveyed indicated that high plasticity soil was not allowed in the backfill material. A common concern of using marginal fill in MSE walls is that the marginal backfill cannot effectively dissipate excessive water pressure. As a result, it increases the lateral force on MSE walls and the backfill material behaves in undrained condition. With regard to this issue, Bobet (2002) conducted extensive laboratory pullout tests along with numerical analyses to determine the relation between drained and undrained pullout capacities for different soil types, overburden pressures, and scale and permeability effects in the dissipation of excess pore pressures. It was observed that:

- Drained and undrained pullout capacities varied depending on the amount of silt. The pullout capacity decreased from clean sand to 5 percent silty sand, increased from 5 to 10 percent silty sand, and then decrease from 10 to 15 and 35 percent silty sand.
- Pullout capacity increased with larger overburden pressure.
- The undrained pullout capacity is always smaller than the drained one except for clean sand, for which it is identical.
- The dissipation of pore pressure is very rapid for hydraulic conductivity larger than  $3.94 \times 10^{-3}$  in/sec and very slow with hydraulic conductivity smaller than  $3.94 \times 10^{-4}$  in/sec.
- For hydraulic conductivity smaller than  $3.94 \times 10^{-4}$  cm/sec, consolidation time increases along with the larger reinforcement length, based on numerical analyses. The deficiency of marginal backfill materials has been reflected in many failure cases (Reddy et al. 2003). Keller (1995) documented case histories with poorly and well-performing MSE walls typically constructed with native soil backfill on low and moderate standard rural roads as presented in Table 3.

**Table 3. Local Marginal Materials Used in Forest Service Structures (after (Keller 1995)).**

| Site                                  | Wall Type                           | USC Unified Soil Classification | % Minus #200 Sieve | PI | $\phi$ (deg) | C (psf) | Comments  |
|---------------------------------------|-------------------------------------|---------------------------------|--------------------|----|--------------|---------|---|
| Goat Hill Plumas NF (National Forest) | Welded wire (4.6 m)                 | SM                              | 21                 | 5  | 34           | 200.5   | 4% settlement on face                           |
|                                       |                                     | SC                              | 20                 | 8  | 31           | 300.7   |   |
|                                       |                                     | SM                              | 23                 | 4  | 27           | 348.8   |   |
| Mosquito R. Tahoe NF                  | Welded wire (8.2 m)                 | SM                              | 22                 | NP | -            | -       | Minor settlement, vegetated                     |
|                                       |                                     | ML                              | 50                 | 6  | -            | -       |   |
| L. North Fork Plumas NF               | Reinforced fill (1:1, 15.2 m)       | SM                              | 38                 | 2  | 34           | 100.2   | Minor slumping, well vegetated                  |
|                                       |                                     | ML                              | 55                 | 3  | 33           | 150.4   |   |
| Gallatin Lassen NF                    | HSE-concrete face with wire (3.8 m) | GW                              | 1+                 | NP | 30+          | -       | Minor face panel separation                     |
| B. Longville Plumas NF                | Welded wire (5.5 m)                 | CL                              | 50+                | -  | 26           | 200.5   | Poor foundation, 3% settlement                  |
|                                       |                                     | SM                              |                    |    |              |         |   |
| Grave Plumas NF                       | Geotextile (2.7 m)                  | SM                              | 26                 | NP | 35           | 850.1   | Irregular face, no fill loss                    |
| Butt Valley Plumas NF                 | Tire-Faced (3.1 m)                  | SC                              | 38                 | 8  | 26           | 401.0   | 10% face settlement                             |
| Thomjac Klamath NF                    | Timber-Faced (4.6 m)                | SM                              | 27                 | NP | 30+          | 0       | Minimal settlement                              |
| Stump Spring Sierra NF                | Welded Wire (6.8 m)                 | SM                              | -                  | -  | -            | -       | Performing well, Min. Settlement                |
|                                       |                                     | SC                              | 42                 | 15 | -            | -       |   |
| Pulga Plumas NF                       | Welded Wire (5.9 m)                 | SM                              | -                  | -  | -            | -       | Mod. Settlement, poor compaction                |
|                                       |                                     | GM                              | 44                 | 4  | 29           | 200.5   |   |
| Agness Siskiyou NF                    | Chainlink Fencing (to 6.7 m)        | GM                              | -                  | -  | -            | -       | Min. settlement, Min. corrosion, face vegetated |
|                                       |                                     | SM                              | 15                 | NP | -            | -       |   |
| Camp 5 Hill Willamette NF             | Wood Chips+ Geotextile (8.5 m)      | GP                              | 0                  | NP | 34           | 0       | 5% Settlement, Continuing chips decomposition   |

Currently, TxDOT recommends use of cement-stabilized Type C backfill when required or as approved along with special drainage provisions. Stabilizing Type C backfill with 5 percent hydraulic cement by dry weight of the backfill material should be followed by compaction of the backfill within 2 hours of mixing. In addition, properties to indicate the potential aggressiveness of the backfill material need to be measured as follows.

- pH between 5.5 and 10.0 as determined by Tex-128-E (TxDOT 1999a).
- Electrical resistivity more than 3000 ohm-cm as determined by Tex-129-E (TxDOT 1999b). Material resistivity between 1500 and 3000 ohm-cm may be used if the chloride content and sulfate content are less than 100 ppm and 200 ppm, respectively, as determined from Tex-620-J (TxDOT 2005).

During the kick-off meeting of this project, project committee members have raised concern on durability of backfill materials. TxDOT project 0-4177 Rathje et al.(2006) conducted a study on using crushed concrete and recycled asphalt pavement (RAP) as backfill to ensure long-term integrity of MSE walls. With respect to durability, expansion of compacted crushed concrete was monitored over a period of 70 to 100 days under various detrimental conditions. The expansion of most samples was negligible except for the samples that had suffered Alkali-Silica Reaction (ASR) or sulfate attack. However, there is a concern on drainage property of crushed concrete. The hydraulic conductivity of crushed concrete ranged from  $3.94 \times 10^{-5}$  to  $3.94 \times 10^{-6}$  in/s over confining pressures of 5 to 50 psi while the typical crushed lime stone backfill material exhibits  $3.94 \times 10^{-4}$  in/s hydraulic conductivity. For the RAP samples, creep testing was conducted to evaluate durability of the material. The results indicated that the creep potential in RAP is significant, similar to that of clays under undrained conditions. Drainage testing of RAP showed hydraulic conductivities ranging from  $1.96 \times 10^{-4}$  to  $1.57 \times 10^{-3}$  in/s over confining pressures of 5 to 50 psi using a triaxial apparatus, exhibiting higher drainage compared to crushed concrete. The study recommended the use of crushed concrete as backfill, unless the material was crushed from concrete structures that have suffered sulfate attack, along with adequate drains and high permittivity filter fabrics. The California Department of Transportation (CalTrans 2004) specifies the following criteria for MSE walls with extensible soil reinforcement (geosynthetics) as shown in Table 4.

**Table 4. Property Requirements for MSE Walls with Extensible Soil Reinforcement (CalTrans 2004).**

| Test             | Requirement | California Test No   |
|------------------|-------------|----------------------|
| Sand Equivalent  | 30 min.     | 217 (CalTrans 2011b) |
| Plasticity Index | 10 max.     | 204 (CalTrans 2008)  |
| Durability Index | 35 min.     | 229 (CalTrans 2011a) |
| pH               | 4.5 to 9.0  | 643 (CalTrans 2007)  |

The durability test is conducted to provide a measure of the relative resistance of an aggregate to producing clay-sized fines when subjected to prescribed methods of interparticle abrasion in the presence of water in accordance with California Test 229 (CalTrans 2011a). As per AASHTO 2002, backfill material should be free of shale or other soft, poor durability particles. Magnesium sulfate soundness should be less than 30 percent after four cycles in accordance with AASHTO T 104 (AASHTO 2007). The organic content in soil should be less than 1 percent measured as per AASHTO T 267 (AASHTO 2008). It is necessary to use clean gravel with minimum fines and to use wet sieve analysis to avoid misrepresentation of clay clumps as a large size particle. The aggressiveness of backfill material should be identified in terms of electrochemical properties, pH, resistivity, and salt contents. For different types of soils, their aggressive soil environments are tabulated below.

**Table 5. Aggressive Soil Environments (Elias et al. 2009).**

| Environment          | Prevalence   | Characteristics   |
|----------------------|--|---|
| Acid-Sulfate soils   | Appalachian Regions                                    | Pyritic, pH<4.5, SO <sub>4</sub> (1000–9000 ppm), Cl <sup>-</sup> (200–600 ppm)   |
| Sodic Soils          | Western States   | pH>9, high in salts including SO <sub>4</sub> and Cl <sup>-</sup>                 |
| Calcareous Soils     | FL, TX, NM, and Western states                         | High in carbonates, alkaline but pH<8.5, mildly corrosive                         |
| Organic Soils        | FL (Everglades), GA, NC, MI, WI, MN                    | Contain organic material in excess of 1% facilitating microbial induced corrosion |
| Coastal Environments | Eastern, Southern and Western Seaboard States and Utah | Atmospheric salts and salts laden soils in marine environments                    |
| Road Deicing Salts   | Northern States  | Deicing liquid contain salts that can infiltrate into soils                       |
| Industrial Fills     | Slag, cinders, fly ash, mine tailings                  | Either acidic or alkaline and may have high sulfate and chloride content          |

## INTERNAL STABILITY DESIGN

The Washington State Department of Transportation (WSDOT) report (Allen et al. 2001) establishes guidelines for a simplified method of analysis for internal stability of MSE walls and a comparison with methods such as the coherent gravity method and FHWA structure stiffness method. This report uses case histories of instrumented MSE walls from 1972 to 1991 to compare the prediction accuracy of the simplified method to that of the other methods in design codes. The simplified method is based on the determination of  $K_r$  using  $K_r/K_a$  vs. depth diagram and FHWA structure stiffness method equation to evaluate horizontal loads in the reinforcement. The difference in these methods is how the vertical soil stress is calculated. The coherent gravity method assumes that internally the wall acts as a rigid body and an overturning moment is transmitted through the reinforced soil mass. The FHWA structure stiffness method and the simplified method do not consider an overturning moment in internal vertical stress computations but do consider it for external bearing stress computation (Allen et al. 2001).

Currently, the simplified method is adopted in AASHTO design specifications for internal stability design. As per AASHTO design specifications, the internal stability of MSE walls is evaluated using a simplified coherent gravity approach. The vertical stress is the result of gravity forces from soil self-weight within and immediately above the reinforced wall backfill and any surcharge loads present. Equations used to calculate vertical stress are stated below. The lateral earth pressure coefficient  $K_r$  is determined by applying a multiplier to the active earth pressure coefficient. The active earth pressure is calculated using the Coulomb method assuming no wall friction.

$$K_a = \tan^2 \left( 45 - \frac{\phi'}{2} \right) \quad (\text{Eq. 1})$$

$$K_a = \frac{\sin^2(\theta + \phi')}{\sin^3\theta \left( 1 + \frac{\sin\phi'}{\sin\theta} \right)} \quad (\text{Eq. 2})$$

$$\sigma_h = \sigma_v K_r + \Delta\sigma_h \quad (\text{Eq. 3})$$

$$T_{\max} = \sigma_h S_v \quad (\text{Eq. 4})$$

where

$K_a$  = Coefficient of active earth pressure



$K_r$  = Coefficient of lateral earth pressure at reinforcement

$\phi$  = Angle of internal friction of retained soils

$\theta$  = Angle of inclination of wall face with vertical axis

$S_v$  = Vertical spacing between reinforcement strips

$\sigma_h$  = Horizontal stress

$\sigma_v$  = Vertical stress

Equation 2 can be used only when the wall face is battered. In Equation 3,  $\Delta\sigma_h$  is the horizontal stress at the reinforcement location resulting from a concentrated horizontal load. As per a report prepared by Liang (2004), the locus of maximum tensile forces in the reinforcement defines the critical limiting failure surface, which is affected by both reinforcement spacing and length. Based on this approach, a new method of analyzing internal stability is developed in this report. The method called Virtual Soil Wedge Analysis has been developed to estimate a reinforcement spacing and length. In this method, the required parameters are:

- Angle of internal friction of backfill material.
- Unit weight of backfill.
- Vertical reinforcement spacing.
- Coverage ratio.

The horizontal earth pressure distribution along the vertical axis is related to the unit weight of the soil, overburden height and a factor that corresponds to the effect of the lateral confinement, and embracement that restrains or prevents the lateral soil movements at the point of consideration. The lateral earth pressure is expressed as:

$$\sigma_h = \gamma h I_c \quad (\text{Eq. 5})$$

where

$I_c$  = The embracement factor, which is different from the lateral earth pressure coefficients

$\gamma$  = Unit weight of soil

$h$  = Height at horizontal stress is calculated.

This embracement factor is related to the slope of the virtual soil wedge and reinforcement layout. This report concludes that the required length of reinforcement is controlled by the internal stability requirements rather than the external stability. This results in significant savings in materials and construction of reinforced earth walls.

As per the TxDOT geotechnical manual (TxDOT 2012), the internal stability design is performed by MSE wall suppliers. Reinforcement loads calculated for internal stability design are dependent on the extensibility and material type of reinforcement. Modes for internal stability failures include:

- Soil reinforcement rupture.
- Soil reinforcement pullout.
- Internal sliding, failure at face connection.
- Bulging of face connections (Holtz and Lee 2002).

The load in the reinforcement is determined at two critical locations, i.e., at the zone of maximum stress and at the connection with the wall face, to assess the internal stability of the wall system. It is important for the engineer in charge to evaluate calculations provided by the wall supplier as these can be useful for calculating external stability of the system.

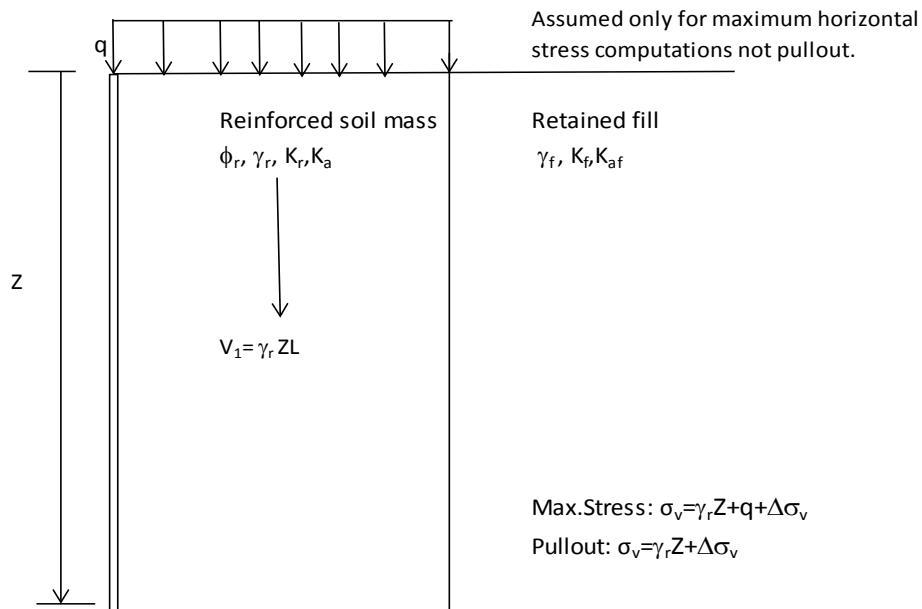


**Figure 2. Calculation of Vertical Stress for Horizontal Back Slope Condition, including Live Load and Dead Load Surcharges for Internal Stability Design (AASHTO 2002).**

### MINIMUM REINFORCEMENT LENGTH

FHWA and AASHTO require minimum length of 0.7H or 8 ft in the public transportation sectors. The NCMA design manual (NCMA 2002) specifies a minimum length of 0.6H, which has been widely used in the private sector. Nowadays, the 0.7H or 8 ft criterion has been used

worldwide based on investigation of simple wall geometries and external stability analyses. However, the 0.7H or 8 ft criteria remain further analysis.

From this perspective, here is the opinion reported below on 8ft or 0.7H reinforcement criterion from a world renowned expert in MSE walls, Dr. Dov Leshchinsky.

“The original FHWA specification on the 0.7H rule was a simple adoption of what has been used by Victor Elias, a pioneer of MSE walls in the US and one of the authors of a few FHWA publications on MSE walls. In the '70s–'80s, the MSE wall designs were implemented in a trial-and-error approach by hand. Considering a backfill of friction angle of  $30^\circ$ , in most instances a metallic strip length of 0.7H would satisfy the stability. Victor Elias personally specified 0.7H for two purposes: 1) it is a good starting point for trial-and-error analysis; and 2) it is a check to warn him about a possible error if the length is significantly longer or shorter than 0.7H.”

Even though the adoption of 0.7H initially seemed unreasonable, a number of studies have shown that the minimum reinforcement length criterion is sometimes conservative and it is effective to ensure the serviceability of constructed MSE walls. Ling and Leshchinsky (2003) and Ling et al. (2005) showed that the deformations increase when reinforcement length decreases. Apart from that, Ling and Leshchinsky (2003) also stated that the spacing of reinforcement affects the distribution of maximum reinforcement force along the wall height. Chew et al. (1991) reported that decreasing reinforcement length from 0.7H to 0.5H resulted in an approximate 50 percent increase in MSE wall deformations. Therefore, the minimum length, though lacking a solid basis, has been kept in the FHWA guidelines. A minimum length of 0.3H and 0.45H has been successfully used in Japan by considering the backfill quality and construction procedure that had a shoring wall in front of the structure to remove any external horizontal loads applying to the reinforced section (Morrison et al. 2006).

The specification of a minimum length of 8 ft for reinforcement is based largely on considerations for constructability rather than stability. Within a 3-ft zone of the MSE wall facing, lightweight compaction equipment is used to avoid exerting excessive pressure on the facing. The width of a typical roller is about 5 ft. To prevent a roller stepping within 3 ft of the facing, 8 ft is about the minimum acceptable length of the reinforced zone.

TxDOT geotechnical manual sets minimum earth reinforcement to 8 ft so as to ensure proper performance of the wall in place. Furthermore, a reinforcement length should be evaluated for project-specific requirements based on wall backfill type, wall embedment, wall drainage, and any conflicts within the reinforced zone of the wall. Special consideration should be given to walls that are subject to inundation. Type B backfill is the default backfill for permanent walls, but Type D backfill must be specified for walls that are subject to inundation. Walls to be placed in front of bridge abutments should have a 1.5-ft minimum and 3-ft desirable clearance from the back of the wall panels to the face of the abutment cap to facilitate wall construction. Standard specification Item 423 governs the design and construction of this wall type (TxDOT 2004).

## **EXTERNAL STABILITY**

The FHWA guidelines for external stability analysis are adopted from guidelines for rigid retaining walls such as gravity walls and cantilever walls. The adopted external stability analysis was claimed “justified” by the FHWA research project titled “Mechanically Stabilized Earth Walls and Reinforced Soil Slopes Design and Construction Guidelines” (FHWA 2001). Overall, sliding and overturning have demonstrated consistency between design and performance. However, disagreement exists on the method used for the bearing capacity analysis. Apart from this, the design of MSE walls for external stability should ensure that there will be adequate FOS as specified in the standards. A proper understanding of the system of forces and the distribution of vertical stress within the reinforced soil mass is important for the evaluation of external stability (Liang 2004). External stability design for MSE walls should include analyses for base sliding failure between wall and foundation soil, bearing capacity failure, and for overall slope stability (Holtz and Lee 2002).

## **BEARING CAPACITY**

Bearing capacity theory was derived by Terzaghi (1943) based on Prandtl’s theory (1920) for plastic failure of metal under rigid punches. For a rigid footing, punching failure occurs when there is compression of the soil under the footing, accompanying by shear in the vertical direction at the edge of the footing as shown in Figure 3. There is no heave at the edge of the footing, but heave may occur at a certain distance from the edge of the footing. Relatively large

settlement is a characteristic of the ultimate bearing capacity failure. Terzaghi proposed the equation below to calculate the ultimate bearing capacity:

$$q_u = cN_c + \gamma D_f N_q + \frac{1}{2} \gamma B N_\gamma \quad (\text{Eq. 6})$$

where

$q_u$  = Ultimate bearing capacity

$c$  = Cohesion of foundation soil

$N_c, N_q, N_\gamma$  = Bearing capacity factors

$\gamma$  = Unit weight of foundation soil

$D_f$  = Embedment factor for foundation

$B$  = Width of footing

However, the usage of the Terzaghi's bearing capacity equation for MSE wall has been in dispute. As described above, the classic Terzaghi's equation was derived based on punching rigid metal, but the MSE wall backfill mass, though reinforced, is still relatively flexible. Using Eq. 6 to calculate bearing capacity yields a conservative result. Another argument against the application of the equation for bearing capacity is that the bearing capacity failure mode for this type of loading seems unrealistic and highly conservative, especially when there is a slope adjacent to the toe of the MSE wall (Leshchinsky 2006). Researchers have attempted to unify global stability and bearing capacity analysis, but no breakthrough has been achieved yet.

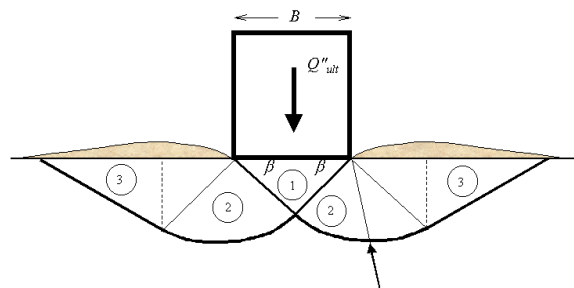


**Figure 3. Ultimate Bearing Capacity of Rigid Footing.**

At the elevation of the leveling pad, only one side is surcharged by backfill materials, thus the surcharge term on the bearing capacity equation is completely ignored in current

practice as shown in Figure 4(a). To increase the bearing capacity, the reinforcement length has to increase to give a larger term of  $\frac{1}{2}\gamma BN\gamma$ . The increase of the reinforcement length becomes crucial, even when the foundation soil is cohesionless. There is a motivation for at least partially considering the surcharge provided by the backfill materials as shown in Figure 4(b). It has been argued that a bearing capacity failure may lead to rotation about the toe of the MSE wall and separation between reinforced zone and retained zone. However, the MSE wall backfills are loose materials and a distinct separation is unlikely to occur. In recent years, there has been a tendency to unify bearing capacity analysis and global stability analysis. An insufficient bearing capacity for MSE wall will not simply induce punching failure, since there is always lateral force. As a result, the MSE wall movement will dominantly be rotation.

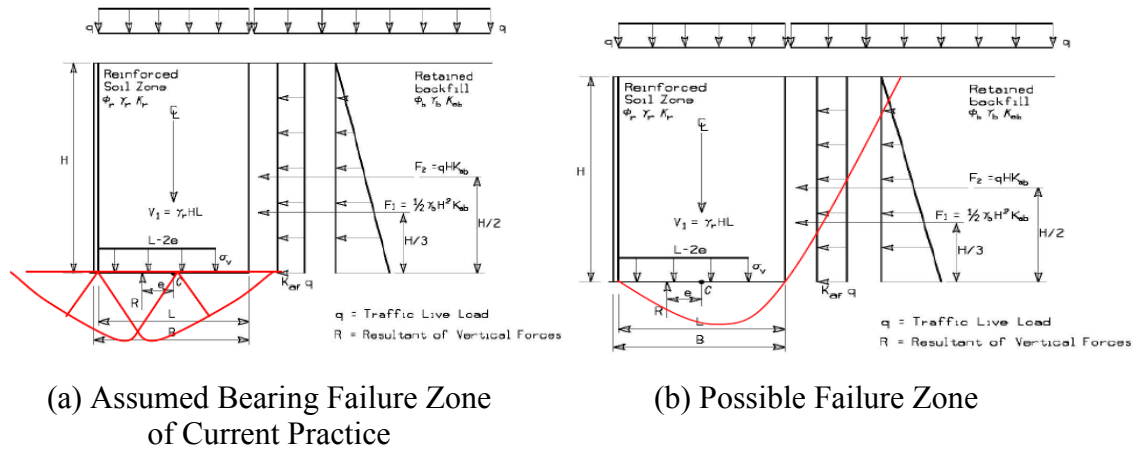


**Figure 4. Bearing Capacity of Retaining Walls.**

## SLIDING AND OVERTURNING

Analysis for the potential for sliding and overturning of rigid wall has been well calibrated by practice. Strictly speaking, sliding analysis based on limit equilibrium is the only analysis that completely satisfies equilibrium (Leshchinsky and Han 2004). Thus, there is almost no dispute on the methods used for checking sliding and overturning. However, researchers and practitioners are concerned about the reliability of calculated FOS for MSE walls against sliding and overturning. A study completed by Chalermyanont and Benson (2005) indicated that the spatial variability of the backfill properties could influence the calculated FOS significantly. For instance, if the target FOS against sliding and overturning are 1.2 and 1.1, respectively, the

material spatial variation along the wall may lead to about 2 percent and 0.4 percent probability of failure (i.e., FOS <1) even without considering uncertainties in FOS calculations. The spatial variation of the properties of backfill materials can influence the results for different reasons, such as non-uniform compaction, construction sequence, and reinforcement. The spatial variation is almost inevitable even though a strict QA/QC procedure is adopted. However, this variability is not considered when calculating the FOS for a rigid retaining wall. Duncan (2000) recommended using reliability analysis as a complement to FOS analysis, but it is often deemed too complicated to be practical. TxDOT has adopted the FOSs listed in Table 6, which are also specified by AASHTO (2002) and NCMA (2002). In the table, the FOSs of other agencies were listed for comparison. No consideration of the spatial variation has been included, which results in higher probability of failure than for rigid retaining wall designed with the same FOS.

**Table 6. Summary of Factor of Safety Used in MSE Design Check.**

| <b>Failure Mode</b> | <b>TxDOT</b>            | <b>WisDOT (WisDOT 2006)</b>                                       | <b>CalTrans (CalTrans 2004)</b>      |
|---------------------|-------------------------|---|--------------------------------------|
| Sliding             | FOS $\geq$ 1.5          | 1.5 for spread footings on soil or rock and 1.0 for pile footings | 1.5                                  |
| Overturning         | FOS $\geq$ 2.0          | 1.5 for footings on piles or rock<br>2.0 for footings on soil     | 1.5                                  |
| Bearing capacity    | FOS $\geq$ 1.3 (global) | 1.3 (Global)  | 3.0                                  |
| Eccentricity, e     | e < L/6 (middle third)  | n/a   | e < L/6, on soil<br>e < L/4, on rock |
| Pullout             | FOS $\geq$ 1.5          | 1.5   | 1.5                                  |

## **COMPOUND FAILURE**

Compound failure, i.e., failure planes passing behind or under and through a portion of the reinforced soil zone, has become a concern as MSE walls have been built in more complicated situations as shown in Figure 5. The FHWA manual discusses four situations where compound failure is a significant concern. AASHTO requires a check for compound failure, but provides no guidelines. FHWA suggests using global stability for a compound failure analysis, which would require information about retained soil, subsurface condition, and reinforcement layout. Thus, the responsibility between the agent and the vendor is not clear. Meyers et al. (1997) summarized how the responsibility was distributed between the agent and the vendor

under different conditions. In TxDOT MSE wall projects, the compound failure analysis is the responsibility of the retaining wall designer.

The analysis of compound failures becomes difficult, since the MSE wall facing units have to be explicitly considered into the slope stability analysis. Appropriate simulation of the interface between facing panels or blocks is critical to obtain reliable results. Hatami and Bathurst (2005) conducted interface tests on modular blocks and found an interface friction angle of  $57^\circ$  and apparent cohesion of 960.8 psf. These properties were used in finite difference numerical modeling and yielded satisfactory results. No study has been done to consider the effect of precast panel on the compound failure. The detailed representation of the interface between facing panels or blocks would not be possible in current limit equilibrium analysis. ReSSA, a computer program based on limit equilibrium analysis and widely used for reinforced soil slope design, may be employed for compound failure analysis, since it directly incorporates reinforcement elements (Berg et al. 2009). However, ReSSA does not explicitly consider facing units. The validity of using ReSSA in checking for safety against compound failure needs to be verified before it can be put into wide usage.

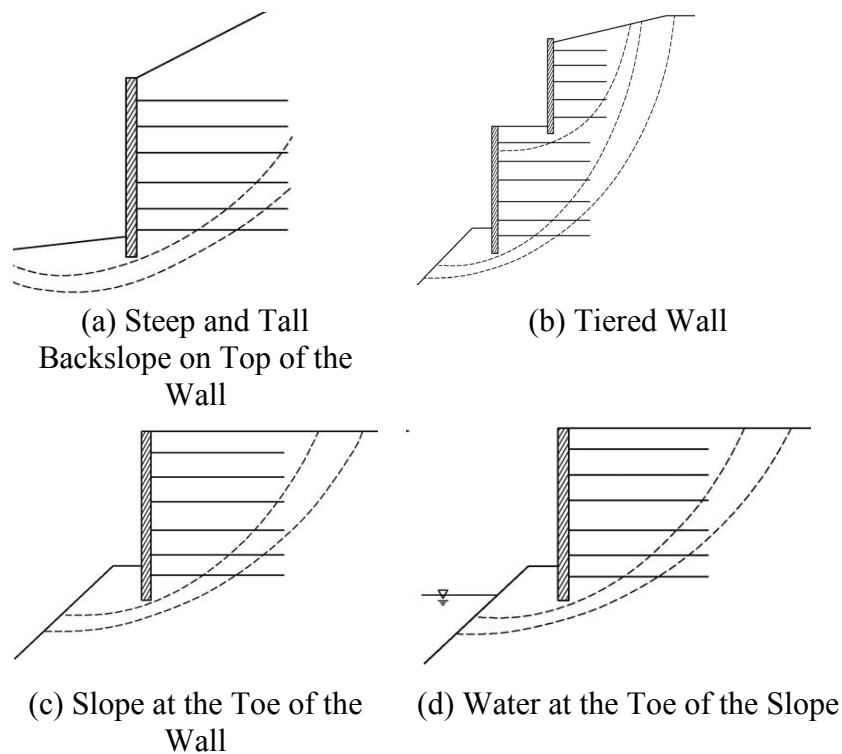


**Figure 5. Compound Failure (Berg et al. 2009).**



## OVERVIEW OF MSE WALL PERFORMANCE

Mr. Marcus J. Galvan of TxDOT presented case studies on performance, cause of failure, and solutions of several retaining walls in Texas (Galvan 2007). He mainly pointed out two aspects about causes of failures:

- Design deficiency in cases where MSE walls are built on slopes to minimize retaining wall square footage as illustrated in Figure 6.
- Construction and inspection problems.

A case history of MSE wall failure due to inadequate construction along with improper backfill material was presented. Gradation of the backfill showed a significant discrepancy in terms of passing No. 200 between the sample supplied by the contractor and samples tested from the stockpile. The latter had 37 percent fines as determined by wet sieve analysis. In addition, a field survey on the failed segment revealed that backfill retained water and presented a large number of voids that might be attributed to inappropriate compaction and bimodal grain size distribution so that the larger particles bridge together, preventing the smaller material from filling in the regions between the particles.



**Figure 6. Example of MSE Wall Failure along the Slope.**

## SUMMARY OF SURVEY OUTCOME

A survey was performed to collect information regarding MSE wall practice. The recipients of this survey questionnaire are experienced geotechnical engineers from state DOTs. In addition to that, a survey questionnaire was sent to Ryan Berg who is a main author of FHWA

design guidelines for MSE walls and reinforced slopes (FHWA 2009). A total of 30 survey questionnaire forms were sent out. The detailed answers to the survey questionnaire are in Appendix A. The personal information on the questionnaire is withheld per a personal information disclosure agreement. The DOTs and the engineer who supplied feedback are:

- Massachusetts DOT.
- Oregon DOT.
- Nevada DOT.
- Idaho DOT.
- Indiana DOT.
- Missouri DOT.
- New Mexico DOT.
- Alabama DOT.
- Kansas DOT.
- Connecticut DOT.
- Illinois DOT.
- Iowa DOT.
- Maryland DOT.
- New Hampshire DOT.
- New York DOT.
- South Carolina DOT.
- Washington DOT.
- Wisconsin DOT.
- California DOT.
- Minnesota DOT.
- Missouri DOT.
- Montana DOT.
- North Carolina DOT.
- Vermont DOT.
- Wyoming DOT.
- Nebraska DOT.

- Louisianan DOT.
- Ryan Berg.

According to the information revealed from the survey forms, all the DOTs have indicated that the FHWA design methodology has been followed to design the MSE walls. The minimum reinforcement length used for design is 0.7H or 8 ft, whichever is longer. In all, thirteen DOTs have different backfill specifications from FHWA guidelines. These specifications deviate slightly from FHWA's in different aspects such as gradation, fine contents, and gravel-size contents, wet sieve analysis, and resistivity, but at the same time they indicate a higher quality of material than the FHWA guidelines specified. All the DOTs showed that the durability of the backfill material was tested for one or multiple of the following:

- Resistivity–AASHTO T288.
- pH –AASHTO T289.
- Chlorides and sulfates–ASTM D4327.
- Magnesium sulfate soundness AASHTO T-104.
- Organics–AASHTO T267.

Vermont DOT indicated its own durability evaluation methods. Oregon DOT and Kansas DOT have indicated that they encountered granular backfill material that can decompose into finer grained soils in the presence of moisture. Oregon DOT defines such backfill as nondurable material and has published guidelines to direct the usage of the material.

According to the frequency of the failure modes being seen, the ranking of the failure modes with frequency descending is bearing capacity, sliding, global stability, compound failure and overturning. The bearing capacity has been constantly checked by using the Terzaghi's bearing capacity formula. The compound failure is checked without considering the effect of the discrete facing units.



## **CHAPTER 3: CASE HISTORIES**

The research team attempted to compile the design and field QA/QC data for some of the constructed TxDOT MSE walls, which should include both poorly performing and well-performing MSE walls. Data mining of the TxDOT construction database did not yield sufficient data to permit meaningful statistical analyses. An alternative approach was taken to obtain relevant information with the assistance from the project directors and TxDOT district engineers. The research team collected information from six sites where the MSE walls were not performing well. Subsequent sections will further describe each site. These six case histories were evaluated to identify:

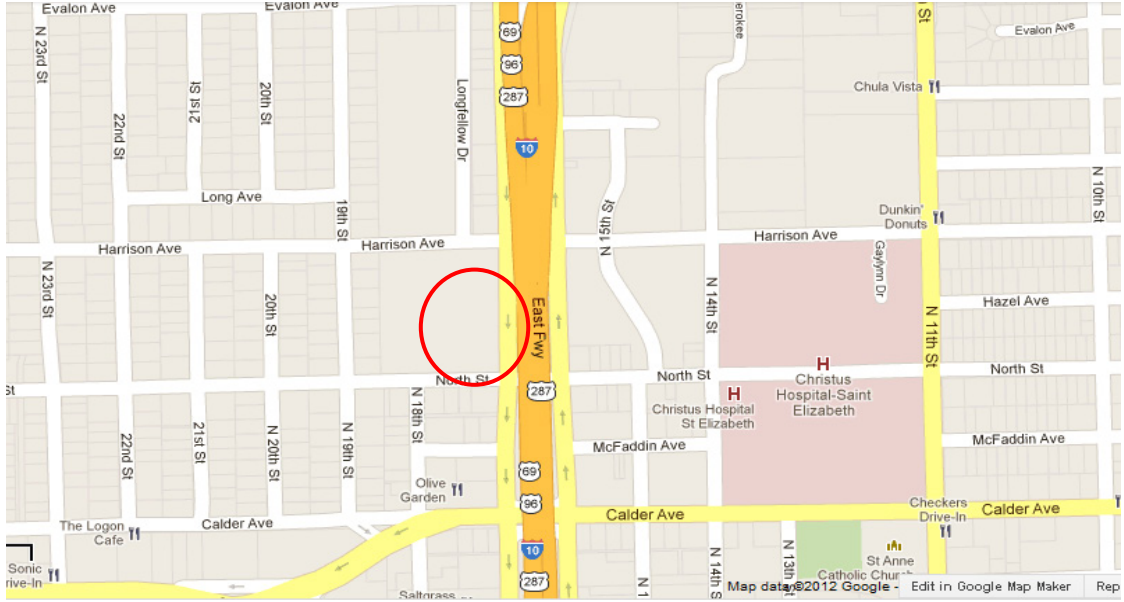
- Which failure mechanisms (e.g., sliding, settlement).
- Whether poor quality backfill contributed to the unsatisfactory performance.

### **CASE HISTORIES OF NOT-WELL PERFORMING MSE WALLS**

#### **IH 10 at Beaumont District**

The existing two MSE walls bounding the east bound (EB) approach and the west bound (WB) departure embankments are located along IH 10 near its intersection with Harrison Avenue in Beaumont, Texas. The geographic location of the MSE walls is shown in Figure 7. The two MSE walls (from Sta. 336+32 to 341+88) are approximately 550 ft long and the maximum heights of the walls at the bridge abutments are approximately 18 ft.

The approach and departure MSE walls constructed in 1980s have experienced some movements indicated by cracks on pavement of travel lanes and tilting of wall panels. The outmost travel lanes settled and separated from the shoulder on both directions. The separation ran about 100 ft long and up to 3 inches wide. Cracking was also observed at the connection between the coping/barrier and the MSE wall panels. To prevent the propagation of the settlement and further separation, a retrofit measure was taken by dowelling the shoulder to the adjacent travel lanes. After the retrofit, cracks appeared in the same travel lanes again, but were shifted toward the centerline of the roadway as shown in Figure 8.



(a) Geographic Location



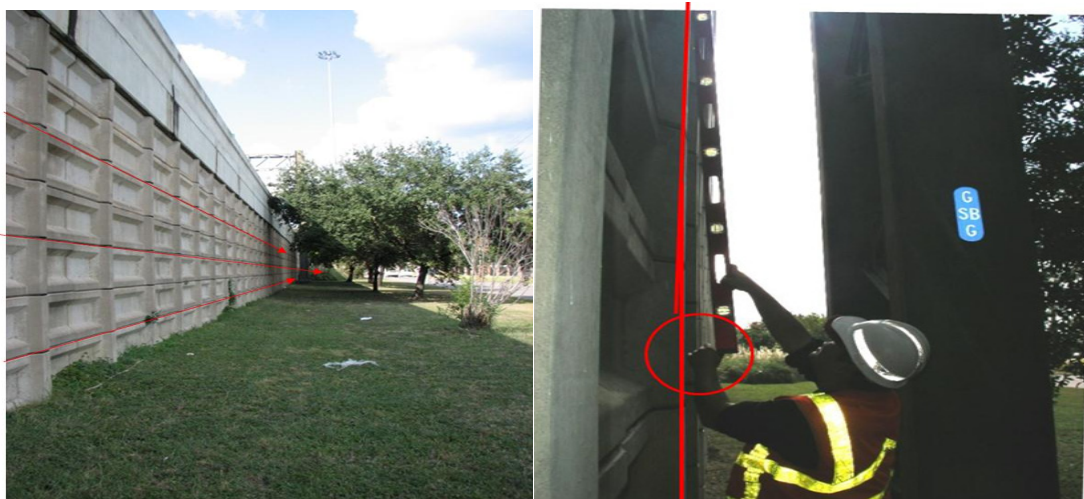
(b) Distressed Portion of the Roadway.

**Figure 7. Locations of the MSE Walls.**



**Figure 8. Recurring of Cracks on the Pavement.**

TxDOT through Professional Service Industries (PSI) conducted a geotechnical study to assess the condition of the MSE walls and pavement, investigate the subsurface conditions, sample and test the backfill materials within the retained and reinforced zones, and determine the possible cause(s) of the movement. Field observations were conducted for the EB and WB walls. As illustrated in Figure 9(a), there was no apparent settlement at the base, material migration through wall panels, and drainage issue at wall facing. However the outward movements of the upper portion of the MSE wall panels were detected as shown in Figure 9(b).



(a) Alignment of the Panels

(b) Wall Movement

**Figure 9. Field Observations.**

A total of five soil borings were drilled as illustrated in Figure 10. Borings B-1 and B-5 were in front of the retaining walls up to 40 ft deep from the existing ground surface, while borings B-2 to B-4 were made through reinforced or retained backfills up to 60 ft. At Borings B-2 and B-4, slope inclinometers were installed so TxDOT personnel can periodically monitor the movements of the walls.

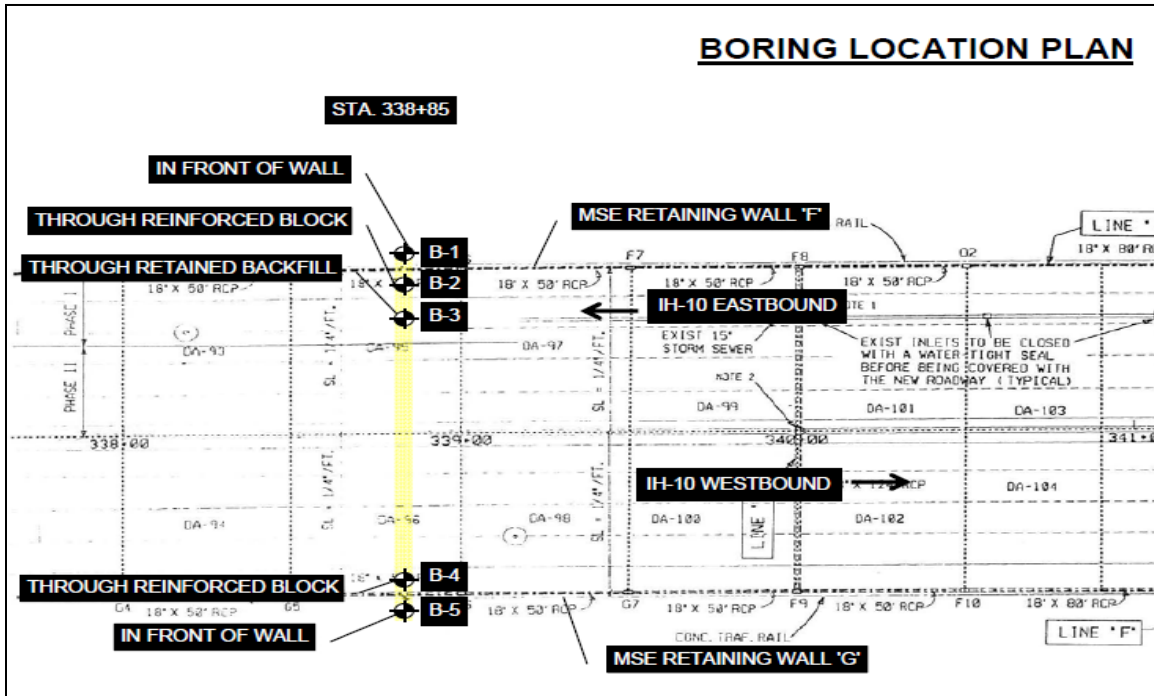


Figure 10. Boring Location Plan.

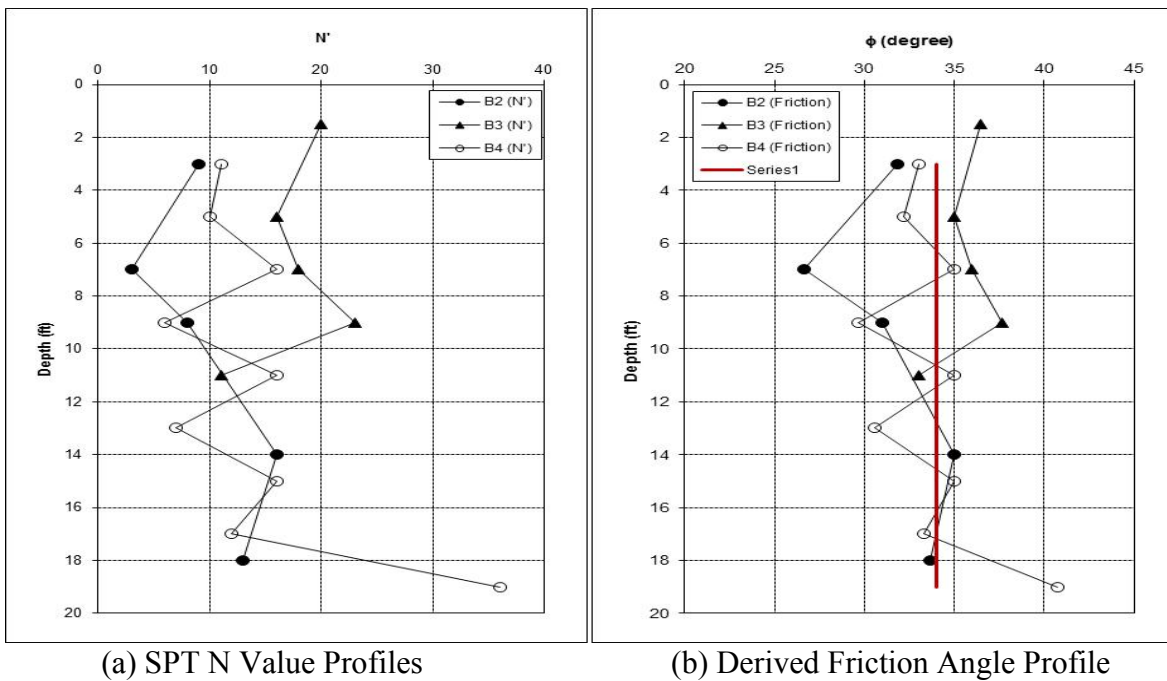
**Extensive laboratory testing was conducted on selected samples.**

Table 7 summarizes the MSE wall fill and subsurface fill. The fill within the reinforced and retained zones was sand with no greater than 5 percent fines. The Standard Penetration Test (SPT) blow counts indicated that the sand ranged from very loose to dense conditions. Figure 11 shows the profiles of SPT blow counts and the derived friction angle from SPT blow counts. The reinforced fill of the WB had higher average blow counts than the EB. The friction angle of reinforced and retained fill ranged from 26° to 38°. The friction angle of the upper 13 ft of reinforced fill was less than 34°, which was the assumed friction angle in the design and was indicated by a red line in Figure 11(b). The subsurface soil was primarily stiff to hard clayey soil. The over-consolidation ratio (OCR) ranged from 2 to greater than 10.



**Table 7. Generalized Soil Properties.**

| Materials       | Description                       | Moisture Content (%) | Passing #200 (%) | SPT N-Values (blow/ft) |
|-----------------|-----------------------------------|----------------------|------------------|------------------------|
| Reinforced fill | sand                              | 3–9                  | 3~5              | 4–39                   |
| Retained fill   | sand                              | 6–21                 | 4                | 6–17                   |
| Subsurface soil | lean to fat clay with sand (fill) | 17–25                | 71 ~ 93          | 8                      |
|                 | clayey sand, sandy clay           | 13–35                | 20–62            | 7–39                   |



**Figure 11. SPT Corrected N and Friction Angle along the Depth.**

The slope inclinometers (SI) were installed in Boring B-2 and B-4 to monitor the movement of the MSE walls. The results of the measurements are shown in Figure 12. Within a short time of monitoring, movements on both EB and WB were observed. Even though the magnitude of the movement was not significant, the movement was steadily increasing during that period and has a tendency of continuous propagation. The movement on the WB was more

pronounced than that at the EB. The lateral movement profile that SI disclosed also indicated salient lateral movement at the bottom of the MSE wall as shown in Figure 12(b).

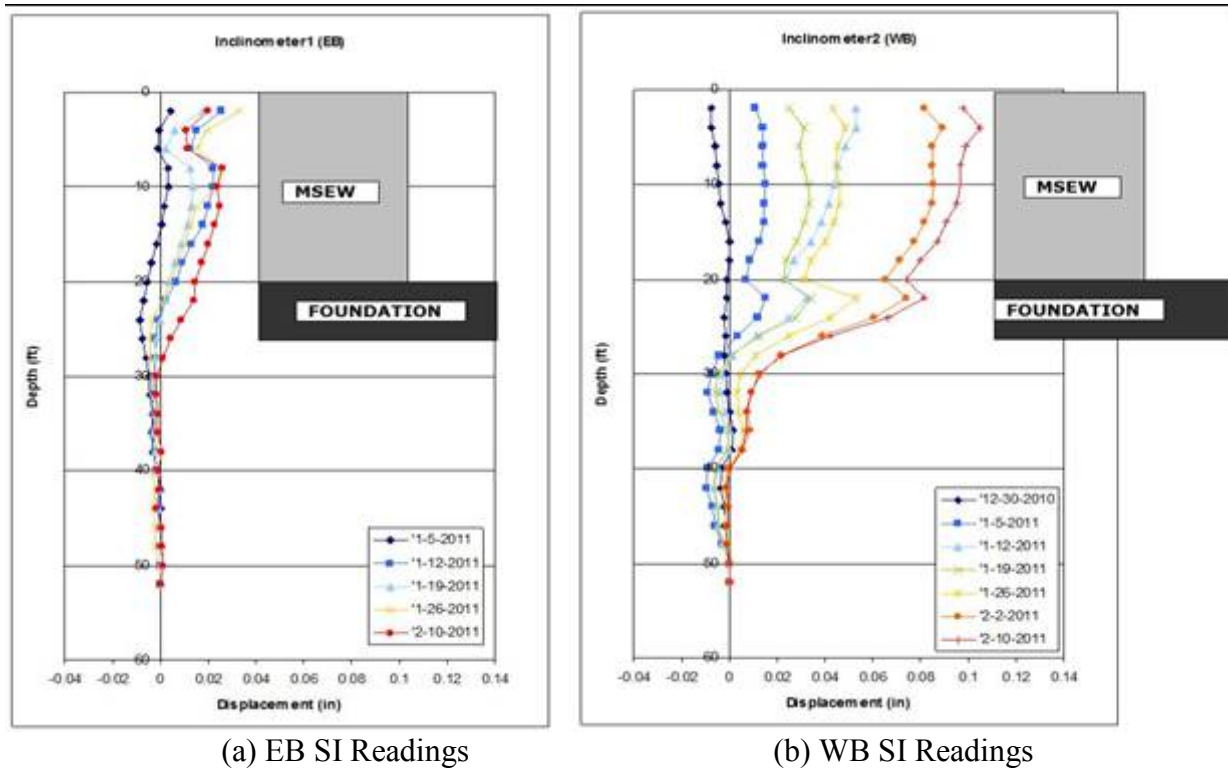


**Figure 12. MSE Retaining Wall Movements Measured by Incliner.**

A back analysis was conducted to investigate the cause(s) of the distress. The back analysis was primarily based on the in-situ SPT data (shown in Figure 11) and the triaxial CU tests performed by PSI (report dated February 2011). Friction angles of the backfill materials were interpreted from SPT blow counts, while the friction angle of foundation soil was based on the triaxial consolidated undrained (CU) test results. The back-analysis included calculating the FOSs for sliding, overturning, bearing capacity, and global stability. The cross-sections of the MSE walls and material properties are presented in Figure 13 below. The summary of the FOSs for both EB and WB MSE walls are presented in Table 8. The critical surface of the global stability of the EB and WB are presented in Figure 14. The eccentricities of EB and WB are 1.7 and 0.7 ft, respectively, which are within the middle third portion of the bases.

Since field evidence strongly suggested that the likely cause of distress was sliding, the back-analysis focused on this slide mechanism. Three inputs were considered in the analysis:

- The friction angle of the reinforced backfill.
- The friction angle of the foundation.
- The unit weight of the reinforced backfill.

The SPT data suggested an average drained friction angle of the backfill of  $31.6^\circ$ , which was taken as the high estimate for the purpose of the parametric study. Since the SPT data also suggested local zones with friction angles as low as  $26^\circ$ , this was taken as a lower bound friction for the backfill. For the foundation, a range of  $28.7^\circ$  to  $22^\circ$  was considered for the friction angle, the latter value was taken as a worst-case estimate corresponding to fully softened conditions. The results in Table 9 shows a factor of safety less than 1.5 only for the case of lower bound strength estimates for both the backfill and the foundation; i.e., fairly extreme lower bound strength estimates are required to obtain safety factors consistent with the observed distress.

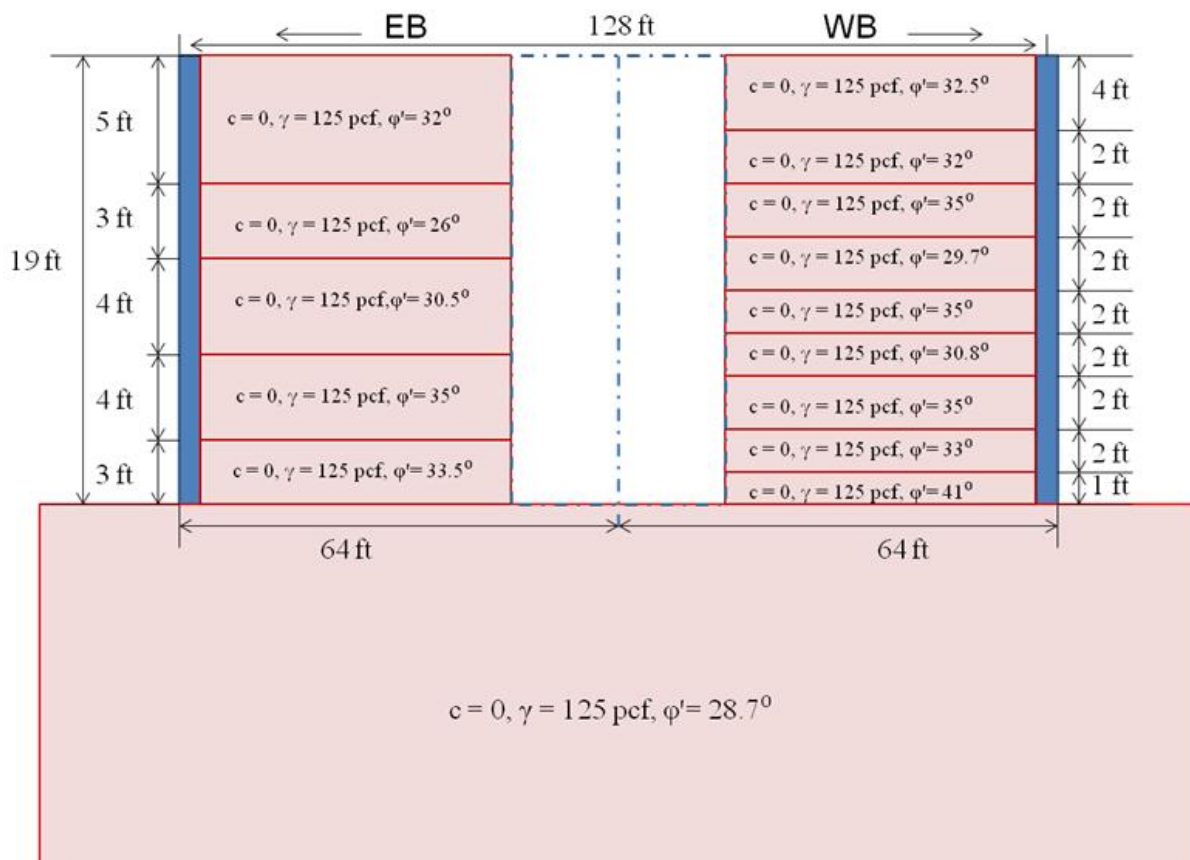


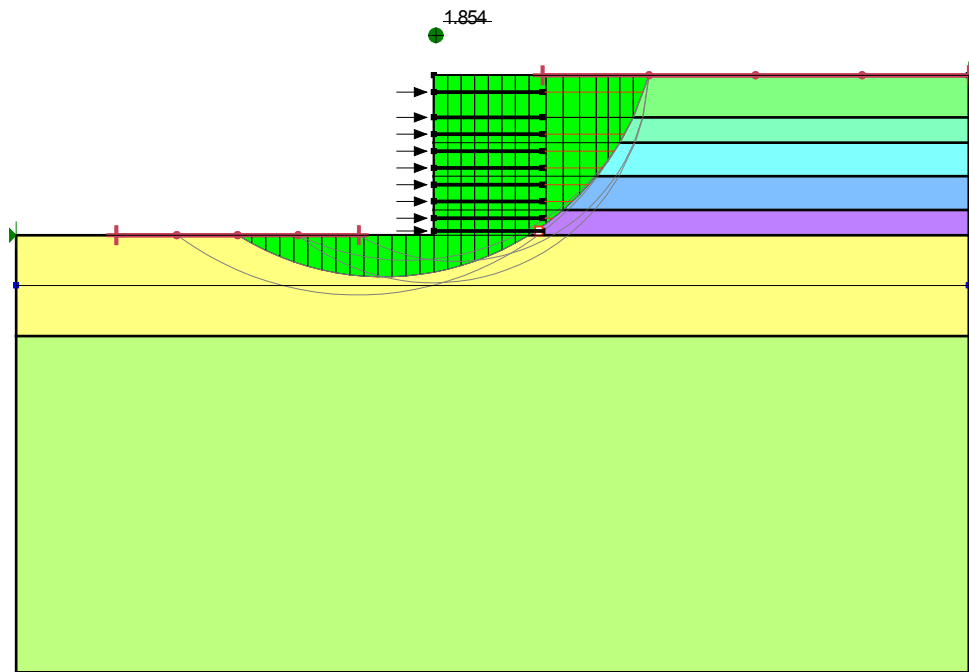
**Figure 13. Cross-Section and Material Properties of Back Analysis.**

**Table 8. Summary of FOSs from Back Analysis.**

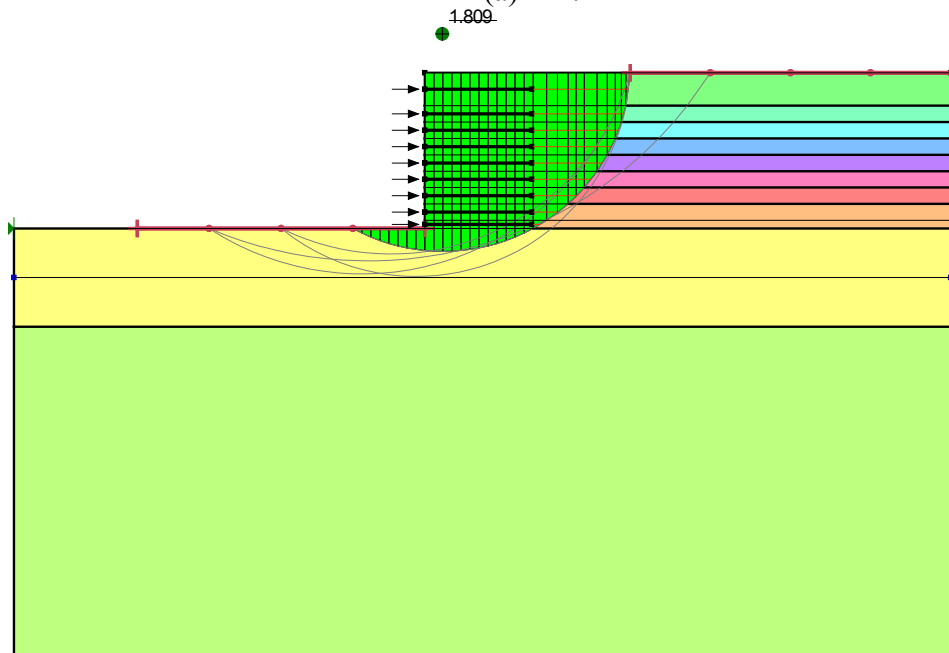
|                  | FOS  |      |
|------------------|------|------|
|                  | EB   | WB   |
| Back analysis    | EB   | WB   |
| Overtuning       | 4.15 | 5.10 |
| Bearing capacity | 6.33 |      |
| Global stability | 1.85 | 1.81 |

**Table 9. Parametric Analysis of Sliding.**

| Condition   | FOS                        |                            |
|---|----------------------------|----------------------------|
|   | $\gamma = 125 \text{ pcf}$ | $\gamma = 105 \text{ pcf}$ |
| $\phi_{\text{retained}} = 31.6, \phi_{\text{found}} = 28.7$ | 2.46                       | 2.06                       |
| $\phi_{\text{retained}} = 31.6, \phi_{\text{found}} = 22$   | 1.81                       | 1.52                       |
| $\phi_{\text{retained}} = 26, \phi_{\text{found}} = 22$     | 1.45                       | 1.22                       |



(a) EB.



(b) WB.

**Figure 14. Global Stability Analysis.**

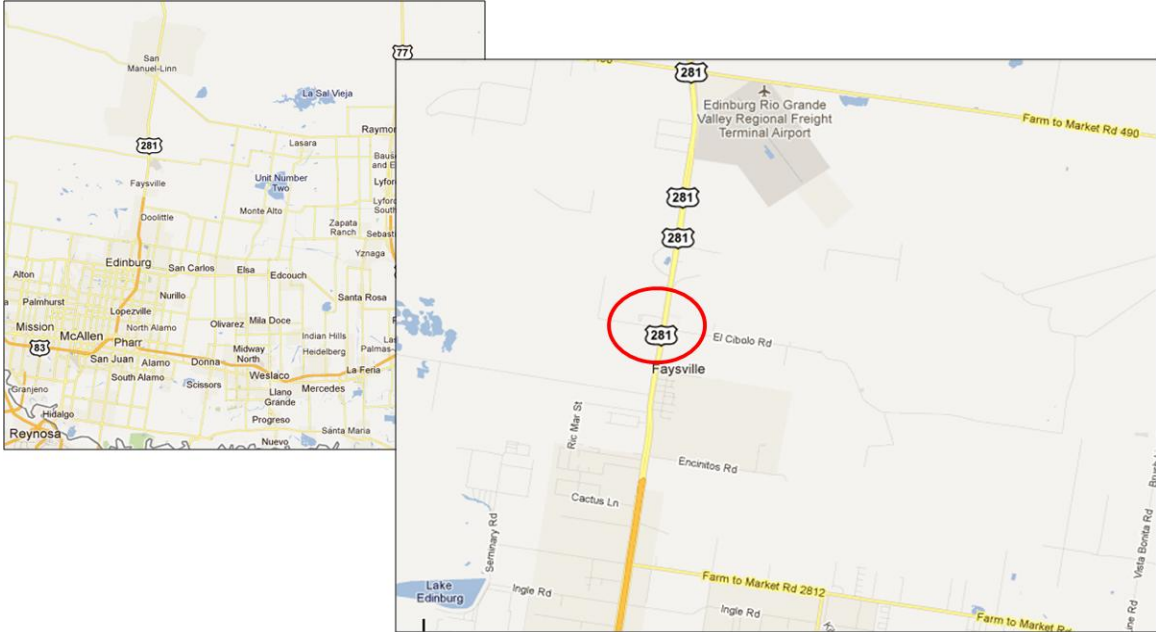
A possible lesson that may be drawn from this case history is that in the case of a MSE wall founded on a clay foundation, the sliding analysis should be based on either: (1) undrained strength rather than drained friction angle for the clay strength, or (2) if a drained friction angle is

used to characterize the clay strength, a greater factor of safety should be required to account for the effects of creep and partial drainage associated with clay soils. These options will be explored later in this project.

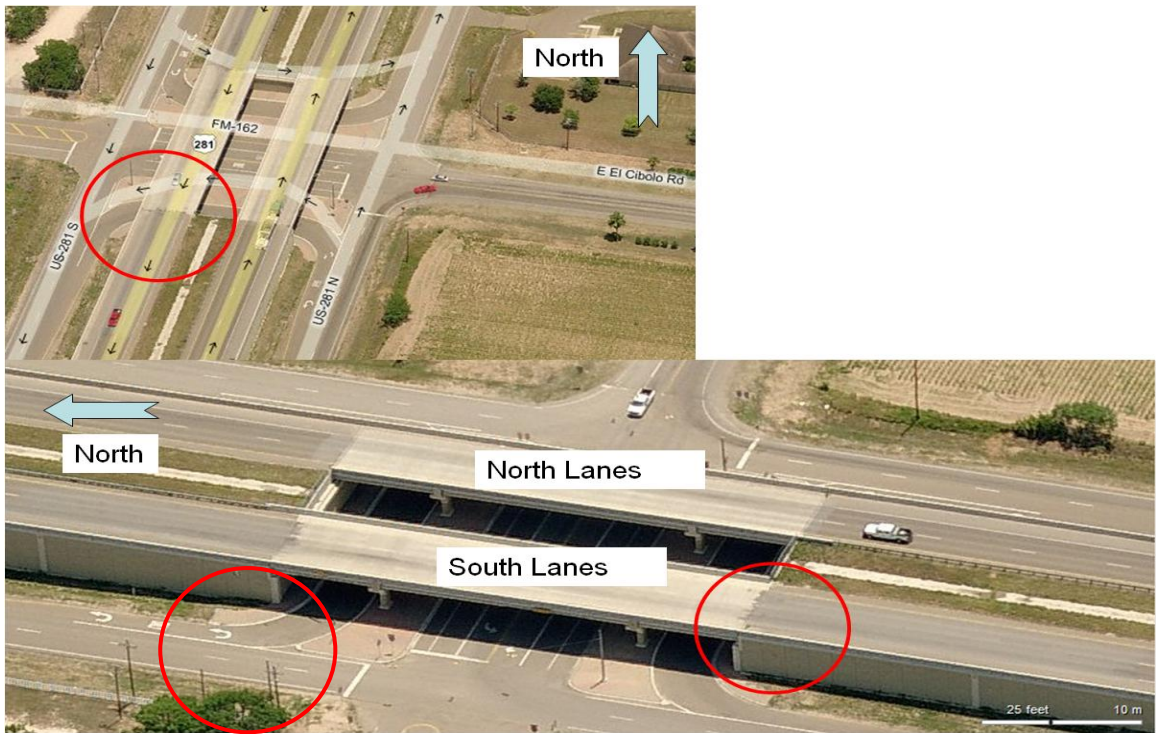
### **US 281 at FM 162 in Pharr District**

An MSE wall of US 281 at the intersection with FM 162 in Pharr District has experienced minor distress. The geographic location of the MSE wall is shown in Figure 15(a). The distress was mainly in the south bound (SB) as shown in Figure 15(b).

The minor distress appeared at various locations as shown in Figure 16. The maximum height of wall was around 22 ft. The pavement showed depression and cracking at the transition zone between the approach/departure embankment and the bridge as shown in Figure 16(a) and (b). The barrier at the approach separated from the bridge barrier up to 2 inches as shown in Figure 16(c), while the barrier at the departure moved toward to the bridge causing localized concrete failure as shown in Figure 16(f). At both the approach and departure, the movement of the MSE walls caused dislocation of the corner panels as shown in Figure 16(d) and (e). In addition, the corner panels appeared to move outward, which induced an apparent gap between the panel and the bridge as shown in Figure 17. At a few other locations, the MSE wall panels showed some minor cracking and dislocation.



(a) Geographic Location of the MSE Wall.



(b) Distressed Locations

**Figure 15. Location of the Distressed MSE Wall.**

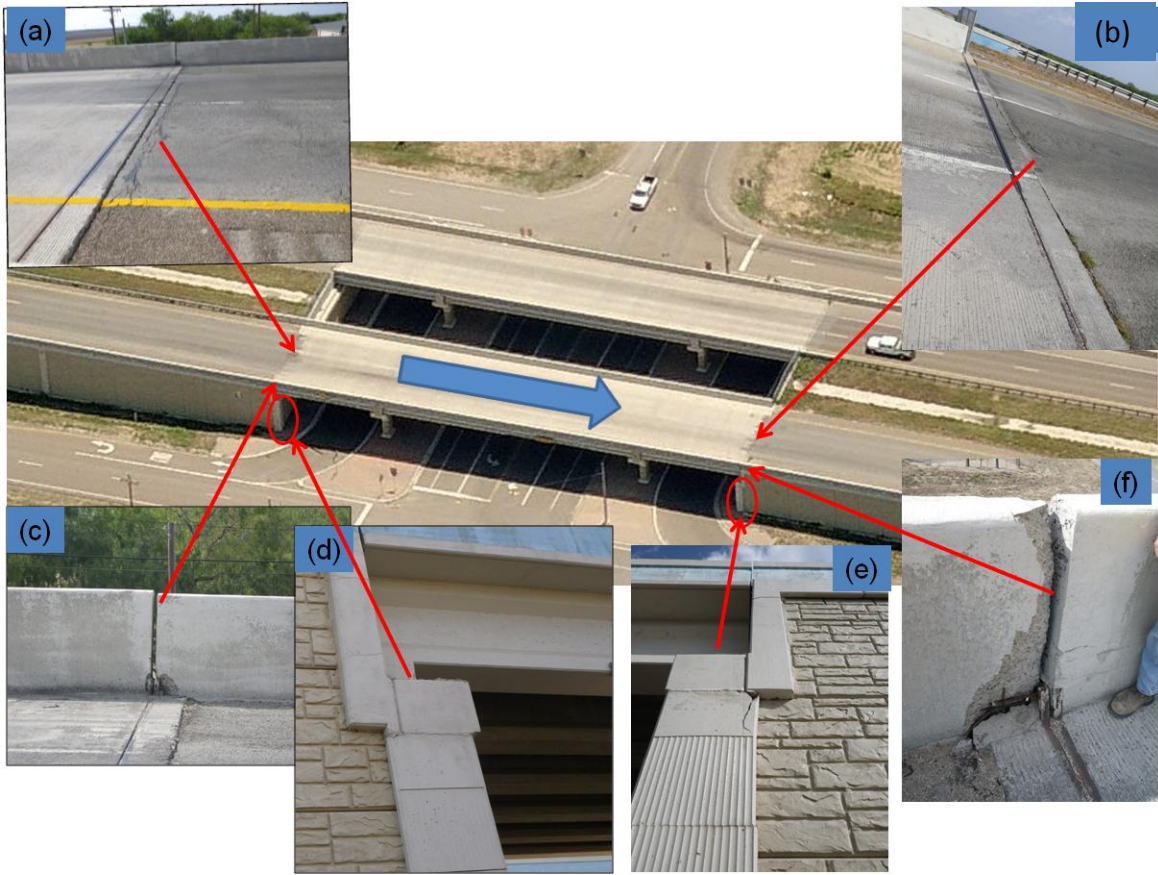


**Figure 16. Distress at Various Locations.**



**Figure 17. Outward Movement of Corner Panel at the Departure.**



In addition, a ground penetrating radar (GPR) survey was attempted to investigate the composition of sublayers. The GPR indicated voids at 4.4 ft below the pavement surface. The research team has obtained some materials from this site for the laboratory testing. The gradation analysis was performed based on dry and wet methods for soil samples taken at different depths. The results are presented in Figure 18. Apparently, the dry and wet methods have yielded different particle distribution curves. All the soil samples seem to meet the requirement of TxDOT Type B backfill based on the dry method. By contrast, sieve analysis by the wet method indicates that none of the samples satisfy the Type B requirements. The explanation for the discrepancy is that the soil samples contain dry soil clumps, which make the soil appear coarser. However, wetting breaks down the soil clumps into fine particles, resulting in a much finer gradation curve.

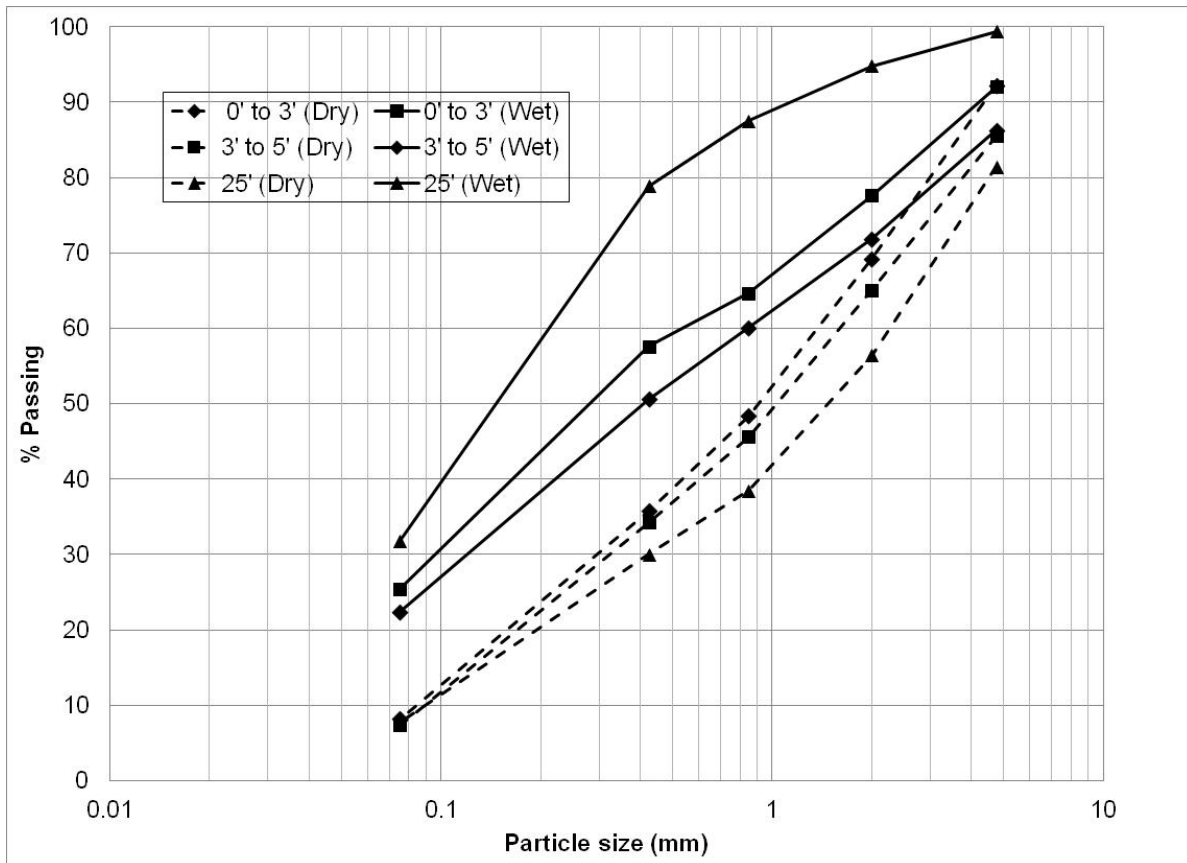


**Figure 18. Particle Size Distribution.**

## Bridge Approaches IH 410 in San Antonio District

The MSE wall was constructed to support the on ramp of the EB IH 410 at Blanco Road as shown in Figure 19. The maximum height of the MSE wall was approximately 20 ft. The bridge approach slab (BAS) experienced distress as shown in Figure 20. The BAS cracked at various locations as shown in Figure 20(a) and (b). The barriers at the MSE wall separated significantly from the barriers of the bridge as shown in Figure 20(c). The MSE wall moved laterally, which led to a sizable gap between the MSE wall and the bridge abutment as shown in Figure 21.

The pavement and BAS were constructed over a thick layer of select fill material. The pavement structure was reported to be 24 inches of hot mix asphalt concrete. The original plans required several feet of flexible base materials to be used; however, the required flexible base material was replaced with recycled asphalt material (RAP) during the construction stage. The movement of BAS was reported as early as 2009 and recurred after a few maintenance repairs.

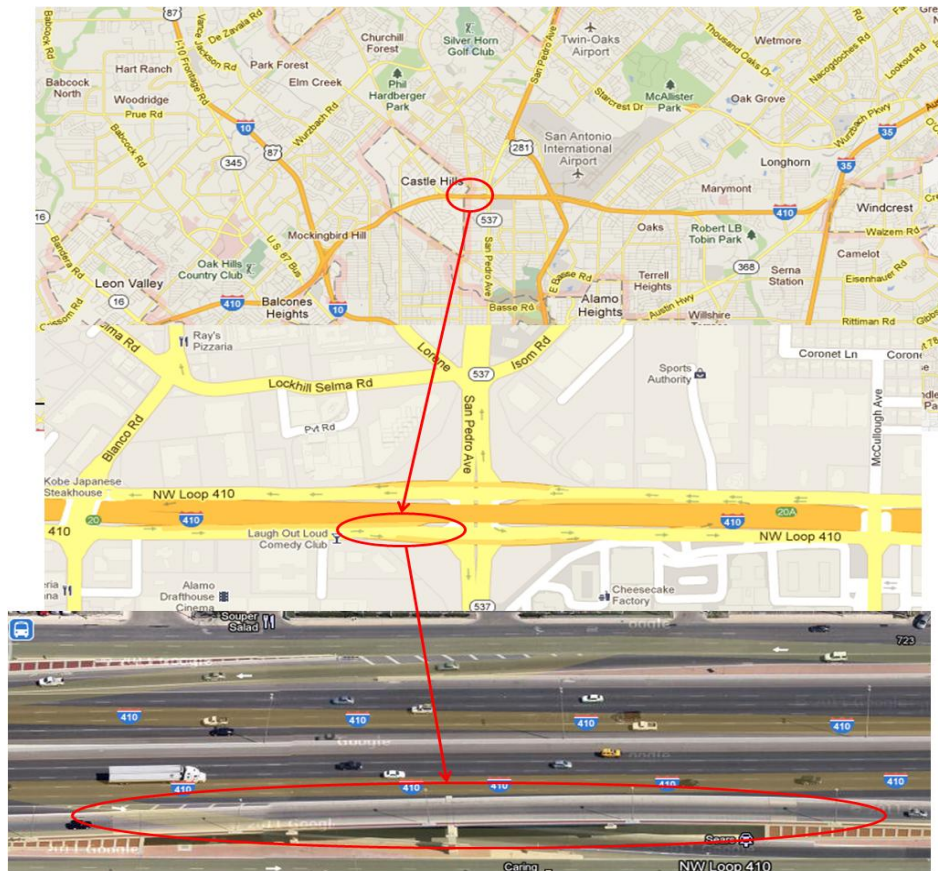
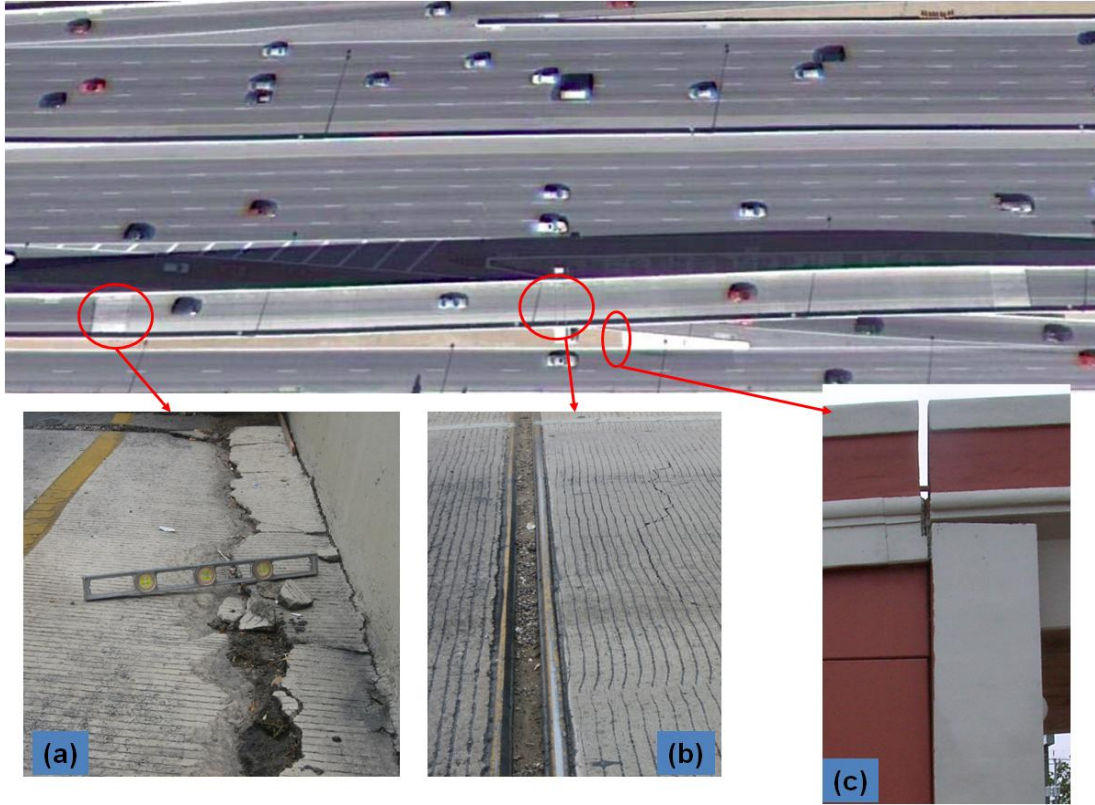


Figure 19. Geographic Location of the MSE Wall of EB IH 410 On ramp at Blanco Road.



**Figure 20. Distress at Pavement, Approach Slab, and Barriers.**



**Figure 21. The Outward Movement of MSE Wall.**

Since 2009, the TxDOT engineers and the researchers of the University of Texas at El Paso (UTEP) and Texas Transportation Institute (TTI) have conducted several investigations to identify the cause of the distress. The investigations conducted included coring, GPR, Dynamic Cone Penetrometer (DCP), and Falling Weight Deflectometer (FWD). The GPR survey was performed longitudinally on the bridge approach and departure slabs as well as the pavement adjacent to the slabs as shown in Figure 22. DCP was performed on both approach and departure sides and 50 ft of pavement adjacent to the approach and departure slabs. The locations of the DCP are shown in Figure 22 as well, and the DCP data are presented in Figure 23. The sudden increase of penetration indicates the existence of voids. The depth was measured from the bottom the pavement. As shown, at the approach side void zones were exhibited at W4, and W5, while at the departure side a void zone was exhibited at E3. In addition, a soft zone on the departure side was identified as shown by the distinct difference in terms of the penetration rate at E4.

Based on the information provided by GPR survey, coring and DCP were performed to locate the voids. The samples retrieved from the coring showed that a layer of high plastic clay material ( $PI = 22 \sim 42$ ) was sandwiched by the pavement and the RAP material (depth ranging from 24 to 48 inches) on the approach side of the bridge as shown in Figure 24(a), while on the departure side of the bridge, a layer of granular material was found at the same depth as shown in Figure 24(b). The materials retrieved were at least 26 inches below the pavement and should be considered as backfill material. Apparently, the backfill material on the approach side did not meet the specification, namely, with excessive fine contents and high PI value. The backfill material on the departure side was also questionable, since it probably possessed a gap gradation.

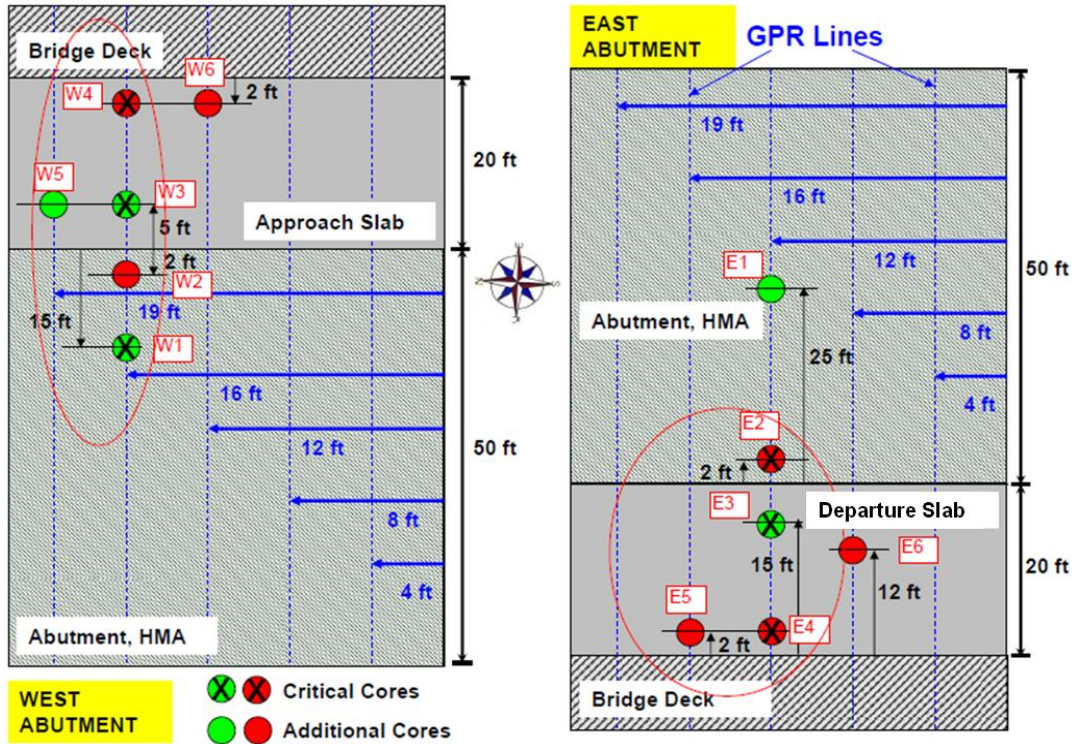


Figure 22. GPR, Coring, and DCP Locations (McDaniel 2011).

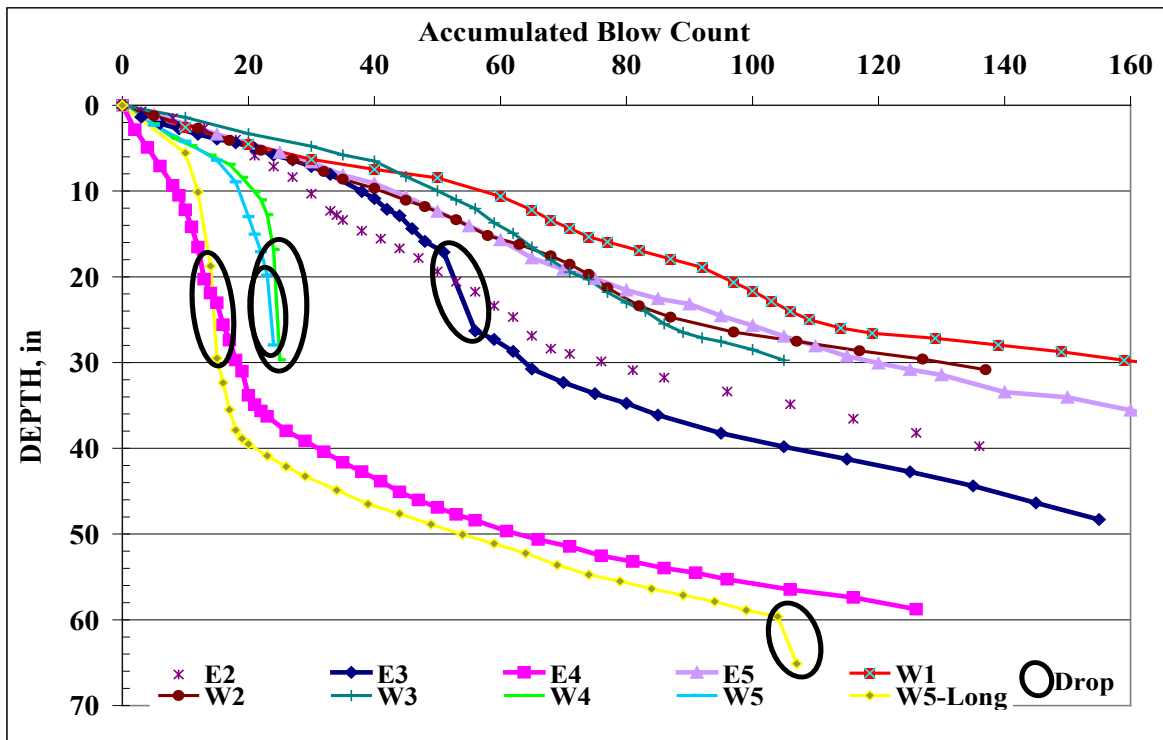
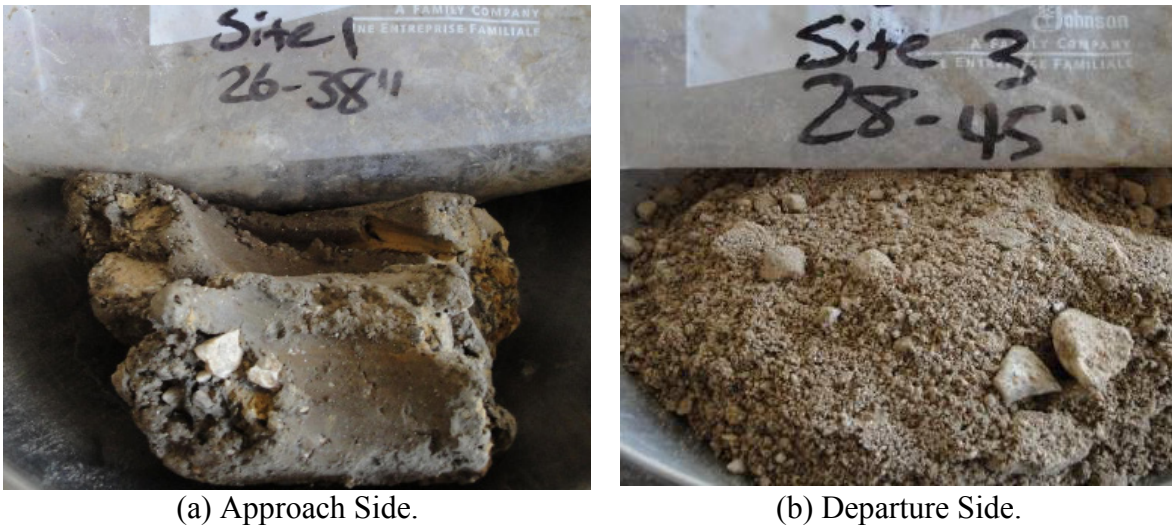


Figure 23. DCP Penetration Data for Both Approach and Departure (McDaniel 2011).



**Figure 24. Fill Material underneath the Pavement.**

The distress of the structures is considered an outcome of the voids underneath the pavement and slabs. The effect of voids on the structures is obvious. The quality of backfill material is of comparable importance. Even though the voids existed on both the approach and departure sides, the distress on the departure side was much less significant, which can be attributed to the high quality backfill material used. Based on the results of the evaluation described above, the TxDOT engineers recommended using polyurethane foam to fill the voids to minimize further settlements.

**IH 35 and FM 310 at Hillsboro, TX**

The MSE walls supporting the approach and departure of the IH35 undercrossing at FM 310 have experienced distress. Figure 25 shows the geographic location of the MSE walls. The MSE walls were approximately 17 ft high at the bridge abutments.

The MSE walls appeared to have moved. The panels at various locations have bulged out as shown in Figure 26(a). The measured maximum movement of the panel was approximately 2.5 inches as shown in Figure 27. This phenomenon has been observed on both approach and departure sides of the bridge. The movement of the MSE walls has caused severe cracking and separation of the barriers as shown in Figure 26(b) and (c). The lateral movement of the MSE wall has also induced up to a 1-inch offset between adjacent barriers. Water stain has been observed at various locations of the panels, which indicated a possible drainage issue within the

MSE walls. The drainage problem is evident from the ongoing seepage at the panels underneath the bridge as shown in Figure 26(d). The wall depicted in Figure 26(d) is a drilled shaft wall. The movement of the MSE walls has also caused some distress on the pavement and the approach slab including cracking, depression, and separation. Due to the severe condition, the BAS was reconstructed. A clay layer that is deemed as the part of subgrade for the pavement structure was identified when the existing BAS was removed as shown in Figure 28. The drainage concern of the MSE wall was verified in the field by injecting water into a drainage inlet at the bridge as shown in Figure 29(a). It was found out that the water could not discharge through the designed drainage path, but had to find its way through the panel joints as shown in Figure 29(b). In summary, the possible causes of the failure would be poor drainage. The effect of the clay soil cannot be evaluated due to lack of information.

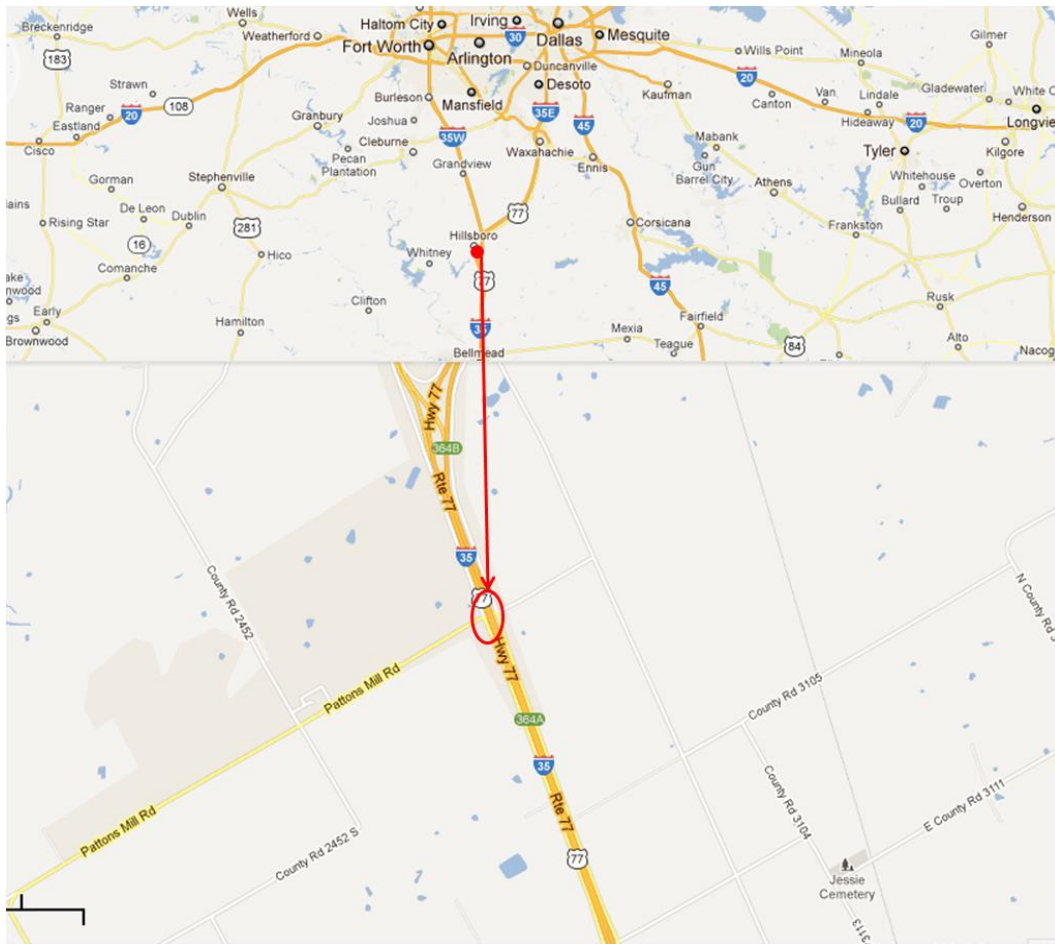


**Figure 25. Geographic Location of the MSE Wall at IH 35 and FM 310.**

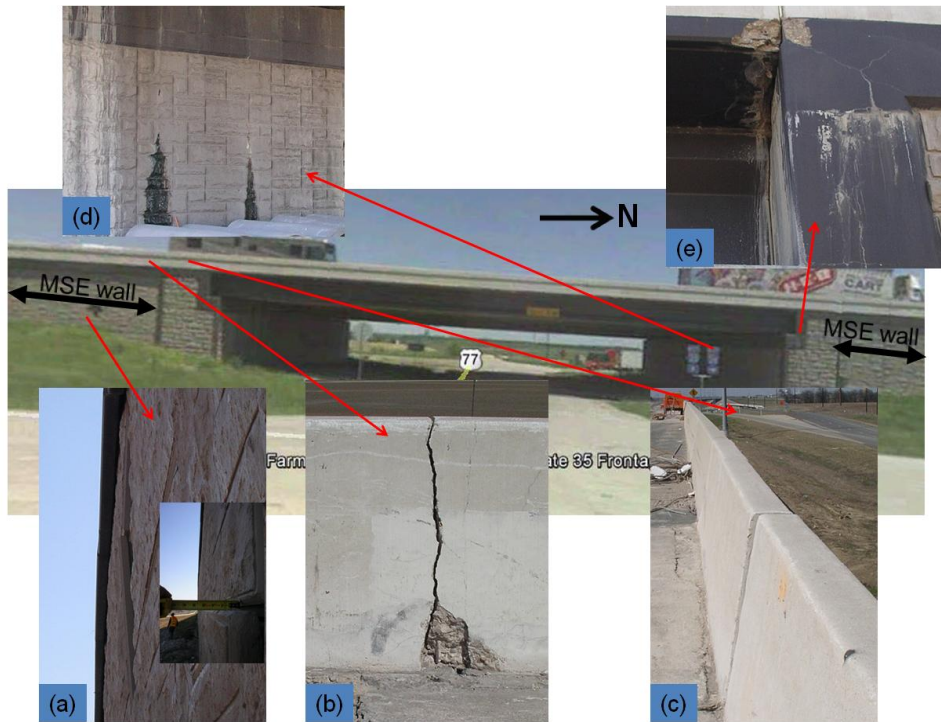


**Figure 26. Distress at Various Locations.**



**Figure 27. Dislocation of the MSE Wall Panels.**





**Figure 28. Clay Layer underneath BAS.**



(a)



(b)

**Figure 29. Water Drainage through Panel Joints.**

### **US 281 at Brook Hollow Blvd, San Antonio**

The MSE wall supporting the US 281 undercrossing at Brook Hollow Blvd. has shown various types of distresses. The pavement and bridge structures have been detrimentally influenced by the distress of the MSE wall. The geographic location of the MSE wall is shown in Figure 30. The distressed MSE walls bounded the east side of the NB US 281.

Even though most of the distresses were localized, at some locations it was so severe that it became a hazard undermining the integrity of the structure. Figure 31 shows the distressed areas. The end of the MSE wall at the departure side was separated from the bridge by 6 inches as shown in Figure 31(a). Significant material loss was observed at that location. The barrier of the MSE wall at the departure side has settled 6 inches and moved outward 7 inches relative to the barrier of the bridge as shown in Figure 31(b). That relative movement has caused a sizable opening at the edge that was found to be the path for material loss. The panels of the MSE walls on both the approach and departure sides have protruded at a few locations as shown in Figure 31(c). The masonry paved slope underneath the bridge has moved downward, which generated a gap between the slope and the bridge abutment as shown in Figure 31(d). The movement of the MSE walls has induced localized bridge structure failure as shown Figure 31(e). In spite of repeated maintenance, new cracks are already apparent as shown in Figure 31(f).

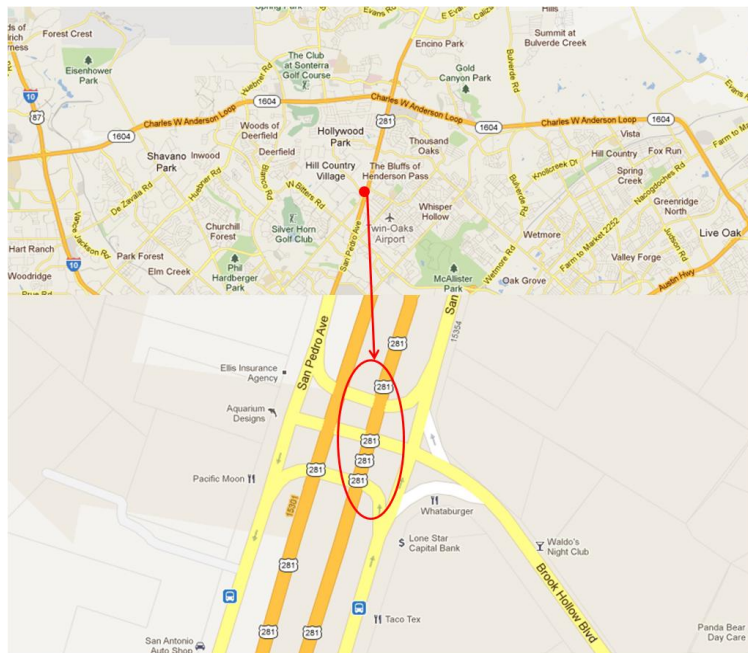


**Figure 30. Geographic Location of the MSE Wall at US 281 and Brook Hollow Blvd.**



(a)



(b)



(c)



(d)



(e)



(f)

**Figure 31. Distress Modes.**

## IH 35 at Walnut Street, Comal County, TX

The distressed MSE walls support the approach and departure of NB IH 35. The geographic location of the MSE walls is shown in Figure 32. At the approach and departure sides, the coping/traffic rail on top of the MSE wall has settled and moved outward as indicated by a significant offset as shown in Figure 33(a) and (b). The pavement has cracked and sizable voids were detected by pushing a rod through the cracks. In the vicinity of the most severe pavement cracking and MSE wall movement, drainage outlets were found on both approach and departure sides.

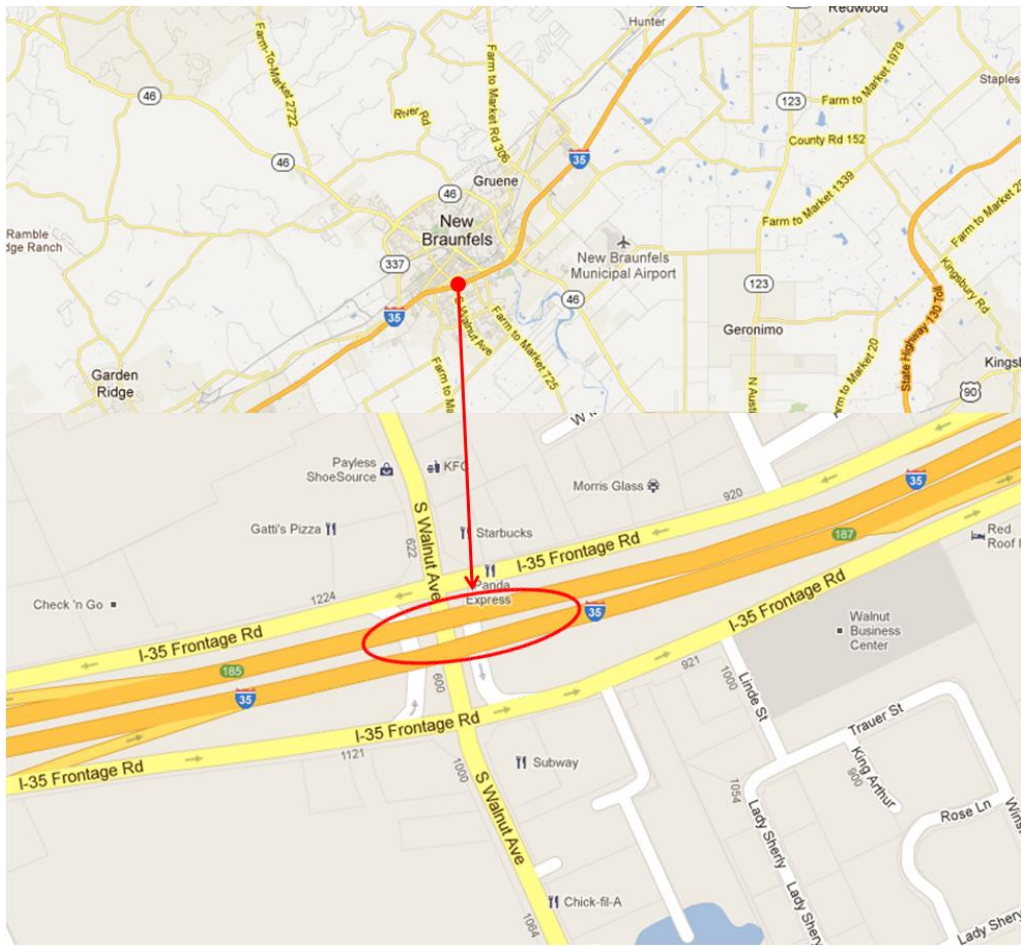
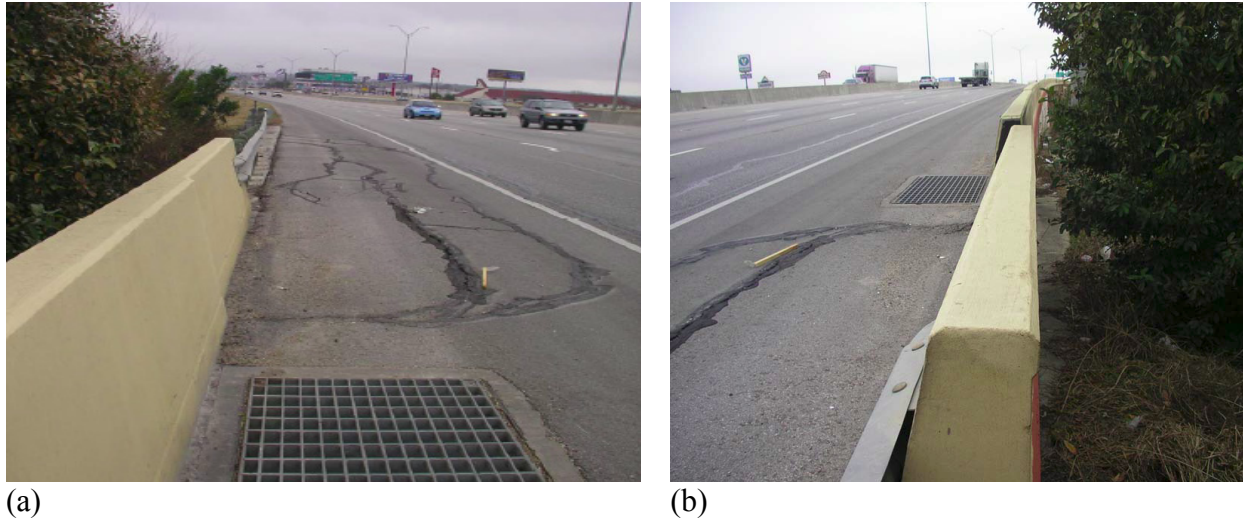


Figure 32. Geographic Locations.



**Figure 33. Distress Modes.**

### **Summary of the Identified Failure/Distress Modes**

The investigated six sites, though being a small sample, are located across Texas and can be deemed representative. These MSE walls have experienced minor to medium distress, which influenced the function of pavement and/or bridge structures, but did not completely lose the functions as earth-retaining structures.

Based on the occurring frequency on the five investigated sites, the failure/distress modes are ranked below, with the pavement cracking being the most frequent and MSE wall sliding the least frequent.

1. Pavement cracking.
2. Pavement depression and separation.
3. MSE wall lateral movement.
4. MSE wall and bridge separation.
5. MSE wall longitudinal movement.
6. MSE wall panel dislocation.
7. MSE wall sliding.

### **Summary of the Possible Causes**

Only two distressed MSE walls have been subjected to forensic study. The rest of the MSE walls were assessed only visually. The possible causes include unsuitable backfill material,

sizeable void within backfill, drainage, and foundation soil. The sizeable void may be the result of poor construction or inappropriate gradation of backfill material.

### LITERATURE REVIEW OF TXDOT 0-5506

Kniss et al. (2007) conducted a study to investigate the design of narrow retaining walls in front of stable faces. Pavement widening has often caused new MSE walls being placed in front of existing stable walls as illustrated in Figure 34.

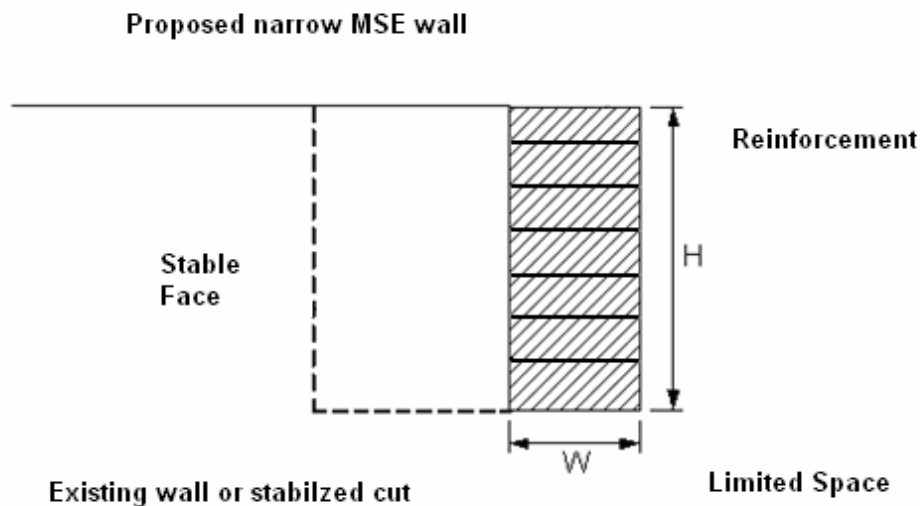


**Figure 34. Illustration of Proposed Narrow MSE Wall in Front of an Existing Stable Face (after Kniss et al. 2007).**

From this study, two primary analyses were conducted as follows:

- Finite element analysis using Plaxis© to evaluate the vertical and horizontal stresses in the backfill behind non-deformable walls constructed in a confined space.
- Limit equilibrium analyses to evaluate the factor of safety such walls placed in a confined space using UTEXAS4.

The nature of wall placed in a confined space results in smaller wall aspect ratio ( $W/H$ ) of MSE walls that may make the walls become stiffer or non-deformable. Researchers attempted to numerically model such non-deformable cases using Plaxis Version 8.2 ©. From this analysis, the following findings were drawn:

1. Modeling the soil-wall interaction was achieved by setting interface elements at the wall face and assigning a total fixity boundary condition to the nodes at the wall face. The interface reduction factor ( $R_{inter}$ ) less than 0.1 shall not be used because they may cause unrealistic results.
2. The proposed models were verified by comparing centrifuge test results performed by Frydman and Keissar (1987) and Take and Valsangkar (2001). A favorable correspondence was found between the measured horizontal earth pressure coefficients and that calculated from Plaxis. In addition, Spangler and Handry's equation given in below was found to be feasible to compute the horizontal earth pressure coefficients.

$$\sigma_h = \frac{\gamma W}{2 \tan(\delta)} \left[ 1 - \exp\left(-2K \left(\frac{z}{W}\right) \tan(\delta)\right) \right] \quad (\text{Eq. 7})$$

where

$W$  = the width of the constrained space

$z$  = the depth of the point of interest below the top of the wall

$\delta$  = the interface friction angle between the soil and wall

$K$  = the horizontal earth pressure coefficient, which is equal to the theoretical at-rest earth pressure coefficient.

3. A parametric study showed that the Hardening-Soil model was deemed the best to model a non-deformable retaining wall with use of  $R_{inter}$  of 0.7.
4. The vertical stress influence factor was found to decrease horizontally from the center of the backfill to the wall face, with depth below the top of the wall and with decreasing wall aspect ratio.
5. The normalized horizontal earth pressure coefficients decreased as the wall aspect ratio decreased. Thus the reduced vertical and horizontal stresses due to the decrease of wall aspect ratio of the wall placed in a confined space could be incorporated into the current design equations to calculate factors of safety with respect to pullout and breakage.
6. Based on the limit equilibrium analysis, the use of noncircular slip surfaces is found to be crucial when the wall aspect ratio of an MSE wall is less than 0.7.

Given the above findings, researchers offered the following recommendations:

1. Use of Plaxis is recommended to model any wall geometry to calculate displacements, stresses, and strains.
2. The current design guide of MSE walls in a confined space in front of a stable face is deemed to be conservative since it ignores the reduction in vertical and horizontal stresses and their effect on the required reinforcement strength. Therefore, it is recommended to use the revised earth pressure coefficients in Figure 35 and the vertical stress influence factor used in Figure 36 in assessing the factors of safety against pullout and breakage.

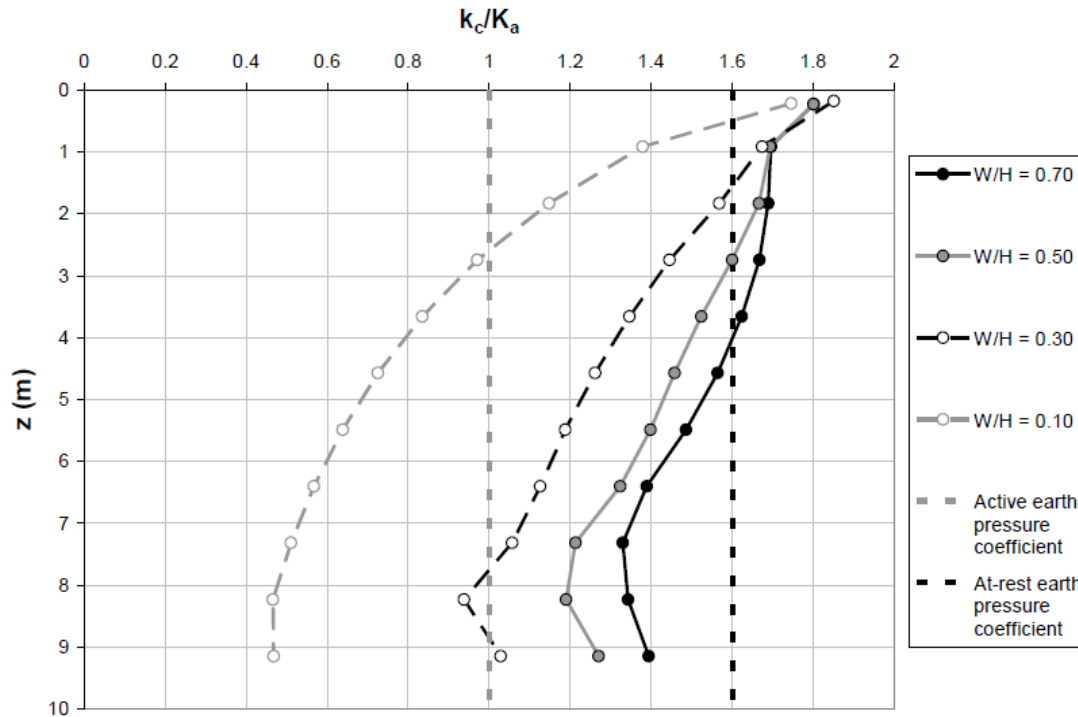


**Figure 35. Proposed Design Chart for Nondeformable Walls Placed in Front of an Existing Stable Face from Plaxis Simulations (after Kniss et al. 2007).**



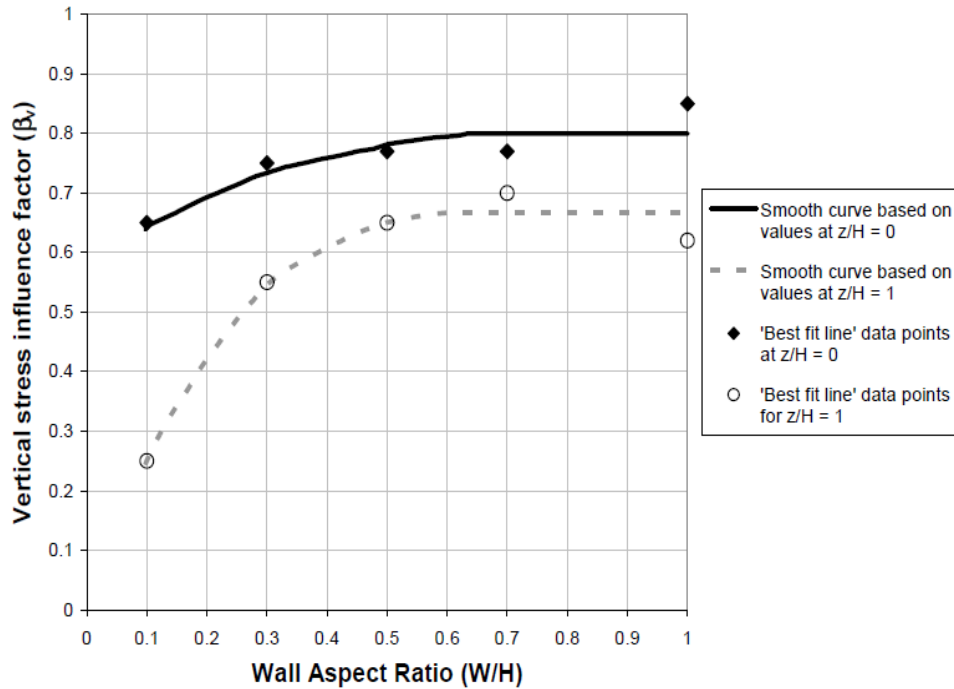


**Figure 36. Values of the Vertical Stress Influence Factor at the Top and Bottom of the Wall (after Kniss et al. 2007).**

3. The impact of the surcharge loads in assessment of MSE wall behaviors needs to be further examined.
4. The external stability of the MSE wall becomes important as the wall aspect ratio decreases since the wall tends to be more susceptible to failure caused by sliding, overturning, and bearing capacity failure. With respect to the external stability of MSE walls placed in front of a stable face, it is recommended that the wall width be greater than 30 percent of the wall height.
5. While anchorage of the reinforcement to the stable face is not recommended, extension of the uppermost levels of reinforcement beyond the nominal stable face appears feasible.
6. Further research is needed to study the design of deformable walls, the effects of surcharge, sloping backfill, and weak foundations using finite element and limit equilibrium analyses.
7. Monitoring the MSE walls with instrumentation is recommended to ensure sufficient field data to verify numerical analyses results.



## **CHAPTER 4: VALIDATION OF DESIGN ASSUMPTIONS**

This chapter addresses the validation of design assumptions for MSE wall design. This involved three sub-tasks. The first task assessed the rationality of design parameters used for TxDOT Types A, B, C, and D backfill materials. The basic methodology for this sub-task involved unit weight and triaxial shear tests for these four types of backfill materials, where the material gradation was systematically varied across the permissible gradation range for each material type. In the case of material Types A, B, and D, large-scale (6-inch diameter) triaxial tests were performed. The laboratory tests provided data on unit weights and friction angles for these backfill materials. The triaxial tests also provided estimates of the elastic modulus  $E$ . While  $E$  is not a direct input for routine design procedures, these data were used for the finite difference studies of MSE wall performance, which was also part of this task. The second sub-task assessed the adequacy of the specified minimum reinforcement length for MSE walls, which is 8 ft or  $0.7 H$ , where  $H$  is wall height. The basic methodology for this design task involved finite difference analysis using the program FLAC of a typical MSE wall section using material data from the first sub-task. Parametric studies were conducted over a range of reinforcement lengths and material types to verify that the typical specified reinforcement lengths will ensure reasonable lateral deflections. The last sub-task assessed whether the factors of safety for sliding and overturning should be modified based on the variability in material parameters. The basic methodology in this sub-task involved performing a statistical evaluation of the material variability measured for the backfill materials in the first sub-task, and inputting that data into Monte Carlo simulations for calculating factors of safety against sliding and overturning.

### **LAB TESTING AND TEST DATA**

A large scale triaxial testing system was developed in April 2012 to conduct consolidated drained triaxial compression testing on MSE wall backfill material. The system, shown in Figure 37, consisted of a triaxial chamber manufactured to our specifications by Trautwein Soil Testing Equipment.

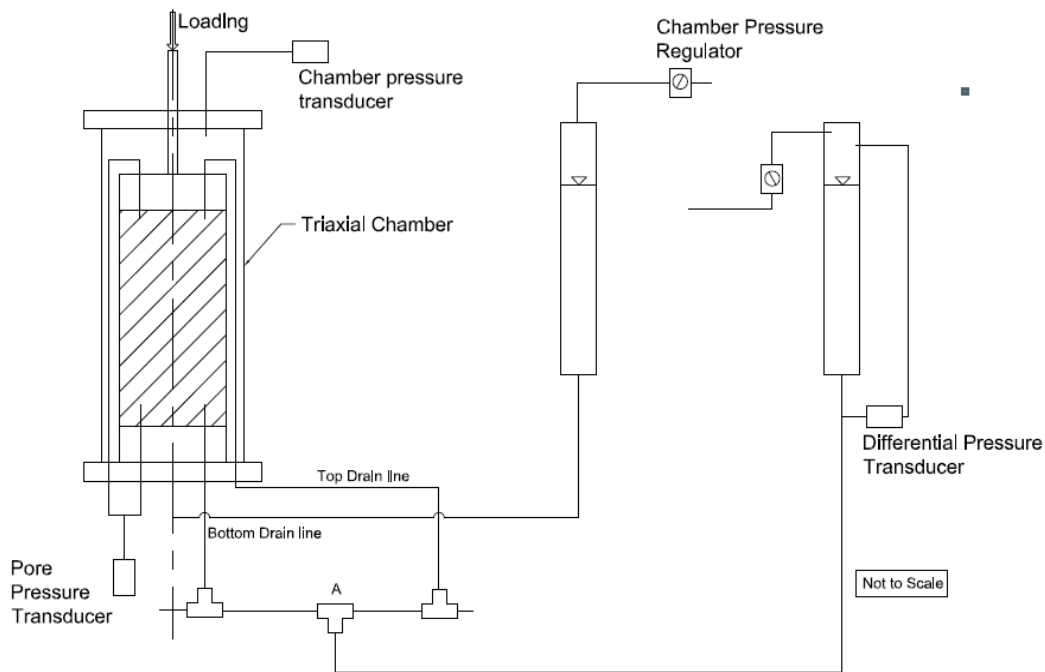


**Figure 37. Large Diameter Triaxial Schematic.**

The exterior chamber size was limited by the 11-inch diameter clearance of an existing 10,000 lb Pro-Loader HM-396 load frame to be used for testing. Based on this limitation, the test apparatus was designed with a 7.5-inch interior diameter acrylic chamber, thus limiting the test specimen diameter to 6 inches.

Following the ASTM D7181 Standard Test Method for Consolidated Drained Triaxial Compression Test for Soils (ASTM 2011a), which requires that the diameter of sample must be at least 6 times of the maximum particle size; a maximum of 1-inch particle was tested in the device. A height to diameter ratio of 2 was used to minimize end friction, resulting in samples approximately 12 inches tall. Samples were tested at full saturation and water was used as the confining medium.

Figure 38 presents a picture of the actual test chamber. The chamber was fitted with a 1-inch linear ball bearing piston at the top for applying axial loading. While the chamber cap contains a port for measuring applied confining pressures, the chamber base is fitted with a port for applying confining pressures and four 1/4-inch drain lines, which connect to the exterior of the chamber with one-way exterior ball valves, to provide adequate drainage to the top and bottom of the sample. Pore pressure measurements are taken by a pressure transducer located

between the top and bottom drain line ports on one side of the sample. Attached to the remaining drain line ports is a series of two-way valves connecting the sample to the back pressure system, which allows air to be flushed from the system during initial sample saturation. In the interior of the chamber, 6-inch diameter top and bottom caps connect the drain lines to the sample. The caps contain a small groove to allow even distribution of flow between the sides of the sample. Thick sintered brass porous stones, 1/8-inch in size, were placed on the top and bottom of the sample along with filter paper to allow for adequate drainage while attempting to slow down the migration of soil particles into the drainage lines.



**Figure 38. Large-Scale Triaxial Chamber.**

A Trautwein pressure panel, shown in Figure 39 with an accuracy of 0.1 psi, was used to regulate back pressure and confining pressure. While the panel connected directly into the chamber to provide confining pressures, it did not have enough capacity to measure continuous volume change. Due to time constraints, early tests were performed taking manual volume change measurements until a volume change apparatus was developed using a  $\frac{3}{4}$  inch transparent PVC pipe with back pressure applied to the top of the water column. The device was connected at the bottom by a tube to the sample drain lines, as seen in

Figure 39. A differential pressure transducer was plumbed in between the top and the bottom of the clear PVC pipe, which recorded the change in differential pressure due to the height of the water column and could thus be calibrated to produce volume change within the known diameter pipe

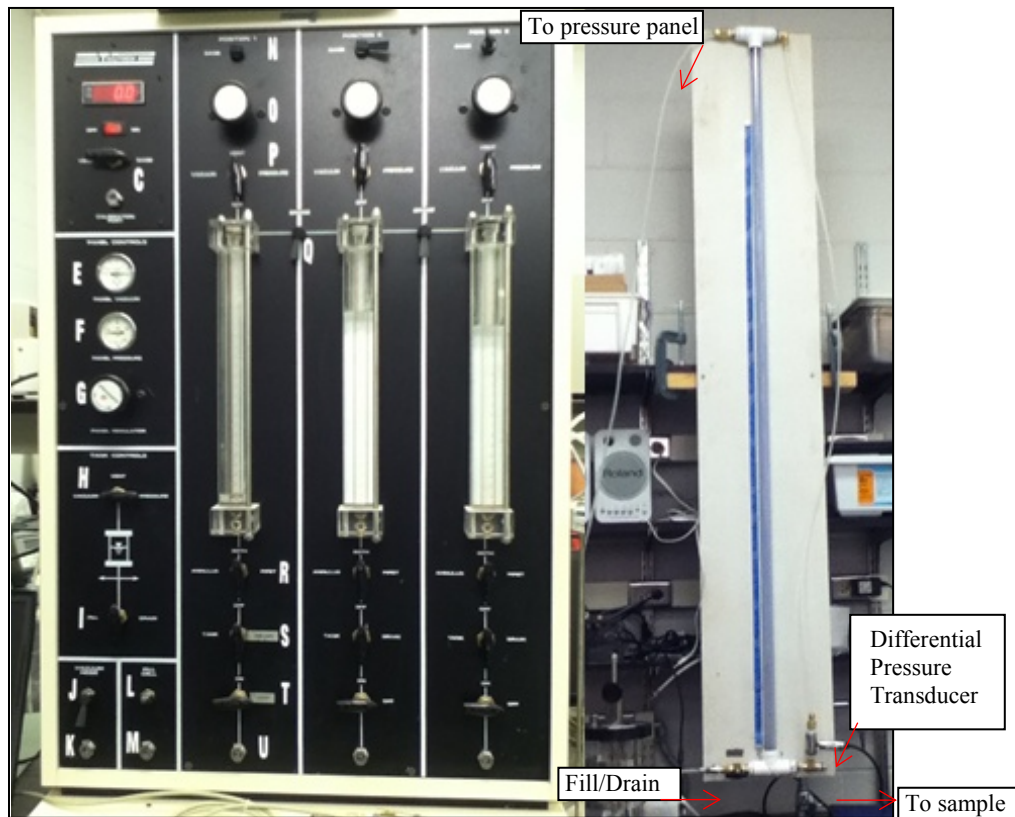


**Figure 39. Trautwein Pressure Panel (Left) and Volume Change Device (Right) Used in Testing.**

An Omega LC101-3k load cell, PX602-100 pressure transducers, and PX409-2.5 differential pressure transducer were used to record force, pressure, and volume change characteristics. The displacement rate was set on the load frame to be 0.0591 inch/min. or a strain rate of 0.005/min. Data were acquired using a National Instruments (NI) Hi-Speed USB Carrier data acquisition box (NI USB 9162) with 24-bit full bridge analog input and a 10 volt external power supply. Data were processed using NI's LabVIEW© program to record time and millivolt readings of the sensors. Figure 40 shows a screenshot of the basic program.



**Figure 40. Data Acquisition Program.**

### Overview of Testing Procedure

As per TxDOT specifications, there are four different types of backfill materials, namely, Types A, B, C, and D. The specification for these types of backfill is given below in Table 10. The backfill materials were obtained from TxDOT-specified borrow sites. The Types A and D

backfills were obtained in Waco, Type B was obtained in Bryan, and Type C was obtained in Beaumont. A total of 72 6-inch diameter consolidated drained triaxial compression tests were conducted according to ASTM D7181 on Types A, B, and D materials. A total of 24 2-inch consolidated undrained tests were performed according to ASTM D4767 (ASTM 2011b) on Type C backfill material.

**Table 10. Select Backfill Gradation Limits (TxDOT 2004).**

| Type | Sieve Size | Percent Retained |
|------|------------|------------------|
| A    | 3 in.      | 0                |
|      | 1/2 in.    | 50-100           |
|      | No. 4      | See Note         |
|      | No. 40     | 85-100           |
| B    | 3 in.      | 0                |
|      | No. 4      | See Note         |
|      | No. 40     | 40-100           |
|      | No. 200    | 85-100           |
| C    | 3 in.      | 0                |
|      | No. 4      | See Note         |
|      | No. 200    | 85-100           |
| D    | 3 in.      | 0                |
|      | 3/8 in.    | 85-100           |

Note: Backfill is considered rock backfill only if 85% or more material is retained on the No. 4 sieve

As the specifications allow a range of gradations for each type of material, it was necessary to test over that range to determine the boundary limits of the behavior associated with each type of material. Four different gradations were tested for each type of material.

Table 11 lists the gradations tested. Additionally, three different confining stresses were tested as confining stress increases with depth in MSE walls. These confining stresses were found by assuming a backfill unit weight of 125 pcf and assuming a coefficient of lateral earth pressure at rest of 0.5. Wall heights of 10, 15, and 20 ft resulted in confining stresses of 4.3, 6.5, and 8.7 psi, respectively.



**Table 11. Tested Backfill Gradations.**

| Type | Particle Size -mm<br>(Sieve Size) | % Passing |           |           |           |
|------|-----------------------------------|-----------|-----------|-----------|-----------|
|      |                                   | A1        | A2        | A3        | A4        |
| A    | 75 (3")                           | 100       | 100       | 100       | 100       |
|      | 12.5 (1/2")                       | 0         | 16.67     | 33.33     | 45.00     |
|      | 4.75 (#4)                         | 0         | 10.00     | 20.00     | 30.00     |
|      | 0.425 (#40)                       | 0         | 5.00      | 10.00     | 15.00     |
|      | 0.075 (#200)                      | 0         | 3.33      | 6.67      | 10.00     |
| B    |                                   | <b>B1</b> | <b>B2</b> | <b>B3</b> | <b>B4</b> |
|      | 75 (3")                           | 100       | 100       | 100       | 100       |
|      | 12.5 (1/2")                       | 35        | 45        | 60        | 75        |
|      | 4.75 (#4)                         | 15        | 25        | 45        | 60        |
|      | 0.425 (#40)                       | 0         | 6         | 10        | 30        |
|      | 0.075 (#200)                      | 0         | 4         | 6         | 15        |
| C    |                                   | <b>C1</b> | <b>C2</b> | <b>C3</b> | <b>C4</b> |
|      | 4.75 (#4)                         | 100       | 100       | 100       | 100       |
|      | 2 (#10)                           | 50        | 60        | 70        | 80        |
|      | 0.85 (#20)                        | 35        | 45        | 55        | 65        |
|      | 0.425 (#40)                       | 25        | 35        | 45        | 55        |
|      | 0.075 (#200)                      | 0         | 10        | 20        | 30        |
| D    |                                   | <b>D1</b> | <b>D2</b> | <b>D3</b> | <b>D4</b> |
|      | 75 (3")                           | 100       | 100       | 100       | 100       |
|      | 12.5 (1/2")                       | 0         | 5.00      | 10.00     | 15.00     |
|      | 4.75 (#4)                         | 0         | 3.33      | 6.67      | 10.00     |
|      | 0.425 (#40)                       | 0         | 3.33      | 6.67      | 10.00     |
|      | 0.075 (#200)                      | 0         | 3.33      | 6.67      | 10.00     |

**Material Classification**

Sieve analysis was performed according to ASTM D422 (ASTM 2007) on backfill material to classify the received backfill material in its field conditions, as well as to anticipate the need for additional material. The borrow gradation curve in comparison to the TXDOT specification limits is shown for Type A material in Figure 41, Type B in Figure 42, and Type D in Figure 44. For Types B and D, actual gradations were outside of the TXDOT specifications; however, as each material was sieved into separate particle size and remixed at desired percentages, this meant additional material was required to have adequate quantities of each particle size for testing. Type C gradation limits in Figure 43 were estimated due to the

ambiguity in the backfill specifications of having a minimum of 85 percent retained on the No. 4 sieve, while 70 percent can be retained on the No. 200 sieve.

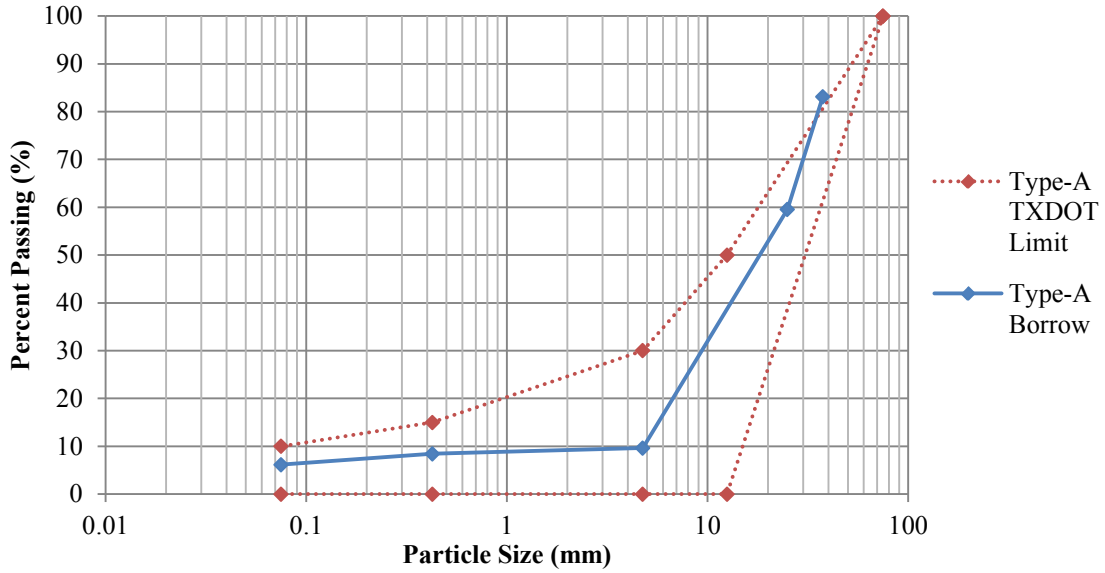


**Figure 41. Type A Borrow Gradation.**

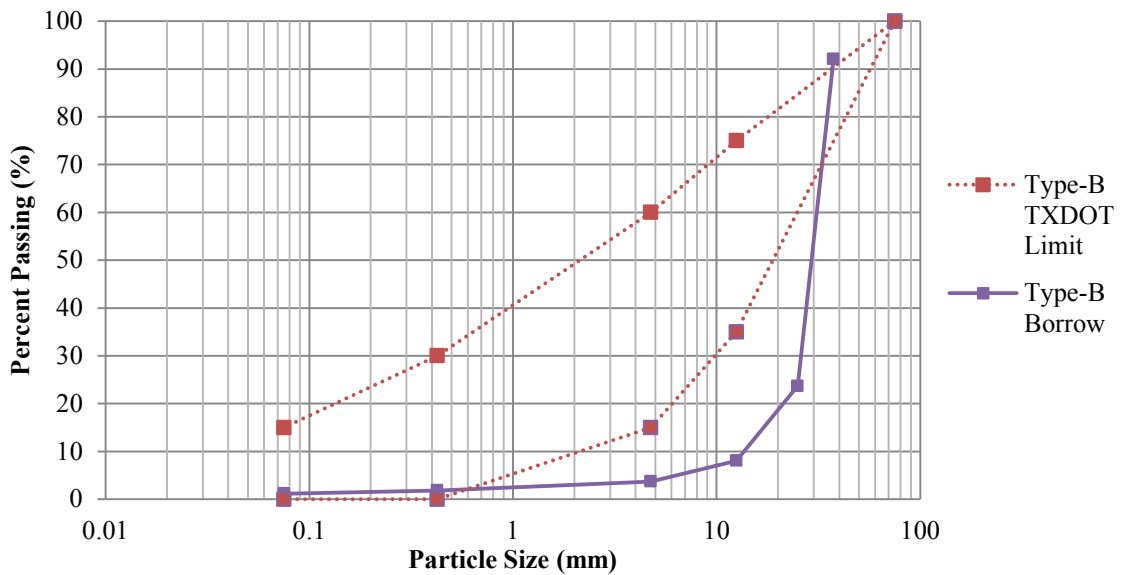


**Figure 42. Type B Borrow Gradation.**

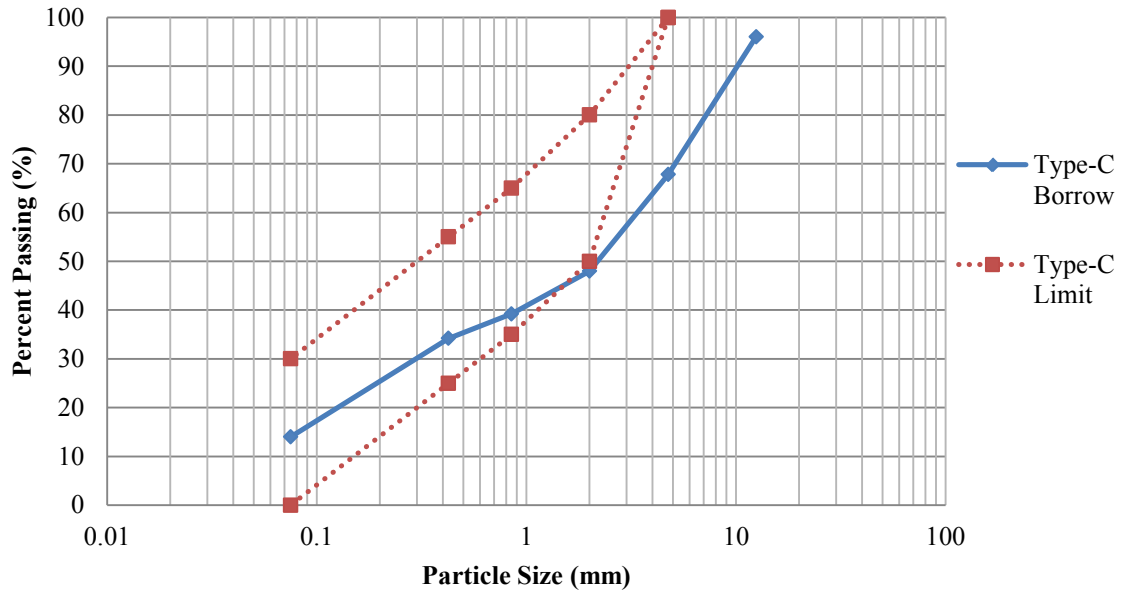


**Figure 43. Type C Borrow Gradation.**

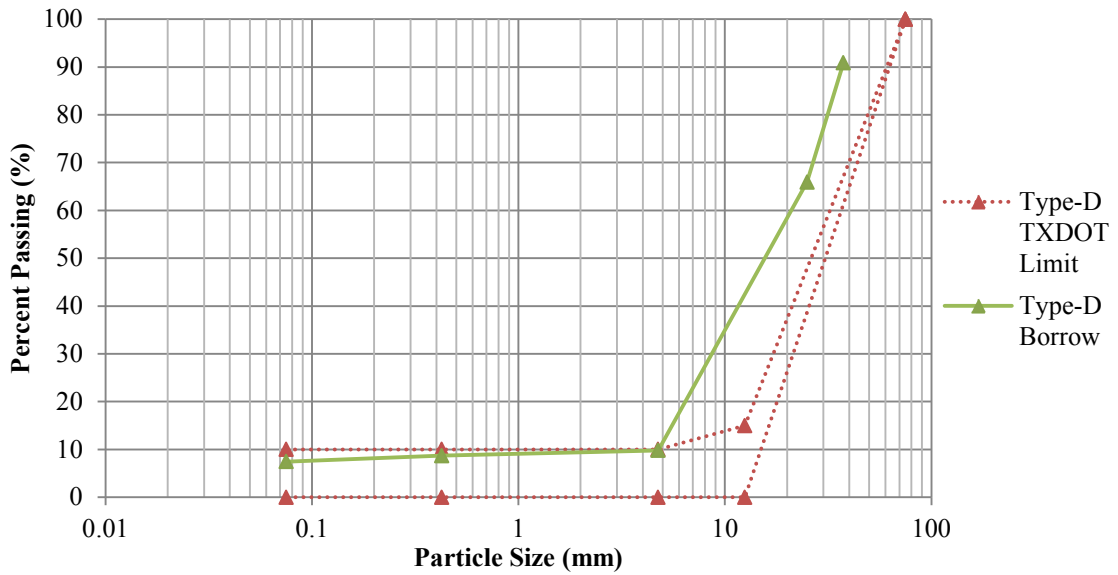


**Figure 44. Type D Borrow Gradation.**

Due to differences in the parent rock of the borrow material, bulk-specific gravity testing was performed according to ASTM C29 (ASTM 2009) on the 1-inch particles of each material. Table 12 summarizes the results of this testing. All three backfill materials are limestone; however, Type B limestone seemed to be a more dense material than Types A and D. The specific gravity test for Type C was performed according to ASTM D854 (ASTM 2010) on each particle size used in Type C and then weight average for different gradation used. The results are presented in Table 13.

**Table 12. Specific Gravity Test Results.**

| <b>Type</b> | <b>Bulk Specific Gravity</b> | <b>Bulk Saturated Surface Dry Specific Gravity</b> | <b>Apparent Specific Gravity</b> |
|-------------|------------------------------|--|----------------------------------|
| A           | 2.20                         | 2.35   | 2.60                             |
| B           | 2.52                         | 2.56   | 2.64                             |
| D           | 2.31                         | 2.46   | 2.71                             |

**Table 13. Specific Gravity Test Results for Type C.**

| <b>Gradation</b> | <b>Specific Gravity</b> |
|------------------|-------------------------|
| C1               | 2.647                   |
| C2               | 2.654                   |
| C3               | 2.661                   |
| C4               | 2.669                   |

Fines were classified using the Atterberg Limits tests to determine plasticity. Test results in Table 14 show that all of the fines used were of relatively low plasticity.

**Table 14. Atterberg Limits of Passing the #200 Sieve**

| <b>Type</b> | <b>LL</b> | <b>PL</b>   | <b>PI</b> | <b>Fines Classification</b> |
|-------------|-----------|-------------|-----------|-----------------------------|
| A           | 18        | 13.4        | 4.6       | CL-ML                       |
| B           | -         | Non-Plastic | -         | ML                          |
| C           | 24.6      | 14.1        | 10.5      | CL                          |
| D           | 20.2      | 11.5        | 8.7       | CL                          |

Maximum density testing was performed on large particulate backfill (Types A, B, and D) by compacting a sample with blows from a modified proctor hammer in a 1/3 cubic foot unit

weight bucket. The unit weight bucket had a diameter of 8 inches and a height of 11.5 inches, which allowed more particle organization, while simulating the test specimen compacted inside the split mold. Initial tests were performed to determine the optimum number of layers and blows per layer, which were 5 layers at 50 blows per layer. Results of maximum density testing are shown below in Table 15. Standard Proctor compaction was performed on Type C materials at different gradation to find optimum moisture content and maximum dry density; test data are shown below in Table 15.

**Table 15. Maximum Density Test Results.**

| <b>Gradation</b> | <b>Dry Unit Weight (pcf)</b> | <b>Gradation</b> | <b>Dry Unit Weight (pcf)</b> | <b>Gradation</b> | <b>Dry Unit Weight (pcf)</b> | <b>Gradation</b> | <b>Optimum MC (%)</b> | <b>Maximum Dry Unit Weight (pcf)</b> |
|------------------|------------------------------|------------------|------------------------------|------------------|------------------------------|------------------|-----------------------|--------------------------------------|
| A1               | 94.65                        | B1               | 98                           | D1               | 93.45                        | C1               | 7.2                   | 120.6                                |
| A2               | 99.7                         | B2               | 113.4                        | D2               | 98                           | C2               | 8.9                   | 129.4                                |
| A3               | 99.1                         | B3               | 122.7                        | D3               | 98.1                         | C3               | 9.7                   | 128.4                                |
| A4               | 109.8                        | B4               | 137.9                        | D4               | 98.3                         | C4               | 9.5                   | 126.3                                |

### **Sample Preparation**

Samples were prepared for testing in three major steps: mixing, compacting, and mounting. The first step was to mix the proper gradation of soil according to specifications listed in Table 10. Prior to testing, particles had been wet sieved into individual particle size shown in Figure 45. All particles except those passing the #200 sieve were oven dried in order to control the moisture content of the sample.

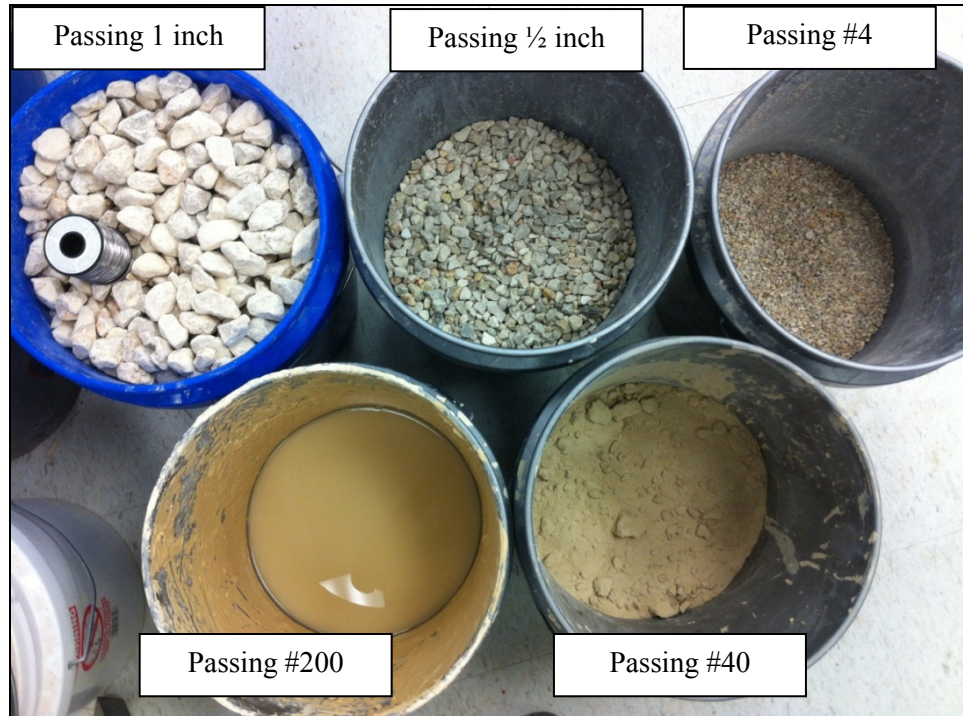


**Figure 45. Sorted Particle Sizes of Type B Material.**

Samples weights were estimated using values slightly above maximum dry unit weights and assuming a sample height of 12 inches with a diameter of 6 inches. Individual particle sizes were weighed and added to the mix. The moisture content was taken on the passing #200 material, thus allowing for the correct amount of solid particles to be added and the moisture content of the total sample to be calculated. To avoid particle segregation as much as possible, judgment was used in determining total sample moisture contents, and water was added if deemed necessary, in order for the particles to clump together. Typically, more well-graded samples required more water. Samples were then thoroughly mixed for even distribution of particles (see Figure 46).



**Figure 46. Sample Mixing of Passing #200 for Type D Material.**

The next step was to compact the specimen inside a 6-inch diameter split mold construction on the base of the triaxial chamber to avoid difficult maneuvers required to mount the 20-plus pound specimen. A 0.025-inch latex membrane was attached to the bottom cap using a rubber O-ring and stretched over the top of the split mold. Vacuum was applied to the exterior of the split mold to pull the membrane tight to avoid pinching. A porous stone and filter paper were then placed at the bottom of the mold. A wet paper towel was placed around the O-ring of the chamber base to prevent granular material from falling into the seal.

Material was poured in one 400 mL scoop per layer. Each layer was then heavily tamped using a rubber mallet. Six 4.45-lb lab weights were then placed on top of the material and 50 blows of the rubber mallet were evenly distributed around the outside of the split mold as shown in Figure 47. This was repeated for a total of about 8 layers, until the level of backfill reached approximately 12 inches in height.



**Figure 47. Compaction of Specimen.**

Particles at the top of the cylinder were then arranged to provide as level of a surface as possible. Filter paper, a porous stone, and a top cap were then placed on top of the specimen and the latex membrane was fastened to the top cap using a rubber O-ring. A regulated partial vacuum of 1.5 psi was then applied through a drain line at the bottom of the sample to help confine the sample. The split mold was released, and the initial sample height was recorded.

Because of the high occurrence of membrane rupture due to compaction, an additional 0.025-inch membrane was checked for leaks and then placed around the sample. The interior was lubricated with petroleum jelly and the ends were fastened with O-rings to provide a water-tight seal. The sample was then leveled to provide complete axial loading from the piston as shown in Figure 48. Drain lines were then connected to the top of the sample and vacuum was moved from the bottom to the top of the sample.



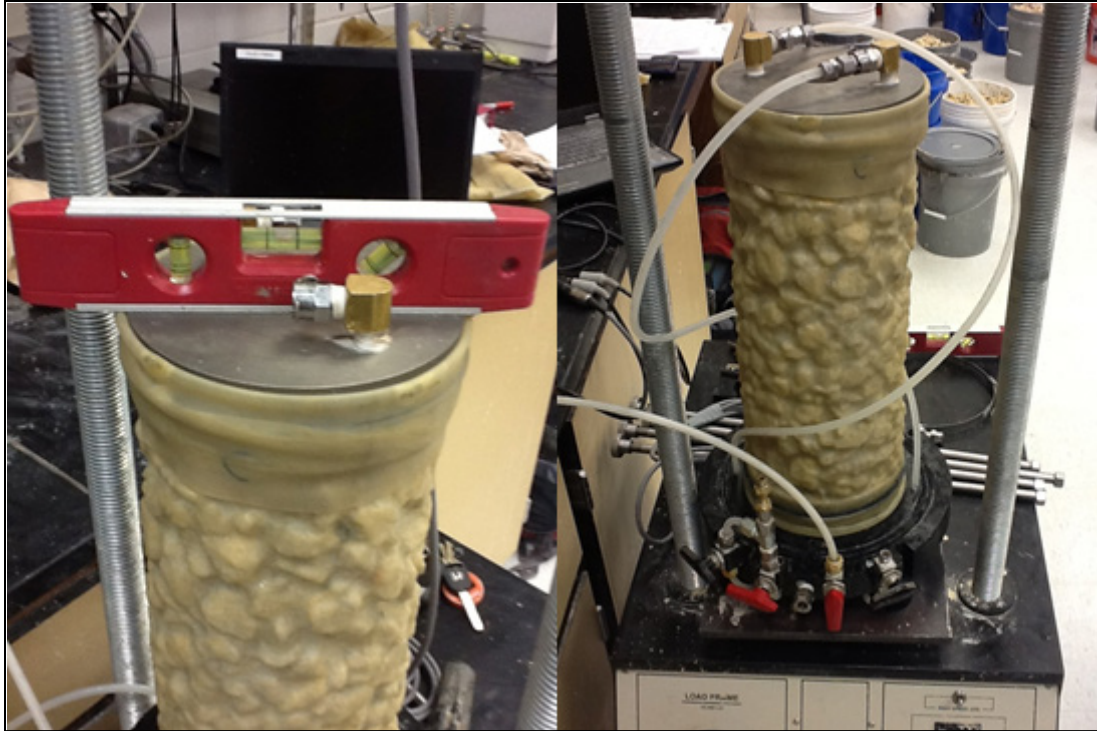


**Figure 48. Leveling Top Cap of Specimen and Final Prepared Specimen.**

The acrylic chamber and piston were then placed on top of the base and fastened with threaded metal bars to seal the chamber. The piston was set and locked in its designated indentation on the top cap of the specimen.

The chamber was then filled from the bottom with water and vented at the top to avoid excess pressure build up and to expel air out of the top of the chamber. Once air bubbles were removed, a pressure transducer was placed in the top port and the bottom port was connected to the pressure panel, where an initial confining stress of 0.5 psi was placed on the sample to confine the sample during saturation. Between the confining stress and the vacuum, the sample received a net confinement of 2.0 psi prior to consolidation and shearing.

### **Testing**

The sample must be saturated in order to measure volumetric changes in the sample during shearing. De-aired water was introduced into the bottom of the specimen from a pressurized water tank and pulled upward with the help of the vacuum at the top until water began to run into the vacuum line. At this point, the vacuum was removed and the sample drain lines were connected to the volume change apparatus, which was filled to the top with water.

Even with the filter paper as a preventative against fines migration, some fines still escaped the sample. Water was allowed to run through the sample and drain through the air bubble bleed out in order to drive air bubbles out of the specimen. At this time, the second pressure transducer was connected in between the drain lines on the left side of the chamber. Once satisfactory air bubble removal had occurred, the chamber pressure and back pressure inside the sample were slowly raised above atmospheric pressure to allow for the solution of any air voids left in the sample. This process, known as back pressure saturation, was allowed to occur for a minimum of 30 minutes, before a B-value check was performed to verify saturation. During the B-value check, drain lines to the sample were closed and initial confining and pore pressure readings were taken. The confining pressure was increased by 0.5 psi, and the pore pressure response was recorded. The B-value is equal to the change in pore pressure over the change in confining pressure and theoretically should equal 1 at 100 percent saturation. As reaching this goal could take multiple days, it was decided that a B-value of at least 0.9 was reasonable to continue testing due to the scale of the test and the stiffness of the specimen.

Once the desired saturation was reached, the sample was isotropically consolidated at the desired confining pressure of the test. Volume change of the specimen was recorded to find the initial volume of the specimen for volumetric strain calculations and to monitor the end of consolidation. Typically, this happened within minutes due to the high porosity and stiffness of the sample. This also served as a good indicator of membrane leakage if volume change did not stabilize.

Following consolidation, the piston was unlocked and the sample was sheared at a constant strain rate of 0.5 percent/min. Ideally, samples were sheared to 15 percent strain, however, in Type B materials, the radial deformation of the sample exceeded the interior chamber diameter prior to 15 percent strain.

### **Consolidated Undrained Triaxial Testing**

Type C material obtained from Beaumont, Texas, was classified as gravely-sand and as per TxDOT specification, this material can be used as backfill for temporary MSE walls. It is important to know an undrained strength and effective friction angle of these materials and to assess the effect of pore pressure on the strength of material. Therefore, a consolidated undrained (CU) triaxial test was performed as per ASTM 4767 to obtain these parameters.

### *Sample Preparation*

The material obtained for Type C was sieved and separated in required particle size and then mixed to appropriate proportions to meet the tested backfill gradation criteria. For each gradation, a standard proctor compaction test ASTM 698 (ASTM 2012) was performed to find the optimum moisture content and maximum dry density. Using this optimum water content, researchers prepared a sample in a 2-inch split mold by taking the required weight of sample to compact as much as possible in a 14.9-in<sup>3</sup> volume of sample as shown in Figure 49. The relative compaction for samples was greater than 95 percent. The sample is then placed on a bottom cap of triaxial chamber and then a latex membrane is placed around the sample as shown in Figure 50.



**Figure 49. Sample Placed on the Bottom Cap of Triaxial Chamber.**

### *Testing*

The testing procedure for CU test is followed as per ASTM-4767. The procedure is similar to the one explained for the CD test, except that during the shearing phase, the drain lines are closed so that the pore pressure will develop during the test. The correction applied during

calculations is different than one applied for large scale CD test. The corrections were used from ASTM-4767 (ASTM 2011b). The consolidated undrained test has three important steps to follow: (1) saturation, (2) consolidation, and (3) undrained shearing.

During saturation stage, the sample is connected to a panel to allow water to pass through, the chamber pressure port is connected to a panel, and a small pressure differential is applied between confining pressure and back pressure. The pore pressure line from the top cap is opened to atmosphere so the air bubbles can escape out easily. After all the bubbles from system are removed, the cell pressure and back pressure are increased slowly to 16.00 psi and 15.50 psi, respectively; this way, the effective confining pressure to the sample is 0.50 psi. The sample is left 6–8 hours for saturation and then a B-value check is performed. Once the B-value is reached to a desired value, sample is then consolidated to required effective confining pressure.

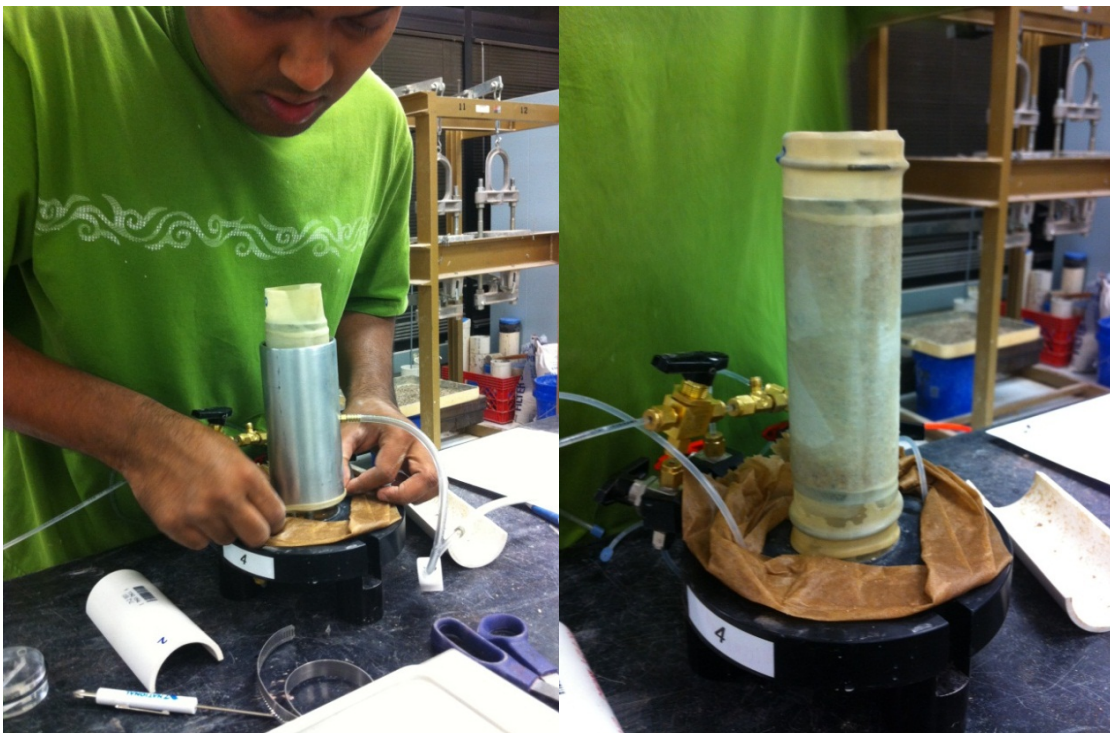


**Figure 50. Stretching Membrane on Spreader and Placing Membrane on Sample.**

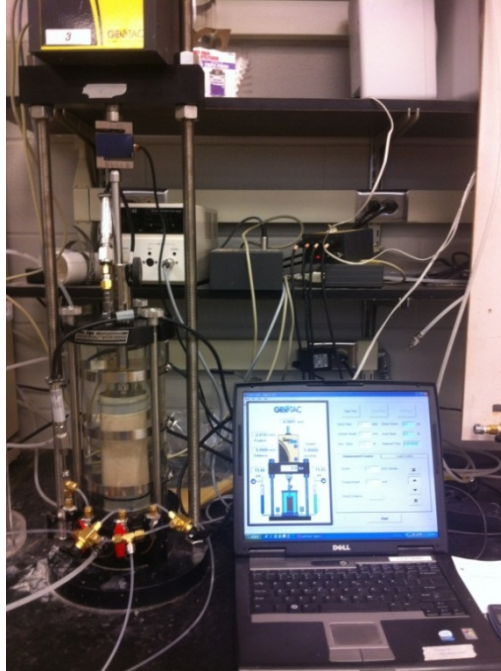


**Figure 51. Geotec Loading Frame and Geotec Sigma-CU Program Used to Perform Triaxial CU Test.**

The consolidation stage is performed for 4–5 hours to confirm that the sample is gone through a primary consolidation phase. During this stage, a volume of water leaving the sample is recorded using differential transducer. The load frame used for this test is servo controlled and maintains a constant load on the sample to compensate the piston uplift due to a confining pressure. The Geotec load frame shown in Figure 51 also allows to record the displacement of piston while maintaining the constant load. These measurements are essential in calculating consolidated area of sample. All the calculations are performed per ASTM-4767 for the CU test. The shearing stage is performed after the consolidation stage. The rate of shearing used for these tests was 5 percent axial strain per hour and sample was sheared to 20 percent axial strain. The sample usually failed at 4–6 percent axial strain. During shearing, the pore pressure ports connecting to panel were closed to ensure there was no drainage. Four parameters were recorded during the test, i.e., axial load, axial displacement, pore pressure, and cell pressure.

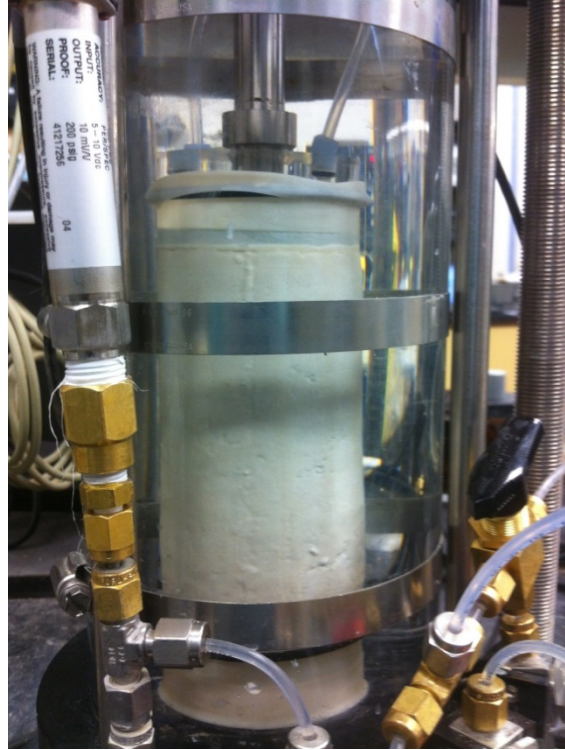


**Figure 52. Sample during Consolidation.**

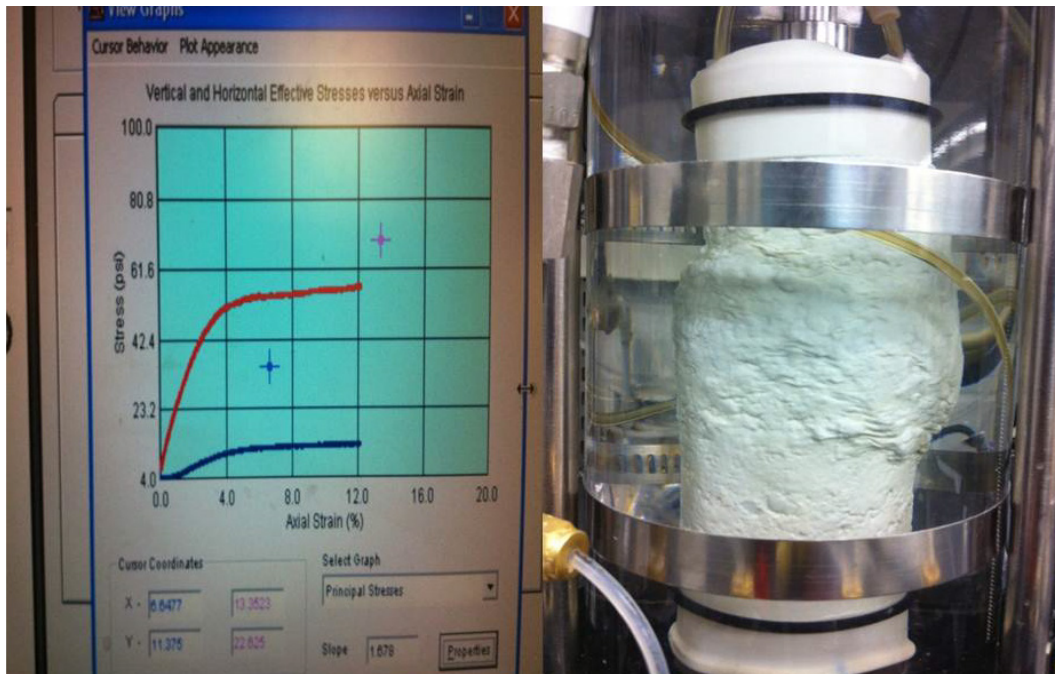


**Figure 53. Stress-Strain Curve on Sigma-CU Program and Deformed Sample at 20 percent Axial Strain.**

## Calculations and Corrections

The calculations and data reduction are done per ASTM 4767. Initially the height of sample and wet density of sample are measured. During consolidation phase the volume of water leaving the sample is measured as well as the change in height of sample. These two measured values are used to calculate consolidated area of sample before shearing.

$$H_c = H_o - \Delta H_o \quad (\text{Eq. 8})$$

where

$H_c$  = Height of sample after consolidation.

$H_o$  = Initial height of sample.

$\Delta H_o$  = Change in height of sample at end of consolidation.

$$A_c = (V_o - \Delta V_o) / H_c \quad (\text{Eq. 9})$$

where

$A_c$  = Consolidated area of sample.

$V_o$  = Initial volume of sample.

$\Delta V_c$  = Change in volume of sample during consolidation.

These values are used to calculate stresses and strains during shearing phase. During the shearing phase, additional data were measured such as axial load, cell pressure, pore pressure, and displacement by measuring the position of servo motor. During undrained shearing, the current area of the specimen must be updated as follows:

$$A = A_c / (1 - \varepsilon_1) \quad (\text{Eq. 10})$$

where

$A$  = Current area during shearing.

$\varepsilon_1$  = Axial strain in decimal format.

The deviator stress is then:

$$\sigma_1 - \sigma_3 = \frac{P}{A} \quad (\text{Eq. 11})$$

A membrane correction is applied to the above deviator stress:

$$\Delta(\sigma_1 - \sigma_3) = \frac{4E_m t_m \varepsilon}{D_c} \quad (\text{Eq. 12})$$

where

$E_m$  = Young's modulus for the membrane material.

$t_m$  = Thickness of the membrane

$\varepsilon$  = Axial strain

$D_c$  = Diameter of specimen after consolidation

The data obtained from these calculations are plotted in three types of graph, i.e., stress-axial strain curve, pore pressure-axial strain, and p-q curve for effective and total stresses. Note  $p = (\sigma_1 + \sigma_3)/2$  and  $q = (\sigma_1 - \sigma_3)/2$ .

### Overview of Data Interpretation

Test data were corrected for piston friction, piston uplift, membrane effects, and changing cross-sectional area. The piston friction was calculated using the procedure outlined by Germaine and Ladd where the pressure inside the empty chamber is increased until the piston lifts up and then decreased until the piston drops. The average of these pressures times the cross-sectional area of the piston was used to correct the load for a piston friction of 6.5 lb. The piston uplift was compensated by zeroing the load when contact was made with the sample during loading. Axial and radial effects of the membrane were corrected using the following equations from Kuerbis and Vaid 1990:

$$\sigma_{am} = \sigma_a - \frac{4E_M t_0 (2 + \varepsilon_v + \varepsilon_{Ma})(\varepsilon_v + 3\varepsilon_{Ma})}{3D_0 (2 - \varepsilon_v + \varepsilon_{Ma})} \quad (\text{Eq. 13})$$

$$\sigma_{rm} = \sigma_r - \frac{4E_M t_0 (2 + \varepsilon_v + \varepsilon_{Ma}) \varepsilon_v}{3D_0 (2 - \varepsilon_v + \varepsilon_{Ma})} \quad (\text{Eq. 14})$$



where

$\sigma_{am}$  and  $\sigma_{rm}$  = the corrected axial and radial stresses.

$\sigma_a$  and  $\sigma_r$  = the applied axial and radial stress.

$E_M$  = the elastic modulus of the membrane.

$t_0$  = the unstretched membrane thickness.

$D_0$  = the unstretched membrane diameter.

$\varepsilon_{Ma}$  and  $\varepsilon_V$  = the axial strain and the volumetric strain.

This equation assumes a thin hollow cylindrical shell and is only applicable if no visible membrane buckling occurs.

Finally, the cross-sectional area was corrected according to Germaine and Ladd where the sample experiences an idealized parabolic or barreling deformation as shown in Figure 54.

The equation for this area correction is:

$$A_c = A_0 \left[ -\frac{1}{4} + \frac{\sqrt{25 - 20\varepsilon_a - 5\varepsilon_a^2}}{4(1 - \varepsilon_a)} \right]^2 \quad \text{(Eq. 15)}$$

where

$A_c$  = the corrected area.

$A_0$  = the initial cross sectional area of the specimen.

$\varepsilon_a$  = the axial strain in the specimen.



**Figure 54. Parabolic Deformation of Test Specimen.**

Friction angles for each test were calculated using the differential stress at 10 percent strain and assuming cohesion of the material was zero. Data for each gradation were plotted in p-q space, where p is equal to the average of the major and minor principal stress, and q is equal to half of the differential stress. A friction angle was determined using a linear regression of the data to find the slope of the line ( $K_f$ ), while again forcing the intercept to be zero. The sine of the friction angle is equal to the slope of the line in p-q space.

### **Overview of Testing Results**

Consolidated drained triaxial compression testing of backfill material resulted in reasonably consistent trends such as a decrease in the angle of internal friction with an increase in confining pressure, as well as an increase in fines due to the increasing suppression of dilation.

Type A had a range of friction angles from 39.8° to 49.9°. Type B friction angles ranged from 31.8° to 53.4°. Type D friction angles ranged between 35.8° to 47.2°. Since the test on Type C material was consolidated undrained test, therefore the data presented are effective internal friction angle (only for Type C). Table 16 and Table 17 summarize relevant results. The detailed test results on backfill material are presented in Appendix -B. In this appendix, a test summary data, stress-strain plots, volumetric strain plots and p-q plots are presented for different types of backfill materials. Few specimen plots are shown below from Figure 55 to Figure 57 for Type A backfill material.

**Table 16. Friction Angles for Types A, B, and D Backfill Tested.**

| <b>Gradation</b> | <b>Maximum Friction Angles (°)</b> | <b>Minimum Friction Angles (°)</b> | <b>p-q Friction Angles (°)</b> |
|------------------|------------------------------------|------------------------------------|--------------------------------|
| A1               | 49.9                               | 43.0                               | 45.5                           |
| A2               | 46.8                               | 41.8                               | 43.7                           |
| A3               | 47.5                               | 41.8                               | 42.9                           |
| A4               | 45.9                               | 39.8                               | 42.8                           |
| B1               | 53.4                               | 48.5                               | 51.9                           |
| B2               | 53.2                               | 48.3                               | 52.5                           |
| B3               | 48.4                               | 43.5                               | 45.7                           |
| B4               | 41.7                               | 31.8                               | 39.2                           |
| D1               | 47.2                               | 41.6                               | 44.2                           |
| D2               | 47.0                               | 36.5                               | 40.7                           |
| D3               | 51.6                               | 38.4                               | 43.8                           |
| D4               | 41.7                               | 35.8                               | 38.0                           |

**Table 17. Friction Angles for Type C Backfill Material.**

| <b>Gradation</b> | <b>Maximum Undrained Friction Angles (°)</b> | <b>Minimum Undrained Friction Angles (°)</b> | <b>Maximum Drained Friction Angles (°)</b> | <b>Minimum Drained Friction Angles (°)</b> |
|------------------|--|--|--|--|
| C1               | 29.4   | 26.2   | 40.3                                       | 27.8                                       |
| C2               | 28.3   | 26.2   | 47.4                                       | 30.1                                       |
| C3               | 32.0   | 22.6   | 50.9                                       | 33.7                                       |
| C4               | 32.3   | 23.6   | 26.4                                       | 23.0                                       |

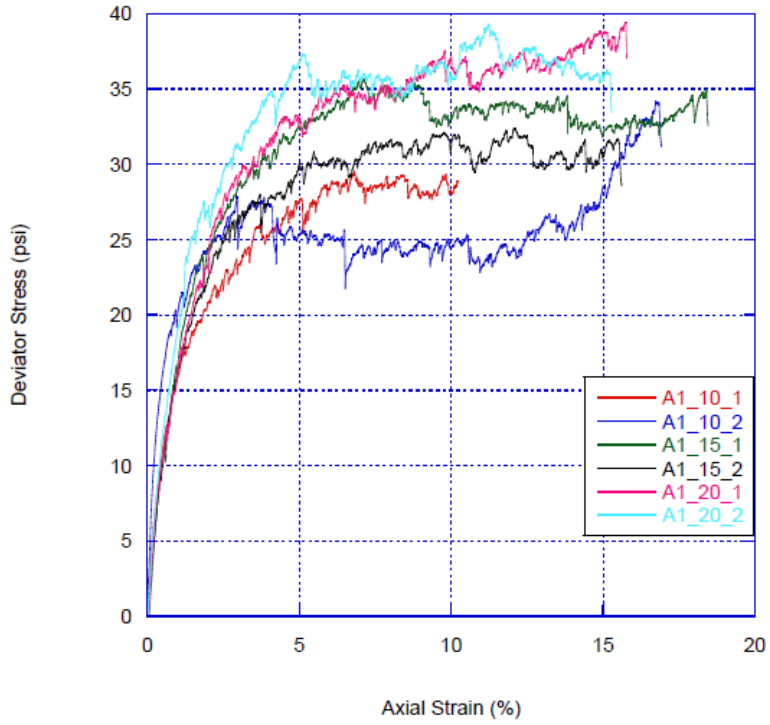


**Figure 55. Stress-Strain for a Gradation Type A1.**

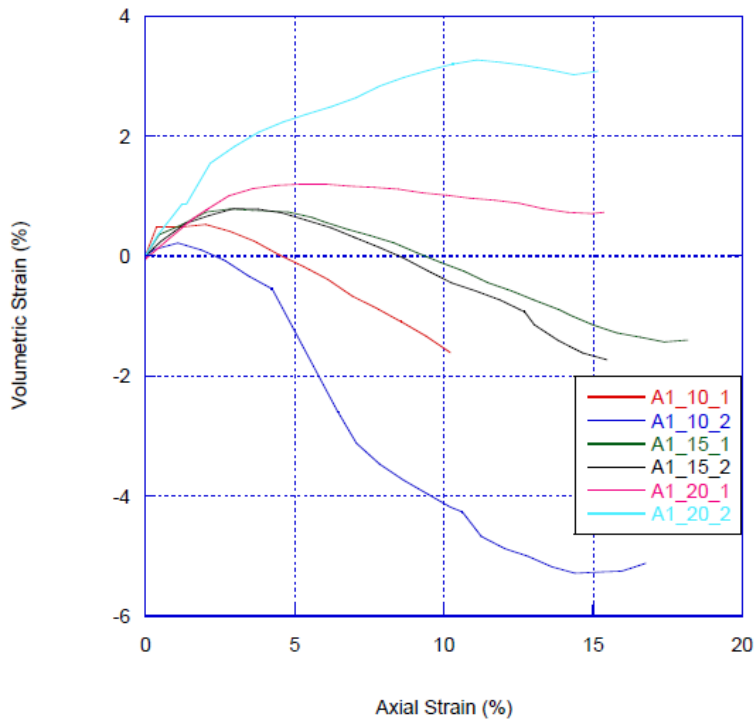


**Figure 56. Volumetric Strain Curves for a Gradation Type A1.**

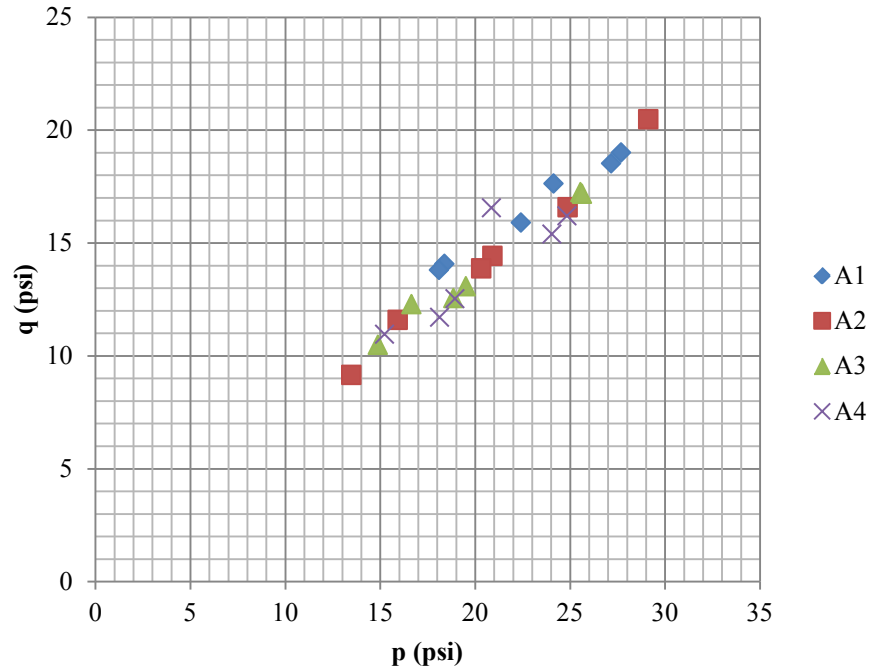


**Figure 57. Type A Material p-q Diagram.**

## STATISTICAL ANALYSES

The statistical analysis of this study includes:

- Analyzing the test data of friction angle and unit weight to establish their distribution.
- Performing a Monte Carlo analysis to investigate the distribution of FOSs of sliding and overturning by considering the spatial variation of backfill material unit weight.

### Statistical Analysis of Test Data

#### *Results for Friction Angle and Unit Weight Analysis*

A number of triaxial tests were conducted for each of Types A, B, and D backfill materials, and the dry unit weight of each compacted and ready-to-test sample was measured. The test data were analyzed by assuming they fall into a normal distribution pattern. The three-sigma ( $3\sigma$ ) rule (i.e., nearly 99.7 percent of the values fall within three standard deviations of the mean as shown in Figure 58) was used to determine the low bound of the friction angles and unit weights of Types A, B, and D material. Figure 59–Figure 64 show the distributions of the friction angles, and unit weights as well as the determined low bound of each value.

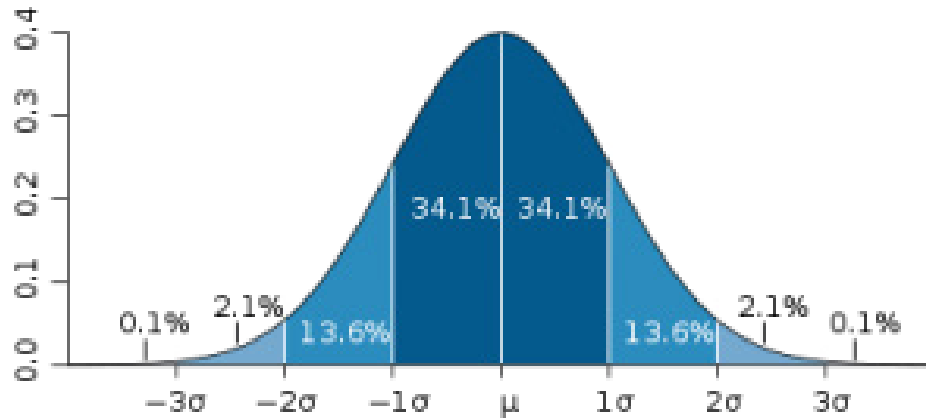
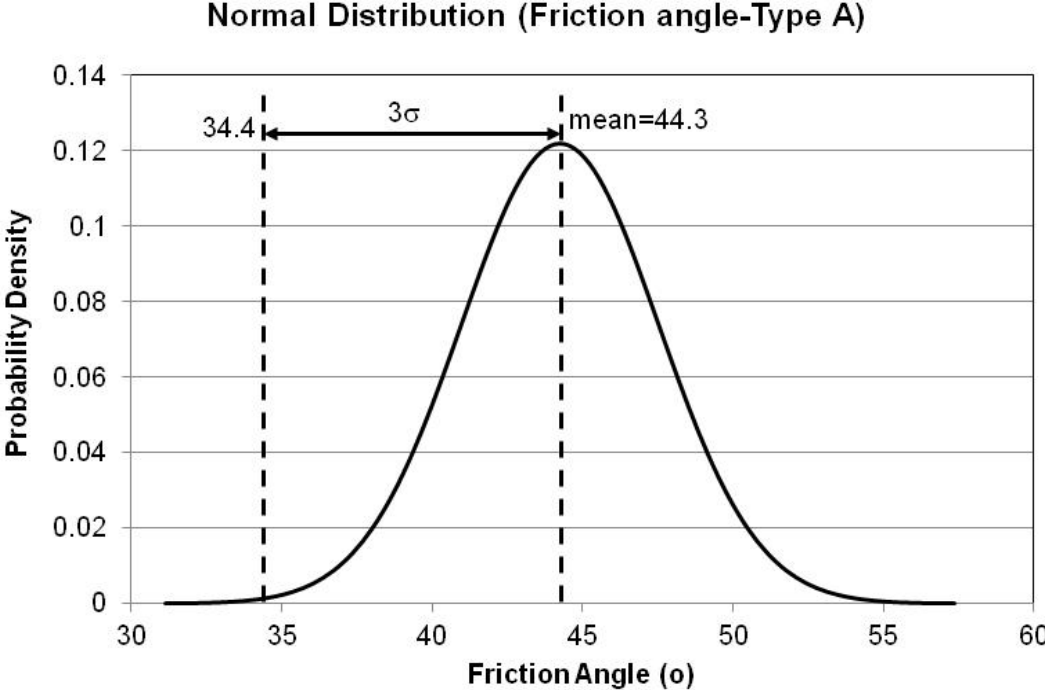


**Figure 58. Statistical Control Limits (www.3sigma.com).**

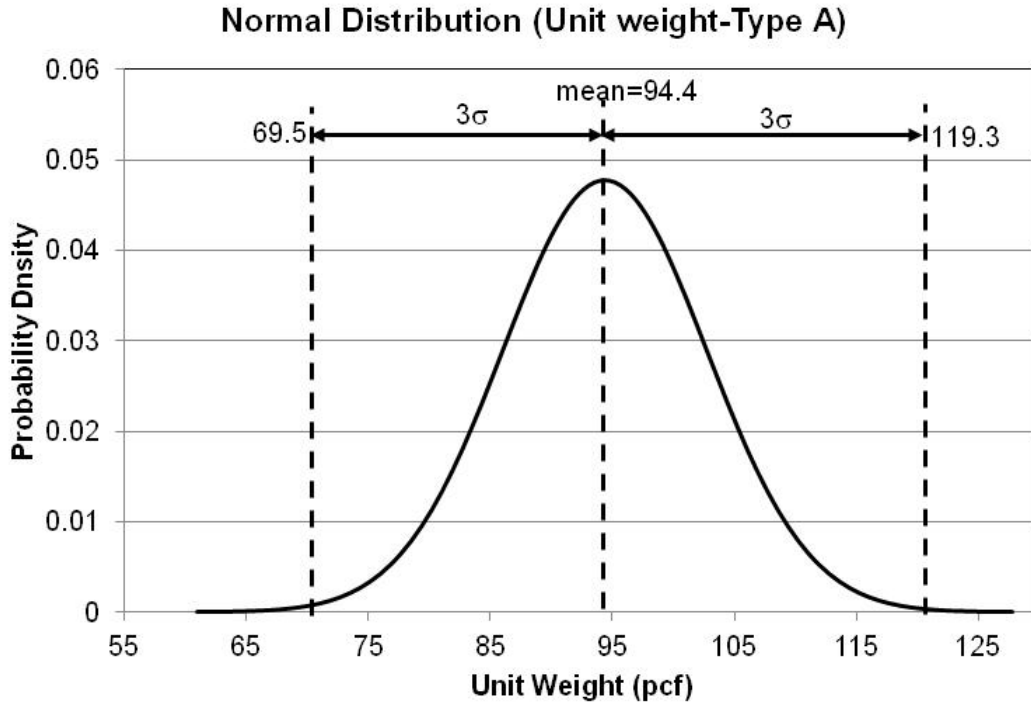
Figure 59, Figure 61 and 63 show the distributions of the friction angle for Types A, B, and D materials. The lower bound of the  $3\sigma$  range is marked in these figures to signify the friction angles for 99.9 percent confidence level. Apparently, the mean values of the friction angles are significantly higher than  $34^\circ$ , which is the value used in the design. However, considering the  $3\sigma$  rule the friction angle is lowered to approximately  $34^\circ$  for Type A material, and  $30^\circ$  for Type B and D materials. In another words, for Types A, B, and D materials, the possibility of the friction angles greater than  $30^\circ$  is at least 99.9 percent. The friction angle is plotted against its confidence level in Figure 65 to assess the possibility of any friction angle. At the confidence level of 95 percent, the friction angles of the three materials are greater than  $35^\circ$ .

Figure 60, Figure 62 and Figure 64 present the distributions of dry unit weights for Types A, B, and D materials. The dry unit weights of the three materials are 94.4, 111.9, and 88.8 pcf, which are lower than the value assumed for design, 125 pcf. The unit weight distributions indicate significant deviations, and the  $3\sigma$  range covers a wide range as shown in the figures. Figure 66 presents the confidence level of the unit weights. The dry unit weight is plotted against relative compaction in Figure 67, which shows that the dry unit weights of the three materials are bounded in a certain range indicated by the lines. For the given relative compaction, the maximum and minimum dry unit weights can be determined. For example, if 95 percent relative compaction is required, the dry unit weight varies from 90 to 115 pcf. The specific gravities of the three types of materials are listed in Table 18. Considering the 100 percent saturation, which

is the worst scenario, the maximum and minimum saturated unit weights at different relative compaction are presented in Table 19.



**Figure 59. Normal Distribution of Friction Angle of Type A.**



**Figure 60. Normal Distribution of Unit Weight of Type A.**

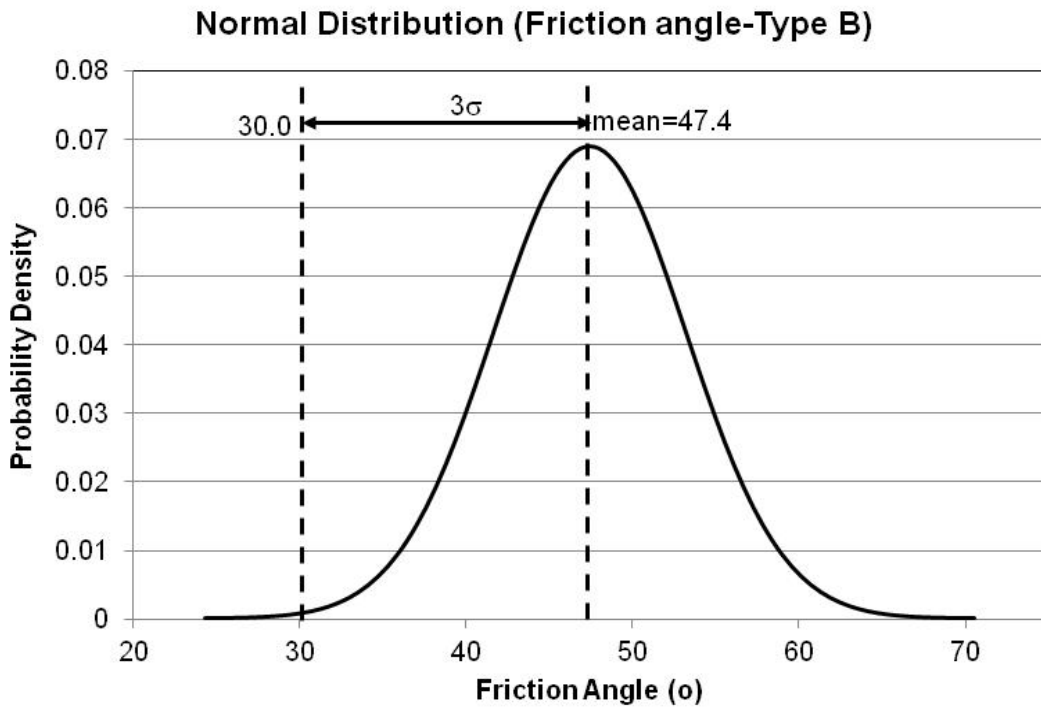


**Figure 61. Normal Distribution of Friction Angle of Type B.**



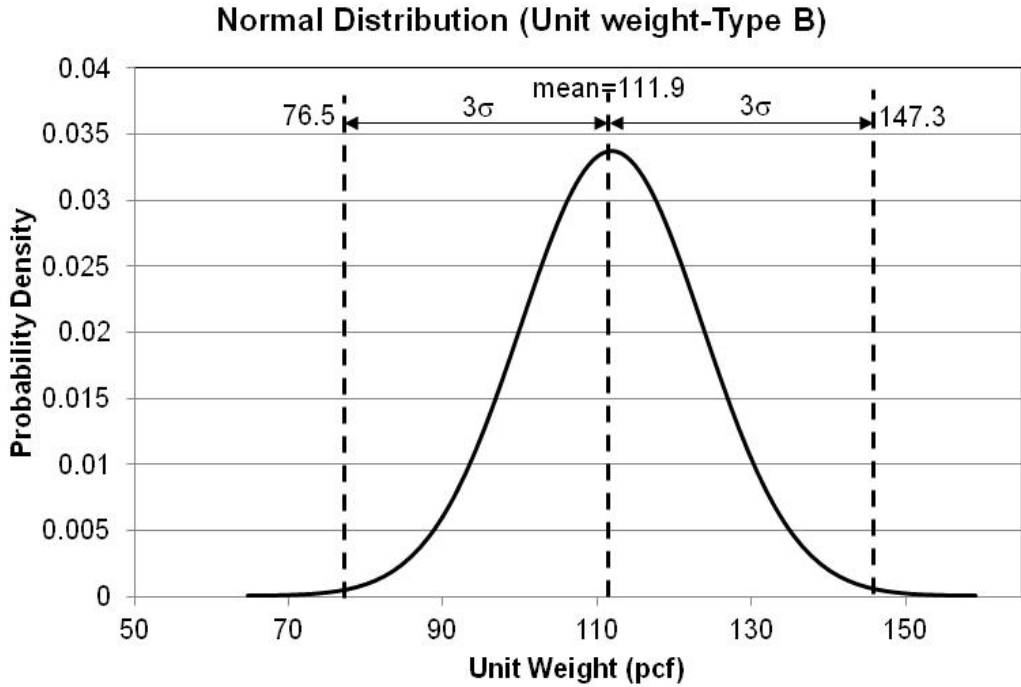


**Figure 62. Normal Distribution of Unit Weight of Type B.**

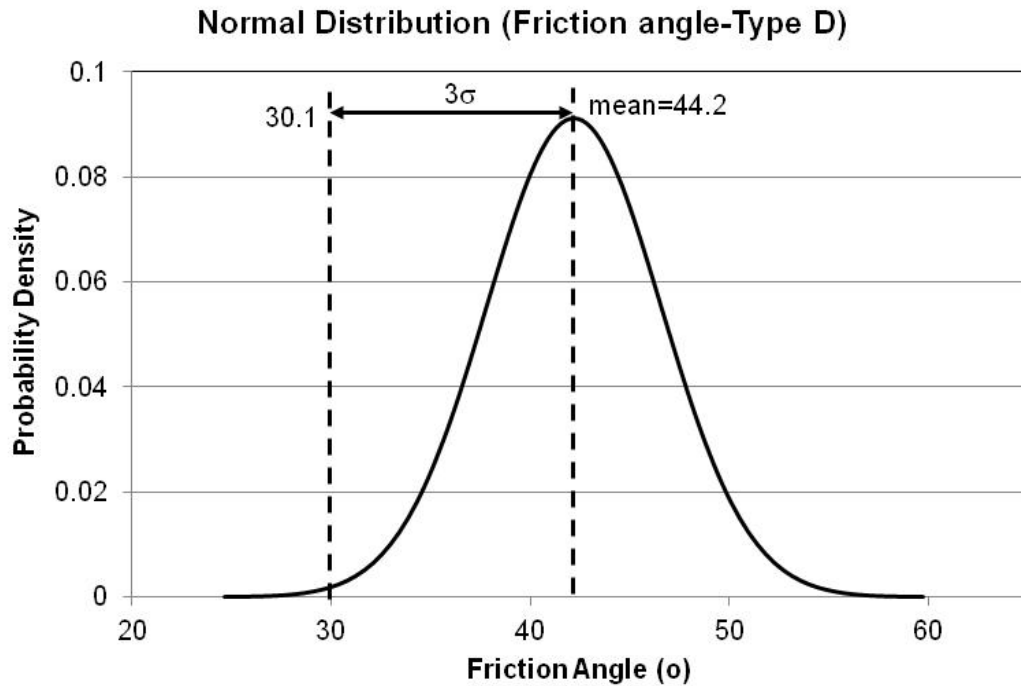


**Figure 63. Normal Distribution of Friction Angle of Type D.**

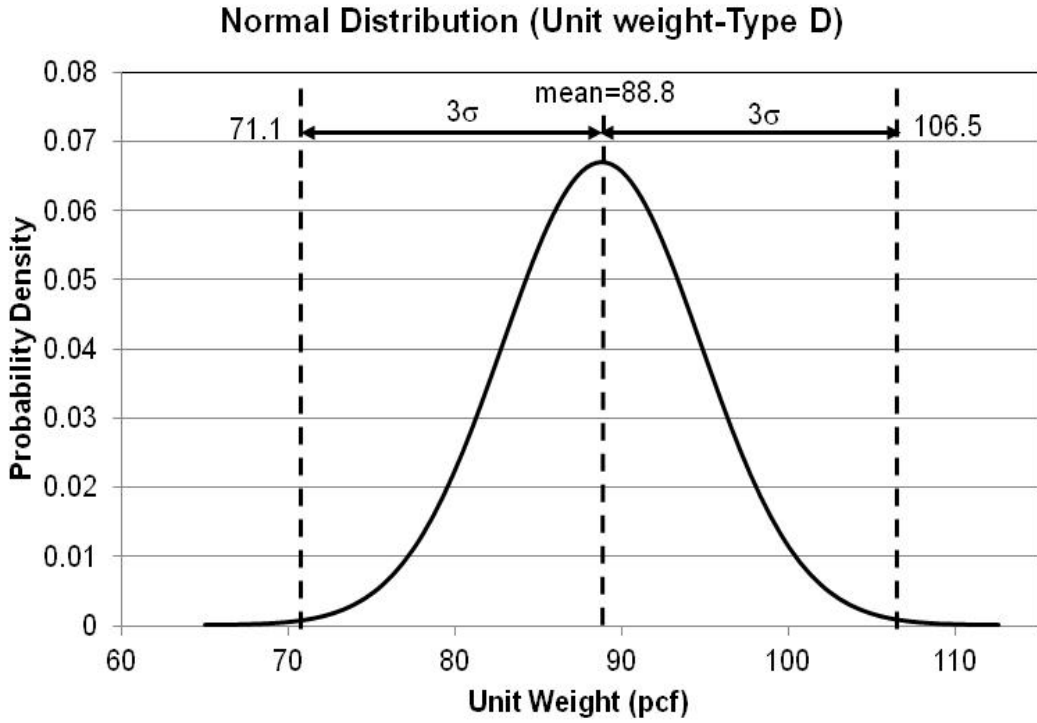


**Figure 64. Normal Distribution of Unit Weight of Type D.**

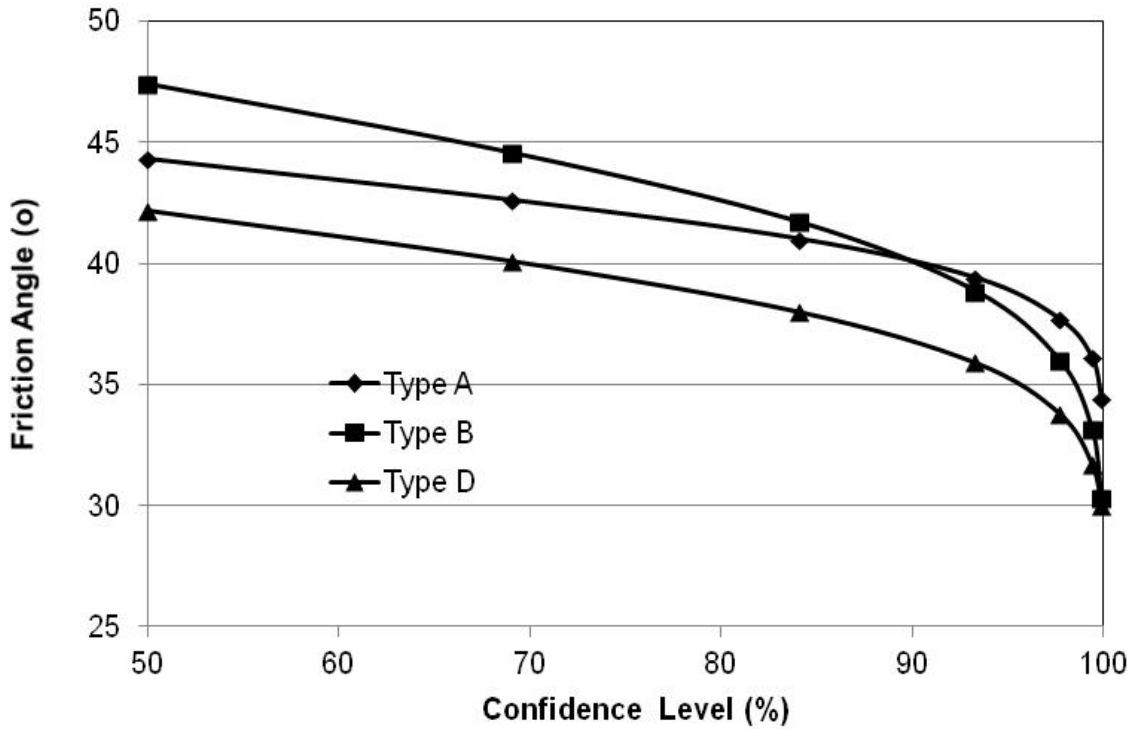


**Figure 65. Friction Angle vs. Confidence Level.**

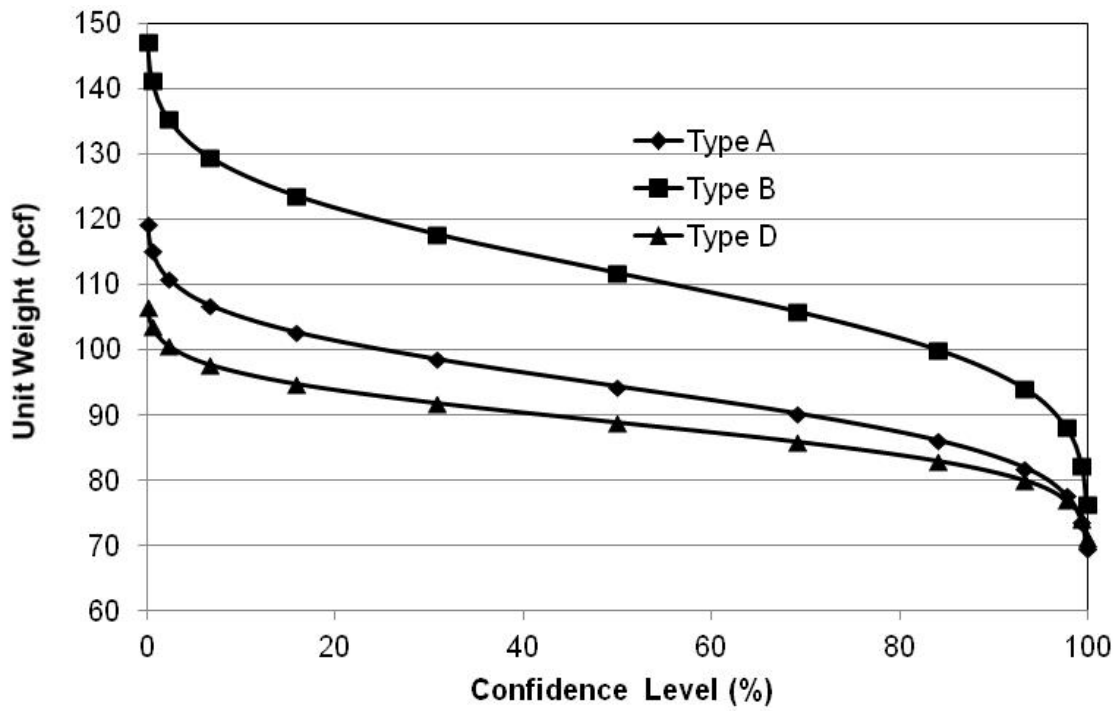


Figure 66. Unit Weight vs. Confidence Level.

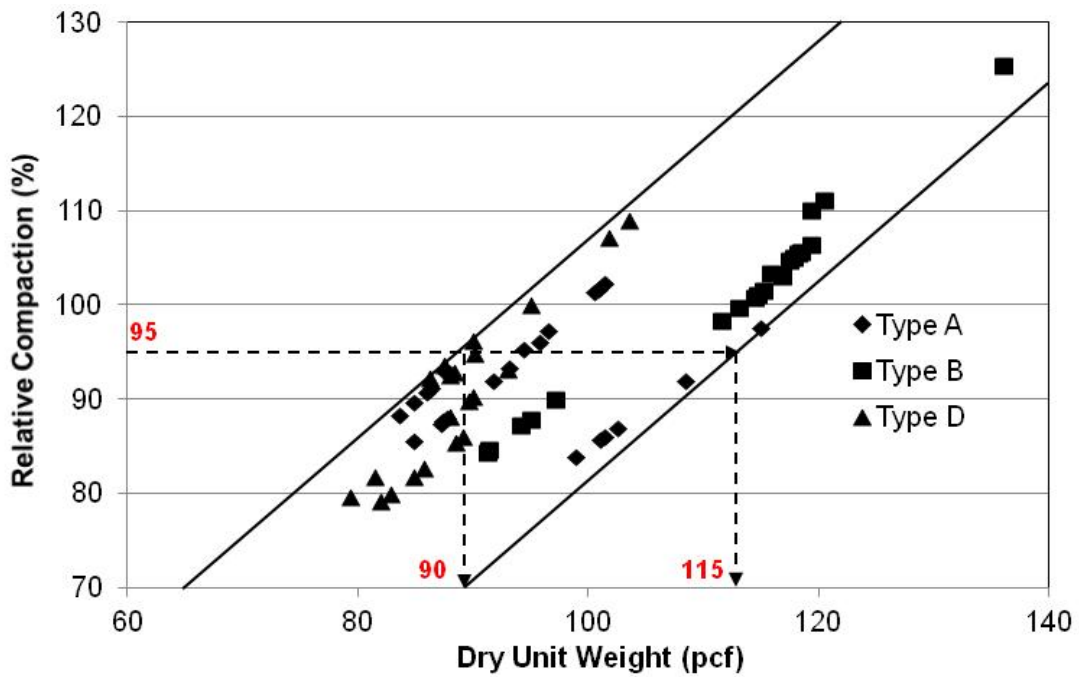


Figure 67. Dry Unit Weight vs. Relative Compaction.

**Table 18. Specific Gravity of Types A, B, and D.**

| <b>Material Type</b> | <b>A</b> | <b>B</b> | <b>D</b> |
|----------------------|----------|----------|----------|
| Specific gravity     | 2.6      | 2.6      | 2.7      |

**Table 19. Unit Weight at Different Compaction.**

| <b>Relative Compaction (%)</b> | <b>Unit weight (pcf)</b> |            |                  |            |
|--------------------------------|--------------------------|------------|------------------|------------|
|                                | <b>Dry</b>               |            | <b>Saturated</b> |            |
|                                | <b>Min</b>               | <b>Max</b> | <b>Min</b>       | <b>Max</b> |
| 90                             | 82                       | 110        | 110              | 128        |
| 95                             | 90                       | 115        | 118              | 134        |

The above statistical analysis was performed based on the available test data. The results can be refined if more test data are available. However, the statistical analysis is still considered meaningful since the results presents a conservative scenario. The limited data form a small sample with great deviation. Thus, the calculated variation ranges of the friction angles and unit weights are broad. With the increase of the sample size, the standard deviation ( $\sigma$ ) likely will be reduced and the variation range covered by  $3\sigma$  will be a subset of the variation range indicated in this analysis.

## **MONTE CARLO ANALYSIS ON FOS**

### **Monte Carlo Method**

Developed by John von Neumann, Stanislaw Ulam, and Nicholas Metropolis in the 1940s, the Monte Carlo method is a computational method for generating suitable random numbers and observing the properties of the numbers or the fraction of the numbers. The Monte Carlo simulation performs analysis by repeated random sampling of any factors from its probability distribution, and then calculates the results or establishes the distribution. A real-world example of the Monte Carlo concept is to find the ratio of the area of the circle to the square shown in Figure 68, if the areas of the square and circle cannot be measured directly. A particle can be repeatedly thrown into the square as shown in Figure 68. The total number of throws is counted as  $T_t$ , which includes the number of throws in the circle inside the square ( $T_c$ ). The ratio of the circle area to the square area can be calculated as  $T_c/T_t$  since the possibility of falling into the circle is equal to the area ratio between the circle and the square.

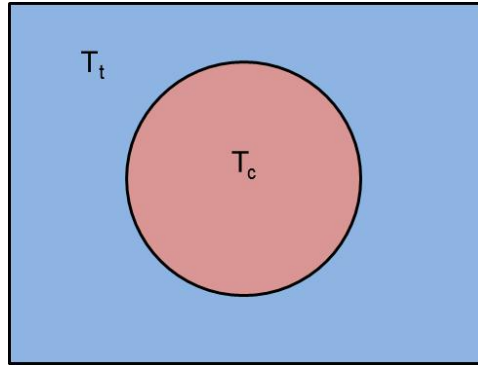


**Figure 68. Monte Carlo Analysis Example.**

From this example, the procedure of the Monte Carlo method is summarized below:

1. Define a domain of possible inputs.
2. Generate inputs randomly from a probability distribution over the domain.
3. Perform a deterministic computation on the inputs.
4. Aggregate the results.

### **FOSs for Sliding and Overturning**

The FOSs for sliding and overturning are evaluated by considering the spatial variation of the unit weight. Due to the compaction energy difference, material gradation difference, and space constraint for compaction, the backfill materials are not compacted uniformly into a unit weight; instead, the unit weight varies at different locations. The effect of unit weight variation on the FOSs for sliding and overturning has been investigated using the Monte Carlo method. Figure 69 presents the prototype of the MSE wall for this analysis. The wall is 20 ft high with a reinforcement of 14 ft (i.e., 0.7H). The reinforced zone was divided into subzones of  $1 \times 1 \text{ ft}^2$  as shown in Figure 69. The unit weight of each zone is randomly selected from its possible distributions such as shown in Figure 60, Figure 62, or Figure 64, and then an FOS is calculated. By repeating the process 100,000 times in this study, 100,000 FOSs have been obtained. The obtained FOSs possess normal distribution patterns, which are plotted in Figure 70–Figure 81. In this study, two friction angles (i.e.,  $30^\circ$  and  $26^\circ$ ) for foundation soil and retained soil are considered. The  $30^\circ$  friction angle is commonly used in practice while the  $26^\circ$  friction angle accounts for the 13 percent deviation as suggested in the research of Harr (1984), and Phoon and Kulhawy (1996).

For all the cases investigated, the FOSs meet the requirements when calculated using TxDOT standard design parameters (i.e., the FOS for overturning=3.7; FOS for sliding=2.0). The Monte Carlo analysis results reveal that for all the cases investigated the overturning meets the FOS requirement ( $>2$ ); however, FOSs for sliding show either insufficiency or limit margin for most of the cases. Of the six conditions assessed (i.e.,  $\phi_f=26^\circ$  and  $30^\circ$  for Types A, B, and D), the FOSs of three conditions are less than 1.5 and the FOS of one condition is barely 1.5. This fact reveals:

- The sliding is usually more critical and often controls the design.
- The current design parameters may not be sufficient in terms of sliding.

Although the figures show significant deviations of unit weights, the Monte Carlo analysis results show that the deviation of the calculated FOS is not significant. The maximum deviation of the FOS is merely 7 percent for the backfill materials investigated.

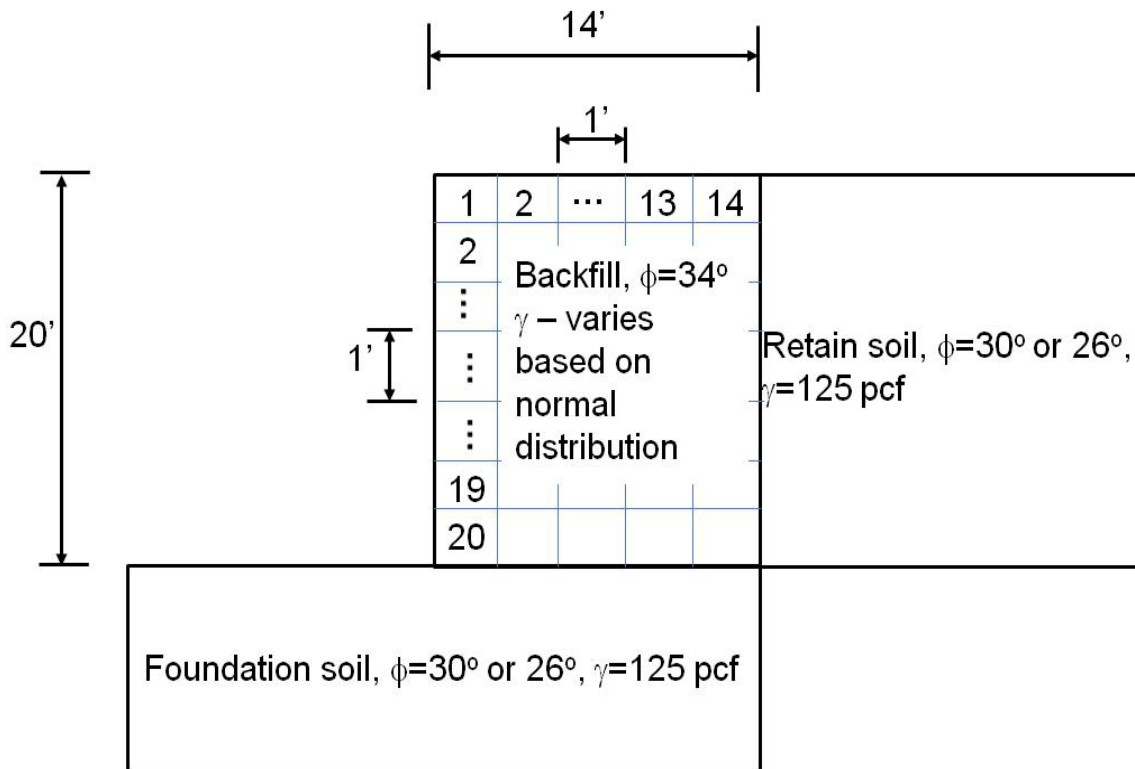


**Figure 69. Monte Carlo Model for Sliding and Overturning FOS Analysis.**

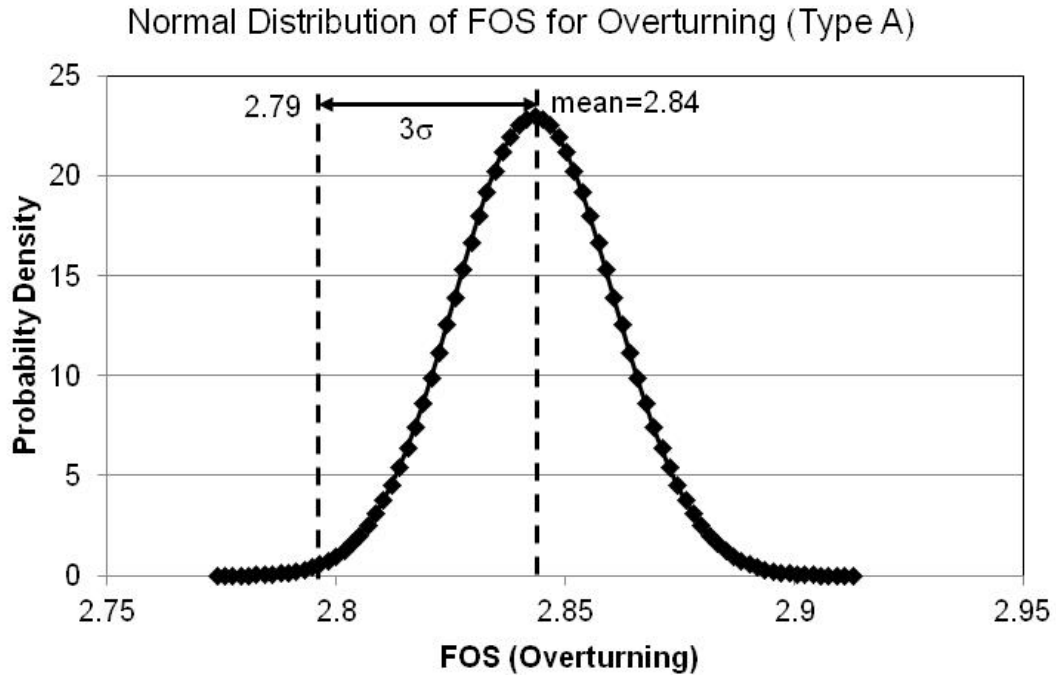


**Figure 70. Overturning FOS of Type A ( $\phi_r=26^\circ$ ).**

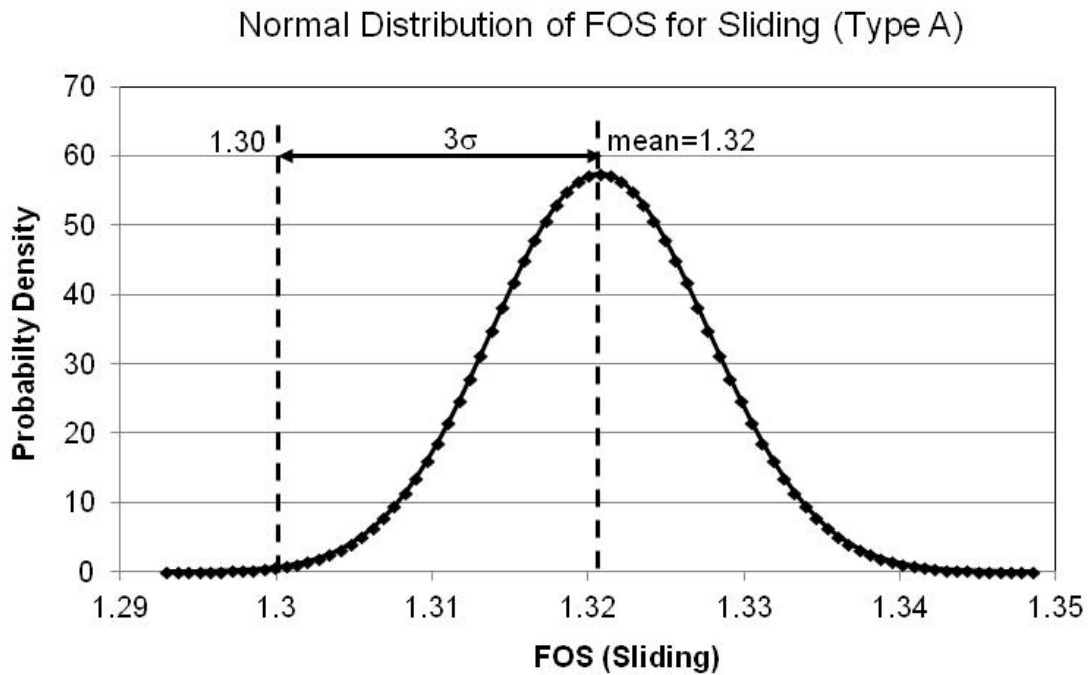


**Figure 71. Sliding FOS of Type A ( $\phi_r=26^\circ$ ).**

Normal Distribution of FOS for Overturning (Type A)

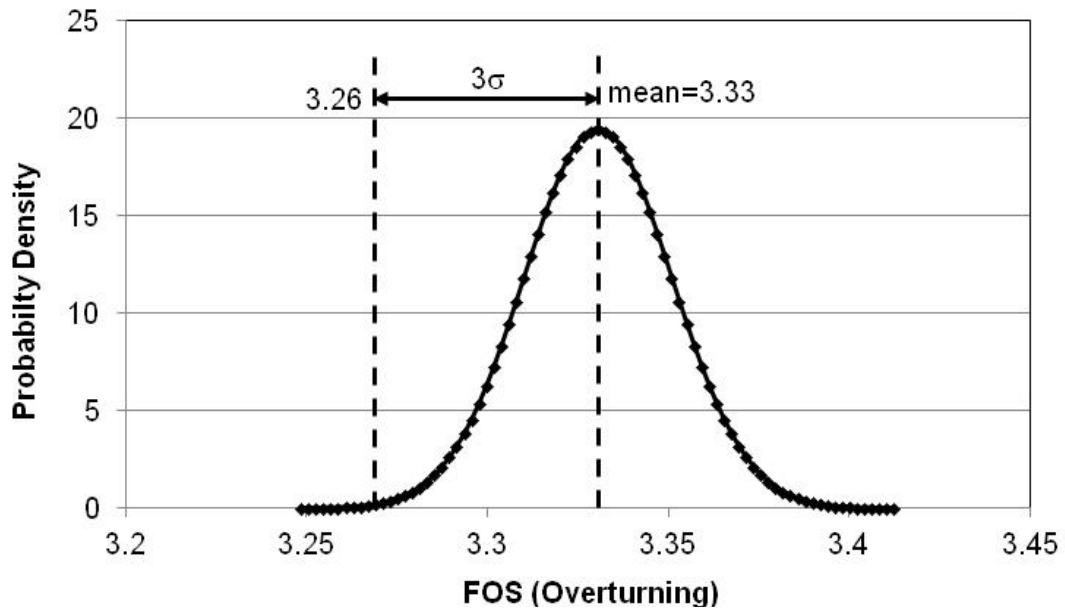


Figure 72. Overturning FOS of Type A ( $\phi_r=30^\circ$ ).

Normal Distribution of FOS for Sliding (Type A)

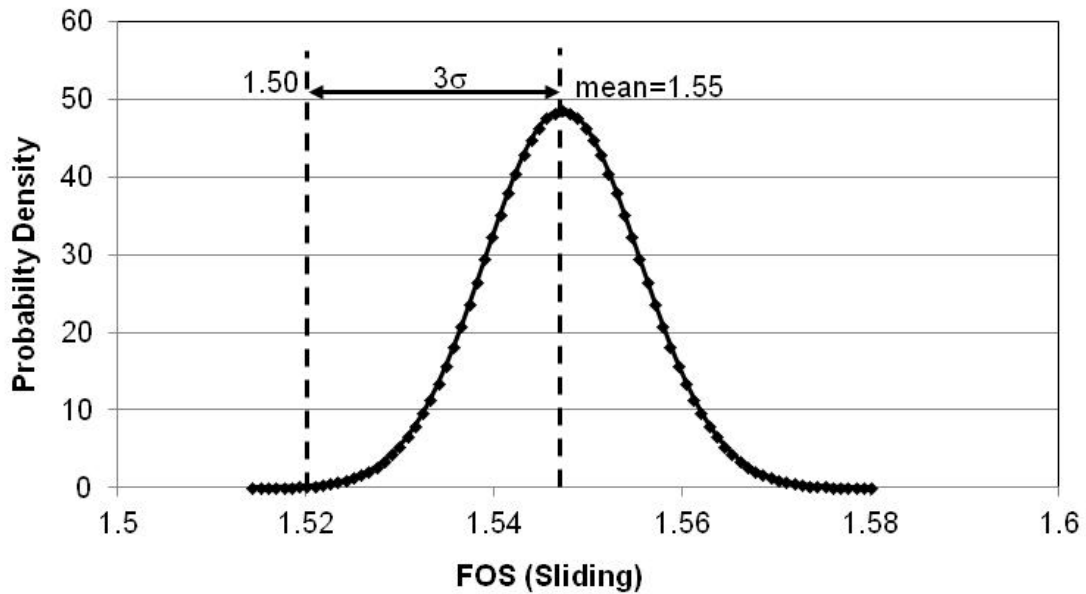


Figure 73. Sliding FOS of Type A ( $\phi_r=30^\circ$ ).



Normal Distribution of FOS for OVerturning (Type B)

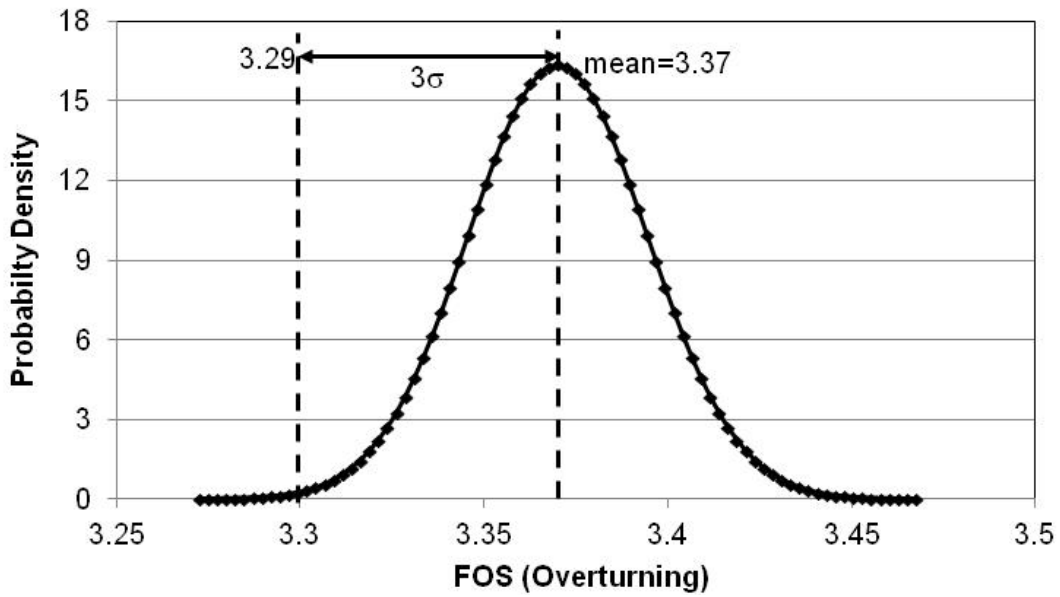


Figure 74. Overturning FOS of Type B ( $\phi_r=26^\circ$ ).

Normal Distribution of FOS for Sliding (Type B)

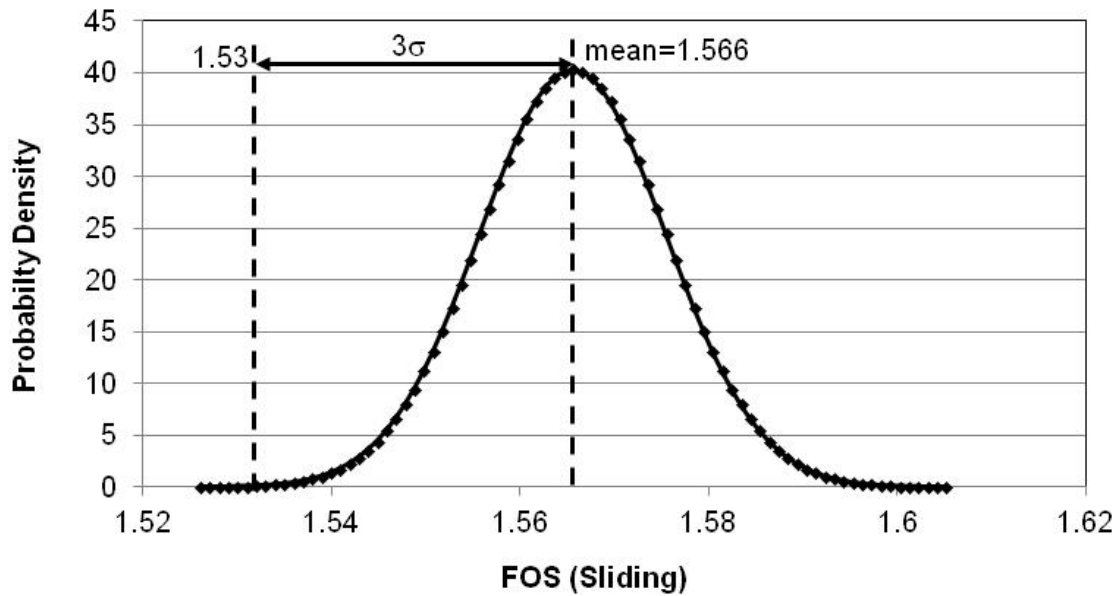


Figure 75. Sliding FOS of Type B ( $\phi_r=26^\circ$ ).

Normal Distribution of FOS for Overturning (Type B)

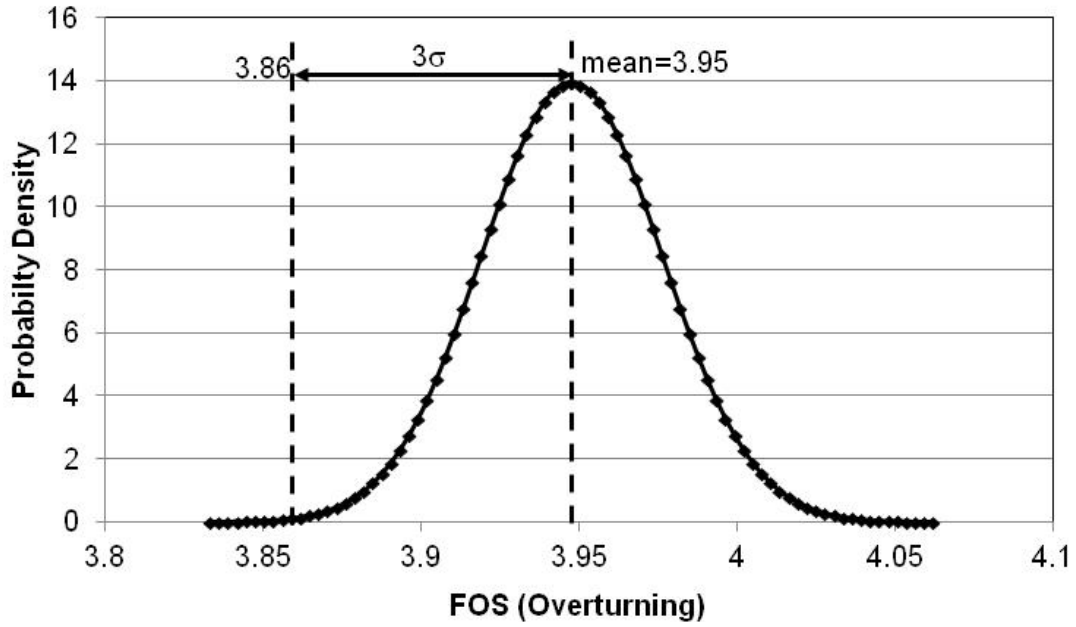


Figure 76. Overturning FOS of Type B ( $\phi_r=30^\circ$ ).

Normal Distribution of FOS for Sliding (Type B)

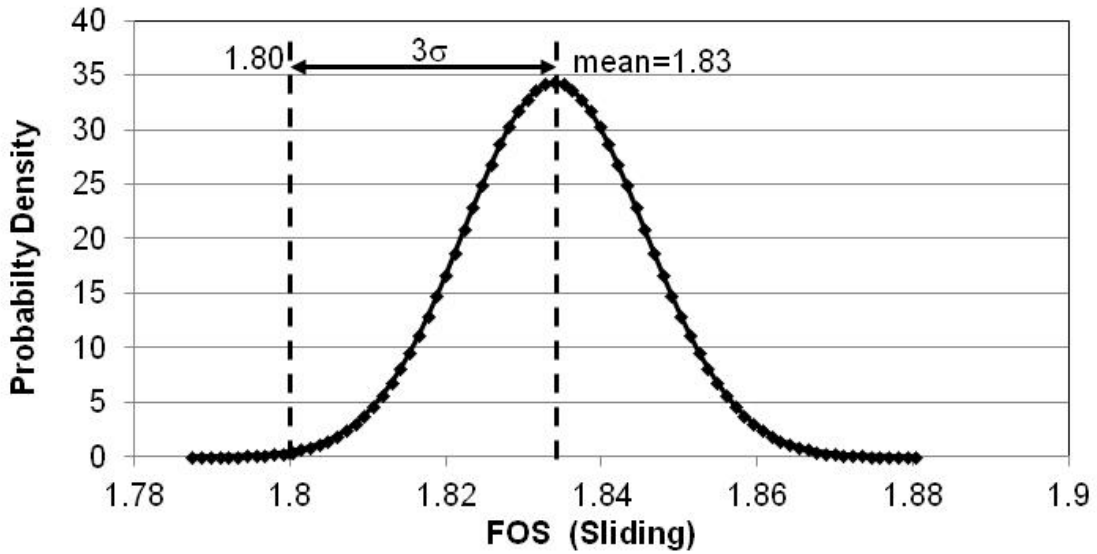


Figure 77. Sliding FOS of Type B ( $\phi_r=30^\circ$ ).

Normal Distribution of FOS for Overturning (Type D)

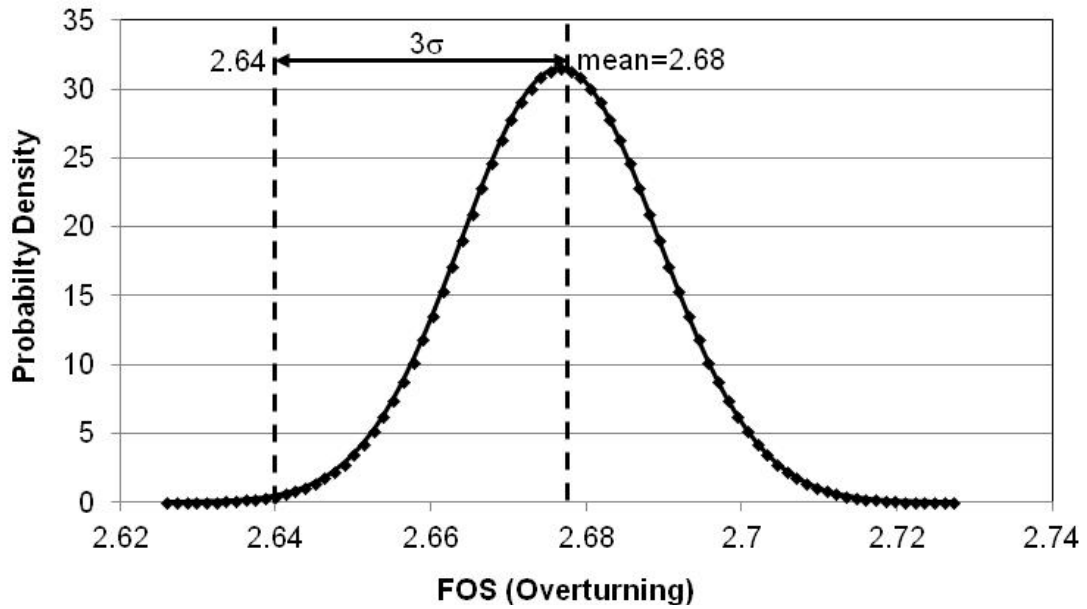


Figure 78. Overturning FOS of Type D ( $\phi_f=26^\circ$ ).

Normal Distribution of FOS for Sliding (Type D)

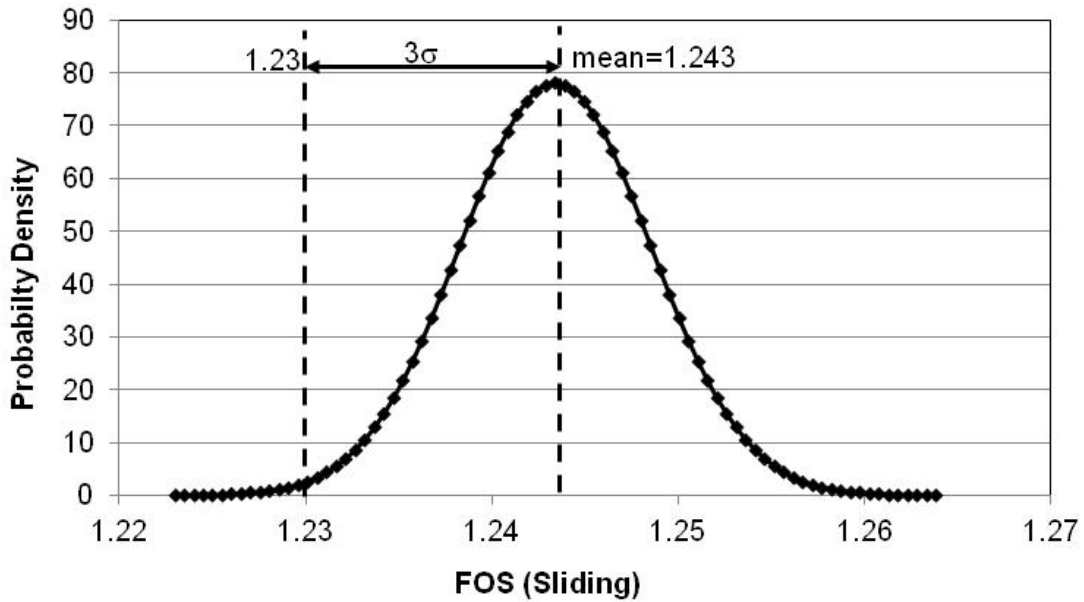


Figure 79. Sliding FOS of Type D ( $\phi_f=26^\circ$ ).

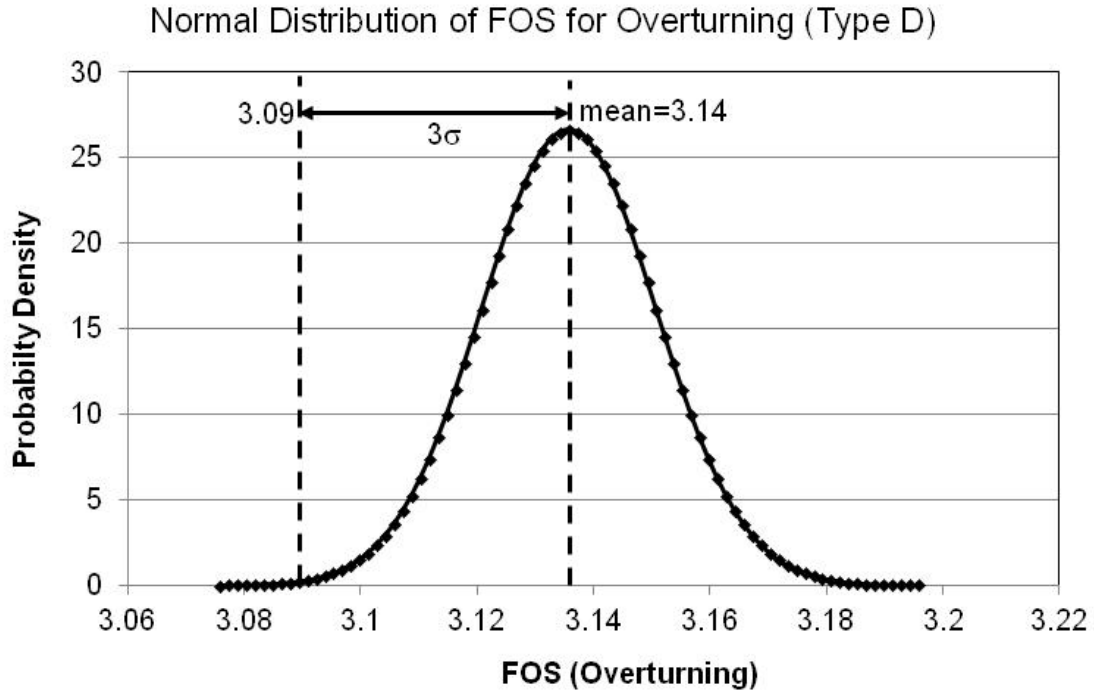


Figure 80. Overturning FOS of Type D ( $\phi_t=30^\circ$ ).

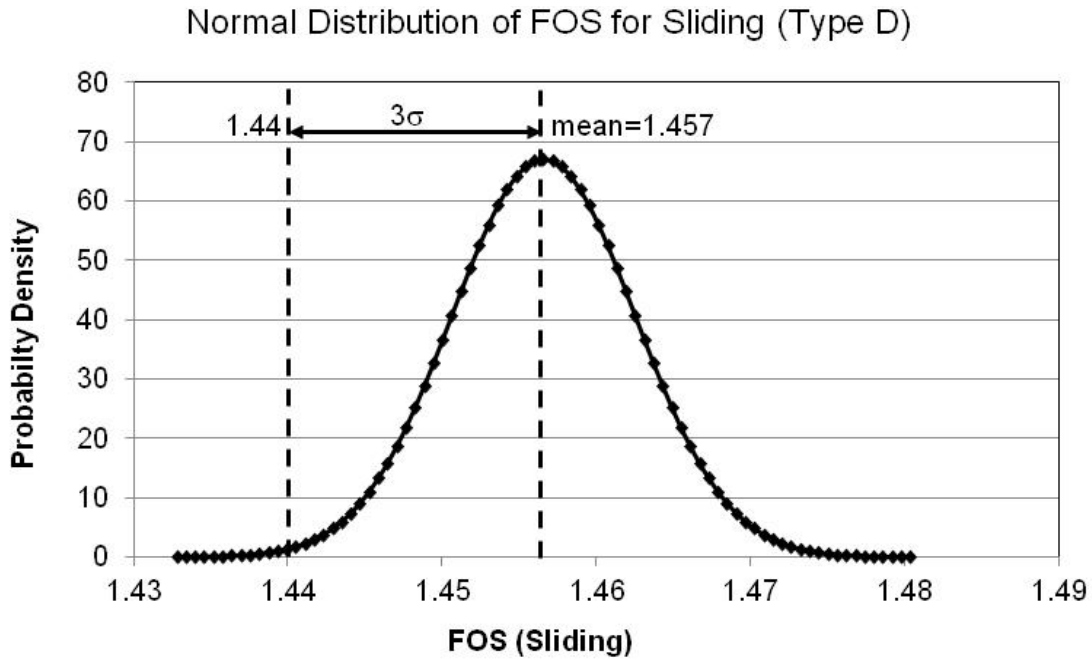
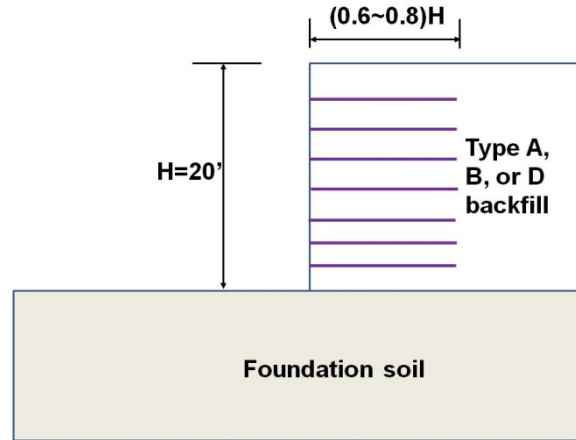


Figure 81. Sliding FOS of Type D ( $\phi_t=30^\circ$ ).

## FLAC ANALYSIS FOR MINIMUM LENGTH

The minimum reinforcement length is evaluated from the lateral deflection point of view. The FLAC, a finite difference software, was used to model the MSE wall and calculate the lateral deflections under different reinforcement length. Figure 82 presents the MSE wall selected for analysis, and FOSs of the MSE wall are presented in Table 20.



**Figure 82. MSE Prototype of Minimum Reinforcement Length Analysis.**

**Table 20. FOSs for Different Reinforcement Length.**

| Reinforcement length | 0.6H | 0.7H | 0.8H |
|----------------------|------|------|------|
| Sliding              | 1.7  | 2.0  | 2.3  |
| Overturning          | 3.2  | 3.7  | 4.2  |
| Global stability     | 2.4  | 2.3  | 2.1  |

Note: for sliding and overturning  $\gamma=105$  pcf; for global stability  $\gamma=125$  pcf.

The Mohr-Coulomb model was used for backfill and retained materials. Friction angles of  $34^\circ$  and  $30^\circ$  were used for the backfill and retained soil, respectively. The elastic modulus of the backfill material is determined below, which indicated a stress-dependent behavior of a granular material (Duncan et al. 1980):

$$E = k \left( \frac{\sigma_3}{p_a} \right)^n \quad (\text{Eq. 16})$$

where

$E$  = the elastic modulus.

$\sigma_3$  = the confining stress.

$k$  and  $n$  = material constants.

$p_a$  = the atmospheric pressure (i.e., 2.1 ksf).

The  $k$  and  $n$  values were determined based on the triaxial test curves for each type of backfill material and are listed in Table 21. In the numerical modeling, the 20-ft backfill material was divided into 20 layers with equal thickness of 1 ft. The elastic modulus was calculated based on the confining stress at the mid-depth of each layer.

**Table 21.  $k$  and  $n$  Values.**

|           | <b>Type A</b> | <b>Type B</b> | <b>Type D</b> |
|-----------|---------------|---------------|---------------|
| $k$ (MPa) | 15            | 34            | 16            |
| $n$       | 0.57          | 0.63          | 0.4           |

The reinforcement consisted of a metallic strap with the cross-section of 2 inches  $\times$  0.16 inches. The interface between the backfill material and the reinforcement was simulated by spring-sliders with Mohr-Coulomb failure criteria. A reduction factor of 0.8 was applied to obtain the interface friction angle. The precast panels were simulated as discrete panels that were connected by hinges. Figure 83 presents the FLAC model.

The maximum deflection is plotted against reinforcement length in Figure 84. Apparently, increasing the reinforcement length leads to less lateral deflection. For the reinforcement length ranging from 0.6~0.8H, the maximum deflection is constantly less than 1 inch for a 20-ft MSE wall.

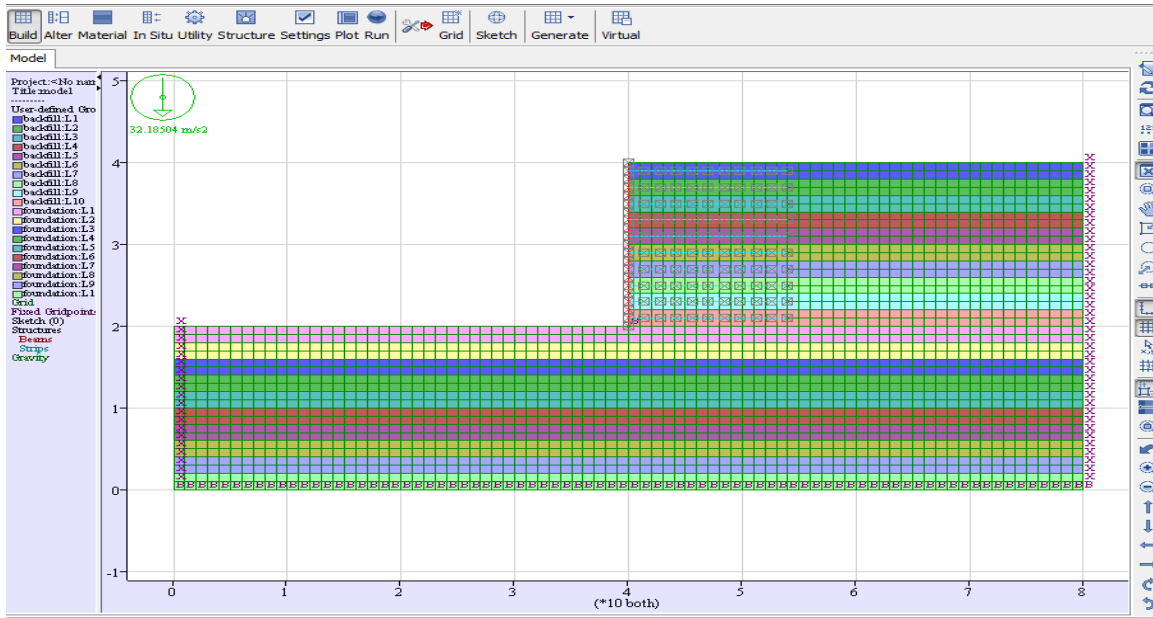


Figure 83. FLAC Model for Minimum Length Analysis.

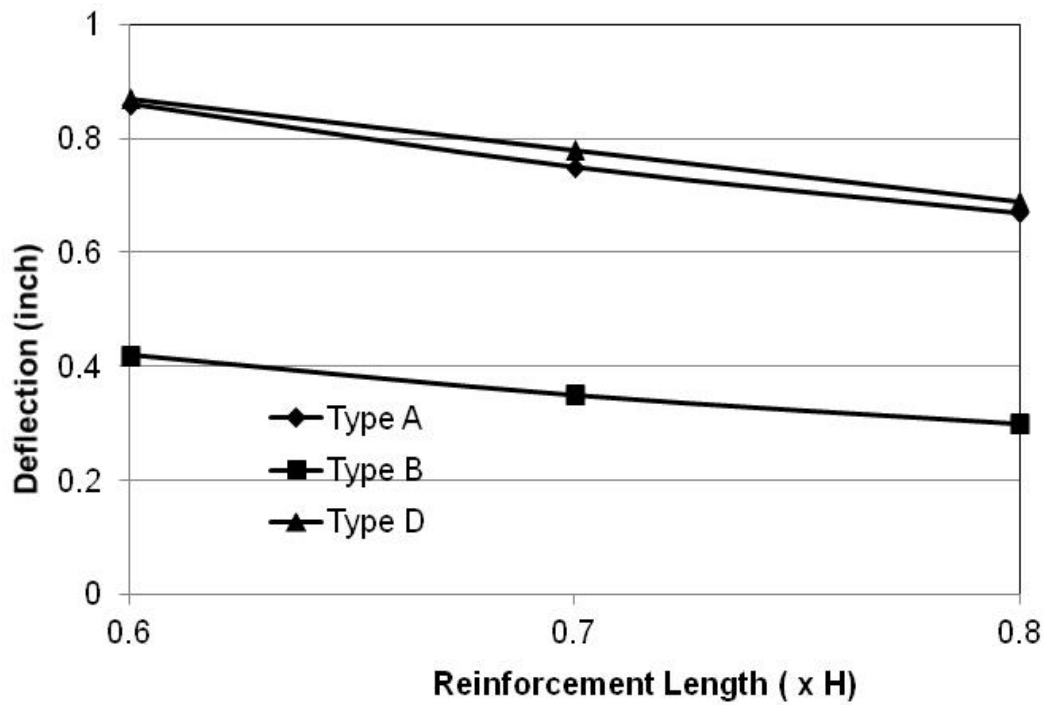


Figure 84. Reinforcement Length vs. Deflection.





## **CHAPTER 5: JUSTIFICATION OF DESIGN METHODOLOGY**

The justification of the design methodology for MSE retaining walls focuses on two issues:

- Whether a classical (Terzaghi) bearing capacity analysis is realistic for MSE walls.
- Whether a potential compound failure mechanism involving the facing panels needs to be considered in MSE wall design and, if so, how it should be analyzed.

The use of the classical bearing capacity theory raises two basic questions. The first question deals with the asymmetric loading associated with retaining walls, which is not strictly accounted for in the classical bearing capacity theory. The bearing capacity section of this chapter addresses this issue. The second question deals with the shearing resistance mobilized by the backfill soil, which leads to failure mechanisms more closely resembling a slope failure rather than a bearing failure. The essence of the second question is whether a classical bearing capacity analysis addresses a realistic possible failure mechanism for MSE walls, or should a global stability analysis be required. Global stability section of this chapter deals with this issue. The compound failure analysis section of this chapter discuss the possibility of the compound failures under complicated geometry and/or groundwater conditions.

Following discussions with TxDOT at the start of this task, the research team decided to perform a parametric study investigating the effects of the following variables on MSE wall stability:

- A variation in foreslope.
- A variation in backslope.
- A two-tiered wall system.
- Rapid drawdown of standing water against the wall.
- Foundation soil strength.
- Backfill soil strength.
- Backfill soil density.

The scope of the parametric study is illustrated in Figure 85–Figure 88. Some portions of the parametric study overlap with the originally planned investigations of bearing capacity and compound failure mechanisms, and are included in those sections.

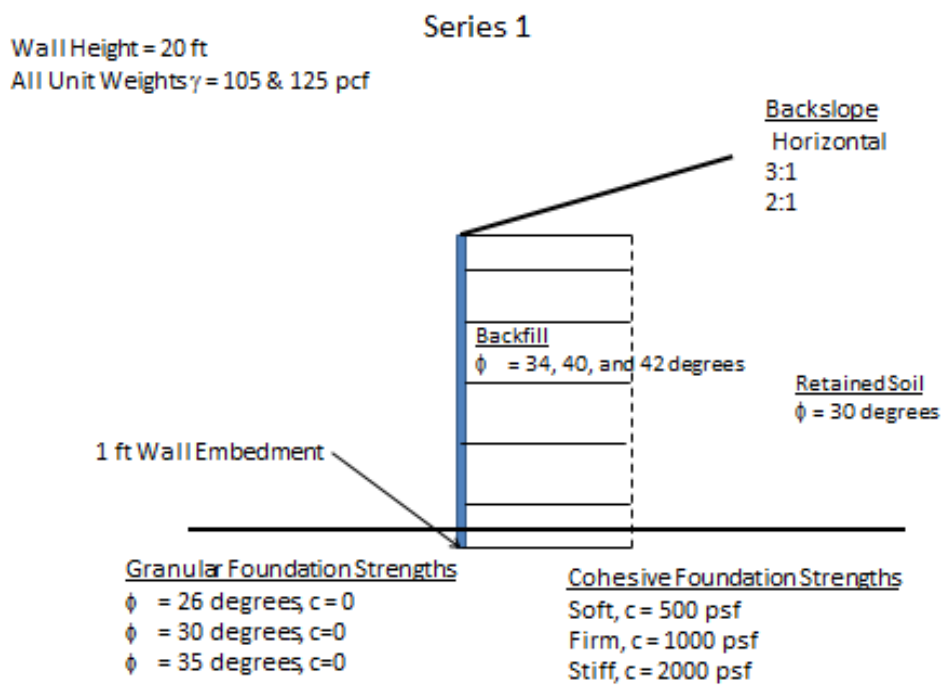


**Figure 85. Effect of Non-Horizontal Back Slope.**

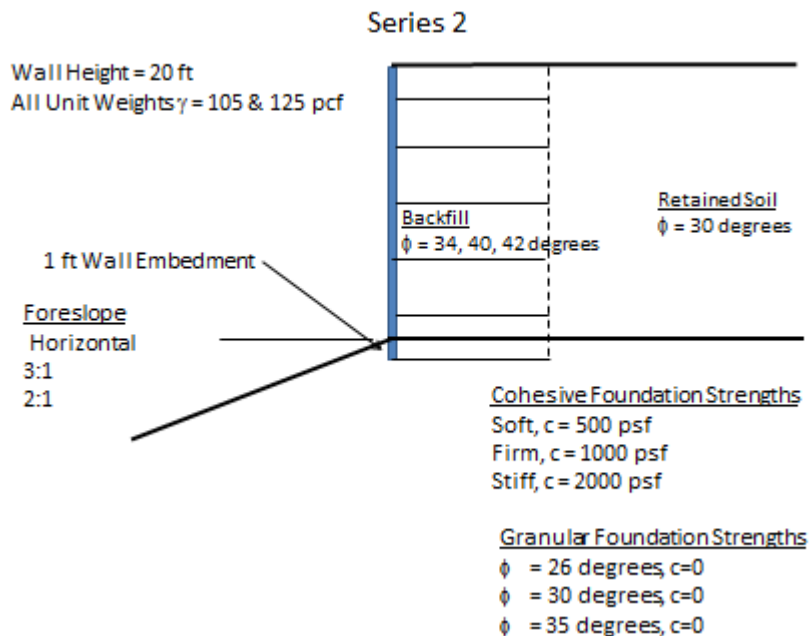


**Figure 86. Effect of Non-Horizontal Fore Slope.**

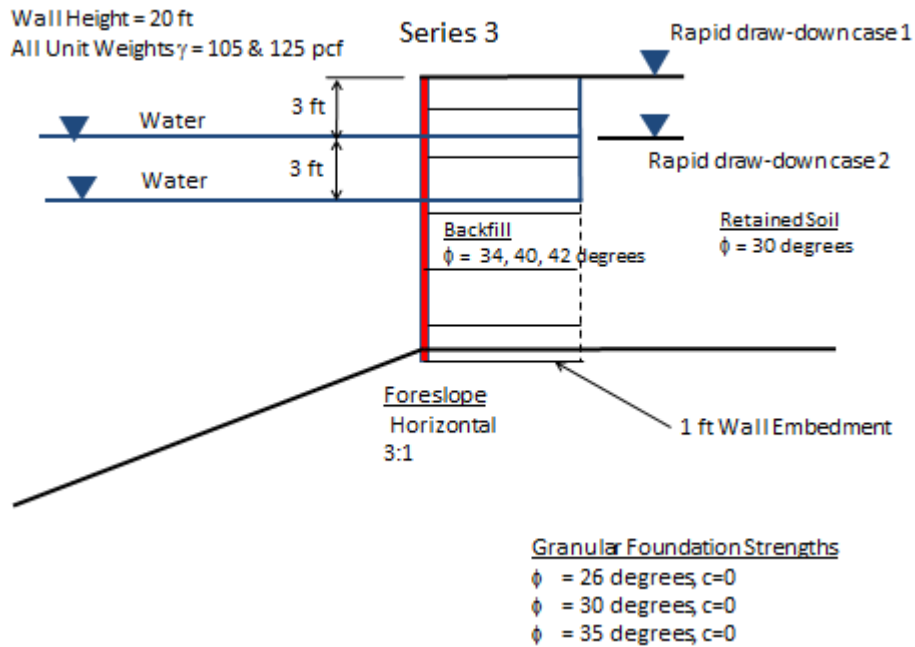


**Figure 87. Effect of Groundwater and Rapid Drawdown.**

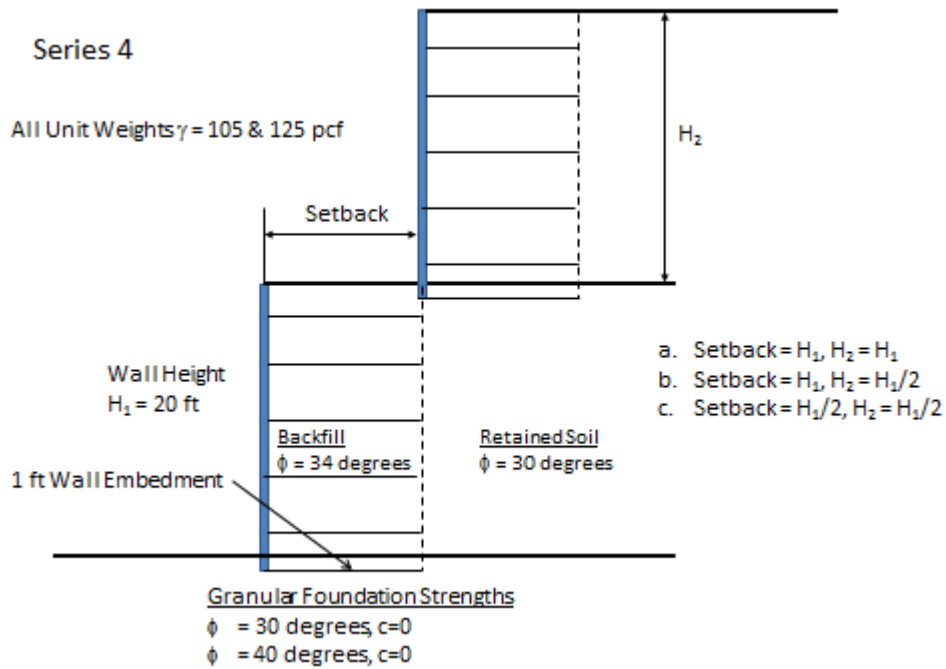


**Figure 88. Stability of Two-Tiered Walls.**

## **BEARING CAPACITY**

The use of Terzaghi's classic bearing capacity theory to check the bearing capacity of an MSE wall has always been in dispute. One of the debates is whether the surcharge term (i.e.,  $qN_q$ ) of the Terzaghi's equation should be completely neglected. For a regular footing, the surcharge term accounts for the effect of surcharge on both sides of the footing. The surcharge is taken as the effective overburden pressure at the base of the footing. MSE walls deviate from the conventional footings in that the surcharge exists only on the backfill side of the footing. The current design of MSE walls usually completely neglects the contribution of surcharge to the bearing capacity. By contrast, it has been argued that the surcharge may still contribute partially to bearing capacity, even though it appears only on one side. In addition, there has been also a trend among researchers such as Leshchinsky et al. (2012) to unify the global stability and bearing capacity analysis. The main objective of this numerical analysis is to assess whether Terzaghi's equation with a surcharge accurately depicts MSE wall behavior.

### **Numerical Analysis**

To fulfill this objective, a numerical analysis was performed to investigate the effect of the one-sided surcharge on bearing capacity. The finite difference software, FLAC, was adopted for this numerical analysis.

#### *Numerical Model*

The geometry, as shown in Figure 89, is 60 ft high and 100 ft wide. The model space was large enough to show the deformation contour accurately and avoid any boundary effect. The footing width was limited to 10 ft and a 1-ft thickness was chosen for the analysis. Each zone was 1 ft in width and height; a total of  $60 \times 100 = 6000$  zones were created. The boundary was fixed in both horizontal and vertical direction at the bottom and only in the horizontal direction on the two sides.



**Figure 89. Model of 10 ft Wide Strip Footing in FLAC.**

### *Material Properties*

Table 22 lists the soil parameters. A single value was given to Young's modulus and Poisson's ratio, since bearing capacity is independent of the elastic properties of the soil. The analyses also considered a single value of unit weight, since the effect of unit weight is relatively minor compared to the effect of the friction angle. The friction angle and cohesion were selected to cover their typical variation ranges. The friction angles were ranged from 30° to 40° and the cohesion was ranged from 0 to 3000 psf. The selection of the friction angle and cohesion covers the shear strength parameters of soil from loose sand to hard clay. The friction angles were paired with cohesion randomly selected from the range. The surcharge was selected to be equivalent to 5, 10, and 15 ft of backfill.

**Table 22. Material Properties for Bearing Capacity Calculation Model.**

| <b>Modulus of Elasticity (psf)</b> | <b>Poisson's Ratio</b> | <b>Shear Modulus (psf)</b> | <b>Bulk Modulus (psf)</b> | <b>Unit Wt. (pcf)</b> | <b><math>\phi</math> (deg)</b> | <b>c (psf)</b> |
|------------------------------------|------------------------|----------------------------|---------------------------|-----------------------|--------------------------------|----------------|
| $7.02 \times 10^6$                 | 0.15                   | $3.048 \times 10^6$        | $3.324 \times 10^6$       | 120                   | 30-40                          | 0-3000         |

### *Model Calibration*

The model was created using the Mohr-Coulomb soil model for the soil and an elastic model for the footing. This model made footing rigid, which is also the assumption of Terzaghi's bearing capacity theory. The model was calibrated by simulating a strip footing situation and then obtained ultimate bearing capacity was compared with the Terzaghi's bearing capacity. The model used for calibration is a 10-ft-wide strip footing built on soil with  $\phi=30^\circ$  and  $c=1000$  psf. The unit weight of the soil is 120 pcf. The surcharge of 600 psf, which is equivalent to 5 ft of fill, was applied on both sides of the footing.

The model was first solved for initial equilibrium under gravity force and then was loaded incrementally until failure occurred. The deformation at the bottom of the footing was recorded for each load increment. The shear zone was detected by plotting the displacement vectors (Figure 90). The maximum curvature point was identified and corresponding pressure is the bearing capacity as shown in Figure 91.

The displacement corresponding to each load increment was recorded and plotted in Figure 91. The failure load was found to be approximately 55,000 psf from the load-displacement curve. The bearing capacity was also calculated using the classic Terzaghi's bearing capacity theory. Bearing capacity factors,  $N_c=30.1$ ,  $N_q=18.4$ , and  $N_\gamma=22.4$ , were obtained from AASHTO Bridge Design Specification (AASHTO 2007a).  $N_c$ ,  $N_q$ , and  $N_\gamma$  are found to be 30.1, 18.4, and 22.4, respectively.

$$\begin{aligned} q_{ult} &= cN_c + qN_q + 0.5\gamma BN_\gamma \\ &= 1000 \times 30.1 + 5 \times 120 \times 18.4 + 0.5 \times 120 \times 10 \times 22.4 \\ &= 54,620 \text{ psf} \end{aligned}$$

It appears that the bearing capacity obtained from numerical modeling is consistent with that of Terzaghi's theory. Thus, the numerical model is considered adequate for further analysis.

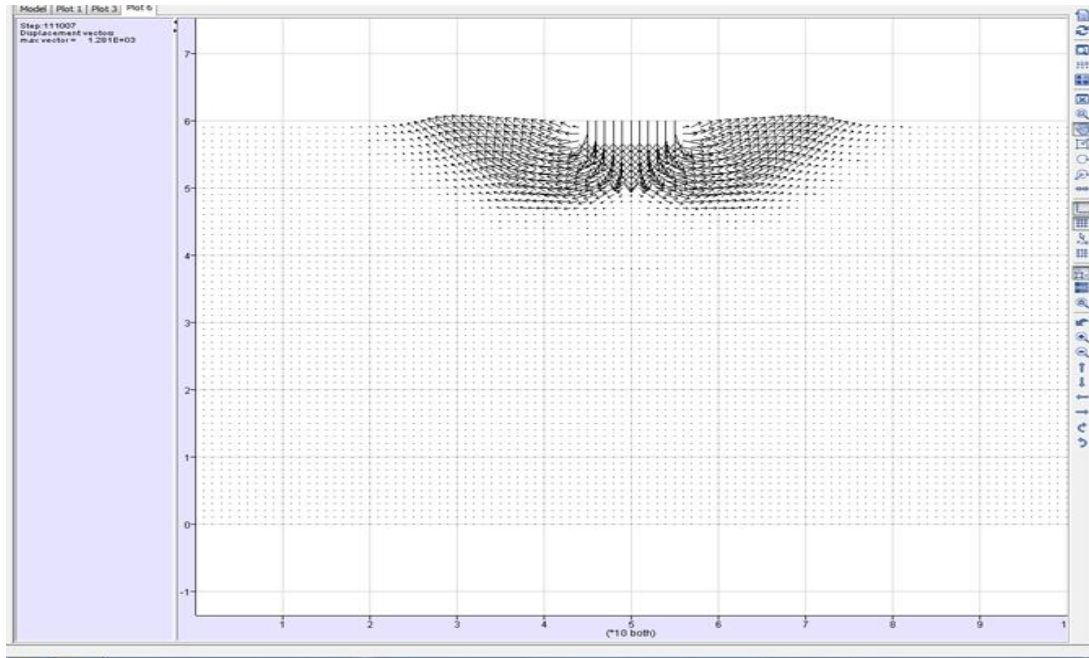


**Figure 90. Displacement Vectors at Failure in FLAC Model.**

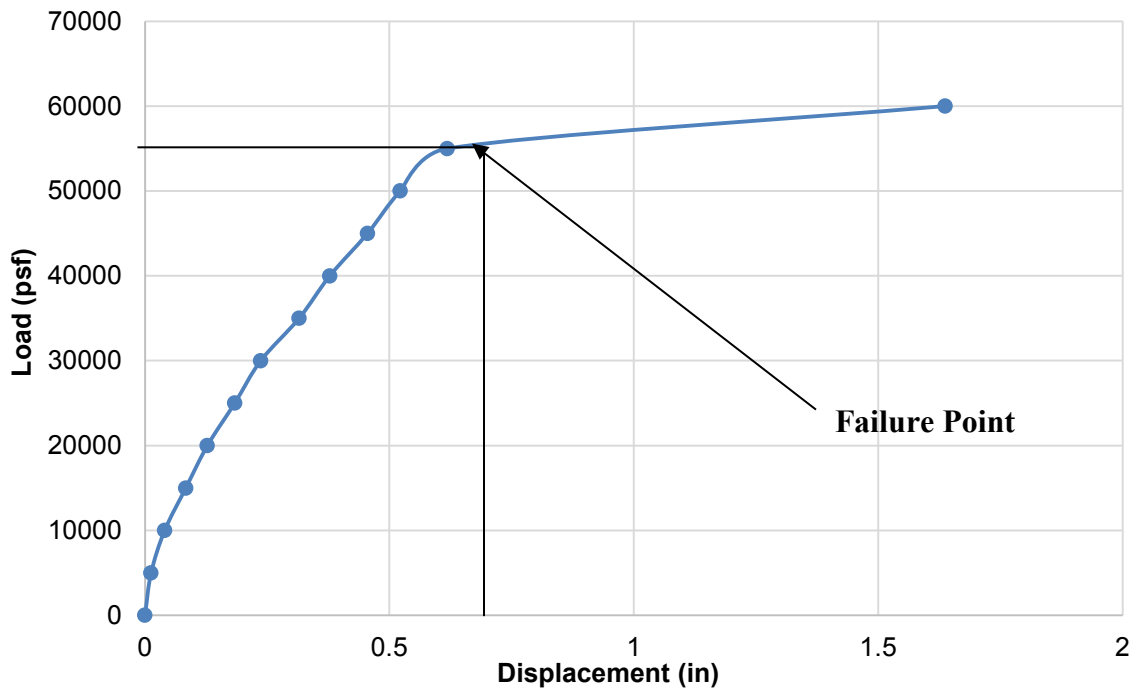


**Figure 91. Load vs. Displacement from FLAC Model ( $\phi = 30^\circ$ ,  $c = 1000$  psf, 600 psf Surcharge on Both Sides).**

## Analysis

After calibration of the model, the bearing capacity problem was modeled by loading the foundation soil with surcharge from only one side (see Figure 92). This simulation simplifies the problem and allows assessment whether one side surcharge can contribute to bearing capacity. Each term of the Terzaghi's equation was calculated separately and the ultimate bearing capacity was compared with the FLAC results. The bearing capacity from FLAC analysis was attained by plotting load vs. settlement curve. A typical load vs. displacement curve is shown in Figure 93. The failure is defined as the point of maximum curvature of the curve indicated in Figure 93.

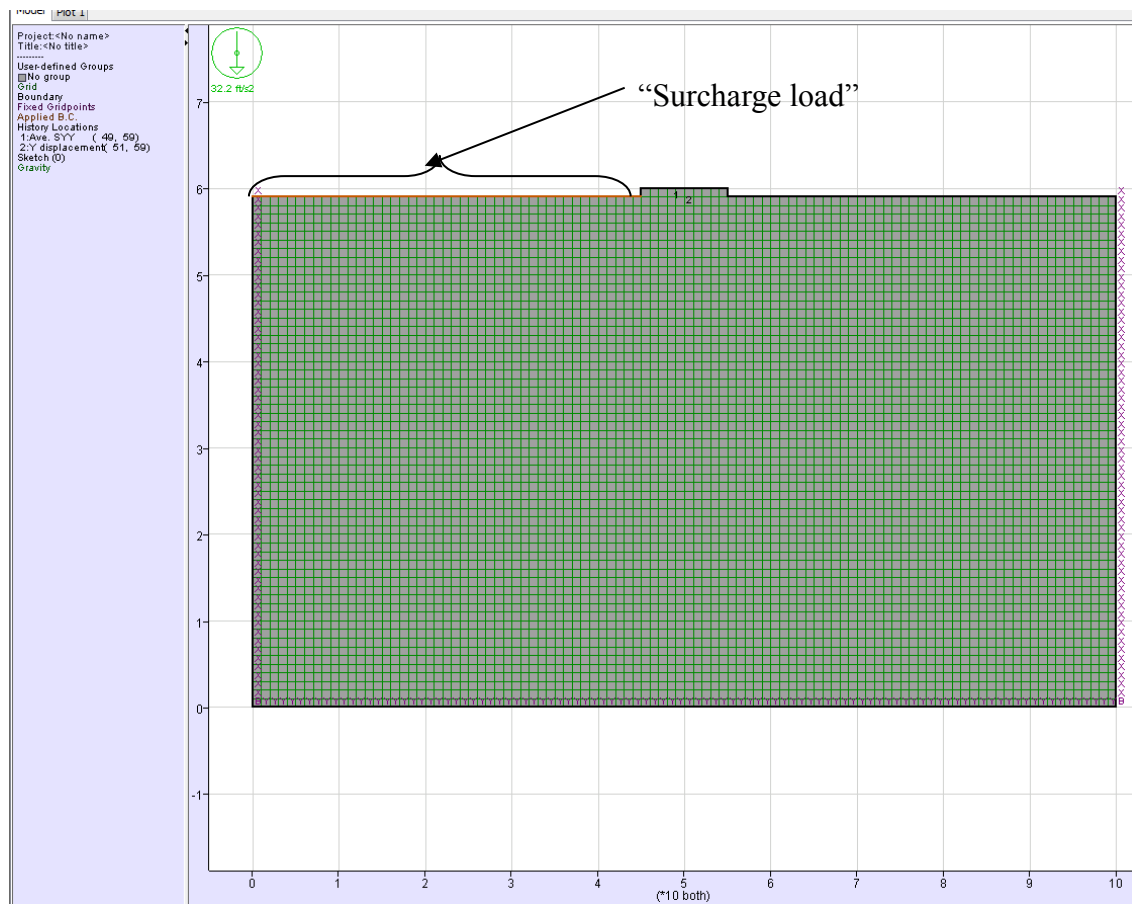


**Figure 92. Numerical Model in FLAC Simulating the Bearing Capacity of MSE Wall (Surcharge Load on One Side Only).**



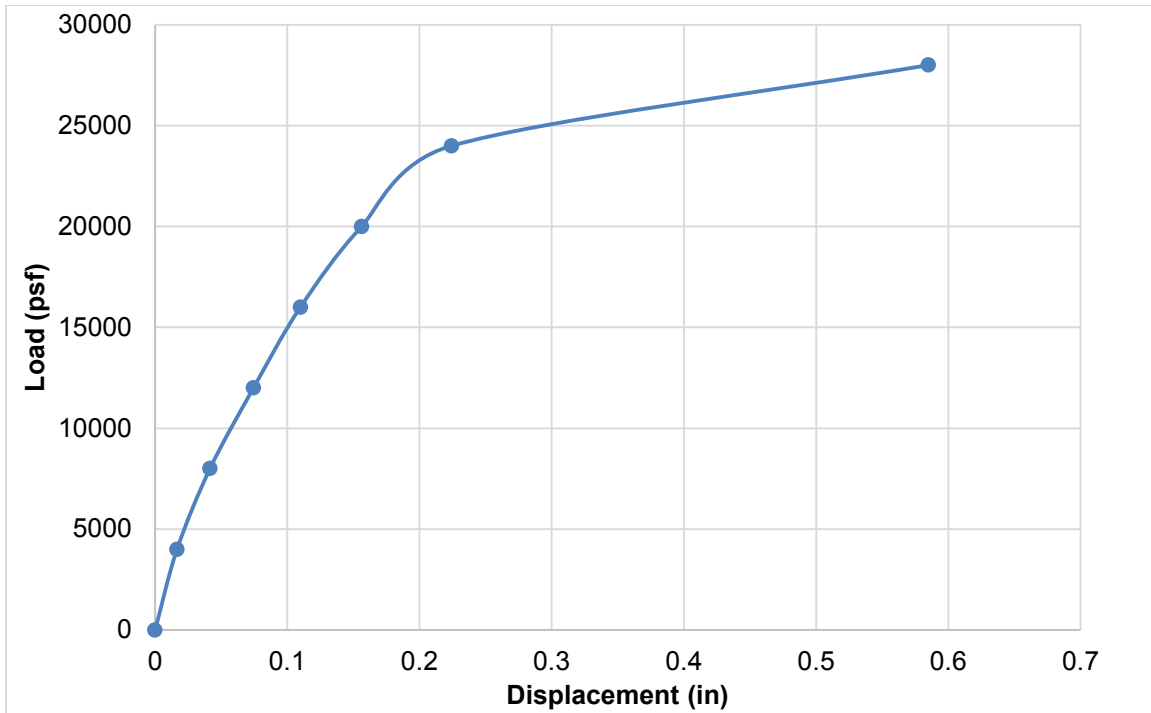


**Figure 93. Typical Load vs. Displacement Curve for Footing Loaded under Uniform Pressure and Surcharged from One Side Only ( $\phi = 35^\circ$ ,  $c = 0$ ,  $\gamma = 120$  pcf, Cohesion = 0, Surcharge Height = 15 ft).**

## Results and Discussion

The ultimate bearing capacities for all the soil properties mentioned above from FLAC analysis and calculated from Terzaghi's theory are tabulated below in Table 23. For the ease of comparison, the bearing capacity obtained from the FLAC analysis was plotted against the bearing capacity calculated from Terzaghi's equation excluding surcharge term in Figure 94. The best fitting line is sloped at  $45^\circ$  and passes through origin. These two facts indicate that the ultimate bearing capacity matched reasonably well with the calculation excluding the surcharge term (i.e.,  $q_u = cN_c + 0.5\gamma BN_\gamma$ ). This conclusion applies to all the soil properties and surcharge combination.

**Table 23. Summary of FLAC Analysis and Manual Calculation.**

| No. | H (ft) | $\phi$ (deg) | c (psf) | $cN_c$ (psf) | $qN_q$ (psf) | $0.5B\gamma N_\gamma$ (psf) | $q_{ult} - qN_q$ (psf) | $q_{ult}$ (FLAC) (psf) |
|-----|--------|--------------|---------|--------------|--------------|-----------------------------|------------------------|------------------------|
| 1   | 5      | 30           | 0       | 0            | 11,040       | 13,440                      | 13,440                 | 12,000                 |
| 2   | 5      | 30           | 1000    | 30,140       | 11,040       | 13,440                      | 43,580                 | 48,000                 |
| 3   | 5      | 30           | 3000    | 90,420       | 11,040       | 13,440                      | 103,860                | 110,000                |
| 4   | 5      | 40           | 1500    | 112,965      | 38,520       | 65,646                      | 178,611                | 140,000                |
| 5   | 5      | 20           | 1000    | 14,830       | 3840         | 3234                        | 18,064                 | 20,000                 |
| 6   | 5      | 20           | 2000    | 29,660       | 3840         | 3234                        | 32,894                 | 36,000                 |
| 7   | 5      | 20           | 3000    | 44,490       | 3840         | 3234                        | 47,724                 | 52,000                 |
| 8   | 10     | 30           | 1000    | 30,140       | 22,080       | 13,440                      | 43,580                 | 45,000                 |
| 9   | 10     | 30           | 3000    | 90,420       | 22,080       | 13,440                      | 103,860                | 110,000                |
| 10  | 10     | 40           | 1500    | 112,965      | 77,040       | 65,646                      | 178,611                | 140,000                |
| 11  | 10     | 20           | 1000    | 14,830       | 7680         | 3234                        | 18,064                 | 20,000                 |
| 12  | 10     | 20           | 2000    | 29,660       | 7680         | 3234                        | 32,894                 | 37,000                 |
| 13  | 10     | 35           | 1500    | 69,180       | 39,960       | 28,818                      | 97,998                 | 104,000                |
| 14  | 10     | 35           | 1000    | 46,120       | 39,960       | 28,818                      | 74,938                 | 80,000                 |
| 15  | 10     | 35           | 2000    | 92,240       | 39,960       | 28,818                      | 121,058                | 120,000                |
| 16  | 10     | 35           | 3000    | 138,360      | 39,960       | 28,818                      | 167,178                | 170,000                |
| 17  | 15     | 40           | 500     | 37,655       | 115,560      | 65,646                      | 103,301                | 95,000                 |
| 18  | 15     | 35           | 500     | 23,060       | 59,940       | 28,818                      | 51,878                 | 55,000                 |
| 19  | 15     | 30           | 500     | 15,070       | 33,120       | 13,440                      | 28,510                 | 32,000                 |
| 20  | 15     | 20           | 0       | 0            | 11,520       | 3234                        | 3234                   | 2500                   |
| 21  | 15     | 20           | 500     | 7415         | 11,520       | 3234                        | 10,649                 | 12,000                 |
| 22  | 15     | 35           | 0       | 0            | 59,940       | 28,818                      | 28,818                 | 28,000                 |
| 23  | 15     | 40           | 0       | 0            | 115,560      | 65,646                      | 65,646                 | 54,000                 |

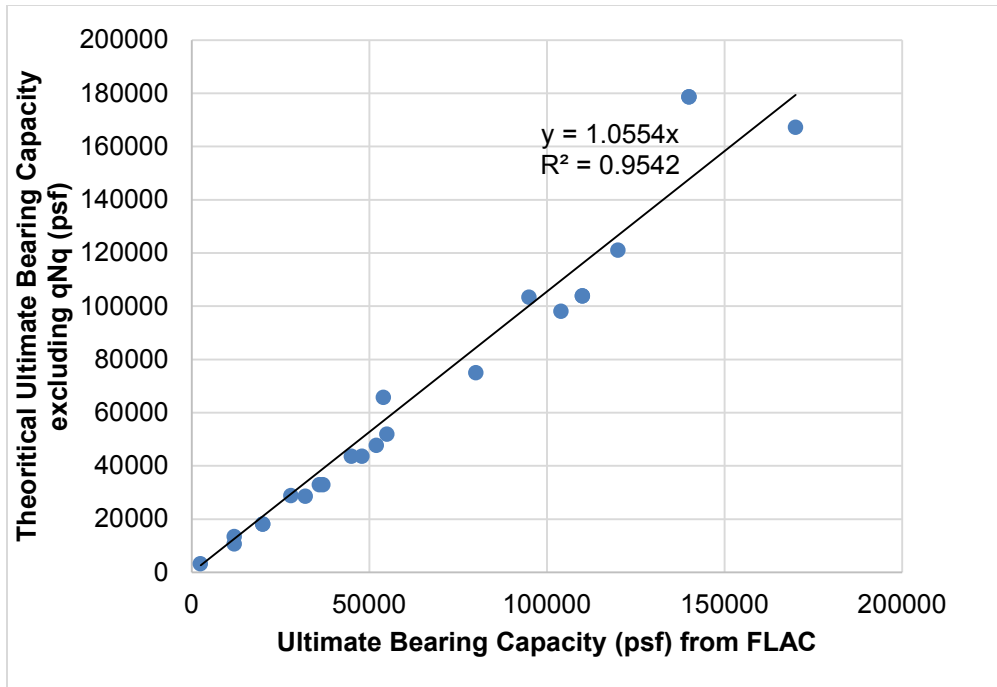


**Figure 94. Comparison between FLAC Results and Terzaghi's Equation Excluding Surcharge Term.**

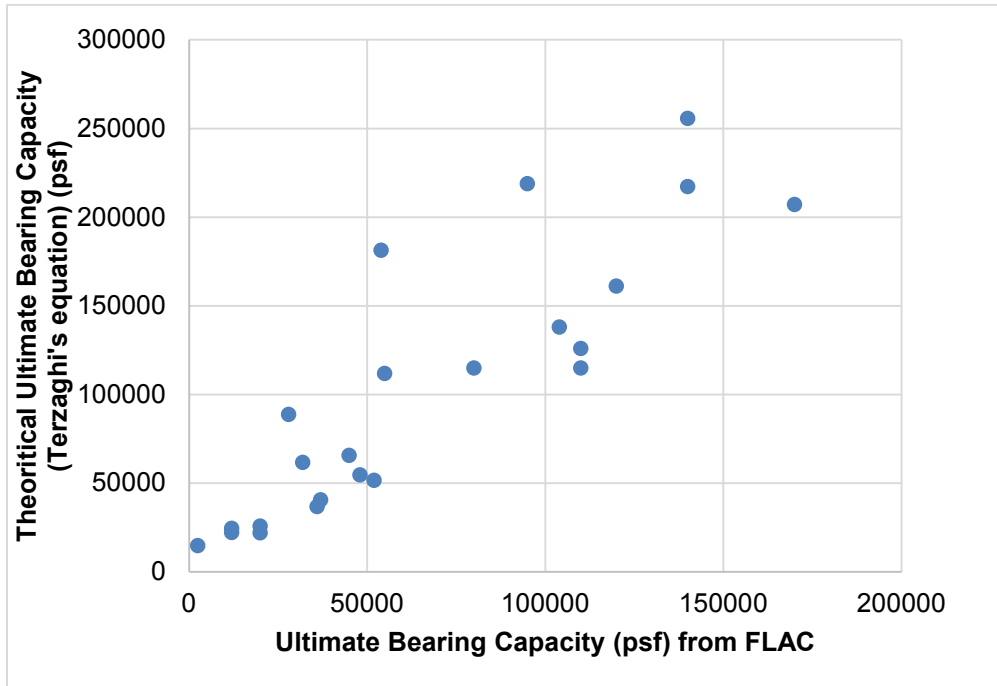


**Figure 95. Comparison between  $q_{ult}$  (FLAC) vs. Terzaghi's Bearing Capacity Including Surcharge Term.**

## Conclusion

It can be concluded that the effect of surcharge on one side of the foundation has a negligible impact on increasing its ultimate bearing capacity. Thus, the surcharge term should not be used for calculating the bearing capacity of MSE walls. The conclusion was drawn based on the FLAC analysis neglecting the lateral earth pressure effect of the retained soil. The lateral earth pressure results in the eccentricity on the footing. AASHTO specifications should be used to consider the eccentricity induced by the lateral earth pressure from retained soil.

## GLOBAL STABILITY

Critics of the use of a bearing capacity analysis to evaluate MSE wall stability maintain that the actual failure mechanism for MSE walls is a global stability failure that is not well represented by a bearing capacity failure mechanism (Leshchinsky et al. 2012). This section assesses whether a classical bearing capacity can provide meaningful inputs for MSE wall design.

### Material Properties Used for Backfill and Foundation Soil

To compute FOS for each case mentioned using the FLAC program, certain material properties are assumed. The friction angles of cohesionless backfill and foundation materials are presented in Table 24. The undrained shear strengths of cohesive foundation materials are tabulated in Table 25, and properties for backfill material are the same for both foundation and backfill materials.

**Table 24. Material Properties for Frictional Backfill and Frictional Foundation Material.**

| Type       | Elastic Modulus* (psf) | Bulk Modulus (psf) | Shear Modulus (psf) | $\nu$ (Poisson's Ratio) | $\phi$ |
|------------|------------------------|--------------------|---------------------|-------------------------|--------|
| Foundation | 2.116 E6               | 3.643 E6           | 0.364 E6            | 0.4516                  | 26     |
|            | 2.116 E6               | 3.643 E6           | 0.364 E6            | 0.4516                  | 30     |
|            | 2.116 E6               | 7.287 E6           | 0.728 E6            | 0.4516                  | 35     |
| Backfill   | 4.232 E6               | 7.287 E6           | 0.728 E6            | 0.4516                  | 34     |
|            |                        |                    |                     |                         | 40     |
|            |                        |                    |                     |                         | 42     |

\* Elastic modulus for sand is taken as  $1000 \cdot P_{atm}$  where  $P_{atm} = 2116.216$  psf (Kulhawy and Mayne 1990)

**Table 25. Material Properties for Cohesive Foundation Material.**

| Type  | Elastic modulus*<br>(psf)  | Bulk modulus<br>(psf) | Shear modulus<br>(psf) | $\nu$<br>(Poisson's ratio) | $c_u$<br>(psf) |
|-------|----------------------------|-----------------------|------------------------|----------------------------|----------------|
| Soft  | $40 * P_{atm} = 84.648 E3$ | 141.081 E3            | 30.231 E3              | 0.4                        | 500            |
| Firm  | $80 * P_{atm}$             | 282.162 E3            | 60.463 E3              |                            | 1000           |
| Stiff | $200 * P_{atm}$            | 705.405 E3            | 151.158 E3             |                            | 2000           |

\* Where  $P_{atm} = 2116.216$  psf (Kulhawy and Mayne 1990)

### Reinforcement Property

The modulus of elasticity of the reinforcement steel was taken as  $30 \times 10^6$  psi and the yield strength was 65,000 psi (AISC 2011). A strip width of 2 inches and thickness of 0.12 inches was assigned for the reinforcement. The  $f^*$  of 2.05 was used according to Rathje et al. 2006. The strips were modeled as metal strips with vertical spacing of 1.5 ft and horizontal spacing of 3 ft.

### Concrete Panel Property

The modulus of elasticity of concrete was estimated from the equation below (Eq. 17) (ACI 318-11):

$$E_c = 57000 \sqrt{f'_c} \quad (\text{Eq. 17})$$

The bulk and shear modulus of the blocks were calculated from Eqs. 18–19.

$$K = \frac{E}{3(1-2\nu)} \quad (\text{Eq. 18})$$

$$G = \frac{E}{2(1+\nu)} \quad (\text{Eq. 19})$$

where

$f'_c$ =compressive strength.

$\nu$ =Poisson's ratio.

Due to the interlocking between panels, the connections between panels were simulated with plastic hinges, which can yield once the stress is beyond the shear strength of concrete and allow vertical separation between the panels. In summary, the hinges provide shear constraint up to the shear strength of the concrete and allow free rotation and vertical separation.

The dimension for a wall panel is used as per TxDOT guidelines and  $0.7H$  for the length of strips. The 20-ft-high MSE wall is built in stages according to individual panel height. The panel height used is 5 ft and total wall height is 20 ft; therefore, the MSE wall is built in four stages. After each stage of the wall, the equilibrium forces were solved for a self-weight condition.

### Horizontal Back Slope

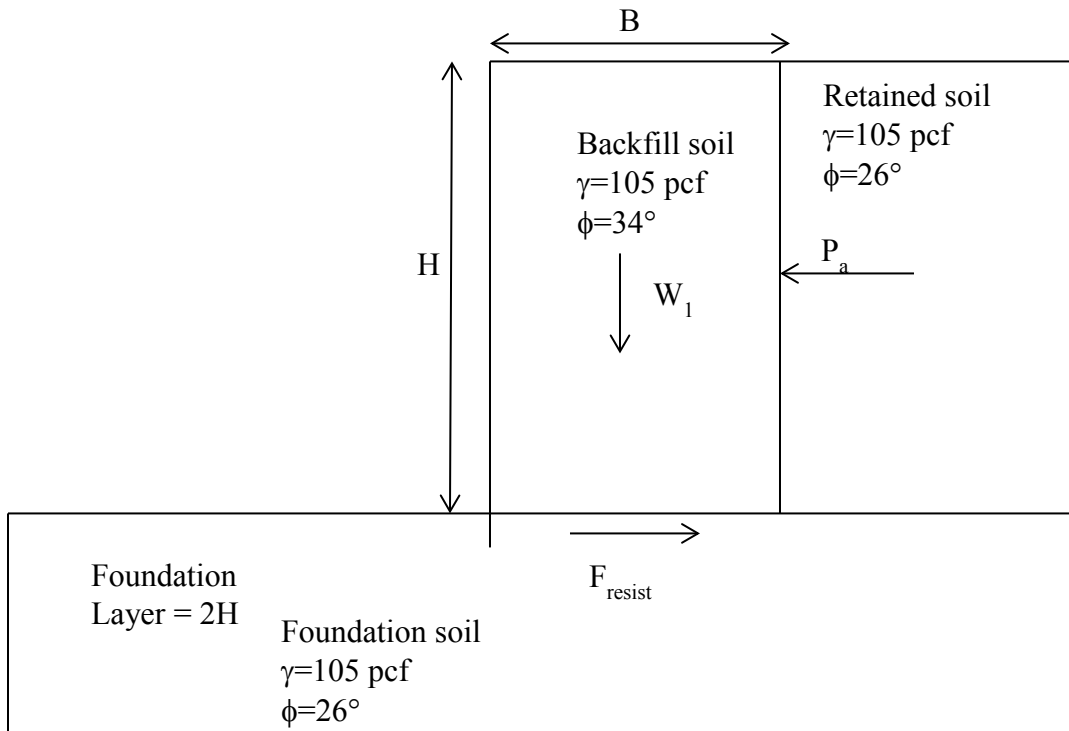


**Figure 96. Dimensions and Properties Used for Series 1 Case 1.**

Table 25 shows the FOSs computed by FLAC for the case of a 20-ft high MSE wall with a reinforcement length of 14 ft and a horizontal back slope as shown in Figure 97. The corresponding plots of maximum shear strain rate for these cases are shown in Figure 98–Figure 102. The foundation soil used in these cases is purely frictional material with no cohesion. The bottom row of Table 25 presents the factors of safety from a classical bearing capacity analysis for the following cases presented. The backfill friction angle and unit weight has no influence on the outcome of the classical bearing analysis. The detailed figures for each case for this series are shown in Appendix C. In this appendix figures for all series for sands and clays are presented.

Figure 98–Figure 102 represent a typical failure mechanism for sands used for foundation layer and for retaining layers.

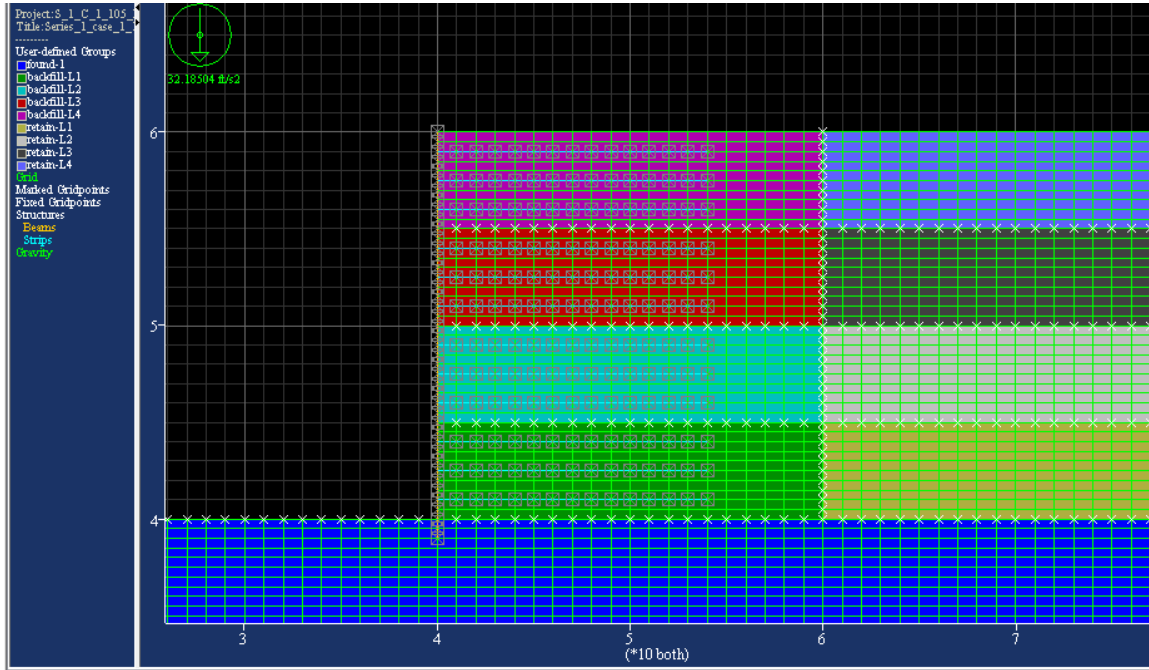


**Figure 97. Concrete Panels and Strips Length Used for Series 1 Case 1.**

The specific equations used in the bearing capacity analysis were as follows:

$$Q = B' [cN_c i_c + B' \gamma N_\gamma i_\gamma g_\gamma / 2] \quad (\text{Eq. 20})$$

where

c = cohesion

$$N_c = (N_q - 1) \cot \phi$$

$$N_\gamma = (N_q - 1) \tan ( 1.4 \phi )$$

$$N_q = \exp ( \pi \tan \phi ) \tan^2 ( \pi/4 + \phi/2 )$$

$$i_c = (1 - 2 \alpha / \pi )^2$$

$$i_\gamma = (1 - \alpha / \phi )^2$$

$$g_\gamma = (1 - \tan \delta)^2.$$

$\phi$  = friction angle.

$$B' = B - 2e.$$

B = base width of MSE wall.

$e$  = eccentricity of load on foundation.

$\delta$  = ground inclination on toe-side of wall.

$\alpha$  = angle of foundation load from vertical.

The eccentricity,  $e$ , and angle of foundation load  $\alpha$  are determined by resolving earth pressure, soil self-weight, and surcharge loads acting on the foundation. Apart from bearing capacity analysis and FOS for bearing capacity, sliding block failure, and FOS of it is also calculated using following equations:

$$P_a = \frac{1}{2} K_a \times \gamma_{ret} \times H_a^2 \quad (\text{Eq. 21})$$

where

$K_a$  = coefficient of active earth pressure.

$\gamma_{ret}$  = unit weight for retained soil.

$H_a$  = Equivalent Height of retained soil exerting active pressure on the wall.

$$F_{resist} = N \tan \phi_{found} \quad (\text{Eq. 22})$$

where

$N$  = total normal acting on the base of wall due to self-weight.

$\phi_{found}$  = friction angle for foundation soil.

$$FOS_{bearing} = \frac{Q}{N} \quad (\text{Eq. 23})$$

$$FOS_{sliding} = \frac{F_{resist}}{P_a} \quad (\text{Eq. 24})$$



**Table 26. Series 1 Case 1: Horizontal Back Slope with Frictional Foundation Soil.**

| Backfill Friction Angle<br>(degrees) | Factor of Safety                 |      |                                  |      |                                  |      |
|--------------------------------------|----------------------------------|------|----------------------------------|------|----------------------------------|------|
|                                      | $\phi_{\text{found}} = 26^\circ$ |      | $\phi_{\text{found}} = 30^\circ$ |      | $\phi_{\text{found}} = 35^\circ$ |      |
|                                      | $\gamma$ - backfill<br>(pcf)     |      | $\gamma$ - backfill<br>(pcf)     |      | $\gamma$ - backfill<br>(pcf)     |      |
|                                      | 105                              | 125  | 105                              | 125  | 105                              | 125  |
| $\phi = 34$                          | 1.01                             | 1.02 | 1.18                             | 1.19 | 1.42                             | 1.36 |
| $\phi = 40$                          | 1.01                             | 1.02 | 1.18                             | 1.19 | 1.42                             | 1.36 |
| $\phi = 42$                          | 1.01                             | 1.02 | 1.18                             | 1.19 | 1.42                             | 1.36 |
| Bearing Capacity Analysis*           | 0.27                             | 0.27 | 1.11                             | 1.11 | 4.49                             | 4.49 |
| Sliding Stability*                   | 1.81                             | 1.81 | 2.55                             | 2.55 | 3.90                             | 3.90 |

\* The factor of safety for these conditions was calculated according to AASHTO 2002.

The analyses indicate the following:

- The dominant failure mechanism involves a wedge behind the reinforced portion of the wall, with a relatively shallow combined bearing-sliding failure at the base of the wall.
- The active wedge behind the wall tends to move downward under the influence of gravity and the wall is pushed horizontally away from active wedge. Therefore, it shows a vertical shear strain line behind the wall, which proves the failure mechanism. There was no interface material used in the simulation between wall and retaining soil.
- The backfill friction angle has negligible influence on global stability.
- At the base of the MSE wall near the interface of the wall face and foundation layer, a strain singularity occurs due to the sharp corner of the wall face. Localized strain singularities commonly occur at such locations and typically have minimal impact on overall equilibrium, particularly for elastoplastic materials where stress levels are limited by the yield strength of the material. For the purpose of computing the FOS against wall failure, the strain concentrations were expected to have minimal impact.
- Increasing or decreasing the unit weight of the backfill in conjunction with the retained soil has no influence on the safety factor. A denser retained soil will increase the active thrust; however, a denser backfill will increase the shearing resistance in similar proportion. The worst-case scenario, a retained soil unit weight  $\gamma = 125$  pcf in conjunction with a backfill unit weight  $\gamma = 105$  pcf, was considered and the results from FLAC simulation for this case were slightly different as the results for a unit weight of  $\gamma = 125$  pcf for both soils. Figure

98 shows the result for this case. The failure mechanism is slightly different in terms of sliding mechanism without an active wedge at the back due to lower unit weight of backfill, which resulted in less force required to slide.

- For weak foundations ( $\phi_{\text{found}} = 26^\circ$  and  $30^\circ$ ), the bearing capacity analysis significantly underestimates the actual factor of safety. This is a likely consequence of the conservative assumption that the full overburden stress due to the backfill acts on the foundation. In actuality, the shearing resistance in the backfill and retained soil will likely reduce the pressure acting on the foundation.
- For strong foundations ( $\phi_{\text{found}} = 35^\circ$ ) the FOS against bearing failure is well above the FOS against a wall failure. This is likely due to the fact that when the foundation is sufficiently strong, the failure mechanism switches to a different mode.
- The FOS against sliding consistently overestimates the FOS against failure. This is a likely consequence of the assumption inherent in a sliding analysis that there is no interaction between bearing resistance and sliding resistance at the base of the backfill. This assumption is generally unconservative, especially when dealing with weak foundations.
- The active wedge behind the reinforced zone tends to move downward under the influence of gravity as the wall moves horizontally away from active wedge. Since the backfill is stiffer than the retained soil, significant strain occurs across the retained-backfill boundary. No interface material used in the simulation between wall and retaining soil. The figures show strain rate contours at the failure state, not the working stress state. Accordingly, the strain rate contours do not represent what would be seen in the field where stresses and strains are well below the failure level.

Given the conservatism of bearing capacity analyses for MSE walls on relatively weak foundations, the following alternatives may be considered:

- Use the bearing capacity as a screening tool for determining whether a more sophisticated global stability analysis is needed.
- Apply a semi-empirical correction to the bearing capacity analysis to match FLAC calculations.
- Discontinue the use of the bearing capacity analysis and only perform the global stability analysis.

In the opinion of the research team, the third alternative is too extreme. Although the existing bearing capacity is conservative, it is simple to perform and, at the least, it can be used as a screening tool for determining if more sophisticated analysis is warranted. In cases of high FOSs, it can avoid more costly analyses.

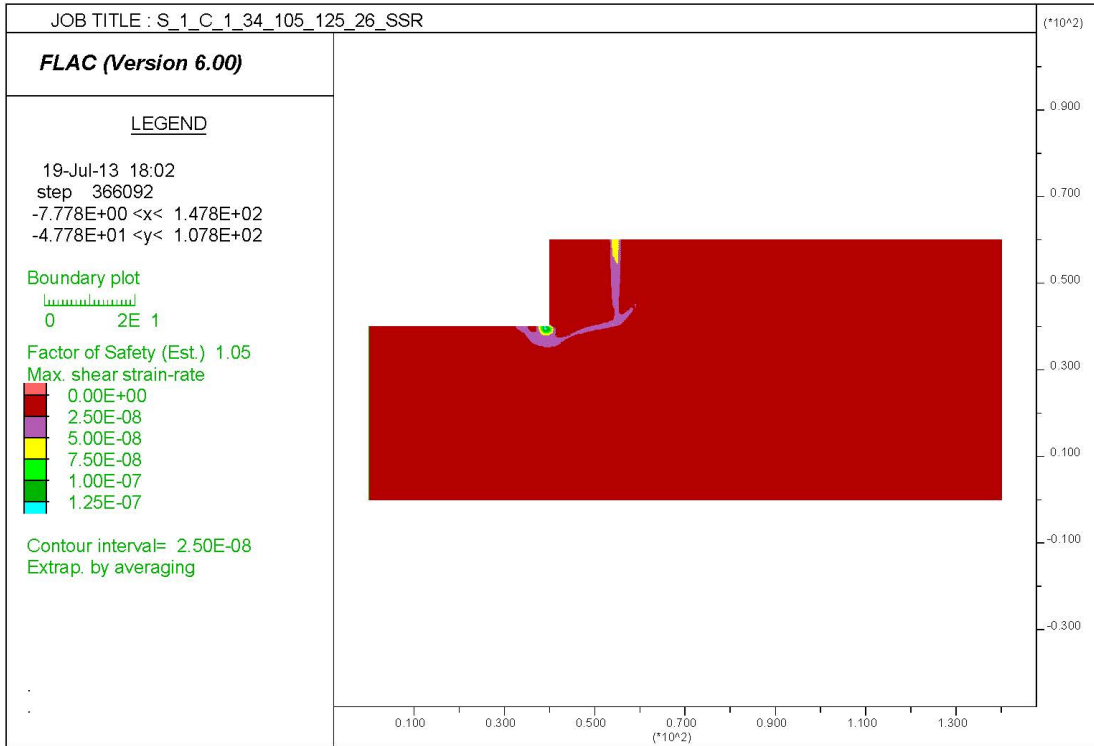


**Figure 98. Series 1 Case 1 Foundation Angle  $\phi=26^\circ$ , Backfill Angle  $\phi=34^\circ$ , and  $\gamma_{back}=105$  pcf  $\gamma_{retain}=125$  pcf Maximum Shear Strain Rate.**

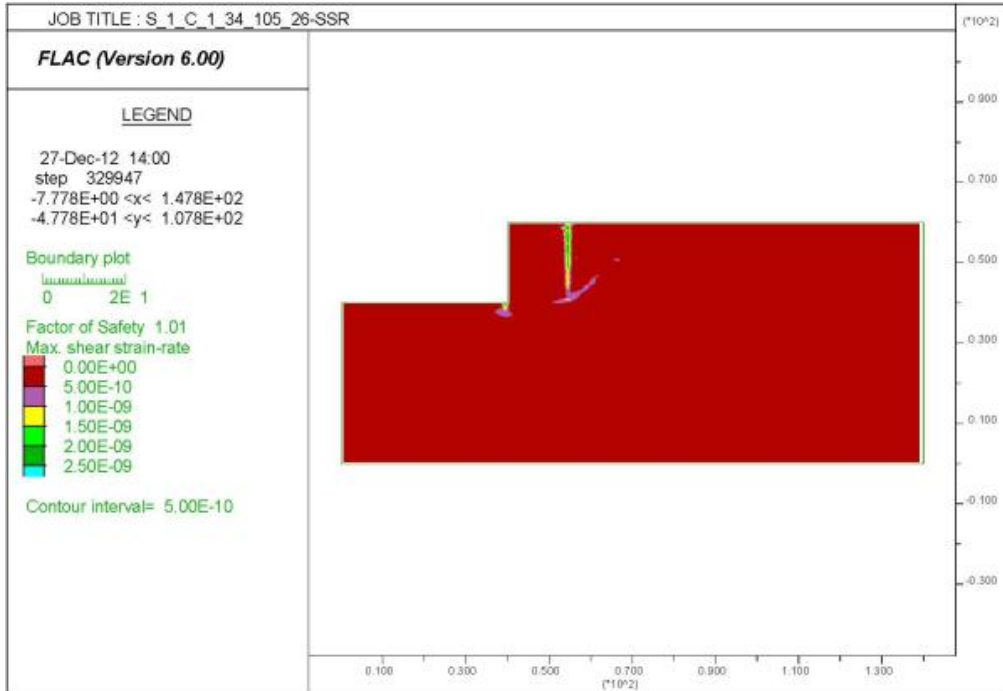


**Figure 99. Series 1 Case 1 Foundation Angle  $\phi=26^\circ$ , Backfill Angle  $\phi=34^\circ$ , and  $\gamma=105$  pcf Maximum Shear Strain Rate.**

The FOS values from FLAC analysis using cohesive soil properties for Series 1 Case 1 are presented in Table 27.  $c_u=500$  psf is considered as soft clays,  $c_u=1000$  psf as firm clays, and  $c_u=2000$  psf as stiff clays.

**Table 27. Series 1 Case 1: Cohesive Foundation Soils.**

| Backfill Friction Angle (degrees) | Factor of Safety          |      |                           |      |                           |      |
|-----------------------------------|---------------------------|------|---------------------------|------|---------------------------|------|
|                                   | $c_u=500$ psf             |      | $c_u=1000$ psf            |      | $c_u=2000$ psf            |      |
|                                   | $\gamma$ - backfill (pcf) |      | $\gamma$ - backfill (pcf) |      | $\gamma$ - backfill (pcf) |      |
|                                   | 105                       | 125  | 105                       | 125  | 105                       | 125  |
| $\phi = 34$                       | 1.03                      | 0.85 | 1.62                      | 1.44 | 2.22                      | 2.09 |
| $\phi = 40$                       | 1.03                      | 0.85 | 1.62                      | 1.44 | 2.22                      | 2.09 |
| $\phi = 42$                       | 1.03                      | 0.85 | 1.62                      | 1.44 | 2.22                      | 2.09 |

Figure 100–Figure 102 show the results for this case. For soft clays the failure is more representative of bearing capacity type failure. The firm and stiff clays show a sliding type failure with stresses more concentrated behind the wall.

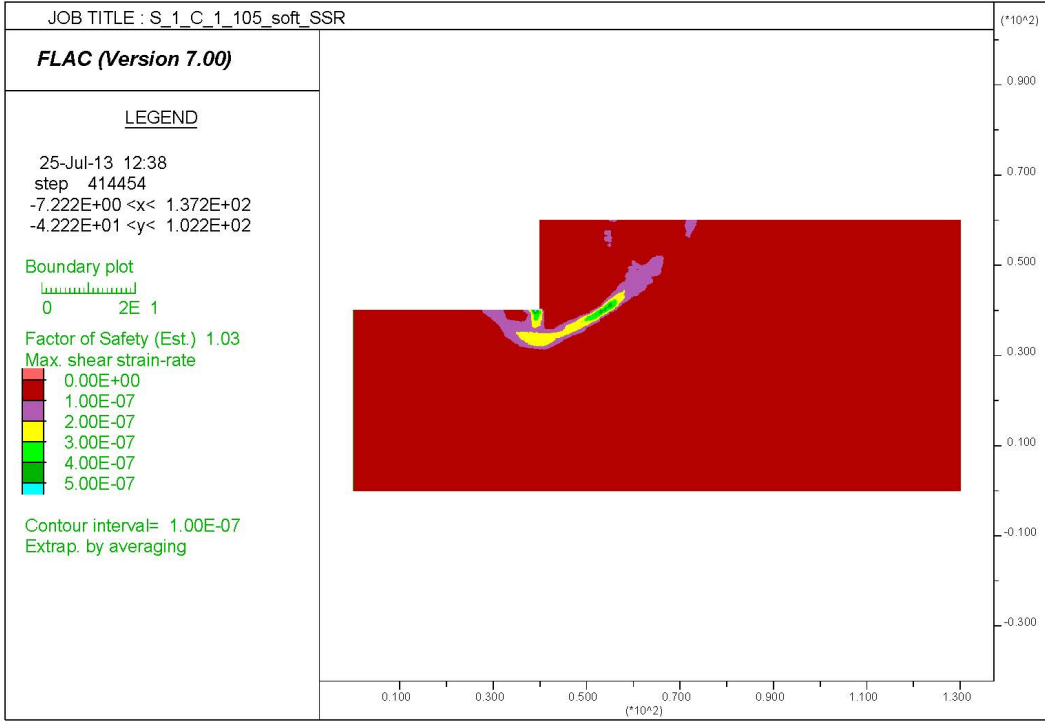


**Figure 100. Series 1 Case 1 Foundation  $c_u=500$  psf, Backfill Angle  $\phi=34^\circ$ , and  $\gamma=105$  pcf Maximum Shear Strain Rate.**

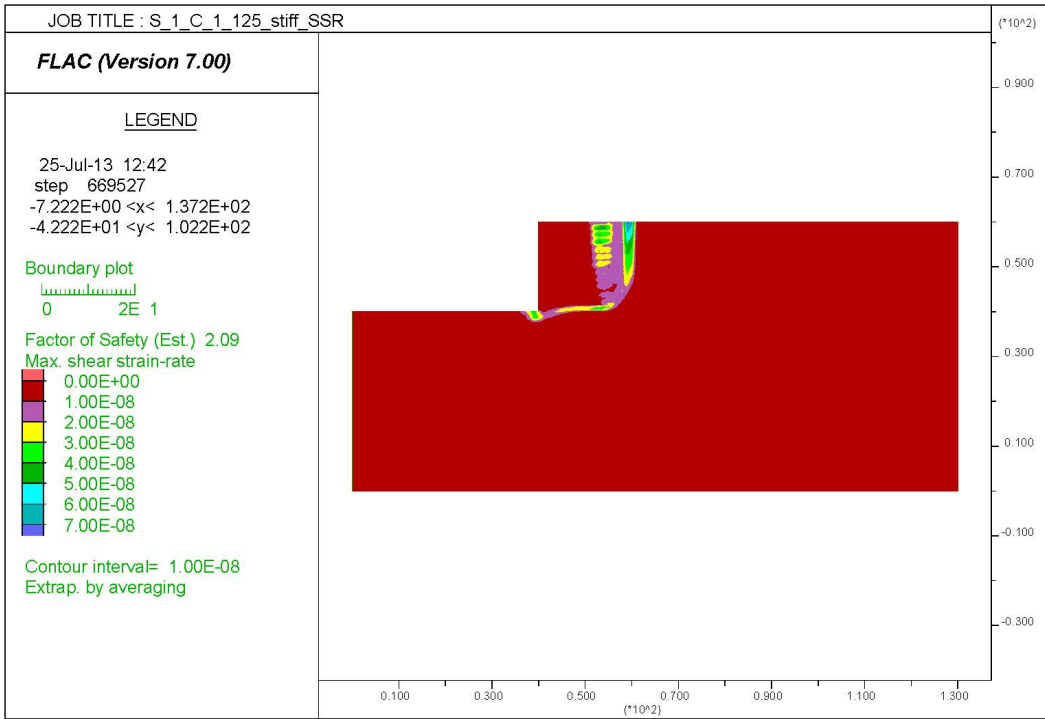


**Figure 101. Series 1 Case 1 Foundation  $c_u=2000$  psf, Backfill Angle  $\phi=34^\circ$ , and  $\gamma=125$  pcf Maximum Shear Strain Rate.**

**Table 28. Factor of Safety Comparison for Series 1 Case 1 with Different Depth.**

| Backfill Friction Angle<br>(degrees) | Factor of Safety          |      |                           |      |  |      |
|--------------------------------------|---------------------------|------|---------------------------|------|--|------|
|                                      | $c_u=2000$ psf (2H)       |      | $c_u=2000$ psf (H)        |      | Percent Different<br>from 2H to H<br>Foundation<br>Depth (%) |      |
|                                      | $\gamma$ – Backfill (pcf) |      | $\gamma$ – Backfill (pcf) |      |  |      |
|                                      | 105                       | 125  | 105                       | 125  | 105  | 125  |
| $\phi = 34$                          | 2.22                      | 2.09 | 1.48                      | 1.37 | 6.22   | 6.22 |
| $\phi = 40$                          | 2.22                      | 2.09 | 1.48                      | 1.37 | 6.22   | 6.22 |
| $\phi = 42$                          | 2.22                      | 2.09 | 1.48                      | 1.37 | 6.22   | 6.22 |

\* It is the difference in FOS when foundation depth is two times the wall height to one time the wall height.

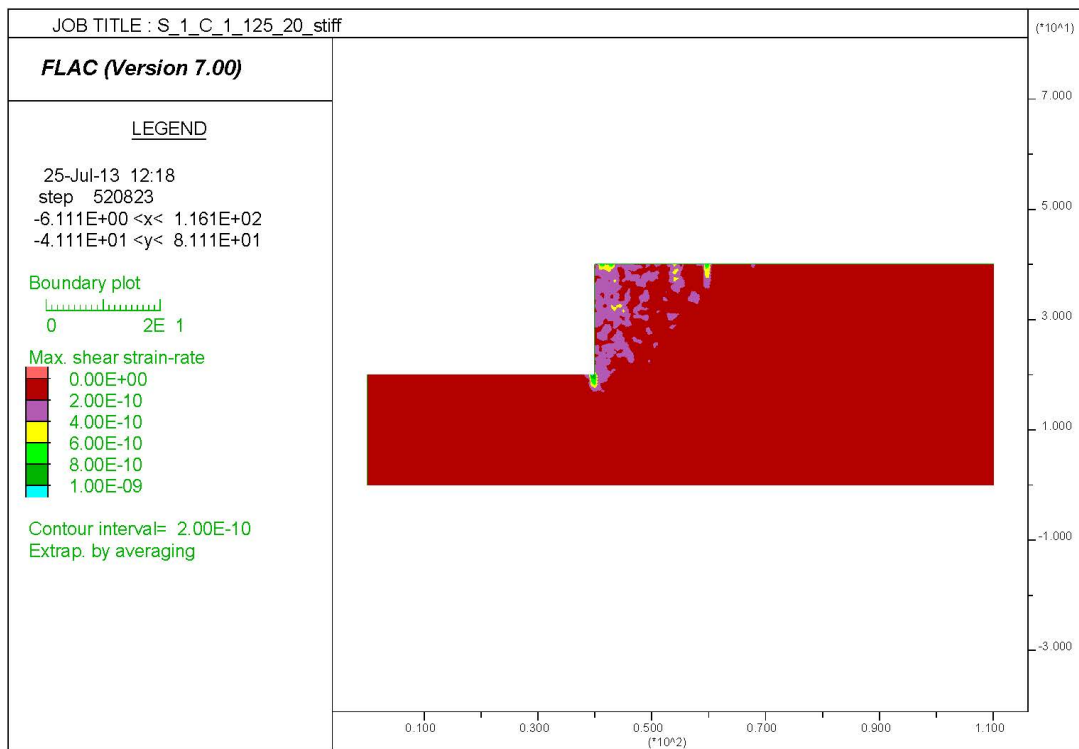


**Figure 102. Series 1 Case 1 Foundation  $c_u=2000$  psf, Backfill Angle  $\phi=34^\circ$ , and  $\gamma=105$  pcf Maximum Shear Strain Rate. Foundation Depth Equals to Wall Height.**

### 3H:1V Back Slope

Table 29 shows the FOSs computed by FLAC for the case of a 20-ft high MSE wall with reinforcement length of 14 ft and a 3H:1V back slope (see Figure 103 below). The corresponding plots of maximum shear strain rate for these cases are shown in the Appendix C. The figures shown below from Figure 104–Figure 108 are with prominent failure surface. The bottom row of Table 29 presents the FOSs from a classical bearing capacity analysis for the cases presented in this section. The backfill friction angle has no influence on the outcome of the classical bearing analysis.

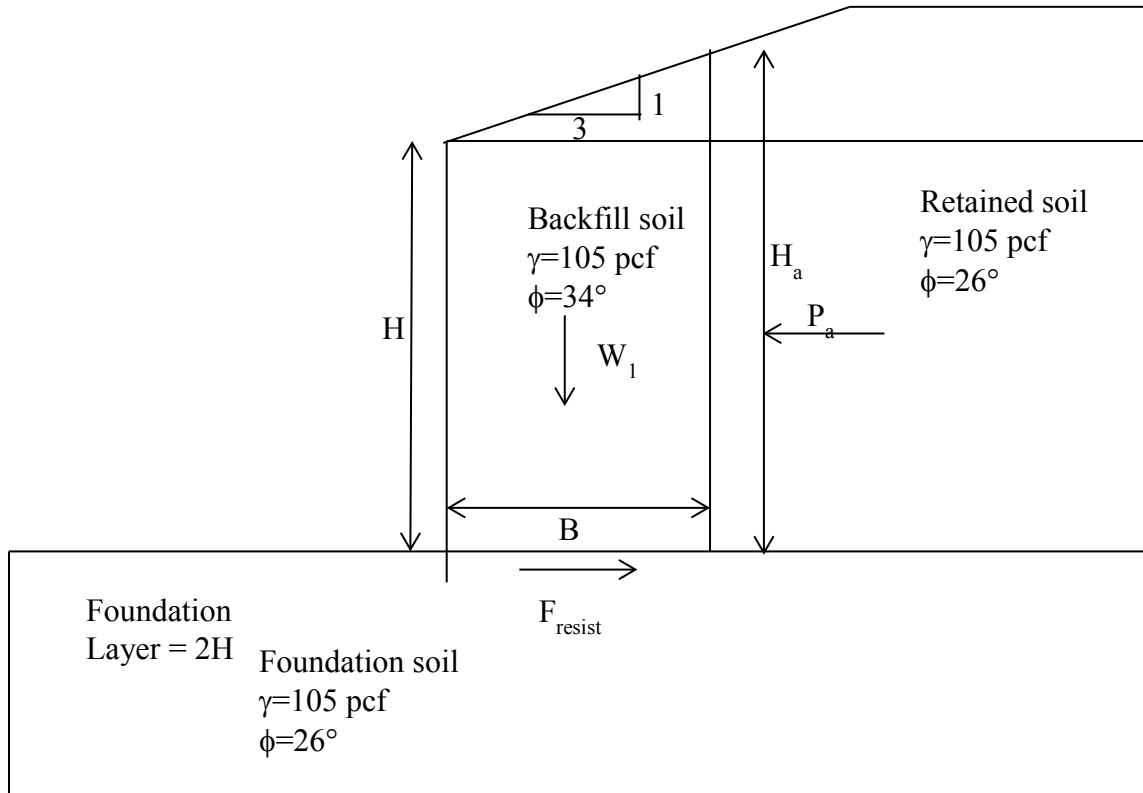


**Figure 103. Dimensions and Properties Used for Series 1 Case 2.**

**Table 29. Series 1 Case 2: Back Slope 3:1 with Frictional Foundation Soil.**

| Backfill Friction Angle<br>(degrees) | Factor of Safety                 |      |                                  |      |                                  |      |
|--------------------------------------|----------------------------------|------|----------------------------------|------|----------------------------------|------|
|                                      | $\phi_{\text{found}} = 26^\circ$ |      | $\phi_{\text{found}} = 30^\circ$ |      | $\phi_{\text{found}} = 35^\circ$ |      |
|                                      | $\gamma$ – Backfill<br>(pcf)     |      | $\gamma$ – Backfill<br>(pcf)     |      | $\gamma$ – Backfill<br>(pcf)     |      |
|                                      | 105                              | 125  | 105                              | 125  | 105                              | 125  |
| $\phi = 34$                          | 0.78                             | 0.78 | 0.90                             | 0.90 | 1.17                             | 1.17 |
| $\phi = 40$                          | 0.78                             | 0.78 | 0.90                             | 0.90 | 1.17                             | 1.17 |

|                           |        |        |      |      |      |      |
|---------------------------|--------|--------|------|------|------|------|
| $\phi = 42$               | 0.78   | 0.78   | 0.90 | 0.90 | 1.17 | 1.17 |
| Bearing Capacity Analysis | 0.0002 | 0.0002 | 0.69 | 0.69 | 3.37 | 3.37 |
| Sliding Analysis          | 0.97   | 0.97   | 2.16 | 2.16 | 3.41 | 3.41 |

For low foundation strengths ( $\phi_{\text{found}}= 26^\circ$  and  $\phi_{\text{found}}= 30^\circ$ ), the classical bearing capacity differs from the finite difference solution significantly maybe because, in the bearing capacity equation the side friction between wall and retained soil is not considered. In the case of  $\phi_{\text{found}}= 26^\circ$ , it is conservative, while it is slightly unconservative in the case of  $\phi_{\text{found}}= 30^\circ$ . For the stronger foundation ( $\phi_{\text{found}}= 35^\circ$ ) the factor of safety against bearing failure exceeds the more accurate finite difference solution by almost two times. As indicated previously, this may be because failure will tend to occur outside the foundation, when the foundation strength is sufficiently high. The failure surface for each case differs slightly. For low unit weight and low foundation friction angles, failure mechanism is mainly a sliding type with a small wedge behind the wall. For higher unit weight and higher friction angle for retained soil, the wedge behind the wall becomes wider with an angle of  $41^\circ$  from horizontal. The angle for wedge of retained soil varies from  $40^\circ$ – $41^\circ$ . The sliding analysis consistently gives a higher safety factor than either the bearing capacity analysis or the finite difference analysis.

These findings again support the notion that, while the bearing capacity analysis is not as reliable as a method that can analyze a global slope/wall failure, it can provide an indicator as to when failure through the foundation can be a problem. Accordingly, at the least it can be used as a preliminary analysis tool for determining when more sophisticated analyses should be used.

**Table 30. Series 1 Case 2: Cohesive Foundation Soils.**

| Backfill Friction Angle<br>(degrees) | Factor of Safety          |      |                           |      |                           |      |
|--------------------------------------|---------------------------|------|---------------------------|------|---------------------------|------|
|                                      | $c_u=500$ psf             |      | $c_u=1000$ psf            |      | $c_u=2000$ psf            |      |
|                                      | $\gamma$ – Backfill (pcf) |      | $\gamma$ – Backfill (pcf) |      | $\gamma$ – Backfill (pcf) |      |
|                                      | 105                       | 125  | 105                       | 125  | 105                       | 125  |
| $\phi = 34$                          | 0.64                      | 0.54 | 1.28                      | 1.08 | 1.98                      | 1.84 |
| $\phi = 40$                          | 0.64                      | 0.54 | 1.28                      | 1.08 | 1.98                      | 1.84 |
| $\phi = 42$                          | 0.64                      | 0.54 | 1.28                      | 1.08 | 1.98                      | 1.84 |



**Table 31. Factor of Safety Comparison for Series 1 Case 2 with Different Depths.**

| Backfill Friction Angle<br>(degrees) | Factor of Safety          |      |                           |      |   |      |
|--------------------------------------|---------------------------|------|---------------------------|------|---|------|
|                                      | $c_u=2000$ psf (2H)       |      | $c_u=2000$ psf (H)        |      | Percent<br>Difference from<br>2H to H<br>Foundation<br>Depth* (%) |      |
|                                      | $\gamma$ - Backfill (pcf) |      | $\gamma$ - Backfill (pcf) |      |   |      |
|                                      | 105                       | 125  | 105                       | 125  | 105   | 125  |
| $\phi = 34$                          | 1.98                      | 1.84 | 1.37                      | 1.44 | 44.5  | 27.7 |
| $\phi = 40$                          | 1.98                      | 1.84 | 1.37                      | 1.44 | 44.5  | 27.7 |
| $\phi = 42$                          | 1.98                      | 1.84 | 1.37                      | 1.44 | 44.5  | 27.7 |

\* It is the difference in FOS when foundation depth is two times the wall height to one time the wall height.

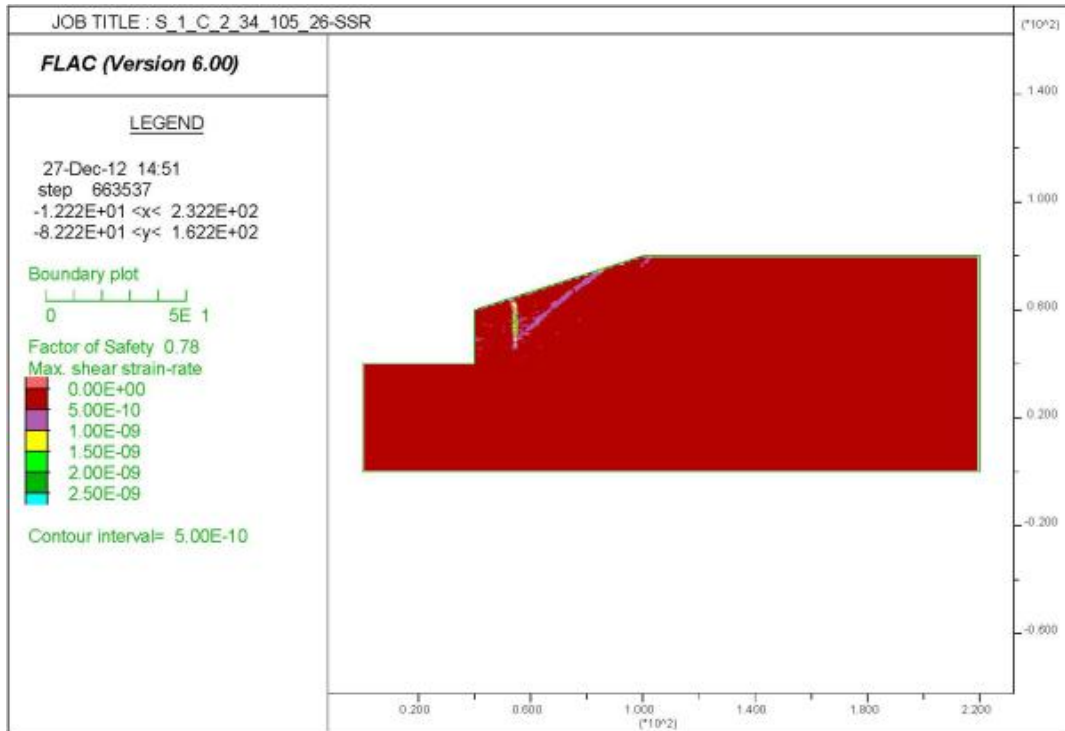


**Figure 104. Series 1 Case 2 Foundation Angle  $\phi=26^\circ$ , Backfill Angle  $\phi=34^\circ$ , and  $\gamma=105$  pcf Maximum Shear Strain Rate.**

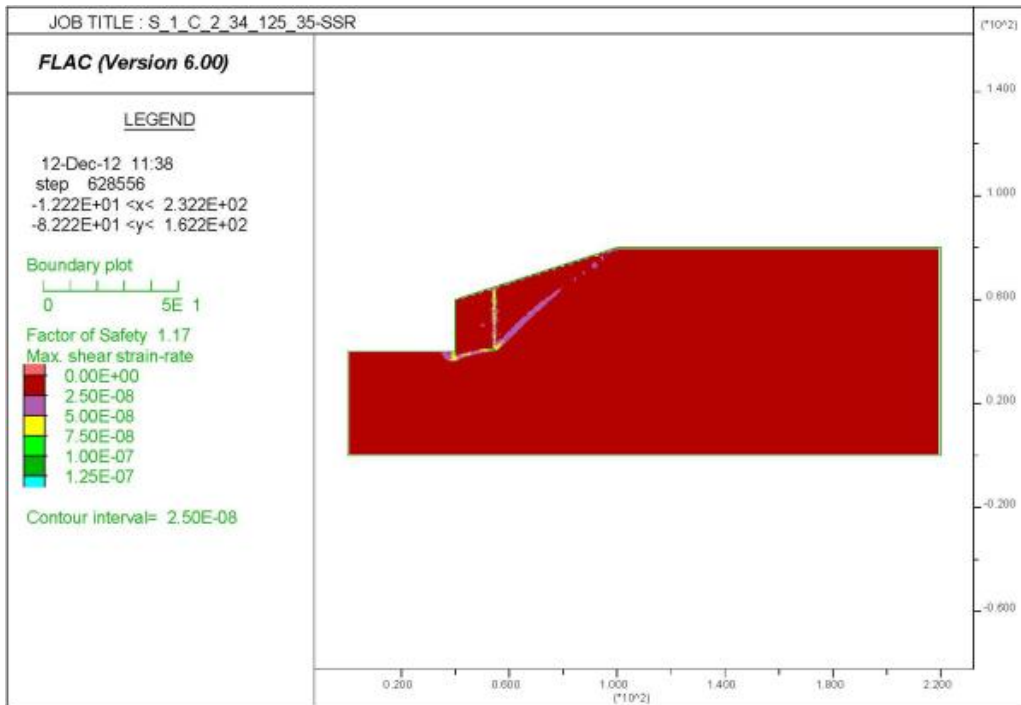


Figure 105. Series 1 Case 2 Foundation Angle  $\phi=35^\circ$ , Backfill Angle  $\phi=34^\circ$ , and  $\gamma=125$  pcf Maximum Shear Strain Rate.

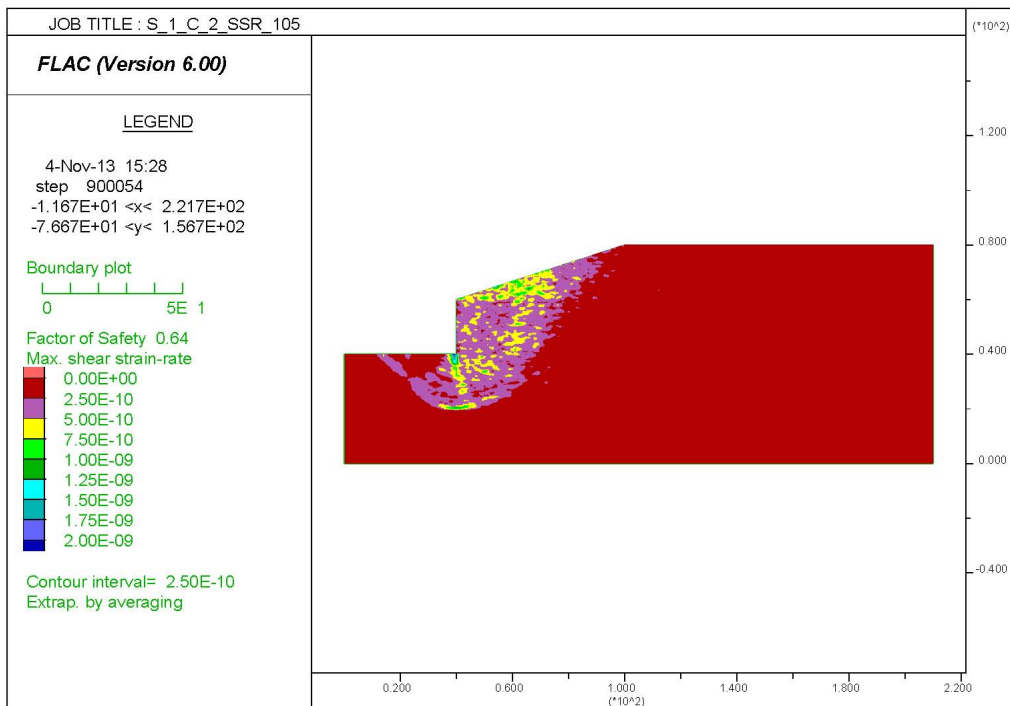
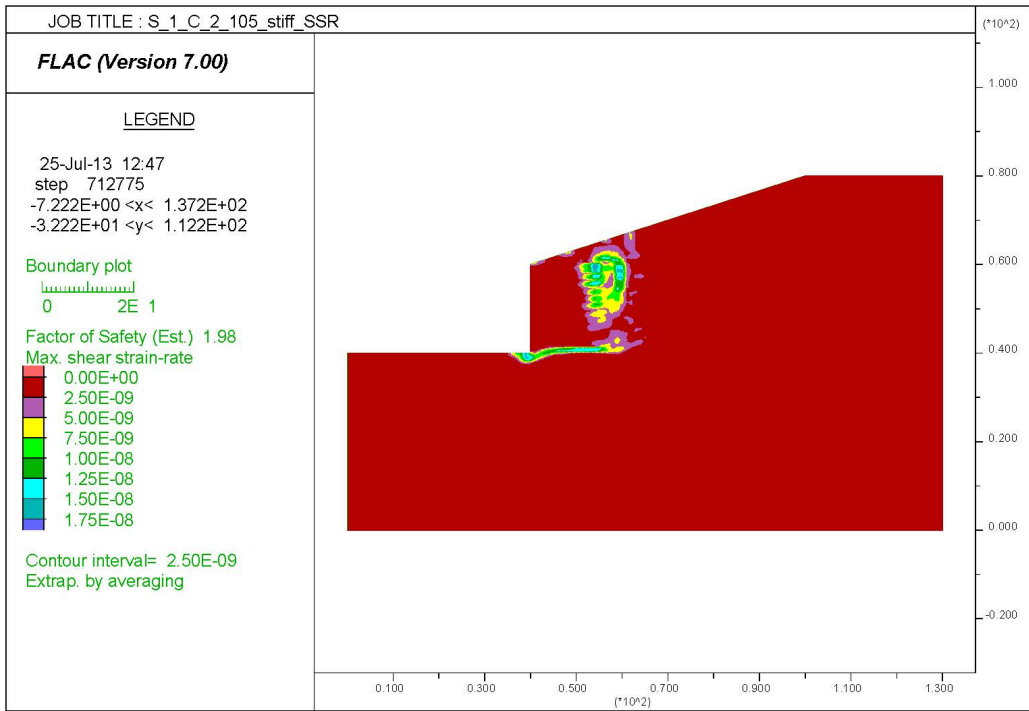
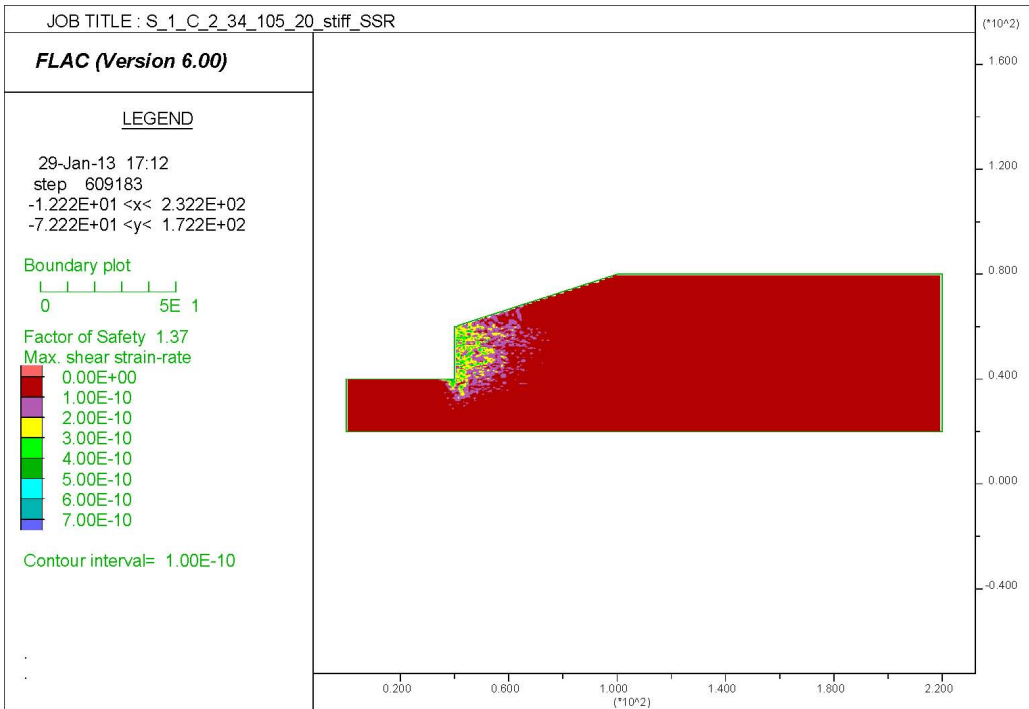


Figure 106. Series 1 Case 2 Foundation  $c_u=500$  pcf, Backfill Angle  $\phi=34^\circ$ , and  $\gamma=105$  pcf Maximum Shear Strain Rate.



**Figure 107. Series 1 Case 2 Foundation  $c_u=2000$  psf, Backfill Angle  $\phi=34^\circ$ , and  $\gamma=105$  pcf Maximum Shear Strain Rate.**



**Figure 108. Series 1 Case 2 Foundation  $c_u=2000$  psf, Backfill Angle  $\phi=34^\circ$ , and  $\gamma=105$  pcf Maximum Shear Strain Rate. Foundation Depth Equals to Wall Height.**

Based on the study, the critical surfaces are summarized into the following situations as shown in Figure 109–Figure 113.

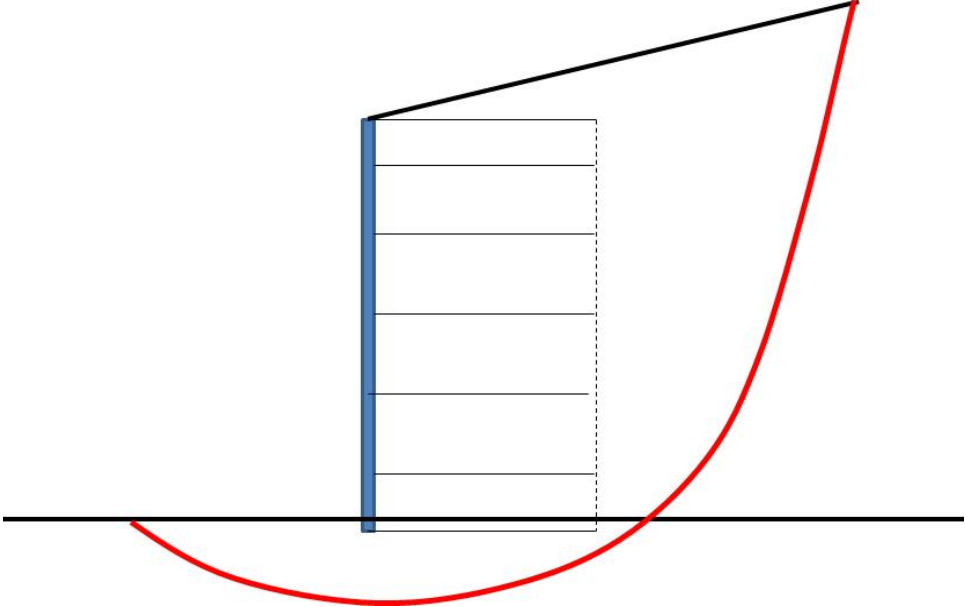


**Figure 109. Circular Failure Surface.**

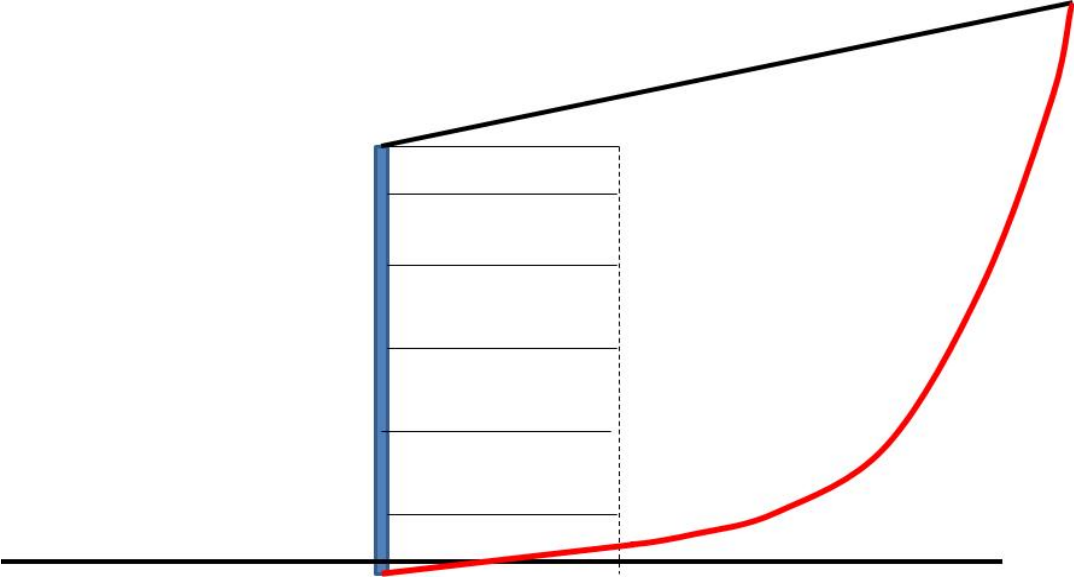


**Figure 110. Circular + Plane Failure Surface.**

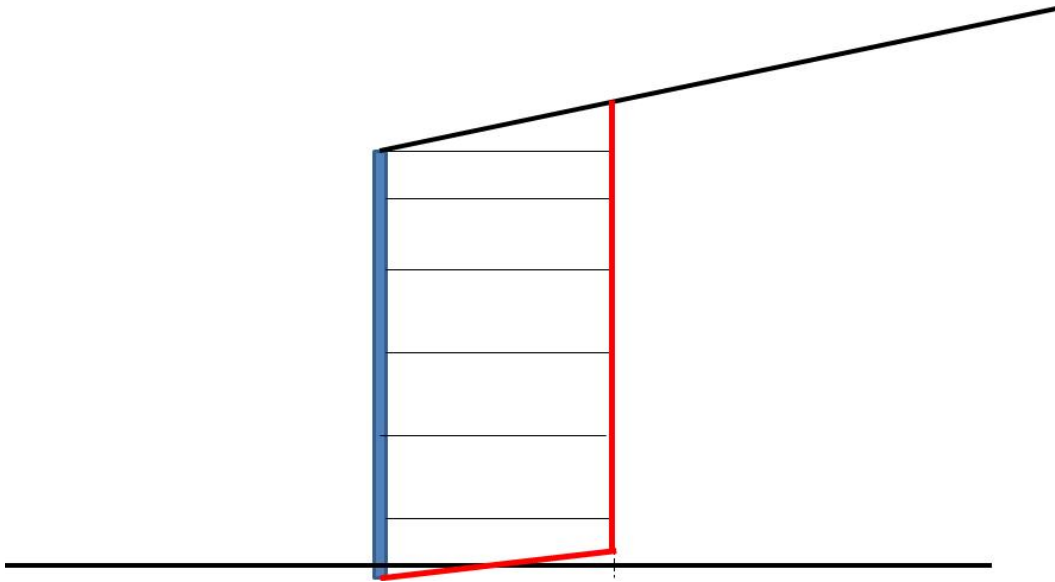


**Figure 111. Vertical Failure Surface.**

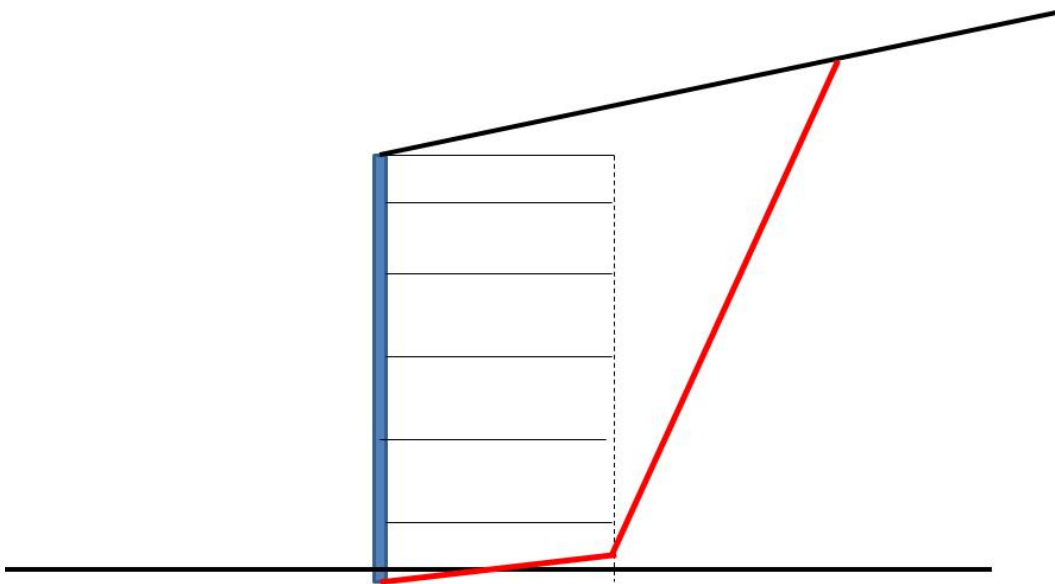


**Figure 112. Wedge Failure Surface.**

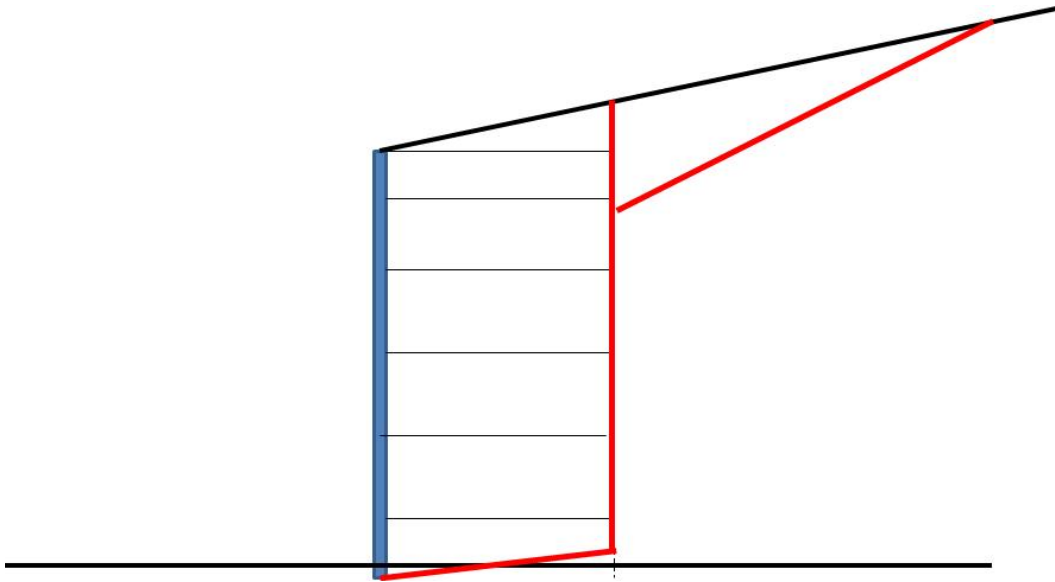


**Figure 113. Wedge + Vertical Failure Surface.**

### **2H:1V Back Slope**

In this case, the back slope angle was taken as 2H:1V, which is steeper than the previous case as shown in Figure 114. Results from FLAC analysis are presented below in Table 32 and Table 33. These tables also present FOSs for bearing capacity and sliding. The figures associated with this case are presented in Appendix C. Figure 115–Figure 118 present a few representative results with visible failure surfaces.

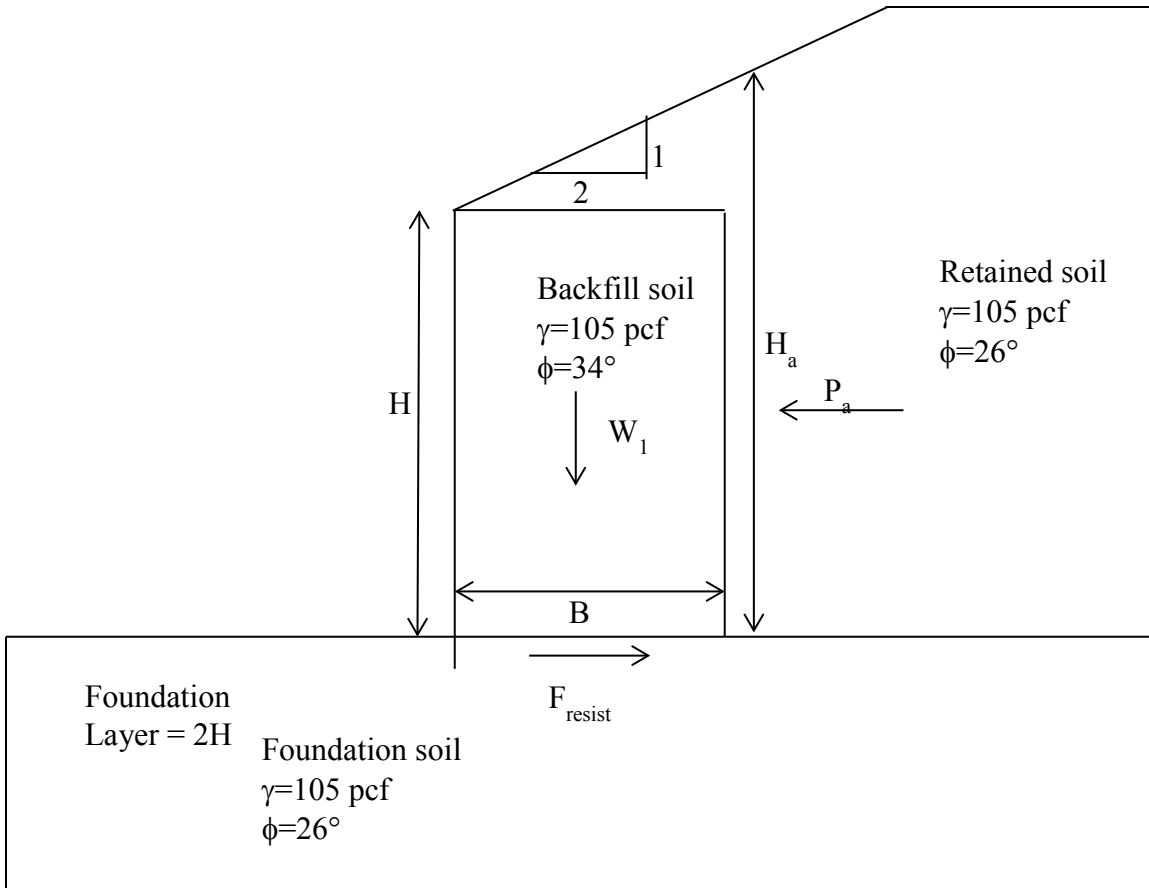


**Figure 114. Dimensions and Properties Used for Series 1 Case 3.**

The results from FLAC analysis show low values for  $\phi_{found}=26^\circ$ , which is due to the fact that failure occurred on a backslope surface instead of a wedge failure influencing the wall.

- The failure surface for  $\phi_{found}=30^\circ$  had a wedge behind the wall with an angle of  $32^\circ$  from horizontal.
- The factor of safety from FLAC simulation for this case compared to 3H:1V back slope are reduced by 20–26 percent.
- The results for this case are different and should be verified with the type of failure surface before considering it.
- The FOSs for bearing capacity are highly conservative, and for sliding, the values are higher than FLAC simulation data.

**Table 32. Series 1 Case 3: Back Slope 2:1 with Frictional Foundation Soil.**

| Backfill Friction Angle<br>(degrees) | Factor of Safety                |       |                                 |        |                                 |      |
|--------------------------------------|---------------------------------|-------|---------------------------------|--------|---------------------------------|------|
|                                      | $\phi_{\text{found}}= 26^\circ$ |       | $\phi_{\text{found}}= 30^\circ$ |        | $\phi_{\text{found}}= 35^\circ$ |      |
|                                      | $\gamma$ - Backfill<br>(pcf)    |       | $\gamma$ - Backfill<br>(pcf)    |        | $\gamma$ - Backfill<br>(pcf)    |      |
|                                      | 105                             | 125   | 105                             | 125    | 105                             | 125  |
| $\phi = 34$                          | 0.61                            | 0.62  | 0.72                            | 0.66   | 0.91                            | 0.92 |
| $\phi = 40$                          | 0.61                            | 0.62  | 0.72                            | 0.66   | 0.91                            | 0.92 |
| $\phi = 42$                          | 0.61                            | 0.62  | 0.72                            | 0.66   | 0.91                            | 0.92 |
| Bearing Capacity Analysis            | 0.000                           | 0.000 | 0.0001                          | 0.0001 | 0.26                            | 0.26 |
| Sliding Analysis                     | 0.65                            | 0.65  | 0.98                            | 0.98   | 1.58                            | 1.58 |

**Table 33. Series 1 Case 3: Cohesive Foundation Soils.**

| Backfill Friction Angle<br>(degrees) | Factor of Safety          |      |                           |      |                           |                   |
|--------------------------------------|---------------------------|------|---------------------------|------|---------------------------|-------------------|
|                                      | $c_u=500$ psf             |      | $c_u=1000$ psf            |      | $c_u=2000$ psf            |                   |
|                                      | $\gamma$ - Backfill (pcf) |      | $\gamma$ - Backfill (pcf) |      | $\gamma$ - Backfill (pcf) |                   |
|                                      | 105                       | 125  | 105                       | 125  | 105                       | 125               |
| $\phi = 34$                          | 0.55                      | 0.49 | 1.16                      | 0.98 | 2.41                      | No<br>Convergence |
| $\phi = 40$                          | 0.55                      | 0.49 | 1.16                      | 0.98 | 2.41                      |                   |
| $\phi = 42$                          | 0.55                      | 0.49 | 1.16                      | 0.98 | 2.41                      |                   |

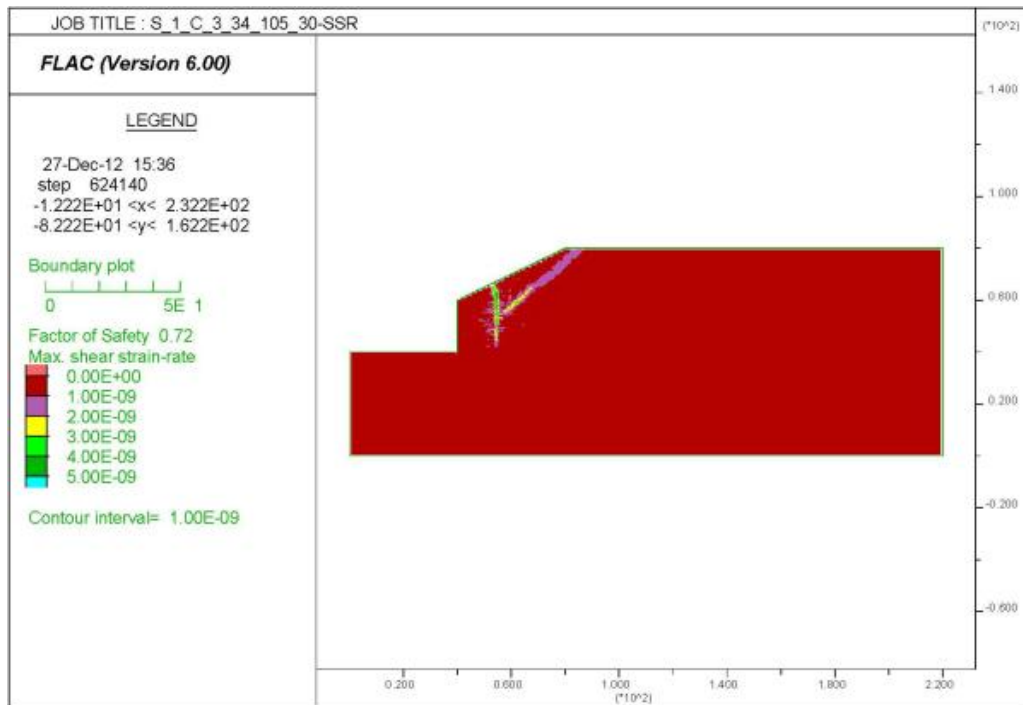


**Figure 115. Series 1 Case 3 Foundation Angle  $\phi=30^\circ$ , Backfill Angle  $\phi=34^\circ$ , and  $\gamma=105$  pcf Maximum Shear Strain Rate.**



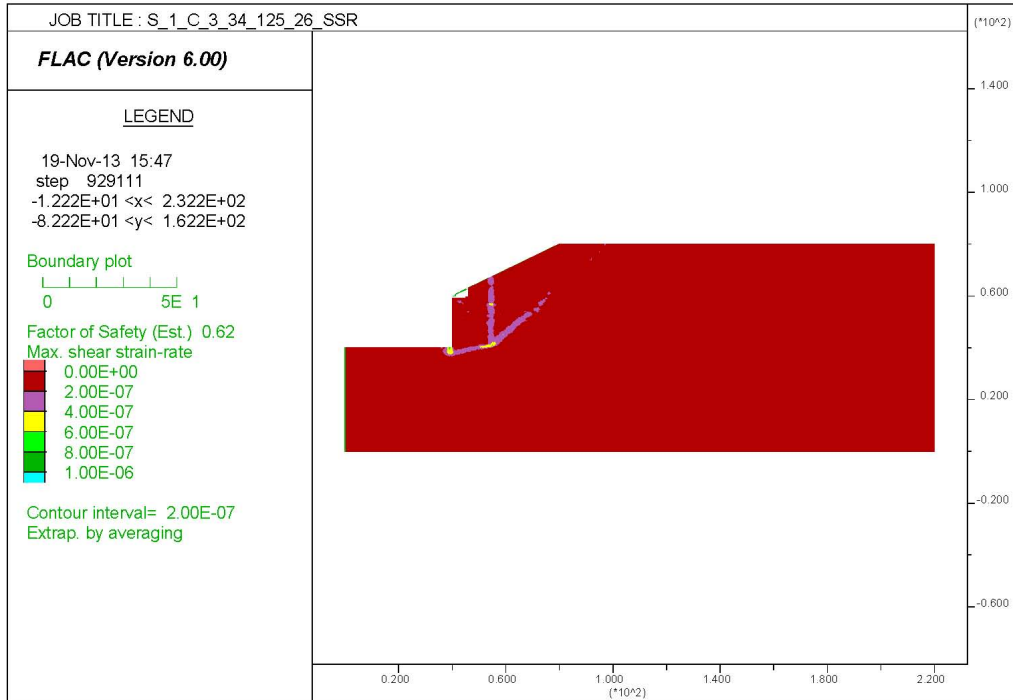


**Figure 116. Series 1 Case 3 Foundation Angle  $\phi=26^\circ$ , Backfill Angle  $\phi=34^\circ$ , and  $\gamma=125$  pcf Maximum Shear Strain Rate.**

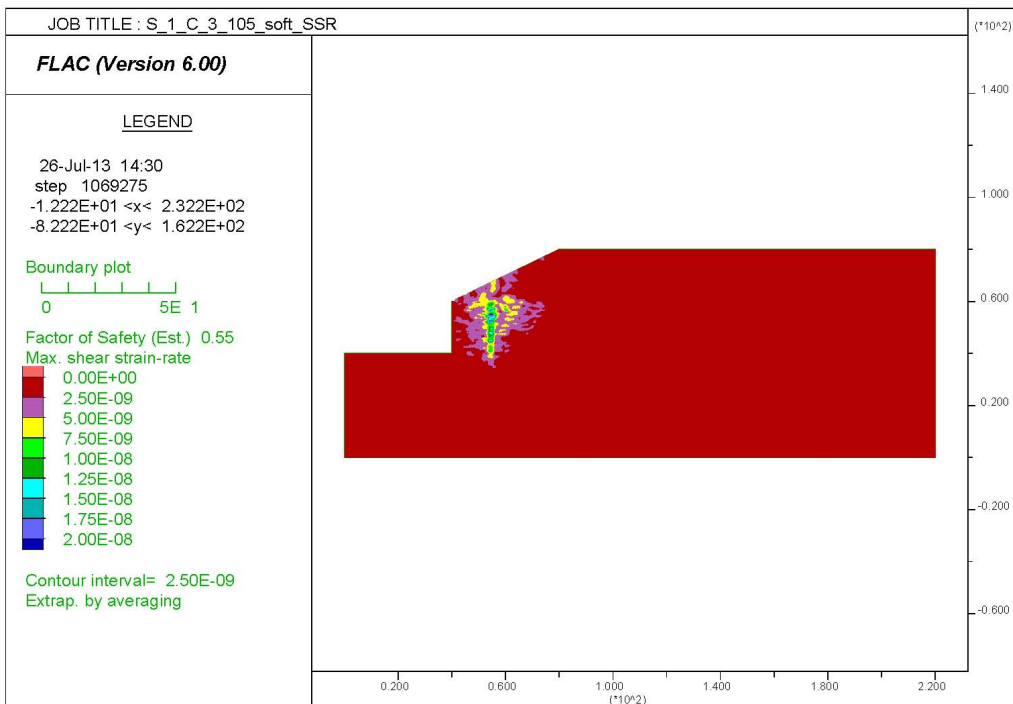


**Figure 117. Series 1 Case 3 Foundation  $c_u=500$  pcf, Backfill Angle  $\phi=34^\circ$ , and  $\gamma=105$  pcf Maximum Shear Strain Rate.**

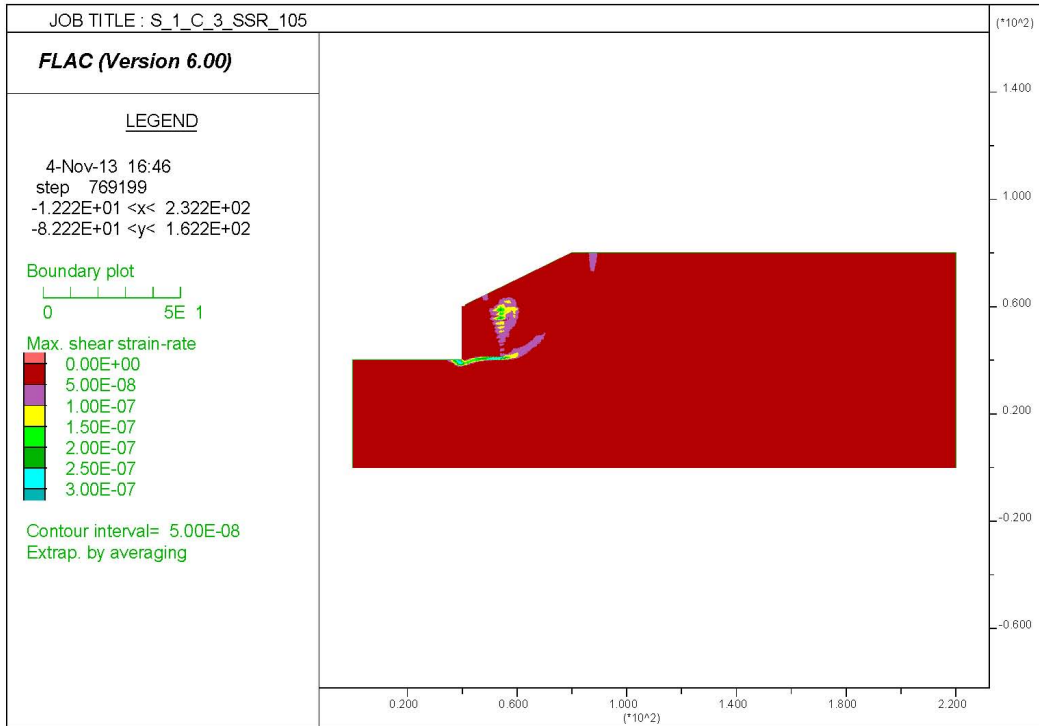


**Figure 118. Series 1 Case 3 Foundation  $c_u=2000$  psf, Backfill Angle  $\phi=34^\circ$ , and  $\gamma=105$  pc Maximum Shear Strain Rate.**

### 3H:1V Fore Slope

In this series 3H:1V, fore slope is considered with depth equals to 1H wall height and the depth of foundation as 2H wall height below the fore slope as shown in Figure 119. Complete results for this case are presented in Appendix C. Figure 120–Figure 124 present a few representative plots from entire analysis for this case.

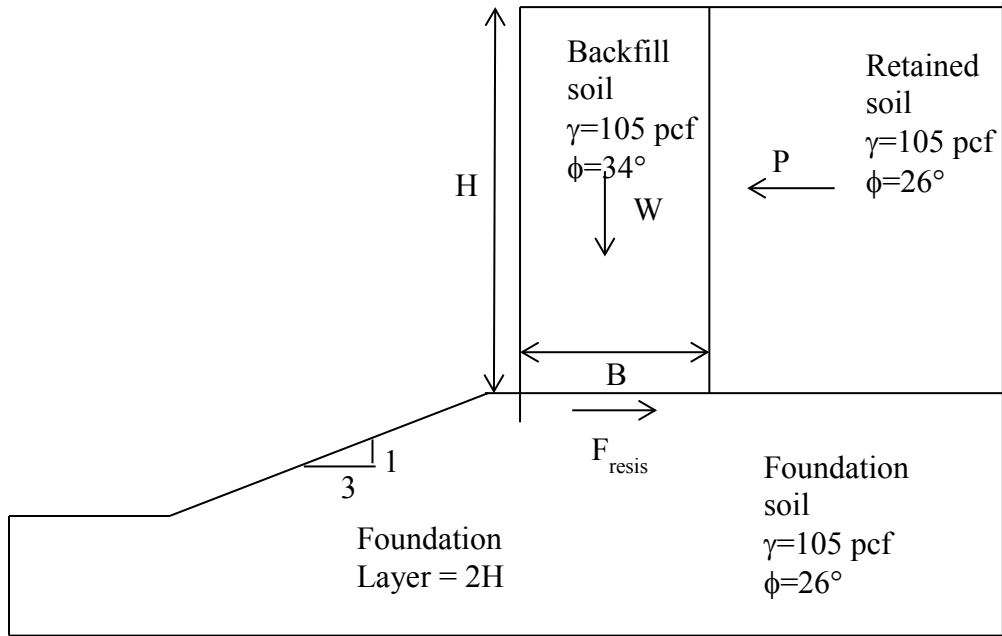


**Figure 119. Dimensions and Properties Used for Series 2 Case 2.**

Table 34 below shows results from FLAC simulation as well as for bearing capacity analysis. The results for ( $\phi_{\text{found}}=26^\circ$  and  $\phi_{\text{found}}=30^\circ$ ) foundations soils have different values for different unit weights. The lower unit weight foundation soils shows sliding failure, whereas the failure surface for stronger foundation soils goes through fore slope showing a general failure surface. The wedge type failure surface formed behind the wall has an angle of  $42^\circ$  with horizontal. The FOS from bearing capacity analysis shows values toward the conservative side while FOSs from sliding analysis show slightly unconservative values.

**Table 34. Series 2 Case 2: Fore Slope 3:1 with Frictional Foundation Soil.**

| Backfill Friction Angle(degrees) | Factor of Safety               |      |                                |      |                                |      |
|----------------------------------|--------------------------------|------|--------------------------------|------|--------------------------------|------|
|                                  | $\phi_{\text{found}}=26^\circ$ |      | $\phi_{\text{found}}=30^\circ$ |      | $\phi_{\text{found}}=35^\circ$ |      |
|                                  | $\gamma$ - Backfill (pcf)      |      | $\gamma$ - Backfill (pcf)      |      | $\gamma$ - Backfill (pcf)      |      |
|                                  | 105                            | 125  | 105                            | 125  | 105                            | 125  |
| $\phi = 34$                      | 0.88                           | 0.83 | 1.03                           | 1.04 | 1.24                           | 1.24 |
| $\phi = 40$                      | 0.88                           | 0.83 | 1.03                           | 1.04 | 1.24                           | 1.24 |
| $\phi = 42$                      | 0.88                           | 0.83 | 1.03                           | 1.04 | 1.24                           | 1.24 |
| Bearing Capacity Analysis        | 0.12                           | 0.12 | 0.49                           | 0.49 | 2.00                           | 2.00 |
| Sliding Analysis                 | 1.81                           | 1.81 | 2.55                           | 2.55 | 3.76                           | 3.76 |

**Table 35. Series 2 Case 2: Cohesive Foundation Soils.**

| Backfill Friction Angle (degrees) | Factor of Safety          |             |                           |             |                           |      |
|-----------------------------------|---------------------------|-------------|---------------------------|-------------|---------------------------|------|
|                                   | $c_u=500$ psf             |             | $c_u=1000$ psf            |             | $c_u=2000$ psf            |      |
|                                   | $\gamma$ - Backfill (pcf) |             | $\gamma$ - Backfill (pcf) |             | $\gamma$ - Backfill (pcf) |      |
|                                   | 105                       | 125         | 105                       | 125         | 105                       | 125  |
| $\phi = 34$                       | No                        | No          | 1.23                      | No          | 2.15                      | 2.03 |
| $\phi = 40$                       | Convergence               | Convergence | 1.23                      | Convergence | 2.15                      | 2.03 |
| $\phi = 42$                       |                           |             | 1.23                      |             | 2.15                      | 2.03 |

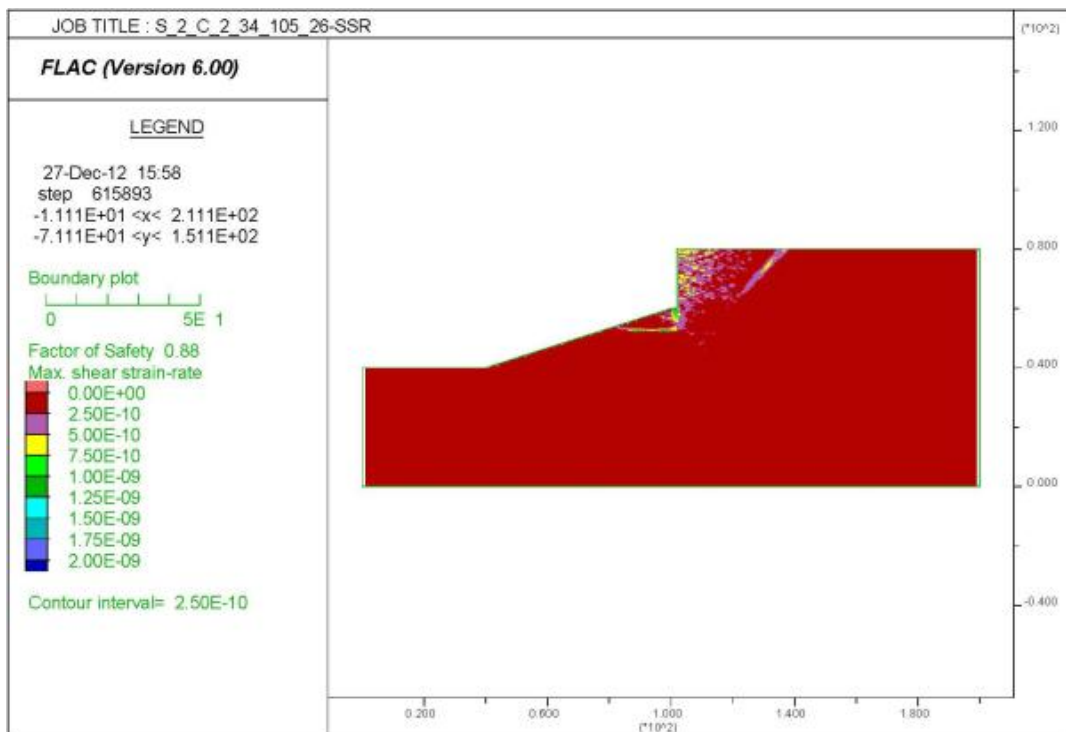


**Figure 120. Series 2 Case 2 Foundation Angle  $\phi=26^\circ$ , Backfill Angle  $\phi=34^\circ$ , and  $\gamma=105$  pcf Maximum Shear Strain Rate.**

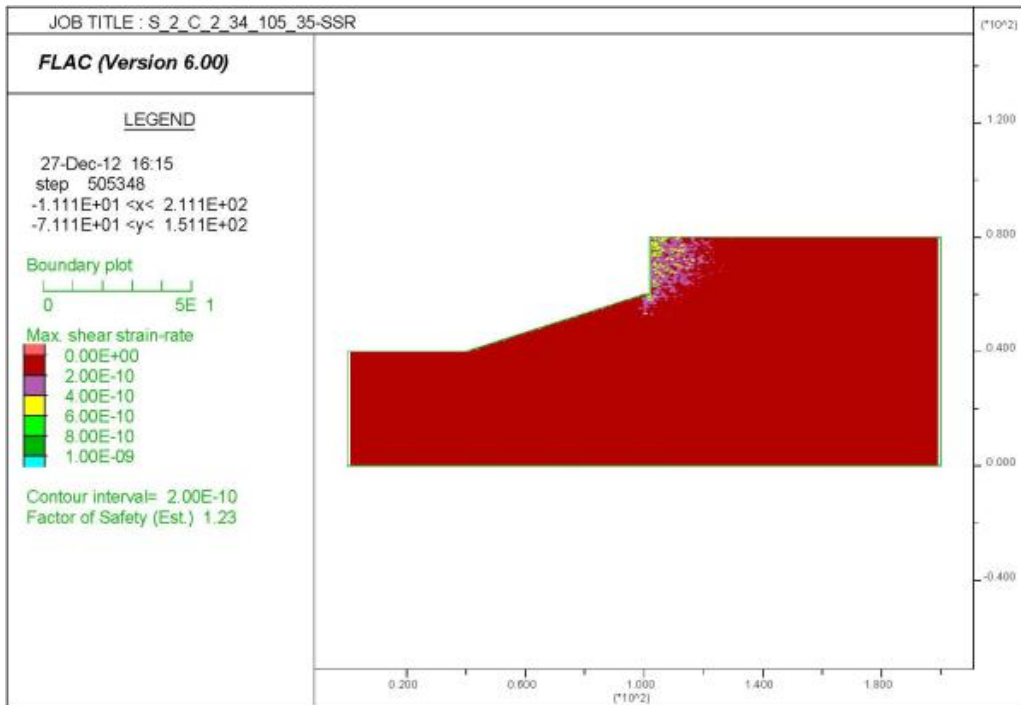


**Figure 121. Series 2 Case 2 Foundation Angle  $\phi=35^\circ$ , Backfill Angle  $\phi=34^\circ$ , and  $\gamma=105$  pcf Maximum Shear Strain Rate.**

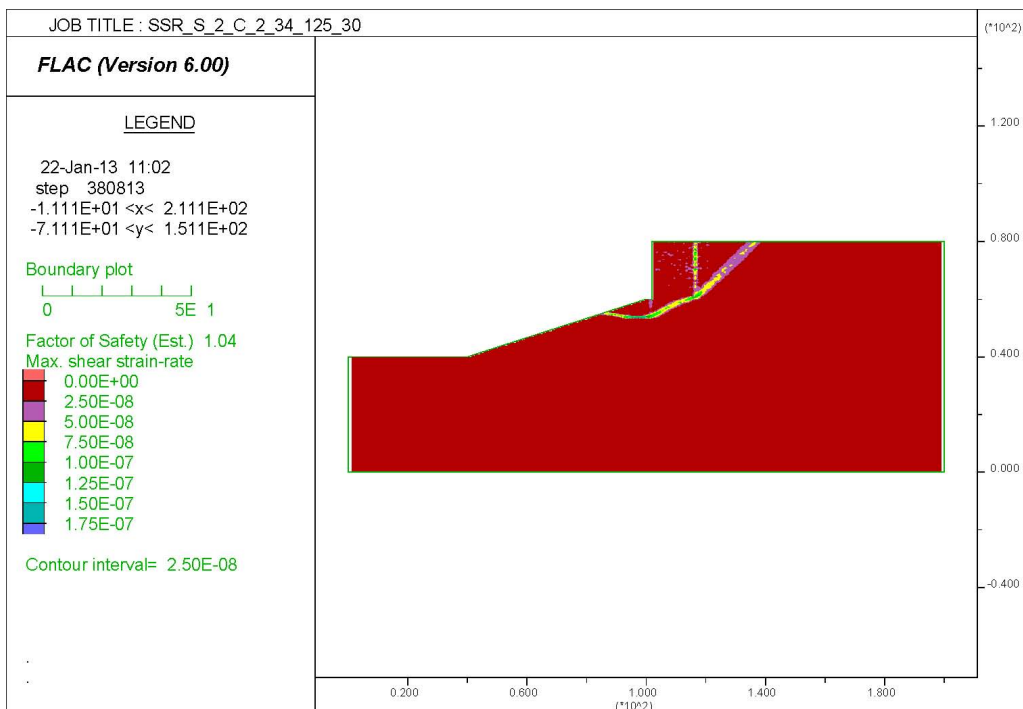


**Figure 122. Series 2 Case 2 Foundation Angle  $\phi=30^\circ$ , Backfill Angle  $\phi=34^\circ$ , and  $\gamma=125$  pcf Maximum Shear Strain Rate.**

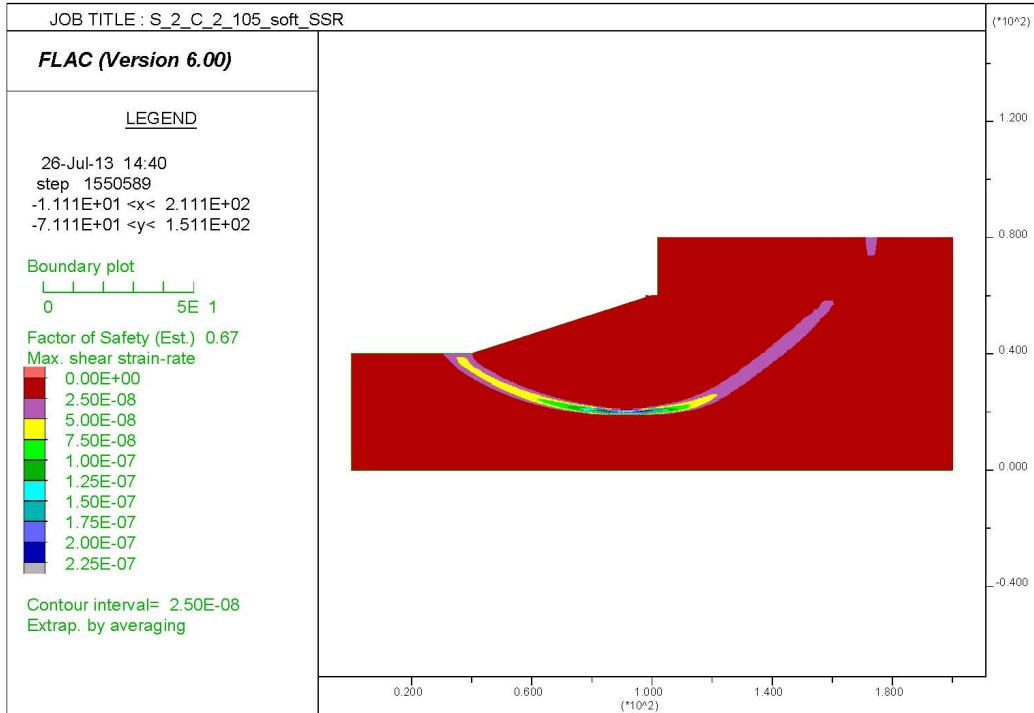


**Figure 123. Series 2 Case 2 Foundation  $c_u=500$  psf, Backfill Angle  $\phi=34^\circ$ , and  $\gamma=105$  pcf Maximum Shear Strain Rate.**

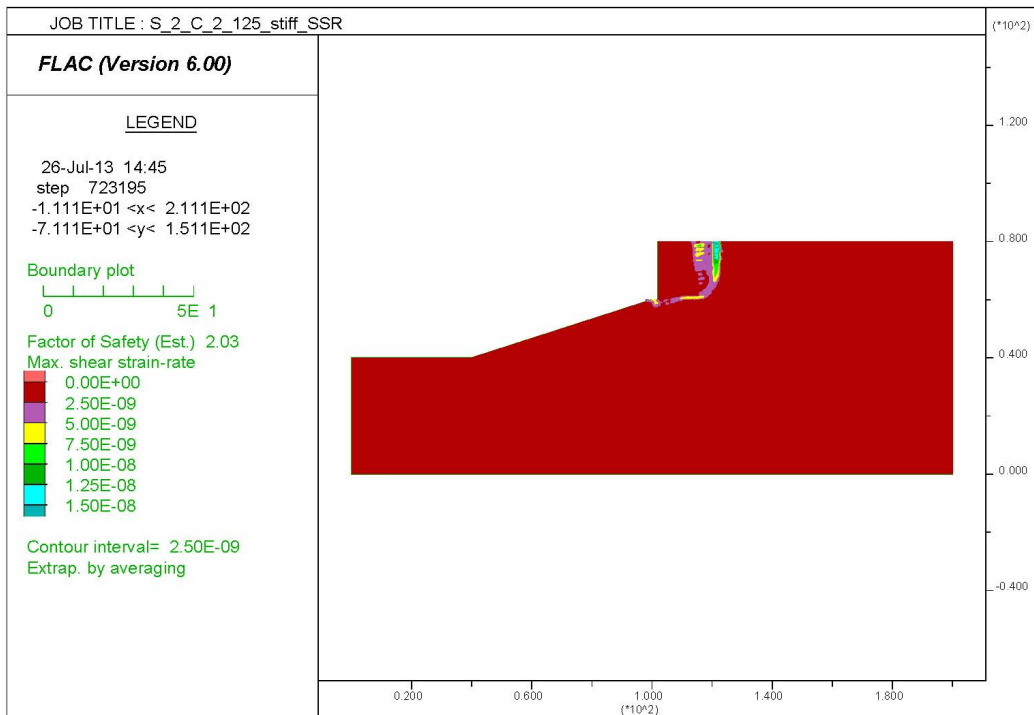


**Figure 124. Series 2 Case 2 Foundation  $c_u=2000$  psf, Backfill Angle  $\phi=34^\circ$ , and  $\gamma=125$  pcf Maximum Shear Strain Rate.**

## 2H:1V Fore Slope

The cases discussed in this section have a higher foreslope angle to see its effects on FLAC simulations. The dimensions for this case are shown in Figure 125. The complete results for this case are presented in Appendix C. Figure 126–Figure 130 present representative plots for this case, which are used here to explain the results for this case.

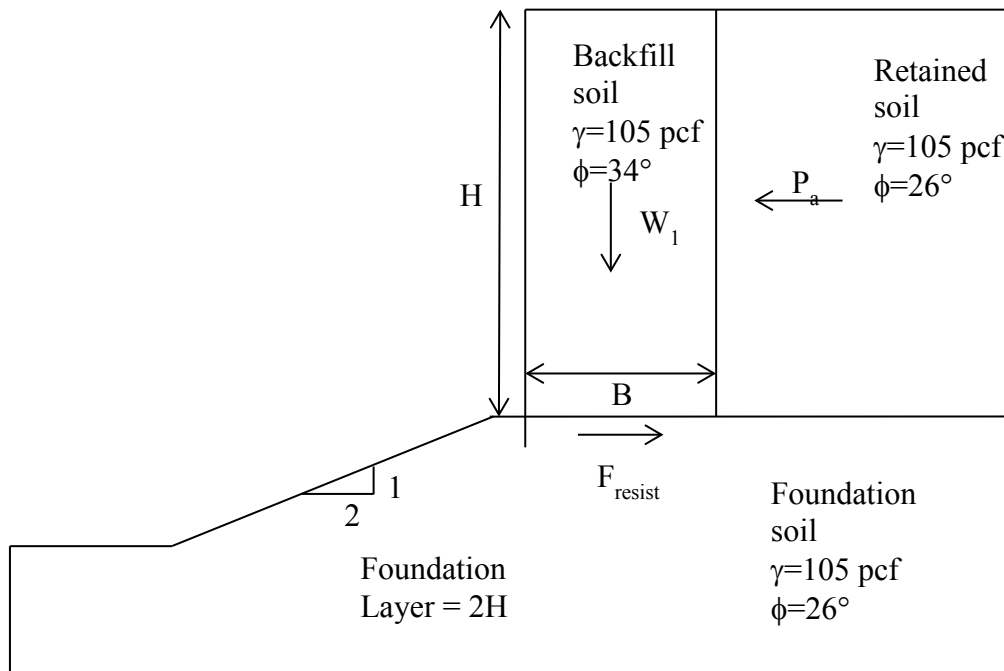


**Figure 125. Dimensions and Properties Used for Series 2 Case 3.**

Table 36 shows FOS values from a FLAC simulation as well as from a bearing capacity and sliding analysis. The results from the bearing capacity analysis are highly conservative for low foundation strengths, but for high foundation strengths, it is close to FLAC analysis, which suggests that failure would be a bearing capacity failure. Values from the sliding analysis lean toward unconservative. With an increase in fore slope angle the FOS values decrease from its previous case by 11–26 percent. The angle of failure wedge behind the wall is  $42.3^\circ$  from horizontal.

**Table 36. Series 2 Case 3: Fore Slope 2:1 with Frictional Foundation Soil.**

| Backfill Friction Angle<br>(degrees) | Factor of Safety                 |       |                                  |       |                                  |      |
|--------------------------------------|----------------------------------|-------|----------------------------------|-------|----------------------------------|------|
|                                      | $\phi_{\text{found}}= 26^\circ$  |       | $\phi_{\text{found}}= 30^\circ$  |       | $\phi_{\text{found}}= 35^\circ$  |      |
|                                      | $\gamma - \text{Backfill (pcf)}$ |       | $\gamma - \text{Backfill (pcf)}$ |       | $\gamma - \text{Backfill (pcf)}$ |      |
|                                      | 105                              | 125   | 105                              | 125   | 105                              | 125  |
| $\phi = 34$                          | 0.78                             | 0.78  | 0.88                             | 0.76  | 1.11                             | 1.11 |
| $\phi = 40$                          | 0.78                             | 0.78  | 0.88                             | 0.76  | 1.11                             | 1.11 |
| $\phi = 42$                          | 0.78                             | 0.78  | 0.88                             | 0.76  | 1.11                             | 1.11 |
| Bearing Capacity Analysis            | 0.068                            | 0.068 | 0.278                            | 0.278 | 1.12                             | 1.12 |
| Sliding Analysis                     | 1.81                             | 1.81  | 2.55                             | 2.55  | 3.76                             | 3.76 |

**Table 37. Series 2 Case 3: Fore Slope 2:1 with Cohesive Foundation Soils.**

| Backfill Friction Angle<br>(degrees) | Factor of Safety                 |      |                                  |      |                                  |      |
|--------------------------------------|----------------------------------|------|----------------------------------|------|----------------------------------|------|
|                                      | $c_u=500 \text{ psf}$            |      | $c_u=1000 \text{ psf}$           |      | $c_u=2000 \text{ psf}$           |      |
|                                      | $\gamma - \text{Backfill (pcf)}$ |      | $\gamma - \text{Backfill (pcf)}$ |      | $\gamma - \text{Backfill (pcf)}$ |      |
|                                      | 105                              | 125  | 105                              | 125  | 105                              | 125  |
| $\phi = 34$                          | 0.64                             | 0.52 | 1.25                             | 1.05 | 2.14                             | 2.12 |
| $\phi = 40$                          | 0.64                             | 0.52 | 1.25                             | 1.05 | 2.14                             | 2.12 |
| $\phi = 42$                          | 0.64                             | 0.52 | 1.25                             | 1.05 | 2.14                             | 2.12 |

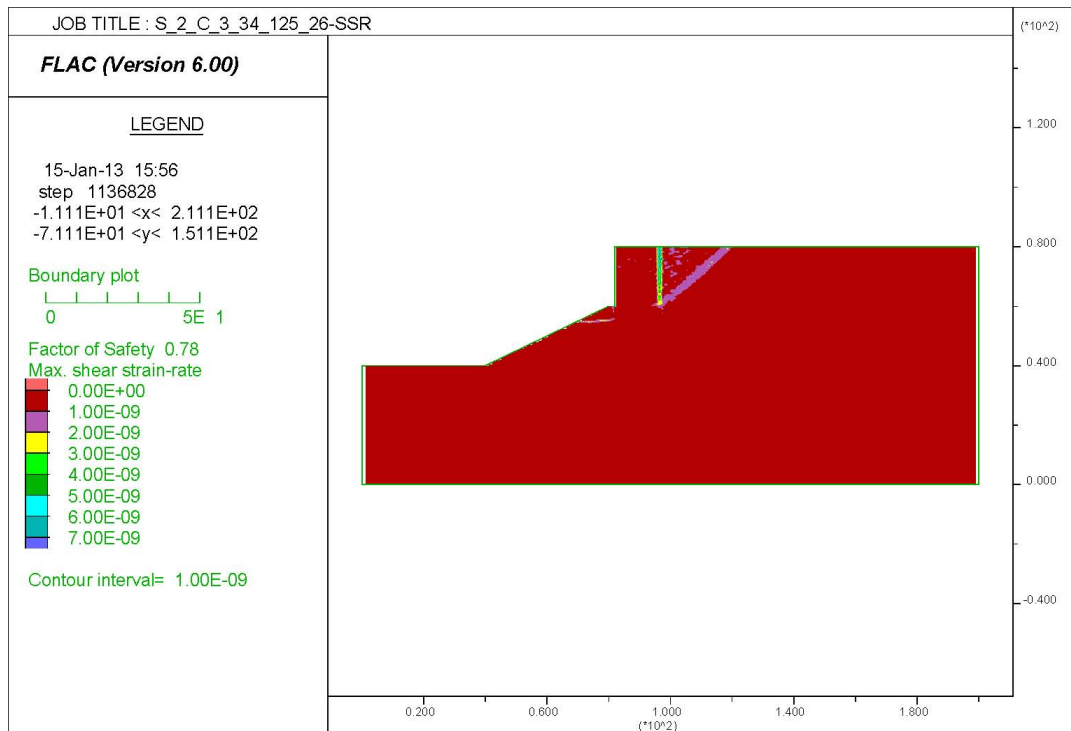


**Figure 126. Series 2 Case 3 Foundation Angle  $\phi=26^\circ$ , Backfill Angle  $\phi=34^\circ$ , and  $\gamma=125$  pcf Maximum Shear Strain Rate.**



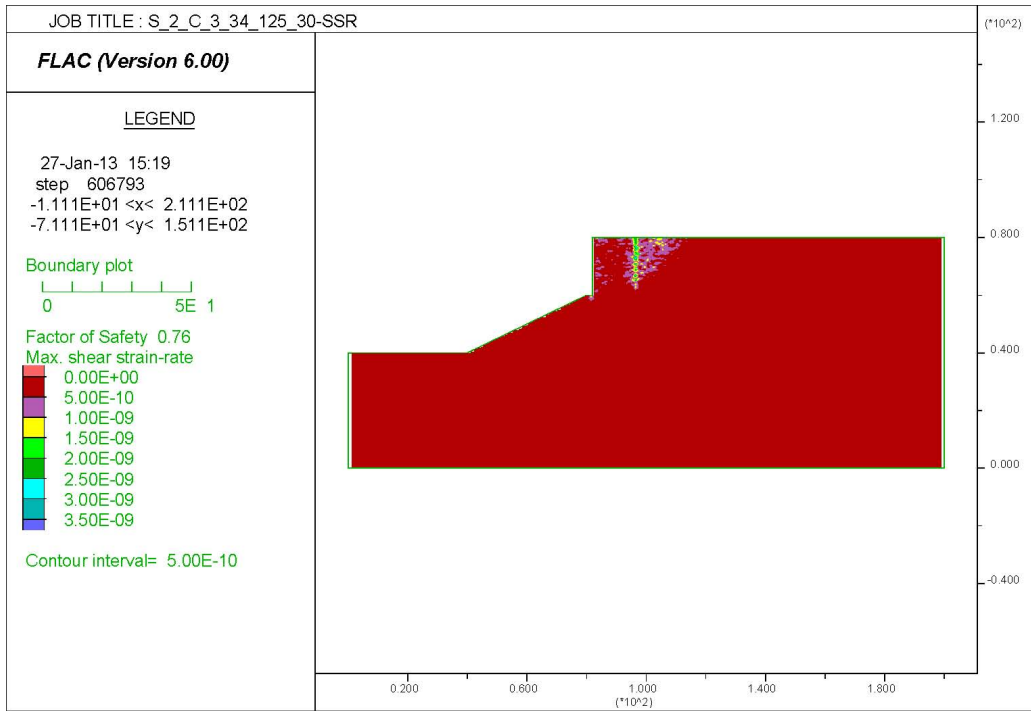


**Figure 127. Series 2 Case 3 Foundation Angle  $\phi=30^\circ$ , Backfill Angle  $\phi=34^\circ$ , and  $\gamma=125$  pcf Maximum Shear Strain Rate.**

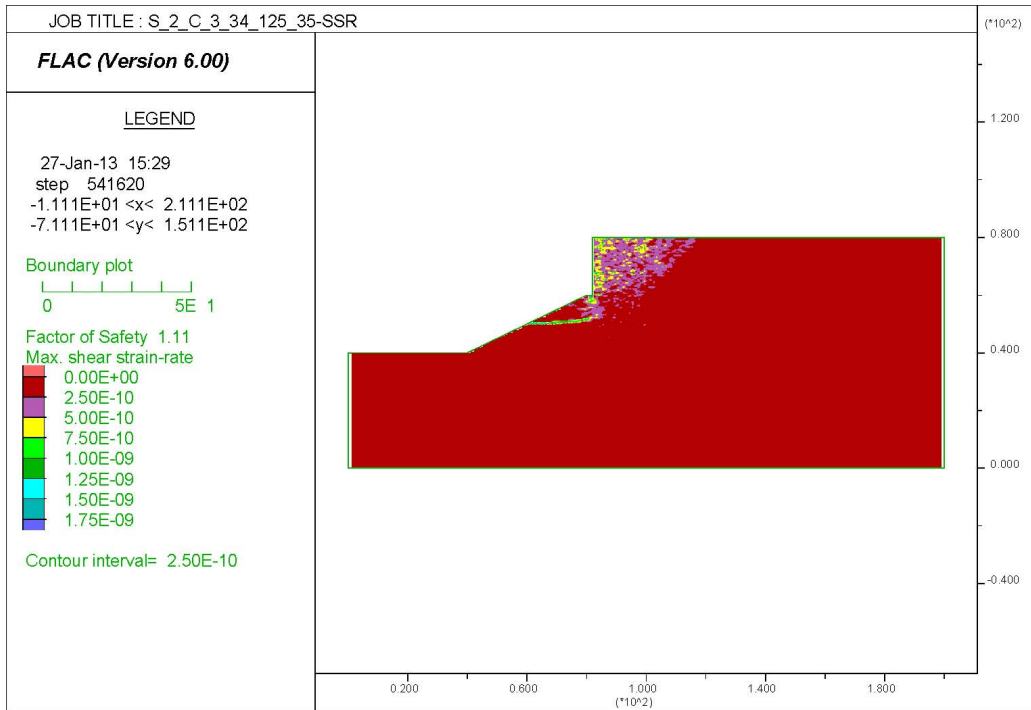


**Figure 128. Series 2 Case 3 Foundation Angle  $\phi=35^\circ$ , Backfill Angle  $\phi=34^\circ$ , and  $\gamma=125$  pcf Maximum Shear Strain Rate.**

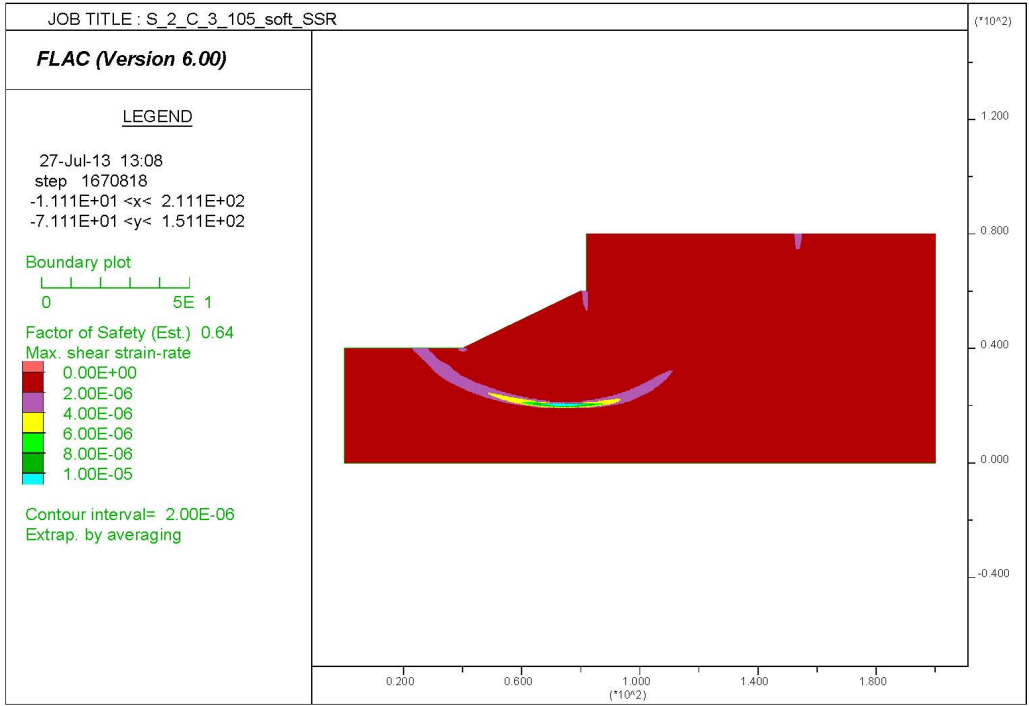


**Figure 129. Series 2 Case 3 Foundation  $c_u=500$  psf, Backfill Angle  $\phi=34^\circ$ , and  $\gamma=105$  pcf Maximum Shear Strain Rate.**

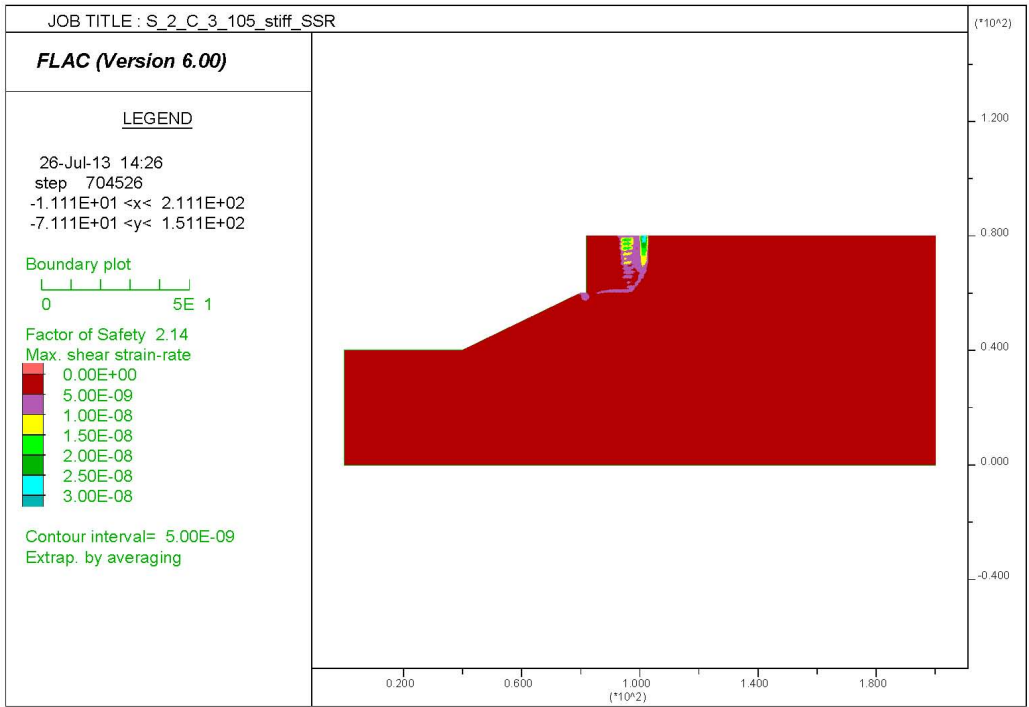


**Figure 130. Series 2 Case 3 Foundation  $c_u=2000$  psf, Backfill Angle  $\phi=34^\circ$ , and  $\gamma=105$  pcf Maximum Shear Strain Rate.**

The failure surfaces for MSE walls with foreslopes are predominantly circular surfaces. The circular surface started from the foreslope surface or the foundation and propagated upward to the retained soil zone. The generalized failure surface will be presented in the next section where the MSE walls with foreslope under rapid drawdown situation are discussed.

### RAPID DRAWDOWN IN FRONT OF THE MSE WALL

The effect of rapid drawdown on the compound failure behavior of an MSE wall was analyzed.

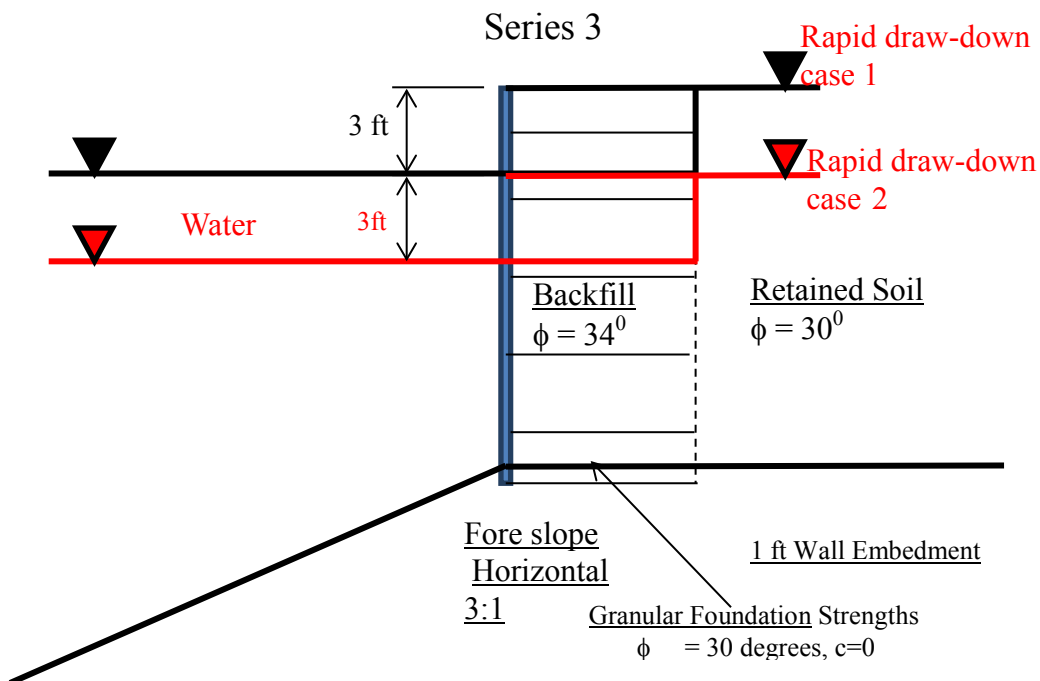


**Figure 131. Analysis Cases for Rapid Drawdown.**

Both horizontal ground and a 3:1 foreslope were considered for the MSE wall. Two cases shown in Figure 131 were considered for the analysis. The backfill material friction angle was assumed  $34^\circ$  and the retained soil was  $30^\circ$ . The friction angle of the foundation soil was taken as  $30^\circ$  and  $40^\circ$ , respectively. The unit weight of both moist and saturated soil was taken as 125 pcf. An impervious boundary between the water and the modular block was applied. Table 38 presents the analysis of the results of the above cases.

**Table 38. Factor of Safety Analysis Results for Case 1.**

| Type of Fore Slope | Foundation Friction Angle | FOS (for Drawdown) | FOS (No Drawdown) | % Change in FOS from No Drawdown |
|--------------------|---------------------------|--------------------|-------------------|----------------------------------|
| Horizontal         | 30                        | 0.83               | 1.20              | 30.83                            |
| Horizontal         | 40                        | 0.98               | 1.48              | 33.78                            |
| 3H:1V              | 30                        | 0.72               | 1.01              | 28.71                            |
| 3H:1V              | 40                        | 0.88               | 1.30              | 32.31                            |

**Table 39. Factor of Safety Analysis Results for Case 2.**

| Type of Fore Slope | Foundation Friction Angle | FOS (for Drawdown) | FOS (No Drawdown) | % Change in FOS from No Drawdown |
|--------------------|---------------------------|--------------------|-------------------|----------------------------------|
| Horizontal         | 30                        | 0.88               | 1.13              | 22.12                            |
| Horizontal         | 40                        | 1.08               | 1.40              | 22.86                            |
| 3H:1V              | 30                        | 0.73               | 0.96              | 23.96                            |
| 3H:1V              | 40                        | 0.94               | 1.24              | 24.19                            |

Based on the data, the FOS is reduced significantly when rapid drawdown occurred. For all the cases analyzed, no compound failure was identified. For the cases with horizontal ground, the critical surface went through the retained soil zone and exited through the interface between the foundation soil and backfill material. The failure surface of the analyzed cases can be simplified as shown in Figure 132. Basically, a circular failure surface was followed by a planar surface. The circular surface started from the top and propagated down to nearly the bottom elevation of the MSE wall. The planar failure surface started from bottom reinforcement layer and extended to the toe of the MSE wall. In addition, for some cases there is a failure plane between the reinforced zone and retained zone. For the cases with foreslopes, the failure plane is circular for global instability (see Figure 133). The contours of the maximum shear rate are presented in Figure 134–Figure 137 for illustration.

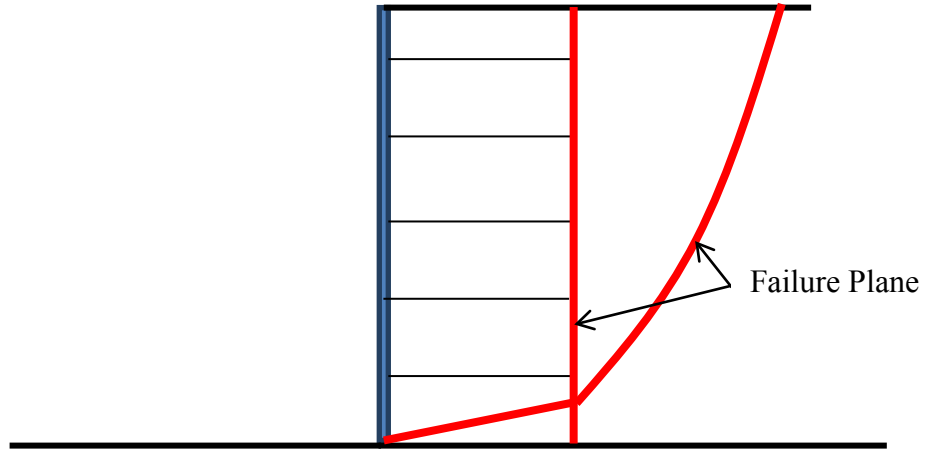


**Figure 132. Failure Plane for MSE Wall Subjected to Rapid Drawdown with Horizontal Fore Slope.**

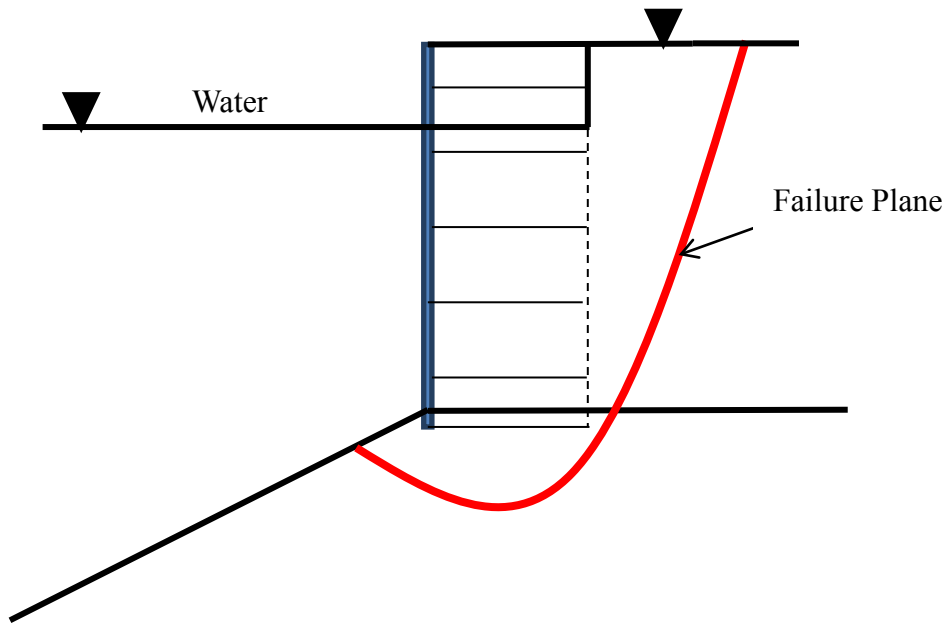


**Figure 133. Global Failure Pattern for MSE Wall with Fore Slope Subjected to Rapid Drawdown.**

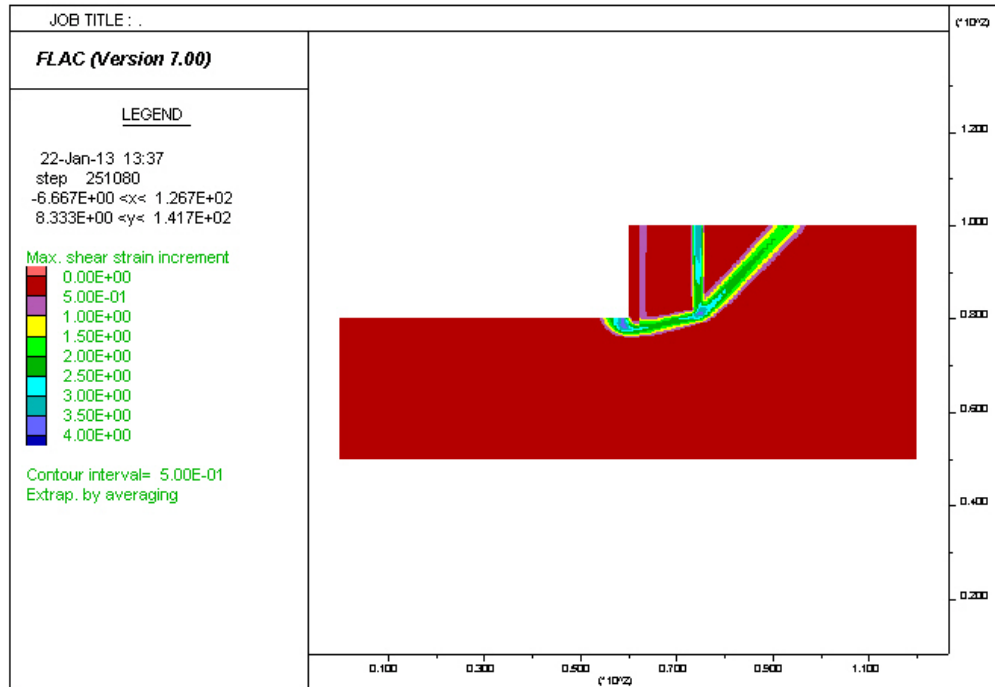


**Figure 134. Maximum Shear Strain for Case 1, Horizontal Fore Slope, Foundation Friction Angle = 30.**

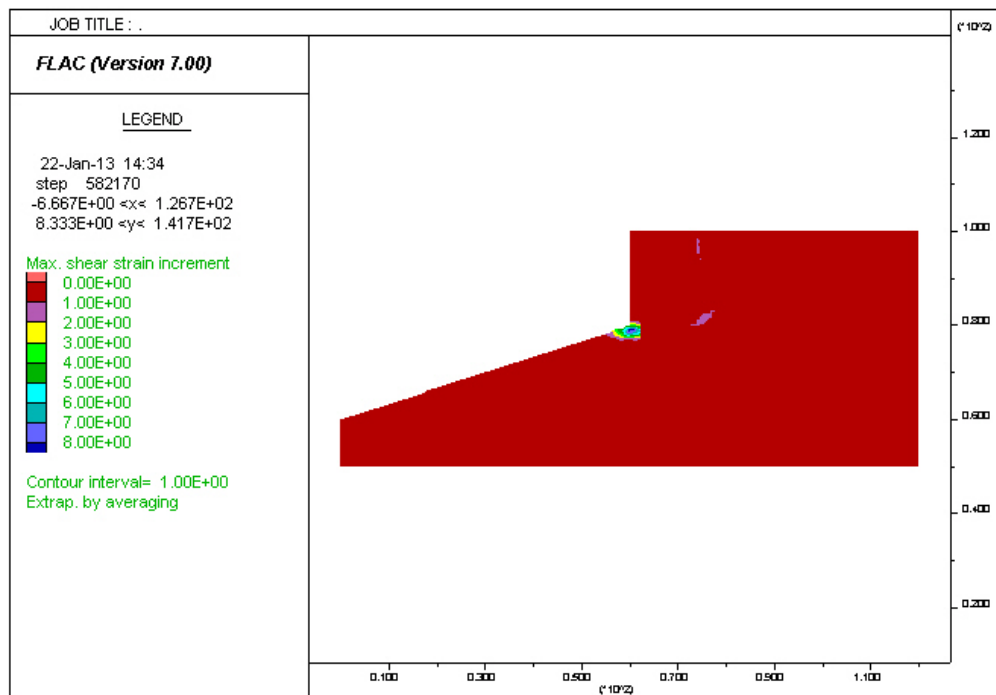


**Figure 135. Max Shear Strain Rate for Case 1, 3:1 Fore Slope, Foundation Friction Angle = 30.**

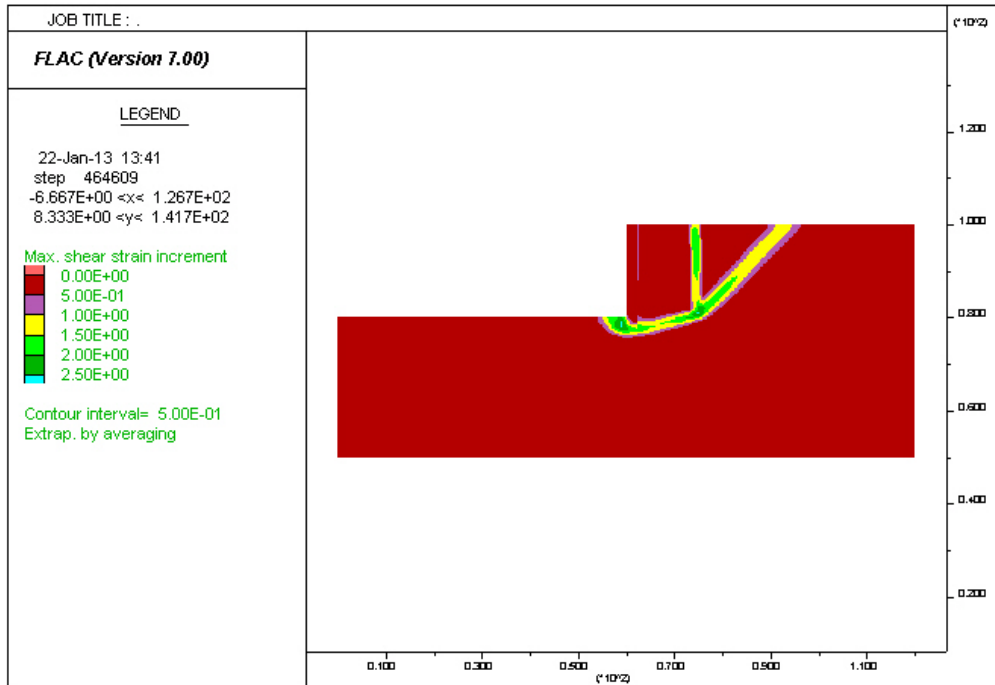


**Figure 136. Maximum Shear Strain for Case 2, Horizontal Fore Slope, Foundation Friction Angle = 30.**

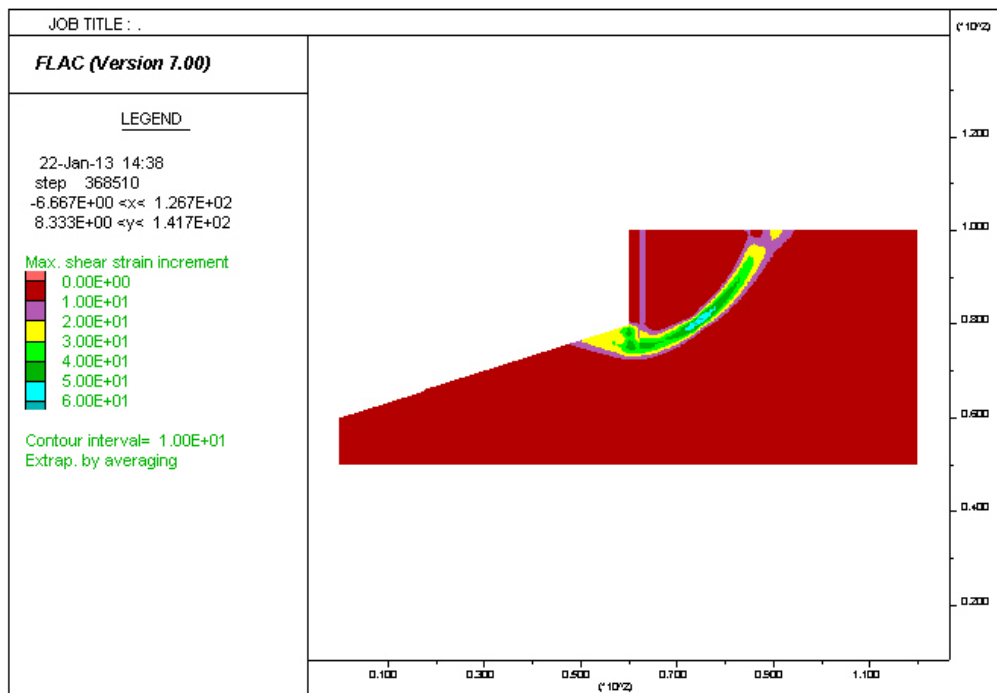


**Figure 137. Max Shear Strain Rate for Case 2, 3:1 Fore Slope, Foundation Friction Angle = 30.**

## **COMPOUND FAILURE ANALYSIS**

The compound failure analyses covered four situations, which are indicated in Figure 5, i.e., MSE walls with backslope (Figure 5(a)), multi-tiered MSE walls (Figure 5 (b)), MSE walls with foreslope (Figure 5 (c)), and MSE walls with foreslopes and shallow groundwater table (Figure 5 (d)). The compound analysis is a part of the global stability analyses for MSE walls with backslopes and the MSE walls with foreslopes since in the global stability analyses the connection between the precast panels were simulated and the critical surface was automatically searched.

### **MSE Walls with Backslopes**

The possible failure surfaces for MSE walls with backslopes are summarized in Figure 109–Figure 113. Clearly, the compound failure is not the governing failure modes.

### **MSE Walls with Foreslopes and with/without Shallow Water Table**

For the MSE walls with foreslopes, the compound failure is not the critical failure mode, namely, the failure plane did not go through the reinforced zones. Three different failure modes have been identified, which are shown in Figure 132, Figure 133, and Figure 139.

### **Two-Tiered MSE Wall**

A FLAC model was created for a two-tier MSE wall to find out the global stability and predict the compound failure for the situation shown in Figure 138. For the bottom tier, the height is 20 ft and the height of the top tier and the setback vary in the analysis. The friction angles of the backfill material, retained soil, and foundation soil were  $34^\circ$ ,  $30^\circ$ , and  $30^\circ$ , respectively. The cohesion was ignored for all the materials. All the unit weights were chosen to be 125 pcf.



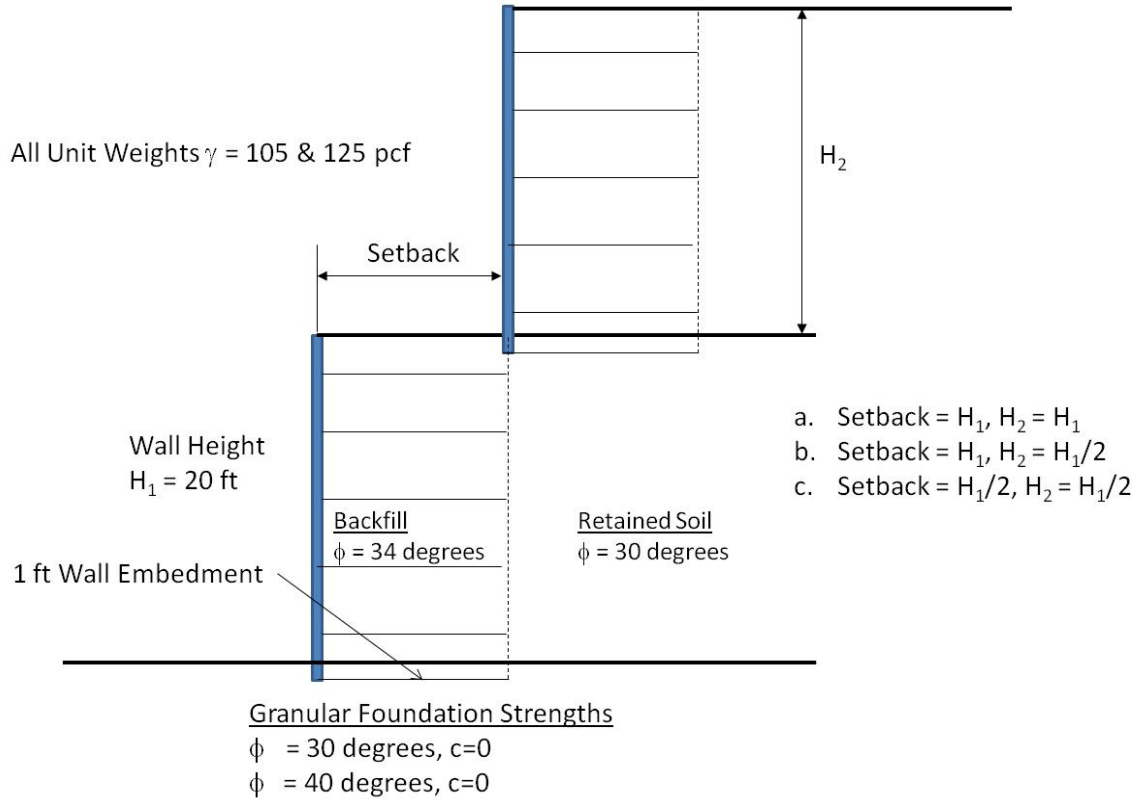


**Figure 138. Analysis of Compound Failure.**

### FLAC Model

The FLAC model was created with  $180 \times 120$  zones; each zone measures  $1 \text{ ft} \times 1 \text{ ft}$ . The boundary conditions were fixed in both horizontal and vertical directions at the bottom and fixed only in the horizontal direction on the right side. The left side, i.e., the block face and the top surface, was free to deform. Details of the FLAC model, such as properties of metallic reinforcement and precast panel, the connection between panels, can be found at the section of global stability of this report.

### Analysis in FLAC

No additional loads were applied, and the model was solved under gravity force only. The Mohr-Coulomb model was used as a constitutive model for all soils.

### Analysis Cases for Series 4

As stated before, there were eight analyses combinations. Eight separate models were developed to run the analysis of each case. Table 40 summarizes the cases and their corresponding FOSs.

**Table 40. Analyzed Cases for Series 4.**

| Case | Foundation Friction Angle (°) | Setback (ft) | H <sub>2</sub> (ft) | Reinforcement Length (ft)* |            | FOS  |
|------|-------------------------------|--------------|---------------------|----------------------------|------------|------|
|      |                               |              |                     | Lower Wall                 | Upper Wall |      |
| 1    | 30                            | 10           | 20                  | 21                         | 18         | 1.65 |
| 2    | 30                            | 10           | 10                  | 17                         | 14         | 1.67 |
| 3    | 30                            | 20           | 20                  | 30                         | 14         | 1.69 |
| 4    | 30                            | 20           | 10                  | 23                         | 9          | 1.67 |
| 5    | 40                            | 10           | 20                  | 21                         | 18         | 1.88 |
| 6    | 40                            | 10           | 10                  | 17                         | 14         | 1.79 |
| 7    | 40                            | 20           | 20                  | 30                         | 14         | 1.74 |
| 8    | 40                            | 20           | 10                  | 23                         | 9          | 1.94 |

\*The reinforcement length is provided by TxDOT.

For all the cases analyzed, no compound failure was identified. The critical surface went through a retained soil zone and exited through the interface between the foundation soil and backfill material. The failure surface of the analyzed cases can be simplified (see Figure 139). For all the cases analyzed, the critical planes are primarily in the upper wall. Basically, a circular failure surface was followed by a planar surface. The circular surface started from the top and propagated down to nearly the bottom elevation of the upper wall. The planar failure surface started from the bottom reinforcement layer and extended to the toe of the upper MSE wall. In addition, for some cases, there was a failure surface between the reinforced zone and retained zone for the bottom tier wall.

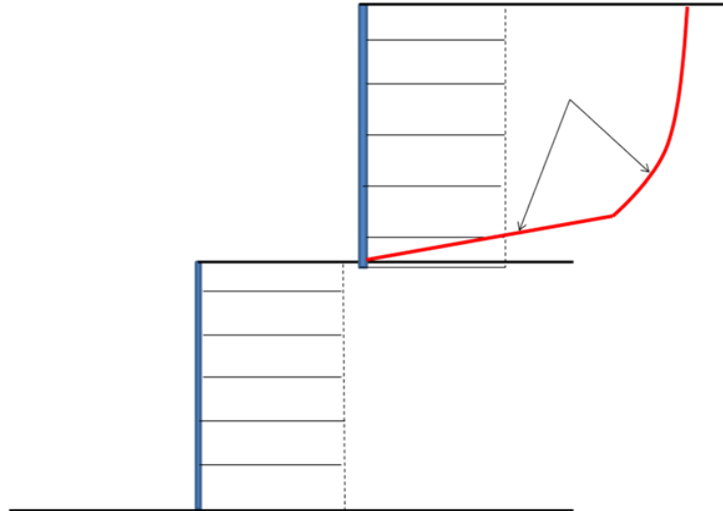


**Figure 139. General Failure Mode of a Two-Tier MSE Wall.**

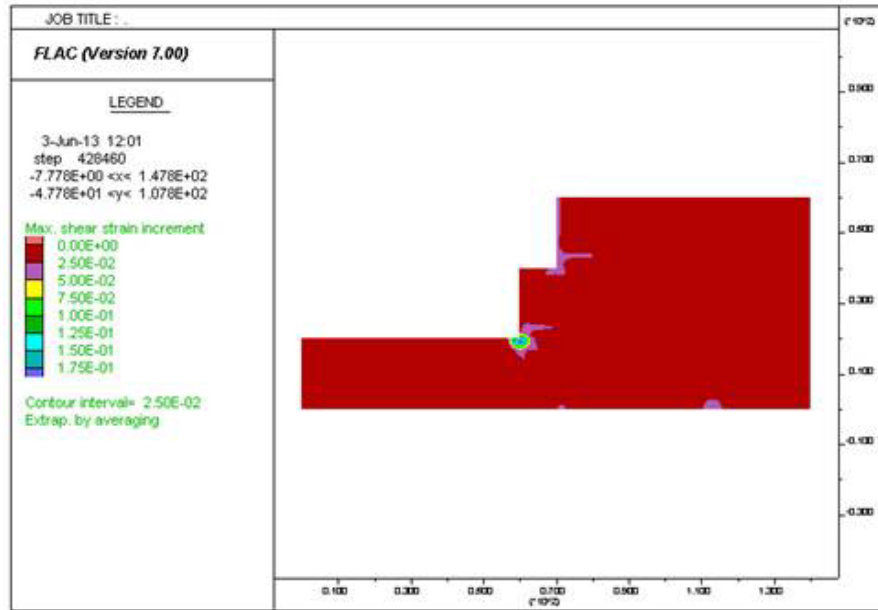


**Figure 140. Maximum Shear Strain for Setback of 10 ft and Second Wall Height of 20 ft with  $\phi=30^\circ$ .**

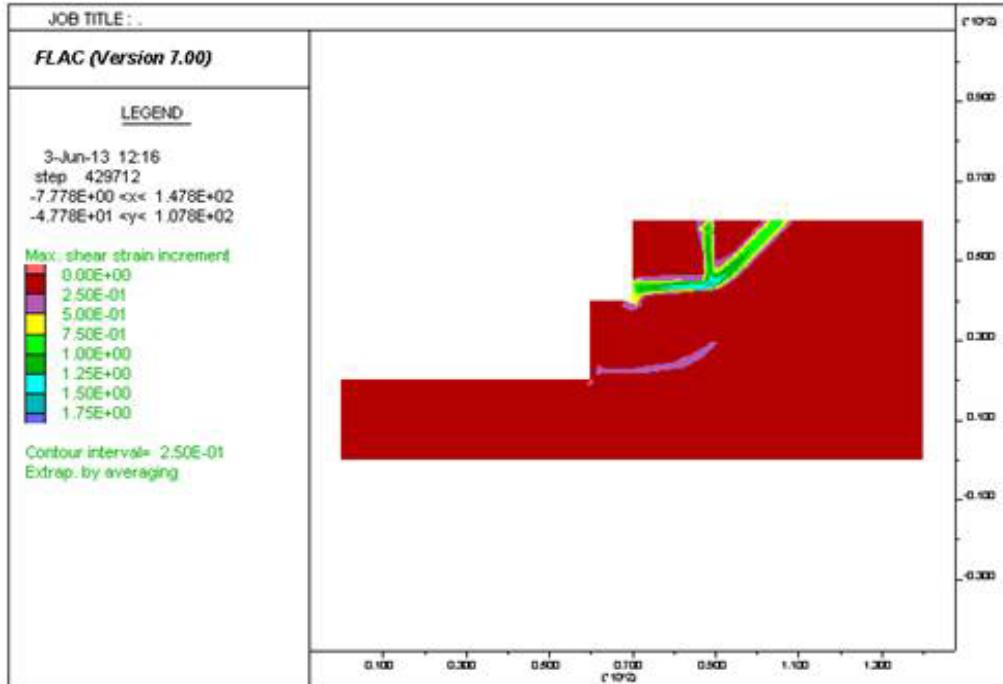


Figure 141. Maximum Shear Strain for Setback of 10 ft and Second Wall Height of 20 ft with  $\phi=40^\circ$ .

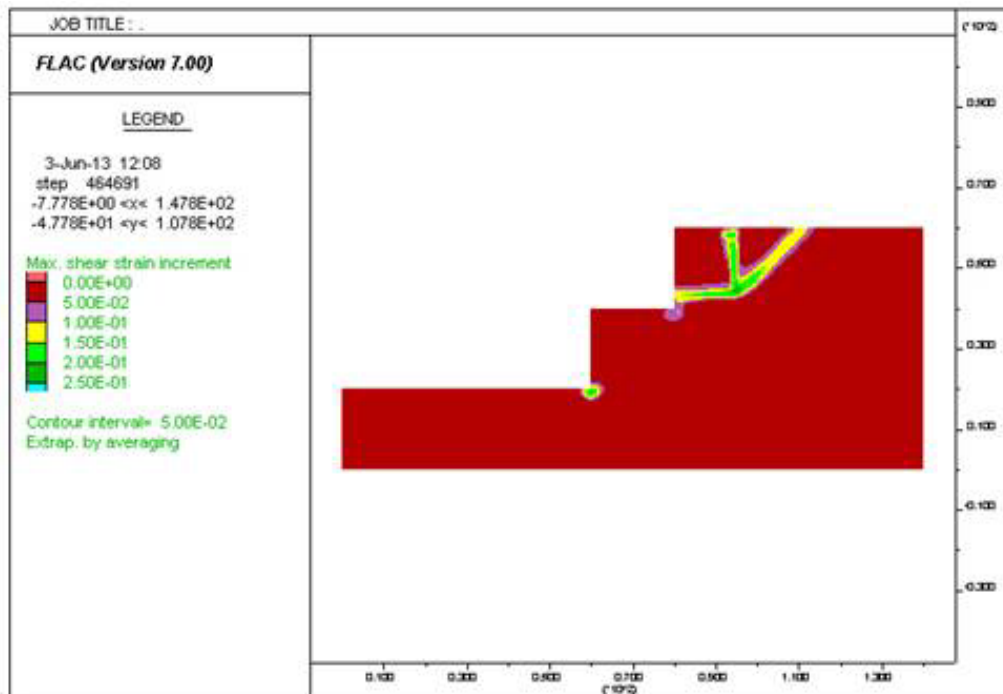
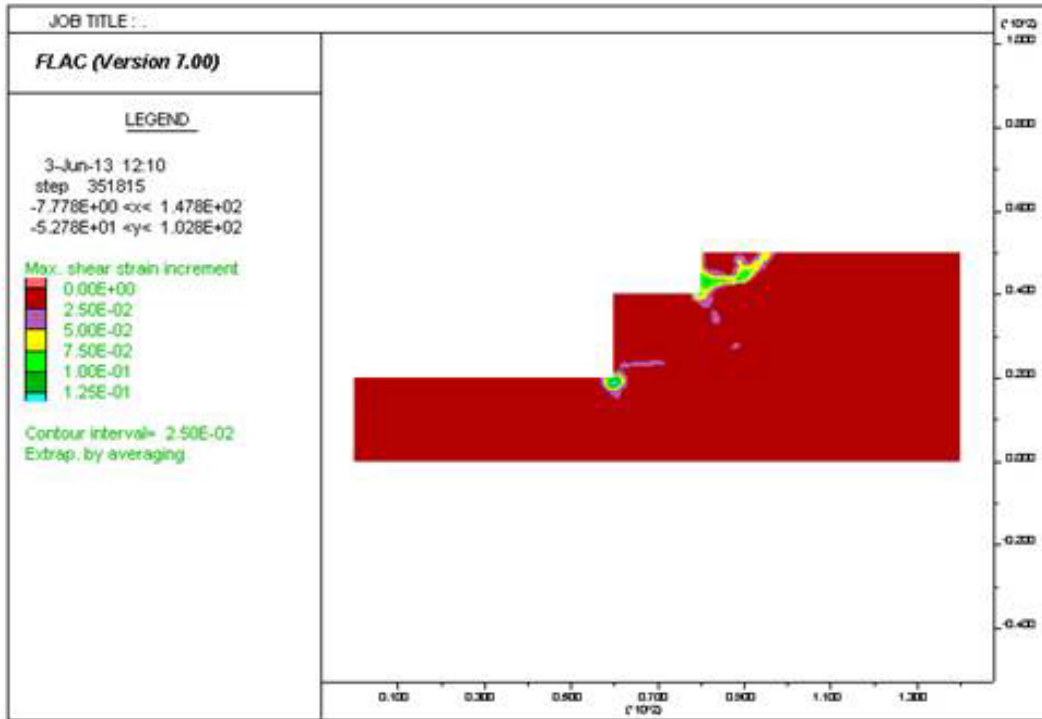


Figure 142. Maximum Shear Strain for Setback of 20 ft and Second Wall Height of 20 ft with  $\phi=30^\circ$ .



**Figure 143. Maximum Shear Strain for Setback of 20 ft and Second Wall Height of 10 ft with  $\phi=30^\circ$ .**



## CHAPTER 6: PARAMETRIC STUDY

### PARAMETRIC STUDY FOR SLIDING AND OVERTURNING ANALYSIS

In this section, researchers assessed the effect of unit weight and strength of the backfill and retaining soils on sliding FOS, as well as overturning FOS. Two different types of wall geometry with cohesionless soil were performed. First, a wall with geometry of 20 ft height and no back slope was considered, and then a wall of 20 ft height with 3H:1V back slope was considered.

#### Horizontal Back Slope

**Figure 144. MSE Wall with 20 ft Wall Height and Horizontal Back Slope.**

For the MSE wall with a geometry shown in Figure 144, initially a unit weight of 105 pcf was assigned to the backfill and retaining soils. Then, this weight was increased to 125 pcf for backfill soil with 105 pcf for retaining soil and vice-versa, to see the effect on FOS against sliding.

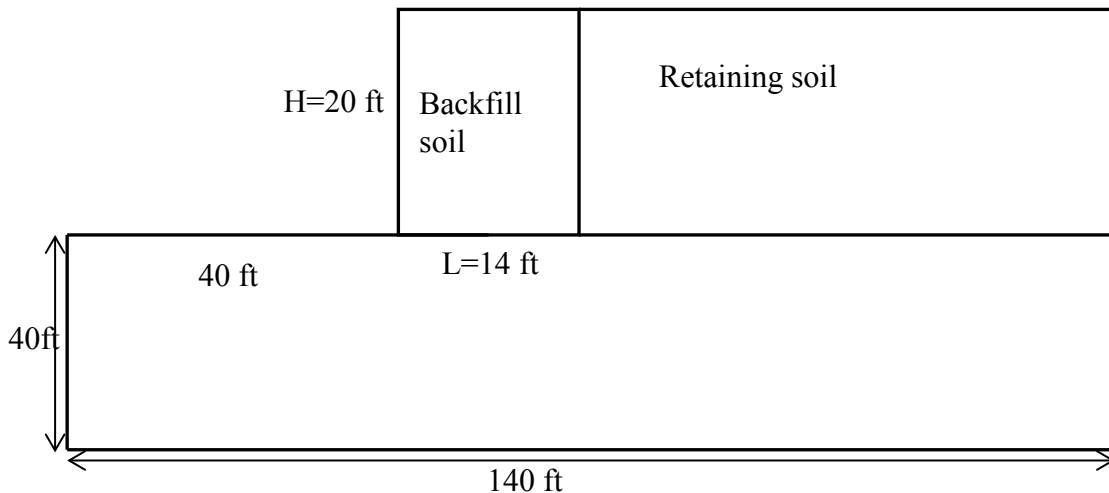


**Figure 145. MSE Wall with 20 ft Wall Height and Horizontal Back Slope.**

The results for this parametric study are presented below. The equations used to calculate FOS for sliding and overturning are shown. These equations are as per AASHTO 2002 manual for MSE retaining walls (AASHTO 2002):

$$F_{driving} = \frac{1}{2} K_a \times \gamma_{ret} \times H^2 \quad (\text{Eq. 25})$$

$$F_{resisting} = W \times \tan \delta_b \quad (\text{Eq. 26})$$

$$W = \gamma_{back} \times L \times H \quad (\text{Eq. 27})$$

$$FOS_{Sliding} = \frac{F_{resisting}}{F_{driving}} \quad (\text{Eq. 28})$$

$$M_{driving} = \frac{1}{2} K_a \times \gamma_{ret} \times H^2 \times \frac{H}{3} \quad (\text{Eq. 29})$$

$$M_{resisting} = W \times \frac{L}{2} \quad (\text{Eq. 30})$$

$$FOS_{overturning} = \frac{M_{resisting}}{M_{driving}} \quad (\text{Eq. 31})$$

To have a better understanding of the effect of unit weight of backfill and retaining soils on FOS for sliding and overturning, it is necessary to plot different FOS values for different  $\phi_{retaining}$  and  $\phi_{foundation}$  with respect to ratio of unit weights. For the above given geometry, FOS values with respect to ratio of unit weights are plotted for three different  $\phi_{retaining}$  in an one plot by fixing  $\phi_{foundation}$  and repeating the same procedure for different  $\phi_{foundation}$ . Noting that retained soil and backfill unit weights can plausibly vary from 105–125 pcf, the unit weight ratio  $\gamma_{back}/\gamma_{retain}$  in Figure 146–Figure 149 can be realistically considered to vary from 0.84–1.19. Thus, an adverse distribution of unit weights—say  $\gamma_{back} = 105$  pcf and  $\gamma_{retain} = 125$  pcf—can lead to FOSs on the order of 20 percent lower than would occur for the case of a homogeneous ( $\gamma_{back}/\gamma_{retain} = 1$ ) unit weight distribution. The overall implications of this issue do not appear very serious. For example, for the case of a relatively low strength foundation,  $\phi_{found} = 26^\circ$ , the FOS for the uniform unit weight case is about 2.1. For a fairly severe adverse case  $\gamma_{back}/\gamma_{retain} = 0.84$ , the FOS reduces to about 1.5, which is still acceptable. Nevertheless, the potential for a reduced safety factor due to an adverse distribution of unit weights should noted, particularly for situations with marginal FOSs.



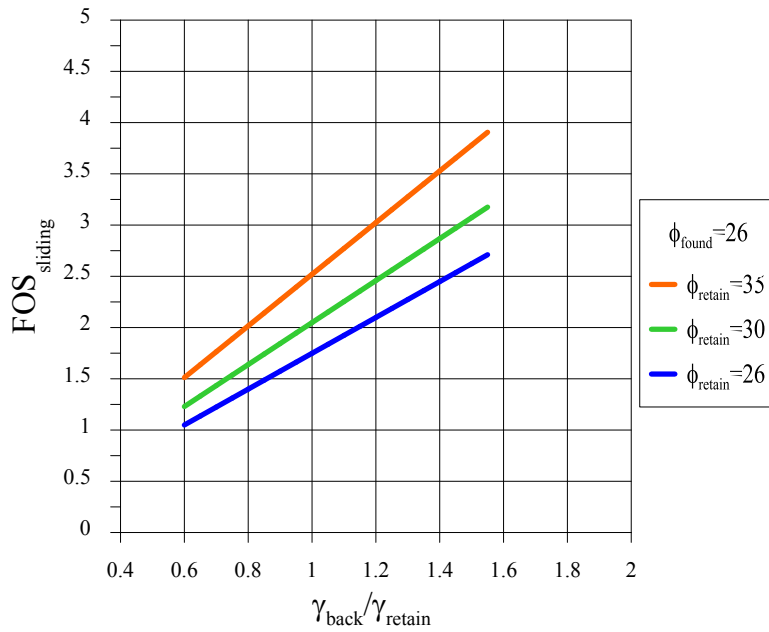


**Figure 146. Factor of Safety against Sliding for a 20-ft Wall Height with No Back Slope for Different  $\phi_{retaining}$  at a Constant  $\phi_{found}=26^\circ$ .**

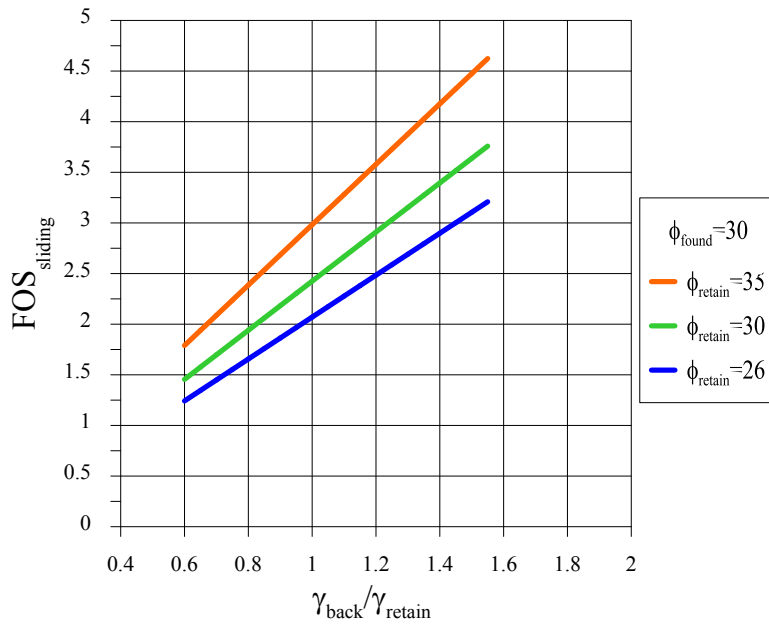


**Figure 147. Factor of Safety against Sliding for a 20-ft Wall Height with No Back Slope for Different  $\phi_{retaining}$  at a Constant  $\phi_{found}=30^\circ$ .**

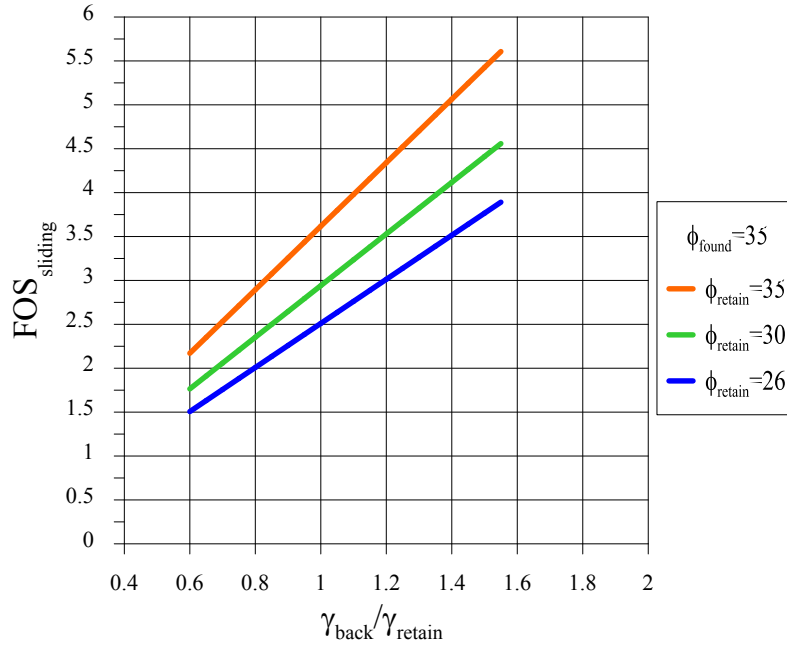


**Figure 148. Factor of Safety against Sliding for a 20-ft Wall Height with No Back Slope for Different  $\phi_{retaining}$  at a Constant  $\phi_{found} = 35^\circ$ .**

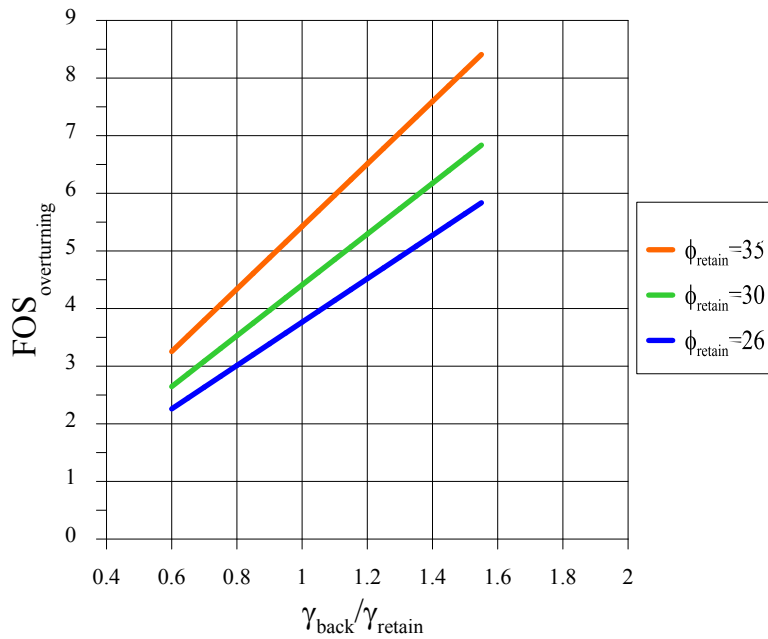


**Figure 149. Factor of Safety against Overturning for a 20-ft Wall Height with No Back Slope for Different  $\phi_{retaining}$ .**

A detailed analysis on FOS influenced by  $\phi$  (retaining) and  $\phi$  (foundation) for two different weights for retaining and backfill soils is plotted below. These plots are mainly to show the contribution of  $\phi$  (foundation) on FOS.

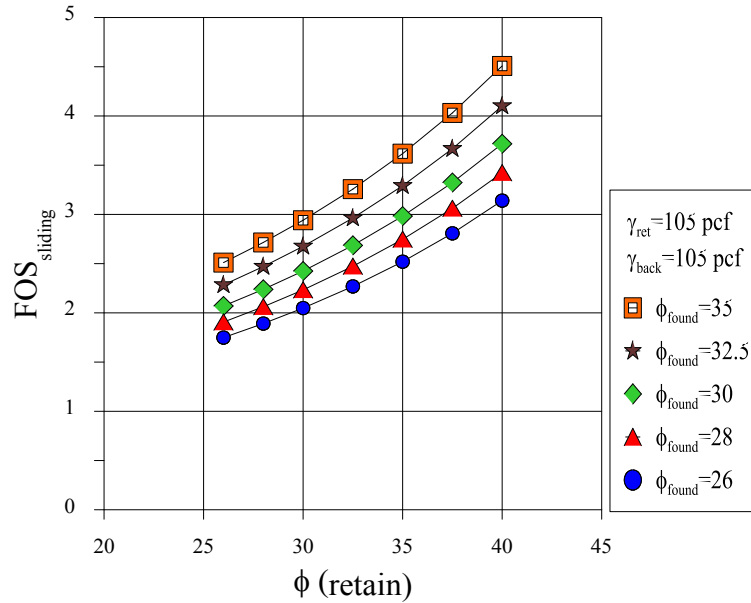


**Figure 150. Factor of Safety against Sliding for a 20-ft Wall Height with No Back Slope with  $\gamma_{\text{ret}}=105$  pcf and  $\gamma_{\text{back}}=105$  pcf for Different Friction Angles.**

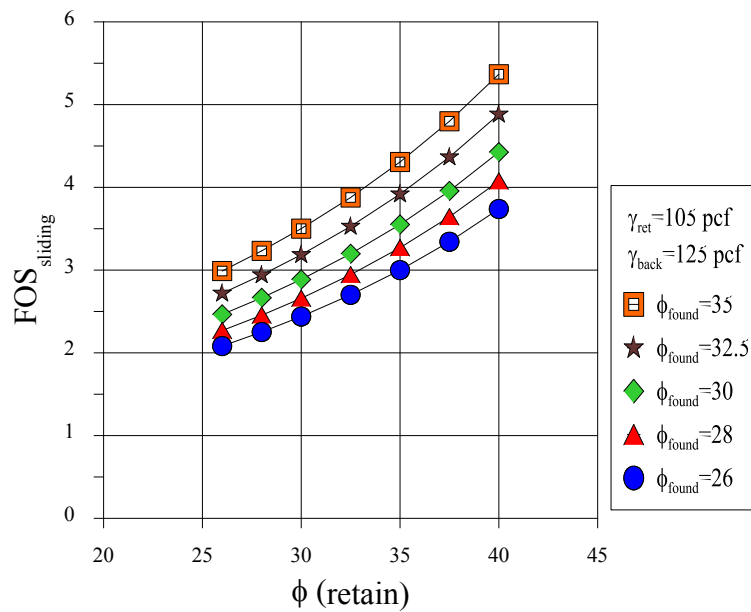


**Figure 151. Factor of Safety against Sliding for a 20-ft Wall Height with No Back Slope with  $\gamma_{\text{ret}}=105$  pcf and  $\gamma_{\text{back}}=125$  pcf for Different Friction Angles.**

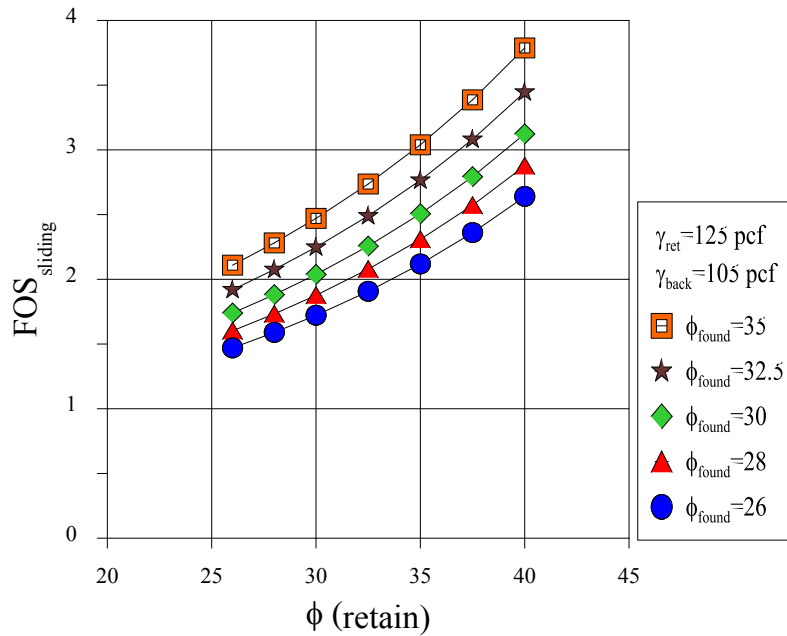


**Figure 152. Factor of Safety against Sliding for a 20-ft Wall Height with No Back Slope with  $\gamma_{ret}=125$  pcf and  $\gamma_{back}=105$  pcf for Different Friction Angles.**

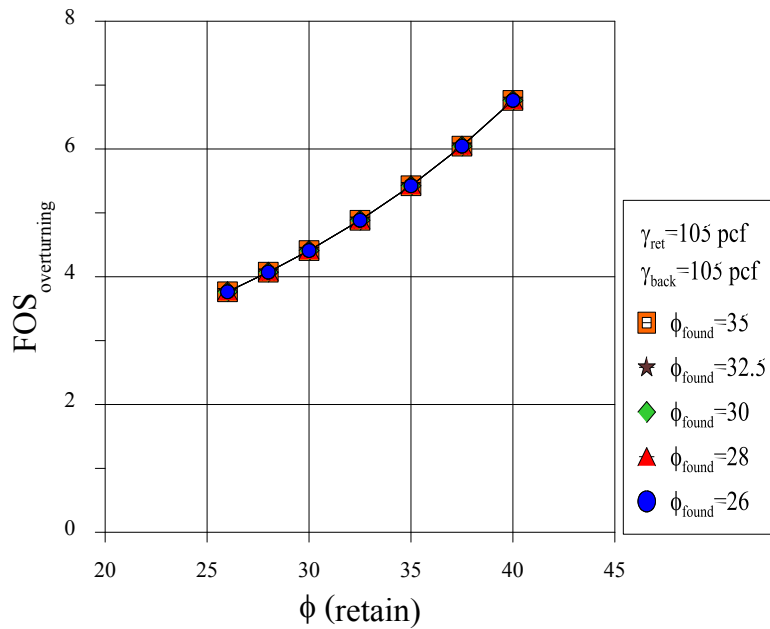


**Figure 153. Factor of Safety against Overturning for a 20-ft Wall Height with No Back Slope with  $\gamma_{ret}=105$  pcf and  $\gamma_{back}=105$  pcf for Different Friction Angles.**

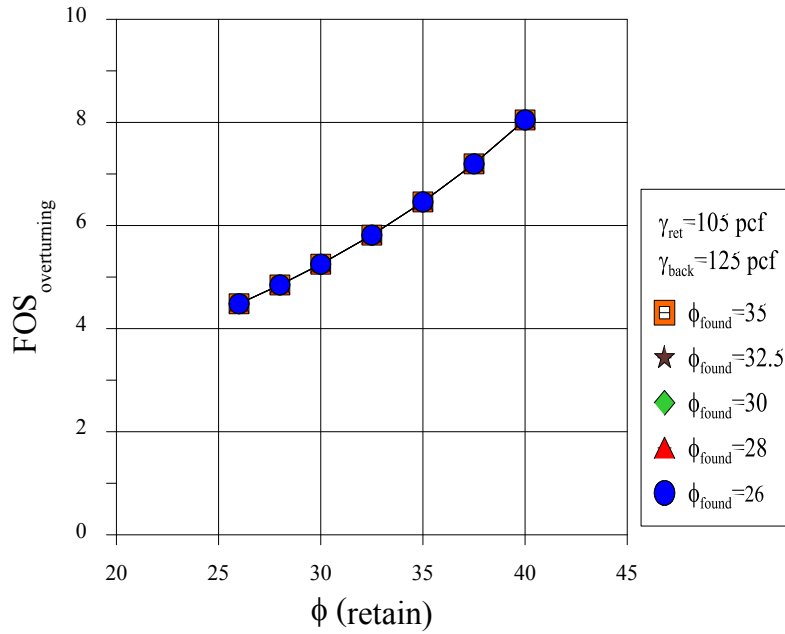


**Figure 154. Factor of Safety against Overturning for a 20-ft Wall Height with No Back Slope with  $\gamma_{ret}=105$  pcf and  $\gamma_{back}=125$  pcf for Different Friction Angles.**

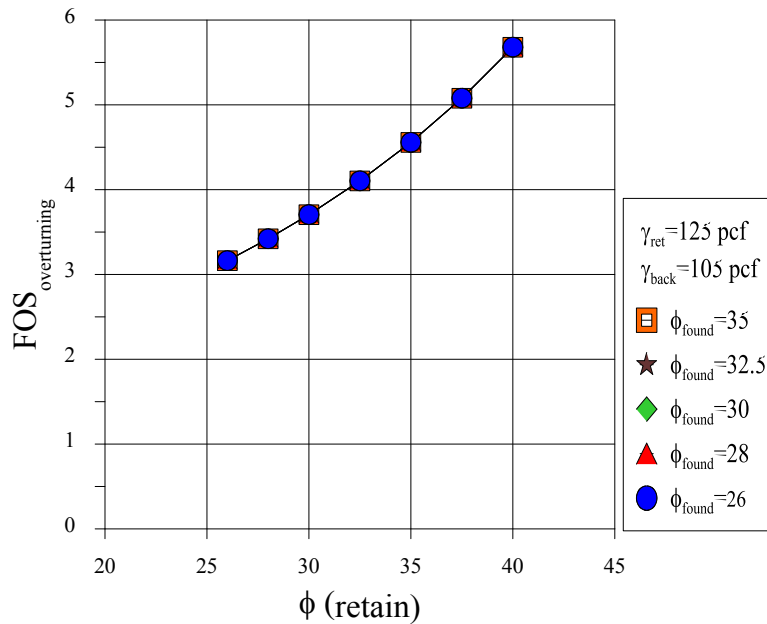


**Figure 155. Factor of Safety against Overturning for a 20-ft Wall Height with No Back Slope with  $\gamma_{ret}=125$  pcf and  $\gamma_{back}=105$  pcf for Different Friction Angles.**

### 3H:1V Back Slope

Similarly a parametric study was conducted on an MSE wall with 3H:1V back slope for a 20-ft wall height. The results are presented below for sliding analysis and overturning analysis with the same criterion used for no back slope case.

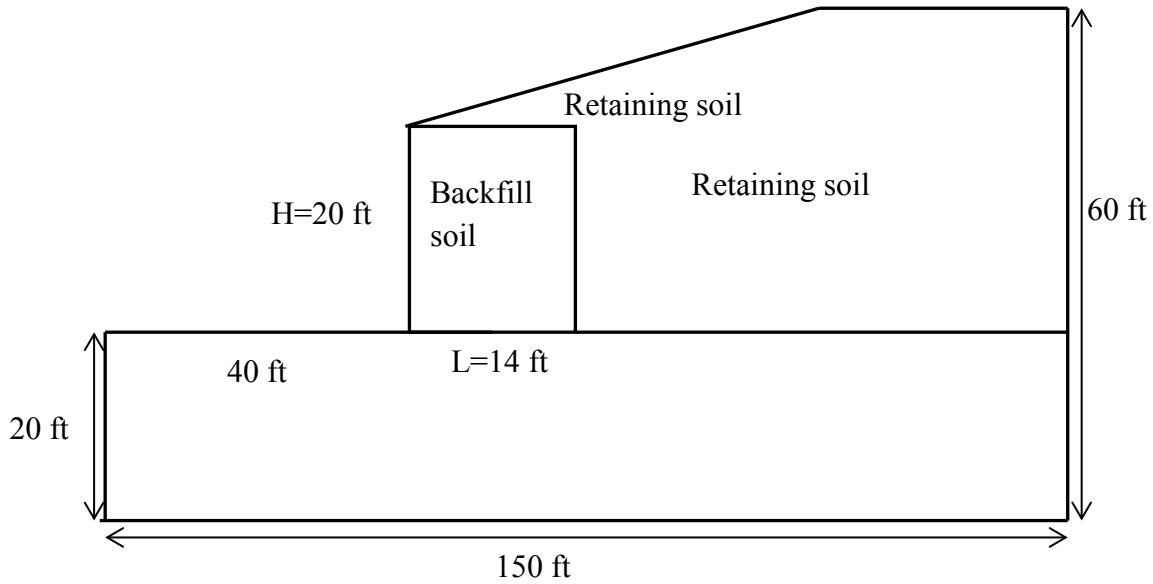


**Figure 156. MSE Wall with 20-ft Wall and 3H:1V Back Slope.**

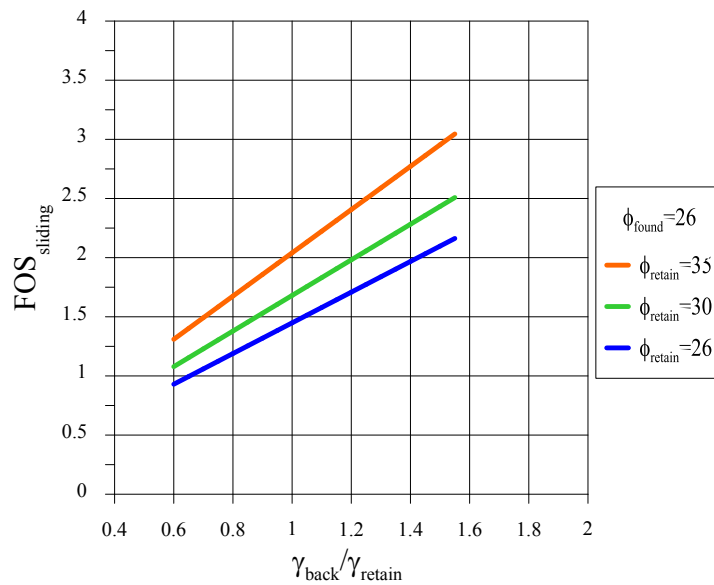


**Figure 157. Factor of Safety against Sliding for a 20-ft Wall Height with 3H:1V Back Slope for Different  $\phi_{retaining}$  at a Constant  $\phi_{found}=26^\circ$ .**

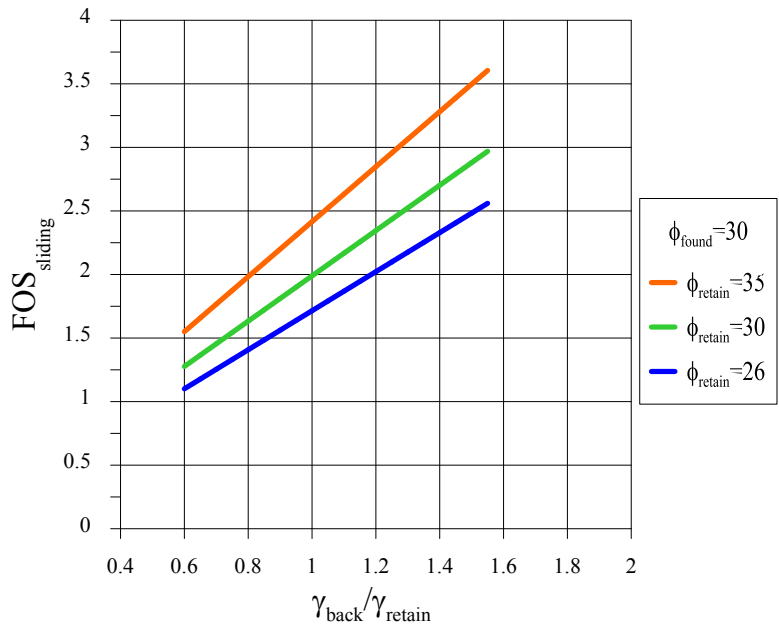


**Figure 158. Factor of Safety against Sliding for a 20-ft Wall Height with 3H:1V Back Slope for Different  $\phi_{retaining}$  at a Constant  $\phi_{found}=30^\circ$ .**

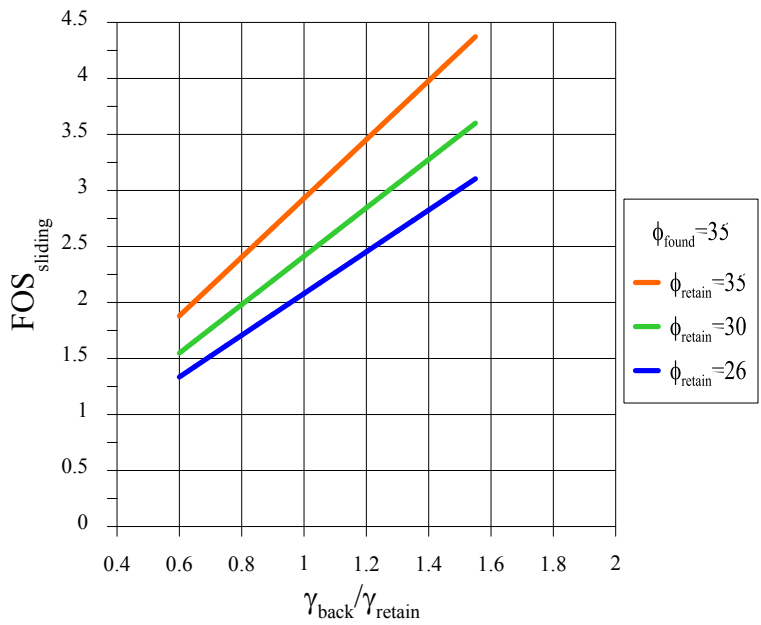


**Figure 159. Factor of Safety against Sliding for a 20-ft Wall Height with 3H:1V Back Slope for Different  $\phi_{retaining}$  at a Constant  $\phi_{found}=35^\circ$ .**

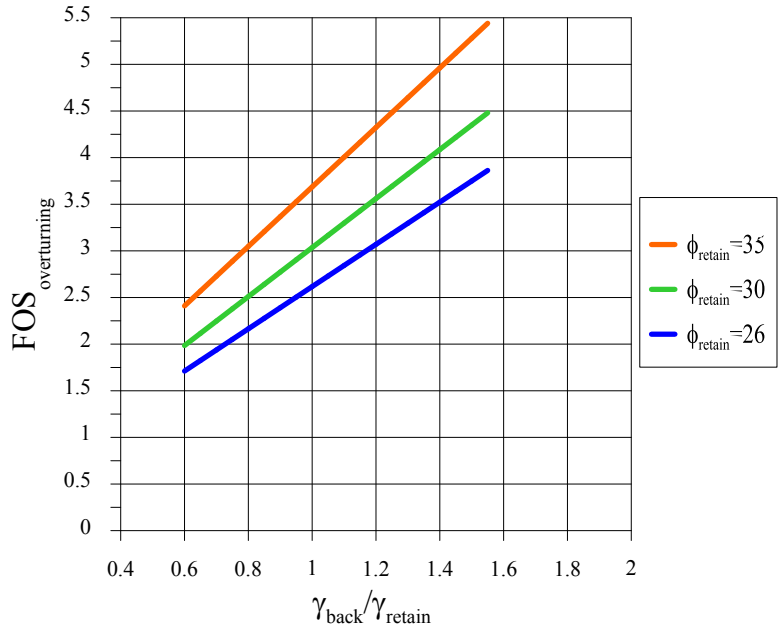


**Figure 160. Factor of Safety against Overturning for a 20-ft Wall Height with 3H:1V Back Slope for Different  $\phi_{retaining}$ .**

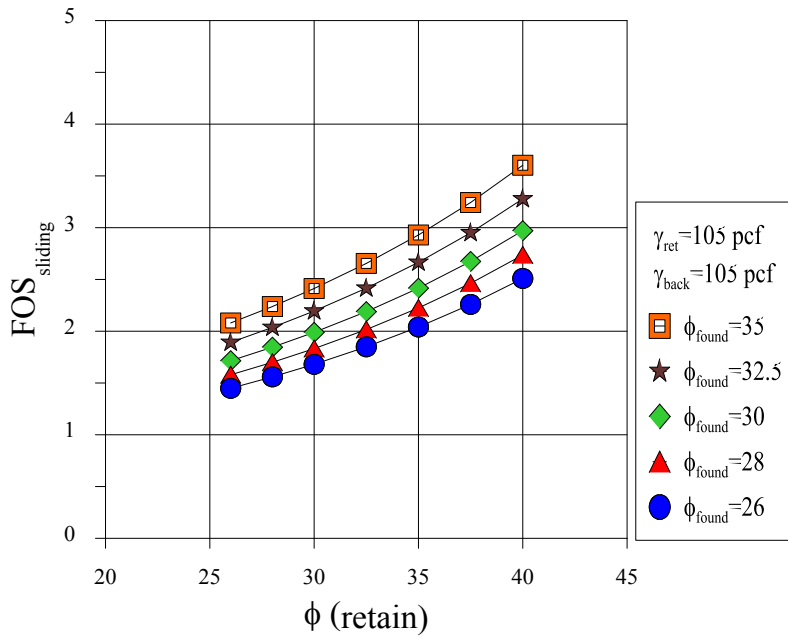


**Figure 161. Factor of Safety against Sliding for a 20-ft Wall Height with 3H:1V Back Slope with  $\gamma_{ret}=105$  pcf and  $\gamma_{back}=105$  pcf for Different Friction Angles.**



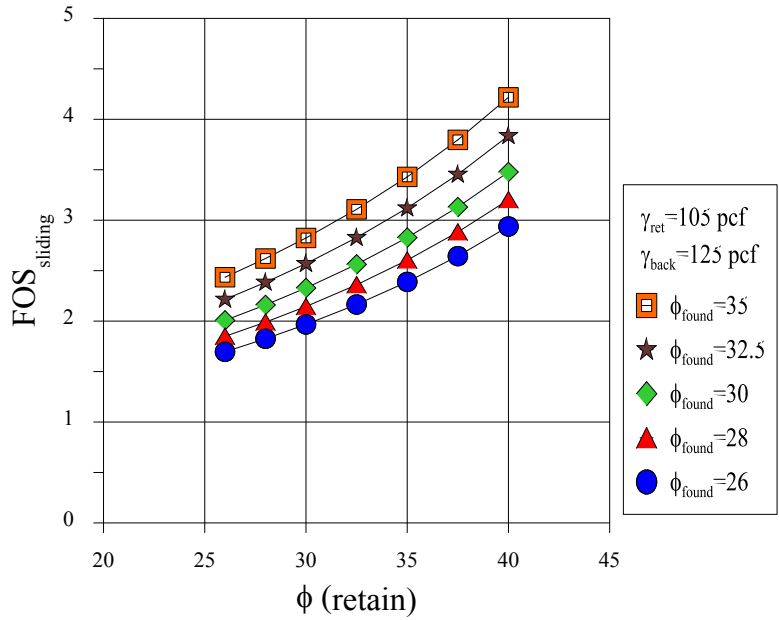


**Figure 162. Factor of Safety against Sliding for a 20-ft Wall Height with 3H:1V Back Slope with  $\gamma_{ret}=105$  pcf and  $\gamma_{back}=125$  pcf for Different Friction Angles.**

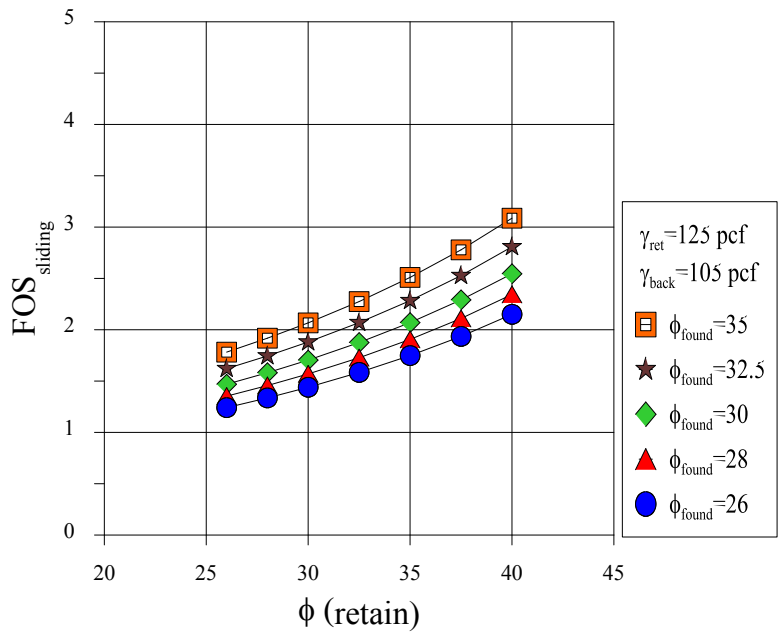


**Figure 163. Factor of Safety against Sliding for a 20-ft Wall Height with 3H:1V Back Slope with  $\gamma_{ret}=125$  pcf and  $\gamma_{back}=105$  pcf for Different Friction Angles.**

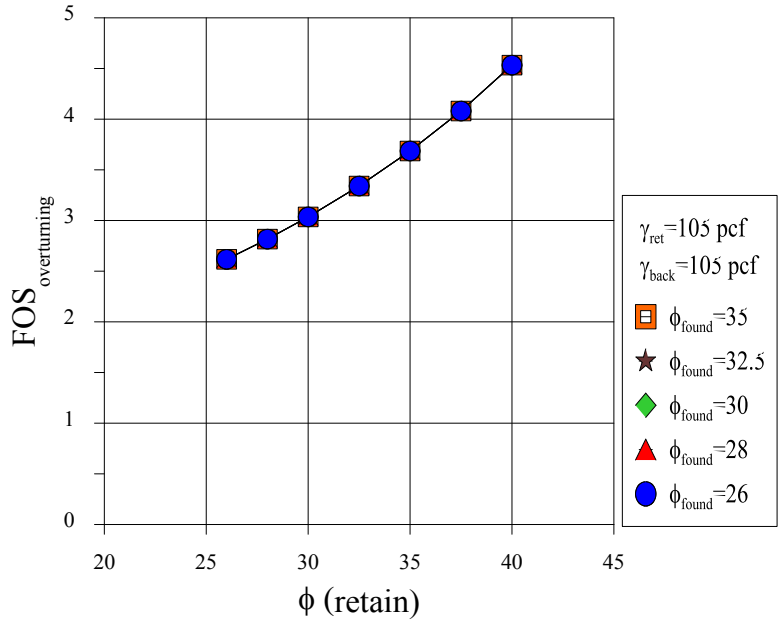


**Figure 164. Factor of Safety against Overturning for a 20-ft Wall Height with 3H:1V Back Slope with  $\gamma_{ret}=105$  pcf and  $\gamma_{back}=105$  pcf for Different Friction Angles.**

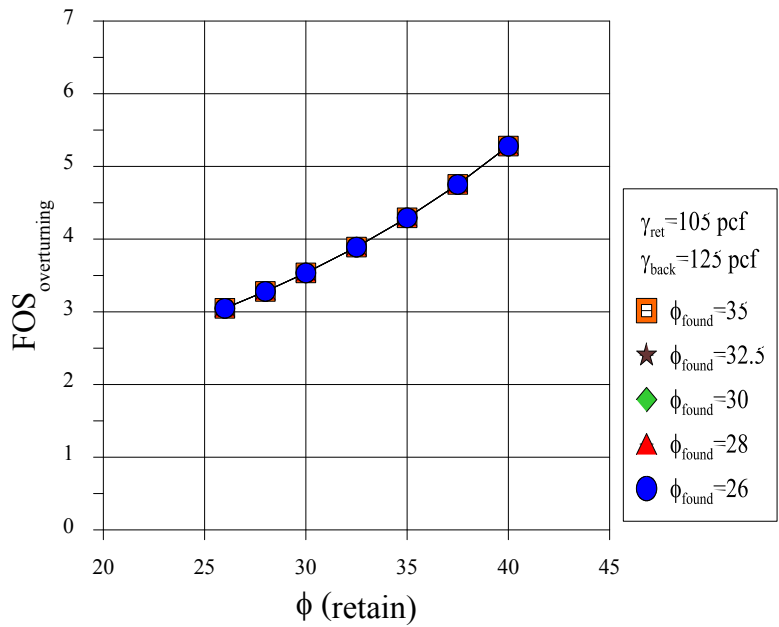


**Figure 165. Factor of Safety against Overturning for a 20-ft Wall Height with 3H:1V Back Slope with  $\gamma_{ret}=105$  pcf and  $\gamma_{back}=125$  pcf for Different Friction Angles.**

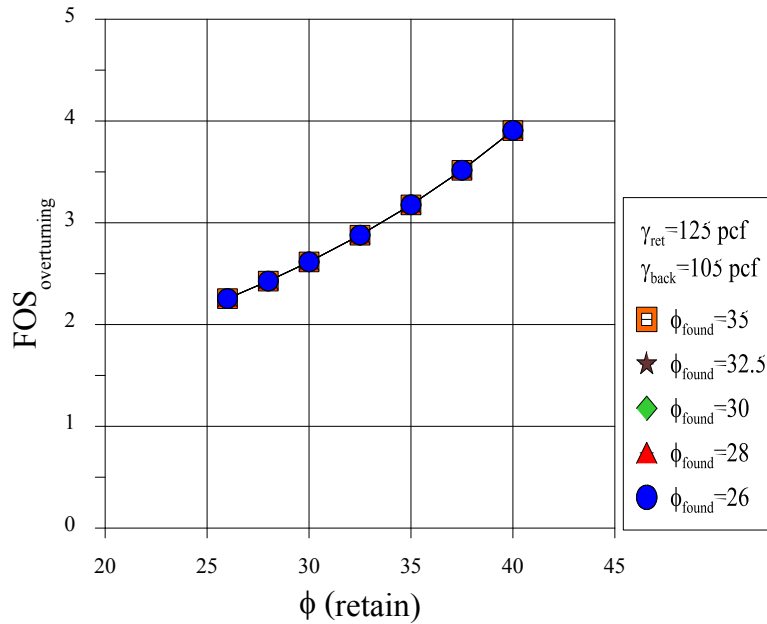


**Figure 166. Factor of Safety against Overturning for a 20-ft Wall Height with 3H:1V Back Slope with  $\gamma_{ret}=125$  pcf and  $\gamma_{back}=105$  pcf for Different Friction Angles.**

## Conclusion

The results from the above cases show that it is important to consider the effect of unit weight of backfill and retaining soils on FOS calculations.

- Increasing  $\gamma_{back}$  from 105 pcf to 125 pcf with  $\gamma_{ret}$  maintained at a constant value of 105 pcf increases the FOS against sliding by 19 percent and FOS against overturning by 19 percent for the case of a wall height of 20 ft with no back slope.
- Increasing  $\gamma_{ret}$  from 105 pcf to 125 pcf with  $\gamma_{back}$  maintained at a constant value of 105 pcf decreases the FOS against sliding and FOS against sliding by 16 percent for the case of a wall height of 20 ft with no back slope.
- For a wall height of 20 ft and 3H:1V back slope, increasing the unit weight of backfill from 105 pcf to 125 pcf increases the FOS against sliding by 17 percent and the FOS against overturning by 16.5 percent as compared to assigning the same unit weights for both types of soils.
- For a wall height of 20 ft and 3H:1V back slope, the FOS against sliding decreases by 14.3 percent and the FOS against overturning decreases by 13.9 percent when the unit

weight of the retained soil is increased from 105 pcf to 125 pcf with a constant backfill unit weight of 105 pcf.

- In general, the ratio  $\gamma_{\text{back}}/\gamma_{\text{retain}}$  has a significant influence on FOS for sliding as well as overturning. The trends are illustrated in Figure 146–Figure 149 and Figure 157–Figure 160.

## PARAMETRIC STUDY USING FLAC SIMULATIONS

### Analysis for Cohesionless Soils

The FLAC simulations are performed for two different geometries and for two different soil types via sands and clays. This section describes the model parameters used in two different wall types and the effect of variation of material parameters.

#### *Model Geometry*

A total of three wall geometries are considered for this parametric study as shown in Figure 167–Figure 169. First, two 20-ft walls are considered: one with no back slope and the other with 3H:1V back slope. In addition, a 10-ft wall with no back slope is analyzed. Figure 167–Figure 169 show the three walls analyzed. All walls use 5-ft panel heights. For the 20-ft wall, the length of reinforcement is 14 ft (0.7H); for the 10-ft wall, an 8-ft reinforcement length is used (AASHTO 2002). The embedment depth was taken as 0 for this study, recognizing that the results will be slightly conservative.

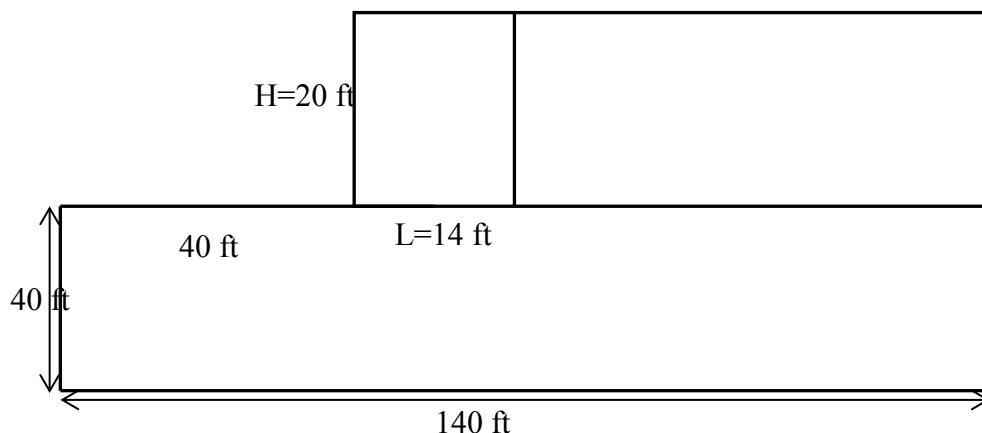


**Figure 167. MSE Wall with a 20-ft Wall Height and No Back Slope Model Geometry for FLAC.**

The dimensions shown in Figure 167 are used for FLAC simulation for a 20-ft wall height. The 90-ft width of the model was sufficiently large to minimize boundary effects. The depth of foundation was taken as twice the wall height, again, to minimize boundary effects. The selected grid size was 0.5 ft in y-direction and 1 ft in x-direction.

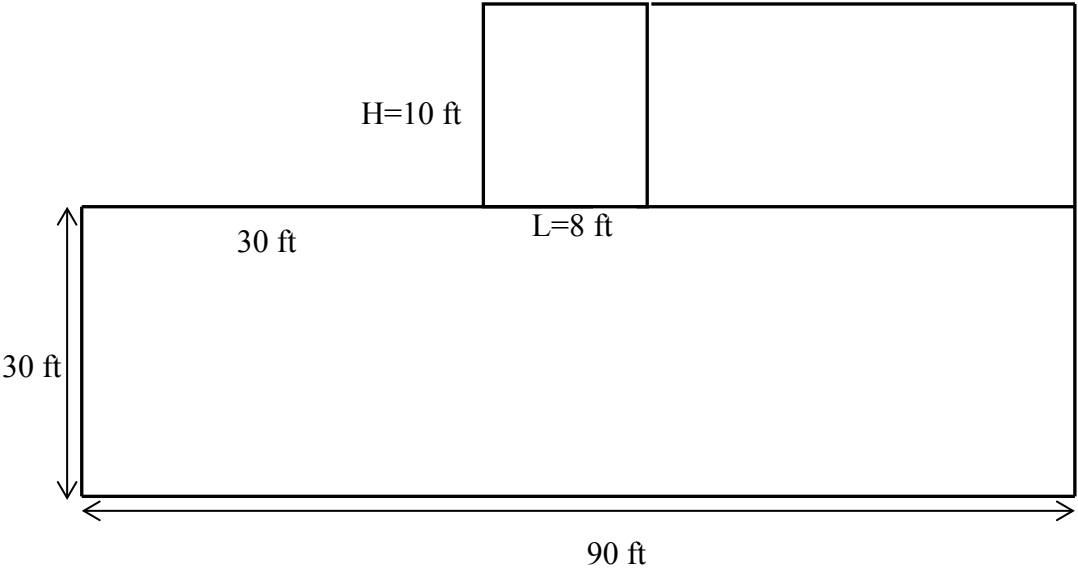


**Figure 168. MSE Wall with a 10-ft Wall Height and No Back Slope.**

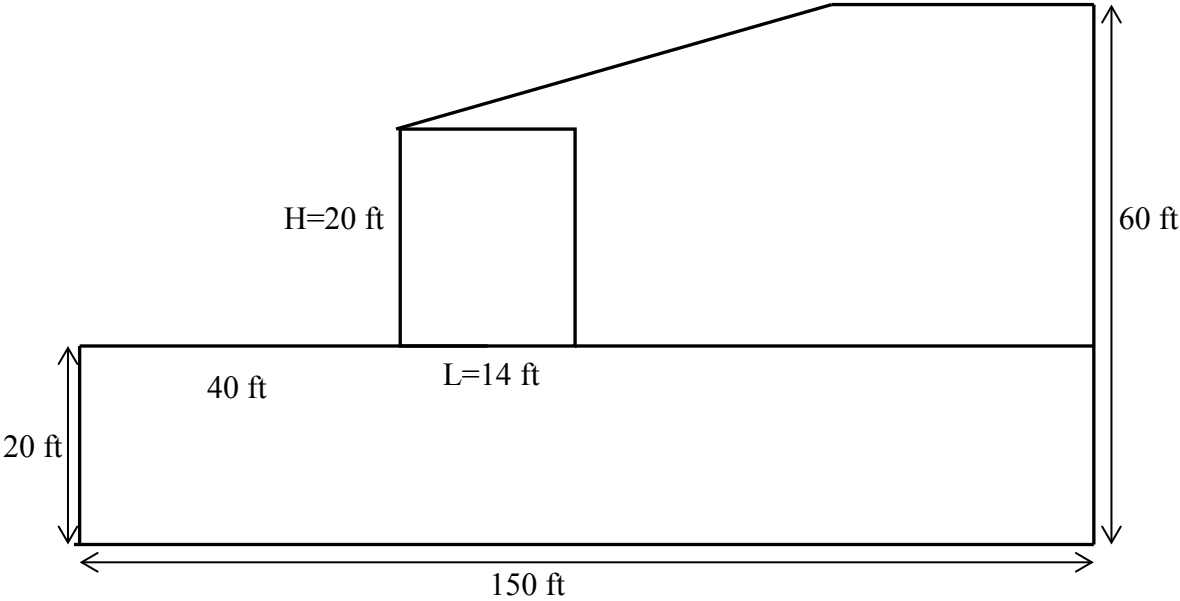


**Figure 169. MSE Wall with a 20-ft Wall and 3H:1V Back Slope.**

Figure 167–Figure 169 show the dimensions used in the FLAC simulations to calculate stresses at the back boundary of the backfill and at the base of the MSE wall. Stresses calculated from FLAC are used to compute design parameters that are used to calculate FOS for sliding and comparing these parameters with AASHTO design (AASHTO 2002).

*Material Parameters*

The soil model used in this study is the Mohr-Coulomb model for backfill, retaining wall, and for foundation soils. Table 41 lists the properties of these soils. The model was run with a dilation angle and without a dilation angle to see the effect on stresses and on FOS. The dilation angle values used in this parametric study was 10°. The friction angle for retaining soils and foundation soils are modified as shown in Table 42 for each case to see the effect of foundation soil on sliding friction as well as the effect of retaining soils on base friction.

**Table 41. Material Properties for Frictional Backfill, Retaining Materials, and Frictional Foundation Material.**

| Type       | Elastic Modulus* (psf) | Bulk Modulus (psf) | Shear Modulus (psf) | v (Poisson's Ratio) | φ    |
|------------|------------------------|--------------------|---------------------|---------------------|------|
| Foundation | 2.116 E6               | 3.643 E6           | 0.364 E6            | 0.4516              | 26   |
|            |                        |                    |                     |                     | 28   |
|            |                        |                    |                     |                     | 30   |
|            |                        |                    |                     |                     | 32.5 |
|            | 4.232 E6               | 7.287 E6           | 0.728 E6            | 0.4516              | 35   |
| Retaining  | 2.116 E6               | 3.643 E6           | 0.364 E6            | 0.4516              | 26   |
|            |                        |                    |                     |                     | 28   |
|            |                        |                    |                     |                     | 30   |
|            |                        |                    |                     |                     | 32.5 |
|            | 4.232 E6               | 7.287 E6           | 0.728 E6            | 0.4516              | 35   |
|            |                        |                    |                     |                     | 37.5 |
|            |                        |                    |                     |                     | 40   |
| Backfill   | 4.232 E6               | 7.287 E6           | 0.728 E6            | 0.4516              | 34   |

\* Elastic modulus for sand is taken as  $1000 \cdot P_{atm}$  where  $P_{atm} = 2116.216$  psf (Kulhawy and Mayne 1990)

**Table 42. Matrix of Properties Changed in FLAC Simulation for Three Different Wall Types.**

|                   |      | MSE Wall with Backfill $\phi=34^\circ$ , $\gamma=105$ pcf |    |    |      |    |      |    |
|-------------------|------|---|----|----|------|----|------|----|
|                   |      | $\phi$ (Retain)   |    |    |      |    |      |    |
|                   |      | 26  | 28 | 30 | 32.5 | 35 | 37.5 | 40 |
| $\phi$<br>(Found) | 26   | x   | x  | x  | x    | x  | x    | x  |
|                   | 28   | x   | x  | x  | x    | x  | x    | x  |
|                   | 30   | x   | x  | x  | x    | x  | x    | x  |
|                   | 32.5 | x   | x  | x  | x    | x  | x    | x  |
|                   | 35   | x   | x  | x  | x    | x  | x    | x  |

*Boundary Conditions*

The boundary conditions for all three wall geometries are as follows. Zero displacement is imposed in the x and y directions at the base of model, and in the x direction on both sides of the model. MSE wall panels used in this model are 5 ft high, and zero relative displacement is imposed at the junctions between the panels. Each panel has three strips in the vertical direction (i.e., y direction) and two strips in the horizontal direction (i.e., z direction) for a total of six strips per panel. The spacing for these strips is shown in Figure 170. The wall is constructed without embedment to simplify the stress calculations. The length for strips used in this model is 14 ft (i.e., 0.7H) for a 20-ft wall and 8 ft for a 10-ft wall height.

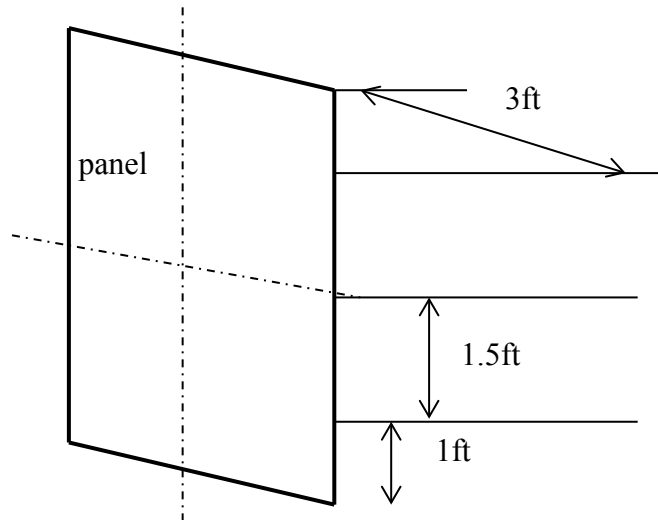


**Figure 170. Strips Spacing for Each Panel of MSE Wall.**

### *FLAC Calculation Process*

Each analysis is solved in stages to simulate the construction sequence for an actual MSE wall. First, a foundation layer is solved for equilibrium conditions under gravity loads and then the first MSE wall layer is added and solved for the same loads for equilibrium conditions. This sequence is continued to build a 20-ft wall in four layers and a 10-ft wall in two layers. Once the wall is solved for equilibrium conditions, the model was solved for failure condition by reducing the strength of material. In this case, strength was reduced gradually until failure occurred. The FOS is defined as:

$$FOS_{flac} = \frac{\tan \phi_{eq}}{\tan \phi_f} \quad \text{(Eq. 32)}$$

where

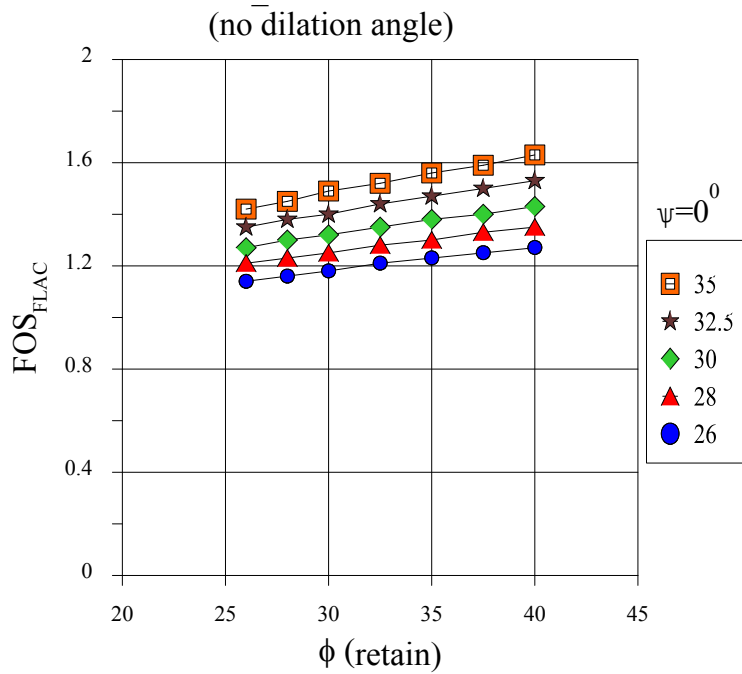
$FOS_{flac}$  = Factor of Safety calculated by FLAC.

$\tan \phi_{eq}$  = Tangent of internal friction angle at equilibrium.

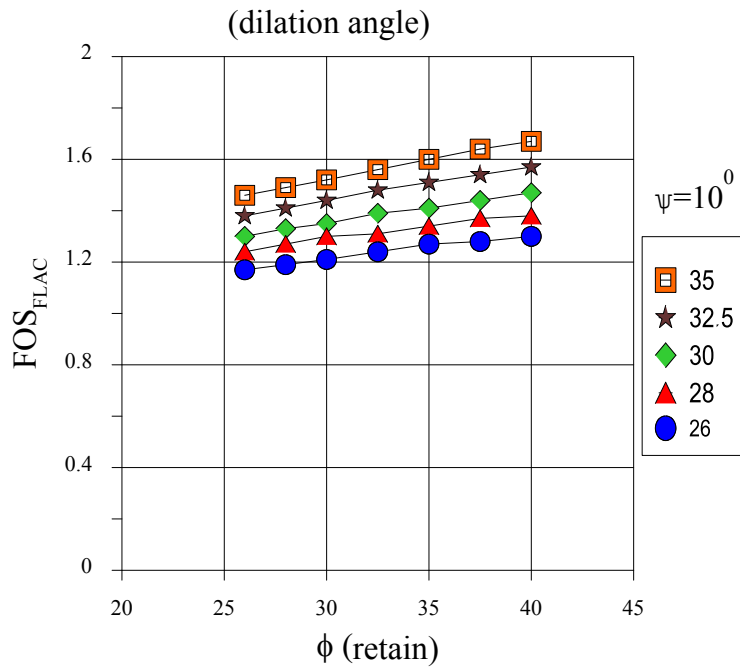
$\tan \phi_f$  = Tangent of internal friction angle at failure.

Figure 171–Figure 176 show FOSs calculated from FLAC for three types of walls with and without dilation angle. After solving for the equilibrium and failure states, the stresses generated in x and y directions are recorded for the entire model. Stresses at the base of the wall and between retain and backfill were used to find the total forces acting on the wall as well as to calculate design parameters. A total of 210 cases were solved for both equilibrium and failure conditions.





**Figure 171. FLAC FOS with Respect to  $\phi$  (Retain) for 10 ft Wall Height with No Dilation Angle.**



**Figure 172. FLAC FOS with Respect to  $\phi$  (Retain) for 10 ft Wall Height with Dilation Angle.**

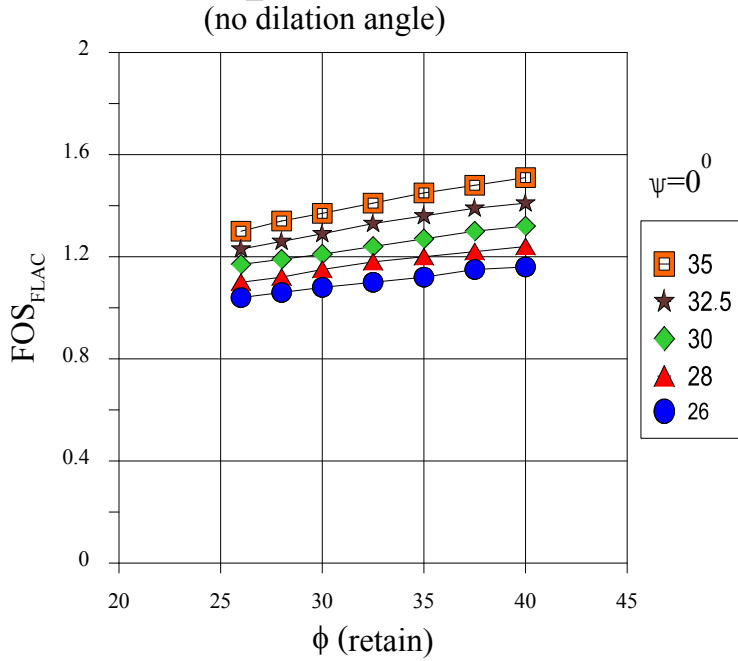


**Figure 173. FLAC FOS with Respect to  $\phi$  (Retain) for 20 ft Wall Height with No Dilation Angle.**

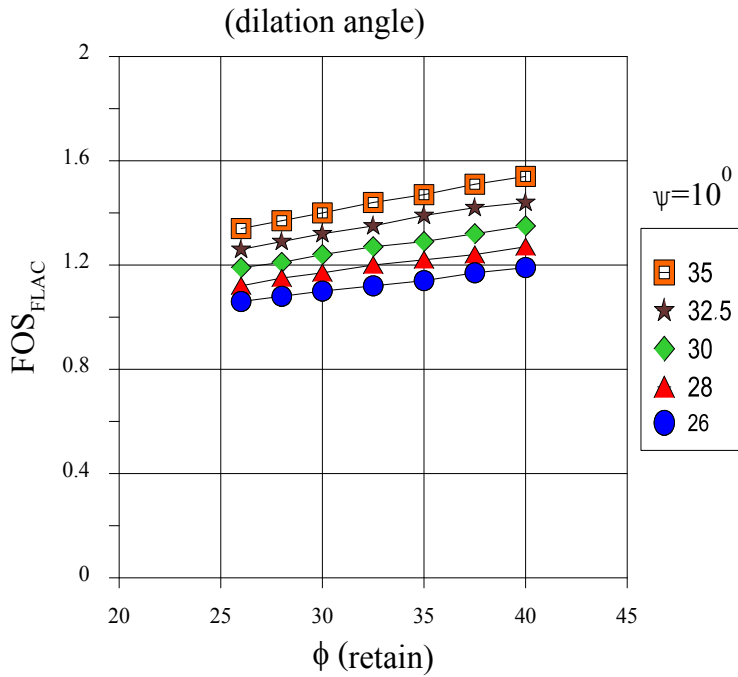


**Figure 174. FLAC FOS with Respect to  $\phi$  (Retain) for 20 ft Wall Height with Dilation Angle.**

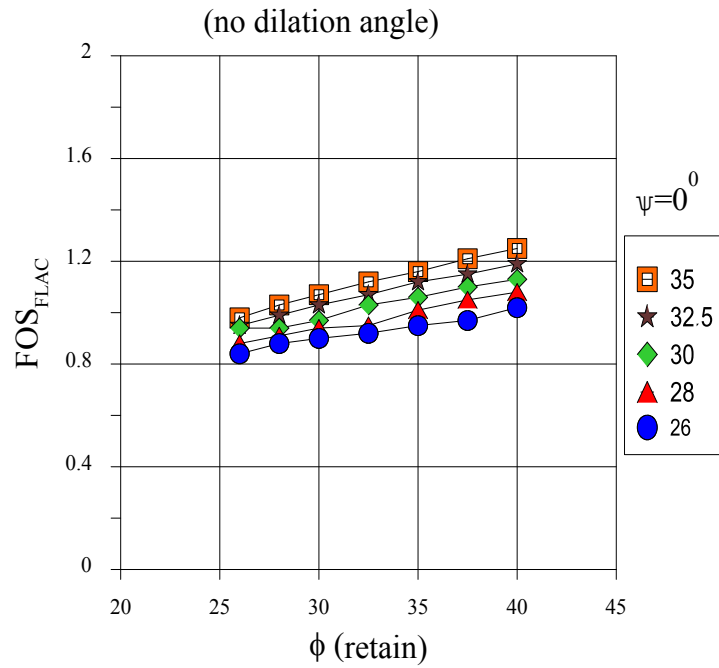


**Figure 175. FLAC FOS with Respect to  $\phi$  (Retain) for 20 ft Wall Height with 3H:1V Back Slope with No Dilation Angle.**

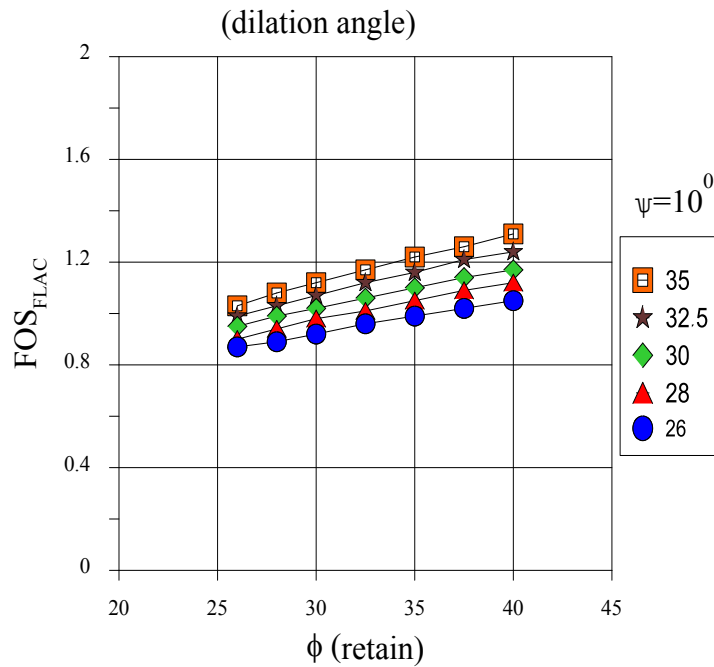


**Figure 176. FLAC FOS with Respect to  $\phi$  (Retain) for 20 ft Wall Height with 3H:1V Back Slope with Dilation Angle.**

### Calculation of Modified Design Parameters from FLAC Simulation

The stresses generated at failure conditions were used to find forces acting on the wall and used to find apparent design parameters such as apparent  $K_a$  (active earth coefficient),  $\delta_w$  (wall friction of angle),  $\delta_b$  (base friction of angle), and comparing them with design parameters that AASHTO (2002) recommended.

The stresses used to find forces are integrated by Simpson's numerical integration rules. The following equations are used to find apparent design parameters. Total horizontal force, vertical force, and shear forces were calculated.

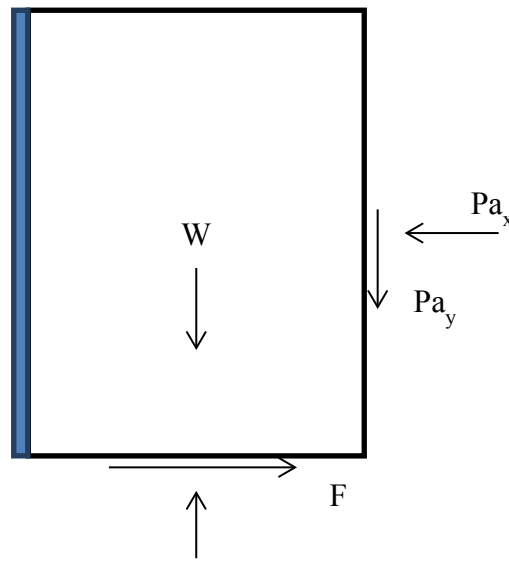


**Figure 177. Free Body Diagram of Forces Acting on MSE Wall.**

The forces in the free body diagram above are evaluated as follows:

$$W = \gamma \times L \times H \quad (\text{Eq. 33})$$

$$N = \int_0^L \sigma_{yy} dx \quad (\text{Eq. 34})$$

$$F = \int_0^L \sigma_{xy} dx \quad (\text{Eq. 35})$$

$$P_{ax} = \int_0^H \sigma_{xx} dy \quad (\text{Eq. 36})$$

$$P_{ay} = \int_0^H \sigma_{xy} dy \quad (\text{Eq. 37})$$

$$K_{a_{app}} = \frac{P_{ax}}{\frac{1}{2} \gamma H^2} \quad (\text{since } P_a = \frac{1}{2} \times K_a \times \gamma \times H^2) \quad (\text{Eq. 38})$$

$$\delta_b = \tan^{-1}\left(\frac{F}{N}\right) \quad (\text{Eq. 39})$$

$$\delta_w = \tan^{-1}\left(\frac{P_{ay}}{P_{ax}}\right) \quad (\text{Eq. 40})$$

*Results*

Figure 178–Figure 183 show parameters starting with the apparent  $K_a$  deduced from the FLAC analyses. The initial analysis series used no dilation angle. This was followed by a series of analyses using a dilation angle of  $10^\circ$ .

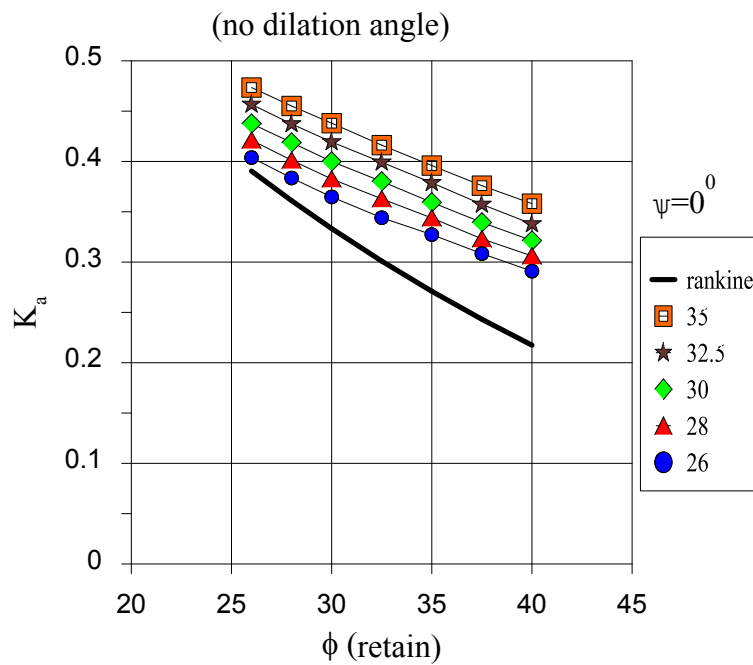


**Figure 178.  $K_a$ \_FLAC Comparison with  $K_a$ \_Rankine for Different  $\phi$  (Retain) for a 10-ft Wall Height with No Dilation Angle.**

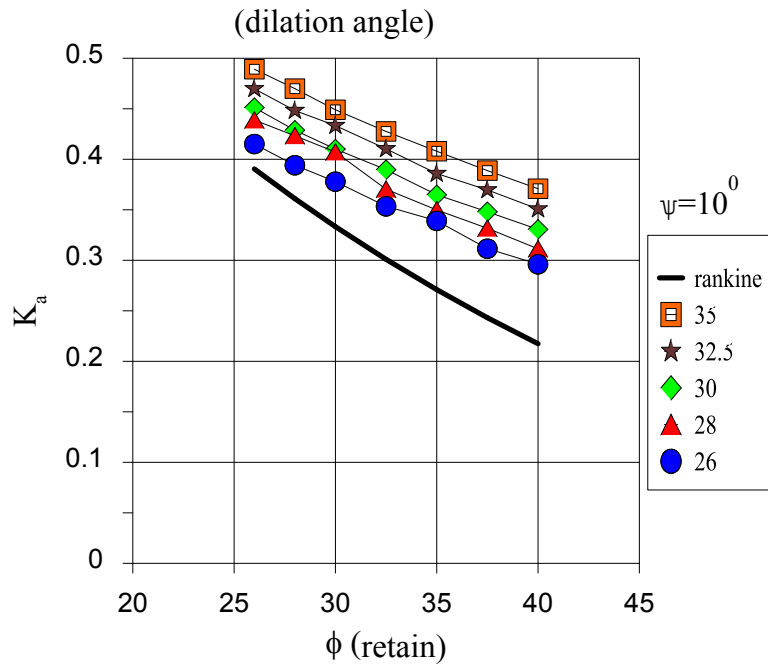


**Figure 179.  $K_a$ \_FLAC Comparison with  $K_a$ \_Rankine for Different  $\phi$  (Retain) for a 10-ft Wall Height with Dilation Angle.**

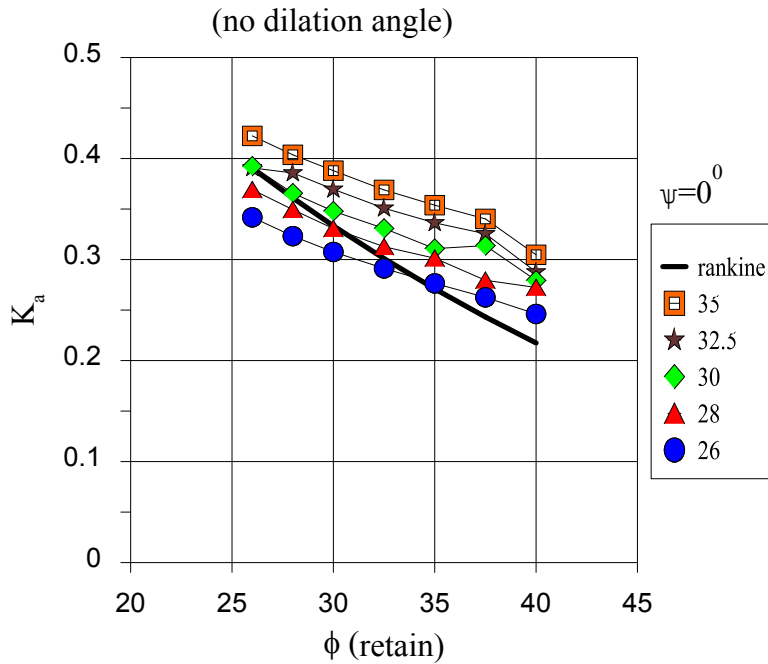


**Figure 180.  $K_a$ \_FLAC Comparison with  $K_a$ \_Rankine for Different  $\phi$  (Retain) for a 20-ft Wall Height with No Dilation Angle.**

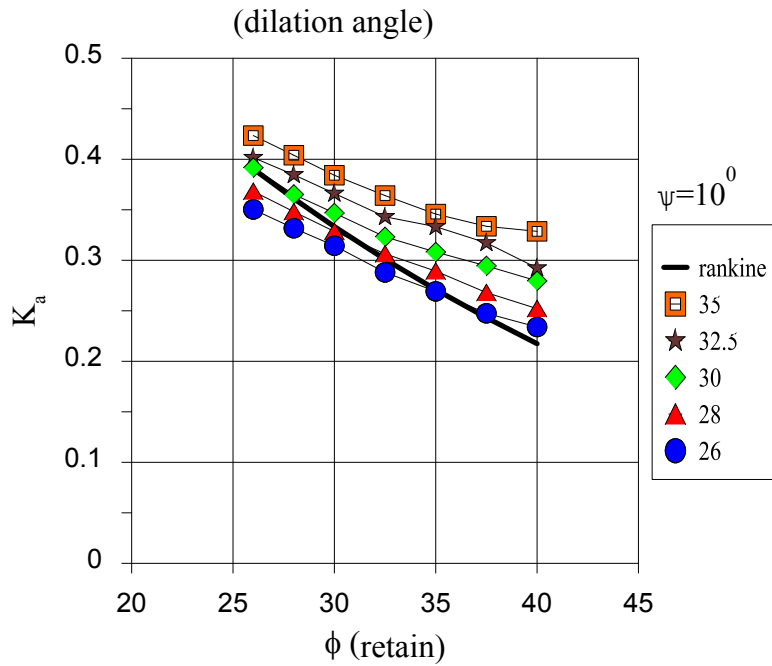


**Figure 181.  $K_a$ \_FLAC Comparison with  $K_a$ \_Rankine for Different  $\phi$  (Retain) for a 20-ft Wall Height with Dilation Angle.**

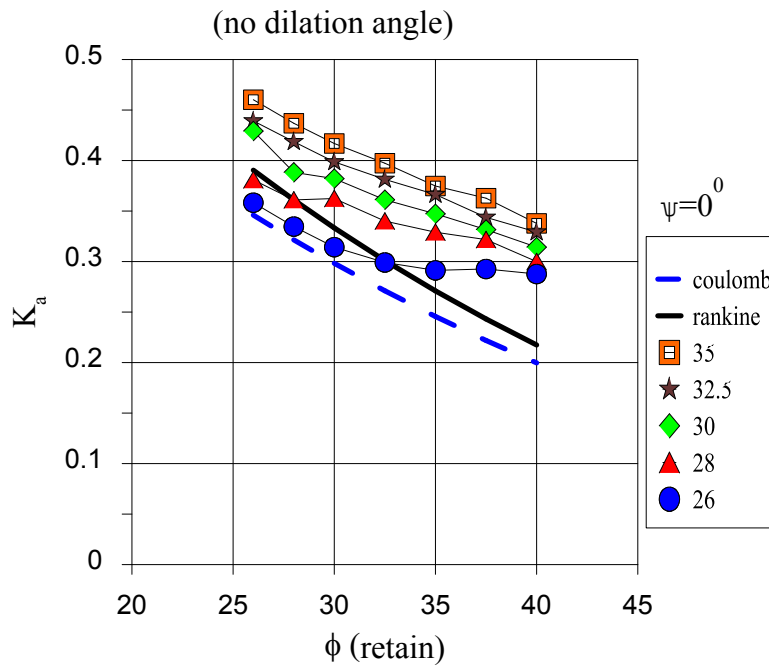


**Figure 182.  $K_a$ \_FLAC Comparison with  $K_a$ \_Rankine for Different  $\phi$  (Retain) for a 20-ft Wall Height with 3H:1V Back Slope with No Dilation Angle.**

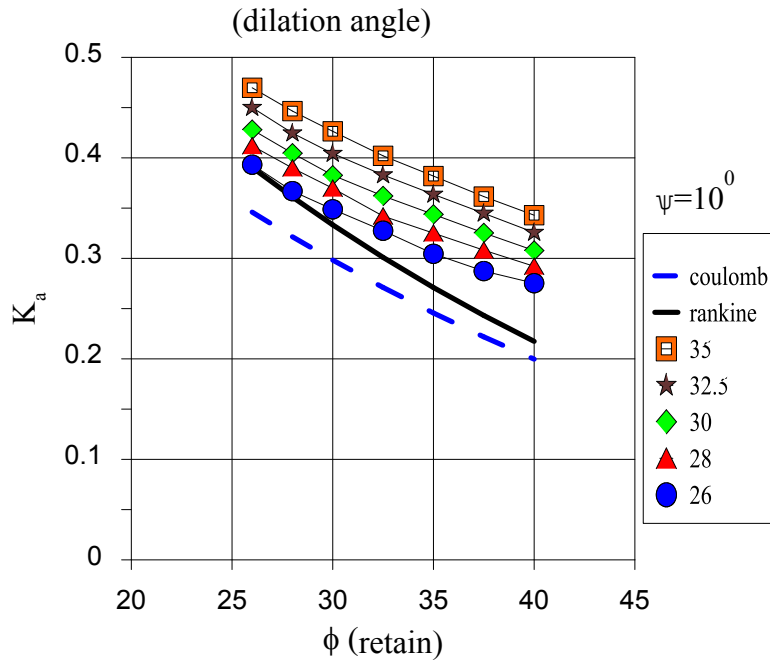


**Figure 183.  $K_a$ \_FLAC Comparison with  $K_a$ \_Rankine for Different  $\phi$  (Retain) for a 20-ft Wall Height with 3H:1V Back Slope with Dilation Angle.**

Once the  $K_a$  from FLAC simulation was calculated, the apparent interface friction was also calculated for the same wall height and same parameters as mentioned earlier by using Eq. 40.

Figure 184–Figure 195 present the results for different cases.

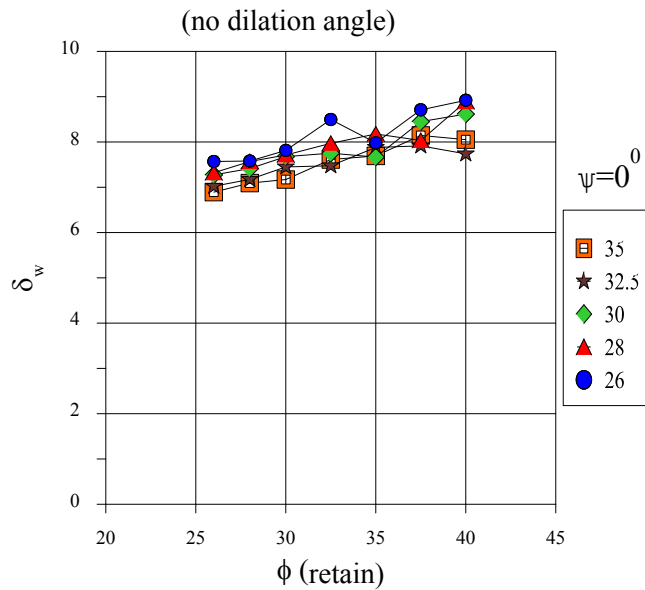


**Figure 184.  $\delta_w$  for Different  $\phi$  (Retain) for a 10-ft Wall Height with No Dilation Angle.**



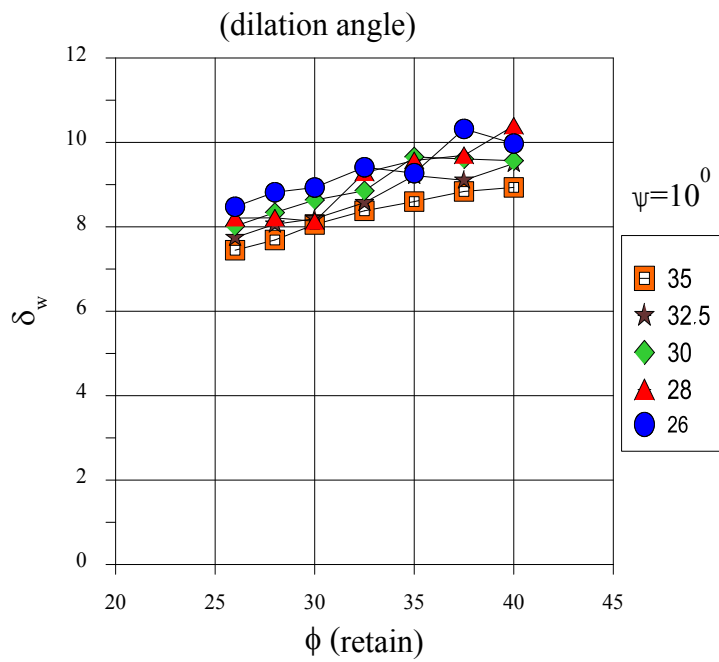


Figure 185.  $\delta_w$  for Different  $\phi$  (Retain) for a 10-ft Wall Height with Dilation Angle.

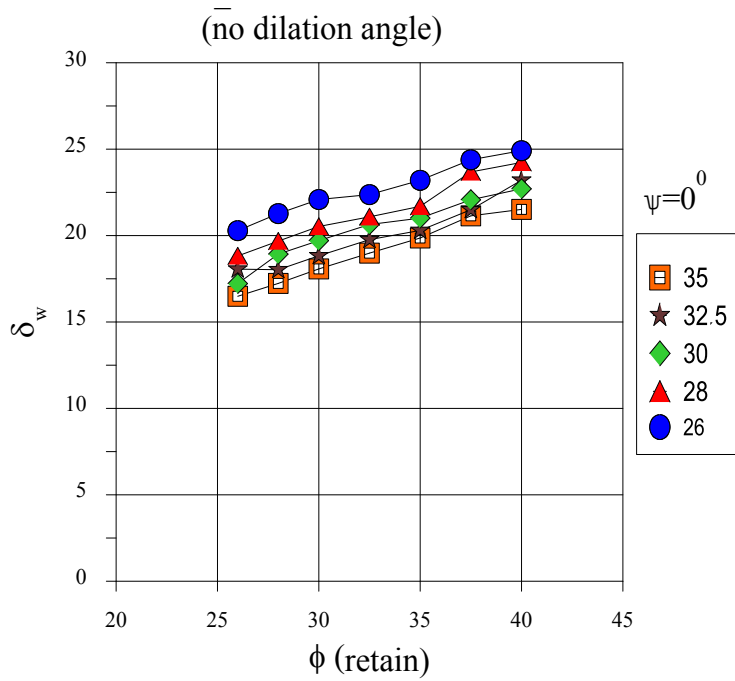


Figure 186.  $\delta_w$  for Different  $\phi$  (Retain) for a 20-ft Wall Height with No Dilation Angle.

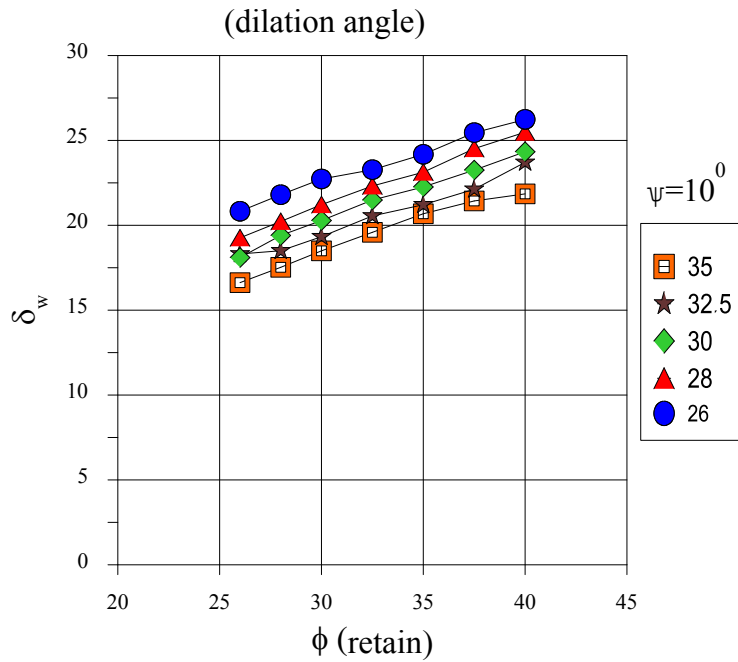


Figure 187.  $\delta_w$  for Different  $\phi$  (Retain) for a 20-ft Wall Height with Dilation Angle.

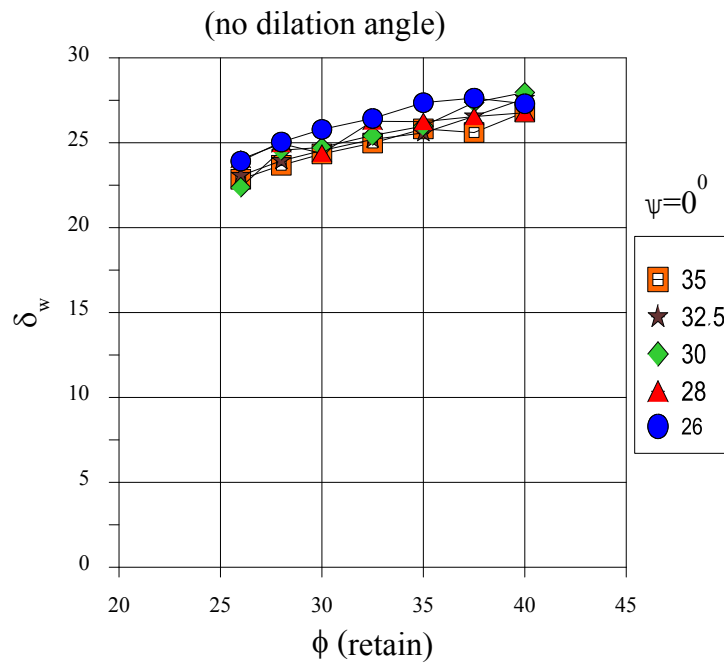
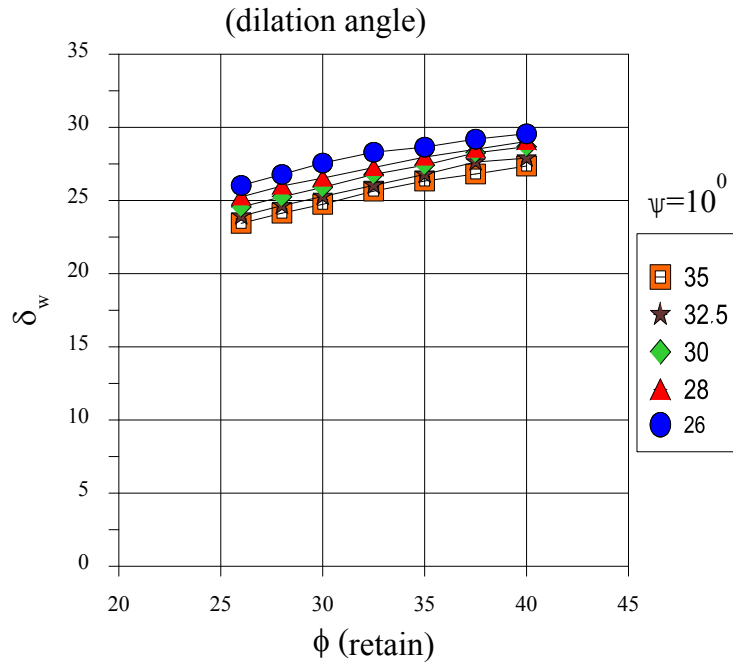
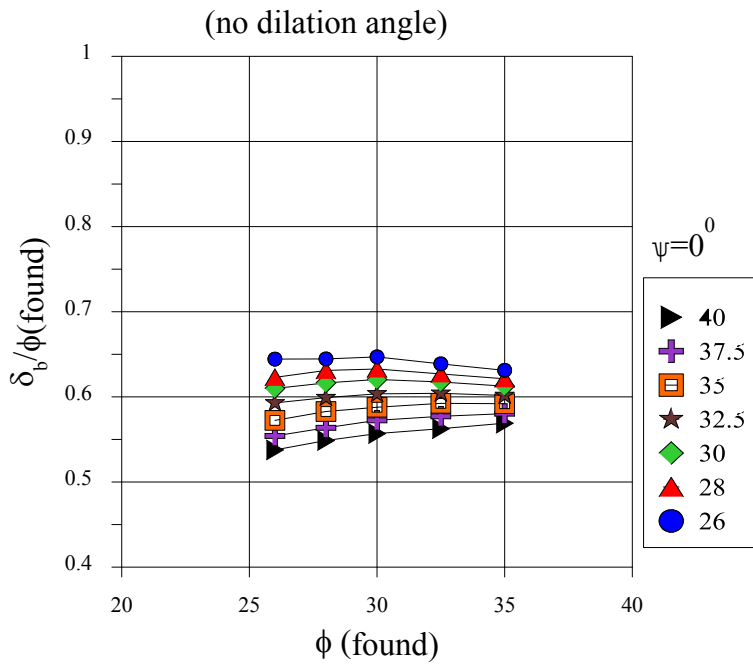


Figure 188.  $\delta_w$  for Different  $\phi$  (Retain) for a 20-ft Wall Height with 3H:1V Back Slope with No Dilation Angle.



**Figure 189.  $\delta_w$  for Different  $\phi$  (Retain) for a 20-ft Wall Height with 3H:1V Back Slope with Dilation Angle.**



**Figure 190.  $\delta_b/\phi$  (Found) for Different  $\phi$  (Found) for a 10-ft Wall Height with No Dilation Angle.**

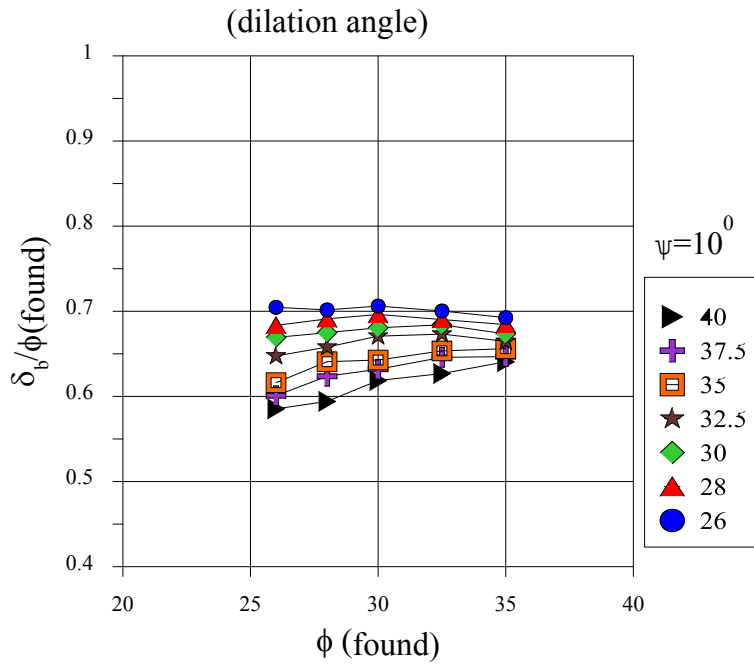


**Figure 191.  $\delta_b/\phi$  (Found) for Different  $\phi$  (Found) for a 10-ft Wall Height with Dilation Angle.**

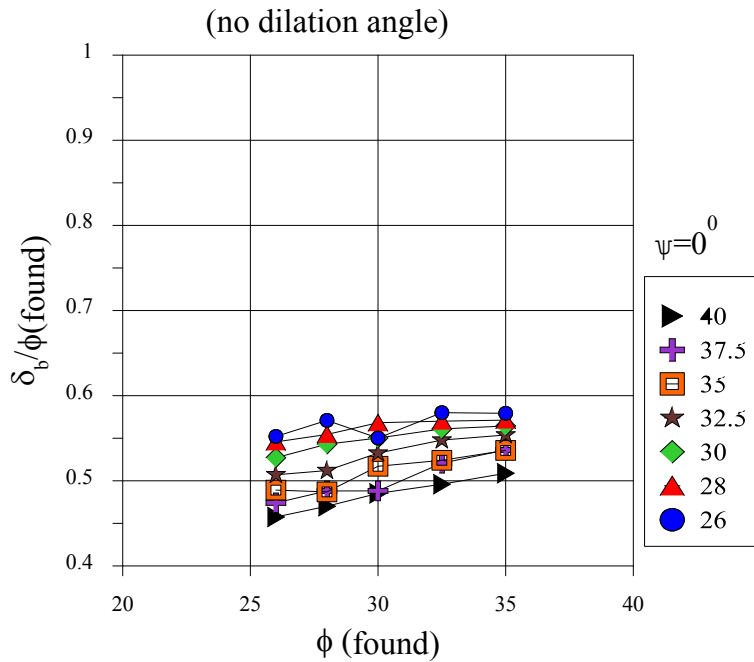


**Figure 192.  $\delta_b/\phi$  (Found) for Different  $\phi$  (Found) for a 20-ft Wall Height with No Dilation Angle.**

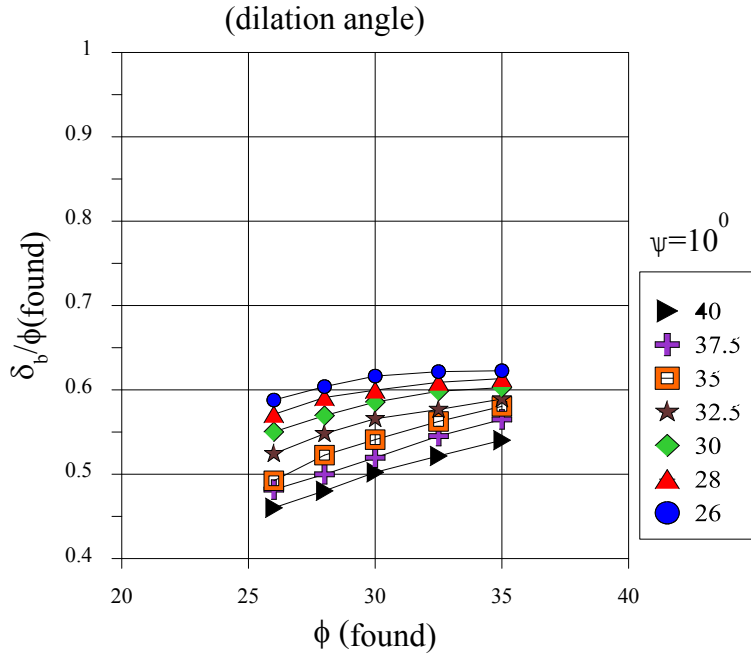


**Figure 193.  $\delta_b/\phi$  (Found) for Different  $\phi$  (Found) for a 20-ft Wall Height with Dilation Angle.**

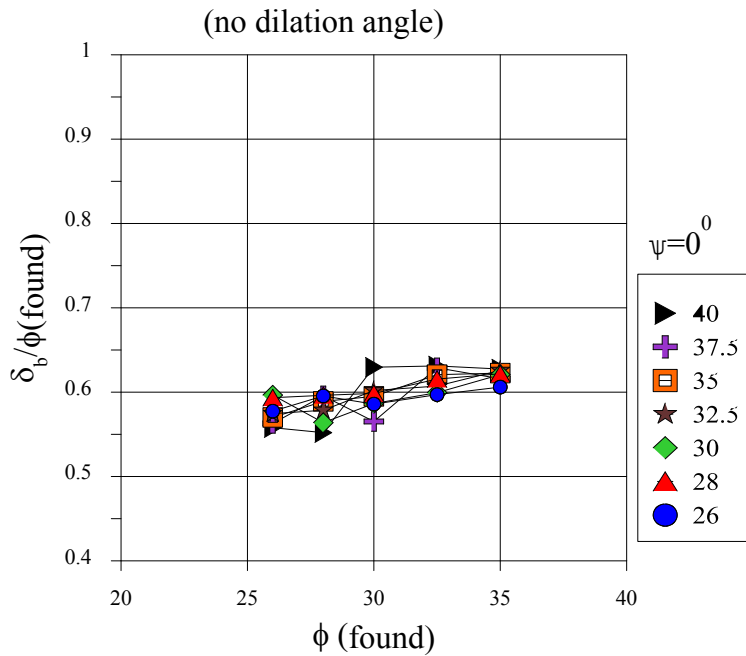


**Figure 194.  $\delta_b/\phi$  (Found) for Different  $\phi$  (Found) for a 20-ft Wall Height with 3H:1V Back Slope with No Dilation Angle.**

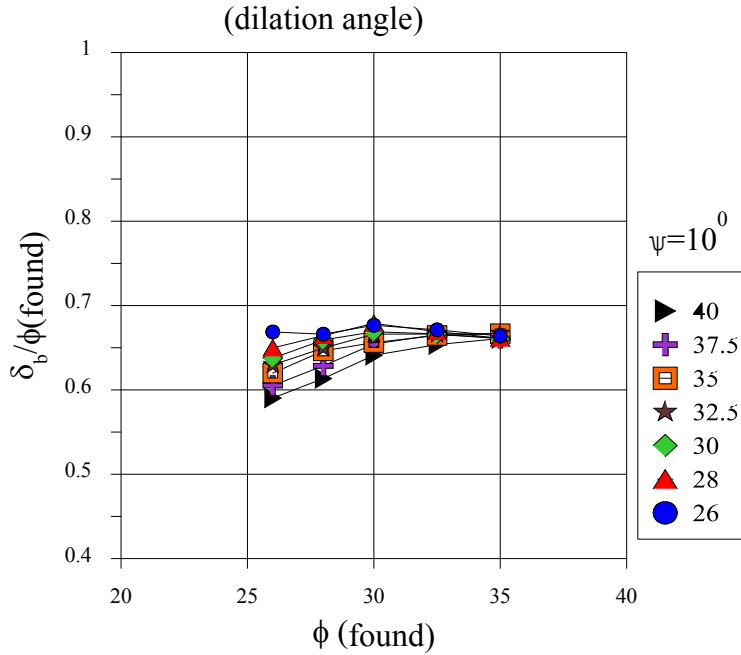


**Figure 195.  $\delta_b/\phi$  (Found) for Different  $\phi$  (Found) for a 20-ft Wall Height with 3H:1V Back Slope with No Dilation Angle.**

The design parameters calculated from FLAC analysis were used to find FOSs against sliding by the following steps. These steps are the same as mentioned in the AASHTO (2002) design manual for MSE walls; the only difference is that  $\delta_b$  in the calculations are from a FLAC analysis.

- Calculate the driving force acting on the wall using  $K_a$  rankine for no back slope and  $K_a$  Coulomb for 3H:1V back slope.

$$F_{driving} = \frac{1}{2} \times K_a \times \gamma \times H^2 \quad \text{(Eq. 41)}$$

- Use  $\delta_b$  from FLAC analysis to find resisting force from base of wall.

$$F_{resisting} = W \times \tan \delta_b \quad \text{(Eq. 42)}$$

$$W = \gamma \times L \times H \quad \text{(Eq. 43)}$$

$$FOS_{Sliding} = \frac{F_{resisting}}{F_{driving}} \quad \text{(Eq. 44)}$$

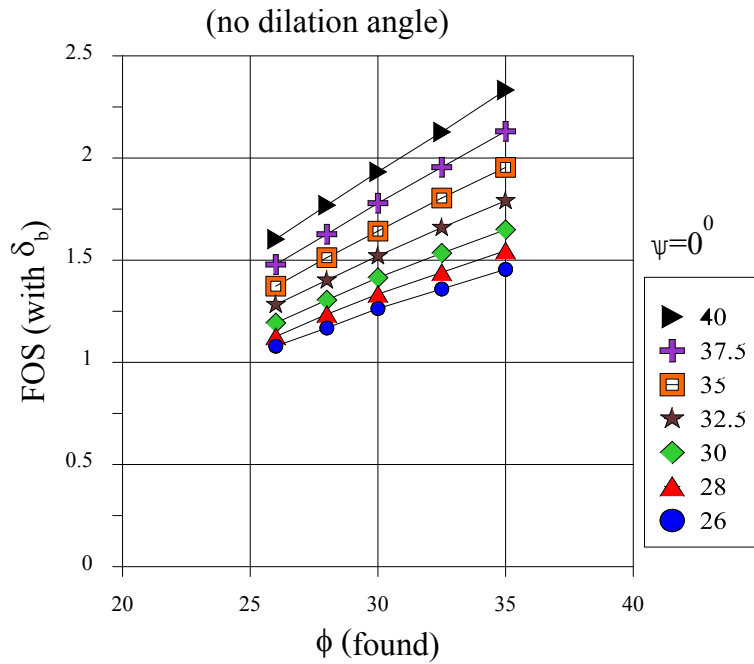


**Figure 196. FOS Calculated with  $\delta_b$  from FLAC for Different  $\phi$  (Found) for a 10-ft Wall Height with No Dilation Angle.**

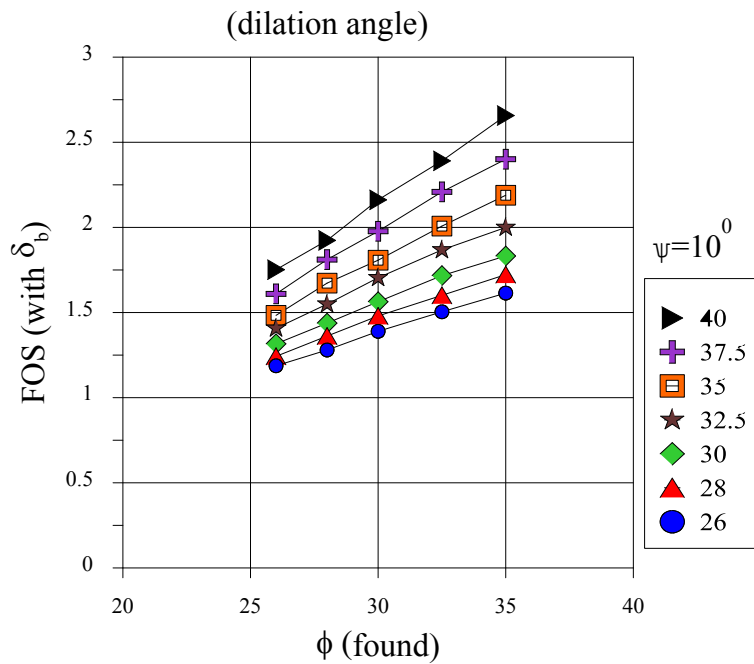


**Figure 197. FOS Calculated with  $\delta_b$  from FLAC for Different  $\phi$  (Found) for a 10-ft Wall Height with Dilation Angle.**

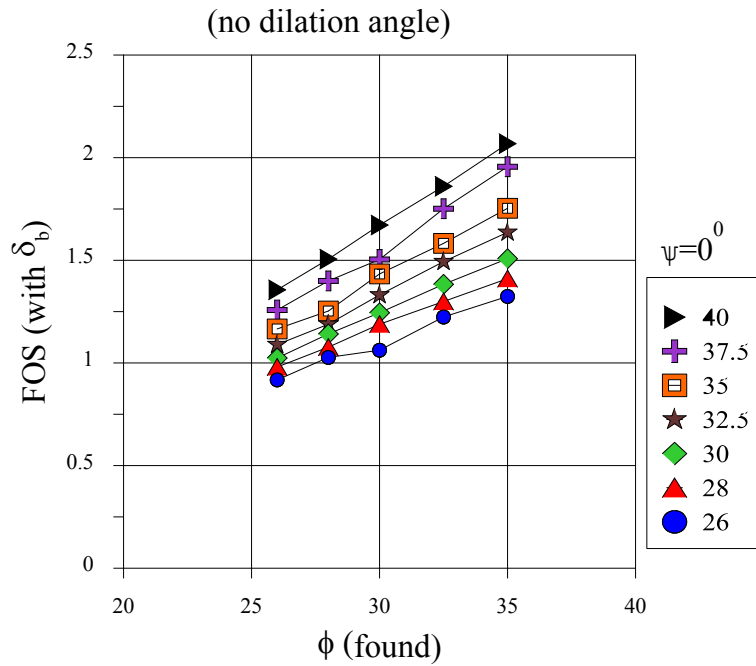


**Figure 198. FOS Calculated with  $\delta_b$  from FLAC for Different  $\phi$  (Found) for a 20-ft Wall Height with No Dilation Angle.**

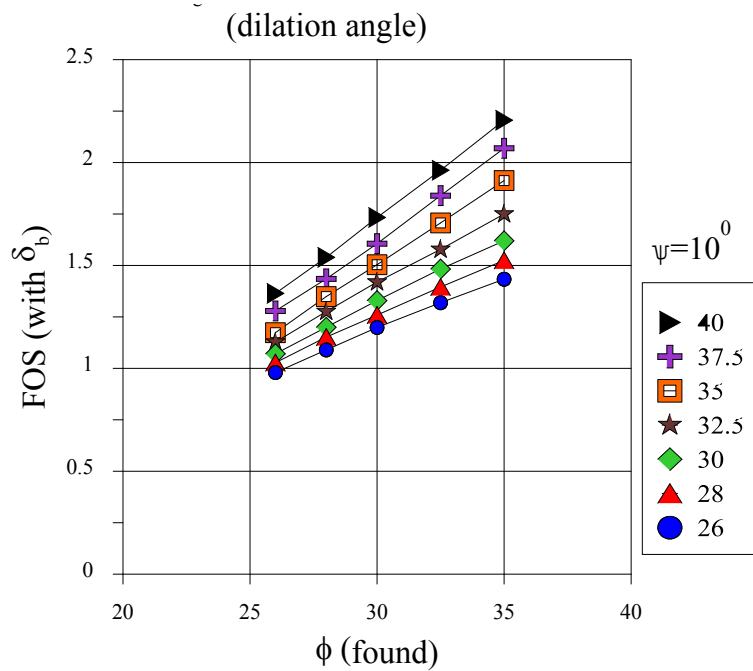


**Figure 199. FOS Calculated with  $\delta_b$  from FLAC for Different  $\phi$  (Found) for a 20-ft Wall Height with Dilation Angle.**



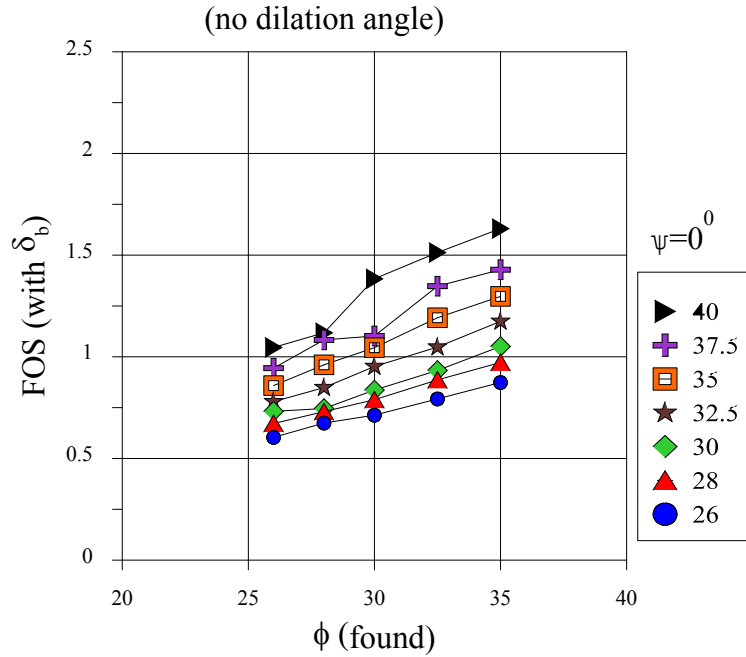


**Figure 200. FOS Calculated with  $\delta_b$  from FLAC for Different  $\phi$  (Found) for a 20-ft Wall Height with 3H:1V Back Slope with No Dilation Angle.**

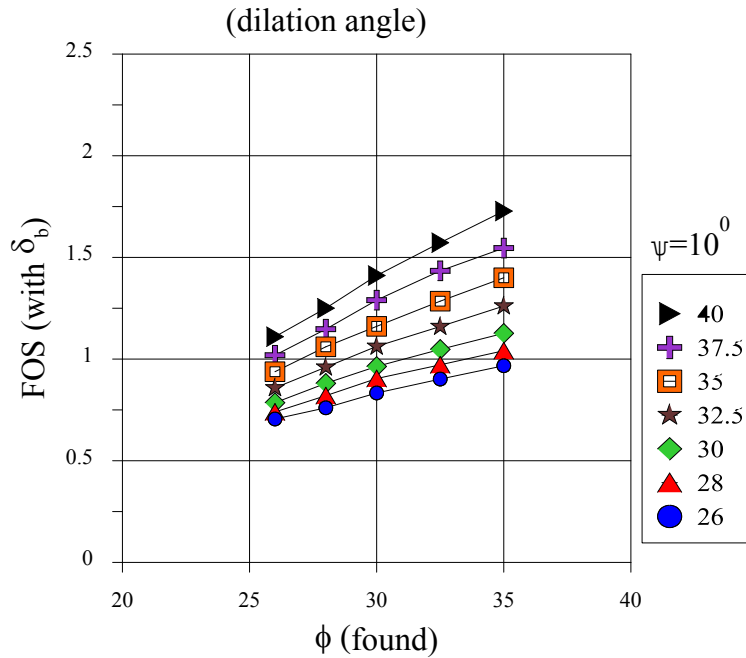


**Figure 201. FOS Calculated with  $\delta_b$  from FLAC for Different  $\phi$  (Found) for a 20-ft Wall Height with 3H:1V Back Slope with No Dilation Angle.**

## **PARAMETRIC STUDY FOR BEARING CAPACITY ANALYSIS**

In this section, an ultimate bearing capacity is calculated using different bearing capacity equations provided in the AASHTO manual (AASHTO 2002), Vesic's equation, and a bearing capacity equation recommended in the German code for MSE walls (as Professor Dov Leshchinsky had recommended). The equation in AASHTO manual is the same as Meyerhof's equation. Using these equations and loads calculated from the FLAC analysis for Figure 167 shown above, researchers carried out a parametric study for cohesionless soils and for undrained cohesive soils as well as for  $c$ - $\phi$  foundation soils with cohesionless retained soils.

### **Bearing Capacity Analysis for Cohesionless Soils**

For cohesionless soils, the friction angle for foundation soils was considered between  $26^\circ$  and  $35^\circ$  and for retaining soils from  $26^\circ$  to  $40^\circ$  with a dilation angle of  $10^\circ$  for both soils. Using these parameters for FLAC simulations, researchers performed a total of 35 simulations. The loads considered for analysis are calculated from FLAC simulations and from Rankine's  $K_a$  to see how it affects the FOS against a bearing failure. The effect of the additional vertical load associated with active thrust is also evaluated.

#### *Loads Acting on the Base of Wall*

According to AASHTO, loads acting on the base of the wall without any external loads are self-weight of the wall and a horizontal load from active thrust from a retaining soil. By contrast, the German code considers the weight of the wall, the horizontal component of active thrust, and the vertical component of active thrust. The horizontal and vertical components are correlated by interface friction angles between backfill and retaining soils. Adding an extra vertical load from active thrust reduces the eccentricity of loads on the base of the wall, which in turn increases the effective width of base in bearing capacity calculations. The loads from active thrust are first calculated from FLAC simulations and from Rankine's  $K_a$  for a geometry shown in Figure 167. Three different retaining soil friction angles were considered for this parametric study. Figure 202 shows the loads acting on the base of wall for AASHTO and German code EBGeo (Johnson 2012).

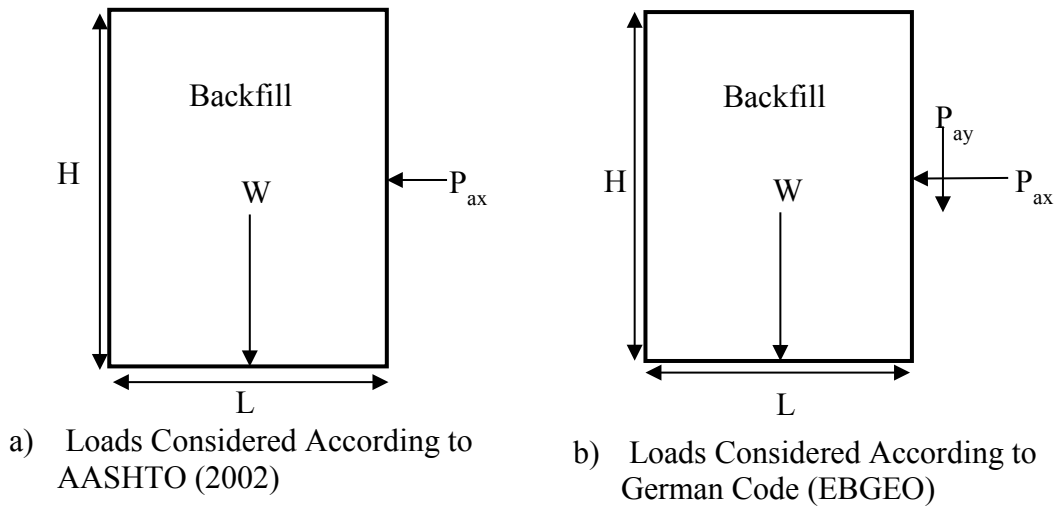


**Figure 202. Loads Acting on the Base of Wall.**

The total vertical load at the base of the wall predicted from the German code is higher than AASHTO, but the eccentricity of the loads is much lower when compared to AASHTO. Reduction of eccentricity has a significant contribution on FOS for bearing. The following equations are used for analysis.

- For eccentricity:

$$\text{AASHTO, 2002 } e = \frac{P_{ax} \times \frac{H}{3}}{W} \quad (\text{Eq. 45})$$

$$\text{EBGEO } e = \frac{P_{ax} \times \frac{H}{3} - P_{ay} \times \frac{L}{2}}{W + P_{ay}} \quad (\text{Eq. 46})$$

where

$$P_{ay} = P_{ax} \times \tan \delta_w.$$

$$\delta_w = 2/3 \times \phi_{\text{found.}}$$

e = Eccentricity of the loads

- Total loads:

$$\text{AASHTO, 2002 } W = \text{weight of the wall} \quad (\text{Eq. 47})$$

$$\text{EBGEO } N_{\text{total}} = W + P_{ay} \quad (\text{Eq. 48})$$

- Load Inclination:

$$\text{AASHTO, 2002 } \tan \delta = \frac{P_{ax}}{W} \quad (\text{Eq. 49})$$

$$\mathbf{EBGEO} \tan \delta = \frac{P_{ax}}{N_{total}} \quad (\text{Eq. 50})$$

### Bearing Capacity Equations Used for Comparison

For this study, equations of bearing capacity used are Meyerhof's, Vesic's, and an equation from German code DIN 4017 for geotechnical structures. The equation provided in AASHTO (2002) is the same as Meyerhof's. To compare an equation from German code and Meyerhof's equation, an additional vertical load from the active thrust is added in Meyerhof's equation to see its effect on FOS for bearing. The factors for bearing capacity equation used for comparison study are tabulated in Table 43 and factors used in bearing capacity equations are for strip footing criteria.

**Table 43. Factors for Bearing Capacity Equations Used from Different Codes and Authors.**

| Description                     | Meyerhof's   | Vesic's   | German Code (DIN 4017)   |
|---------------------------------|--|---|--|
| Bearing capacity factors- $N_q$ | $Nq = [e^{(\pi \tan \phi)}] \tan^2 (45 + \frac{\phi}{2})$                | Same as Meyerhof's  | Same as Meyerhof's   |
| $N_\gamma$                      | $N\gamma = (Nq - 1) \tan(1.4\phi)$                                       | $N\gamma = 2(Nq + 1) \tan(\phi)$  | $Nb = (Nq - 1) \tan \phi$<br>$N_\gamma = 2N_b$   |
| $N_c$                           | $Nc = (Nq - 1) \cot \phi$ when $\phi > 0$<br>$Nc = 5.14$ when $\phi = 0$ | Same as Meyerhof's  | Same as Meyerhof's   |
| Load inclination factors- $i_q$ | $i_q = \left(1 - \frac{2\delta}{\pi}\right)^2$                           | $i_q = (1 - \tan \theta)^2$<br>$\theta$ is same as $\delta$   | $i_q = (1 - 0.7 \tan \theta)^3$  |
| $i_c$                           | $i_c = \left(1 - \frac{2\delta}{\pi}\right)^2$                           | $i_c = \frac{i_q N_q - 1}{N_q - 1}$ when $\phi > 0$<br>$i_c = 1 - \frac{2H}{L * c * N_c}$ when $\phi = 0$ | $i_c = \frac{i_q N_q - 1}{N_q - 1}$ when $\phi > 0$<br>$i_c = 0.5 + 0.5 \sqrt{\left(1 - \frac{H}{L * c}\right)}$ when $\phi = 0$ |
| $i_\gamma$                      | $i_\gamma = \left(1 - \frac{\delta}{\phi}\right)^2$                      | $i_\gamma = (1 - \tan \theta)^3$  | $i_\gamma = (1 - \tan \theta)^3$   |

According to AASHTO (2002) the embedment part of the bearing capacity equation is neglected as most of MSE walls have a minimal embedment depth of one foot or less. The German code also recommends the same and the equations deduced to the overburden part and cohesion part. The bearing capacity equations are as follows.

- For Meyerhof's, Vesic's and for AASHTO (2002), the ultimate bearing capacity equation is:

$$Q = b' (c N_c i_c + 1/2 b' \gamma N_\gamma i_\gamma) \quad (\text{Eq. 51})$$

where

$c$  = Cohesion.

$b' = L - 2e$ .

$\gamma$  = Unit weight of foundation soil.

$$FOS = \frac{Q}{W} \quad (\text{Eq. 52})$$

- From DIN 4017, the equation for ultimate bearing capacity is:

$$Q = b' (c N_c i_c + b' \gamma N_b i_\gamma) \quad (\text{Eq. 53})$$

where

$c$  = Cohesion.

$b' = L - 2e$ .

$\gamma$  = Unit weight of foundation soil.

$$FOS = \frac{Q}{W} \quad (\text{Eq. 54})$$

A FOS for bearing for cohesionless soils is plotted below for different foundation soils. In these plots Meyerhof's equation gives lower estimates of FOS and whereas Vesic's gives higher estimates without considering additional vertical load from active thrust. For DIN4017 equation a vertical component of active thrust was considered in load calculation and it gives a higher estimate than Vesic's equation. A vertical component of active thrust was used in Meyerhof's equations to see the effect on FOS for bearing and was compared with the German code. Figure 203–Figure 205 show FOS for bearing for cohesionless soils using loads from FLAC, and Figure 206–Figure 208 show loads calculated from Rankine's  $K_a$ .

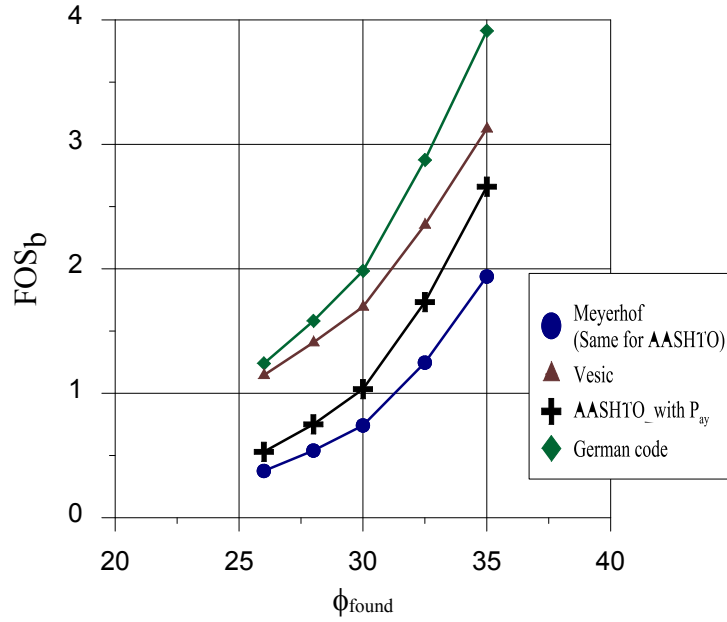


**Figure 203. Factor of Safety for Bearing Using Different Equations for Different  $\phi$  (Found) for a  $\phi_{\text{retain}}=26^\circ$  and Loads Calculated from FLAC Simulation.**

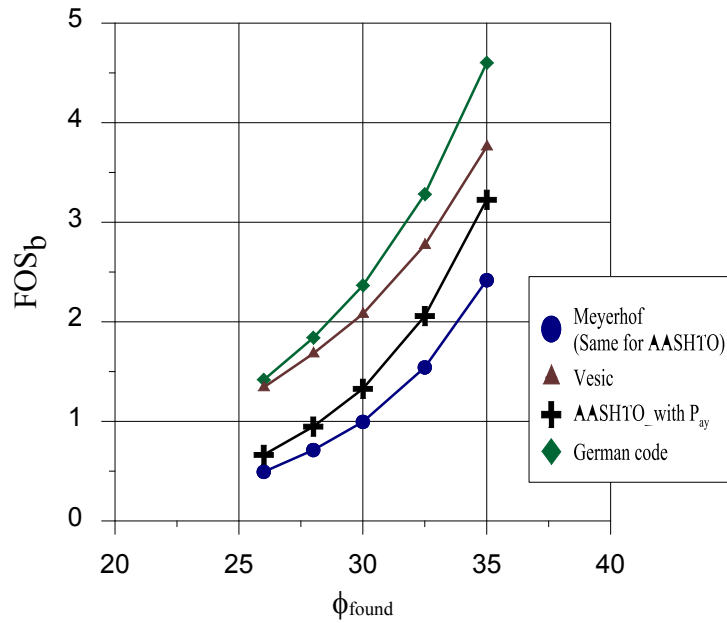


**Figure 204. Factor of Safety for Bearing Using Different Equations for Different  $\phi$  (Found) for a  $\phi_{\text{retain}}=30^\circ$  and Loads Calculated from FLAC Simulation.**

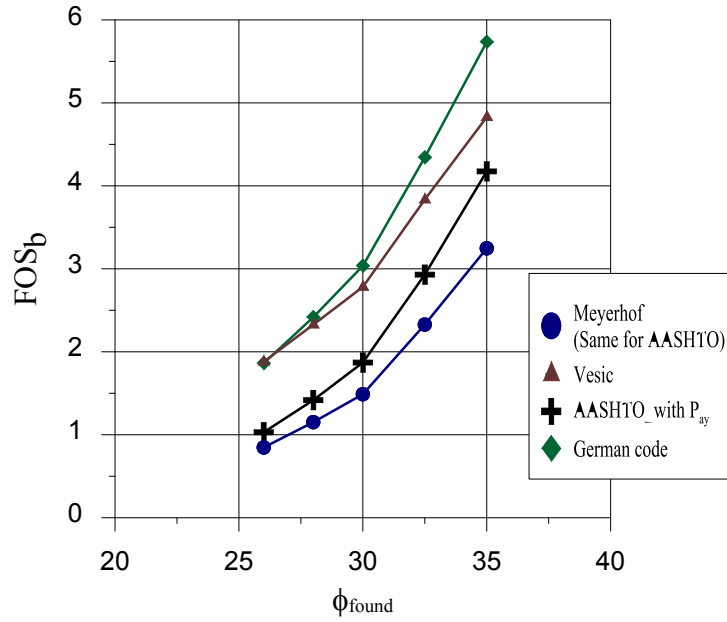


**Figure 205. Factor of Safety for Bearing Using Different Equations for Different  $\phi$  (Found) for a  $\phi_{\text{retain}}=40^\circ$  and Loads Calculated from FLAC Simulation.**

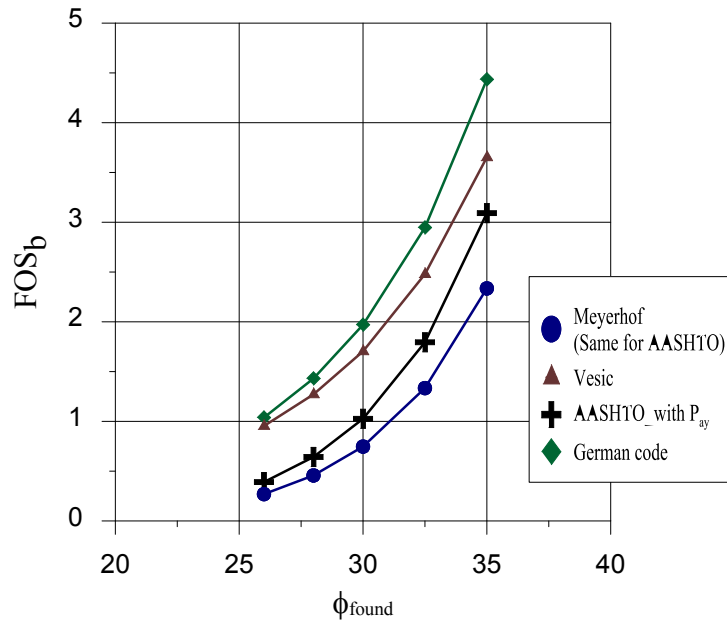


**Figure 206. Factor of Safety for Bearing Using Different Equations for Different  $\phi$  (Found) for a  $\phi_{\text{retain}}=26^\circ$  and Loads Calculated from Rankine's  $K_a$ .**

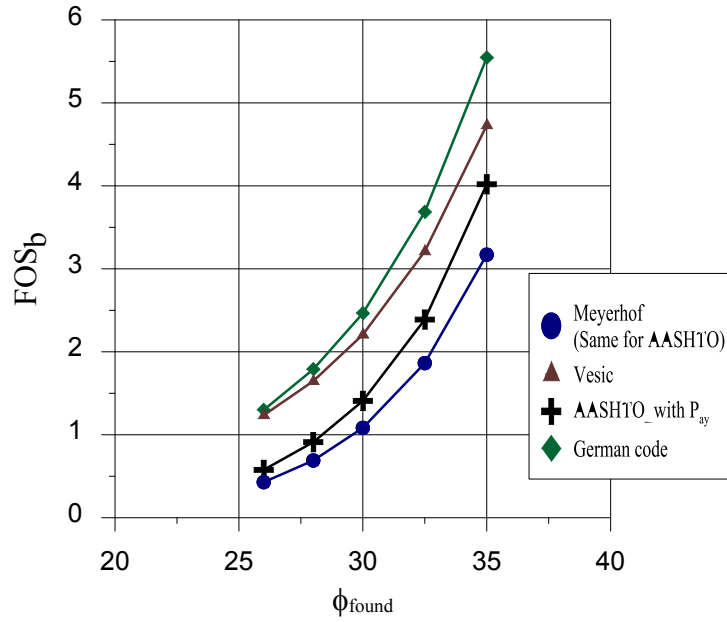


**Figure 207. Factor of Safety for Bearing Using Different Equations for Different  $\phi$  (Found) for a  $\phi_{\text{retain}}=30^\circ$  and Loads Calculated from Rankine's  $K_a$ .**

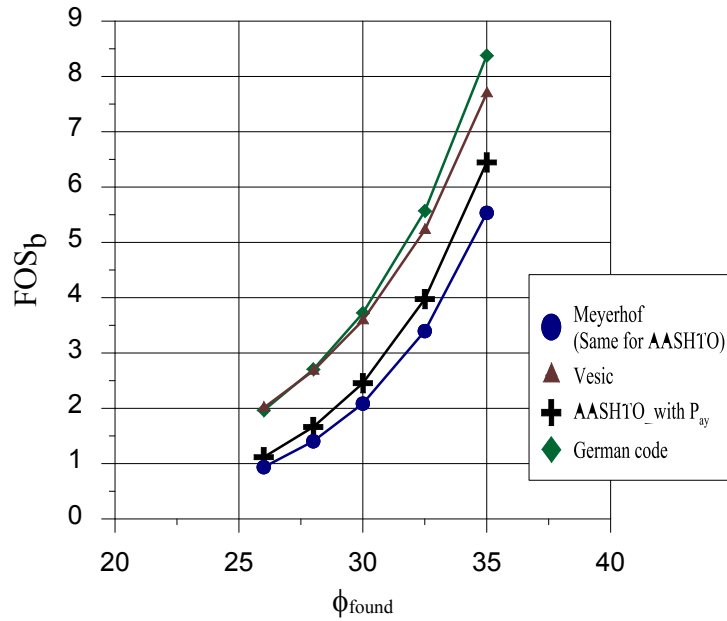


**Figure 208. Factor of Safety for Bearing Using Different Equations for Different  $\phi$  (Found) for a  $\phi_{\text{retain}}=40^\circ$  and Loads Calculated from Rankine's  $K_a$ .**



## *Conclusions*

The researchers made the following conclusions from this parametric study on bearing capacity equations:

- Forces from FLAC simulations are higher than forces calculated from Rankine's theory, especially for higher  $\phi$  (retained) values. The higher lateral loads largely account for the lower FOS values predicted from the FLAC analyses.
- The Meyerhof's equation, which is used in the AASHTO analysis, gives a lower estimate of FOS for bearing than Vesic's equations.
- The German code (EBGEO) considers a vertical force associated with the active thrust. The FLAC simulations can also calculate the vertical component of the earth pressure force based on the stresses generated at the back of the wall. This vertical component increases the total vertical load at the base of the wall, but at the same time it decreases the eccentricity from the center of base of the wall. This decrease in eccentricity is generally beneficial as it increases the effective width of the base in the ultimate bearing capacity equation.
- FOSs for bearing from the German code (EBGEO) give higher values than Vesic's. This is due to the consideration of vertical component of the active thrust that decreases the eccentricity.
- Including the vertical component of active thrust in the Meyerhof analysis will increase the FOS against a bearing failure, but the predicted FOS will still be lower than that predicted from the Vesic analysis.
- Meyerhof's (AASHTO) gives a conservative FOS value for bearing capacity.

## **Bearing Capacity Analysis for Undrained Cohesive Soils**

FLAC simulations were carried out on an MSE wall with no back slope geometry for pure cohesive retaining soils and foundation soils. The unit weight of sandy backfill soil and retaining soils were both equal to 125 pcf. Figure 167 shows the geometry of the model. The model properties are explained below for clays only. After performing the simulations, researchers extracted the stresses from simulations for each case, and calculated the forces acting on the wall from active thrust from stress data.

*Model Properties Used for Pure Clay Used as Retaining and Foundation Soils*

The backfill material used for this model was frictional soils with a dilation angle of 10° and an internal friction angle of 34°. Table 44 presents the properties of retaining and foundation soils.

**Table 44. Material Properties Used for Pure Cohesive Soils for FLAC Simulations.**

| Type                           | Strength    | Unit Weight (pcf) | Elastic Modulus* (psf) | Bulk Modulus (psf) | Shear Modulus (psf) | $c_u$ (psf) |
|--------------------------------|-------------|-------------------|------------------------|--------------------|---------------------|-------------|
| Foundation and Retaining soils | Soft        | 125               | 0.08464 E6             | 0.1410 E6          | 0.0302 E6           | 500         |
|                                | Medium-Firm | 125               | 0.1269 E6              | 0.2116 E6          | 0.0453 E6           | 750         |
|                                | Firm        | 125               | 0.1692 E6              | 0.2821 E6          | 0.0604 E6           | 1000        |
|                                | Medium-Firm | 125               | 0.2962 E6              | 0.4937 E6          | 0.1058 E6           | 1500        |
|                                | Stiff       | 125               | 0.4232 E6              | 0.7054 E6          | 0.1511 E6           | 2000        |

\* Elastic modulus for sand is taken as  $1000 \cdot P_{atm}$  where  $P_{atm} = 2116.216$  psf and Poisson's ratio = 0.45 (Kulhawy and Mayne 1990).

Using these material properties, researchers performed a total of 25 simulations to consider the effects of different foundation properties and different retained soils of the MSE retaining wall. The model was first run for equilibrium condition under gravity and then it was run for failure condition under gravity loads.

*Results*

The loads acting on the wall due to an active thrust from retaining soils are calculated using FLAC simulations. The vertical component of active thrust was fairly small for all cohesive type retaining soils. Therefore, this vertical force was not accounted in bearing capacity calculations. The equations used for bearing capacity are Meyerhof's, Vesic's, and German code (EBGEO). Since there is no vertical component from active thrust, the bearing capacity values for German code and Vesic's are the same. The results presented below from Figure 209–Figure 211 are for soft, firm, and stiff clay retaining soils, and for soft, med-firm, firm, med-stiff, and stiff clay foundation soils. The results are compared with FLAC FOS and the FOS for bearing calculated using Meyerhof's and Vesic's equations.

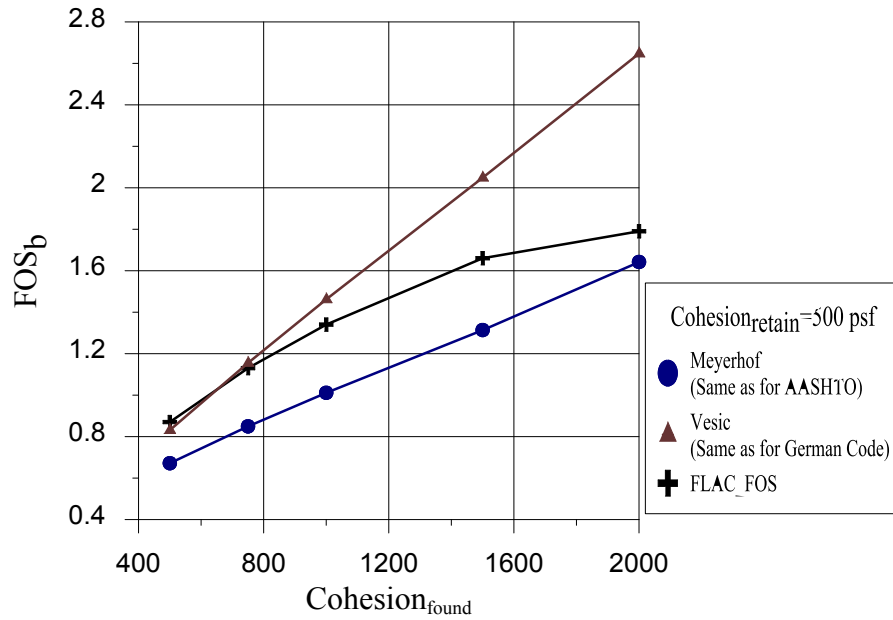


**Figure 209. Factor of Safety for Bearing Using Different Equations for Different Cohesion (Found) for a cohesion<sub>retain</sub>=500 psf and Loads Calculated from FLAC.**

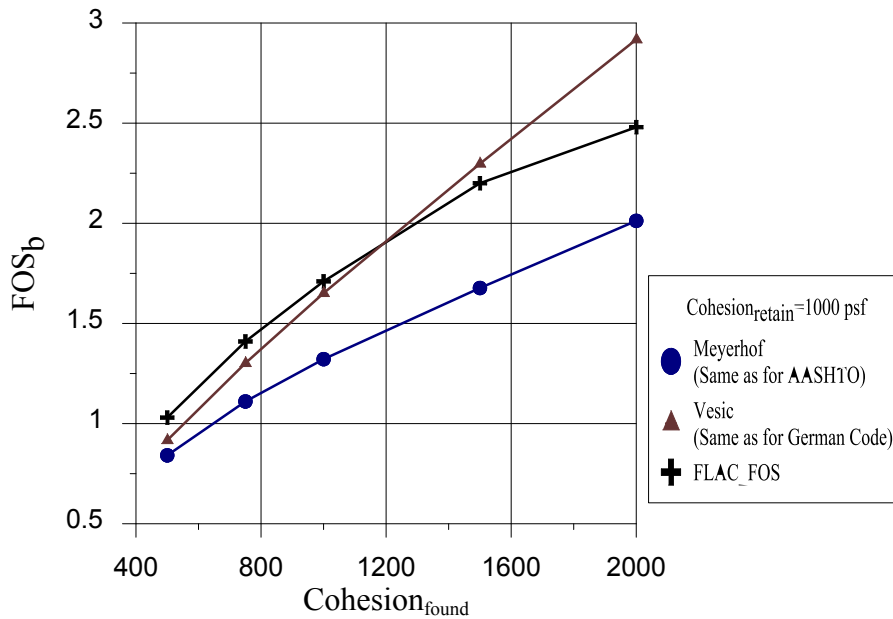


**Figure 210. Factor of Safety for Bearing Using Different Equations for Different Cohesion (Found) for a cohesion<sub>retain</sub>=1000 psf and Loads Calculated from FLAC.**

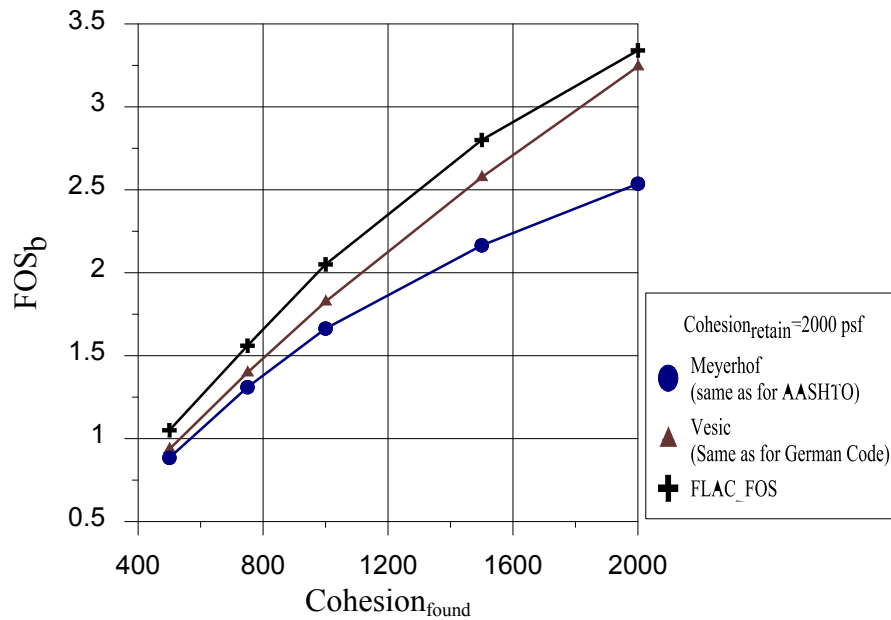


**Figure 211. Factor of Safety for Bearing Using Different Equations for Different Cohesion (Found) for a cohesion<sub>retain</sub>=2000 psf and Loads Calculated from FLAC.**

### Conclusions

The following are the conclusions for using pure cohesive soils as foundation soils:

- The FOSs for soft retained soils are lower because the softer retaining soils exert higher active thrust on the wall, especially horizontal load from active thrust.
- FOSs predicted from the Meyerhof’s (AASHTO) equations are lower than those predicted from Vesic’s equation and FLAC.
- Vesic’s equation agrees reasonably well with FLAC for medium and stiff soils, but appears unconservative for soft soil.
- The primary difference between the Meyerhof’s and Vesic’s equations for purely cohesive soils lies in the load inclination factor. Vesic’s load inclination factor accounts for the dimensions of the wall and cohesion at the base of wall, whereas Meyerhof’s load inclination factor accounts only for the load inclination angle from the vertical axis.
- For stiff clay retained soils, the FOS from FLAC is higher than FOS from the Meyerhof’s and Vesic’s equations, because of the smaller active thrust.

- Meyerhof’s equation for bearing capacity can be used as a preliminary assessment tool for bearing capacity. However, if it gives a very low FOS, a FLAC simulation can be carried out to verify the calculations.

### **Bearing Capacity Analysis for c- $\phi$ Foundation Soils**

To combine the effect of friction angle and cohesion on bearing capacity, researchers performed a FLAC simulation with foundation soils having both friction angle and cohesion. The properties of retaining soils are that of cohesionless soils with 26°, 30°, and 40° with a dilation angle of 10°.

#### *Material Properties Used for FLAC Simulations*

The material properties for retaining soils used here are cohesionless soils to see the full effect of active thrust in both horizontal and vertical directions. Using cohesionless retaining soils also gives an option of comparing all possible bearing capacity equations and to see the effect of load inclination on both cohesion and overburden parts of the bearing capacity equation. Table 45 shows the values used for material properties for FLAC simulations.

**Table 45. Material Properties for FLAC Simulations c- $\phi$  Foundations.**

| Type             | Unit Weight (pcf) | Elastic Modulus* (psf) | Bulk Modulus (psf) | Shear Modulus (psf) | c <sub>u</sub> (psf) | $\phi$ |
|------------------|-------------------|------------------------|--------------------|---------------------|----------------------|--------|
| Foundation Soils | 125               | 2.116 E6               | 3.6435 E6          | 0.3644 E6           | 500                  | 26     |
|                  |                   |                        |                    |                     | 750                  |        |
|                  |                   |                        |                    |                     | 1000                 |        |
| Retaining Soils  | 125               | 2.116 E6               | 3.6435 E6          | 0.3644 E6           | 0                    | 26     |
|                  |                   |                        |                    |                     |                      | 30     |
|                  |                   |                        |                    |                     |                      | 40     |

#### *Results*

Nine simulations were performed with different combinations of retaining and foundation soils. The results plotted below show the FOS for sliding, for bearing using different equations, and FOS from FLAC. The FLAC gives a FOS value by strength reduction method. This FOS is

plotted as a reference for other calculated FOS from forces extracted from FLAC simulations as shown in Figure 212–Figure 214.

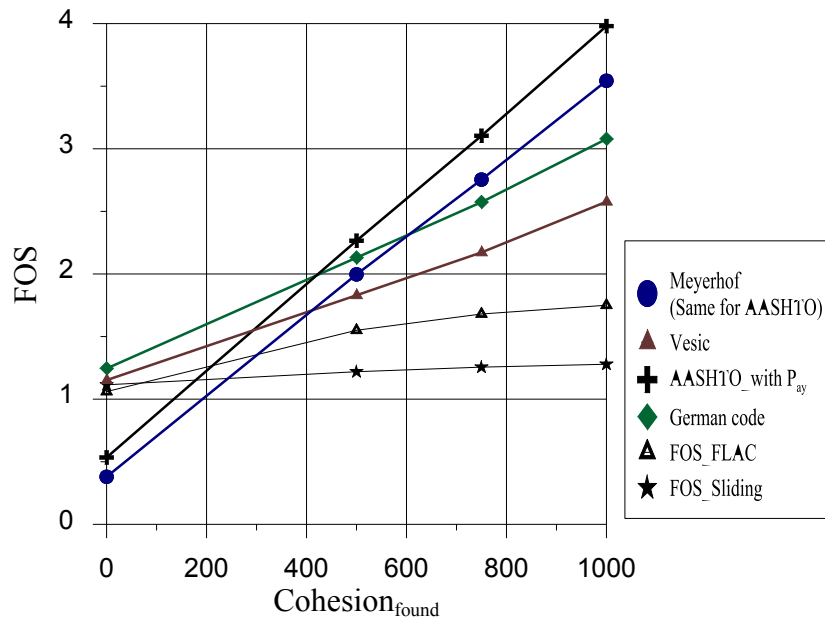


**Figure 212. Factor of Safety Values for Bearing Analysis, Sliding Analysis, and from FLAC Simulation for Different Cohesion (Found) for a Retaining  $\phi=26^\circ$ .**

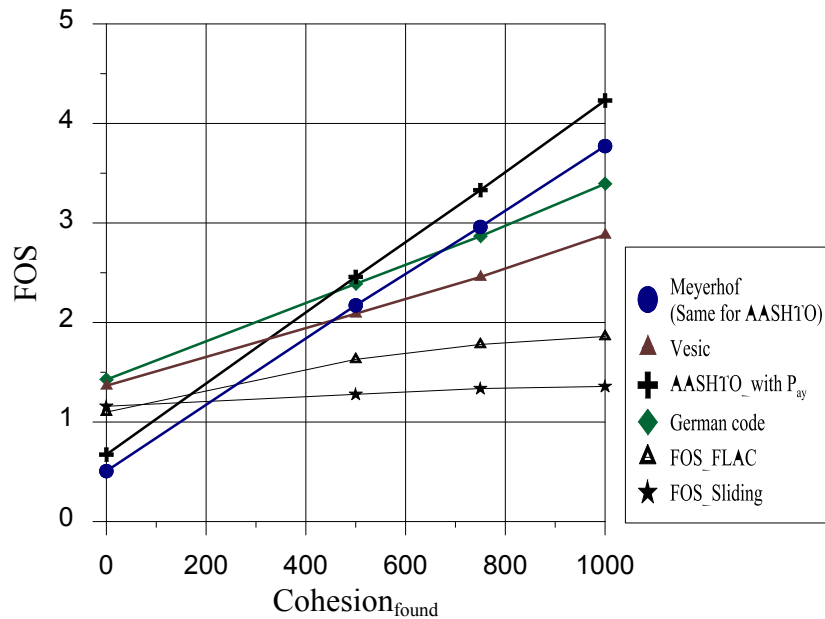


**Figure 213. Factor of Safety Values for Bearing Analysis, Sliding Analysis and from FLAC Simulation for Different Cohesion (Found) for a Retaining  $\phi=30^\circ$ .**

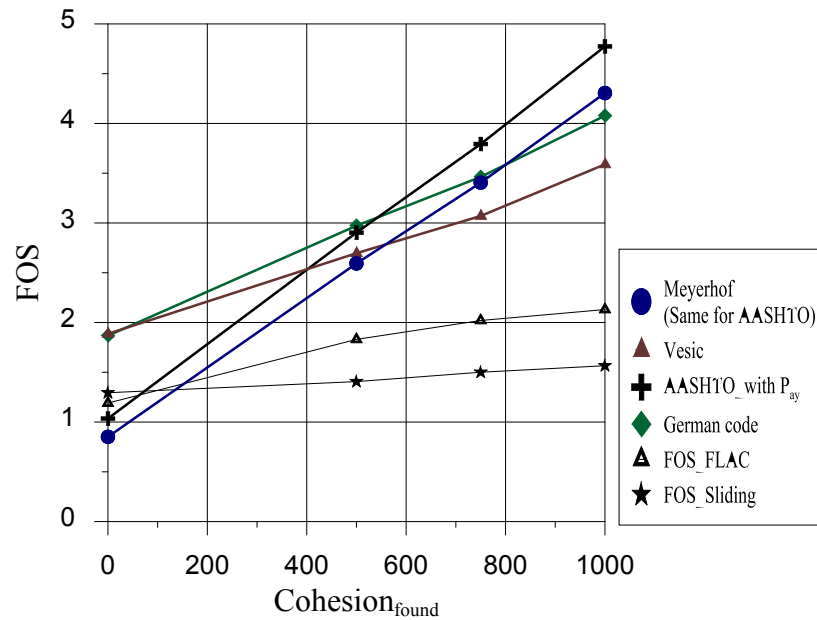


**Figure 214. Factor of Safety Values for Bearing Analysis, Sliding Analysis and from FLAC Simulation for Different Cohesion (Found) for a Retaining  $\phi=40^\circ$ .**

### Conclusions

These are the conclusions for c- $\phi$  soils used as foundation soils.

- The FOS against sliding is calculated using forces from FLAC simulation. These FOS values are lower than FLAC values, because the sliding calculations assumed no cohesion.
- For lower retained soil friction values, the FOS from FLAC has a higher value than the FOS for bearing from the Meyerhof analysis for foundation soils with low cohesion. However, for higher cohesion values, the Meyerhof safety factors exceed the FLAC predictions.
- Accounting for the additional vertical load from active thrust in Meyerhof's equation generates a small increase in the predicted bearing capacity.
- The increase in bearing capacity with increasing cohesion predicted from the Meyerhof equation is nearly linear.
- The load inclination factor has a significant influence on both the embedment and cohesion contributions to bearing capacity predicted from the Meyerhof's and Vesic's equations.

- For lower cohesion and friction angle, FOS for bearing from Meyerhof's should be verified by performing FLAC simulation for a particular case.



## CHAPTER 7: CONCLUSIONS AND RECOMMENDATIONS

### CONCLUSIONS

This chapter summarizes all the outcomes from this research. Conclusions are drawn based on these outcomes. The recommendations for this project are provided at the end of this chapter.

### Laboratory Results for Backfill Materials

The relevant data include the minimum and maximum internal friction angles and unit weights for backfill Types A, B, C, and D. The unit weight of materials was calculated as per ASTM C29 for Types A, B, and D; for Type C, it was calculated by performing a standard compaction test. Table 46–Table 47 show data for the abovementioned materials. Table 47 shows drained and undrained strength parameters for Type C materials. For the confining pressures tested, the Type C soils exhibited dilative behavior; therefore, the drained strength is actually less than the undrained strength, since negative pore pressures develop under such conditions. Since the amount of fines allowed in Type C makes it difficult to dissipate this pore pressure rapidly, this undrained condition stays longer than for other Types A, B and D.

**Table 46. Laboratory Results for Types A, B, and D.**

| Gradation | Friction Angles (°) |      |      |                    | Dry Unit Weight (pcf) | Dry Unit Weight (pcf) |                    |
|-----------|---------------------|------|------|--------------------|-----------------------|-----------------------|--------------------|
|           | Max.                | Min. | Mean | Standard Deviation |                       | Mean                  | Standard Deviation |
| A1        | 49.9                | 43.0 | 44.3 | 3.3                | 94.65                 | 100.81                | 6.40               |
| A2        | 46.8                | 41.8 |      |                    | 99.7                  |                       |                    |
| A3        | 47.5                | 41.8 |      |                    | 99.1                  |                       |                    |
| A4        | 45.9                | 39.8 |      |                    | 109.8                 |                       |                    |
| B1        | 53.4                | 48.5 | 47.4 | 5.8                | 98                    | 118.00                | 16.73              |
| B2        | 53.2                | 48.3 |      |                    | 113.4                 |                       |                    |
| B3        | 48.4                | 43.5 |      |                    | 122.7                 |                       |                    |
| B4        | 41.7                | 31.8 |      |                    | 137.9                 |                       |                    |
| D1        | 47.2                | 41.6 | 44.2 | 4.7                | 93.45                 | 96.96                 | 2.34               |
| D2        | 47.0                | 36.5 |      |                    | 98                    |                       |                    |
| D3        | 51.6                | 38.4 |      |                    | 98.1                  |                       |                    |
| D4        | 41.7                | 35.8 |      |                    | 98.3                  |                       |                    |

**Table 47. Laboratory Test Results for Type C Material.**

| <b>Gradation</b> | <b>Maximum Undrained Friction Angles (°)</b> | <b>Minimum Undrained Friction Angles (°)</b> | <b>Maximum Drained Friction Angles (°)</b> | <b>Minimum Drained Friction Angles (°)</b> | <b>Dry Unit Weight (pcf)</b> |
|------------------|--|--|--|--|------------------------------|
| C1               | 29.4   | 26.2   | 40.3                                       | 27.8                                       | 120.6                        |
| C2               | 28.3   | 26.2   | 47.4                                       | 30.1                                       | 129.4                        |
| C3               | 32.0   | 22.6   | 50.9                                       | 33.7                                       | 128.4                        |
| C4               | 32.3   | 23.6   | 26.4                                       | 23.0                                       | 126.3                        |

Note: For C4 gradation, there were two drained angles below 15°, which were excluded from these test results.

### **FLAC Analysis for Minimum Length**

For the reinforcement length ranging from 0.6~0.8H, the maximum deflection is constantly less than 1 inch for a 20-ft MSE wall. The analysis shows that requiring minimum length of 0.7H is a good practice to ensure that the lateral deflection is less than 1 inch. The analysis was conducted by assuming a wall height of 20 ft. Thus, the conclusion may not be applicable to walls higher than 20 ft, especially, when Types A and D are used as backfill materials.

### **Bearing Capacity**

The effect of retained soil on bearing capacity was evaluated by applying surcharge on only one side of the footing. The study investigated different foundation soils with friction angles ranging from 30–40° and cohesions ranging from 0–3000 psf. The surcharge was varied to be equivalent to different MSE wall heights.

The bearing capacity from the numerical model is consistent with the bearing capacity calculated from the classic Terzaghi's theory. The bearing capacity calculated from Terzaghi's theory did not include the surcharge term. It can be concluded that the surcharge on only one side of the footing would not have significant influence on the bearing capacity. Therefore, the effect of the retained soil on improving bearing capacity is not significant.

The conclusion was drawn based on the FLAC analysis neglecting the lateral earth pressure effect of the retained soil. The lateral earth pressure results in the eccentricity on the footing. The AASHTO specification should be used to consider the eccentricity that the lateral earth pressure induced from retained soil.

## Global Stability

Here are the conclusions for global stability analysis carried out using the FLAC program.

- The active wedge behind the wall is trying to move downward under the influence of gravity and the wall is pushed horizontally away from the active wedge. Therefore, it shows a vertical shear strain line behind the wall, which proves the failure mechanism. There was no interface material used in the simulation between the wall and retaining soil.
- The backfill friction angle has negligible influence on global stability.
- For weak foundations ( $\phi_{\text{found}} = 26^\circ$  and  $30^\circ$ ), the bearing capacity analysis significantly underestimates the actual factor of safety. This is a likely consequence of the conservative assumption that the full overburden stress due to the backfill acts on the foundation. In actuality, the shearing resistance in the backfill and retained soil will likely reduce the pressure acting on the foundation.
- For strong foundations ( $\phi_{\text{found}} = 35^\circ$ ) the FOS against bearing failure is well above the FOS against a wall failure. This is likely due to the fact that when the foundation is sufficiently strong, the failure mechanism switches to a different mode.
- The FOS against sliding consistently overestimates the FOS against failure. This is a likely consequence of the assumption inherent in a sliding analysis that there is no interaction between bearing resistance and sliding resistance at the base of the backfill. Assuming no interaction between sliding and bearing resistance is generally unconservative, especially when dealing with weak foundations.
- The active wedge behind the reinforced zone tends to move downward under the influence of gravity as the wall moves horizontally away from the active wedge. Since the backfill is stiffer than the retained soil, significant strain occurs across the retained-backfill boundary. No interface material is used in the simulation between wall and retaining soil. The figures show strain rate contours at the failure state, not the working stress state. Accordingly, the strain rate contours do not represent what would be seen in the field where stresses and strains are well below the failure level.

## Compound Failure Analysis

The cases of complicated geometry or groundwater conditions (i.e., MSE wall with foreslope, MSE wall with backslope, MSE wall with shallow groundwater tables and two-tier MSE wall) have been analyzed for compound failure. For the cases of the MSE wall with foreslopes, and the MSE wall with backslopes, the slope angles were varied. For the cases of the MSE wall with shallow groundwater tables, both non-rapid drawdown and rapid drawdown conditions were assessed. For the two-tier MSE wall cases, the offset and top MSE wall height were varied. Based on the analyses, the compound failure is not the critical failure mode for the situations considered in this study.

## Conclusions from Parametric Studies

### *Sliding and Overturning Analysis*

The results from the above cases show that it is important to consider the effect of unit weight of backfill and retaining soils on FOS calculations.

- Increasing  $\gamma_{\text{back}}$  from 105 pcf to 125 pcf with  $\gamma_{\text{ret}}$  maintained at a constant value of 105 pcf increases the FOS against sliding by 19 percent and FOS against overturning by 19 percent for the case of a wall height of 20 ft with no back slope.
- Increasing  $\gamma_{\text{ret}}$  from 105 pcf to 125 pcf with  $\gamma_{\text{back}}$  maintained at a constant value of 105 pcf decreases the FOS against sliding and FOS against sliding by 16 percent for the case of a wall height of 20 ft with no back slope.
- For a wall height of 20 ft and 3H:1V back slope, increasing the unit weight of backfill from 105 pcf to 125 pcf increases the FOS against sliding by 17 percent and the FOS against overturning by 16.5 percent as compared to assigning the same unit weights for both types of soils.
- For a wall height of 20 ft and 3H:1V back slope, the FOS against sliding decreases by 14.3 percent and the FOS against overturning decreases by 13.9 percent when the unit weight of the retained soil is increased from 105 pcf to 125 pcf with a constant backfill unit weight of 105 pcf.

### *Bearing Capacity Analysis*

The following conclusions can be drawn from a parametric study carried on bearing capacity analysis using different equations for different soil types.

- Forces from FLAC simulations are higher than the forces calculated from Rankine's theory, especially for higher  $\phi$  (retained) values. The higher lateral loads largely account for the lower FOS values predicted from the FLAC analyses.
- The Meyerhof's equation, which is used in the AASHTO analysis, gives a lower estimate of FOS for bearing than Vesic's equations.
- FOSs for bearing from the German code (EBGEO) give higher values than Vesic's. This is due to the consideration of vertical component of the active thrust that decreases the eccentricity.
- Including the vertical component of active thrust in the Meyerhof analysis will increase the FOS against a bearing failure, but the predicted FOS will still be lower than that predicted from the Vesic analysis.
- Meyerhof's (AASHTO) gives a conservative FOS value for bearing capacity.
- The FOSs for soft retaining soils are lower because the softer retaining soils exert higher active thrust on the wall, especially horizontal load from active thrust.
- Vesic's equation agrees reasonably well with FLAC for medium and stiff soils, but appears unconservative for soft soil.
- The chief difference between the Meyerhof's and Vesic's equations for purely cohesive soils lies in the load inclination factor. Vesic's load inclination factor accounts for the dimensions of the wall and cohesion at the base of the wall, whereas Meyerhof's load inclination factor accounts only for the load inclination angle from vertical.
- For stiff clay retained soils, the FOS from FLAC is higher than the FOS from the Meyerhof's and Vesic's equations, because of the smaller active thrust.
- Meyerhof's equation for bearing capacity can be used as a preliminary assessment tool for bearing capacity. If it gives a very low FOS, however, a FLAC simulation can be carried out to verify the calculations.

- The FOS against sliding is calculated using forces from FLAC simulation. These FOS values are lower than FLAC values, because the sliding calculations assumed no cohesion.
- For lower retained soil friction values, the FOS from FLAC is a higher value than the FOS for bearing from the Meyerhof analysis for foundation soils with low cohesion. However, for higher cohesion values, the Meyerhof safety factors exceed the FLAC predictions.
- Accounting for the additional vertical load from active thrust in Meyerhof's equation generates a small increase in the predicted bearing capacity.
- The increase in bearing capacity with increasing cohesion predicted from Meyerhof's equation is nearly linear.
- The load inclination factor has a significant influence on both the embedment and cohesion contributions to bearing capacity predicted from the Meyerhof's and Vesic's equations.
- For lower cohesion and friction angle, FOS for bearing from Meyerhof's equation should be verified by performing FLAC simulation for a particular case.

## RECOMMENDATIONS

Following are the researchers' recommendations:

- The unit weight values for Types A, B and D from tests shows that it is close to the lower range of unit weight values TxDOT had specified; for Type C, it is close to the higher range.
- The material classification for backfill plays an important role in the variability of soil parameters. For example, the amount of fines has a significant contribution on friction values for a given backfill material. Therefore, it is necessary to perform a wet sieve analysis when possible to quantify an exact amount of fines present in backfill material.
- The soil parameters for Type C backfill material should be quantified based on drainage condition at failure loading. Since the amount of fines that TxDOT recommended for Type C is between 0–30 percent, this amount changes the behavior of backfill material from cohesionless to cohesive. The friction values presented in this project are for drained and undrained conditions. Depending on the amount of fines present in this

backfill, a corresponding friction angle should be used as a soil parameter for Type C backfill material.

- The FLAC simulations performed for minimum reinforcement length using Types A, B, and D shows that current AASHTO recommendation (i.e., 0.7H) is sufficient.
- The FLAC simulations conducted for global stability on different geometries with cohesionless soil parameters for retaining and foundation soils shows that for lower friction values the failure surface is in the form of a wedge behind the wall. The overall failure mechanism for these soil parameters is a sliding failure type mechanism.
- For undrained cohesive soil parameters, the failure mechanism for soft type soils shows a bearing type failure, whereas firm and stiff type soils show a sliding type failure. Therefore, it is important to assess the failure mechanism using FLAC simulations before recommending a design procedure for lower friction/strength type of soils.
- For the conditions investigated (i.e., MSE walls with backslope, MSE wall with foreslopes, MSE walls with foreslopes, and shallow groundwater table and two-tiered MSE walls), the compound failure is not the governing failure mode.
- For two-tier walls, the compound failure represents a more circular surface outside the backfill zone. It also shows that the geometry of tiered walls influences the failure surface.
- The parametric study performed using AASHTO-recommended soil parameters shows that the ratio of unit weight backfill to unit weight of retain soils plays an important role on sliding FOS and overturning FOS. For a lower retaining friction angle, a ratio of 0.85 gives a FOS of 1.5 for sliding with horizontal back slope geometry. For 3H:1V back slope, a ratio of 1.1 gives a FOS of 1.5 for sliding.
- A FLAC simulation performed using cohesionless soil parameters on retaining and foundation soils shows that there is an interaction effect on the base friction factor used in sliding analysis and it should be considered in the design process.
- The bearing capacity analysis for cohesionless soil parameters using FLAC simulations has shown that a load eccentricity has an important role on ultimate bearing capacity. A lower eccentricity gives a higher FOS for bearing capacity.
- The comparison of bearing capacity equations that AASHTO and EBGE0 recommended shows that an additional vertical load from active thrust reduces the eccentricity of loads.

- The comparison between Meyerhof's equation and Vesic's equation shows that a different load inclination factor gives different ultimate bearing capacity values. The Meyerhof's equation gives a lower estimate and Vesic's gives a higher estimate; if compared with FLAC simulations, the FLAC FOS falls between FOS for bearing from Meyerhof's and Vesic's.
- The addition of cohesion value in lower frictional soils improves the FOS for bearing more than for sliding. Certainly, an addition of cohesion in frictional foundation soils improves the stability of the MSE walls.



## REFERENCES

- AASHTO (2002). "Standard Specifications for Highway Bridges (17th Edition) Retaining Walls." American Association of State Highway and Transportation Officials, Inc., Washington, D.C.
- AASHTO (2007). "T104-Standard Method of Test for Soundness of Aggregate by Use of Sodium Sulfate or Magnesium Sulfate." American Association of State Highway and Transportation Officials, Inc, Washington, D.C., 10.
- AASHTO (2007a). *Load and Resistance Factor Design Movable Highway Bridge Design Specifications*, American Association of State Highway and Transportation Officials, Inc.
- AASHTO (2008). "T267-Standard Method of Test for Determination of Organic Content in Soils by Loss of Ignition." American Association of State Highway and Transportation Officials, Inc, Washington, D.C., 2.
- Adams, M., Nicks, J., Stabile, T., Wu, J., Schlatter, W., and Hartmann, J. (2011). "Geosynthetic Reinforced Soil Integrated Bridge System, FHWA Synthesis Report." 68.
- AISC (2011). *Steel Construction Manual*. American Institute of Steel Construction, Chicago, IL.
- Allen, T., Christopher, B., Elias, V., and DeMaggio, J. (2001). "Development of the simplified method for internal stability design of mechanically stabilized earth walls." *FHWA Publication No. WA-RD*, 79.
- Alzamora, D., and Barrows, R. J. (2007). "Research Pays Off: Mechanically Stabilized Earth Walls on the Interstate Highway System: Thirty Years of Experience." *TR News* (249).
- ASTM (2007). "D422-63-Standard Test Method for Particle-Size Analysis of Soils." American Society for Testing and Materials, International, West Conshohocken, PA.
- ASTM (2009). "C29-Standard Test Method for Bulk Density ("Unit Weight") and Voids in Aggregate." American Society for Testing and Materials, International, West Conshohocken, PA.
- ASTM (2010). "D854-Standard Test Methods for Specific Gravity of Soil Solids by Water Pycnometer." American Society for Testing and Materials, International, West Conshohocken, PA.
- ASTM (2011a). "D7181-Consolidated Drained Triaxial Compression Test for Soils." American Society for Testing and Materials, International, West Conshohocken, PA.
- ASTM (2011b). "D4767-Standard Test Method for Consolidated Undrained Triaxial Compression Test for Cohesive Soils." American Society for Testing and Materials, International, West Conshohocken, PA.
- ASTM (2012). "D698-12-Standard Test Method for Laboratory Compaction Characteristics of Soil Using Standard Effort." American Society for Testing and Materials, International, West Conshohocken, PA, 13.
- Berg, R. R., Christopher, B. R., and Samtani, N. C. (2009). "Design of Mechanically Stabilized Earth Walls and Reinforced Soil Slopes—Volume II."

- Bobet, A. (2002). "Design of MSE Walls for Fully Saturated Conditions." Joint Transportation Research Program, Purdue University, West Lafayette, IN, 163.
- CalTrans (2004). "Bridge Design Specifications " *Retaining Walls*, California Department of Transportation, Sacramento, CA.
- CalTrans (2007). "California Test 643–Method for Determining Field and Laboratory Resistivity and pH Measurements for Soil and Water." California Department of Transportation, Sacramento, CA, 14.
- CalTrans (2008). "California Test 204–Method of Tests for Plasticity Index of Soils." California Department of Transportation, Sacramento, CA, 2.
- CalTrans (2011a). "California Test 229- Method of Test for Durability Index." California Department of Transportation, Sacramento, CA, 15.
- CalTrans (2011b). "California Test 217- Method of Test for Sand Equivalent." California Department of Transportation, Sacramento, CA, 11.
- Chalermyanont, T., and Benson, C. H. (2005). "Reliability-Based Design for External Stability of Mechanically Stabilized Earth Walls." *International Journal of Geomechanics*, 5(3), 196–205.
- Chew, S., Schmertmann, G., and Mitchell, J. (1991). "Reinforced soil wall deformations by finite element method." *Performance of Reinforced Soil Structures*, A. McGown, K. Yeo and KZ Andrawes (Eds.), London: Thomas Telford Ltd, 35–40.
- Christopher, B. R., Leshchinsky, D., and Stulgis, R. (2005). "Geosynthetic-Reinforced Soil Walls and Slopes: U.S. Perspective." *Proc., Geo-Frontiers Congress 2005*, Austin, TX, ASCE, 12.
- Dodson, M. D. (2010). "Lessons Learned from Settlement of Three Highway Embankment MSE Walls." *Earth Retention Conference 3*, 588-595.
- Duncan, J. M. (2000). "Factors of Safety and Reliability in Geotechnical Engineering." *Journal of Geotechnical and Geoenvironmental Engineering*, 126(4), 307–316.
- Duncan, J. M., Wong, K. S., and Mabry, P. (1980). "Strength, stress-strain and bulk modulus parameters for finite element analyses of stresses and movements in soil masses." *Journal of Geotechnical Engineering*.
- Elias, V., Fishman, K. L., Christopher, B. R., and Berg, R. R. (2009). "Corrosion/Degradation of Soil Reinforcements for Mechanically Stabilized Earth Walls and Reinforced Soil Slopes." Federal Highway Administration, Washington, D.C., 142.
- FHWA (2001). "Mechanically Stabilized Earth Walls and Reinforced Soil Slopes Design and Construction Guidelines." V. Elias, Christopher, B. R., Berg, R. R., ed., Federal Highway Administration, Washington, D.C.
- FHWA (2009). "Design and Construction of Mechanically Stabilized Earth Walls and Reinforced Soil Slopes-Vol.1." Federal Highway Administration, Washington, D.C.
- Galvan, M. (2007). Presentation titled "Retaining wall design and construction issues." <[https://ftp.dot.state.tx.us/pub/txdot-info/des/presentations/desbrgconf07/galvan%20retaining\\_wall\\_issues.pdf](https://ftp.dot.state.tx.us/pub/txdot-info/des/presentations/desbrgconf07/galvan%20retaining_wall_issues.pdf)>. (2011).

- Harr, M. E. (1984). *Reliability-based design in civil engineering*, Dept. of Civil Engineering, School of Engineering, North Carolina State University, Raleigh, N.C.
- Hatami, K., and Bathurst, R. J. (2005). "Development and verification of a numerical model for the analysis of geosynthetic-reinforced soil segmental walls under working stress conditions." *Canadian Geotechnical Journal*, 42(4), 1066–1085.
- Holtz, R. D., and Lee, W. F. (2002). "Internal stability analyses of geosynthetic reinforced retaining walls." Washington State Dept. of Transportation, 379.
- Johnson, A. (2012). *Recommendations for Design and Analysis of Earth Structures Using Geosynthetic Reinforcements-EBGEO*, John Wiley & Sons.
- Keller, G. R. (1995). "Experiences with Mechanically Stabilized Structures and Native Soil Backfill." *Journal of the Transportation Research Record*, 1474, 30–38.
- Kniss, K. T., Wright, S. G., Zornberg, J. G., and Yang, K. H. (2007). "Design considerations for MSE retaining walls constructed in confined spaces." University of Texas, Austin, Austin, TX, 176.
- Kuerbis, R. H., and Vaid, Y. P. (1990). "Corrections for Membrane Strength in the Triaxial Test." *Geotechnical Testing Journal, ASTM*, 13(4), 9.
- Kulhawy, F. H. (1992). "On the evaluation of soil properties." *ASCE Geotech. Spec. Publ.*, 31, 95–115.
- Kulhawy, F. H., and Mayne, P. W. (1990). "Manual on estimating soil properties for foundation design." Electric Power Research Inst., Palo Alto, CA (USA); Cornell Univ., Ithaca, NY (USA). Geotechnical Engineering Group.
- Leshchinsky, D. (2006). "ASD and LRFD of Reinforced SRW with the Use of Software Program MSEW (3.0)." *Geosynthetics*, 14–20.
- Leshchinsky, D., and Han, J. (2004). "Geosynthetic reinforced multitiered walls." *Journal of Geotechnical and Geoenvironmental Engineering*, 130, 1225.
- Leshchinsky, D., Vahedifard, F., and Leshchinsky, B. A. (2012). Revisiting bearing capacity analysis of MSE walls." *Journal of Geotextiles and Geomembranes*, 34(0), 100-107.
- Liang, R. Y. (2004). "MSE Wall and Reinforcement Testing at MUS-16-7.16 Bridge Site." University of Akron, Dept. of Civil Engineering. FHWA, 616.
- Ling, H., and Leshchinsky, D. (2003). "Finite element parametric study of the behavior of segmental block reinforced-soil retaining walls." *Geosynthetics International*, 10(3), 77-94.
- Ling, H. I., Liu, H., and Mohri, Y. (2005). "Parametric studies on the behavior of reinforced soil retaining walls under earthquake loading." *Journal of Engineering Mechanics*, 131, 1056.
- Meyers, M. S., Schwanz, N. T., and Berg, R. R. (1997). "Specifying and Bidding Segmental Concrete Faced MSE Walls on U.S. Army Corps of Engineers, St. Paul District Projects." *Proc., Geosynthetics '97 Conference proceedings*, 789-801.
- Mooney, M. A., Nocks, C. S., Selden, K. L., Bee, G. T., and Senseney, C. T. (2008). "Improving Quality Assurance of MSE Wall and Bridge Approach Earthwork Compaction." Colorado Dept. of Transportation, DTD Applied Research and Innovation Branch.

- Morrison, K. F., Harrison, F. E., Collin, J. G., Dodds, A. M., and Arndt, B. (2006). "Shored Mechanically Stabilized Earth (SMSE) Wall systems Design Guidelines." Golder Associates Inc, Lakewood, CO, 230.
- NCMA (2002). "Segmental Retaining Wall Design Manual: 2nd edition." National Concrete Masonry Association Herndon, VA, 289.
- Phoon, K. K., and Kulhawy, F. H. (1996). "On quantifying inherent soil variability." *Uncertainty in the Geologic Environment* C. D. Shackelford, P. P. Nelson, and M. J. S. Roth, eds., ASCE, New York, 326–340.
- Rathje, E. M., Rauch, A. F., Trejo, D., Folliard, K. J., Viyanant, C., Esfellar, M., Jain, A., and Ogalla, M. (2006). "Evaluation of crushed concrete and recycled asphalt pavement as backfill for mechanically stabilized earth walls." Center for Transportation Research, Austin, TX., 182.
- Reddy, D., Navarrete, F., Rosay, C., Cira, A., Ashmawy, A., and Gunaratne, M. (2003). "Long-Term Behavior of Geosynthetic Reinforced Mechanically Stabilized Earth (MSE) Wall System-Numerical/Analytical Studies, Full-Scale Field Testing, and Design Software Development." 281.
- Terzaghi, K. (1943). *Theoretical Soil Mechanics*, Wiley, New York.
- TxDOT (1999a). "Tex-128-E Determining Soil pH." Texas Department of Transportation, Austin, TX, 3.
- TxDOT (1999b). "Tex-129-E Measuring the Resistivity of Soil Materials." Texas Department of Transportation, Austin, TX.
- TxDOT (2004). "Standard Specifications for Construction and Maintenance of Highways, Streets, and Bridges." Texas Department of Transportation, Austin, Texas, 1028.
- TxDOT (2005). "Tex-620-J Determining Chloride and Sulfate Contents in Soil." Texas Department of Transportation, Austin, TX.
- TxDOT (2011). "Retaining Wall Information."  
<[http://www.txdot.gov/business/contractors\\_consultants/bridge/retaining\\_wall.htm](http://www.txdot.gov/business/contractors_consultants/bridge/retaining_wall.htm)>.  
(10/17, 2011).
- TxDOT (2012). "Geotechnical Manual." Texas Department of Transportation, Austin, Texas, 60.
- WisDOT (2006). "Bridge Manual." *Retaining Walls*, Wisconsin Department of Transportation, Madison, WI.
- Yoon, S. (2011). "Backfill Material Parameters used by TxDOT (Personal Communication)." Austin, TX.

**APPENDIX A:  
SURVEY ON MSE WALL PRACTICE**

(The participants' personal information is erased from the forms due to the agreement on personal information disclosure.)

| <b>Survey Questionnaire TxDOT Research (RTI 0-6716)<br/>Design Parameters and Methodology for MSE Walls<br/>PD: Sean Yoon, Bridge Div.    RS: Charles Aubeny, TTI</b> |   |  |  |
|---|---|--|--|
| <b>Participant Information</b>  |   |  |  |
| Name of Participant   |   | Contact phone number                         |  |
| Name of the affiliation   |   | Contact email                                |  |
| <b>Survey Questions</b>   |   |  |  |
| 1   | Is the FHWA/AASHTO manual used as guideline for MSE wall design?<br>If no, please list the guideline used for your design.  | __yes <input checked="" type="checkbox"/> no |  |
| 2   | Is the minimum length criteria used, i.e., 8 feet or 0.7H?<br>If no, please explain the minimum length criteria being used.   | <input checked="" type="checkbox"/> yes __no |  |
| 3   | Is the FHWA specification of backfill material followed?<br>If no, please provide a brief description of the classifications and material parameters for the backfill.  | <input checked="" type="checkbox"/> yes __no |  |
| 4.  | Is the durability of backfill material evaluated?<br><i>Yes, as/if appropriate as a function of geologic source and agency experience.</i><br>If yes, what is evaluated and what methods are used?<br><i>Durability and electro-chemical limits per FHWA and AASHTO.</i>  | <input checked="" type="checkbox"/> yes __no |  |
| 5.  | Have you encountered granular material that can decompose into finer grained soils in the presence of moisture?<br>If yes, please list them.<br><i>Shales, but not used for MSE fill.</i>   | <input checked="" type="checkbox"/> yes __no |  |
| 6.  | Please rank the following potential failure modes on a scale of 1 to 5, with 1 being the least common, 5 being the most common. If the failure has not been seen in your practice, please mark as N/A.<br><u>3</u> sliding <u>N/A</u> overturning <u>4</u> bearing capacity <u>2</u> global stability <u>5</u> pullout<br><u>1</u> compound failure |  |  |
| 7.  | What factor of safety (FOS) do you require for the following failure modes?<br><i>Use and LRFD capacity to demand ratio of <math>\geq 1.0</math>; which correlates to following FS values.</i><br>Sliding <u>1.5</u> ; Overturning <u>N/A</u> ; Bearing capacity <u>3.0</u> ; Pullout <u>1.5</u>  |  |  |

|  |  |  |
|--|--|--|
| 8.   | Do you use the following equation to evaluate bearing capacity?<br>$q_u = cN_c + 0.5L'\gamma_i N_\gamma$   | <input type="checkbox"/> yes<br><input checked="" type="checkbox"/> no |
| If no, please specify what method is used to check bearing capacity.<br><i>Only when appropriate. Simple equation does not incorporate groundwater or sloping toe fill conditions – that are commonly encountered.</i> |  |  |
| 9.   | Do you evaluate stability for failure modes that consider the effect of discrete wall facing units?  | <input type="checkbox"/> yes <input checked="" type="checkbox"/> no    |
| If yes, please brief how.<br><i>Generally no, except for unusual cases.</i>  |  |  |
| 10.  | Failure case of compound failure. Please mark on the dashed critical curves. Use “√” for being seen in the field; use “X” for modes considered in design analysis. |  |
|  |  |  |
| <b>Additional Comments</b>   |  |  |
| Please make any comments on the current MSE design methodology.  |  |  |

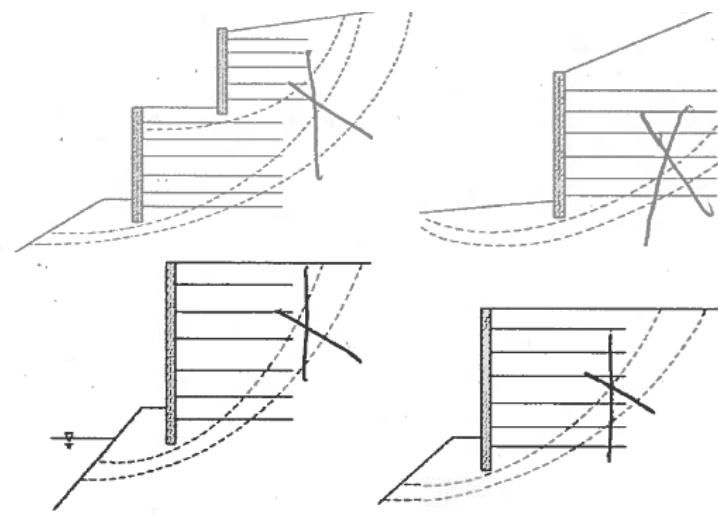
**Survey Questionnaire TxDOT Research (RTI 0-6716)  
Design Parameters and Methodology for MSE Walls  
PD: Sean Yoon, Bridge Div. RS: Charles Aubeny, TTI**

**Participant Information**

|                         |                             |                      |                                  |
|-------------------------|-----------------------------|----------------------|----------------------------------|
| Name of Participant     |                             | Contact phone number |                                  |
| Name of the affiliation | <i>MassDOT,<br/>Highway</i> | Contact email        | <i>Peter.Connors@state.ma.us</i> |

**Survey Questions**

|    |   |   |
|----|---|---|
| 1  | Is the FHWA/AASHTO manual used as guideline for MSE wall design?<br>If no, please list the guideline used for your design.  | <input checked="" type="checkbox"/> yes <input type="checkbox"/> no |
| 2  | Is the minimum length criteria used, i.e., 8 feet or 0.7H?<br>If no, please explain the minimum length criteria being used.   | <input checked="" type="checkbox"/> yes <input type="checkbox"/> no |
| 3  | Is the FHWA specification of backfill material followed?<br><i>We may use a standard material gradation that closely matches.</i><br>If no, please provide a brief description of the classifications and material parameters for the backfill.   | <input checked="" type="checkbox"/> yes <input type="checkbox"/> no |
| 4. | Is the durability of backfill material evaluated?<br>If yes, what is evaluated and what methods are used?<br><i>Los Angeles Abrasion AASHTO T96</i>   | <input checked="" type="checkbox"/> yes <input type="checkbox"/> no |
| 5. | Have you encountered granular material that can decompose into finer grained soils in the presence of moisture?<br>If yes, please list them.  | <input type="checkbox"/> yes <input checked="" type="checkbox"/> no |
| 6. | Please rank the following potential failure modes on a scale of 1 to 5, with 1 being the least common, 5 being the most common. If the failure has not been seen in your practice, please mark as N/A.<br><i>N/A sliding N/A overturning N/A bearing capacity N/A global stability<br/>N/A pullout N/A compound failure</i> |   |
| 7. | What factor of safety (FOS) do you require for the following failure modes?<br><i>LRFD<br/>Sliding 1.0; Overturning N/A Bearing capacity 0.65; Pullout Table 11.5.6-1</i>   |   |
| 8. | Do you use the following equation to evaluate bearing capacity?<br>$q_u = cN_c + 0.5L'\gamma_i N_\gamma$<br>If no, please specify what method is used to check bearing capacity.<br><i>EQN 10.6.3.1.2a-1</i>  | <input type="checkbox"/> yes <input checked="" type="checkbox"/> no |
| 9. | Do you evaluate stability for failure modes that consider the effect of discrete wall facing units?<br>If yes, please brief how.<br><i>AASHTO Chapter 11</i>  | <input checked="" type="checkbox"/> yes <input type="checkbox"/> no |

|  |  |  |
|--|--|--|
| 10.  | Failure case of compound failure. Please mark on the dashed critical curves. Use “√” for being seen in the field; use “X” for modes considered in design analysis. |  |
|  |  |  |
| 11.  | Is the AASHTO MSE wall backfill specification for the electrochemical requirements followed?   | <input checked="" type="checkbox"/> yes __no |

**Additional Comments**

Please make any comments on the current MSE design methodology.

*Current AASHTO code does not adequately address Integral Abutment Bridges behind MSE walls.*



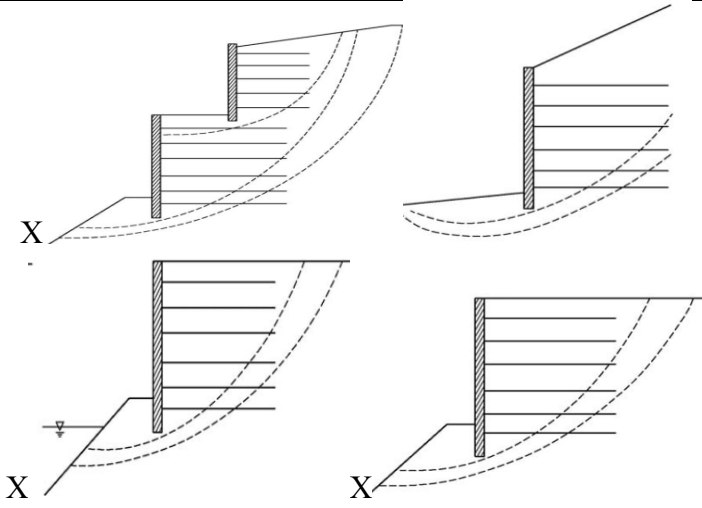
**Survey Questionnaire TxDOT Research (RTI 0-6716)  
Design Parameters and Methodology for MSE Walls  
PD: Sean Yoon, Bridge Div. RS: Charles Aubeny, TTI**

**Participant Information**

|                         |                   |                      |  |
|-------------------------|-------------------|----------------------|--|
| Name of Participant     | .                 | Contact phone number |  |
| Name of the affiliation | <i>Oregon DOT</i> | Contact email        |  |

**Survey Questions**

|    |  |   |
|----|--|---|
| 1  | Is the FHWA/AASHTO manual used as guideline for MSE wall design?<br>If no, please list the guideline used for your design.   | <input checked="" type="checkbox"/> yes <input type="checkbox"/> no |
| 2  | Is the minimum length criteria used, i.e., 8 feet or 0.7H?<br>If no, please explain the minimum length criteria being used.  | <input checked="" type="checkbox"/> yes <input type="checkbox"/> no |
| 3  | Is the FHWA specification of backfill material followed?<br>If no, please provide a brief description of the classifications and material parameters for the backfill.<br><i>Oregon DOT Special Provision 0A596.11 (Backfill) defines gradation, plasticity, and electrochemical requirements for MSE Granular Wall Backfill described at the following weblink:</i><br><br><a href="http://www.oregon.gov/ODOT/HWY/SPECS/docs/08specials/00500/SP596A.doc">http://www.oregon.gov/ODOT/HWY/SPECS/docs/08specials/00500/SP596A.doc</a><br><br><i>MSE Granular Wall Backfill is a graded, 1" or ¾" base aggregate material (crushed rock) with sand and 40–60% passing the No. 10 Sieve.</i> | <input type="checkbox"/> yes <input checked="" type="checkbox"/> no |
| 4. | Is the durability of backfill material evaluated?<br>If yes, what is evaluated and what methods are used?  | <input checked="" type="checkbox"/> yes <input type="checkbox"/> no |
| 5. | Have you encountered granular material that can decompose into finer grained soils in the presence of moisture?<br>If yes, please list them.<br><i>We have various sedimentary bedrock units classified as nondurable rock in portions of the state that rapidly degrade when wet. Embankment construction criteria for nondurable rock is provided in Oregon DOT Standard Specification 00330.42(c)(2)(e).</i>  | <input checked="" type="checkbox"/> yes <input type="checkbox"/> no |
| 6. | Please rank the following potential failure modes on a scale of 1 to 5, with 1 being the least common, 5 being the most common. If the failure has not been seen in your practice, please mark as N/A.<br><u>1</u> sliding <u>N/A</u> overturning <u>N/A</u> bearing capacity <u>3</u> global stability <u>N/A</u> pullout<br><u>2</u> compound failure  |   |

|  |  |  |
|--|--|--|
| 7.   | What factor of safety (FOS) do you require for the following failure modes?<br><i>Use AASHTO LRFD Sections 10 and 11.</i>  |  |
| Sliding _____ ; Overturning _____ ; Bearing capacity _____ ; Pullout _____   |  |  |
| 8.   | Do you use the following equation to evaluate bearing capacity?<br>$q_u = cN_c + 0.5L'\gamma_i N_\gamma$   | __yes <input checked="" type="checkbox"/> no |
| If no, please specify what method is used to check bearing capacity.<br><i>Use AASHTO LRFD Sections 11.10.5.4, 10.6.3.1, and 10.6.3.2.</i>   |  |  |
| 9.   | Do you evaluate stability for failure modes that consider the effect of discrete wall facing units?  | __yes <input checked="" type="checkbox"/> no |
| If yes, please brief how.  |  |  |
| 10.  | Failure case of compound failure. Please mark on the dashed critical curves. Use “√” for being seen in the field; use “X” for modes considered in design analysis. |  |
|   |  |  |
| <b>Additional Comments</b>   |  |  |
| <p>Please make any comments on the current MSE design methodology.</p> <p><i>The Oregon DOT MSE design methodology is described in Chapter 15 of the ODOT Geotechnical Design Manual at the following web link:</i></p> <p><a href="ftp://ftp.odot.state.or.us/techserv/Geo-Environmental/Geotech/GeoManual/FinalGDMApril2011/FinalGDMApril2011.pdf">ftp://ftp.odot.state.or.us/techserv/Geo-Environmental/Geotech/GeoManual/FinalGDMApril2011/FinalGDMApril2011.pdf</a></p> |  |  |

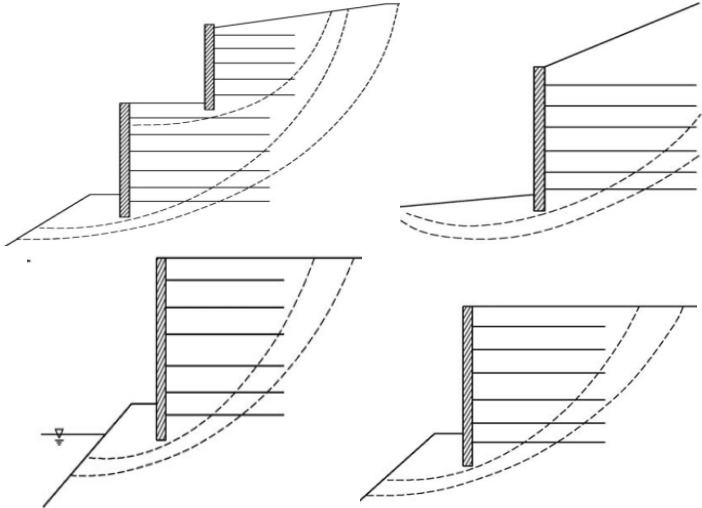
**Survey Questionnaire TxDOT Research (RTI 0-6716)**  
**Design Parameters and Methodology for MSE Walls**  
**PD: Sean Yoon, Bridge Div. RS: Charles Aubeny, TTI**

**Participant Information**

|                         |              |                      |  |
|-------------------------|--------------|----------------------|--|
| Name of Participant     |              | Contact phone number |  |
| Name of the affiliation | <i>SDDOT</i> | Contact email        |  |

**Survey Questions**

|    |  |   |
|----|--|---|
| 1  | Is the FHWA/AASHTO manual used as guideline for MSE wall design?   | <input checked="" type="checkbox"/> yes <input type="checkbox"/> no |
|    | If no, please list the guideline used for your design.   |   |
| 2  | Is the minimum length criteria used, i.e., 8 feet or 0.7H?   | <input checked="" type="checkbox"/> yes <input type="checkbox"/> no |
|    | If no, please explain the minimum length criteria being used.  |   |
| 3  | Is the FHWA specification of backfill material followed?   | <input type="checkbox"/> yes <input checked="" type="checkbox"/> no |
|    | If no, please provide a brief description of the classifications and material parameters for the backfill.<br><i>The backfill material spec has been modified from 100% passing the 4" sieve to 100% passing the 1.5" sieve.</i>   |   |
| 4. | Is the durability of backfill material evaluated?  | <input checked="" type="checkbox"/> yes <input type="checkbox"/> no |
|    | If yes, what is evaluated and what methods are used?<br><i>We have a Special Provision that states that the soundness of the backfill material shall be free of soft, poor durability particles. The material shall have a sodium sulfate soundness loss of less than 15 percent after five cycles determined in accordance with AASHTO T-104 or SD 220.</i> |   |
| 5. | Have you encountered granular material that can decompose into finer grained soils in the presence of moisture?  | <input type="checkbox"/> yes <input checked="" type="checkbox"/> no |
|    | If yes, please list them.  |   |
| 6. | Please rank the following potential failure modes on a scale of 1 to 5, with 1 being the least common, 5 being the most common. If the failure has not been seen in your practice, please mark as N/A.   |   |
|    | <i><u>N/A</u> sliding <u>3</u> overturning <u>5</u> bearing capacity <u>1</u> global stability <u>N/A</u> pullout <u>N/A</u> compound failure</i>  |   |
| 7. | What factor of safety (FOS) do you require for the following failure modes?  |   |
|    | <i>Sliding <u>1.5</u>; Overturning <u>2.0</u>; Bearing capacity <u>2.0</u>; Pullout <u>1.5</u></i>   |   |
| 8. | Do you use the following equation to evaluate bearing capacity?<br>$q_u = cN_c + 0.5L'\gamma_i N_\gamma$   | <input checked="" type="checkbox"/> yes <input type="checkbox"/> no |
|    | If no, please specify what method is used to check bearing capacity.   |   |

|  |  |  |
|--|--|--|
| 9.   | Do you evaluate stability for failure modes that consider the effect of discrete wall facing units?<br>If yes, please brief how.                                   | <input type="checkbox"/> yes <input checked="" type="checkbox"/> no                |
| 10.  | Failure case of compound failure. Please mark on the dashed critical curves. Use “√” for being seen in the field; use “X” for modes considered in design analysis. |  |
| 11.  | Is the AASHTO MSE wall backfill specification for the electrochemical requirements followed?   | <input checked="" type="checkbox"/> yes <input type="checkbox"/> no                |
| <b>Additional Comments</b>   |  |  |
| <p>Please make any comments on the current MSE design methodology.</p> <p><i>All the cases in item number 10 are looked and run accordingly for worst-case scenario. Global stability is checked on all walls that are designed.</i></p> |  |  |

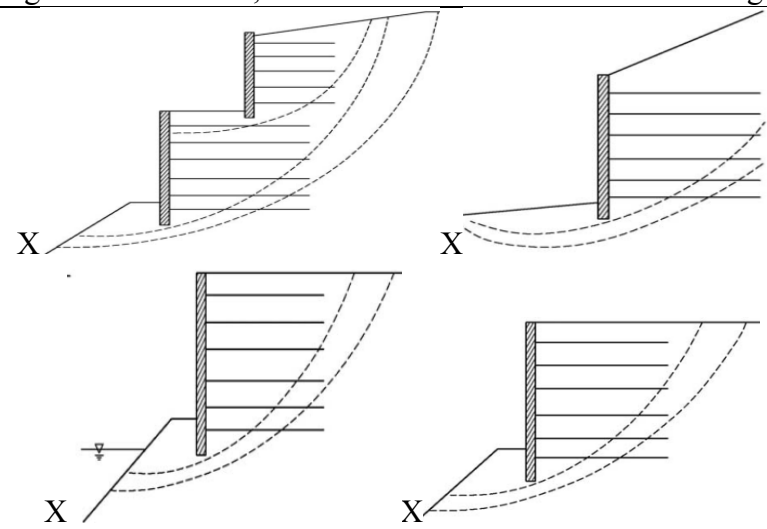
**Survey Questionnaire TxDOT Research (RTI 0-6716)**  
**Design Parameters and Methodology for MSE Walls**  
**PD: Sean Yoon, Bridge Div. RS: Charles Aubeny, TTI**

**Participant Information**

|                         |                   |                      |  |
|-------------------------|-------------------|----------------------|--|
| Name of Participant     |                   | Contact phone number |  |
| Name of the affiliation | <i>Nevada DOT</i> | Contact email        |  |

**Survey Questions**

|    |   |   |
|----|---|---|
| 1  | Is the FHWA/AASHTO manual used as guideline for MSE wall design?<br>If no, please list the guideline used for your design.  | <input checked="" type="checkbox"/> yes <input type="checkbox"/> no |
| 2  | Is the minimum length criteria used, i.e., 8 feet or 0.7H?<br>If no, please explain the minimum length criteria being used.   | <input checked="" type="checkbox"/> yes <input type="checkbox"/> no |
| 3  | Is the FHWA specification of backfill material followed?<br>If no, please provide a brief description of the classifications and material parameters for the backfill.  | <input checked="" type="checkbox"/> yes <input type="checkbox"/> no |
| 4. | Is the durability of backfill material evaluated?<br>If yes, what is evaluated and what methods are used?<br><i>AASHTO T104: Magnesium Sulfate Soundness, AASHTO T267: Organic Content.</i>   | <input checked="" type="checkbox"/> yes <input type="checkbox"/> no |
| 5. | Have you encountered granular material that can decompose into finer grained soils in the presence of moisture?<br>If yes, please list them.  | <input type="checkbox"/> yes <input checked="" type="checkbox"/> no |
| 6. | Please rank the following potential failure modes on a scale of 1 to 5, with 1 being the least common, 5 being the most common. If the failure has not been seen in your practice, please mark as N/A.<br><i>N/A</i> sliding <i>N/A</i> overturning <i>N/A</i> bearing capacity <i>N/A</i> global stability<br><i>N/A</i> pullout <i>N/A</i> compound failure |   |
| 7. | What factor of safety (FOS) do you require for the following failure modes?<br>Sliding <u>1.5</u> ; Overturning <u>2</u> ; Bearing capacity <u>2.5</u> ; Pullout <u>1.5</u>   |   |
| 8. | Do you use the following equation to evaluate bearing capacity?<br>$q_u = cN_c + 0.5L'\gamma_iN_\gamma$<br>If no, please specify what method is used to check bearing capacity.   | <input checked="" type="checkbox"/> yes <input type="checkbox"/> no |
| 9. | Do you evaluate stability for failure modes that consider the effect of discrete wall facing units?<br>If yes, please brief how.  | <input type="checkbox"/> yes <input checked="" type="checkbox"/> no |

|     |  |
|-----|--|
| 10. | <p>Failure case of compound failure. Please mark on the dashed critical curves. Use “√” for being seen in the field; use “X” for modes considered in design analysis.</p>  |
| 11. | <p>Is the AASHTO MSE wall backfill specification for the electrochemical requirements followed? <input checked="" type="checkbox"/>yes ___no</p>   |

**Additional Comments**

Please make any comments on the current MSE design methodology.

*We use AASHTO LRFD Method. For maximum reinforced loads, we use Simplified Method.*

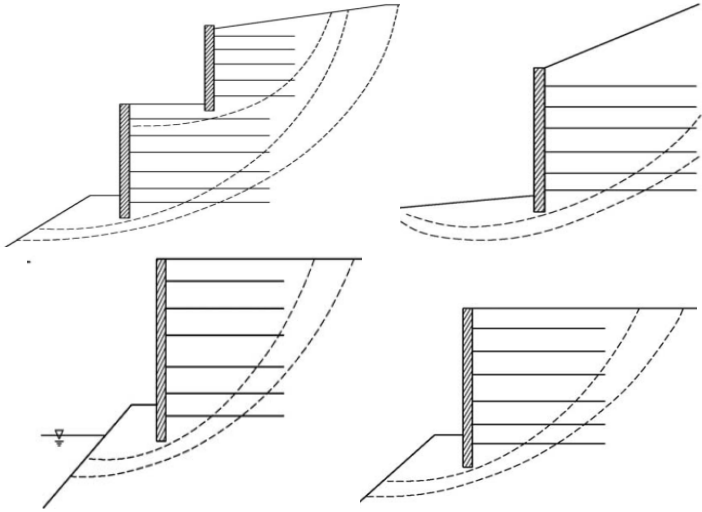
**Survey Questionnaire TxDOT Research (RTI 0-6716)  
 Design Parameters and Methodology for MSE Walls  
 PD: Sean Yoon, Bridge Div. RS: Charles Aubeny, TTI**

**Participant Information**

|                         |                               |                      |  |
|-------------------------|-------------------------------|----------------------|--|
| Name of Participant     |                               | Contact phone number |  |
| Name of the affiliation | <i>Idaho Dept. of Transp.</i> | Contact email        |  |

**Survey Questions**

|    |   |   |
|----|---|---|
| 1  | Is the FHWA/AASHTO manual used as guideline for MSE wall design?<br>If no, please list the guideline used for your design.  | <input checked="" type="checkbox"/> yes <input type="checkbox"/> no |
| 2  | Is the minimum length criteria used, i.e., 8 feet or 0.7H?<br>If no, please explain the minimum length criteria being used.   | <input checked="" type="checkbox"/> yes <input type="checkbox"/> no |
| 3  | Is the FHWA specification of backfill material followed?<br>If no, please provide a brief description of the classifications and material parameters for the backfill.  | <input checked="" type="checkbox"/> yes <input type="checkbox"/> no |
| 4. | Is the durability of backfill material evaluated?<br>If yes, what is evaluated and what methods are used?   | <input type="checkbox"/> yes <input checked="" type="checkbox"/> no |
| 5. | Have you encountered granular material that can decompose into finer grained soils in the presence of moisture?<br>If yes, please list them.  | <input type="checkbox"/> yes <input checked="" type="checkbox"/> no |
| 6. | Please rank the following potential failure modes on a scale of 1 to 5, with 1 being the least common, 5 being the most common. If the failure has not been seen in your practice, please mark as N/A.<br><u>N/A</u> sliding <u>N/A</u> overturning <u>N/A</u> bearing capacity <u>N/A</u> global stability<br><u>N/A</u> pullout <u>N/A</u> compound failure |   |
| 7. | What factor of safety (FOS) do you require for the following failure modes?<br>Sliding <u>N/A</u> ; Overturning <u>N/A</u> ; Bearing capacity <u>N/A</u> ; Pullout <u>N/A</u>   |   |
| 8. | Do you use the following equation to evaluate bearing capacity?<br>$q_u = cN_c + 0.5L'\gamma_i N_\gamma$<br>If no, please specify what method is used to check bearing capacity.<br><i>Methods in AASHTO LRFD Bridge Design Specifications</i>  | <input type="checkbox"/> yes <input checked="" type="checkbox"/> no |
| 9. | Do you evaluate stability for failure modes that consider the effect of discrete wall facing units?<br>If yes, please brief how.  | <input type="checkbox"/> yes <input checked="" type="checkbox"/> no |

|   |  |         |  |
|---|--|---------|--|
| 10.   | Failure case of compound failure. Please mark on the dashed critical curves. Use “√” for being seen in the field; use “X” for modes considered in design analysis.   |         |  |
|   |  |         |  |
| 11.   | Is the AASHTO MSE wall backfill specification for the electrochemical requirements followed? <table border="1" data-bbox="1136 821 1352 898"> <tr> <td data-bbox="1136 821 1250 898">___ yes</td> <td data-bbox="1250 821 1352 898"><input checked="" type="checkbox"/> no</td> </tr> </table> | ___ yes | <input checked="" type="checkbox"/> no |
| ___ yes   | <input checked="" type="checkbox"/> no   |         |  |
| <b>Additional Comments</b>  |  |         |  |
| <p>Please make any comments on the current MSE design methodology.</p> <p><i>Because we don't design walls with ASD design method, we don't have answers for question #7 regarding FOS.</i></p> |  |         |  |



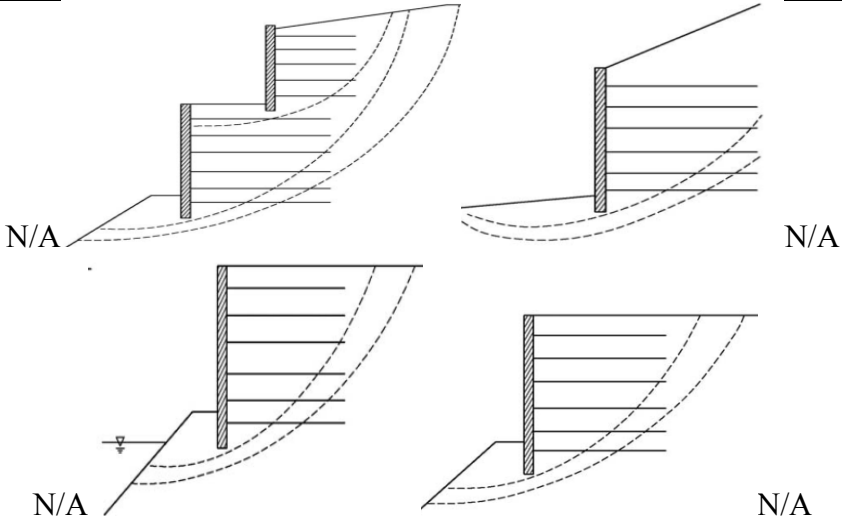
**Survey Questionnaire TxDOT Research (RTI 0-6716)  
 Design Parameters and Methodology for MSE Walls  
 PD: Sean Yoon, Bridge Div. RS: Charles Aubeny, TTI**

**Participant Information**

|                         |       |                      |  |
|-------------------------|-------|----------------------|--|
| Name of Participant     |       | Contact phone number |  |
| Name of the affiliation | INDOT | Contact email        |  |

**Survey Questions**

|    |   |   |
|----|---|---|
| 1  | Is the FHWA/AASHTO manual used as guideline for MSE wall design?<br>If no, please list the guideline used for your design.  | <input checked="" type="checkbox"/> yes <input type="checkbox"/> no |
| 2  | Is the minimum length criteria used, i.e., 8 feet or 0.7H?<br>If no, please explain the minimum length criteria being used.   | <input checked="" type="checkbox"/> yes <input type="checkbox"/> no |
| 3  | Is the FHWA specification of backfill material followed?<br>If no, please provide a brief description of the classifications and material parameters for the backfill.  | <input checked="" type="checkbox"/> yes <input type="checkbox"/> no |
| 4. | Is the durability of backfill material evaluated?<br>If yes, what is evaluated and what methods are used?   | <input checked="" type="checkbox"/> yes <input type="checkbox"/> no |
| 5. | Have you encountered granular material that can decompose into finer grained soils in the presence of moisture?<br>If yes, please list them.  | <input type="checkbox"/> yes <input checked="" type="checkbox"/> no |
| 6. | Please rank the following potential failure modes on a scale of 1 to 5, with 1 being the least common, 5 being the most common. If the failure has not been seen in your practice, please mark as N/A.<br><u>N/A</u> sliding <u>N/A</u> overturning <u>N/A</u> bearing capacity <u>3</u> global stability<br><u>N/A</u> pullout <u>N/A</u> compound failure |   |
| 7. | What factor of safety (FOS) do you require for the following failure modes?<br>Sliding <u>1.5</u> ; Overturning <u>1.5</u> ; Bearing capacity <u>≥2.5</u> ; Pullout <u>1.5</u>  |   |
| 8. | Do you use the following equation to evaluate bearing capacity?<br>$q_u = cN_c + 0.5L'\gamma_i N_\gamma$<br>If no, please specify what method is used to check bearing capacity.  | <input checked="" type="checkbox"/> yes <input type="checkbox"/> no |
| 9. | Do you evaluate stability for failure modes that consider the effect of discrete wall facing units?<br>If yes, please brief how.  | <input type="checkbox"/> yes <input checked="" type="checkbox"/> no |

|   |   |   |                             |
|---|---|---|-----------------------------|
| 10.   | Failure case of compound failure. Please mark on the dashed critical curves. Use “√” for being seen in the field; use “X” for modes considered in design analysis.  |   |                             |
|  <p>The figure contains four diagrams of MSE wall cross-sections, arranged in a 2x2 grid. Each diagram shows a wall with horizontal reinforcement layers and dashed lines representing critical failure curves. The diagrams are labeled 'N/A'.</p> |   |   |                             |
| 11.   | Is the AASHTO MSE wall backfill specification for the electrochemical requirements followed? <table border="1" data-bbox="1149 835 1352 909"> <tr> <td><input checked="" type="checkbox"/> yes</td> <td><input type="checkbox"/> no</td> </tr> </table> | <input checked="" type="checkbox"/> yes | <input type="checkbox"/> no |
| <input checked="" type="checkbox"/> yes   | <input type="checkbox"/> no   |   |                             |
| <b>Additional Comments</b>  |   |   |                             |
| Please make any comments on the current MSE design methodology.   |   |   |                             |

**Survey Questionnaire TxDOT Research (RTI 0-6716)**  
**Design Parameters and Methodology for MSE Walls**  
**PD: Sean Yoon, Bridge Div. RS: Charles Aubeny, TTI**

**Participant Information**

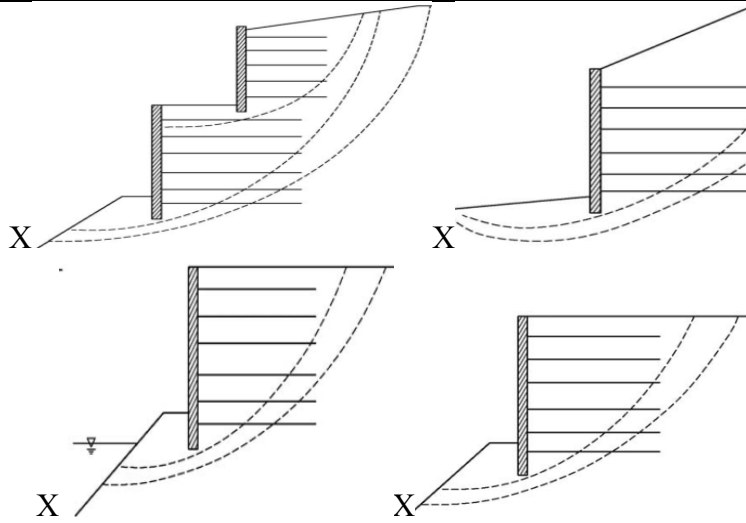
|                         |   |                      |  |
|-------------------------|---|----------------------|--|
| Name of Participant     |   | Contact phone number |  |
| Name of the affiliation | <i>Missouri Dept. of Transportation</i> | Contact email        |  |

**Survey Questions**

|    |   |   |
|----|---|---|
| 1  | Is the FHWA/AASHTO manual used as guideline for MSE wall design?<br>If no, please list the guideline used for your design.  | <input checked="" type="checkbox"/> yes <input type="checkbox"/> no |
| 2  | Is the minimum length criteria used, i.e., 8 feet or 0.7H?<br>If no, please explain the minimum length criteria being used.   | <input checked="" type="checkbox"/> yes <input type="checkbox"/> no |
| 3  | Is the FHWA specification of backfill material followed?<br>If no, please provide a brief description of the classifications and material parameters for the backfill.<br><i>Allow 2000 ohm-cm material for resistivity</i>   | <input checked="" type="checkbox"/> yes <input type="checkbox"/> no |
| 4. | Is the durability of backfill material evaluated?<br>If yes, what is evaluated and what methods are used?<br><i>Resistivity – AASHTO T288/pH- AASHTO T289/Chlorides &amp; Sulfates – ASTM D4327/ Organics- AASHTO T267</i>  | <input checked="" type="checkbox"/> yes <input type="checkbox"/> no |
| 5. | Have you encountered granular material that can decompose into finer grained soils in the presence of moisture?<br>If yes, please list them.  | <input type="checkbox"/> yes <input checked="" type="checkbox"/> no |
| 6. | Please rank the following potential failure modes on a scale of 1 to 5, with 1 being the least common, 5 being the most common. If the failure has not been seen in your practice, please mark as N/A.<br><i>NA sliding NA overturning 2 bearing capacity 1 global stability<br/>NA pullout NA compound failure</i> |   |
| 7. | What factor of safety (FOS) do you require for the following failure modes?<br>Sliding _____ ; Overturning _____ ; Bearing capacity _____ ; Pullout _____   |   |
| 8. | Do you use the following equation to evaluate bearing capacity?<br>$q_u = cN_c + 0.5L'\gamma_iN_\gamma$<br>If no, please specify what method is used to check bearing capacity.   | <input checked="" type="checkbox"/> yes <input type="checkbox"/> no |
| 9. | Do you evaluate stability for failure modes that consider the effect of discrete wall facing units?<br>If yes, please brief how.  | <input type="checkbox"/> yes <input checked="" type="checkbox"/> no |

10.

Failure case of compound failure. Please mark on the dashed critical curves. Use “√” for being seen in the field; use “X” for modes considered in design analysis.



**Additional Comments**

Please make any comments on the current MSE design methodology.

**Survey Questionnaire TxDOT Research (RTI 0-6716)**  
**Design Parameters and Methodology for MSE Walls**  
**PD: Sean Yoon, Bridge Div. RS: Charles Aubeny, TTI**

**Participant Information**

|                         |   |                      |  |
|-------------------------|---|----------------------|--|
| Name of Participant     |   | Contact phone number |  |
| Name of the affiliation | <i>NMDOT<br/>Geotechnical<br/>Section</i> | Contact email        |  |

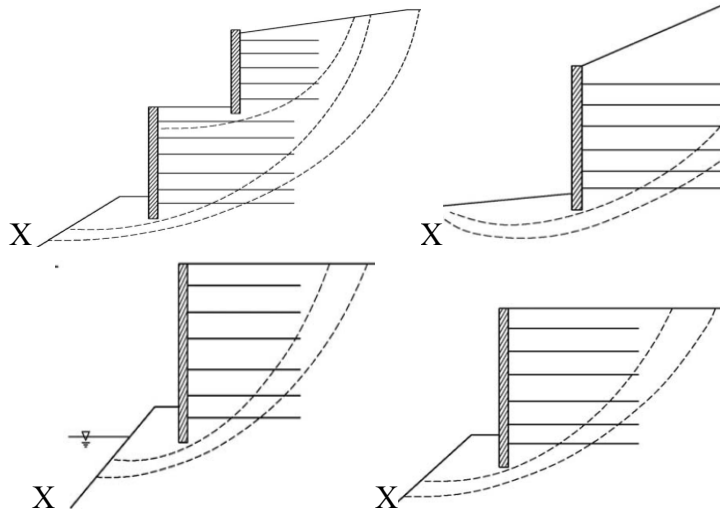
**Survey Questions**

|    |   |   |
|----|---|---|
| 1  | Is the FHWA/AASHTO manual used as guideline for MSE wall design?<br>If no, please list the guideline used for your design.  | <input checked="" type="checkbox"/> yes <input type="checkbox"/> no |
| 2  | Is the minimum length criteria used, i.e., 8 feet or 0.7H?<br>If no, please explain the minimum length criteria being used.   | <input checked="" type="checkbox"/> yes <input type="checkbox"/> no |
| 3  | Is the FHWA specification of backfill material followed?<br>If no, please provide a brief description of the classifications and material parameters for the backfill.<br><i>All same except Resistivity max at 2500 ohm-cm</i>   | <input type="checkbox"/> yes <input checked="" type="checkbox"/> no |
| 4. | Is the durability of backfill material evaluated?<br>If yes, what is evaluated and what methods are used?   | <input checked="" type="checkbox"/> yes <input type="checkbox"/> no |
| 5. | Have you encountered granular material that can decompose into finer grained soils in the presence of moisture?<br>If yes, please list them.  | <input type="checkbox"/> yes <input checked="" type="checkbox"/> no |
| 6. | Please rank the following potential failure modes on a scale of 1 to 5, with 1 being the least common, 5 being the most common. If the failure has not been seen in your practice, please mark as N/A.<br><input type="checkbox"/> sliding <input type="checkbox"/> overturning <input type="checkbox"/> bearing capacity <input type="checkbox"/> global stability <input type="checkbox"/> pullout<br><input type="checkbox"/> compound failure <input checked="" type="checkbox"/> - Differential Settlement of panels |   |
| 7. | What factor of safety (FOS) do you require for the following failure modes?<br>Sliding <u>1.5</u> ; Overturning <u>2.0</u> ; Bearing capacity <u>2.0</u> ; Pullout <u>1.5</u> 100-year service life LRFD Being Used   |   |
| 8. | Do you use the following equation to evaluate bearing capacity?<br>$q_u = cN_c + 0.5L'\gamma_i N_\gamma$<br>If no, please specify what method is used to check bearing capacity.  | <input checked="" type="checkbox"/> yes <input type="checkbox"/> no |

9. Do you evaluate stability for failure modes that consider the effect of discrete wall facing units?  yes  no

If yes, please brief how.

10. Failure case of compound failure. Please mark on the dashed critical curves. Use “√” for being seen in the field; use “X” for modes considered in design analysis.



11. Is the AASHTO MSE wall backfill specification for the electrochemical requirements followed?  yes  no  
*2500 ohm-cm max.*

**Additional Comments**

Please make any comments on the current MSE design methodology.

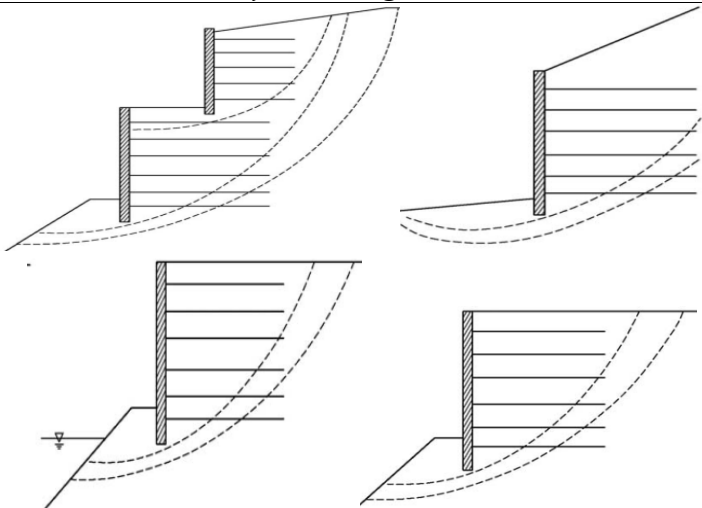
**Survey Questionnaire TxDOT Research (RTI 0-6716)**  
**Design Parameters and Methodology for MSE Walls**  
**PD: Sean Yoon, Bridge Div. RS: Charles Aubeny, TTI**

**Participant Information**

|                         |                    |                      |  |
|-------------------------|--------------------|----------------------|--|
| Name of Participant     |                    | Contact phone number |  |
| Name of the affiliation | <i>Alabama DOT</i> | Contact email        |  |

**Survey Questions**

|    |   |   |
|----|---|---|
| 1  | Is the FHWA/AASHTO manual used as guideline for MSE wall design?<br>If no, please list the guideline used for your design.  | <input checked="" type="checkbox"/> yes <input type="checkbox"/> no |
| 2  | Is the minimum length criteria used, i.e., 8 feet or 0.7H?<br>If no, please explain the minimum length criteria being used.   | <input checked="" type="checkbox"/> yes <input type="checkbox"/> no |
| 3  | Is the FHWA specification of backfill material followed?<br>If no, please provide a brief description of the classifications and material parameters for the backfill.<br><ul style="list-style-type: none"> <li>• <i>Concrete sand meeting the requirements of 802, Fine Aggregates (FM waived) of ALDOT Standard Specifications for Highway Construction</i></li> <li>• <i>Section 801 Coarse Aggregate crushed material that is smaller than #467 with 10% or less passing the #200 sieve</i></li> <li>• <i>Crusher run material with 100% passing the 2-inch sieve and with 10% or less passing the #200 sieve</i></li> </ul> | <input type="checkbox"/> yes <input checked="" type="checkbox"/> no |
| 4. | Is the durability of backfill material evaluated?<br>If yes, what is evaluated and what methods are used?<br><i>Per 801 and 802 as noted above, a soundness test is performed per AASHTO T104</i>   | <input checked="" type="checkbox"/> yes <input type="checkbox"/> no |
| 5. | Have you encountered granular material that can decompose into finer grained soils in the presence of moisture?<br>If yes, please list them.<br><i>Chert gravels</i>  | <input checked="" type="checkbox"/> yes <input type="checkbox"/> no |
| 6. | Please rank the following potential failure modes on a scale of 1 to 5, with 1 being the least common, 5 being the most common. If the failure has not been seen in your practice, please mark as N/A.<br><input type="checkbox"/> sliding <input type="checkbox"/> overturning <input type="checkbox"/> bearing capacity <input type="checkbox"/> global stability <input type="checkbox"/> pullout<br><input type="checkbox"/> compound failure<br><i>N/A to all as we or the contractor check all the above failure modes, before building the wall.</i>   |   |
| 7. | What factor of safety (FOS) do you require for the following failure modes?<br>Sliding <u>1.5</u> ; Overturning <u>2.0</u> ; Bearing capacity <u>2.0</u> ; Pullout <u>1.5</u>   |   |
| 8. | Do you use the following equation to evaluate bearing capacity?<br>$q_u = cN_c + 0.5L'\gamma_i N_\gamma$<br>If no, please specify what method is used to check bearing capacity.  | <input checked="" type="checkbox"/> yes <input type="checkbox"/> no |

|   |  |  |
|---|--|--|
| 9.  | Do you evaluate stability for failure modes that consider the effect of discrete wall facing units?  | <input checked="" type="checkbox"/> yes __no |
| <p>If yes, please brief how.<br/> <i>Contractor required to submit internal stability checks when submit for construction approval.</i></p> |  |  |
| 10.   | <p>Failure case of compound failure. Please mark on the dashed critical curves. Use “√” for being seen in the field; use “X” for modes considered in design analysis.<br/> <i>All cases would be checked during the design analysis. Have not had a failure of this type on an ALDOT wall to my knowledge.</i></p>  |  |
| 11.   | Is the AASHTO MSE wall backfill specification for the electrochemical requirements followed?   | <input checked="" type="checkbox"/> yes __no |
| <b>Additional Comments</b>  |  |  |
| <p>Please make any comments on the current MSE design methodology.</p>  |  |  |



**Survey Questionnaire TxDOT Research (RTI 0-6716)  
 Design Parameters and Methodology for MSE Walls  
 PD: Sean Yoon, Bridge Div. RS: Charles Aubeny, TTI**

**Participant Information**

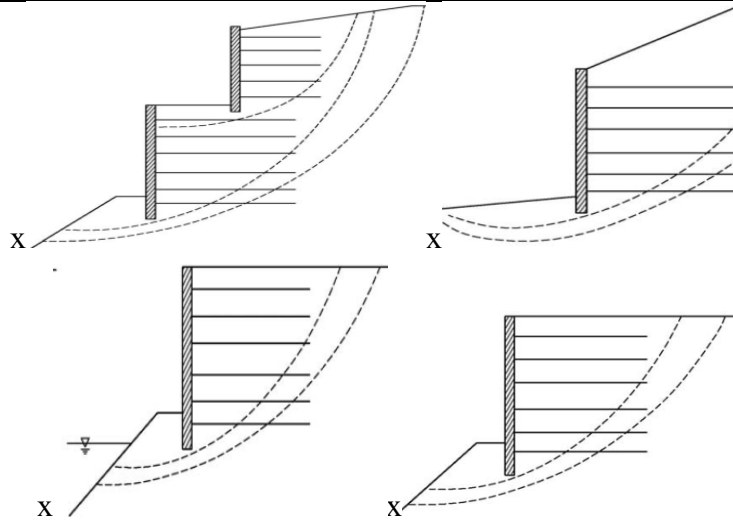
|                         |             |                      |  |
|-------------------------|-------------|----------------------|--|
| Name of Participant     |             | Contact phone number |  |
| Name of the affiliation | <i>KDOT</i> | Contact email        |  |

**Survey Questions**

|    |   |   |
|----|---|---|
| 1  | Is the FHWA/AASHTO manual used as guideline for MSE wall design?<br>If no, please list the guideline used for your design.  | <input checked="" type="checkbox"/> yes <input type="checkbox"/> no |
| 2  | Is the minimum length criteria used, i.e., 8 feet or 0.7H?<br>If no, please explain the minimum length criteria being used.   | <input checked="" type="checkbox"/> yes <input type="checkbox"/> no |
| 3  | Is the FHWA specification of backfill material followed?<br>If no, please provide a brief description of the classifications and material parameters for the backfill.<br><i>We are more stringent and only allow 5 percent passing the #200 sieve.</i>   | <input type="checkbox"/> yes <input checked="" type="checkbox"/> no |
| 4. | Is the durability of backfill material evaluated?<br>If yes, what is evaluated and what methods are used?<br><i>Has to meet our durability criteria.</i>  | <input checked="" type="checkbox"/> yes <input type="checkbox"/> no |
| 5. | Have you encountered granular material that can decompose into finer grained soils in the presence of moisture?<br>If yes, please list them.<br><i>Chalky limestones.</i>   | <input checked="" type="checkbox"/> yes <input type="checkbox"/> no |
| 6. | Please rank the following potential failure modes on a scale of 1 to 5, with 1 being the least common, 5 being the most common. If the failure has not been seen in your practice, please mark as N/A.<br><u>5</u> sliding <u>N/A</u> overturning <u>4</u> bearing capacity <u>3</u> global stability <u>N/A</u> pullout<br><u>N/A</u> compound failure |   |
| 7. | What factor of safety (FOS) do you require for the following failure modes?<br>Sliding <u>1.5</u> ; Overturning <u>2.0</u> ; Bearing capacity <u>2.0</u> ; Pullout <u>1.5</u>   |   |
| 8. | Do you use the following equation to evaluate bearing capacity?<br>$q_u = cN_c + 0.5L'\gamma_iN_\gamma$<br>If no, please specify what method is used to check bearing capacity.   | <input checked="" type="checkbox"/> yes <input type="checkbox"/> no |
| 9. | Do you evaluate stability for failure modes that consider the effect of discrete wall facing units?<br>If yes, please brief how.  | <input type="checkbox"/> yes <input checked="" type="checkbox"/> no |

10.

Failure case of compound failure. Please mark on the dashed critical curves. Use “√” for being seen in the field; use “X” for modes considered in design analysis.



**Additional Comments**

Please make any comments on the current MSE design methodology.

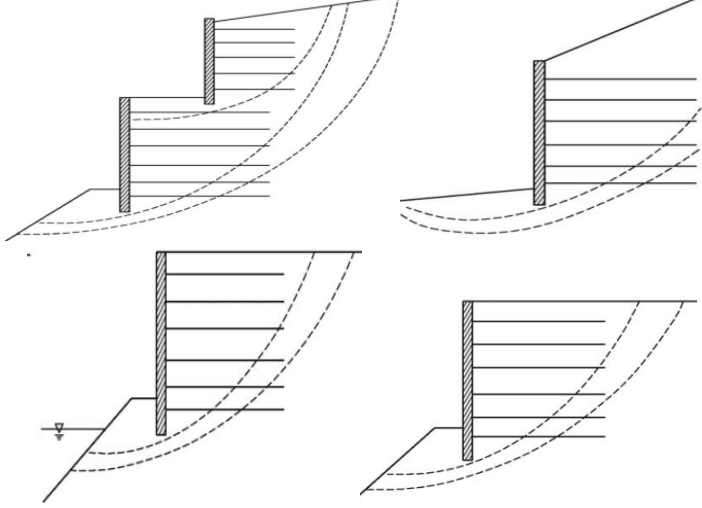
**Survey Questionnaire TxDOT Research (RTI 0-6716)  
Design Parameters and Methodology for MSE Walls  
PD: Sean Yoon, Bridge Div. RS: Charles Aubeny, TTI**

**Participant Information**

|                         |                |                      |  |
|-------------------------|----------------|----------------------|--|
| Name of Participant     |                | Contact phone number |  |
| Name of the affiliation | <i>ConnDOT</i> | Contact email        |  |

**Survey Questions**

|    |  |   |
|----|--|---|
| 1  | Is the FHWA/AASHTO manual used as guideline for MSE wall design?<br>If no, please list the guideline used for your design.   | <input checked="" type="checkbox"/> yes <input type="checkbox"/> no |
| 2  | Is the minimum length criteria used, i.e., 8 feet or 0.7H?<br>If no, please explain the minimum length criteria being used.  | <input checked="" type="checkbox"/> yes <input type="checkbox"/> no |
| 3  | Is the FHWA specification of Backfill material followed?<br>If no, please provide a brief description of the classifications and material parameters for the backfill.<br><i>Our standard structure backfill is required refer to the material requirements of pervious structure backfill in our standard specifications</i><br><br><a href="http://www.ct.gov/dot/lib/dot/documents/dpublications/816/012004/2004_816_original.pdf">http://www.ct.gov/dot/lib/dot/documents/dpublications/816/012004/2004_816_original.pdf</a> | <input type="checkbox"/> yes <input checked="" type="checkbox"/> no |
| 4. | Is the durability of backfill material evaluated?<br>If yes, what is evaluated and what methods are used?<br><i>See material specs referred to above</i>   | <input checked="" type="checkbox"/> yes <input type="checkbox"/> no |
| 5. | Have you encountered granular material that can decompose into finer grained soils in the presence of moisture?<br>If yes, please list them.   | <input type="checkbox"/> yes <input checked="" type="checkbox"/> no |
| 6. | Please rank the following potential failure modes on a scale of 1 to 5, with 1 being the least common, 5 being the most common. If the failure has not been seen in your practice, please mark as N/A.<br><input type="checkbox"/> sliding <input type="checkbox"/> overturning <input type="checkbox"/> bearing capacity <input type="checkbox"/> global stability <input type="checkbox"/> pullout<br><input type="checkbox"/> compound failure<br><i>N/A no failures to report</i>  |   |
| 7. | What factor of safety (FOS) do you require for the following failure modes?<br><i>AASHTO no local design requirements</i><br>Sliding _____ ; Overturning _____ ; Bearing capacity _____ ; Pullout _____  |   |
| 8. | Do you use the following equation to evaluate bearing capacity?<br>$q_u = cN_c + 0.5L'\gamma_iN_\gamma$<br>If no, please specify what method is used to check bearing capacity.  | <input checked="" type="checkbox"/> yes <input type="checkbox"/> no |

|   |  |  |
|---|--|--|
| 9.  | Do you evaluate stability for failure modes that consider the effect of discrete wall facing units?<br>If yes, please brief how.   | __yes <input checked="" type="checkbox"/> no |
| 10.   | <p>Failure case of compound failure. Please mark on the dashed critical curves. Use “√” for being seen in the field; use “X” for modes considered in design analysis.</p>  |  |
| 11.   | Is the AASHTO MSE wall backfill specification for the electrochemical requirements followed?   | <input checked="" type="checkbox"/> yes __no |
| <b>Additional Comments</b>                                      |  |  |
| Please make any comments on the current MSE design methodology. |  |  |

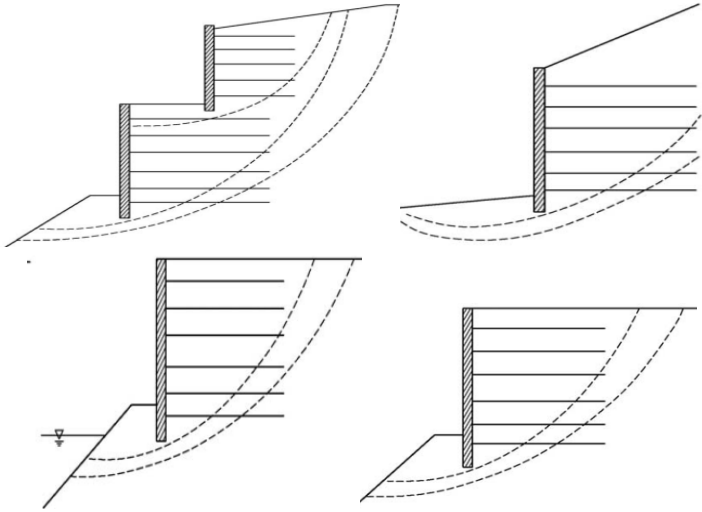
**Survey Questionnaire TxDOT Research (RTI 0-6716)  
 Design Parameters and Methodology for MSE Walls  
 PD: Sean Yoon, Bridge Div. RS: Charles Aubeny, TTI**

**Participant Information**

|                         |               |                      |  |
|-------------------------|---------------|----------------------|--|
| Name of Participant     |               | Contact phone number |  |
| Name of the affiliation | <i>IL-DOT</i> | Contact email        |  |

**Survey Questions**

|    |  |               |
|----|--|---------------|
| 1  | Is the FHWA/AASHTO manual used as guideline for MSE wall design?<br>If no, please list the guideline used for your design.   | <u>  </u> yes |
| 2  | Is the minimum length criteria used, i.e., 8 feet or 0.7H?<br>If no, please explain the minimum length criteria being used.  | <u>  </u> yes |
| 3  | Is the FHWA specification of Backfill material followed?<br>If no, please provide a brief description of the classifications and material parameters for the backfill.   | <u>  </u> yes |
| 4. | Is the durability of backfill material evaluated?<br>If yes, what is evaluated and what methods are used?<br><i>NasSO4 Soundness 5 cycles 15% max loss.</i>  | <u>  </u> yes |
| 5. | Have you encountered granular material that can decompose into finer grained soils in the presence of moisture?<br>If yes, please list them.   | <u>  </u> no  |
| 6. | Please rank the following potential failure modes on a scale of 1 to 5, with 1 being the least common, 5 being the most common. <u>  </u> sliding <u>  </u> overturning<br><u>  </u> bearing capacity <u>  </u> global stability <u>  </u> pullout <u>  </u> compound failure . If the failure has not been seen in your practice, please mark as N/A.<br><i>N/A</i> |               |
| 7. | What factor of safety (FOS) do you require for the following failure modes?<br><i>Sliding 1.5; Overturning 2.0; Bearing capacity 2.5; Pullout 1.5</i>  |               |
| 8. | Do you use the following equation to evaluate bearing capacity?<br>$q_u = cN_c + 0.5L'\gamma_iN_\gamma$<br>If no, please specify what method is used to check bearing capacity.  | <u>  </u> yes |
| 9. | Do you evaluate stability for failure modes that consider the effect of discrete wall facing units?<br>If yes, please brief how.   | <u>  </u> no  |

|   |  |       |
|---|--|-------|
| 10.   | Failure case of compound failure. Please mark on the dashed critical curves. Use “√” for being seen in the field; use “X” for modes considered in design analysis. |       |
|   |  |       |
| <i>We do not look a compound Failure modes, only global, external and internal</i>  |  |       |
| 11.   | Is the AASHTO MSE wall backfill specification for the electrochemical requirements followed?   | __yes |
| <b>Additional Comments</b>  |  |       |
| <p><i>We have been having problems with our coarse agg. passing the Resistivity requirements AASHTO would like. Not sure the test is proper for a coarse aggregate.</i></p> |  |       |

| <b>Survey Questionnaire TxDOT Research (RTI 0-6716)</b><br><b>Design Parameters and Methodology for MSE Walls</b><br><b>PD: Sean Yoon, Bridge Div. RS: Charles Aubeny, TTI</b> |  |   |  |
|--|--|---|--|
| Participant Information  |  |   |  |
| Name of Participant  |  | Contact phone number                    |  |
| Name of the affiliation  | <i>Iowa DOT</i>  | Contact email                           |  |
| Survey Questions   |  |   |  |
| 1  | Is the FHWA/AASHTO manual used as guideline for MSE wall design?<br><i>Internal design is done by MSE vendor. External design done by Iowa DOT. Both generally according to AASHTO.</i><br>If no, please list the guideline used for your design.  | <input checked="" type="checkbox"/> yes | <input type="checkbox"/> no            |
| 2  | Is the minimum length criteria used, i.e., 8 feet or 0.7H?<br>If no, please explain the minimum length criteria being used.  | <input checked="" type="checkbox"/> yes | <input type="checkbox"/> no            |
| 3  | Is the FHWA specification of backfill material followed?<br>If no, please provide a brief description of the classifications and material parameters for the backfill.<br><i>Iowa DOT has its own specification for backfill, which is granular material (sand) with no more than 5% fines.</i>  | <input type="checkbox"/> yes            | <input checked="" type="checkbox"/> no |
| 4.   | Is the durability of backfill material evaluated?<br><i>However, Iowa DOT does have electrochemical requirements.</i><br>If yes, what is evaluated and what methods are used?  | <input type="checkbox"/> yes            | <input checked="" type="checkbox"/> no |
| 5.   | Have you encountered granular material that can decompose into finer grained soils in the presence of moisture?<br>If yes, please list them.   | <input type="checkbox"/> yes            | <input checked="" type="checkbox"/> no |
| 6.   | Please rank the following potential failure modes on a scale of 1 to 5, with 1 being the least common, 5 being the most common. If the failure has not been seen in your practice, please mark as N/A.<br><u>N/A</u> sliding <u>N/A</u> overturning <u>N/A</u> bearing capacity <u>N/A</u> global stability <u>N/A</u> pullout <u>N/A</u> compound failure |   |  |
| 7.   | What factor of safety (FOS) do you require for the following failure modes?<br>Sliding <u>1.5</u> ; Overturning <u>2.0</u> ; Bearing capacity <u>2.5</u> ; Pullout <u>By MSE Vendor, as per AASHTO</u>   |   |  |
| 8.   | Do you use the following equation to evaluate bearing capacity?<br>$q_u = cN_c + 0.5L'\gamma_iN_\gamma$<br>If no, please specify what method is used to check bearing capacity.  | <input checked="" type="checkbox"/> yes | <input type="checkbox"/> no            |

|   |   |   |
|---|---|---|
| 9.  | Do you evaluate stability for failure modes that consider the effect of discrete wall facing units?<br>If yes, please brief how.  | <input checked="" type="checkbox"/> yes <input type="checkbox"/> no |
| 10.   | Failure case of compound failure. Please mark on the dashed critical curves. Use “√” for being seen in the field; use “X” for modes considered in design analysis.        |   |
|   |   |   |
| <i>X...All failure modes are considered in design by either Iowa DOT (external) or by MSE vendor (internal). No failures seen in the field.</i> |   |   |
| 11.   | Is the AASHTO MSE wall backfill specification for the electrochemical requirements followed?<br><i>As noted above, Iowa DOT has its own electrochemical requirements.</i> | <input type="checkbox"/> yes <input checked="" type="checkbox"/> no |
| <b>Additional Comments</b>  |   |   |
| Please make any comments on the current MSE design methodology.   |   |   |



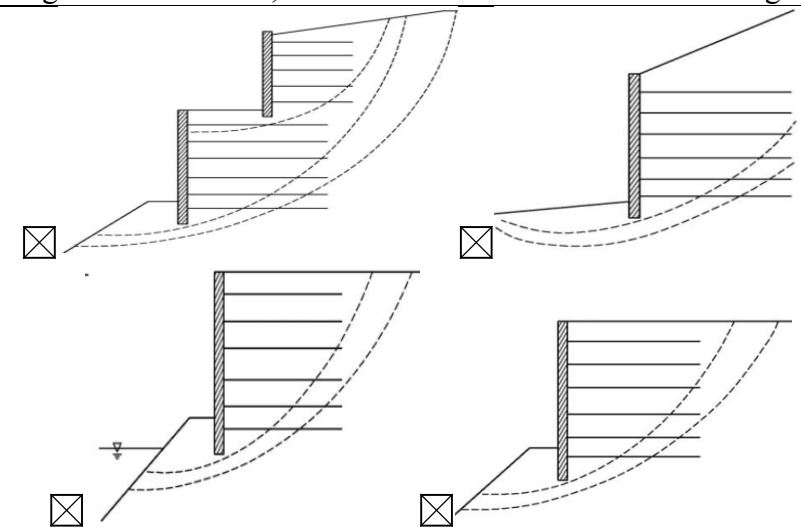
**Survey Questionnaire TxDOT Research (RTI 0-6716)**  
**Design Parameters and Methodology for MSE Walls**  
**PD: Sean Yoon, Bridge Div. RS: Charles Aubeny, TTI**

**Participant Information**

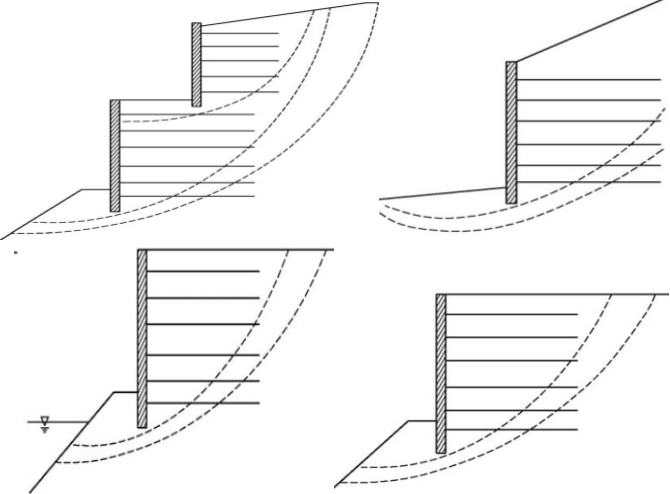
|                         |               |                      |  |
|-------------------------|---------------|----------------------|--|
| Name of Participant     |               | Contact phone number |  |
| Name of the affiliation | <i>MD SHA</i> | Contact email        |  |

**Survey Questions**

|   |  |   |
|---|--|---|
| 1 | Is the FHWA/AASHTO manual used as guideline for MSE wall design?<br>If no, please list the guideline used for your design.   | <input checked="" type="checkbox"/> yes ___no |
| 2 | Is the minimum length criteria used, i.e., 8 feet or 0.7H?<br>If no, please explain the minimum length criteria being used.  | <input checked="" type="checkbox"/> yes ___no |
| 3 | Is the FHWA specification of backfill material followed?<br>If no, please provide a brief description of the classifications and material parameters for the backfill.<br><i>Response: No. 57 stone is used as backfill.</i>   | ___yes <input checked="" type="checkbox"/> no |
| 4 | Is the durability of backfill material evaluated?<br>If yes, what is evaluated and what methods are used?<br><i>Sodium sulfate soundness, LA Abrasion, pH.</i>   | <input checked="" type="checkbox"/> yes ___no |
| 5 | Have you encountered granular material that can decompose into finer grained soils in the presence of moisture?<br>If yes, please list them.   | ___yes <input checked="" type="checkbox"/> no |
| 6 | Please rank the following potential failure modes on a scale of 1 to 5, with 1 being the least common, 5 being the most common. If the failure has not been seen in your practice, please mark as N/A.<br><u>1</u> sliding <u>2</u> overturning <u>4</u> bearing capacity ___ global stability <u>5</u> pullout<br><u>3</u> compound failure |   |
| 7 | What factor of safety (FOS) do you require for the following failure modes?<br>Sliding <u>1.5</u> ; Overturning <u>1.5</u> ; Bearing capacity <u>2.5</u> ; Pullout <u>1.5</u>  |   |
| 8 | Do you use the following equation to evaluate bearing capacity?<br>$q_u = cN_c + 0.5L'\gamma_iN_\gamma$<br>If no, please specify what method is used to check bearing capacity.  | <input checked="" type="checkbox"/> yes ___no |
| 9 | Do you evaluate stability for failure modes that consider the effect of discrete wall facing units?<br>If yes, please brief how.   | ___yes <input checked="" type="checkbox"/> no |

|  |  |
|--|--|
| 10.  | <p>Failure case of compound failure. Please mark on the dashed critical curves. Use “√” for being seen in the field; use “X” for modes considered in design analysis.</p>  |
| 11.  | <p>Is the AASHTO MSE wall backfill specification for the electrochemical requirements followed? <input checked="" type="checkbox"/>yes ___no</p>   |
| <b>Additional Comments</b>   |  |
| <p>Please make any comments on the current MSE design methodology.</p> |  |

| <b>Survey Questionnaire TxDOT Research (RTI 0-6716)</b><br><b>Design Parameters and Methodology for MSE Walls</b><br><b>PD: Sean Yoon, Bridge Div. RS: Charles Aubeny, TTI</b> |   |   |  |
|--|---|---|--|
| <b>Participant Information</b>   |   |   |  |
| Name of Participant  |   | Contact phone number                    |  |
| Name of the affiliation  | <i>NHDOT</i>  | Contact email                           |  |
| <b>Survey Questions</b>  |   |   |  |
| 1  | Is the FHWA/AASHTO manual used as guideline for MSE wall design?  | <input checked="" type="checkbox"/> yes | <input type="checkbox"/> no            |
|  | If no, please list the guideline used for your design.  |   |  |
| 2  | Is the minimum length criteria used, i.e., 8 feet or 0.7H?  | <input checked="" type="checkbox"/> yes | <input type="checkbox"/> no            |
|  | If no, please explain the minimum length criteria being used.   |   |  |
| 3  | Is the FHWA specification of backfill material followed?  | <input checked="" type="checkbox"/> yes | <input type="checkbox"/> no            |
|  | If no, please provide a brief description of the classifications and material parameters for the backfill.  |   |  |
| 4.   | Is the durability of backfill material evaluated?   | <input checked="" type="checkbox"/> yes | <input type="checkbox"/> no            |
|  | If yes, what is evaluated and what methods are used?<br><i>Soundness loss &lt; 30 percent per AASHTO T104</i>   |   |  |
| 5.   | Have you encountered granular material that can decompose into finer grained soils in the presence of moisture?   | <input type="checkbox"/> yes            | <input checked="" type="checkbox"/> no |
|  | If yes, please list them.   |   |  |
| 6.   | Please rank the following potential failure modes on a scale of 1 to 5, with 1 being the least common, 5 being the most common. If the failure has not been seen in your practice, please mark as N/A.  |   |  |
|  | <input type="checkbox"/> sliding <input type="checkbox"/> overturning <input type="checkbox"/> bearing capacity <input type="checkbox"/> global stability <input type="checkbox"/> pullout<br><input type="checkbox"/> compound failure<br><i>N/A</i> |   |  |
| 7.   | What factor of safety (FOS) do you require for the following failure modes?   |   |  |
|  | Sliding <i>1.5</i> ; Overturning <i>2.0</i> ; Bearing capacity <i>2.5</i> ; Pullout <i>1.5</i><br><i>Above are for ASD design methods, not LRFD.</i>  |   |  |
| 8.   | Do you use the following equation to evaluate bearing capacity?   | <input type="checkbox"/> yes            | <input checked="" type="checkbox"/> no |
|  | $q_u = cN_c + 0.5L'\gamma_i N_\gamma$ If no, please specify what method is used to check bearing capacity.<br><i>Methods described in LRFD AASHTO code section 10.6.3 are used.</i>   |   |  |

|  |   |   |
|--|---|---|
| 9.   | <p>Do you evaluate stability for failure modes that consider the effect of discrete wall facing units?<br/> <i>This is part of the internal stability analysis of the MSE wall system by the MSE proprietor (MSE wall systems are approved in advance by NHDOT – this is reviewed during the approval process).</i></p>   | <p><input type="checkbox"/> yes <input checked="" type="checkbox"/><br/> no</p> |
| <p>If yes, please brief how.</p>   |   |   |
| 10.  | <p>Failure case of compound failure. Please mark on the dashed critical curves. Use “√” for being seen in the field; use “X” for modes considered in design analysis.</p> <div style="text-align: center;">  </div> <p><i>All potential global stability failure modes are checked as part of the design analysis.</i></p> |   |
| 11.  | <p>Is the AASHTO MSE wall backfill specification for the electrochemical requirements followed?</p>   | <p><input checked="" type="checkbox"/> yes<br/> <input type="checkbox"/> no</p> |
| <p><b>Additional Comments</b></p>  |   |   |
| <p>Please make any comments on the current MSE design methodology.</p> <p><i>NHDOT generally follows the 2012 AASHTO LRFD code and the 2009 FHWA GEC 011 manual.</i></p> |   |   |

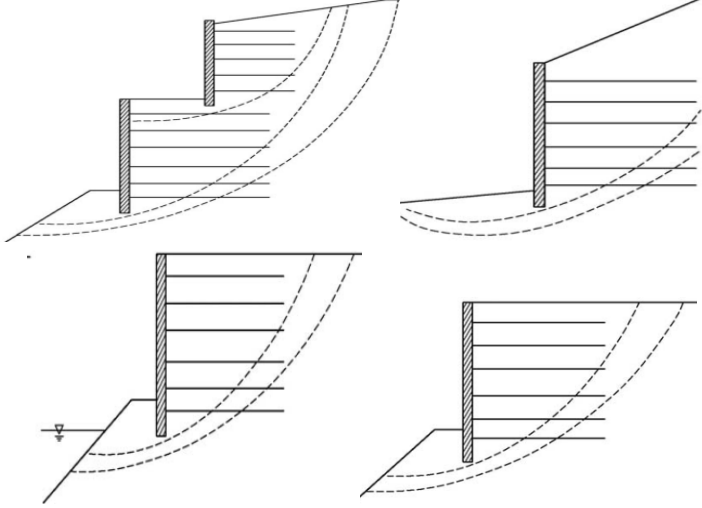
**Survey Questionnaire TxDOT Research (RTI 0-6716)  
 Design Parameters and Methodology for MSE Walls  
 PD: Sean Yoon, Bridge Div. RS: Charles Aubeny, TTI**

**Participant Information**

|                         |  |                      |  |
|-------------------------|--|----------------------|--|
| Name of Participant     |  | Contact phone number |  |
| Name of the affiliation | <i>NYS<br/>DOT<br/>Geotechnical<br/>Engineering Bureau</i> | Contact email        |  |

**Survey Questions**

|    |   |   |
|----|---|---|
| 1  | Is the FHWA/AASHTO manual used as guideline for MSE wall design?<br>If no, please list the guideline used for your design.  | <input checked="" type="checkbox"/> yes <input type="checkbox"/> no |
| 2  | Is the minimum length criteria used, i.e., 8 feet or 0.7H?<br>If no, please explain the minimum length criteria being used.   | <input checked="" type="checkbox"/> yes <input type="checkbox"/> no |
| 3  | Is the FHWA specification of backfill material followed?<br>If no, please provide a brief description of the classifications and material parameters for the backfill.<br><i>Section 554 of the Standard Specification covers the construction of Fill Type Retaining Walls where MSE walls fall. This and the backfill requirements for MSES walls can be found in Section 733-02 of our Standard Specification at the following link:<br/><a href="https://www.dot.ny.gov/main/business-center/engineering/specifications/english-spec-repository/espec5-3-12english.pdf">https://www.dot.ny.gov/main/business-center/engineering/specifications/english-spec-repository/espec5-3-12english.pdf</a></i> | <input checked="" type="checkbox"/> yes <input type="checkbox"/> no |
| 4. | Is the durability of backfill material evaluated?<br>If yes, what is evaluated and what methods are used?<br><i>Durability requirements can be found under Section 733-02 of our Standard Specification through the same link as above.</i>   | <input checked="" type="checkbox"/> yes <input type="checkbox"/> no |
| 5. | Have you encountered granular material that can decompose into finer grained soils in the presence of moisture?<br>If yes, please list them.  | <input type="checkbox"/> yes <input checked="" type="checkbox"/> no |
| 6. | Please rank the following potential failure modes on a scale of 1 to 5, with 1 being the least common, 5 being the most common. If the failure has not been seen in your practice, please mark as N/A.<br><i>N/A sliding N/A overturning N/A bearing capacity N/A global stability<br/>N/A pullout N/A compound failure</i>   |   |
| 7. | What factor of safety (FOS) do you require for the following failure modes?<br><i>Sliding 1.5; Overturning 2.0; Bearing capacity 2.5; Pullout 1.5</i>   |   |

|  |   |  |
|--|---|--|
| 8.   | Do you use the following equation to evaluate bearing capacity?<br>$q_u = cN_c + 0.5L'\gamma_iN_\gamma$<br>If no, please specify what method is used to check bearing capacity  | <input checked="" type="checkbox"/> yes __no |
| 9.   | Do you evaluate stability for failure modes that consider the effect of discrete wall facing units<br>If yes, please brief how.   | <input checked="" type="checkbox"/> yes __no |
| 10.  | Failure case of compound failure. Please mark on the dashed critical curves. Use “√” for being seen in the field; use “X” for modes considered in design analysis.<br><i>All of the failure modes shown are considered and checked. The two tiered wall system is rarely constructed by NYSDOT</i><br> |  |
| 11.  | Is the AASHTO MSE wall backfill specification for the electrochemical requirements followed?<br><i>See 3 above.</i>   | <input checked="" type="checkbox"/> yes __no |
| <b>Additional Comments</b>   |   |  |
| Please make any comments on the current MSE design methodology.<br><br><i>AASHTO Code is followed for the design of MSES Walls. Please be aware that almost everything being submitted now is in LRFD so factors of safety will no longer apply.</i> |   |  |

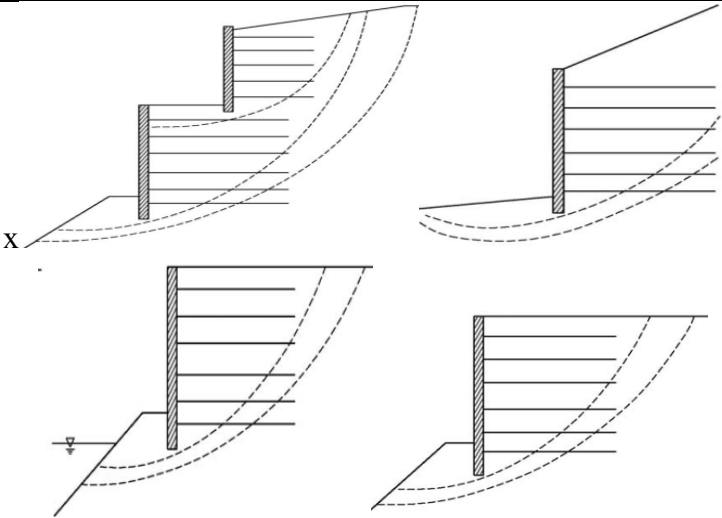
**Survey Questionnaire TxDOT Research (RTI 0-6716)  
 Design Parameters and Methodology for MSE Walls  
 PD: Sean Yoon, Bridge Div. RS: Charles Aubeny, TTI**

**Participant Information**

|                         |       |                      |  |
|-------------------------|-------|----------------------|--|
| Name of Participant     |       | Contact phone number |  |
| Name of the affiliation | SCDOT | Contact email        |  |

**Survey Questions**

|    |  |   |
|----|--|---|
| 1  | Is the FHWA/AASHTO manual used as guideline for MSE wall design?<br>If no, please list the guideline used for your design.   | <input checked="" type="checkbox"/> yes ___no |
| 2  | Is the minimum length criteria used, i.e., 8 feet or 0.7H?<br>If no, please explain the minimum length criteria being used.  | <input checked="" type="checkbox"/> yes ___no |
| 3  | Is the FHWA specification of backfill material followed?<br>If no, please provide a brief description of the classifications and material parameters for the backfill.   | <input checked="" type="checkbox"/> yes ___no |
| 4. | Is the durability of backfill material evaluated?<br>If yes, what is evaluated and what methods are used?  | ___yes <input checked="" type="checkbox"/> no |
| 5. | Have you encountered granular material that can decompose into finer grained soils in the presence of moisture?<br>If yes, please list them.   | ___yes <input checked="" type="checkbox"/> no |
| 6. | Please rank the following potential failure modes on a scale of 1 to 5, with 1 being the least common, 5 being the most common. If the failure has not been seen in your practice, please mark as N/A.<br><u>NA</u> sliding <u>NA</u> overturning <u>NA</u> bearing capacity <u>5</u> global stability<br><u>NA</u> pullout <u>NA</u> compound failure |   |
| 7. | What factor of safety (FOS) do you require for the following failure modes?<br>Sliding____; Overturning____; Bearing capacity____; Pullout____<br><i>We use LRFD resistance factors from AASHTO.</i>   |   |
| 8. | Do you use the following equation to evaluate bearing capacity?<br>$q_u = cN_c + 0.5L'\gamma_iN_\gamma$<br>If no, please specify what method is used to check bearing capacity.  | <input checked="" type="checkbox"/> yes ___no |
| 9. | Do you evaluate stability for failure modes that consider the effect of discrete wall facing units?<br>If yes, please brief how.   | ___yes <input checked="" type="checkbox"/> no |

|  |  |
|--|--|
| 10.  | Failure case of compound failure. Please mark on the dashed critical curves. Use “√” for being seen in the field; use “X” for modes considered in design analysis. |
|  |  |
| 11.  | Is the AASHTO MSE wall backfill specification for the electrochemical requirements followed? <input checked="" type="checkbox"/> yes ___no                         |
| <b>Additional Comments</b>   |  |
| Please make any comments on the current MSE design methodology.                    |  |



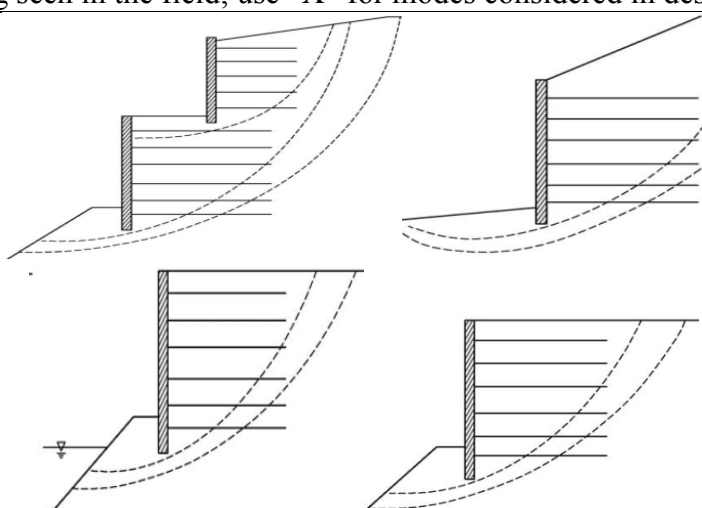
**Survey Questionnaire TxDOT Research (RTI 0-6716)  
Design Parameters and Methodology for MSE Walls  
PD: Sean Yoon, Bridge Div. RS: Charles Aubeny, TTI**

**Participant Information**

|                         |              |                      |  |
|-------------------------|--------------|----------------------|--|
| Name of Participant     |              | Contact phone number |  |
| Name of the affiliation | <i>WSDOT</i> | Contact email        |  |

**Survey Questions**

|    |  |   |
|----|--|---|
| 1  | Is the FHWA/AASHTO manual used as guideline for MSE wall design?<br>If no, please list the guideline used for your design.<br><i>In addition, our WSDOT Geotechnical Design Manual has additional design procedures/requirements (see Chapter 15).</i>   | <input checked="" type="checkbox"/> yes ___no |
| 2  | Is the minimum length criteria used, i.e., 8 feet or 0.7H?<br><i>Actually, 6 ft is allowed under certain circumstances by AASHTO.</i><br>If no, please explain the minimum length criteria being used.   | <input checked="" type="checkbox"/> yes ___no |
| 3  | Is the FHWA specification of backfill material followed?<br>If no, please provide a brief description of the classifications and material parameters for the backfill.<br><i>We are more restrictive because of our typically wet conditions – fines are limited to less than 7%. We also restrict max. particle size for geosynthetic walls to 1.25 inches or less. See our Gravel Borrow specifications in our Std. Spec. Book.</i>      | ___yes <input checked="" type="checkbox"/> no |
| 4. | Is the durability of backfill material evaluated?<br>If yes, what is evaluated and what methods are used?<br><i>LA abrasion.</i>   | <input checked="" type="checkbox"/> yes ___no |
| 5. | Have you encountered granular material that can decompose into finer grained soils in the presence of moisture?<br>If yes, please list them.<br><i>Marine basalts typically found on our west coast and along the western Columbia river – see Chapter 5 of our Geotech Design Manual.</i>   | <input checked="" type="checkbox"/> yes ___no |
| 6. | Please rank the following potential failure modes on a scale of 1 to 5, with 1 being the least common, 5 being the most common. If the failure has not been seen in your practice, please mark as N/A.<br><i>Note: failures are rare, but when they happen, the ratings below reflect what is most common. Note that you have not listed failure of the connection between the facing and reinforcement, which does occur on occasion.</i> |   |
|    | <u>2</u> sliding <u>NA</u> overturning <u>2</u> bearing capacity <u>5</u> global stability <u>2</u> pullout<br><u>4</u> compound failure   |   |

|     |  |   |
|-----|--|---|
| 7.  | What factor of safety (FOS) do you require for the following failure modes?<br><i>We use AASHTO Standards, and we use load and resistance factors, not FOS.</i>    |   |
|     | Sliding _____ ; Overturning _____ ; Bearing capacity _____ ; Pullout _____   |   |
| 8.  | Do you use the following equation to evaluate bearing capacity? $q_u = cN_c + 0.5L'\gamma_iN_\gamma$   | <input type="checkbox"/> yes <input type="checkbox"/> no            |
|     | If no, please specify what method is used to check bearing capacity<br>We use what is specified in AASHTO. The above equation is a simplification of that.         |   |
| 9.  | Do you evaluate stability for failure modes that consider the effect of discrete wall facing units   | <input checked="" type="checkbox"/> yes <input type="checkbox"/> no |
|     | If yes, please brief how.<br><i>I am not sure what you mean, but we do consider the structural stability of the facing and the connection strength.</i>            |   |
| 10. | Failure case of compound failure. Please mark on the dashed critical curves. Use “√” for being seen in the field; use “X” for modes considered in design analysis. |   |
|     |   |   |
|     | <i>I am not sure how to respond to this one.</i>   |   |
| 11. | Is the AASHTO MSE wall backfill specification for the electrochemical requirements followed?   | <input checked="" type="checkbox"/> yes <input type="checkbox"/> no |

### Additional Comments

Please make any comments on the current MSE design methodology.

*My comments would be too extensive for this survey form. However, I suggest you look at the following papers:*

1. *Allen, T.M. and Bathurst, R.J., 2002, Observed Long-Term Performance of Geosynthetic Walls, and Implications for Design, Geosynthetics International, Vol. 9, Nos. 5-6, pp. 567-606.*
2. *Allen, T.M. and Bathurst, R.J., 2002, Soil Reinforcement Loads in Geosynthetic Walls at Working Stress Conditions, Geosynthetics International, Vol. 9, Nos. 5-6, pp. 525-566.*

3. Allen, T.M., Bathurst, R.J., and Berg, R.R., 2002, *Global Level of Safety and Performance of Geosynthetic Walls: An Historical Perspective*, *Geosynthetics International*, Vol. 9, Nos. 5-6, pp. 395-450.
4. Allen, T.M., Bathurst, R.J., Holtz, R.D., Walters, D.L. and Lee, W.F., 2003. "A New Working Stress Method for Prediction of Reinforcement Loads in Geosynthetic Walls", *Canadian Geotechnical Journal*, Vol. 40, No. 5, pp. 976-994.
5. Allen, T.M., Bathurst, R.J., Lee, W. F., Holtz, R.D., and Walters, D.L., 2004, "A New Method for Prediction of Loads in Steel Reinforced Walls", *ASCE Journal of Geotechnical and Geo-environmental Engineering*, Vol. 130, No. 11, pp. 1109-1120.
6. Bathurst, R.J., Allen, T.M., and Nowak, A.S., 2008, "Calibration Concepts for Load and Resistance Factor Design (LRFD) of Reinforced Soil Walls," *Canadian Geotechnical Journal*, Vol. 45, pp. 1377-1392.
7. Bathurst, R.J., Allen, T. and Walters, D., 2005, "Reinforcement Loads in Geosynthetic Walls and the Case for a New Working Stress Design Method, 2002-2004 Mercer Lecture," *Geotextiles and Geomembranes*, Vol. 23, pp. 287-322.
8. Bathurst, R.J., Allen, T.M., and Walters, D.L., 2002, *Short-Term Strain and Deformation Behavior of Geosynthetic Walls at Working Stress Conditions*, *Geosynthetics International*, Vol. 9, Nos. 5-6, pp. 451-482.
9. Bathurst, R.J., Nernheim, A., and Allen, T.M. 2009. "Predicted loads in steel reinforced soil walls using the AASHTO Simplified Method," *ASCE Journal of Geotechnical and Geoenvironmental Engineering*, Vol. 135, No. 2, pp. 177-184. See also discussion published in *ASCE* December 2011, pp. 1305-1310.
10. Bathurst, R.J., Nernheim, A. and Allen, T.M. 2008. "Comparison of measured and predicted loads using the Coherent Gravity Method for steel soil walls." *Ground Improvement*, Vol. 161, No. 3, 113-120.
11. Bathurst, R.J., Vlachopoulos, N., Walters, D.L., Burgess, P.G. and Allen, T.M. 2006. "The influence of facing rigidity on the performance of two geosynthetic reinforced soil retaining walls," *Canadian Geotechnical Journal*, Vol. 43, pp. 1225-1237.
12. Bathurst, R.J., Vlachopoulos, N., Walters, D.L., Burgess, P.G. and Allen, T.M. 2007, Reply to the Discussions on "The influence of facing rigidity on the performance of two geosynthetic reinforced soil retaining walls," Vol. 44, pp. 1484-1490.
13. Huang, B., Bathurst, R.J., Hatami, K., and Allen, T.M., 2010, "Influence of Toe Restraint on Reinforced Soil Segmental Walls," *Canadian Geotechnical Journal*, Vol. 47, No. 8, pp. 885-904.
14. Walters, D.L., Allen, T.M., and Bathurst, R.J., 2002, *Conversion of Geosynthetic Strain to Load using Reinforcement Stiffness*, *Geosynthetics International*, Vol. 9, Nos. 5-6, pp. 483-523.
15. Bathurst, R.J., Miyata, Y., Nernheim, A. and Allen, T.M. (2008). "Refinement of K-stiffness method for geosynthetic reinforced soil walls." *Geosyn. Int.*, 15(4), 269-295.
16. Allen, T. M., Christopher, B. R., Elias, V., and DiMaggio, J. D., 2001, *Development of the Simplified Method for Internal Stability Design of Mechanically Stabilized Earth (MSE) Walls*, *WSDOT Research Report WA-RD 513.1*, 96 pp.

17. Allen, T.M., and Bathurst, R.J., in press, "Comparison of Working Stress and Limit Equilibrium Behavior of Reinforced Soil Walls," ASCE GSP-?? In Honor of R. D. Holtz.
18. Bathurst, R.J., Allen, T.M. and Huang B. 2010. Invited panel paper, Current issues for the internal stability design of geosynthetic reinforced soil. 9th International Geosynthetics Conference, Guarujá, Brazil, 23-27 May, pp. 533-546.

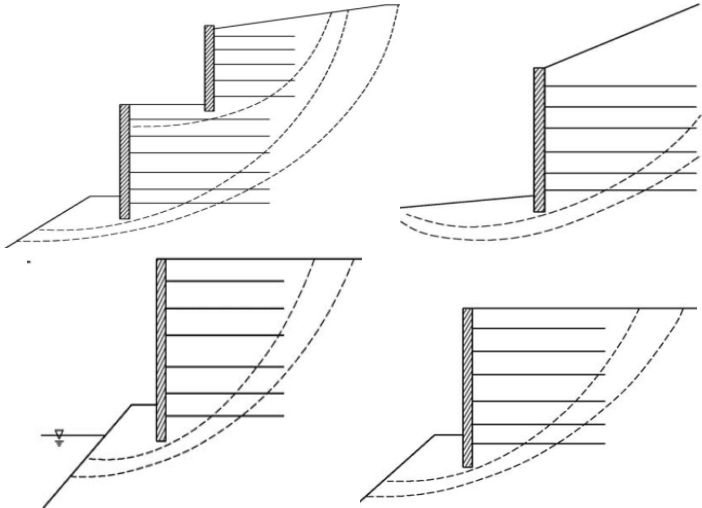
**Survey Questionnaire TxDOT Research (RTI 0-6716)  
 Design Parameters and Methodology for MSE Walls  
 PD: Sean Yoon, Bridge Div. RS: Charles Aubeny, TTI**

**Participant Information**

|                         |                      |                      |  |
|-------------------------|----------------------|----------------------|--|
| Name of Participant     |                      | Contact phone number |  |
| Name of the affiliation | <i>Wisconsin DOT</i> | Contact email        |  |

**Survey Questions**

|    |  |   |
|----|--|---|
| 1  | Is the FHWA/AASHTO manual used as guideline for MSE wall design?<br>If no, please list the guideline used for your design.   | <input checked="" type="checkbox"/> yes <input type="checkbox"/> no |
| 2  | Is the minimum length criteria used, i.e., 8 feet or 0.7H?<br>If no, please explain the minimum length criteria being used.<br><i>8 feet or 0.7H is used for MSE precast panels, but we allow a minimum of 6' for MSE modular block walls.</i>   | <input type="checkbox"/> yes <input checked="" type="checkbox"/> no |
| 3  | Is the FHWA specification of backfill material followed?<br><i>See note below</i>  | <input checked="" type="checkbox"/> yes <input type="checkbox"/> no |
|    | If no, please provide a brief description of the classifications and material parameters for the backfill.<br><br><i>Note: We have found that some of our uniform, rounded sands have somewhat low internal angles of friction. For design purposes, we limit the internal angle of friction of the reinforced granular material to 30 degrees, unless a direct shear test of the backfill confirms a larger value. If a test is performed and confirms higher values, we allow up to a maximum value of 36 degrees.</i> |   |
| 4. | Is the durability of backfill material evaluated?<br>If yes, what is evaluated and what methods are used?<br><i>Wear and soundness</i>   | <input checked="" type="checkbox"/> yes <input type="checkbox"/> no |
| 5. | Have you encountered granular material that can decompose into finer grained soils in the presence of moisture?<br>If yes, please list them.   | <input type="checkbox"/> yes <input checked="" type="checkbox"/> no |
| 6. | Please rank the following potential failure modes on a scale of 1 to 5, with 1 being the least common, 5 being the most common. If the failure has not been seen in your practice, please mark as N/A.<br><br><u>3</u> sliding <u>1</u> overturning <u>2</u> bearing capacity <u>2</u> global stability <u>1</u> pullout<br><u>1</u> compound failure  |   |
| 7. | What factor of safety (FOS) do you require for the following failure modes?<br>Sliding <u>1.5</u> ; Overturning <u>2.0</u> ; Bearing capacity <u>2.0–2.5</u> ; Pullout <u>2.0</u><br><i>Note: We currently use LRFD design with CDRs.</i>  |   |

|   |   |   |
|---|---|---|
| 8.  | Do you use the following equation to evaluate bearing capacity?<br>$q_u = cN_c + 0.5L'\gamma_i N_\gamma$  | <input type="checkbox"/> yes <input checked="" type="checkbox"/> no |
| If no, please specify what method is used to check bearing capacity.<br><i>We use the general bearing capacity equation, including the depth/embedment component.</i>   |   |   |
| 9.  | Do you evaluate stability for failure modes that consider the effect of discrete wall facing units?<br>If yes, please brief how.  | <input type="checkbox"/> yes <input checked="" type="checkbox"/> no |
| 10.   | Failure case of compound failure. Please mark on the dashed critical curves. Use “√” for being seen in the field; use “X” for modes considered in design analysis. <div style="text-align: center;">  </div> |   |
| 11.   | Is the AASHTO MSE wall backfill specification for the electrochemical requirements followed?  | <input checked="" type="checkbox"/> yes <input type="checkbox"/> no |
| <b>Additional Comments</b>  |   |   |
| Please make any comments on the current MSE design methodology.<br><br><i>See comments noted above. WisDOT also has freeze/thaw requirements for modular blocks used for MSE walls. Modular block MSE walls are not used to support roadways or structures.</i> |   |   |

**Survey Questionnaire TxDOT Research (RTI 0-6716)**  
**Design Parameters and Methodology for MSE Walls**  
**PD: Sean Yoon, Bridge Div. RS: Charles Aubeny, TTI**

**Participant Information**

|                         |                 |                      |  |
|-------------------------|-----------------|----------------------|--|
| Name of Participant     |                 | Contact phone number |  |
| Name of the affiliation | <i>Caltrans</i> | Contact email        |  |

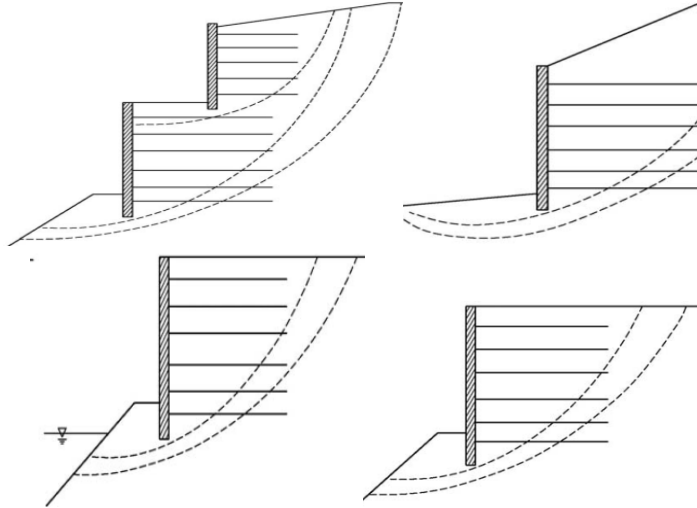
**Survey Questions**

|    |  |   |
|----|--|---|
| 1  | Is the FHWA/AASHTO manual used as guideline for MSE wall design?   | <input checked="" type="checkbox"/> yes <input type="checkbox"/> no |
|    | If no, please list the guideline used for your design.   |   |
| 2  | Is the minimum length criteria used, i.e., 8 feet or 0.7H?   | <input checked="" type="checkbox"/> yes <input type="checkbox"/> no |
|    | If no, please explain the minimum length criteria being used.  |   |
| 3  | Is the FHWA specification of backfill material followed?   | <input checked="" type="checkbox"/> yes <input type="checkbox"/> no |
|    | If no, please provide a brief description of the classifications and material parameters for the backfill.   |   |
| 4. | Is the durability of backfill material evaluated?  | <input checked="" type="checkbox"/> yes <input type="checkbox"/> no |
|    | If yes, what is evaluated and what methods are used?   |   |
| 5. | Have you encountered granular material that can decompose into finer grained soils in the presence of moisture?  | <input type="checkbox"/> yes <input checked="" type="checkbox"/> no |
|    | If yes, please list them.  |   |
| 6. | Please rank the following potential failure modes on a scale of 1 to 5, with 1 being the least common, 5 being the most common. If the failure has not been seen in your practice, please mark as N/A. |   |
|    | <u>NA</u> sliding <u>NA</u> overturning <u>3</u> bearing capacity <u>5</u> global stability<br><u>NA</u> pullout <u>1</u> compound failure   |   |
| 7. | What factor of safety (FOS) do you require for the following failure modes?  |   |
|    | Sliding <u>1.5</u> ; Overturning <u>1.5</u> ; Bearing capacity <u>2</u> ; Pullout <u>1.5</u>   |   |
| 8. | Do you use the following equation to evaluate bearing capacity?<br>$q_u = cN_c + 0.5L'\gamma_iN_\gamma$  | <input checked="" type="checkbox"/> yes <input type="checkbox"/> no |
|    | If no, please specify what method is used to check bearing capacity.   |   |

9. Do you evaluate stability for failure modes that consider the effect of discrete wall facing units?  yes  no

If yes, please brief how.

10. Failure case of compound failure. Please mark on the dashed critical curves. Use “√” for being seen in the field; use “X” for modes considered in design analysis.



**Additional Comments**

Please make any comments on the current MSE design methodology.



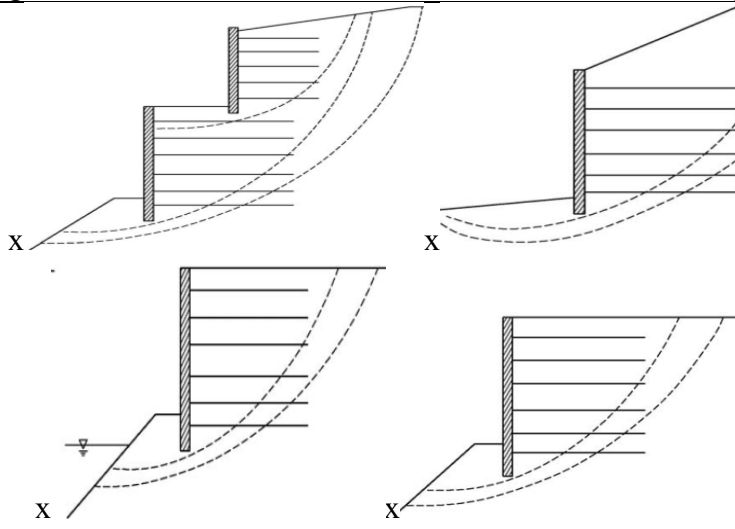
**Survey Questionnaire TxDOT Research (RTI 0-6716)  
 Design Parameters and Methodology for MSE Walls  
 PD: Sean Yoon, Bridge Div. RS: Charles Aubeny, TTI**

**Participant Information**

|                         |                              |                      |  |
|-------------------------|------------------------------|----------------------|--|
| Name of Participant     |                              | Contact phone number |  |
| Name of the affiliation | <i>MnDOT<br/>Foundations</i> | Contact email        |  |

**Survey Questions**

|    |   |   |
|----|---|---|
| 1  | Is the FHWA/AASHTO manual used as guideline for MSE wall design?<br>If no, please list the guideline used for your design.  | <input checked="" type="checkbox"/> yes <input type="checkbox"/> no |
| 2  | Is the minimum length criteria used, i.e., 8 feet or 0.7H?<br>If no, please explain the minimum length criteria being used.<br><i>Depends on the wall type, for large blocks yes and small blocks no o the 8' min. but we do require the 0.7H.</i>  | <input type="checkbox"/> yes <input checked="" type="checkbox"/> no |
| 3  | Is the FHWA specification of backfill material followed?<br>If no, please provide a brief description of the classifications and material parameters for the backfill.<br><i>Large block walls (wet-cast) we use pretty much the FHWA spec. but for small dry-cast block we have another spec. but it is basically the same.</i>  | <input type="checkbox"/> yes <input checked="" type="checkbox"/> no |
| 4. | Is the durability of backfill material evaluated?<br>If yes, what is evaluated and what methods are used?<br><i>Depends on the material source. If it is good mineral aggregates from known sources then no need to run a bunch of tests on it so that is what we try to use. We know of some problem sources and that material is either banned or tested if we must use it per the recommendations of our geologists.</i> | <input checked="" type="checkbox"/> yes <input type="checkbox"/> no |
| 5. | Have you encountered granular material that can decompose into finer grained soils in the presence of moisture?<br>If yes, please list them.<br><i>Our glacial sands typically do not do that.</i>  | <input type="checkbox"/> yes <input checked="" type="checkbox"/> no |
| 6. | Please rank the following potential failure modes on a scale of 1 to 5, with 1 being the least common, 5 being the most common. If the failure has not been seen in your practice, please mark as N/A.<br><i>N/A</i> sliding    2 overturning <i>N/A</i> bearing capacity <u>1</u> global stability<br><i>N/A</i> pullout <i>N/A</i> compound failure   |   |

|   |   |
|---|---|
| 7.  | What factor of safety (FOS) do you require for the following failure modes?<br>Sliding <u>1.0 resistance factor</u> ; Overturning <u>Eccentricity max limit of L/4 on soil and 3/8 L on rock</u> ; Bearing capacity <u>0.65 res. Factor (1.5)</u> ; Pullout <u>3 foot min. beyond failure surface</u> |
| 8.  | Do you use the following equation to evaluate bearing capacity? <input checked="" type="checkbox"/> yes <input type="checkbox"/> no<br>$q_u = cN_c + 0.5L'\gamma_iN_\gamma$<br>If no, please specify what method is used to check bearing capacity.   |
| 9.  | Do you evaluate stability for failure modes that consider the effect of discrete wall facing units? <input type="checkbox"/> yes <input checked="" type="checkbox"/> no<br>If yes, please brief how.  |
| 10.   | Failure case of compound failure. Please mark on the dashed critical curves. Use “√” for being seen in the field; use “X” for modes considered in design analysis.<br>   |
| 11.   | Is the AASHTO MSE wall backfill specification for the electrochemical requirements followed? <input checked="" type="checkbox"/> yes <input type="checkbox"/> no  |
| <b>Additional Comments</b>                                      |   |
| Please make any comments on the current MSE design methodology. |   |

**Survey Questionnaire TxDOT Research (RTI 0-6716)**  
**Design Parameters and Methodology for MSE Walls**  
**PD: Sean Yoon, Bridge Div.    RS: Charles Aubeny, TTI**

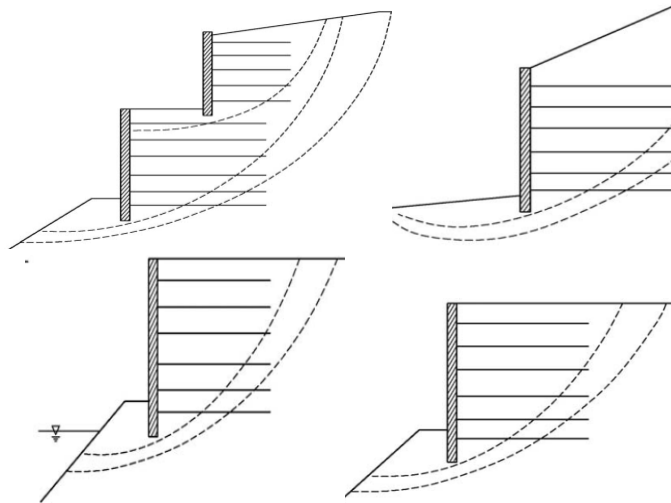
**Participant Information**

|                         |             |                 |  |
|-------------------------|-------------|-----------------|--|
| Name of Participant     |             | Contact phone # |  |
| Name of the affiliation | <i>MDOT</i> | Contact email   |  |

**Survey Questions**

|    |  |   |
|----|--|---|
| 1  | Is the FHWA/AASHTO manual used as guideline for MSE wall design?<br>If no, please list the guideline used for your design.   | <input checked="" type="checkbox"/> yes <input type="checkbox"/> no |
| 2  | Is the minimum length criteria used, i.e., 8 feet or 0.7H?<br>If no, please explain the minimum length criteria being used.<br><i>However, for walls with sloping backfill 8 ft or 0.8H is specified.</i>  | <input checked="" type="checkbox"/> yes <input type="checkbox"/> no |
| 3  | Is the FHWA specification of Backfill material followed?<br>If no, please provide a brief description of the classifications and material parameters for the backfill.<br><i>With the following exception: MDOT granular material Class II meeting gradation requirements specified in section 902 of MDOT's Standard Specifications for Construction.</i> | <input checked="" type="checkbox"/> yes <input type="checkbox"/> no |
| 4. | Is the durability of backfill material evaluated?<br>If yes, what is evaluated and what methods are used?<br><i>Backfill for the reinforced soil mass is tested per AASHTO T-104 (magnesium sulfate soundness).</i>  | <input checked="" type="checkbox"/> yes <input type="checkbox"/> no |
| 5. | Have you encountered granular material that can decompose into finer grained soils in the presence of moisture?<br>If yes, please list them.   | <input type="checkbox"/> yes <input checked="" type="checkbox"/> no |
| 6. | Please rank the following potential failure modes on a scale of 1 to 5, with 1 being the least common, 5 being the most common. If the failure has not been seen in your practice, please mark as N/A.<br><i>N/A sliding   N/A overturning   N/A bearing capacity   N/A global stability<br/>N/A pullout   N/A compound failure</i>                        |   |
| 7. | What <b>LRFD resistance factors</b> do you require for the following failure modes?<br><i>Sliding <math>\phi=1.0</math>; Overturning <math>e &lt; B/4</math>; Bearing capacity <math>\phi=0.65</math>; Pullout <math>\phi=0.90</math></i>  |   |
| 8. | Do you use the following equation to evaluate bearing capacity?<br>$q_u = cN_c + 0.5L'\gamma_i N_\gamma$<br>If no, please specify what method is used to check bearing capacity.   | <input checked="" type="checkbox"/> yes <input type="checkbox"/> no |
| 9. | Do you evaluate stability for failure modes that consider the effect of discrete wall facing units<br>If yes, please brief how.  | <input type="checkbox"/> yes <input checked="" type="checkbox"/> no |

10. Failure case of compound failure. Please mark on the dashed critical curves. Use “√” for being seen in the field; use “X” for modes considered in design analysis.



#### Additional Comments

Please make any comments on the current MSE design methodology.

*MDOT's MSE walls are designed following the LRFD design methodology.*

*At this point in time, MDOT uses SLIDE by Rocscience to perform classical slope stability analyses considering the reinforced soil zone as a rigid body and only failure surfaces completely outside of this zone are considered. Tiered MSE walls have yet to be designed/constructed by/for MDOT.*

*Only MSE-related failure resulted from saturated backfill from broken water line.*

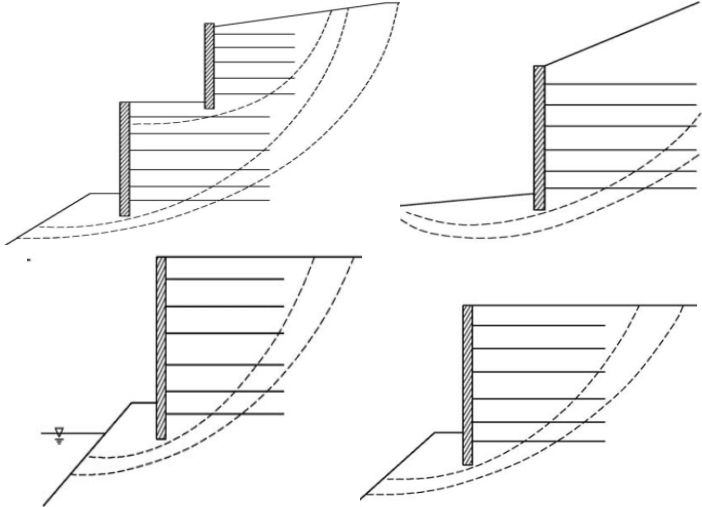
**Survey Questionnaire TxDOT Research (RTI 0-6716)  
Design Parameters and Methodology for MSE Walls  
PD: Sean Yoon, Bridge Div. RS: Charles Aubeny, TTI**

**Participant Information**

|                         |                    |                      |  |
|-------------------------|--------------------|----------------------|--|
| Name of Participant     |                    | Contact phone number |  |
| Name of the affiliation | <i>Montana DOT</i> | Contact email        |  |

**Survey Questions**

|    |   |   |
|----|---|---|
| 1  | Is the FHWA/AASHTO manual used as guideline for MSE wall design?<br>If no, please list the guideline used for your design.  | <input checked="" type="checkbox"/> yes <input type="checkbox"/> no |
| 2  | Is the minimum length criteria used, i.e., 8 feet or 0.7H?<br>If no, please explain the minimum length criteria being used.   | <input checked="" type="checkbox"/> yes <input type="checkbox"/> no |
| 3  | Is the FHWA specification of backfill material followed?<br>If no, please provide a brief description of the classifications and material parameters for the backfill.<br><i>We use a more stringent gradation for the backfill and also require a percentage of fractured face on the plus No. 4 Sieve as part of our specifications. We will occasionally evaluate other gradations, if the actual backfill material is tested for friction angle using direct shear.</i> | <input type="checkbox"/> yes <input checked="" type="checkbox"/> no |
| 4. | Is the durability of backfill material evaluated?<br>If yes, what is evaluated and what methods are used?<br><i>Soundness using AASHTO T-104</i>  | <input checked="" type="checkbox"/> yes <input type="checkbox"/> no |
| 5. | Have you encountered granular material that can decompose into finer grained soils in the presence of moisture?<br>If yes, please list them.  | <input type="checkbox"/> yes <input checked="" type="checkbox"/> no |
| 6. | Please rank the following potential failure modes on a scale of 1 to 5, with 1 being the least common, 5 being the most common. If the failure has not been seen in your practice, please mark as N/A)<br><i>N/A sliding N/A overturning 4 bearing capacity 2 global stability 1 pullout 3 compound failure</i>   |   |
| 7. | What factor of safety (FOS) do you require for the following failure modes?<br><i>Sliding 1.5; Overturning 1.5; Bearing capacity 2.5; Pullout 1.5</i>   |   |
| 8. | Do you use the following equation to evaluate bearing capacity?<br>$q_u = cN_c + 0.5L'\gamma_i N_\gamma$<br>If no, please specify what method is used to check bearing capacity   | <input checked="" type="checkbox"/> yes <input type="checkbox"/> no |

|  |  |  |
|--|--|--|
| 9.   | Do you evaluate stability for failure modes that consider the effect of discrete wall facing units?<br>If yes, please brief how.                                   | <input type="checkbox"/> yes <input checked="" type="checkbox"/> no                |
| 10.  | Failure case of compound failure. Please mark on the dashed critical curves. Use “√” for being seen in the field; use “X” for modes considered in design analysis. |  |
| 11.  | Is the AASHTO MSE wall backfill specification for the electrochemical requirements followed?   | <input checked="" type="checkbox"/> yes <input type="checkbox"/> no                |
| <b>Additional Comments</b>   |  |  |
| <p>Please make any comments on the current MSE design methodology.</p> <p><i>Note: I cannot get the “X” to work on question number 10; however, we check walls for all of these types of compound failure modes during design. We have not observed a failure in the field.</i></p> <p><i>General comment: Montana DOT does not typically construct very many MSE walls. I would say on average we have one or two per year.</i></p> |  |  |

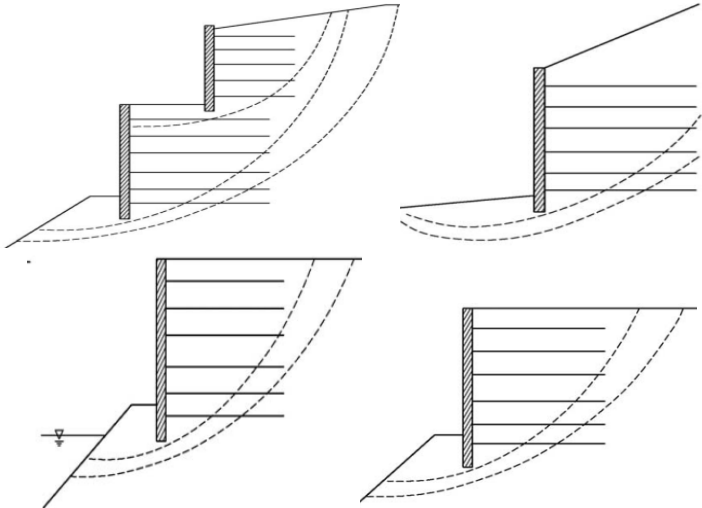
**Survey Questionnaire TxDOT Research (RTI 0-6716)  
 Design Parameters and Methodology for MSE Walls  
 PD: Sean Yoon, Bridge Div. RS: Charles Aubeny, TTI**

**Participant Information**

|                         |              |                      |  |
|-------------------------|--------------|----------------------|--|
| Name of Participant     |              | Contact phone number |  |
| Name of the affiliation | <i>NCDOT</i> | Contact email        |  |

**Survey Questions**

|    |   |   |
|----|---|---|
| 1  | Is the FHWA/AASHTO manual used as guideline for MSE wall design?<br><i>Predominately AASHTO LRFD Bridge Design Specs but FHWA MSE Wall Manual for traffic impact analysis.</i>  | <input checked="" type="checkbox"/> yes <input type="checkbox"/> no |
|    | If no, please list the guideline used for your design.  |   |
| 2  | Is the minimum length criteria used, i.e., 8 feet or 0.7H?<br><i>Except 6 ft instead of 8 ft.</i>   | <input checked="" type="checkbox"/> yes <input type="checkbox"/> no |
|    | If no, please explain the minimum length criteria being used.   |   |
| 3  | Is the FHWA specification of Backfill material followed?  | <input type="checkbox"/> yes <input checked="" type="checkbox"/> no |
|    | If no, please provide a brief description of the classifications and material parameters for the backfill.<br><i>Clean washed coarse aggregate or fine aggregate with less than 8% fines.</i>   |   |
| 4. | Is the durability of backfill material evaluated?   | <input checked="" type="checkbox"/> yes <input type="checkbox"/> no |
|    | If yes, what is evaluated and what methods are used?<br><i>Soundness for coarse and fine aggregate and abrasion for coarse aggregate.</i>   |   |
| 5. | Have you encountered granular material that can decompose into finer grained soils in the presence of moisture?   | <input type="checkbox"/> yes <input checked="" type="checkbox"/> no |
|    | If yes, please list them.   |   |
| 6. | Please rank the following potential failure modes on a scale of 1 to 5, with 1 being the least common, 5 being the most common. If the failure has not been seen in your practice, please mark as N/A.<br><i><u>NA</u> sliding <u>NA</u> overturning <u>2</u> bearing capacity <u>NA</u> global stability<br/><u>NA</u> pullout <u>1</u> compound failure</i> |   |
| 7. | What factor of safety (FOS) do you require for the following failure modes?<br><i>We use LRFD, not ASD.</i>   |   |
|    | Sliding _____; Overturning _____; Bearing capacity _____; Pullout _____   |   |

|  |  |   |
|--|--|---|
| 8.   | Do you use the following equation to evaluate bearing capacity?<br>$q_u = cN_c + 0.5L'\gamma_i N_\gamma$   | <input type="checkbox"/> yes <input checked="" type="checkbox"/> no |
| If no, please specify what method is used to check bearing capacity.<br><i>Eqn. above is close but we use AASHTO Eqn. 10.6.3.1.2a-1.</i> |  |   |
| 9.   | Do you evaluate stability for failure modes that consider the effect of discrete wall facing units?<br>If yes, please brief how.   | <input checked="" type="checkbox"/> yes <input type="checkbox"/> no |
| 10.  | Failure case of compound failure. Please mark on the dashed critical curves. Use “√” for being seen in the field; use “X” for modes considered in design analysis. <div style="text-align: center;">  </div> <p><i>These pictures seem to show failure planes through the reinforcement. We evaluate the reinforcement for strength (rupture) and pullout and global stability with failure planes outside the reinforced zone but we assume the failure plane would not occur through the reinforcement. I am aware of only one case in NC where the rapid rise and fall of the water level below the MSE wall caused a failure.</i></p> |   |
| 11.  | Is the AASHTO MSE wall backfill specification for the electrochemical requirements followed?   | <input checked="" type="checkbox"/> yes <input type="checkbox"/> no |
| <b>Additional Comments</b>   |  |   |
| Please make any comments on the current MSE design methodology.  |  |   |



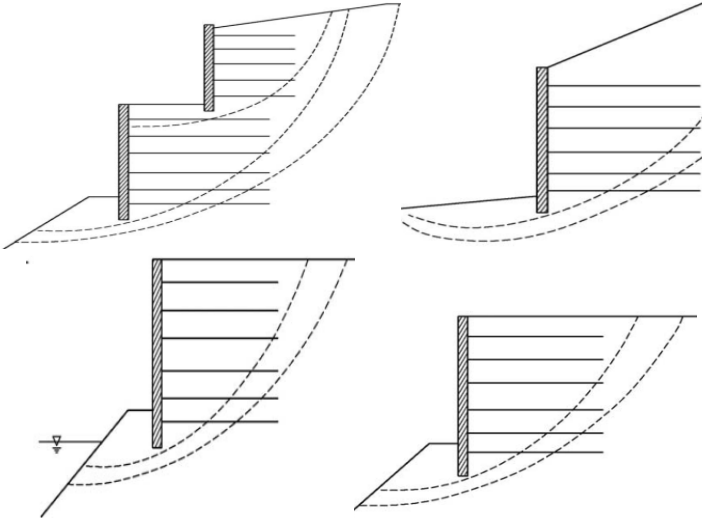
**Survey Questionnaire TxDOT Research (RTI 0-6716)  
 Design Parameters and Methodology for MSE Walls  
 PD: Sean Yoon, Bridge Div. RS: Charles Aubeny, TTI**

**Participant Information**

|                         |               |                      |  |
|-------------------------|---------------|----------------------|--|
| Name of Participant     |               | Contact phone number |  |
| Name of the affiliation | <i>VTrans</i> | Contact email        |  |

**Survey Questions**

|    |   |   |
|----|---|---|
| 1  | Is the FHWA/AASHTO manual used as guideline for MSE wall design?<br>If no, please list the guideline used for your design.  | <input checked="" type="checkbox"/> yes <input type="checkbox"/> no |
| 2  | Is the minimum length criteria used, i.e., 8 feet or 0.7H?<br>If no, please explain the minimum length criteria being used.<br><i>0.7H.</i>   | <input checked="" type="checkbox"/> yes <input type="checkbox"/> no |
| 3  | Is the FHWA specification of backfill material followed?<br>If no, please provide a brief description of the classifications and material parameters for the backfill.<br><i>Please see 704.18. Select Backfill for Mechanically Stabilized Earth (MSE) Walls. In the VTrans Standard Specifications</i><br><a href="http://www.aot.state.vt.us/conadmin/Documents/2011%20Spec%20Book%20for%20Construction/2011Division700.pdf">http://www.aot.state.vt.us/conadmin/Documents/2011%20Spec%20Book%20for%20Construction/2011Division700.pdf</a> | <input type="checkbox"/> yes <input checked="" type="checkbox"/> no |
| 4. | Is the durability of backfill material evaluated?<br>If yes, what is evaluated and what methods are used?<br><i>Please see 704.18. Select Backfill for Mechanically Stabilized Earth (MSE) Walls. In the VTrans Standard Specifications</i><br><a href="http://www.aot.state.vt.us/conadmin/Documents/2011%20Spec%20Book%20for%20Construction/2011Division700.pdf">http://www.aot.state.vt.us/conadmin/Documents/2011%20Spec%20Book%20for%20Construction/2011Division700.pdf</a>  | <input checked="" type="checkbox"/> yes <input type="checkbox"/> no |
| 5. | Have you encountered granular material that can decompose into finer grained soils in the presence of moisture?<br>If yes, please list them.  | <input type="checkbox"/> yes <input checked="" type="checkbox"/> no |
| 6. | Please rank the following potential failure modes on a scale of 1 to 5, with 1 being the least common, 5 being the most common. If the failure has not been seen in your practice, please mark as N/A.<br><i>N/A sliding N/A overturning N/A bearing capacity N/A global stability<br/>N/A pullout N/A compound failure</i>   |   |
| 7. | What factor of safety (FOS) do you require for the following failure modes?<br><i>We design using the resistance factors specified in the 2010 AASHTO LRFD Bridge Design Specifications.</i><br>Sliding _____ ; Overturning _____ ; Bearing capacity _____ ; Pullout _____  |   |

|   |  |   |
|---|--|---|
| 8.  | Do you use the following equation to evaluate bearing capacity?<br>$q_u = cN_c + 0.5L'\gamma_iN_\gamma$  | <input checked="" type="checkbox"/> yes (see below) <input type="checkbox"/> no |
| If no, please specify what method is used to check bearing capacity<br><i>Yes for a level grade in front of the wall and no groundwater</i>                               |  |   |
| 9.  | Do you evaluate stability for failure modes that consider the effect of discrete wall facing units?<br><i>Can you elaborate here?</i>  | <input type="checkbox"/> yes <input type="checkbox"/> no                        |
| If yes, please brief how.   |  |   |
| 10.   | Failure case of compound failure. Please mark on the dashed critical curves. Use “√” for being seen in the field; use “X” for modes considered in design analysis.<br><i>Questions is not clear; what is meant by “seen in the field” - the failure is seen or this type of design? All combinations are generally considered.</i> |   |
|    |  |   |
| <b>Additional Comments</b>  |  |   |
| Please make any comments on the current MSE design methodology.<br><br><i>We use the AASHTO 2010 LRFD Bridge Specifications and MSEW Version 3.0 for MSE wall design.</i> |  |   |

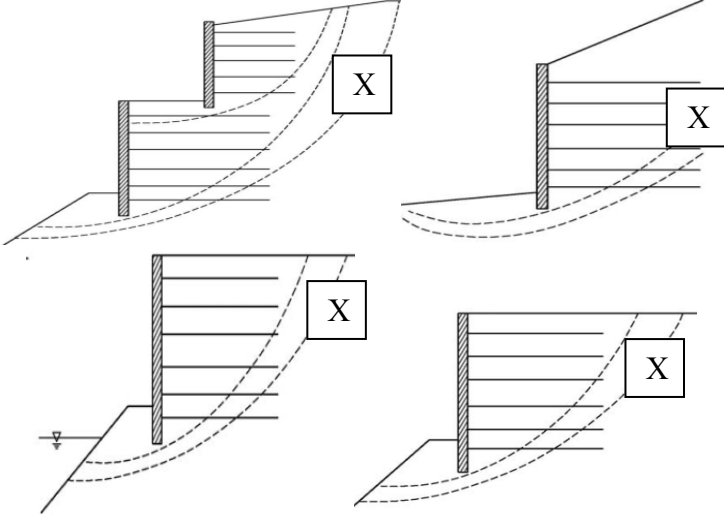
**Survey Questionnaire TxDOT Research (RTI 0-6716)  
 Design Parameters and Methodology for MSE Walls  
 PD: Sean Yoon, Bridge Div. RS: Charles Aubeny, TTI**

**Participant Information**

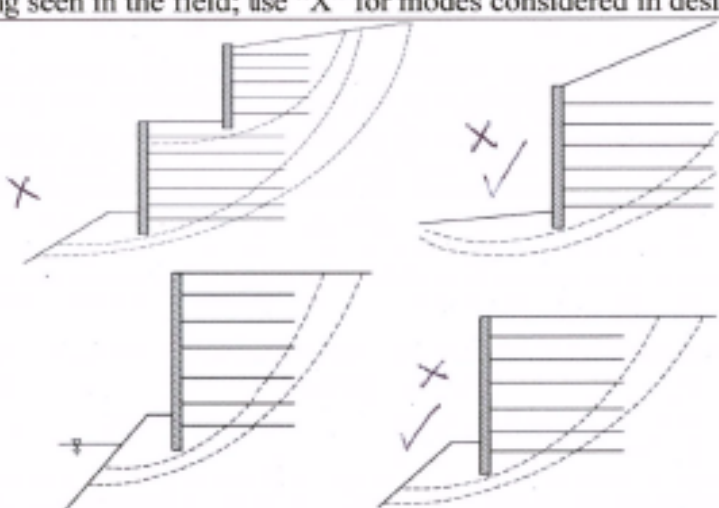
|                         |             |                      |  |
|-------------------------|-------------|----------------------|--|
| Name of Participant     |             | Contact phone number |  |
| Name of the affiliation | Wyoming DOT | Contact email        |  |

**Survey Questions**

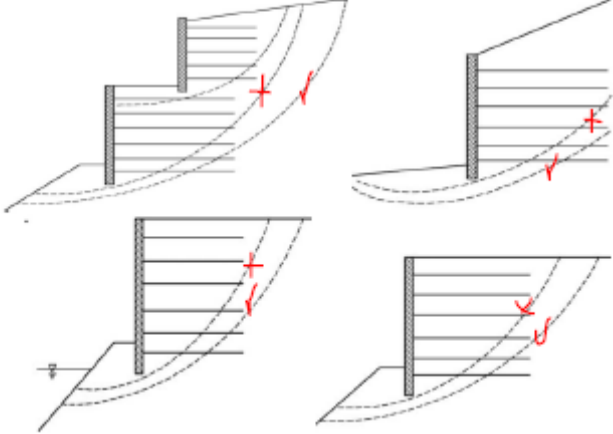
|               |   |   |              |                        |               |            |           |                |             |
|---------------|---|---|--------------|------------------------|---------------|------------|-----------|----------------|-------------|
| 1             | Is the FHWA/AASHTO manual used as guideline for MSE wall design?  | <input checked="" type="checkbox"/> yes <input type="checkbox"/> no |              |                        |               |            |           |                |             |
|               | If no, please list the guideline used for your design.  |   |              |                        |               |            |           |                |             |
| 2             | Is the minimum length criteria used, i.e., 8 feet or 0.7H?  | <input checked="" type="checkbox"/> yes <input type="checkbox"/> no |              |                        |               |            |           |                |             |
|               | If no, please explain the minimum length criteria being used.   |   |              |                        |               |            |           |                |             |
| 3             | Is the FHWA specification of Backfill material followed?  | <input checked="" type="checkbox"/> yes <input type="checkbox"/> no |              |                        |               |            |           |                |             |
|               | <p>If no, please provide a brief description of the classifications and material parameters for the backfill.</p> <p><i>The following is from our specs for mse walls.</i></p> <p><i>Ensure the backfill material within the reinforced area is a crusher run subbase material as approved by the engineer, free from organic or otherwise deleterious material and conforming to the requirements of Subsection 803.4 - Aggregate for Subbase and Base, except the R-value requirements will not apply. Ensure the unit weight is at least 125 lb/ft<sup>2</sup> and the angle of internal friction (phi angle) is at least 34°. Ensure the crusher run subbase is crushed material having the following gradation:</i></p> <table border="0"> <tr> <td><i>Sieve</i></td> <td><i>Percent Passing</i></td> </tr> <tr> <td><i>2 inch</i></td> <td><i>100</i></td> </tr> <tr> <td><i>#4</i></td> <td><i>30 - 50</i></td> </tr> <tr> <td><i>#200</i></td> <td><i>0-9</i></td> </tr> </table> <p><i>Section 803.4 can be found at:</i><br/> <a href="http://www.dot.state.wy.us/wydot/engineering_technical_programs/manuals_publications/2010_Standard_Specifications">http://www.dot.state.wy.us/wydot/engineering_technical_programs/manuals_publications/2010_Standard_Specifications</a></p> |   | <i>Sieve</i> | <i>Percent Passing</i> | <i>2 inch</i> | <i>100</i> | <i>#4</i> | <i>30 - 50</i> | <i>#200</i> |
| <i>Sieve</i>  | <i>Percent Passing</i>  |   |              |                        |               |            |           |                |             |
| <i>2 inch</i> | <i>100</i>  |   |              |                        |               |            |           |                |             |
| <i>#4</i>     | <i>30 - 50</i>  |   |              |                        |               |            |           |                |             |
| <i>#200</i>   | <i>0-9</i>  |   |              |                        |               |            |           |                |             |
| 4.            | Is the durability of backfill material evaluated?   | <input checked="" type="checkbox"/> yes <input type="checkbox"/> no |              |                        |               |            |           |                |             |
|               | <p>If yes, what is evaluated and what methods are used?</p> <p><i>See Section 803.4 (noted in Item 3)</i></p>   |   |              |                        |               |            |           |                |             |
| 5.            | Have you encountered granular material that can decompose into finer grained soils in the presence of moisture?   | <input type="checkbox"/> yes <input checked="" type="checkbox"/> no |              |                        |               |            |           |                |             |
|               | If yes, please list them.   |   |              |                        |               |            |           |                |             |

|   |  |   |
|---|--|---|
| 6.  | Please rank the following potential failure modes on a scale of 1 to 5, with 1 being the least common, 5 being the most common. If the failure has not been seen in your practice, please mark as N/A. |   |
|   | <i>N/A</i> sliding <i>N/A</i> overturning <i>N/A</i> bearing capacity <i>N/A</i> global stability<br><i>N/A</i> pullout <i>N/A</i> compound failure  |   |
| 7.  | What factor of safety (FOS) do you require for the following failure modes?<br><i>See comments</i>   |   |
|   | Sliding _____; Overturning _____; Bearing capacity _____; Pullout _____  |   |
| 8.  | Do you use the following equation to evaluate bearing capacity?<br>$q_u = cN_c + 0.5L'\gamma_i N_\gamma$   | <input type="checkbox"/> yes <input checked="" type="checkbox"/> no |
|   | If no, please specify what method is used to check bearing capacity<br><i>AASHTO LRFD eqn 10.6.3.1.2a-1</i>  |   |
| 9.  | Do you evaluate stability for failure modes that consider the effect of discrete wall facing units?  | <input type="checkbox"/> yes <input checked="" type="checkbox"/> no |
|   | If yes, please brief how.  |   |
| 10.   | Failure case of compound failure. Please mark on the dashed critical curves. Use “√” for being seen in the field; use “X” for modes considered in design analysis.                                     |   |
|   |   |   |
| 11.   | Is the AASHTO MSE wall backfill specification for the electrochemical requirements followed?   | <input checked="" type="checkbox"/> yes <input type="checkbox"/> no |
| <b>Additional Comments</b>                                      |  |   |
| Please make any comments on the current MSE design methodology. |  |   |
| <i>Using AASHTO LRFD specifications for all mse wall design</i> |  |   |



|   |  |  |
|---|--|--|
| 9.  | Do you evaluate stability for failure modes that consider the effect of discrete wall facing units<br>If yes, please brief how.  | <input type="checkbox"/> yes<br><input checked="" type="checkbox"/> no |
| 10.   | <p>Failure case of compound failure (Please mark on the dashed critical curves. Use "√" for being seen in the field; use "X" for modes considered in design analysis)</p>  |  |
| 11.   | Is the AASHTO MSE wall backfill specification for the electrochemical requirements followed?   | <input checked="" type="checkbox"/> yes<br><input type="checkbox"/> no |
| <b>Additional Comments</b>  |  |  |
| <p>Please make any comments on the current MSE design methodology.</p> <p>We do not allow construction of MSE walls at water crossings in Nebraska for our roadway projects.</p> <p>We have recently adopted the LRFD method of analysis and therefore no longer use the ASD method for external stability.</p> |  |  |

| Survey Questionnaire TxDOT Research (RTI 0-6716)<br>Design Parameters and Methodology for MSE walls |  |  |   |
|---|--|--|---|
| PD: Sean Yoon, TxDOT  |  | RS: Charles Aubeny, TTI  |   |
| Information of the Participants   |  |  |   |
| Name of Participant   |  | Contact phone number   |   |
| Name of the affiliation   | LA DOTD  | Contact email  |   |
| Survey Questions  |  |  |   |
| 1   | Whether FHWA/AASHTO manual is used as guideline of designing MSE wall?<br>If no, please list the guideline used for your design.   | <input checked="" type="checkbox"/> _x_                                  | <input type="checkbox"/> _yes<br><input type="checkbox"/> _no |
| 2   | Is the minimum length criteria used, i.e., of 8 feet or 0.7H?<br>If no, please explain the minimum length criteria being used.   | <input checked="" type="checkbox"/> _x_                                  | <input type="checkbox"/> _yes<br><input type="checkbox"/> _no |
| 3   | Is the FHWA specification of Backfill material followed?<br>If no, please brief the classifications and major parameters of the backfill.  | <input checked="" type="checkbox"/> _x_                                  | <input type="checkbox"/> _yes<br><input type="checkbox"/> _no |
| 4   | Is the durability of backfill material evaluated?<br>If yes, what are aspects evaluated and corresponding methods used?  | <input checked="" type="checkbox"/> _x_                                  | <input type="checkbox"/> _yes<br><input type="checkbox"/> _no |
| 5   | Have you encountered granular materials, which can be decomposed into fine grained soil with the presence of moisture?<br>If yes, please list them.  | <input type="checkbox"/> _yes<br><input checked="" type="checkbox"/> _x_ | <input type="checkbox"/> _no                                  |
| 6   | Common failure modes identified (Please rate them as 1 to 5, as 1 being the least common, 5 being the most common. If the failure has not been seen in your practice, please mark as N/A)<br>_1_sliding _1_overturning _1_bearing capacity _2_global stability _3_pullout<br>_3_compound failure |  |   |
| 7   | Stability criteria used for sliding, overturning, and pullout, i.e., factors of safety (FOS) used for these stability analyses.<br>Factor of Safety Used: sliding_1.5_; overturning_1.2_; bearing capacity_2_; pullout_3_  |  |   |
| 8   | Whether this equation is used to check bearing capacity? $q_u = cN_c + 0.5L\gamma_iN_\gamma$<br>If no, please specify what method is used to check bearing capacity  | <input checked="" type="checkbox"/> _x_                                  | <input type="checkbox"/> _yes<br><input type="checkbox"/> _no |

|   |  |  |
|---|--|--|
| 9.  | Compound failure check methods: considering the effect of discrete wall facing units<br>If yes, please brief how.  | <input checked="" type="checkbox"/> _x_ yes<br><input type="checkbox"/> _no        |
| 10.   | Failure case of compound failure (Please mark on the dashed critical curves. Use “√” for being seen in the field; use “X” for identified in design analysis) |  |
| <b>Additional Comments</b>                                      |  |  |
| Please make any comments on the current MSE design methodology. |  |  |



## APPENDIX B: LABORATORY TEST RESULTS

The results presented here are for Types A, B, and D, which were tested under consolidated drained conditions. Meanwhile, a consolidated undrained test was performed on a Type C backfill material and the results are also presented. The table shows an overview of test results and the detailed test results for each type of backfill materials.

**Table B. 1. Friction Angles for Type A, B, and D Backfill Tested.**

| <b>Gradation</b> | <b>Maximum Friction Angles (°)</b> | <b>Minimum Friction Angles (°)</b> | <b>p-q Friction Angles (°)</b> |
|------------------|------------------------------------|------------------------------------|--------------------------------|
| A1               | 49.9                               | 43.0                               | 45.5                           |
| A2               | 46.8                               | 41.8                               | 43.7                           |
| A3               | 47.5                               | 41.8                               | 42.9                           |
| A4               | 45.9                               | 39.8                               | 42.8                           |
| B1               | 53.4                               | 48.5                               | 51.9                           |
| B2               | 53.2                               | 48.3                               | 52.5                           |
| B3               | 48.4                               | 43.5                               | 45.7                           |
| B4               | 41.7                               | 31.8                               | 39.2                           |
| D1               | 47.2                               | 41.6                               | 44.2                           |
| D2               | 47.0                               | 36.5                               | 40.7                           |
| D3               | 51.6                               | 38.4                               | 43.8                           |
| D4               | 41.7                               | 35.8                               | 38.0                           |

**Table B. 2. Laboratory Test Results for Type C Material.**

| <b>Gradation</b> | <b>Maximum Undrained Friction Angles (°)</b> | <b>Minimum Undrained Friction Angles (°)</b> | <b>Maximum Drained Friction Angles (°)</b> | <b>Minimum Drained Friction Angles (°)</b> | <b>Dry Unit Weight (pcf)</b> |
|------------------|--|--|--|--|------------------------------|
| C1               | 29.4   | 26.2   | 40.3                                       | 27.8                                       | 120.6                        |
| C2               | 28.3   | 26.2   | 47.4                                       | 30.1                                       | 129.4                        |
| C3               | 32.0   | 22.6   | 50.9                                       | 33.7                                       | 128.4                        |
| C4               | 32.3   | 23.6   | 26.4                                       | 14.5                                       | 126.3                        |

**Table B. 3. Type A Test Results.**

| Test Name     | Date   | Gradation | Cell Pressure (psi) | Unit Weight of Sample Tested | Void Ratio | RC (%) | Friction Angle | Comments  |
|---------------|--------|-----------|---------------------|------------------------------|------------|--------|----------------|---|
| A1_10_1_52012 | 20-May | A1        | 4.3                 | 87.90                        | 0.85       | 93     | 49.9           |   |
| A1_10_2_60412 | 4-Jun  | A1        | 4.3                 | 87.80                        | 0.85       | 93     | 49.7           | Possible leak: dilation up to 5%                    |
| A1_15_1_60512 | 5-Jun  | A1        | 6.5                 | 86.00                        | 0.89       | 91     | 47.0           |   |
| A1_15_2_61412 | 14-Jun | A1        | 6.5                 | 86.40                        | 0.88       | 91     | 45.2           |   |
| A1_20_1_60512 | 5-Jun  | A1        | 8.7                 | 83.60                        | 0.94       | 88     | 43.3           |   |
| A1_20_2_61412 | 14-Jun | A1        | 8.7                 | 84.90                        | 0.91       | 90     | 43.0           | Contraction at 3%                                   |
| A2_10_1_70312 | 3-Jul  | A2        | 4.3                 | 87.80                        | 0.85       | 88     | 46.8           |   |
| A2_10_2_71312 | 13-Jul | A2        | 4.3                 | 95.82                        | 0.69       | 96     | 42.7           | Compliant load curve                                |
| A2_15_1_71612 | 16-Jul | A2        | 6.5                 | 87.24                        | 0.86       | 88     | 43.6           |   |
| A2_15_2_71712 | 17-Jul | A2        | 6.5                 | 87.43                        | 0.86       | 88     | 43.1           |   |
| A2_20_1_71812 | 18-Jul | A2        | 8.7                 | 91.80                        | 0.77       | 92     | 44.7           |   |
| A2_20_2_71812 | 18-Jul | A2        | 8.7                 | 93.17                        | 0.74       | 93     | 41.8           | Leak: volume change=24%                             |
| A3_10_1_71912 | 19-Jul | A3        | 4.3                 | 96.49                        | 0.68       | 97     | 47.5           | Inconsistent load curve trend                       |
| A3_10_2_72012 | 20-Jul | A3        | 4.3                 | 84.90                        | 0.91       | 86     | 44.8           |   |
| A3_15_1_73012 | 30-Jul | A3        | 6.5                 | 100.89                       | 0.61       | 102    | 42.1           |   |
| A3_15_2_73012 | 30-Jul | A3        | 6.5                 | 94.44                        | 0.72       | 95     | 41.7           | Large jump in load curve at 7.5%, volume change 11% |
| A3_20_1_73112 | 31-Jul | A3        | 8.7                 | 101.45                       | 0.60       | 102    | 42.4           | Leak: volume change=18%                             |
| A3_20_2_73112 | 31-Jul | A3        | 8.7                 | 100.49                       | 0.61       | 101    | 42.1           | Leak: volume change 14%                             |
| A4_10_2_62212 | 22-Jun | A4        | 4.3                 | 115.00                       | 0.41       | 98     | 52.5           | Inconsistent load curve trend                       |
| A4_10_3_62412 | 24-Jun | A4        | 4.3                 | 108.40                       | 0.50       | 92     | 45.9           |   |
| A4_15_1_62612 | 26-Jun | A4        | 6.5                 | 102.50                       | 0.58       | 87     | 41.4           | Leak: volume change=8%                              |
| A4_15_2_62712 | 27-Jun | A4        | 6.5                 | 98.90                        | 0.64       | 84     | 40.2           | Compliant load curve                                |
| A4_20_1_70212 | 2-Jul  | A4        | 8.7                 | 101.40                       | 0.60       | 86     | 39.8           |   |
| A4_20_2_70212 | 2-Jul  | A4        | 8.7                 | 101.00                       | 0.61       | 86     | 40.7           |   |

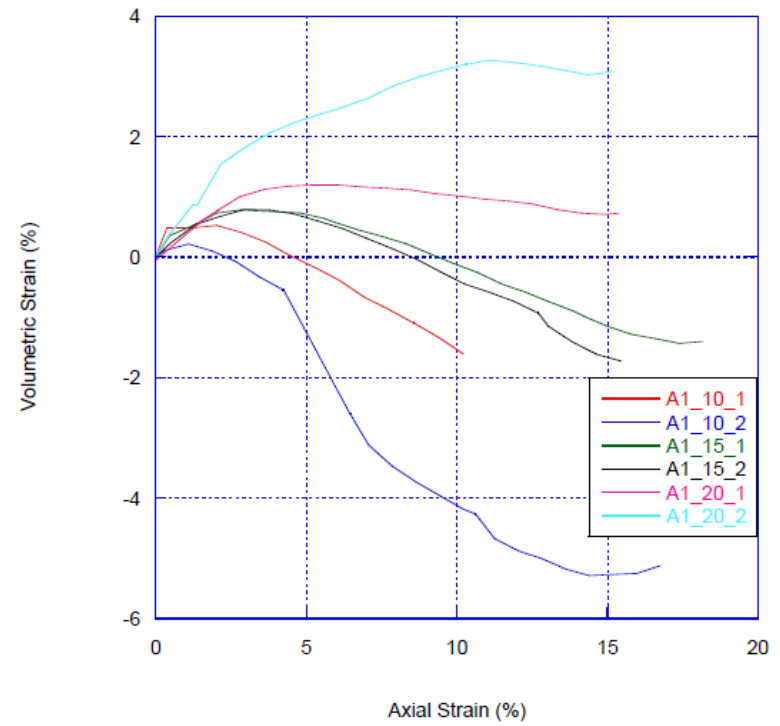
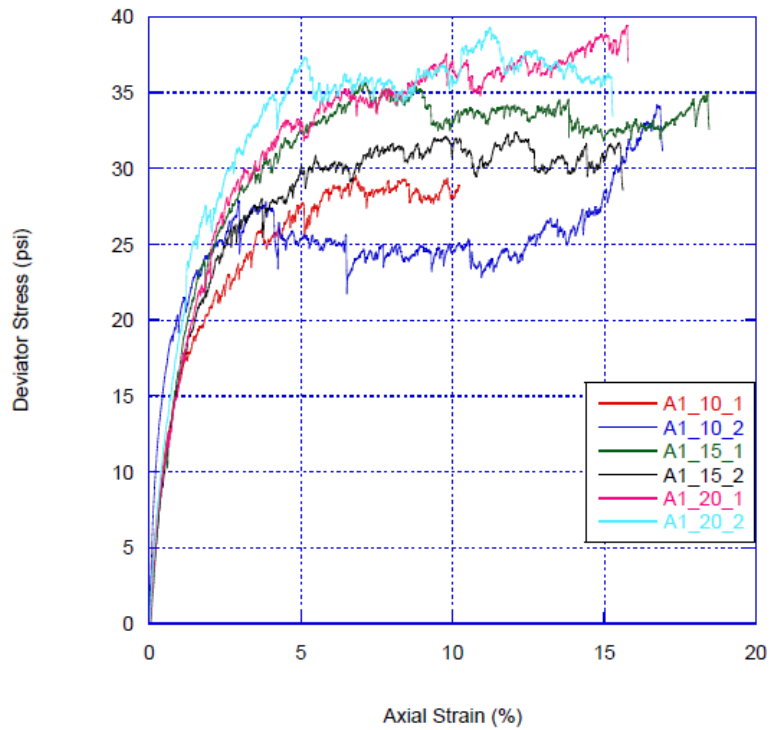


**Figure B. 1. Gradation A1 Stress-Strain and Volumetric Strain Curves.**

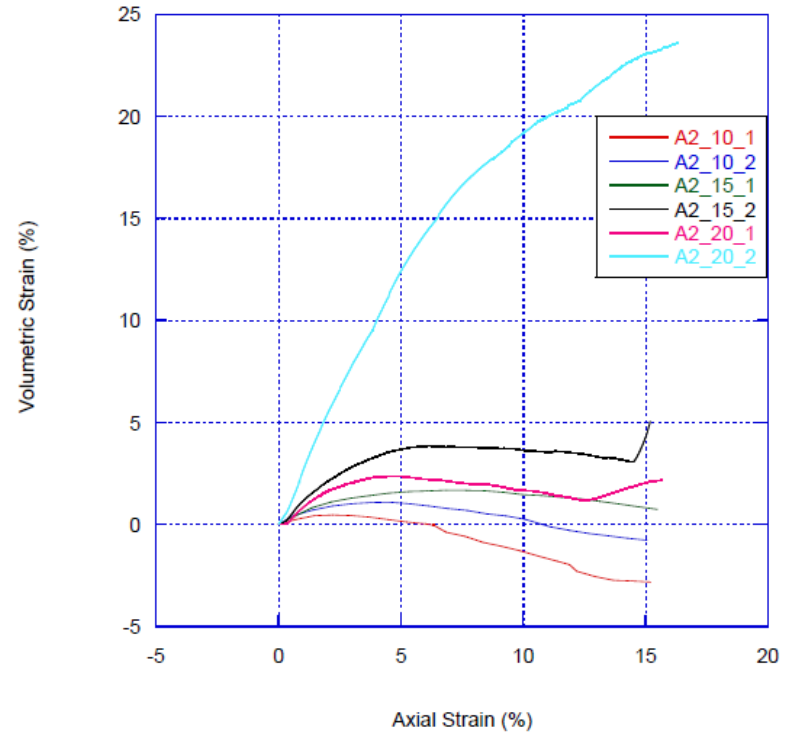
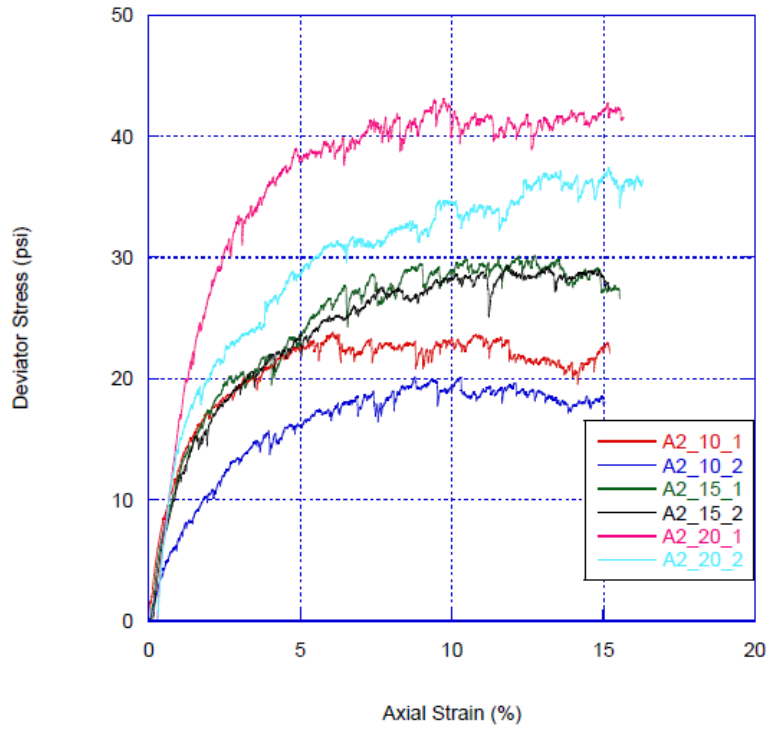


**Figure B. 2. Gradation A2 Stress-Strain and Volumetric Strain Curves.**

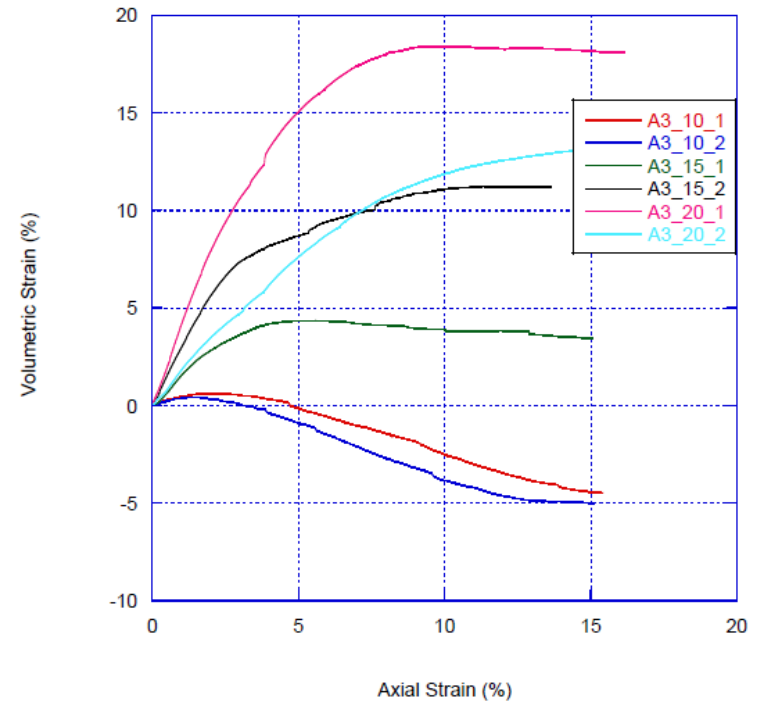
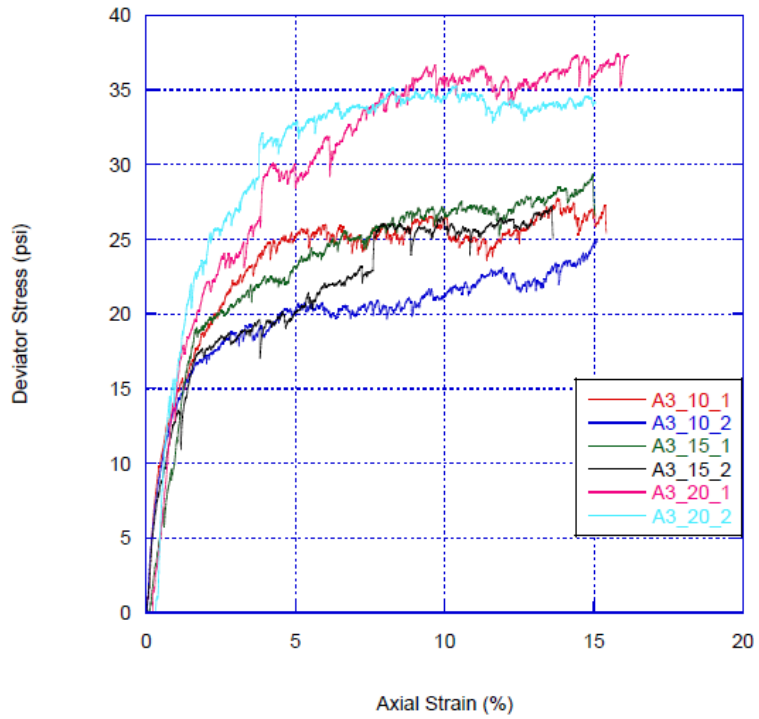


**Figure B. 3. Gradation A3 Stress-Strain and Volumetric Strain Curves.**

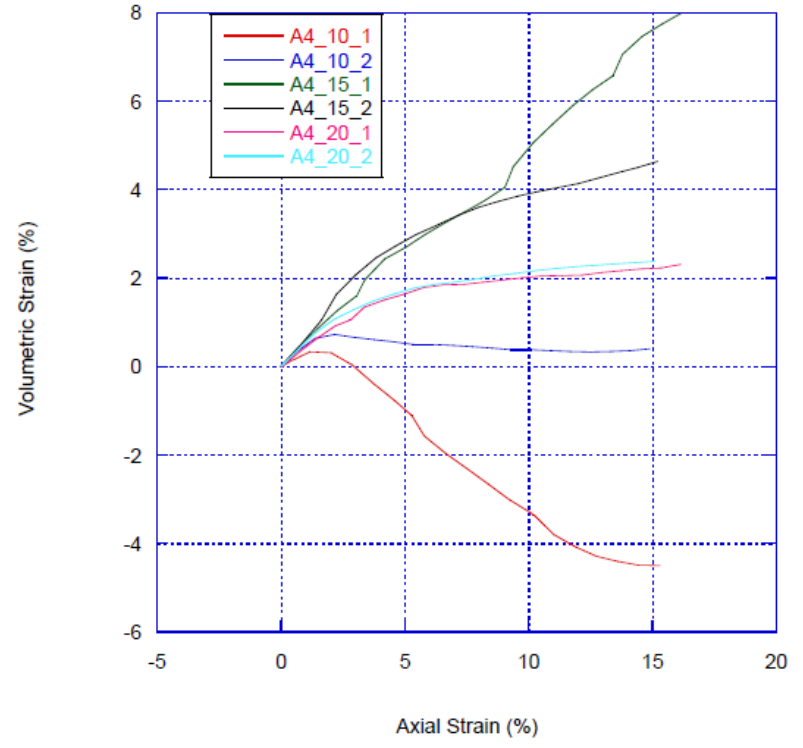
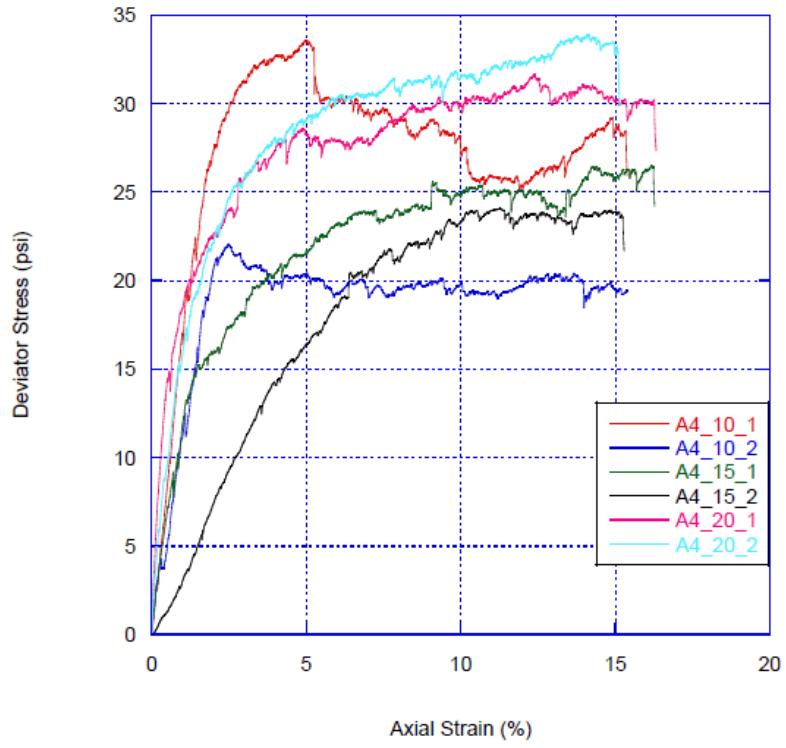


**Figure B. 4. Gradation A4 Stress-Strain and Volumetric Strain Curves.**

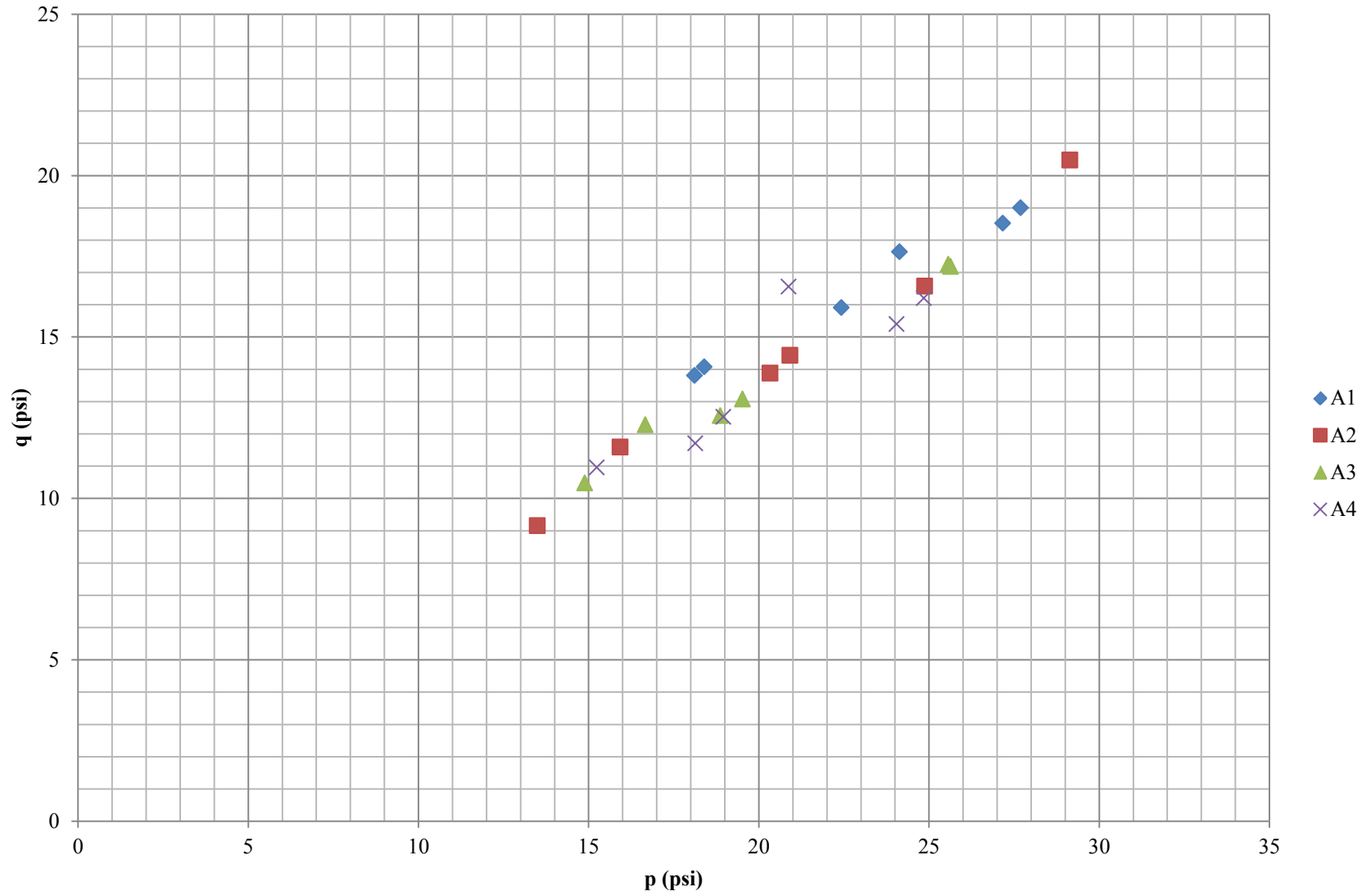


Figure B. 5. Type A Material p-q Diagram.

**Table B. 4. Type B Test Results.**

| Test Name     | Date   | Gradation | Cell Pressure (psi) | Unit Weight of Sample Tested | Void Ratio | RC (%) | Friction Angle | Comments                                      |
|---------------|--------|-----------|---------------------|------------------------------|------------|--------|----------------|---|
| B1_10_1_60612 | 6-Jun  | B1        | 4.3                 | -                            | -          | -      | 53.3           |   |
| B1_10_2_61312 | 13-Jun | B1        | 4.3                 | 94.20                        | 0.75       | 87     | 53.4           |   |
| B1_15_1_60712 | 7-Jun  | B1        | 6.5                 | 95.00                        | 0.73       | 88     | 51.5           |   |
| B1_15_2_61212 | 12-Jun | B1        | 6.5                 | 97.20                        | 0.69       | 90     | 51.4           | Sample touching chamber at strain <10%        |
| B1_20_1_61112 | 11-Jun | B1        | 8.7                 | 91.20                        | 0.81       | 84     | 53.8           |   |
| B1_20_2_61212 | 12-Jun | B1        | 8.7                 | 91.40                        | 0.80       | 85     | 48.5           |   |
| B2_10_1_80112 | 1-Aug  | B2        | 4.3                 | 114.40                       | 0.44       | 101    | 49.6           |   |
| B2_10_2_80112 | 1-Aug  | B2        | 4.3                 | 114.70                       | 0.44       | 101    | 49.4           |   |
| B2_15_1_80212 | 2-Aug  | B2        | 6.5                 | 113.10                       | 0.46       | 100    | 53.2           | Leak: volume change=100%                      |
| B2_15_2_80212 | 2-Aug  | B2        | 6.5                 | 111.60                       | 0.48       | 98     | 48.3           |   |
| B2_20_1_80312 | 3-Aug  | B2        | 8.7                 | 115.20                       | 0.43       | 102    | 50.7           |   |
| B2_20_2_80312 | 3-Aug  | B2        | 8.7                 | 116.90                       | 0.41       | 103    | 48.4           |   |
| B3_10_1_80412 | 4-Aug  | B3        | 4.3                 | 119.33                       | 0.38       | 106    | 45.9           | Membrane rupture volume change large after 8% |
| B3_10_2_80612 | 6-Aug  | B3        | 4.3                 | 117.44                       | 0.40       | 105    | 48.4           |   |
| B3_15_1_80612 | 6-Aug  | B3        | 6.5                 | 118.27                       | 0.39       | 106    | 47.1           |   |
| B3_15_2_80712 | 7-Aug  | B3        | 6.5                 | 117.79                       | 0.40       | 105    | 46.0           |   |
| B3_20_1_80712 | 7-Aug  | B3        | 8.7                 | 118.48                       | 0.39       | 106    | 43.5           | Inconsistent load curve trend                 |
| B3_20_2_80812 | 8-Aug  | B3        | 8.7                 | 115.89                       | 0.42       | 103    | 45.4           |   |
| B4_10_1_71812 | 18-Jul | B4        | 4.3                 | 120.53                       | 0.37       | 111    | 31.8           |   |
| B4_15_1_82012 | 20-Aug | B4        | 6.5                 | 119.40                       | 0.38       | 110    | 34.5           |   |
| B4_20_2_82312 | 23-Aug | B4        | 8.7                 | 136.00                       | 0.21       | 125    | 41.7           |   |



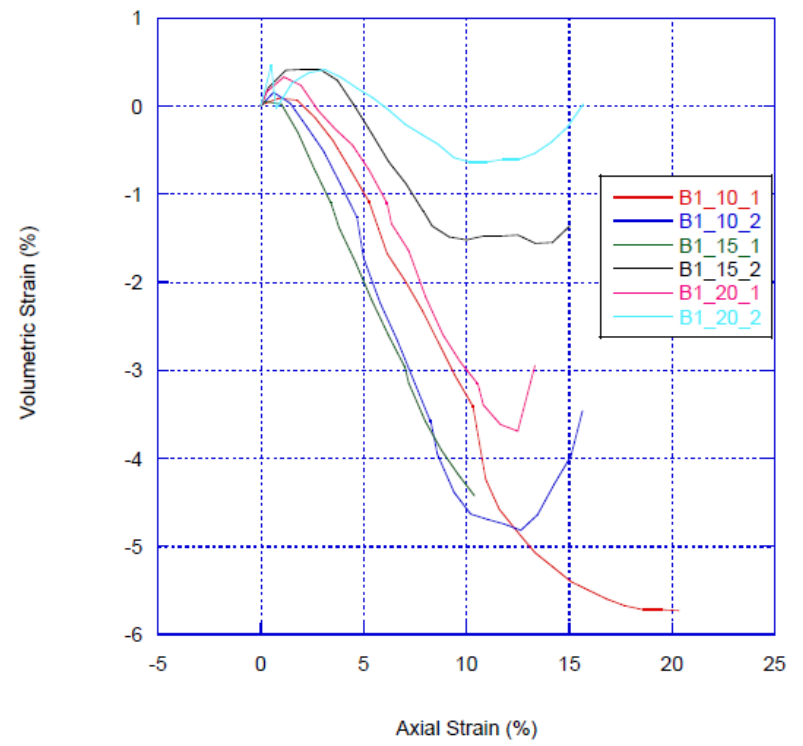
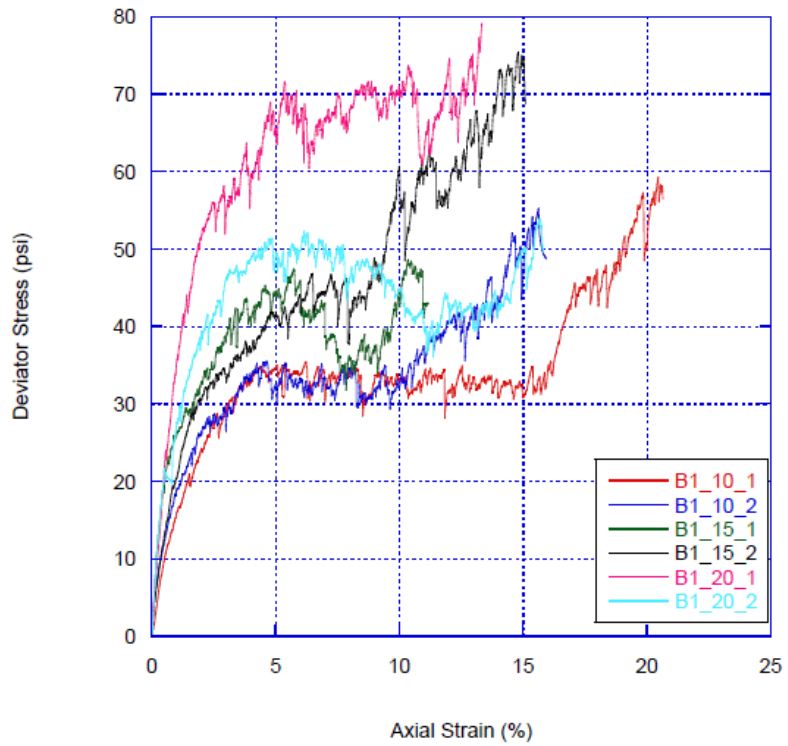
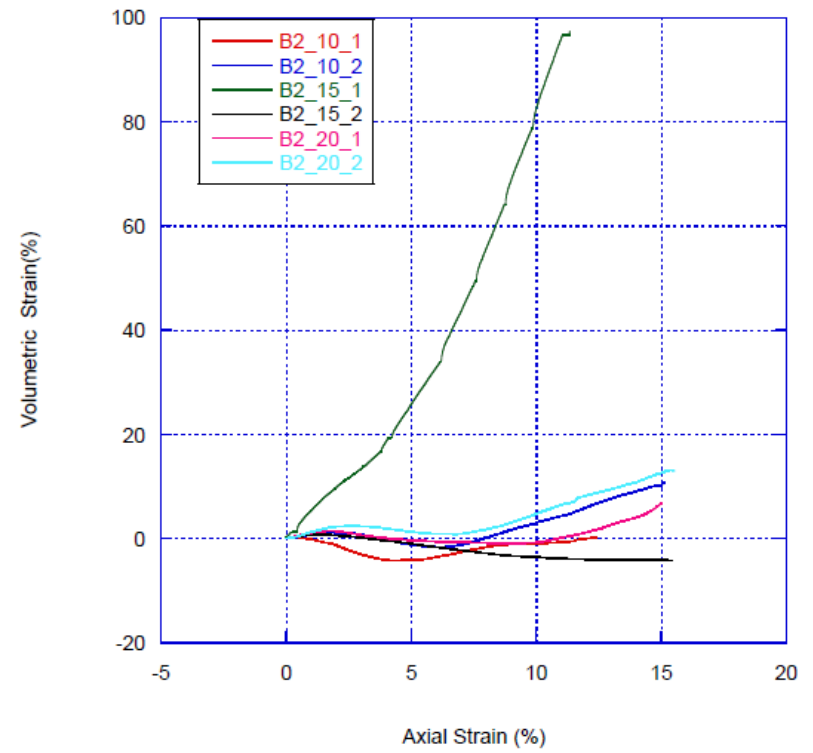
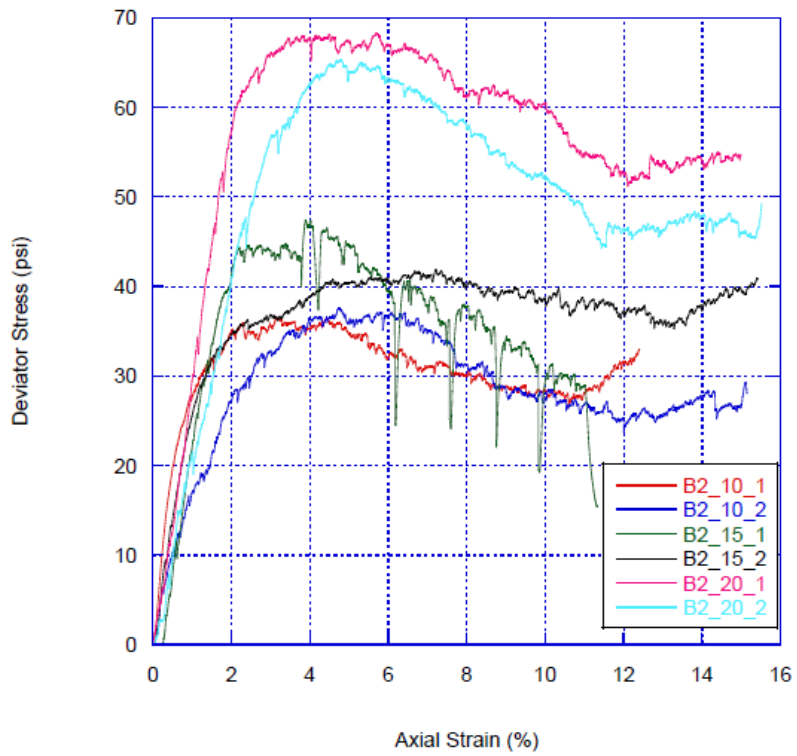


Figure B. 6. Gradation B1 Stress-Strain and Volumetric Strain Curves.



**Figure B. 7. Gradation B2 Stress-Strain and Volumetric Strain Curves.**

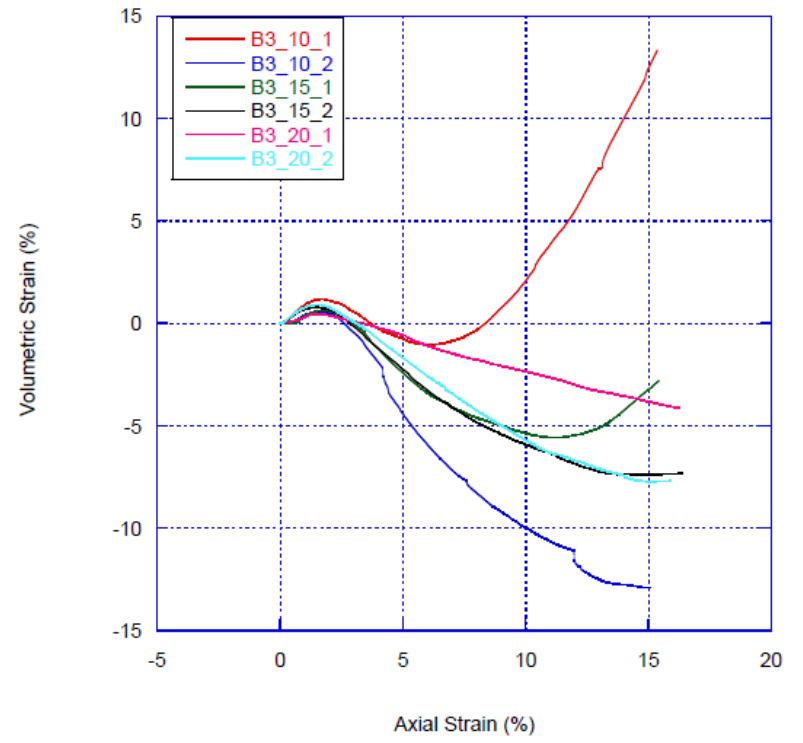
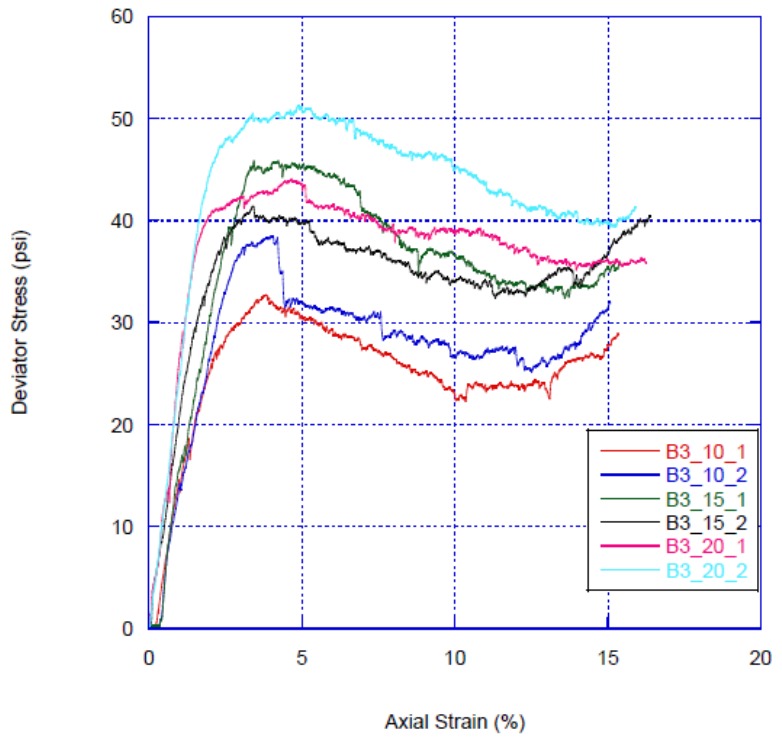


Figure B. 8. Gradation B3 Stress-Strain and Volumetric Strain Curves.

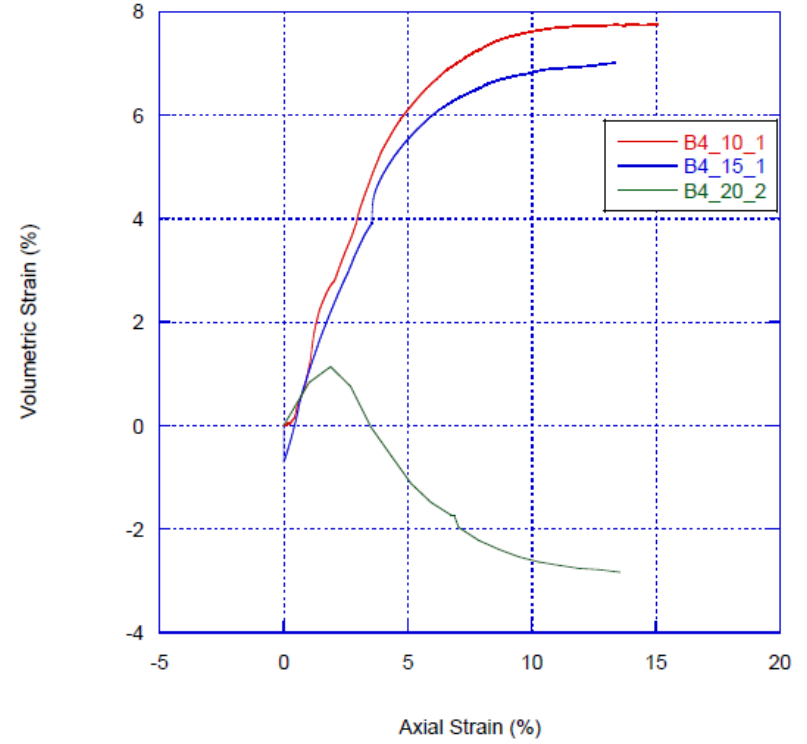
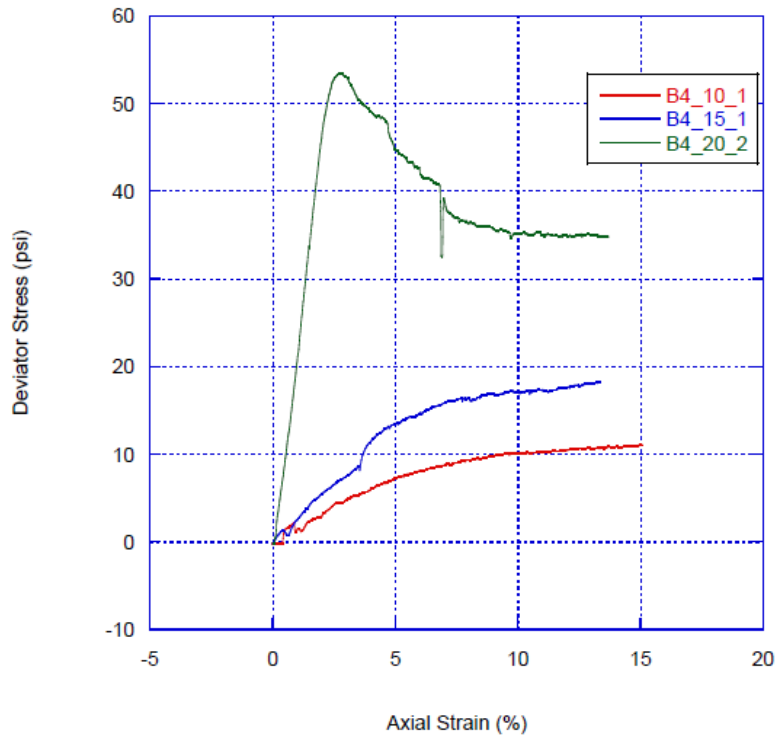


Figure B. 9. Gradation B4 Stress-Strain and Volumetric Strain Curves.

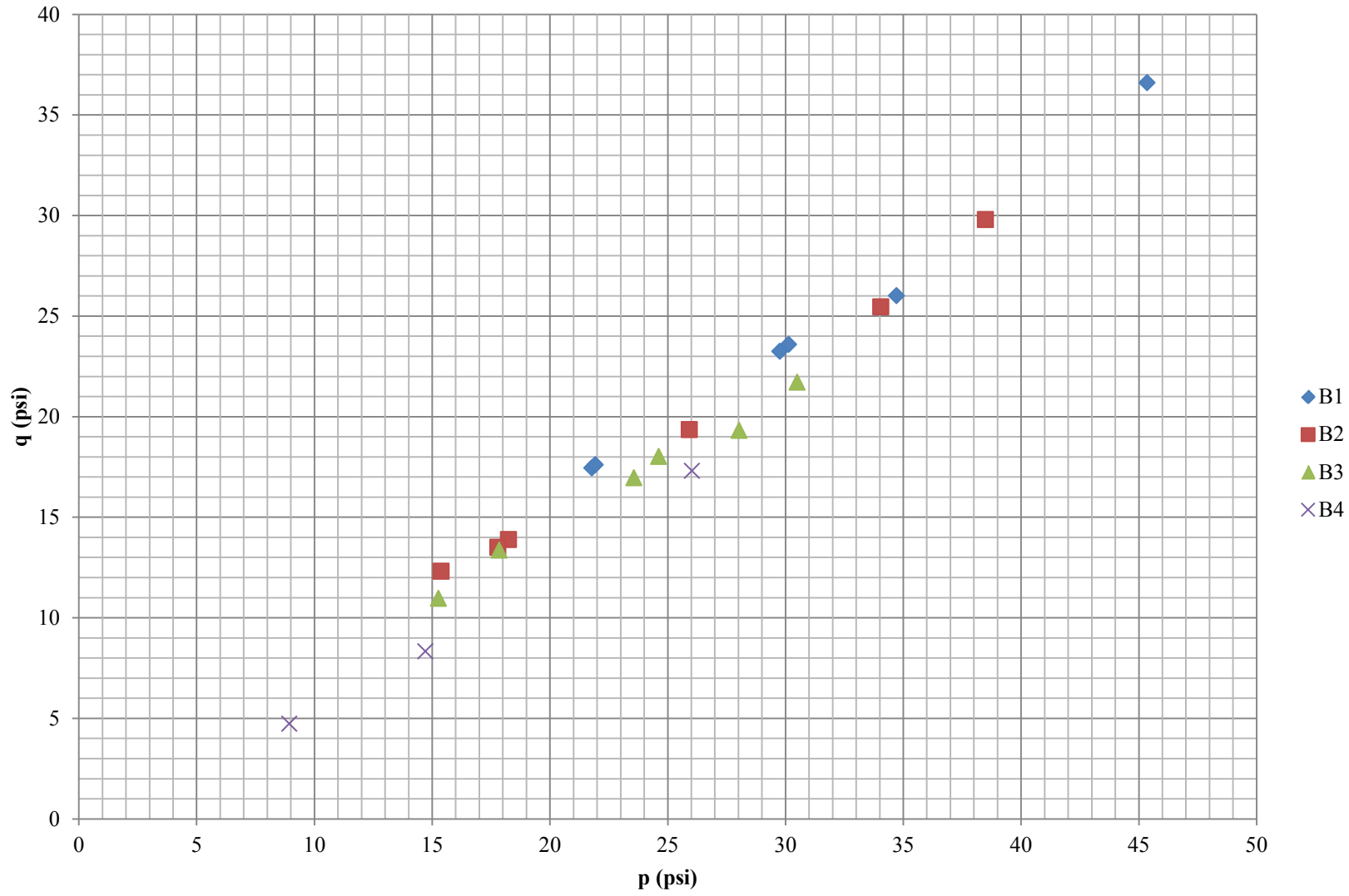


Figure B. 10. Type B Material p-q Diagram.

**Table B. 5. Type C Test Results.**

| Test Name        | Date   | Soil Type | Gradation | Confining Stress (psf) | Confining Stress (psi) | Wall Height (ft) | Unit Weight of Sample Tested | Void Ratio | % RC   | Friction Angle (undrained) | Friction Angle (drained) | Comments |
|------------------|--------|-----------|-----------|------------------------|------------------------|------------------|------------------------------|------------|--------|----------------------------|--------------------------|----------|
| C1_10_1_S_10412  | 4-Oct  | C         | C1        | 625                    | 4.34                   | 10               | 120.12                       | -          | 99.60  | 27.50                      | 40.27                    |          |
| C1_10_2_S_10412  | 4-Oct  | C         | C1        | 625                    | 4.34                   | 10               | 123.44                       | -          | 102.35 | 29.19                      | 39.08                    |          |
| C1_15_1_S_10612  | 6-Oct  | C         | C1        | 937.5                  | 6.51                   | 15               | 119.96                       | -          | 99.48  | 27.23                      | 34.49                    |          |
| C1_15_2_S_10612  | 6-Oct  | C         | C1        | 937.5                  | 6.51                   | 15               | 125.31                       | -          | 103.93 | 29.45                      | 34.48                    |          |
| C1_20_1_S_10812  | 8-Oct  | C         | C1        | 1250                   | 8.68                   | 20               | 117.73                       | -          | 97.62  | 26.23                      | 27.97                    |          |
| C1_20_2_S_10812  | 8-Oct  | C         | C1        | 1250                   | 8.68                   | 20               | 124.11                       | -          | 102.91 | 28.10                      | 30.94                    |          |
| C2_10_1_S_92812  | 28-Sep | C         | C2        | 625                    | 4.34                   | 10               | 125.86                       | -          | 97.57  | 26.91                      | 47.45                    |          |
| C2_10_2_S_10112  | 1-Oct  | C         | C2        | 625                    | 4.34                   | 10               | 131.97                       | -          | 101.52 | 28.33                      | 44.24                    |          |
| C2_15_1_S_92812  | 28-Sep | C         | C2        | 937.5                  | 6.51                   | 15               | 130.05                       | -          | 100.04 | 28.20                      | 45.39                    |          |
| C2_15_2_S_10312  | 3-Oct  | C         | C2        | 937.5                  | 6.51                   | 15               | 128.70                       | -          | 99.00  | 29.22                      | 35.96                    |          |
| C2_20_1_S_93012  | 30-Sep | C         | C2        | 1250                   | 8.68                   | 20               | 124.96                       | -          | 96.12  | 26.24                      | 30.06                    |          |
| C2_20_2_S_10112  | 1-Oct  | C         | C2        | 1250                   | 8.68                   | 20               | 131.79                       | -          | 101.38 | 28.82                      | 41.12                    |          |
| C3_10_1_S_101012 | 10-Oct | C         | C3        | 625                    | 4.34                   | 10               | 129.33                       | -          | 100.72 | 22.66                      | 41.10                    |          |
| C3_10_2_S_101012 | 10-Oct | C         | C3        | 625                    | 4.34                   | 10               | 133.23                       | -          | 103.76 | 32.02                      | 50.90                    |          |
| C3_15_1_S_101112 | 11-Oct | C         | C3        | 937.5                  | 6.51                   | 15               | 129.26                       | -          | 100.67 | 26.18                      | 35.37                    |          |
| C3_15_2_S_101112 | 11-Oct | C         | C3        | 937.5                  | 6.51                   | 15               | 132.89                       | -          | 103.49 | 28.48                      | 44.03                    |          |
| C3_20_1_S_101212 | 12-Oct | C         | C3        | 1250                   | 8.68                   | 20               | 133.02                       | -          | 103.60 | 26.99                      | 33.67                    |          |
| C3_20_2_S_101212 | 12-Oct | C         | C3        | 1250                   | 8.68                   | 20               | 129.99                       | -          | 101.24 | 27.80                      | 35.41                    |          |
| C4_10_1_S_101612 | 16-Oct | C         | C4        | 625                    | 4.34                   | 10               | 125.10                       | -          | 98.97  | 25.82                      | 26.41                    |          |
| C4_10_1_S_101612 | 16-Oct | C         | C4        | 625                    | 4.34                   | 10               | 121.01                       | -          | 95.81  | 32.31                      | 20.44                    |          |
| C4_15_1_S_101912 | 19-Oct | C         | C4        | 937.5                  | 6.51                   | 15               | 119.57                       | -          | 94.59  | 23.66                      | 14.49                    |          |
| C4_15_2_S_101712 | 17-Oct | C         | C4        | 937.5                  | 6.51                   | 15               | 126.87                       | -          | 100.29 | 30.68                      | 22.00                    |          |
| C4_20_1_S_101812 | 18-Oct | C         | C4        | 1250                   | 8.68                   | 20               | 128.64                       | -          | 101.69 | 27.68                      | 22.79                    |          |
| C4_20_1_S_101812 | 18-Oct | C         | C4        | 1250                   | 8.68                   | 20               | 124.28                       | -          | 98.32  | 32.29                      | 13.37                    |          |

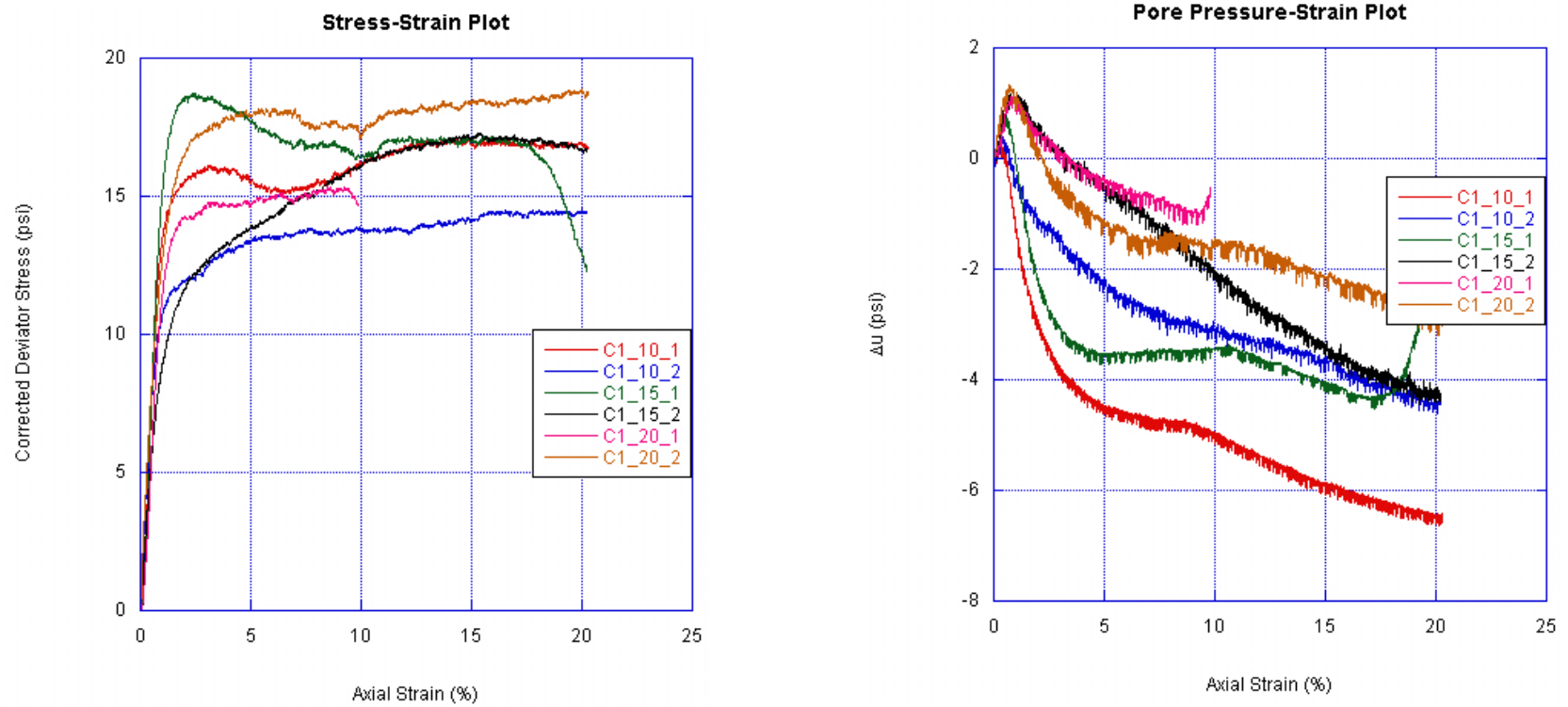


Figure B. 11. Gradation C1 Stress-Strain and Pore Pressure-Strain Curves.

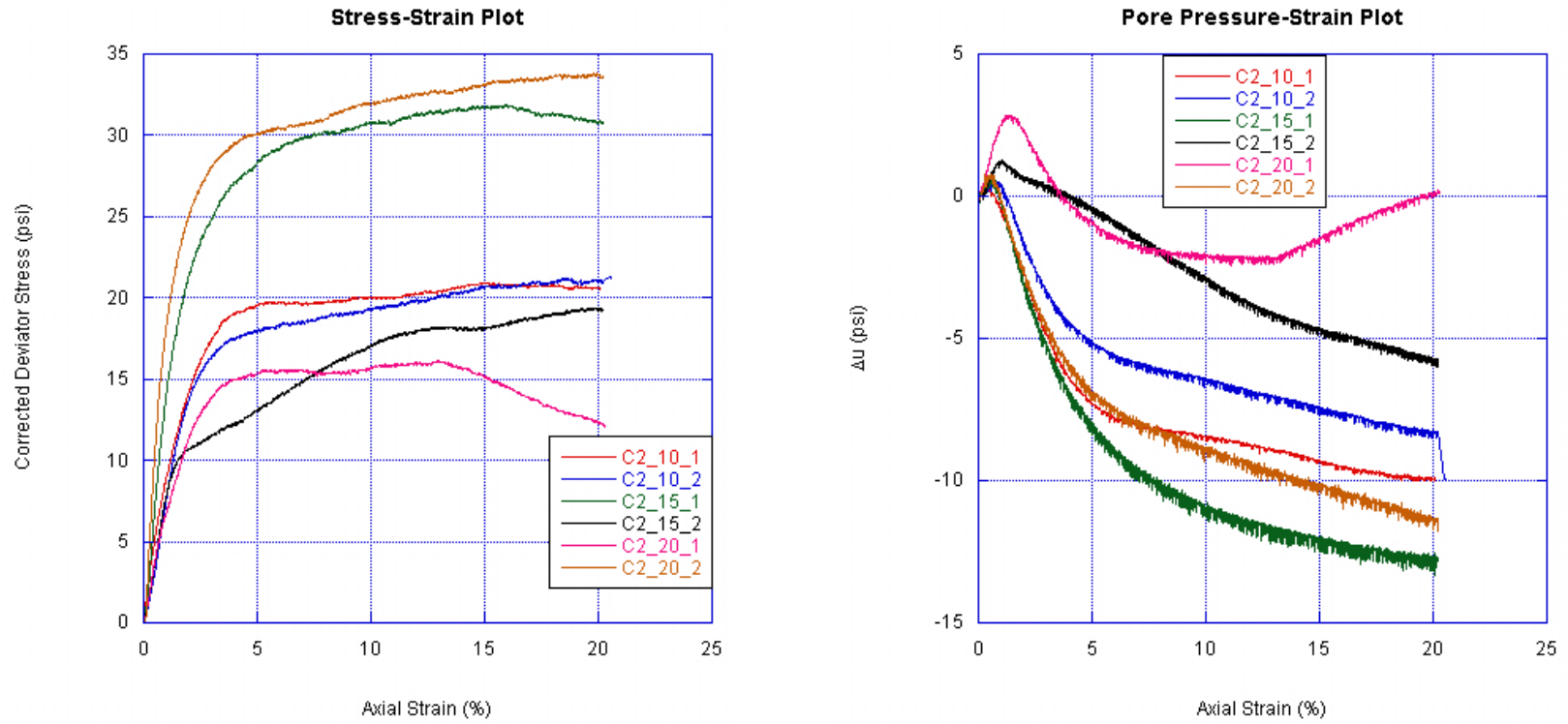
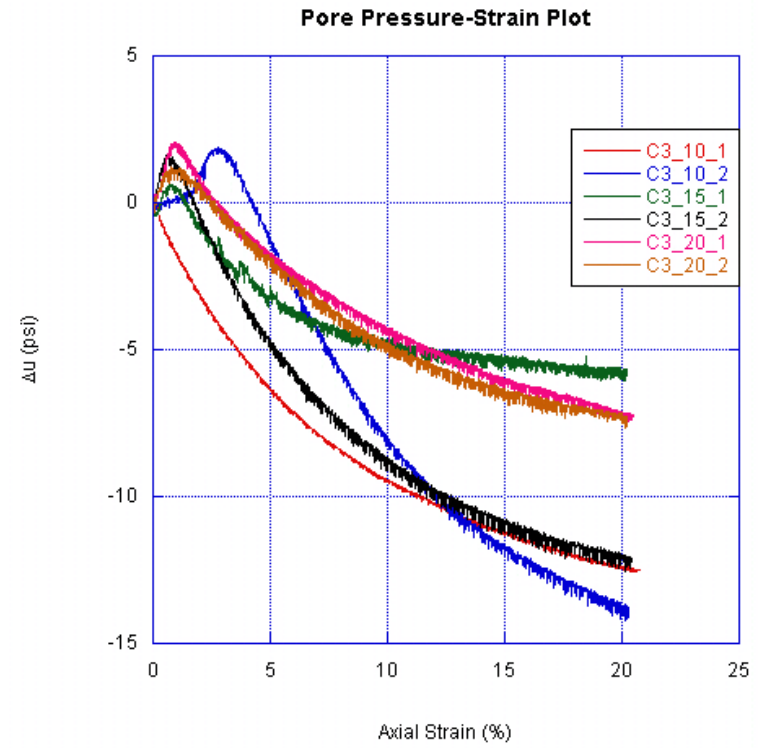
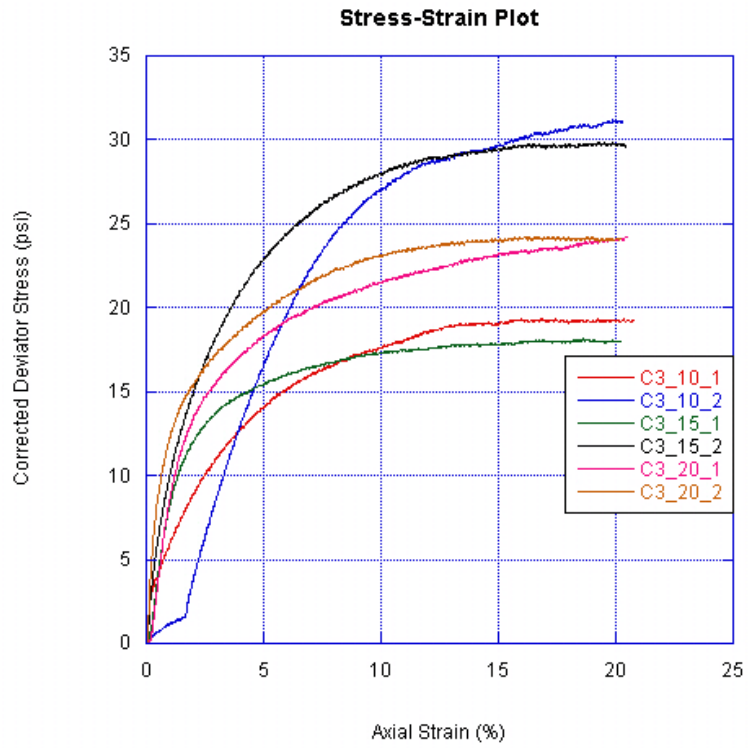


Figure B. 12. Gradation C2 Stress-Strain and Pore Pressure-Strain Curves.





**Figure B. 13. Gradation C3 Stress-Strain and Pore Pressure-Strain Curves.**

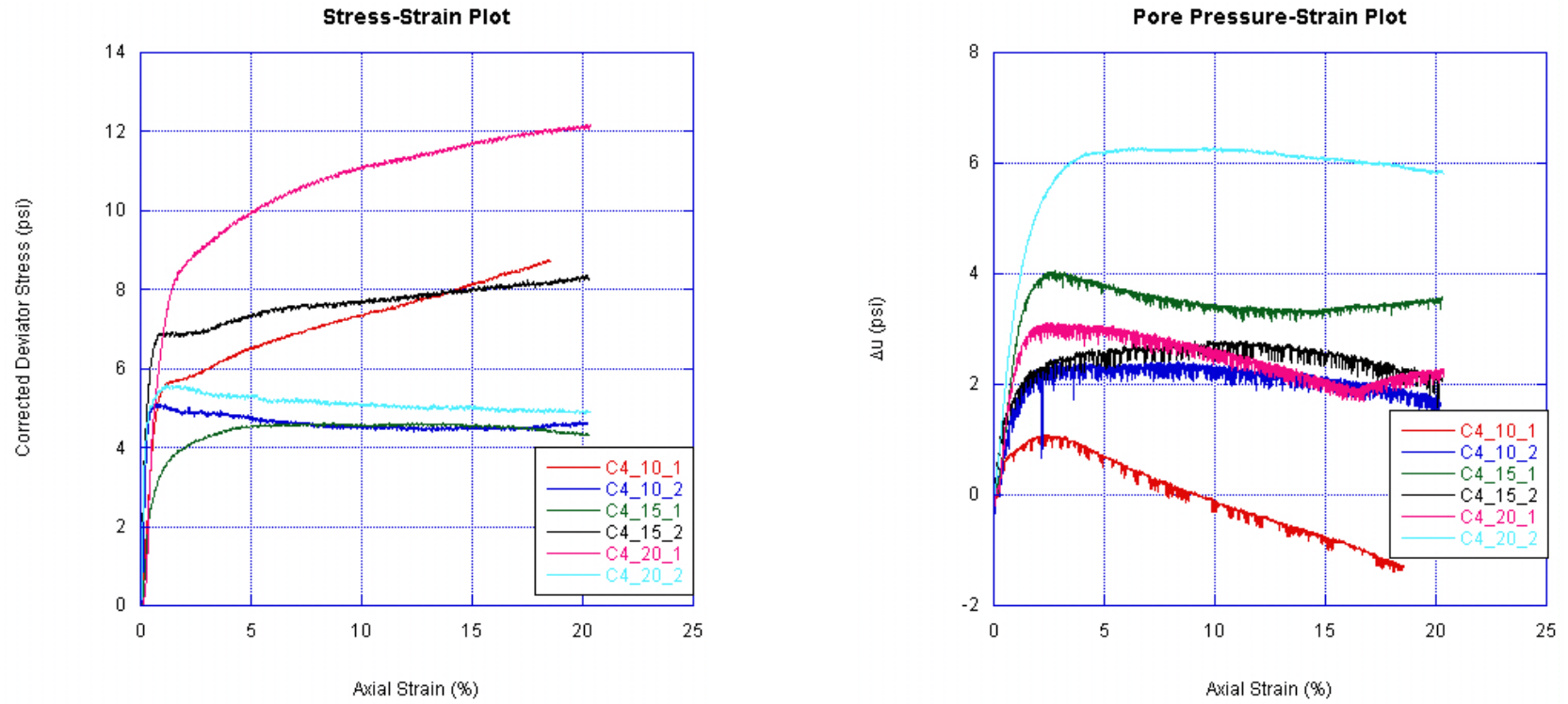


Figure B. 14. Gradation C4 Stress-Strain and Pore Pressure-Strain Curves.

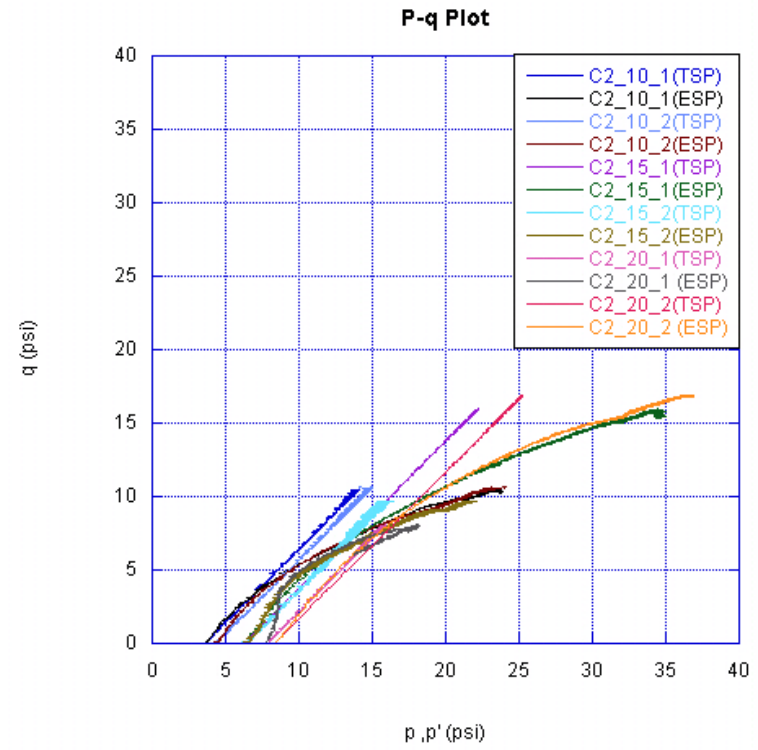
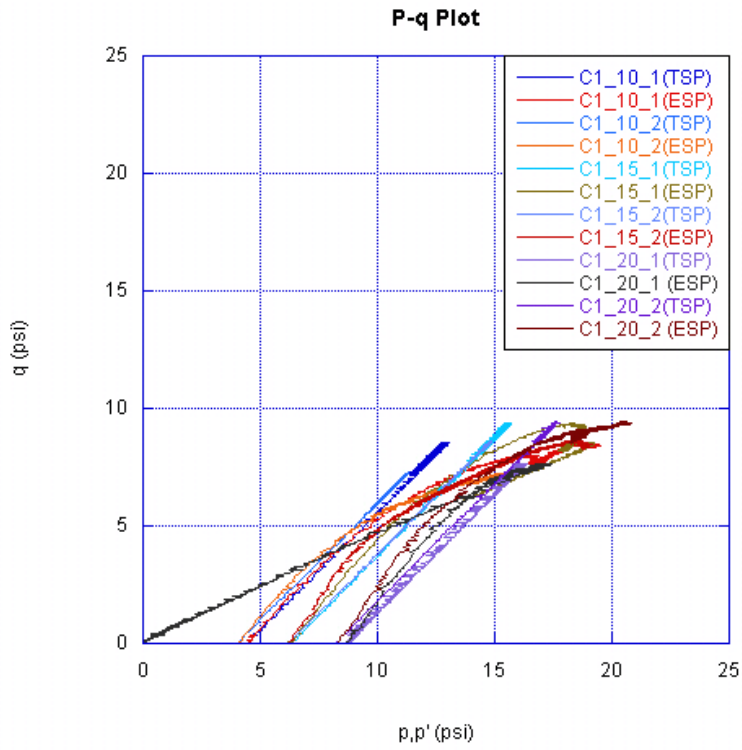


Figure B. 15. Type C-1 and C-2 p-q Plots.

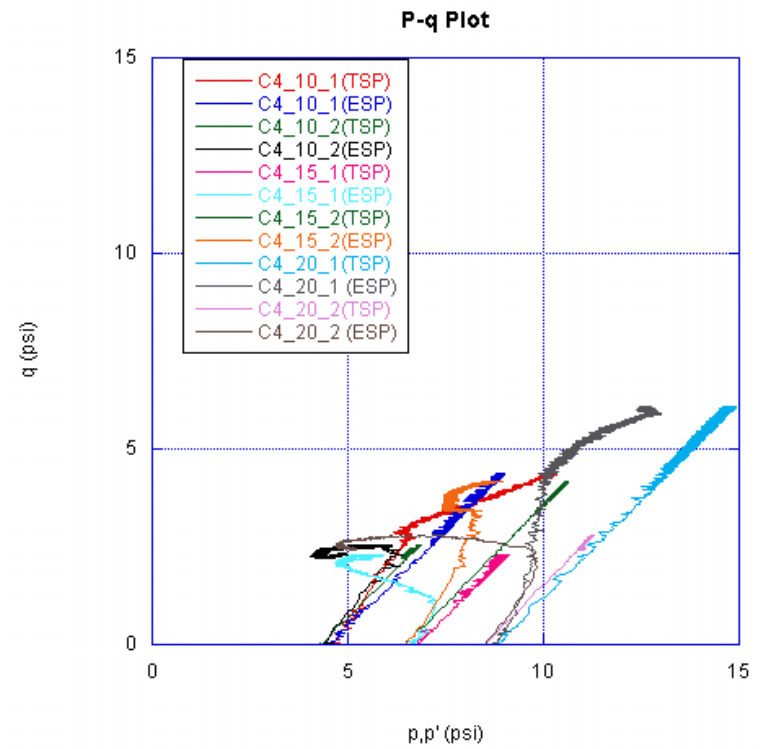
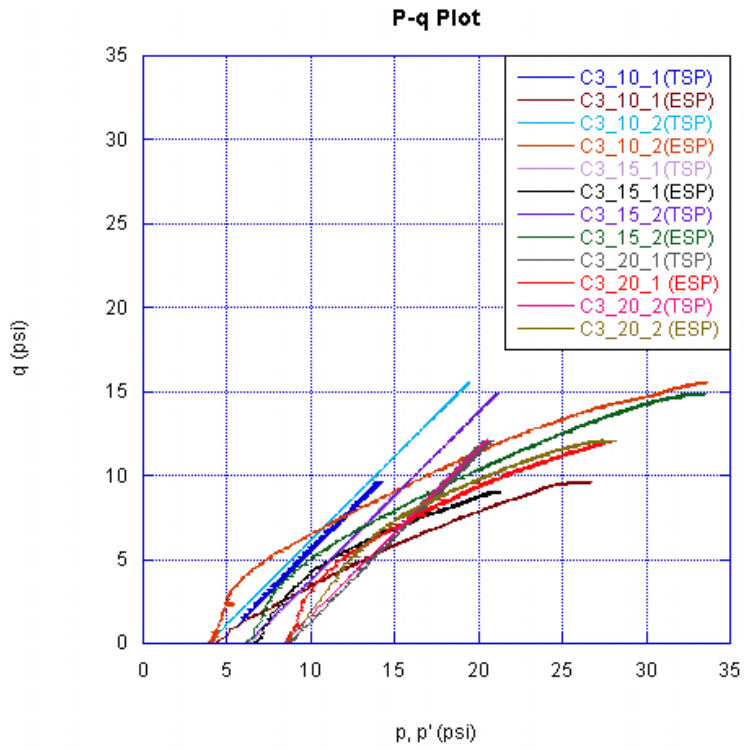


Figure B. 16. Type C-3 and C-4 p-q Plots.

**Table B. 6. Type D Test Results.**

| Test Name     | Date   | Gradation | Cell Pressure (psi) | Unit Weight of Sample Tested | Void Ratio | RC (%) | Friction Angle | Comments  |
|---------------|--------|-----------|---------------------|------------------------------|------------|--------|----------------|---|
| D1_10_1_52012 | 20-May | D1        | 4.3                 | -                            |            | -      | 46.9           |   |
| D1_10_2_53012 | 30-May | D1        | 4.3                 | 87.50                        | 0.93       | 94     | 47.2           |   |
| D1_15_1_52112 | 21-May | D1        | 6.5                 | -                            |            | -      | 42.3           |   |
| D1_15_2_61812 | 18-Jun | D1        | 6.5                 | 86.20                        | 0.95       | 92     | 45.2           |   |
| D1_20_1_52212 | 22-May | D1        | 8.7                 | -                            |            | -      | 41.6           |   |
| D1_20_2_61912 | 19-Jun | D1        | 8.7                 | 90.00                        | 0.87       | 96     | 45.0           | Leak. volume change=10%                                 |
| D2_10_1_71112 | 11-Jul | D2        | 4.3                 | 89.10                        | 0.89       | 86     | 47.0           |   |
| D2_10_2_71112 | 11-Jul | D2        | 4.3                 | 82.00                        | 1.05       | 79     | 39.6           | Inconsistent load curve trend, leak. volume change 9%   |
| D2_15_1_71212 | 12-Jul | D2        | 6.5                 | 88.50                        | 0.90       | 85     | 44.6           | Inconsistent load curve trend                           |
| D2_15_2_71212 | 12-Jul | D2        | 6.5                 | 84.80                        | 0.99       | 82     | 41.2           |   |
| D2_20_1_71312 | 13-Jul | D2        | 8.7                 | 82.90                        | 1.03       | 80     | 36.5           |   |
| D2_20_2_71312 | 13-Jul | D2        | 8.7                 | 85.68                        | 0.97       | 83     | 38.0           |   |
| D3_10_1_72312 | 23-Jul | D3        | 4.3                 | 101.80                       | 0.66       | 107    | 51.59          | Inconsistent load curve trend, possible material change |
| D3_10_2_72312 | 23-Jul | D3        | 4.3                 | 103.60                       | 0.63       | 109    | 50.95          | Inconsistent load curve trend, possible material change |
| D3_15_1_72412 | 24-Jul | D3        | 6.5                 | 95.00                        | 0.77       | 100    | 39.93          | Leak, volume change=16%                                 |
| D3_15_2_72412 | 24-Jul | D3        | 6.5                 | 88.00                        | 0.91       | 93     | 42.06          |   |
| D3_20_1_72512 | 25-Jul | D3        | 8.7                 | 90.11                        | 0.87       | 95     | 38.40          |   |
| D3_20_2_73112 | 31-Jul | D3        | 8.7                 | 88.33                        | 0.91       | 93     | 42.41          |   |
| D4_10_1_62512 | 25-Jun | D4        | 4.3                 | 90.00                        | 0.87       | 90     | 41.00          | Inconsistent volumetric behavior                        |
| D4_10_2_62612 | 26-Jun | D4        | 4.3                 | 89.60                        | 0.88       | 90     | 41.70          |   |
| D4_15_1_62712 | 27-Jun | D4        | 6.5                 | 93.00                        | 0.81       | 93     | 39.40          | Inconsistent load curve trend                           |
| D4_15_2_62912 | 29-Jun | D4        | 6.5                 | 79.40                        | 1.12       | 80     | 35.80          | Compliant load curve                                    |
| D4_20_1_62812 | 28-Jun | D4        | 8.7                 | 81.50                        | 1.07       | 82     | 36.10          |   |
| D4_20_2_62912 | 29-Jun | D4        | 8.7                 | 88.00                        | 0.91       | 88%    | 37.90          |   |

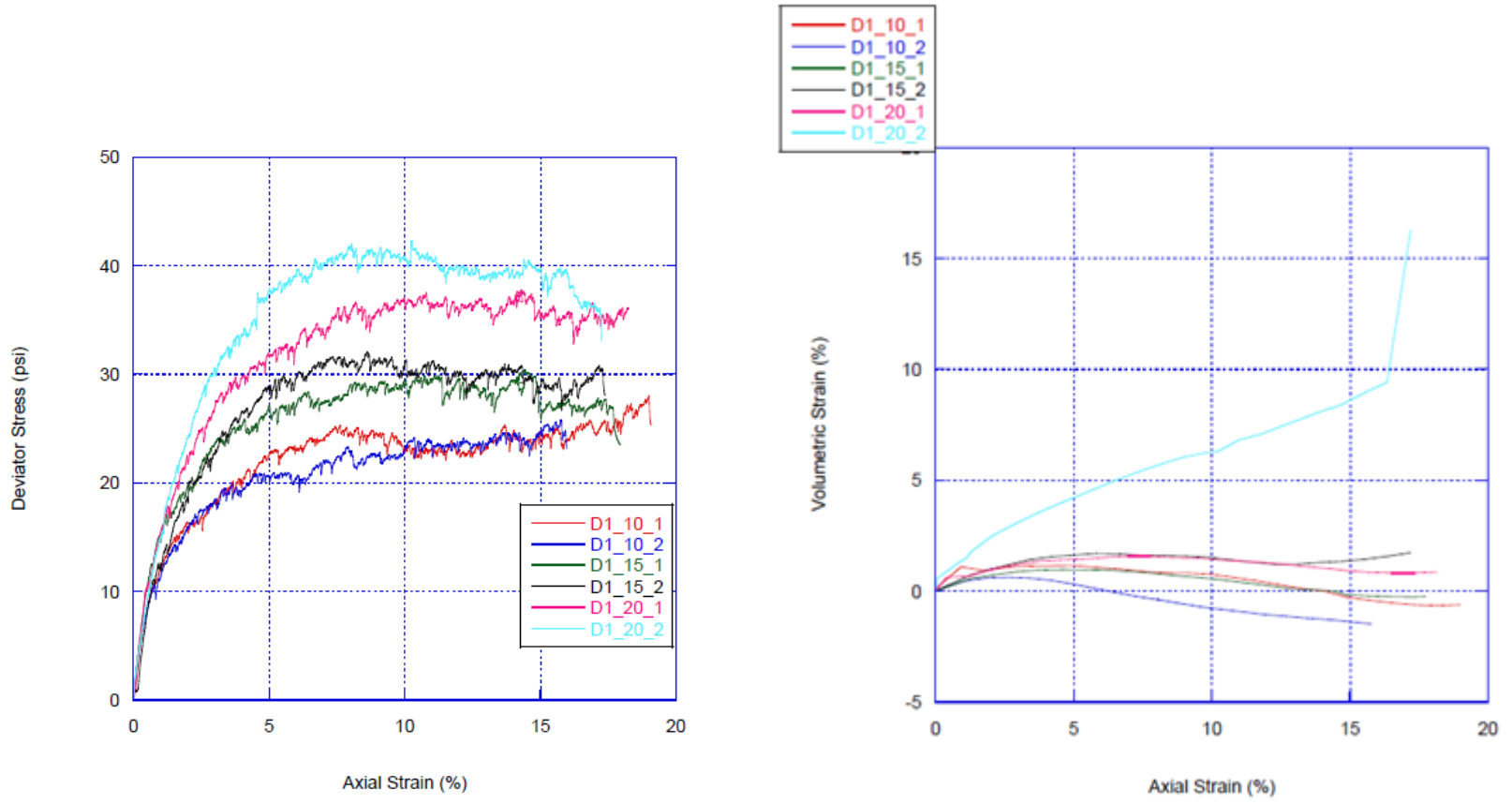
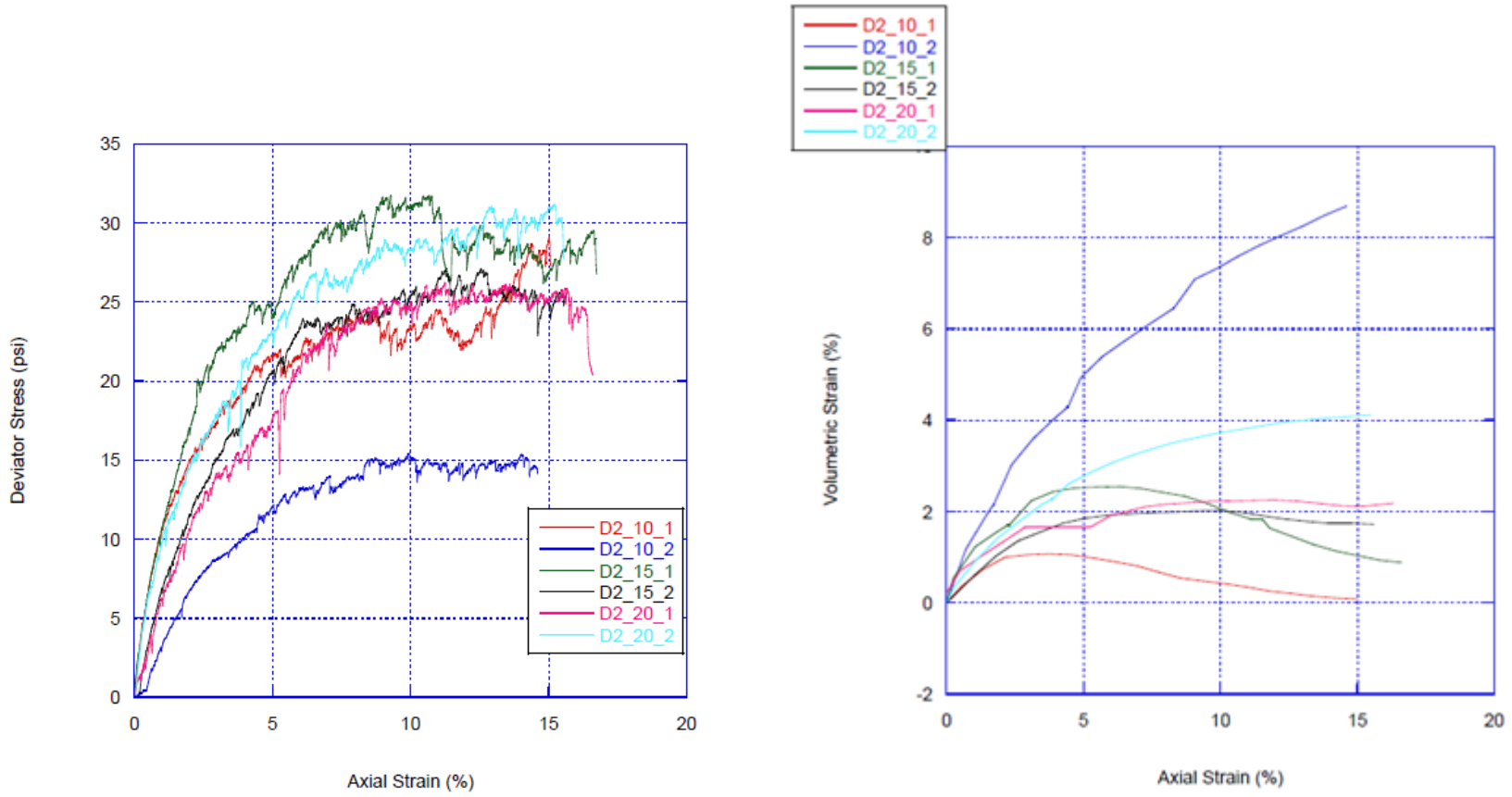


Figure B. 17. Gradation D1 Stress-Strain and Volumetric Strain Curves.



**Figure B. 18. Gradation D2 Stress-Strain and Volumetric Strain Curves.**

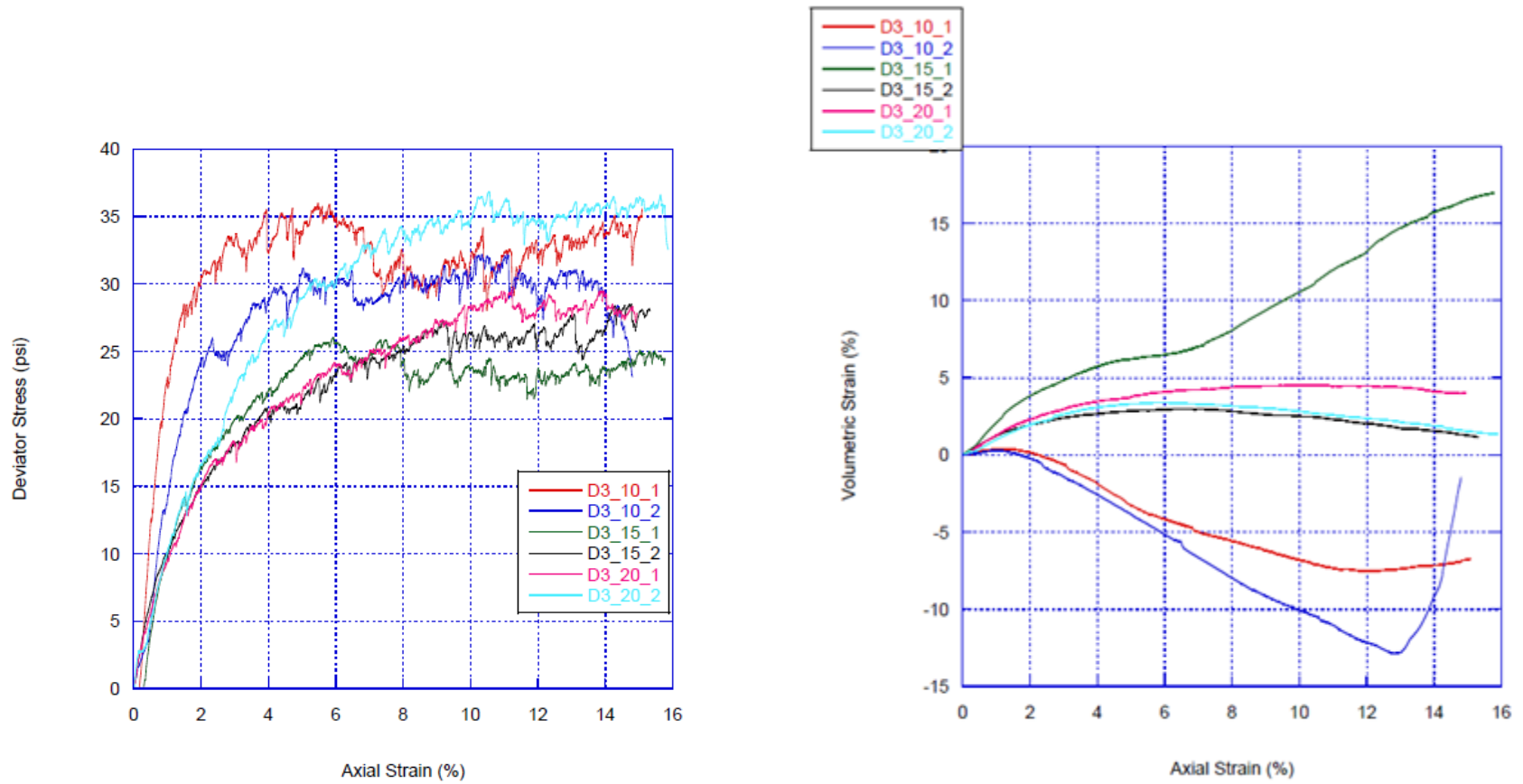


Figure B. 19. Gradation D3 Stress-Strain and Volumetric Strain Curves.



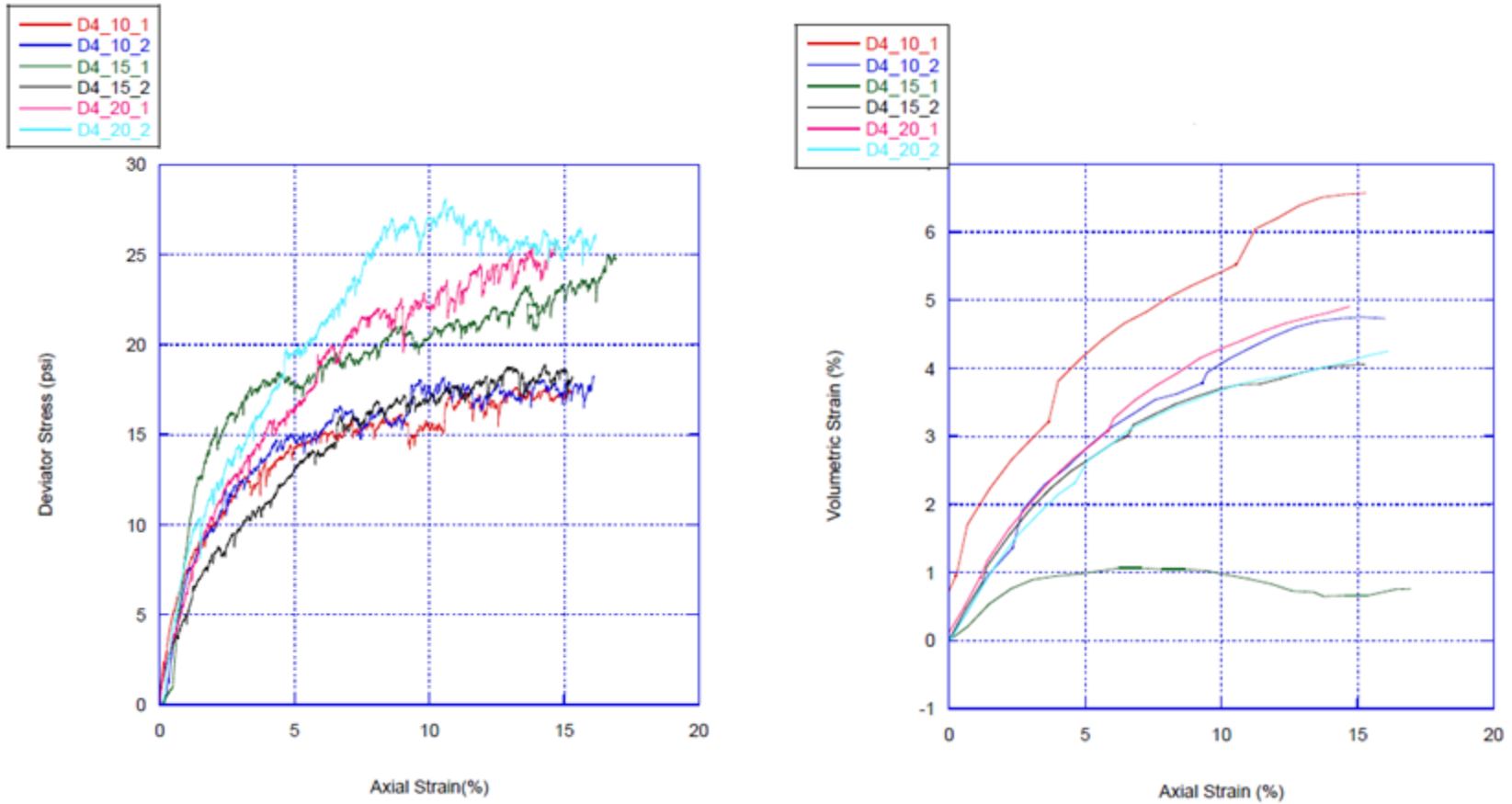


Figure B. 20. Gradation D4 Stress-Strain and Volumetric Strain Curves.

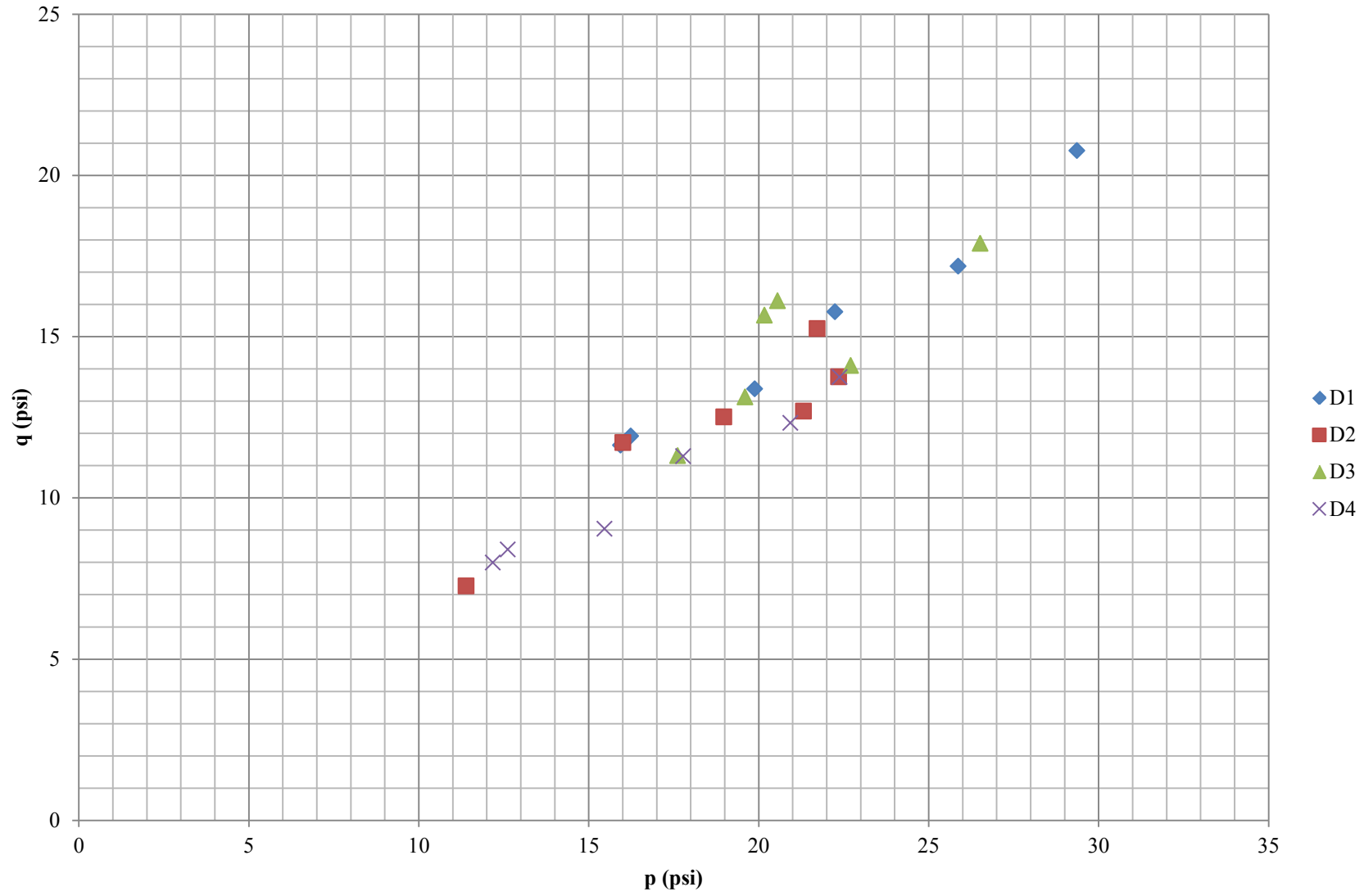
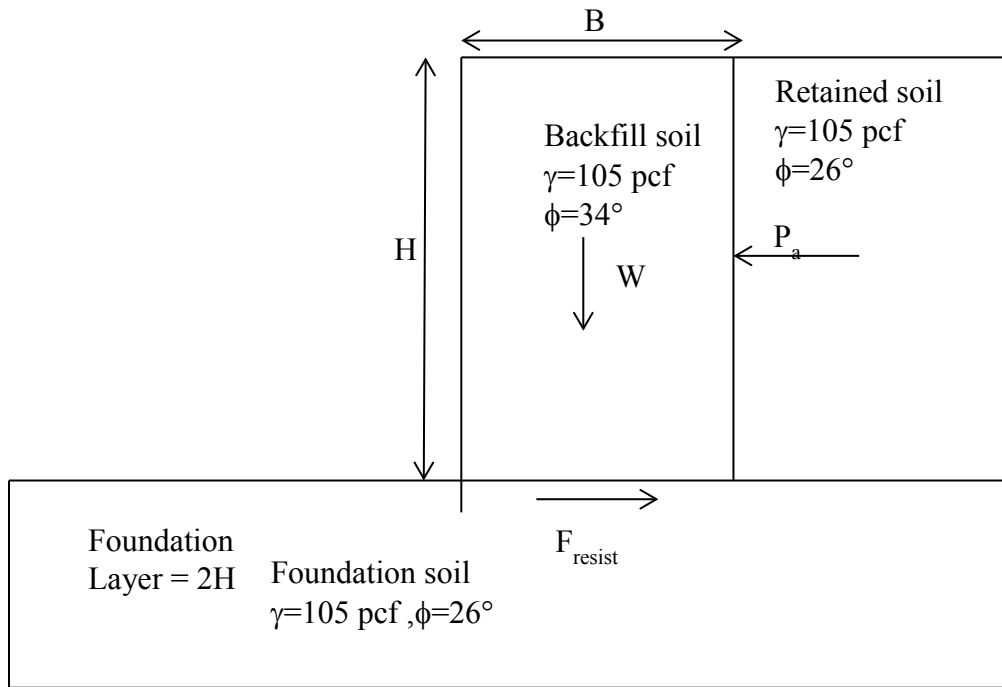
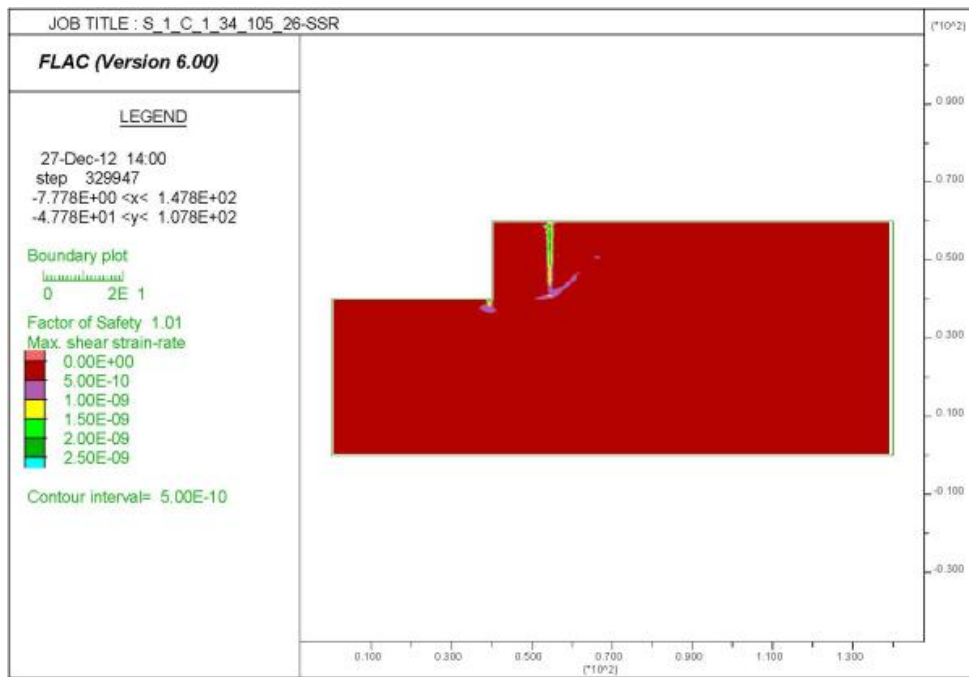


Figure B. 21. Type D Material p-q Diagram.

## APPENDIX C: RESULTS FROM FLAC SIMULATIONS



**Figure C. 1. Dimensions and Properties Used for Series 1 Case 1.**



**Figure C. 2. Series 1 Case 1 Foundation Angle  $\phi=26^\circ$ , Backfill Angle  $\phi=34^\circ$ , and  $\gamma=105 \text{ pcf}$  Maximum Shear Strain Rate.**

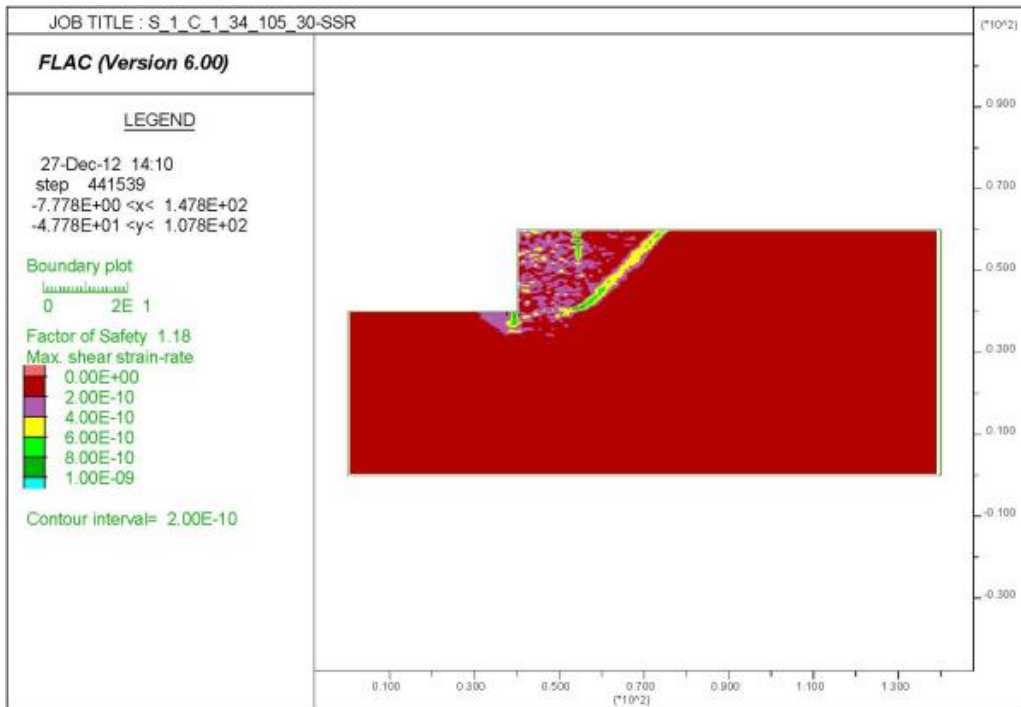


Figure C. 3. Series 1 Case 1 Foundation Angle  $\phi=30^\circ$ , Backfill Angle  $\phi=34^\circ$ , and  $\gamma=105$  pcf Maximum Shear Strain Rate.

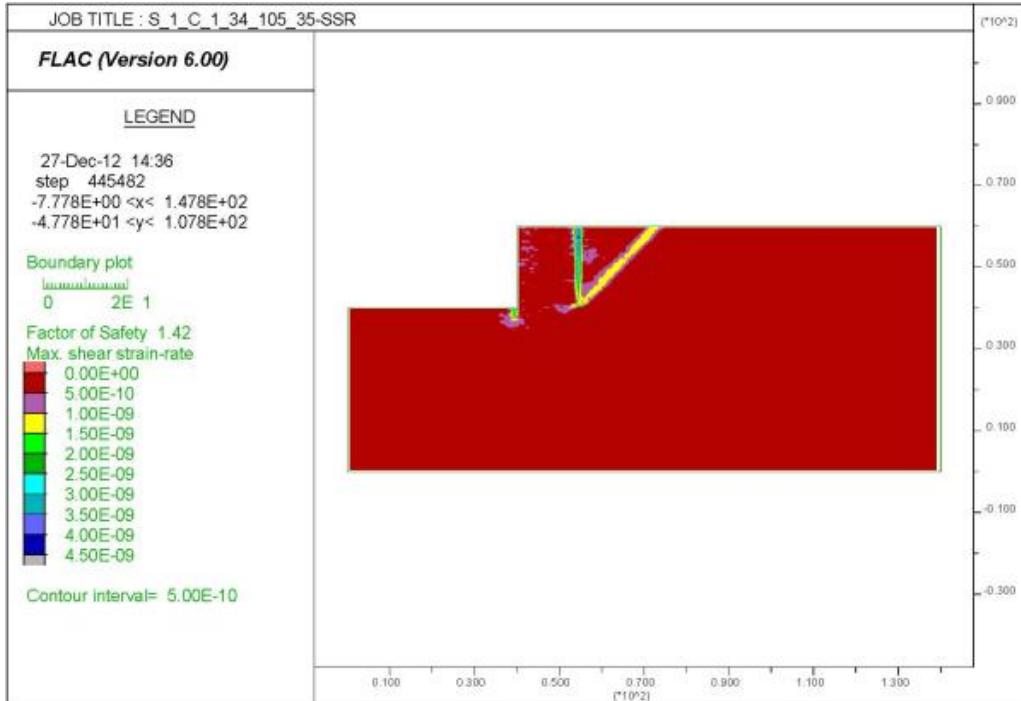


Figure C. 4. Series 1 Case 1 Foundation Angle  $\phi=35^\circ$ , Backfill Angle  $\phi=34^\circ$ , and  $\gamma=105$  pcf Maximum Shear Strain Rate.

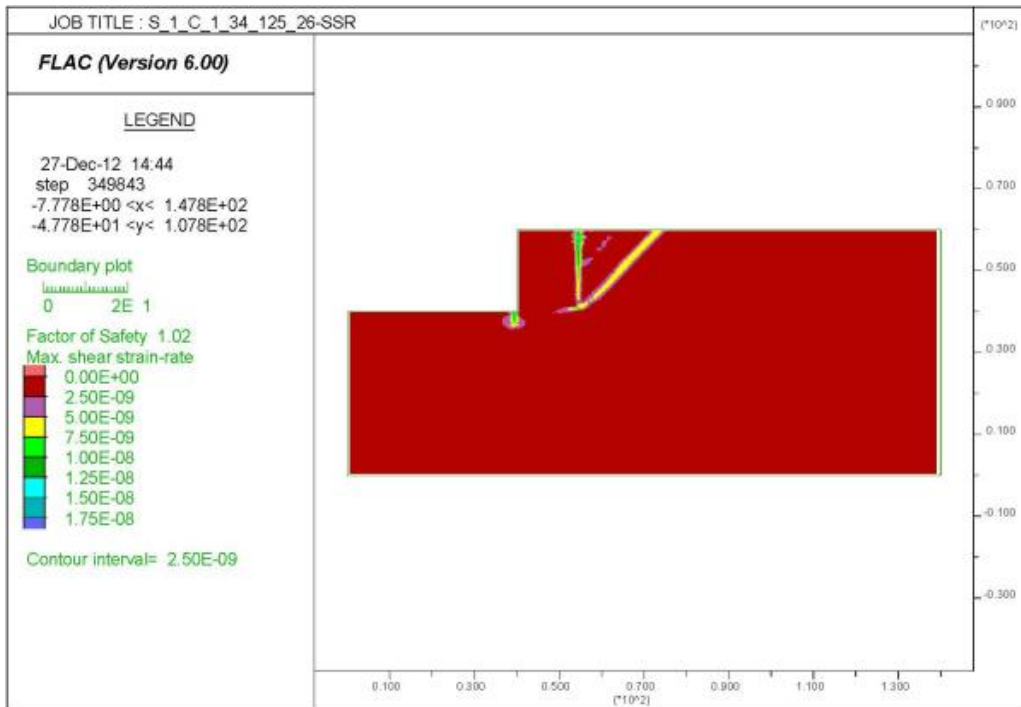


Figure C. 5. Series 1 Case 1 Foundation Angle  $\phi=26^\circ$ , Backfill Angle  $\phi=34^\circ$ , and  $\gamma=125$  pcf Maximum Shear Strain Rate.

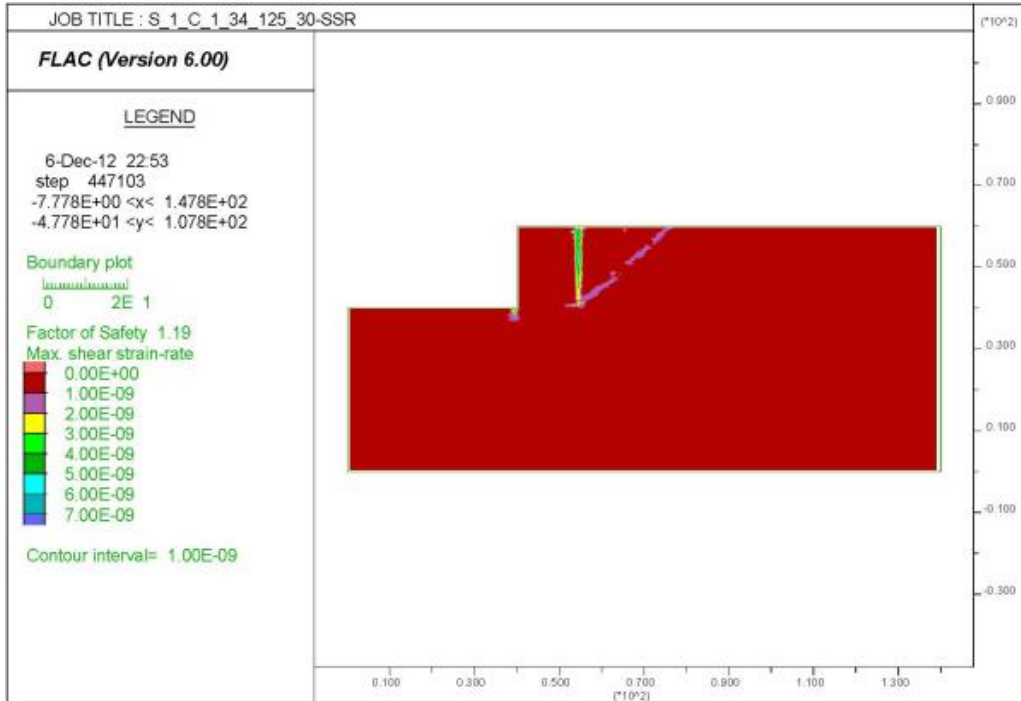
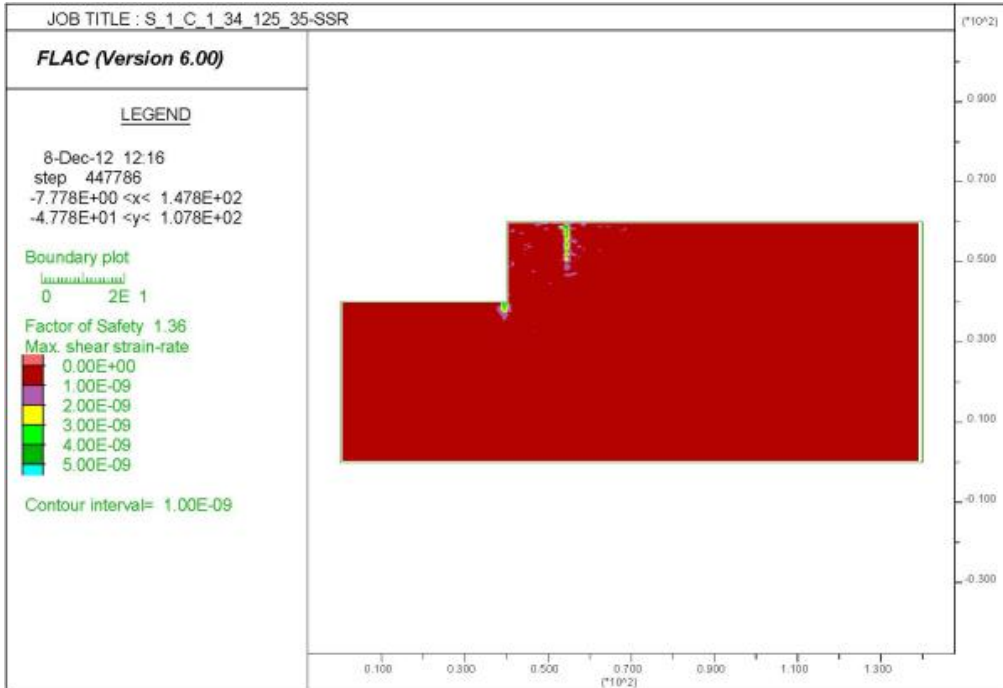
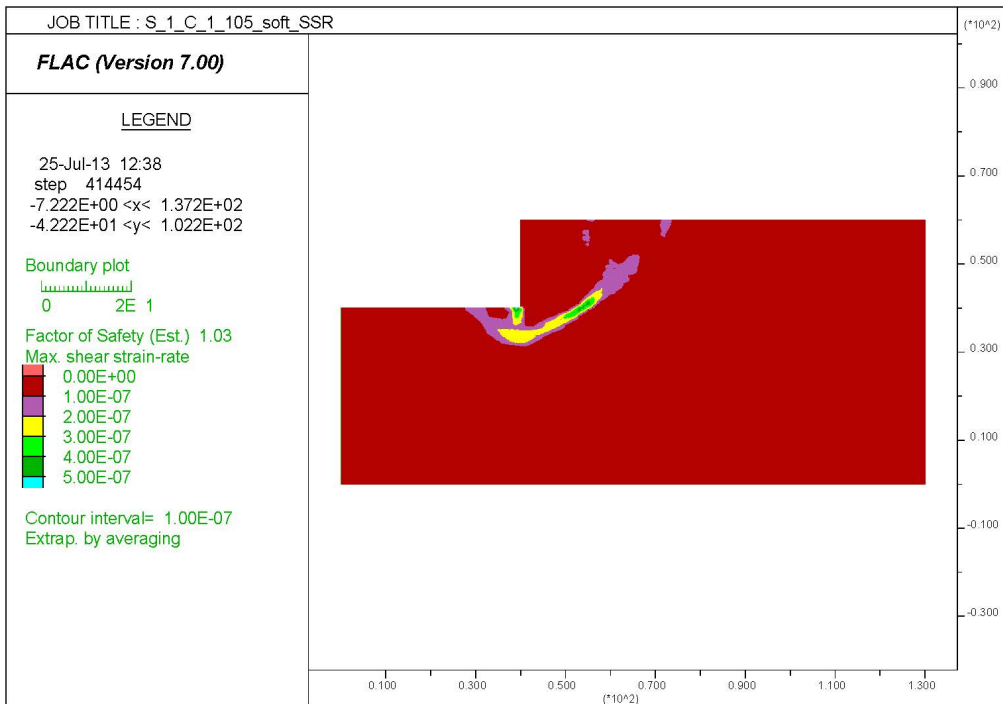


Figure C. 6. Series 1 Case 1 Foundation Angle  $\phi=30^\circ$ , Backfill Angle  $\phi=34^\circ$ , and  $\gamma=125$  pcf Maximum Shear Strain Rate.



**Figure C. 7. Series 1 Case 1 Foundation Angle  $\phi=35^\circ$ , Backfill Angle  $\phi=34^\circ$ , and  $\gamma=125$ pcf Maximum Shear Strain Rate.**



**Figure C. 8. Series 1 Case 1 Foundation  $c_u=500$  pcf, Backfill Angle  $\phi=34^\circ$ , and  $\gamma=105$ pcf Maximum Shear Strain Rate.**

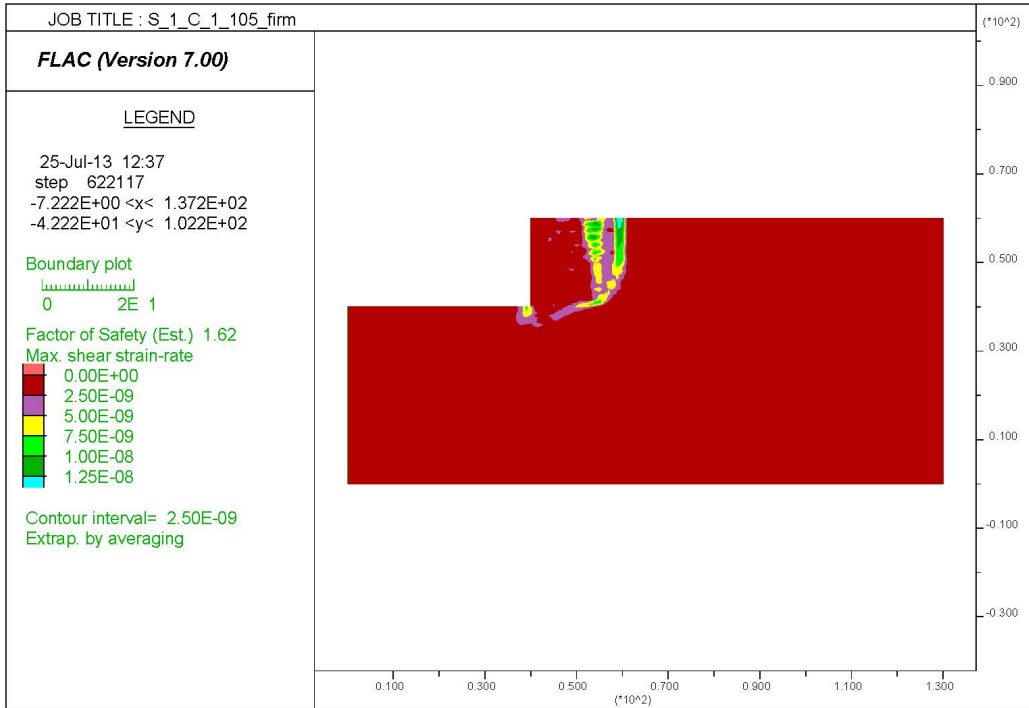


**Figure C. 9. Series 1 Case 1 Foundation  $c_u=1000$  psf, Backfill Angle  $\phi=34^\circ$ , and  $\gamma=105$  pcf Maximum Shear Strain Rate.**

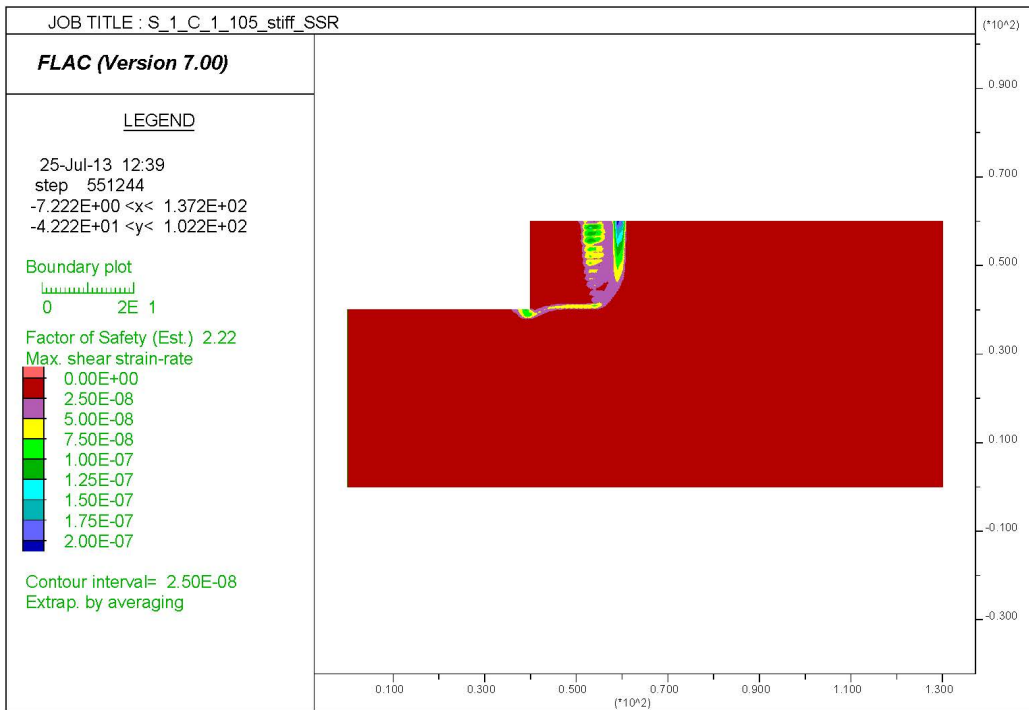


**Figure C. 10. Series 1 Case 1 Foundation  $c_u=2000$  psf, Backfill Angle  $\phi=34^\circ$ , and  $\gamma=105$  pcf Maximum Shear Strain Rate.**

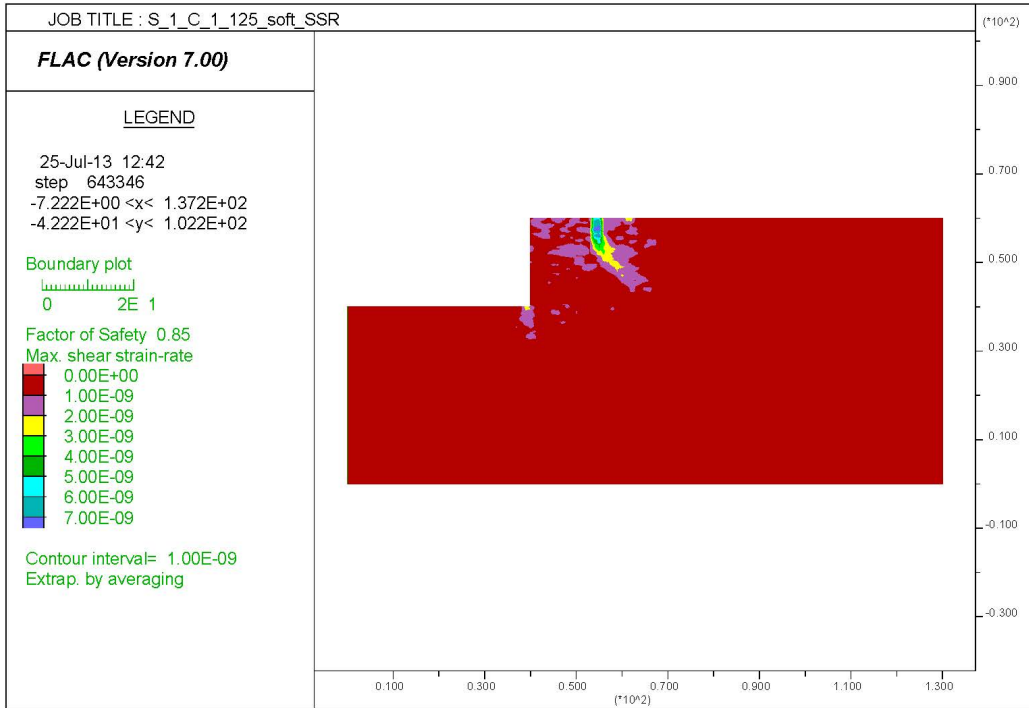


**Figure C. 11. Series 1 Case 1 Foundation  $c_u=500$  psf, Backfill Angle  $\phi=34^\circ$ , and  $\gamma=125$  pcf Maximum Shear Strain Rate.**

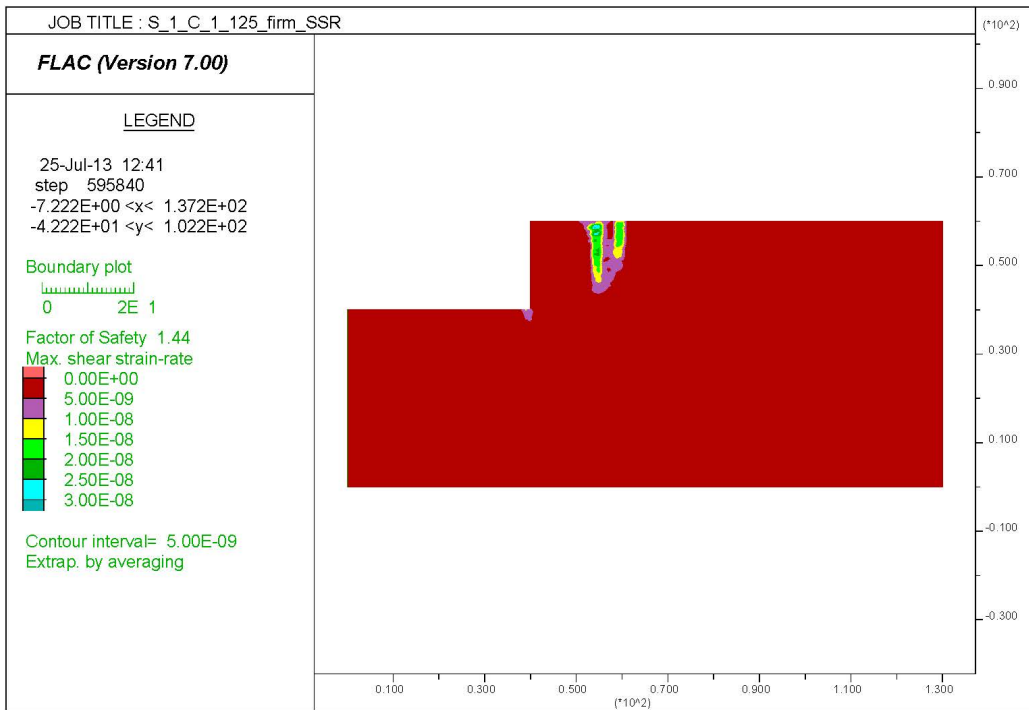


**Figure C. 12. Series 1 Case 1 Foundation  $c_u=1000$  psf, Backfill Angle  $\phi=34^\circ$ , and  $\gamma=125$  pcf Maximum Shear Strain Rate.**



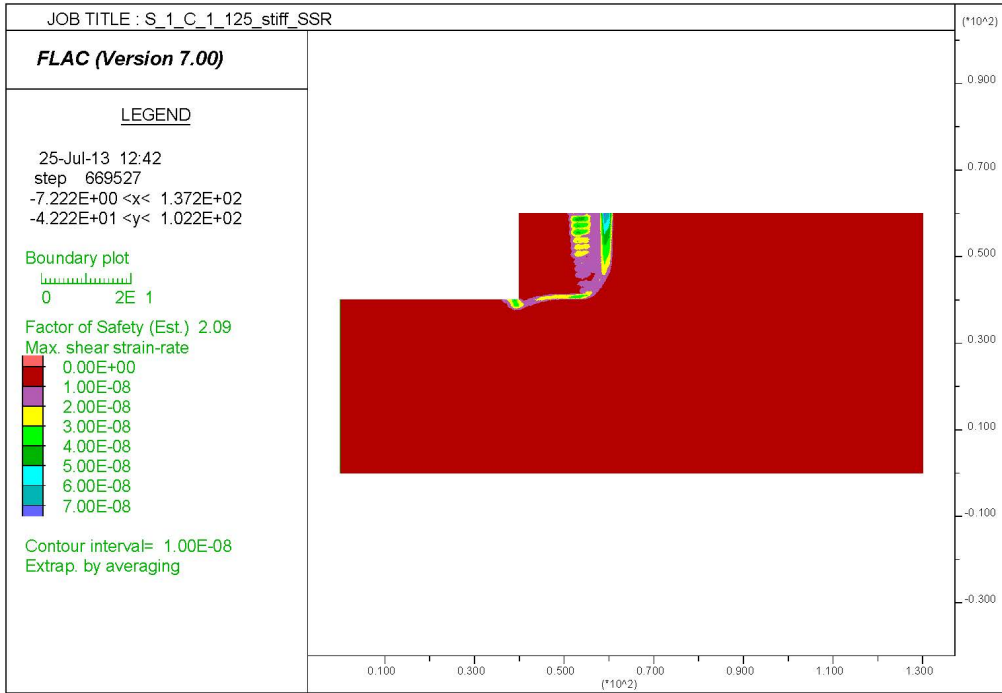


Figure C. 13. Series 1 Case 1 Foundation  $c_u=2000$  psf, Backfill Angle  $\phi=34^\circ$ , and  $\gamma=125$  pcf Maximum Shear Strain Rate.

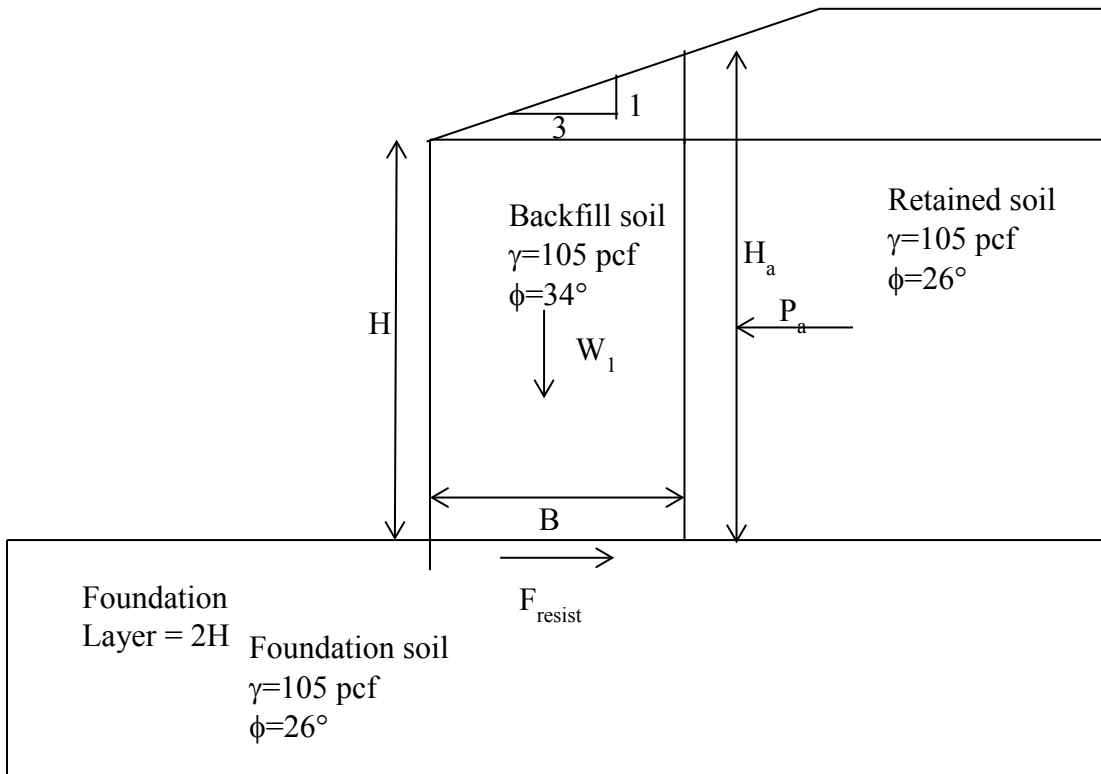


Figure C. 14. Dimensions and Properties Used for Series 1 Case 2.

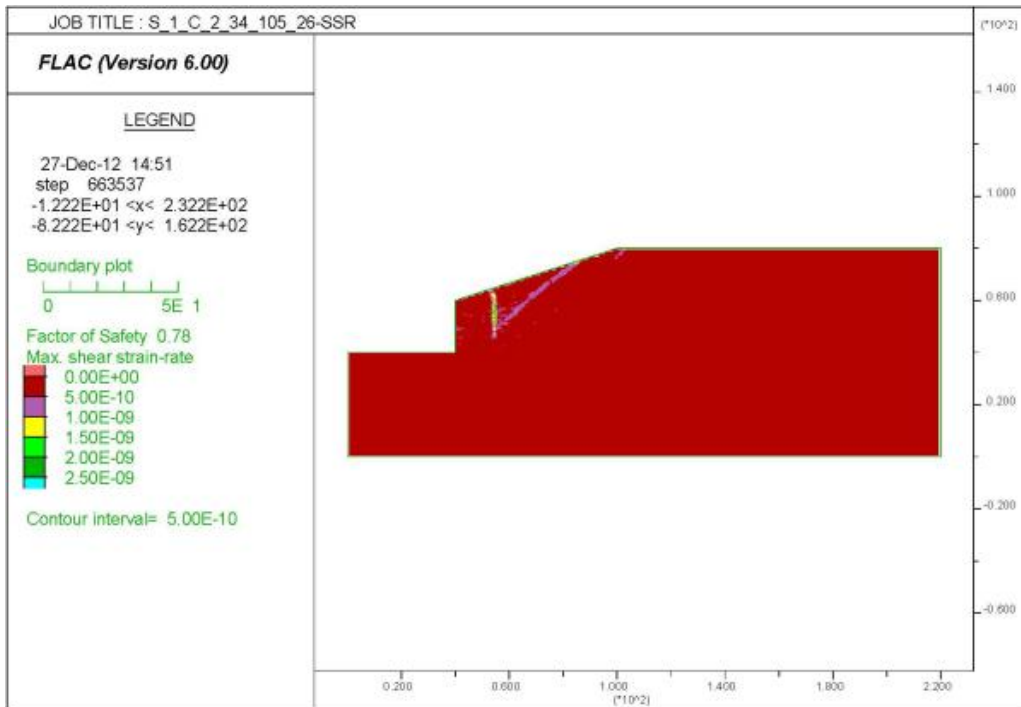


Figure C. 15. Series 1 Case 2 Foundation Angle  $\phi=26^\circ$ , Backfill Angle  $\phi=34^\circ$ , and  $\gamma=105$  pcf Maximum Shear Strain Rate.

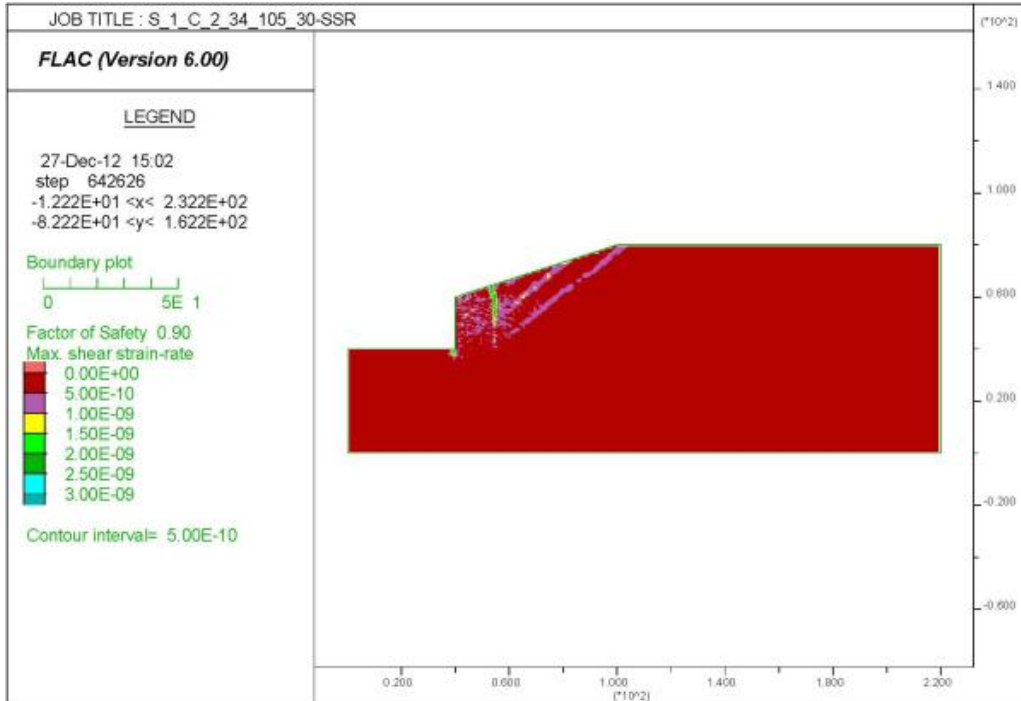


Figure C. 16. Series 1 Case 2 Foundation Angle  $\phi=30^\circ$ , Backfill Angle  $\phi=34^\circ$ , and  $\gamma=105$  pcf Maximum Shear Strain Rate.

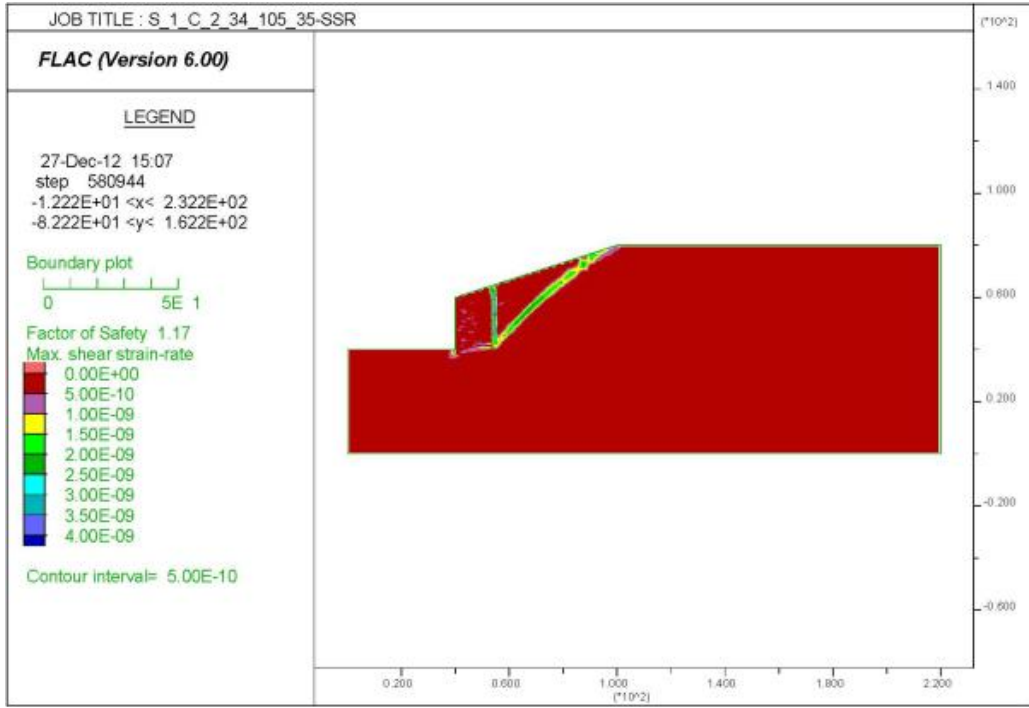


Figure C. 17. Series 1 Case 2 Foundation Angle  $\phi=35^\circ$ , Backfill Angle  $\phi=34^\circ$ , and  $\gamma=105$  pcf Maximum Shear Strain Rate.

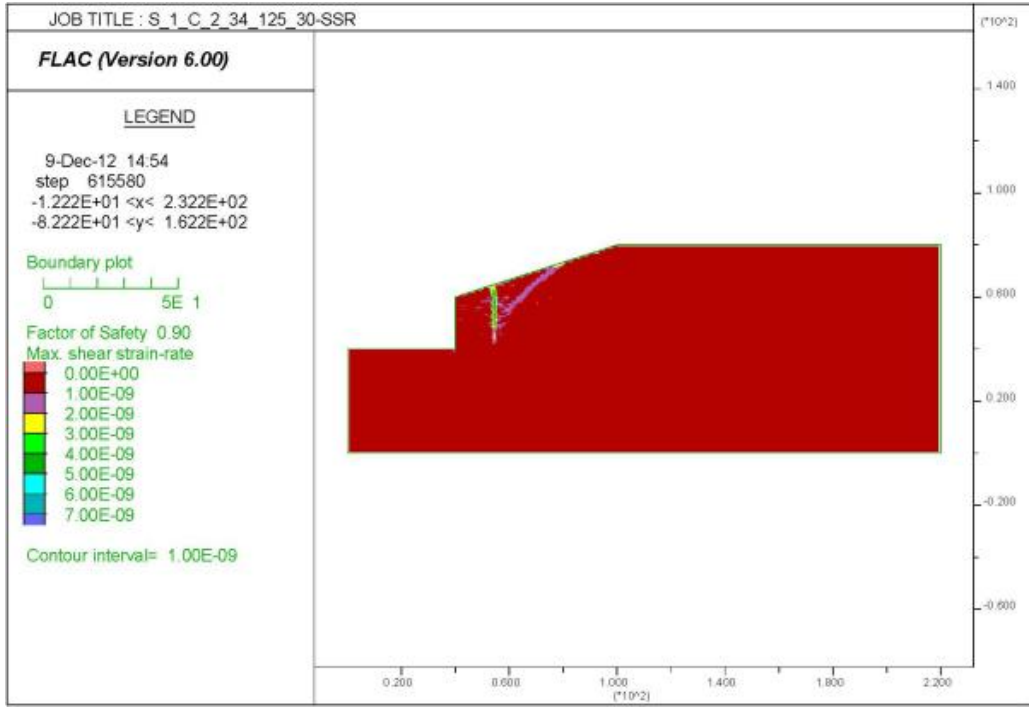


Figure C. 18. Series 1 Case 2 Foundation Angle  $\phi=26^\circ$ , Backfill Angle  $\phi=34^\circ$ , and  $\gamma=125$  pcf Maximum Shear Strain Rate.

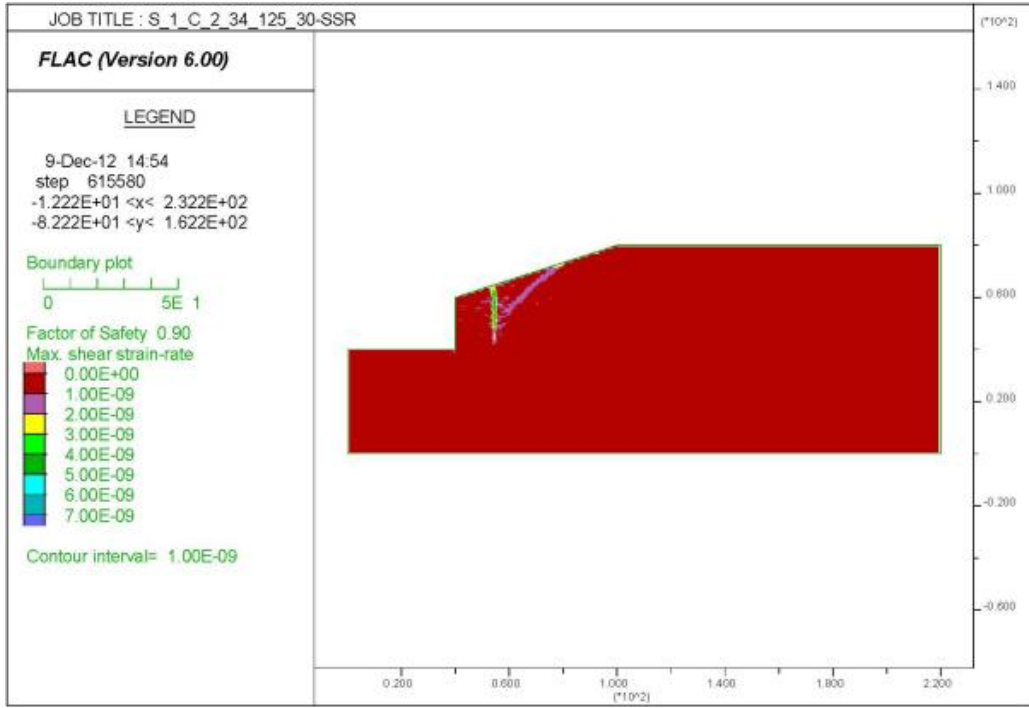


Figure C. 19. Series 1 Case 2 Foundation Angle  $\phi=30^\circ$ , Backfill Angle  $\phi=34^\circ$ , and  $\gamma=125$  pcf Maximum Shear Strain Rate.

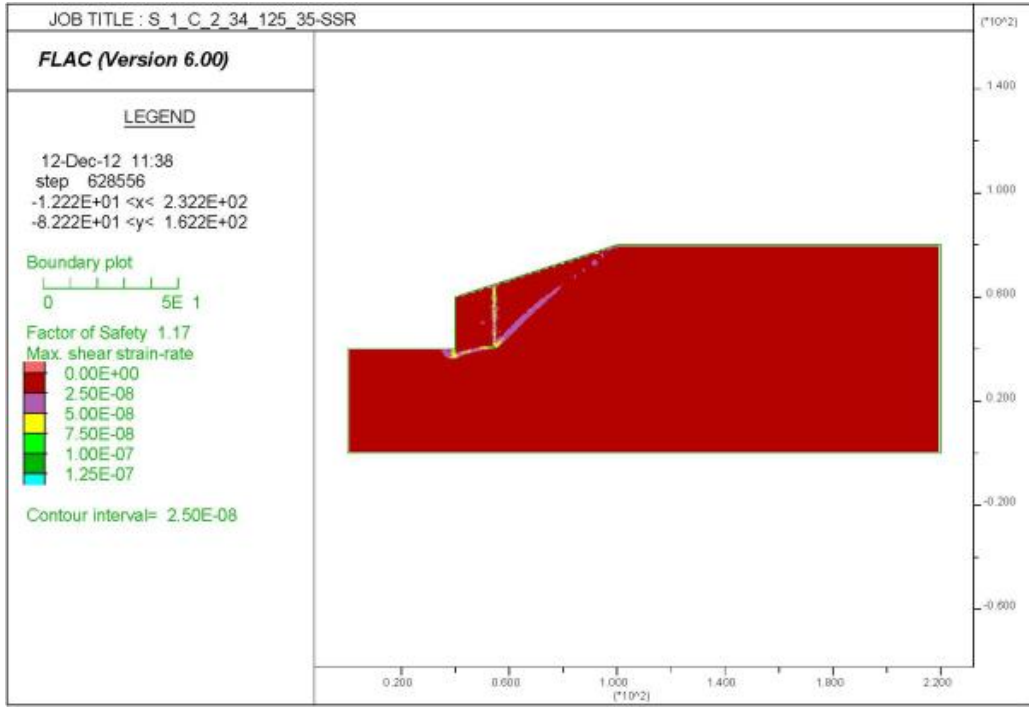
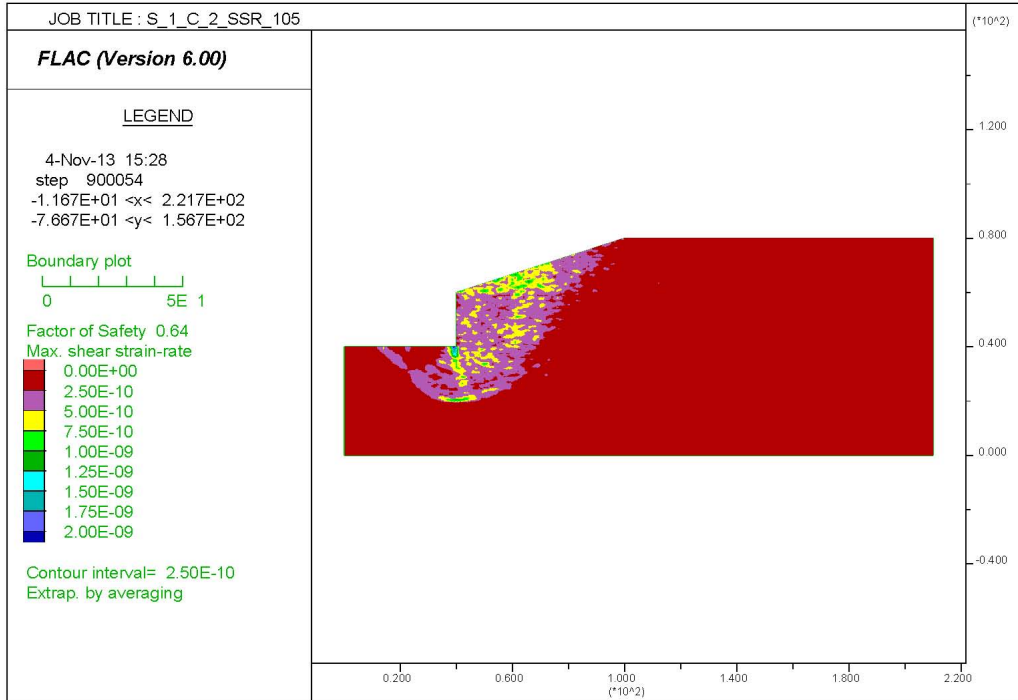
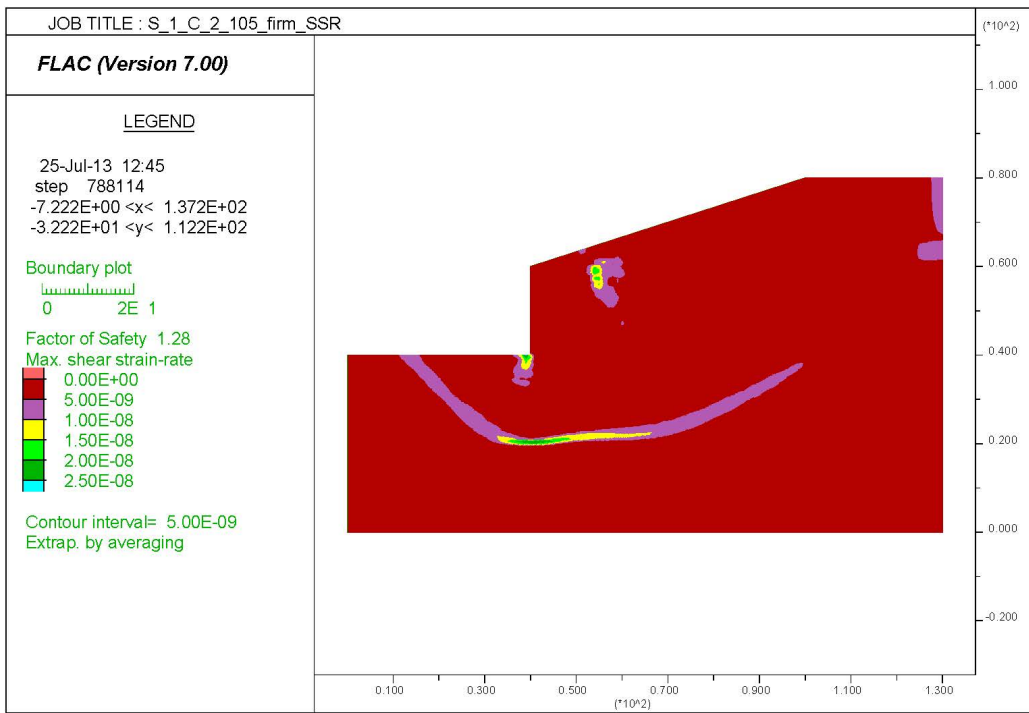


Figure C. 20. Series 1 Case 2 Foundation Angle  $\phi=35^\circ$ , Backfill Angle  $\phi=34^\circ$ , and  $\gamma=125$  pcf Maximum Shear Strain Rate.



**Figure C. 21. Series 1 Case 2 Foundation  $c_u=500$  psf, Backfill Angle  $\phi=34^\circ$ , and  $\gamma=105$  pcf Maximum Shear Strain Rate.**



**Figure C. 22. Series 1 Case 2 Foundation  $c_u=1000$  psf, Backfill Angle  $\phi=34^\circ$ , and  $\gamma=105$  pcf Maximum Shear Strain Rate.**

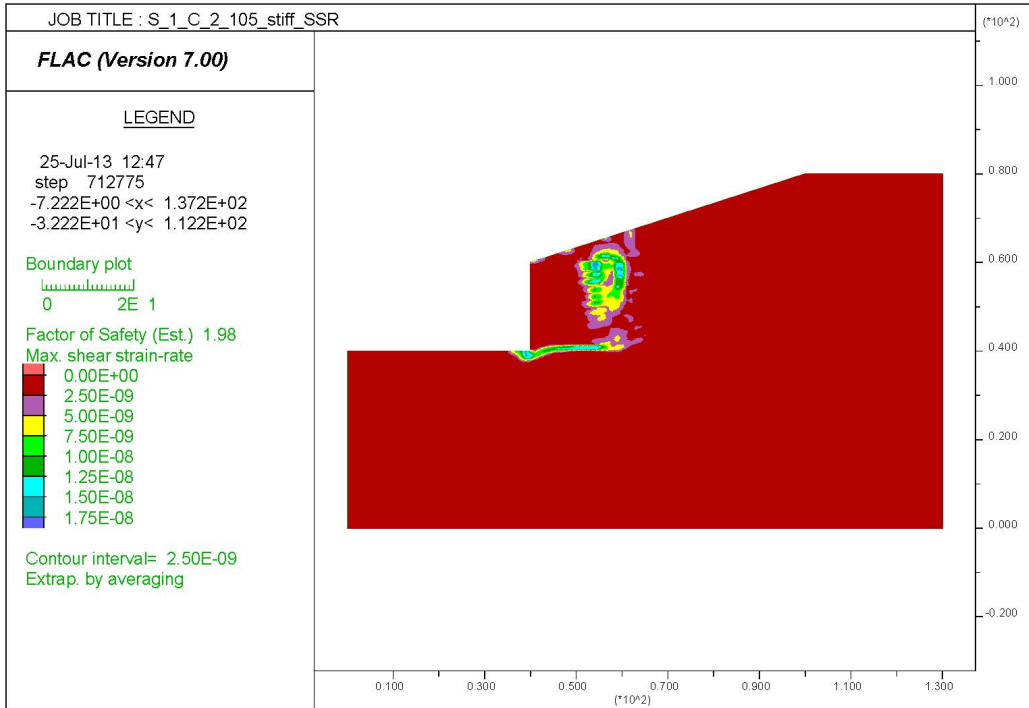


**Figure C. 23. Series 1 Case 2 Foundation  $c_u=2000$  psf, Backfill Angle  $\phi=34^\circ$ , and  $\gamma=105$  pcf Maximum Shear Strain Rate.**

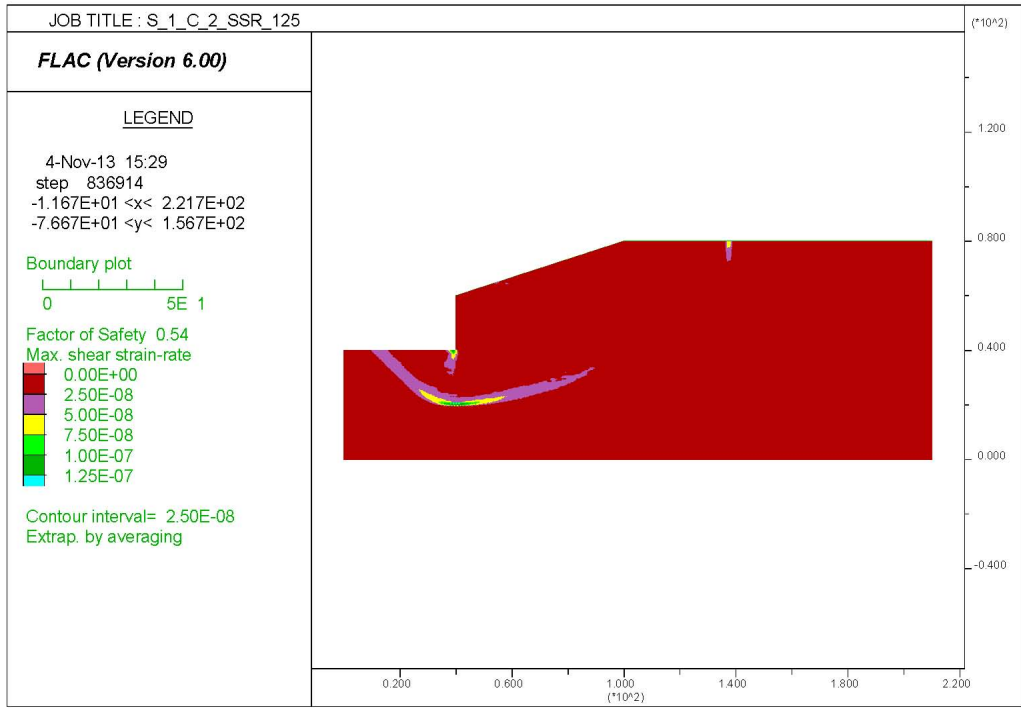


**Figure C. 24. Series 1 Case 2 Foundation  $c_u=500$  psf, Backfill Angle  $\phi=34^\circ$ , and  $\gamma=125$  pcf Maximum Shear Strain Rate.**

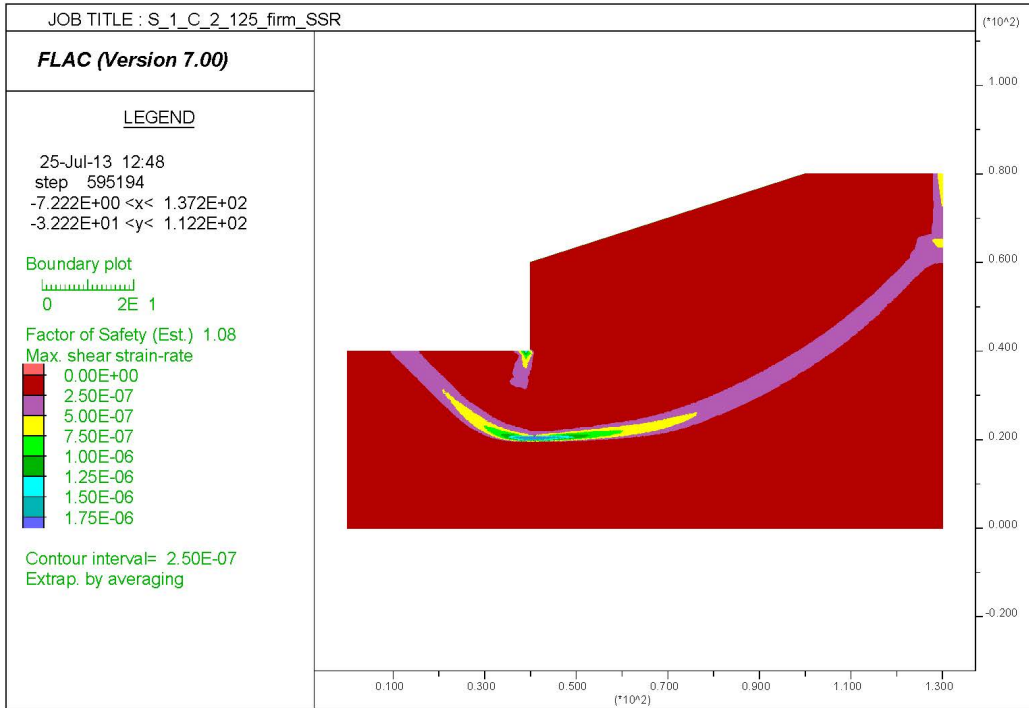


**Figure C. 25. Series 1 Case 2 Foundation  $c_u=1000$  psf, Backfill Angle  $\phi=34^\circ$ , and  $\gamma=125$  pcf Maximum Shear Strain Rate.**

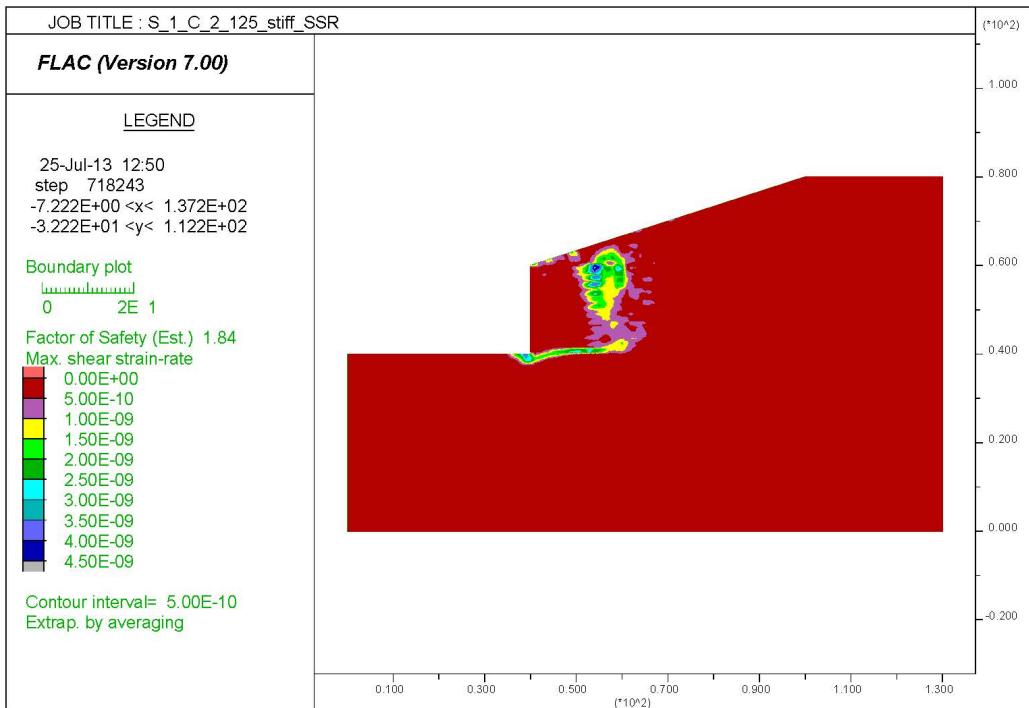


**Figure C. 26. Series 1 Case 2 Foundation  $c_u=2000$  psf, Backfill Angle  $\phi=34^\circ$ , and  $\gamma=125$  pcf Maximum Shear Strain Rate.**

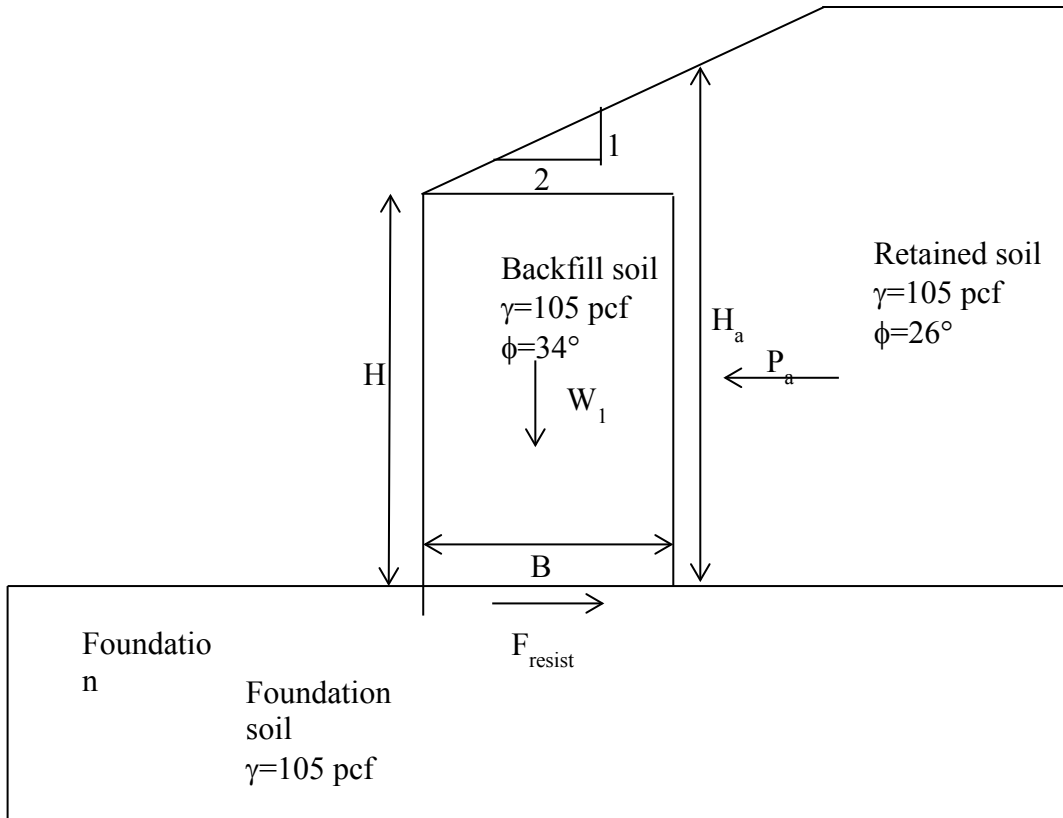


Figure C. 27. Dimensions and Properties Used for Series 1 Case 3.

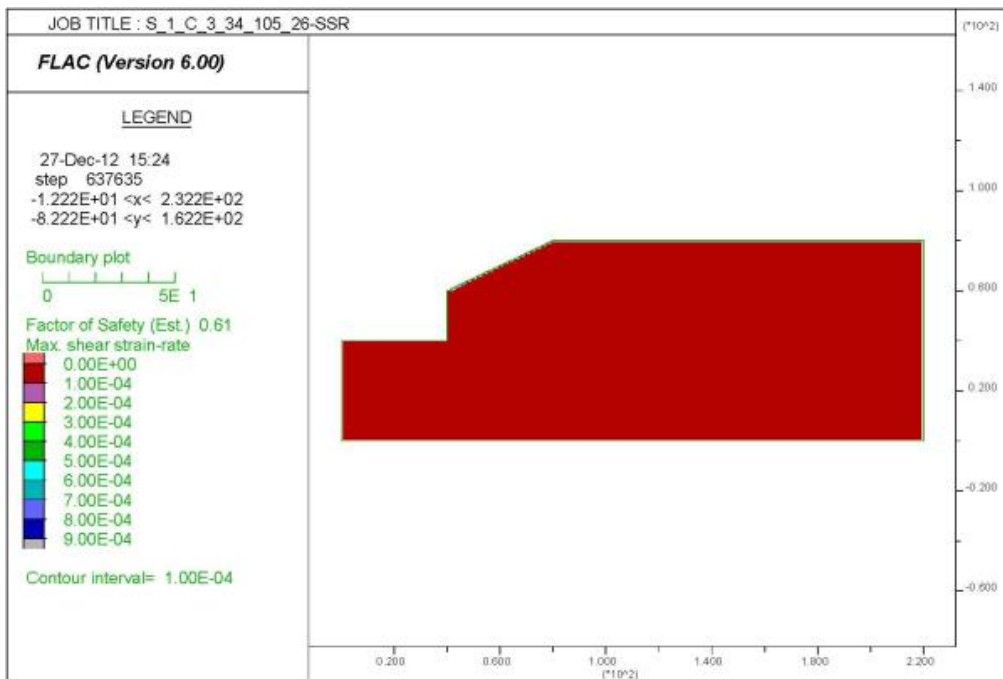


Figure C. 28. Series 1 Case 3 Foundation Angle  $\phi=26^\circ$ , Backfill Angle  $\phi=34^\circ$ , and  $\gamma=105$  pcf Maximum Shear Strain Rate.





Figure C. 29. Series 1 Case 3 Foundation Angle  $\phi=30^\circ$ , Backfill Angle  $\phi=34^\circ$ , and  $\gamma=105$  pcf Maximum Shear Strain Rate.

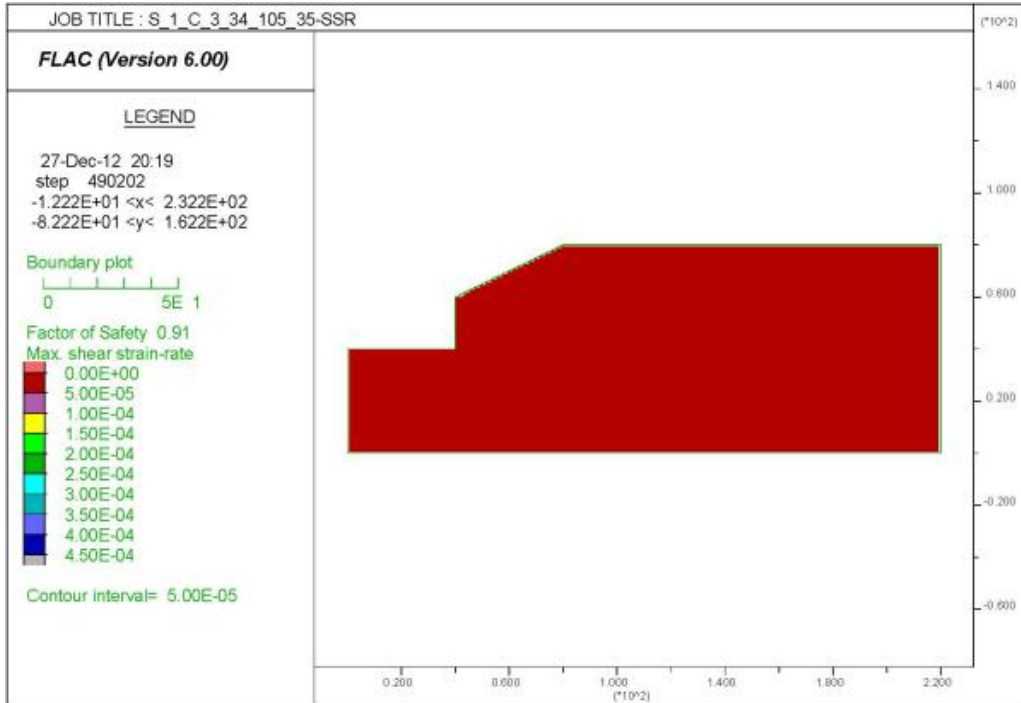


Figure C. 30. Series 1 Case 3 Foundation Angle  $\phi=35^\circ$ , Backfill Angle  $\phi=34^\circ$ , and  $\gamma=105$  pcf Maximum Shear Strain Rate.

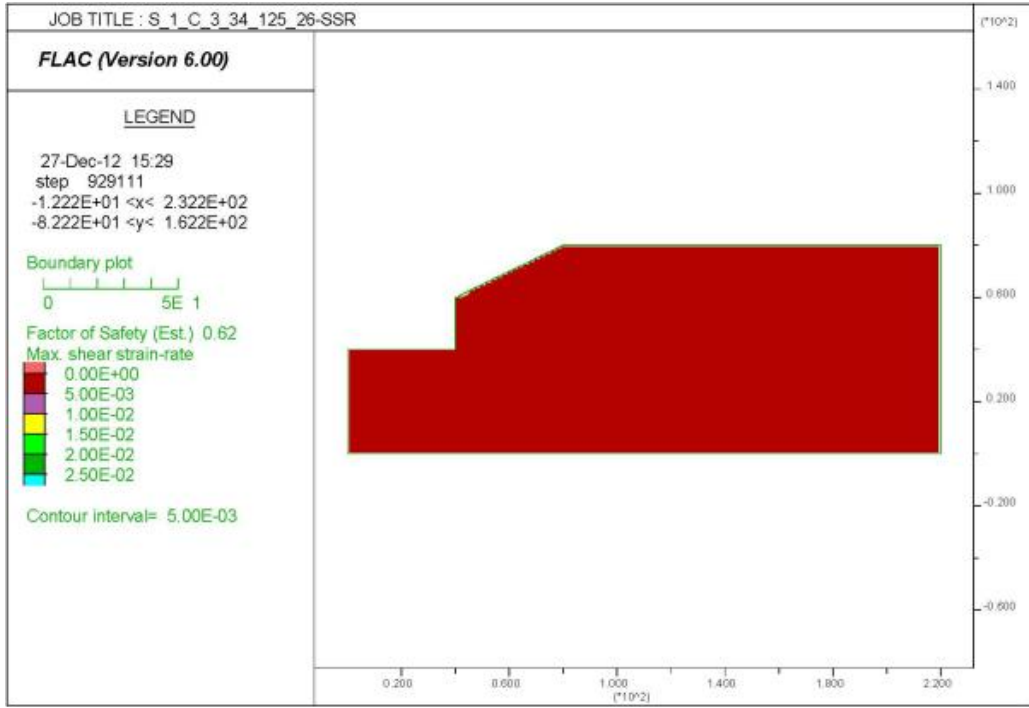


Figure C. 31. Series 1 Case 3 Foundation Angle  $\phi=26^\circ$ , Backfill Angle  $\phi=34^\circ$ , and  $\gamma=125$  pcf Maximum Shear Strain Rate.

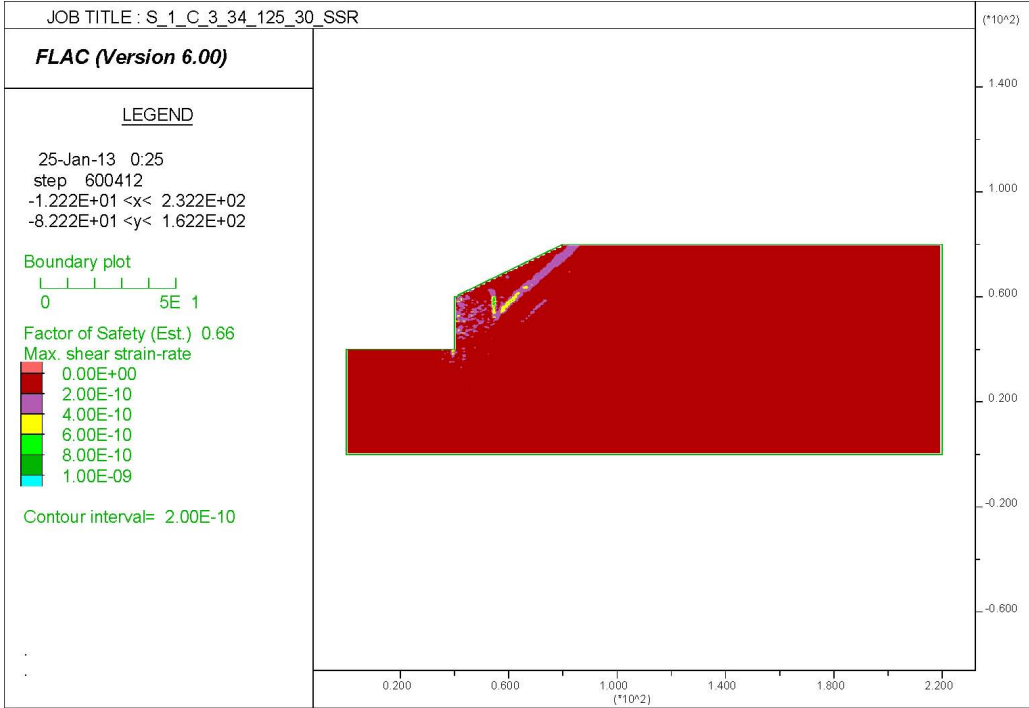
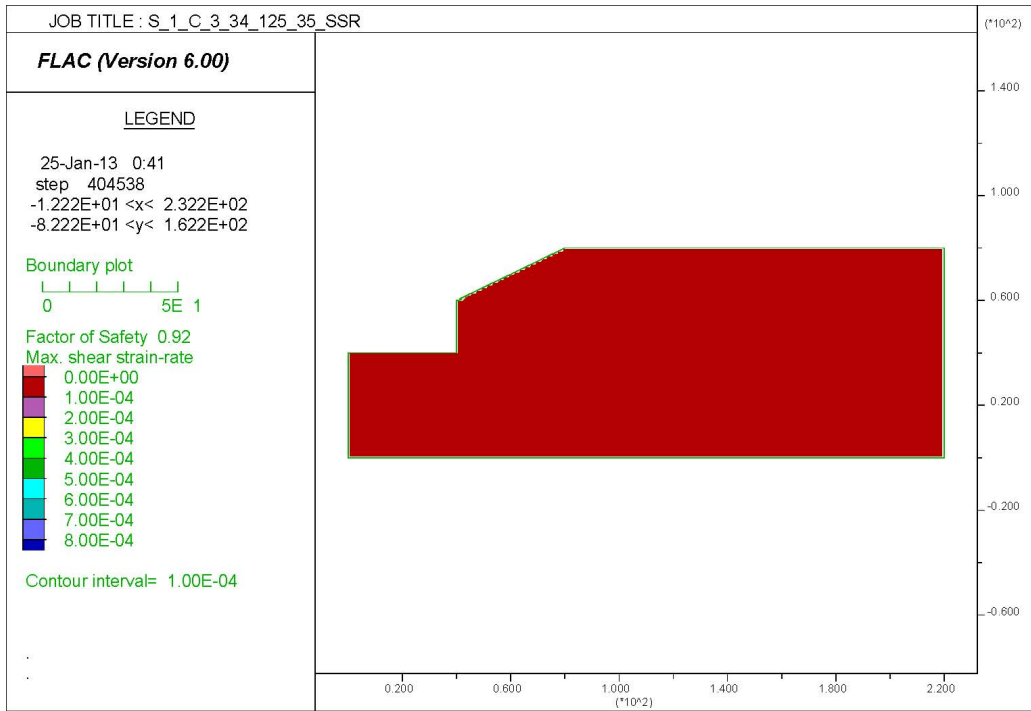
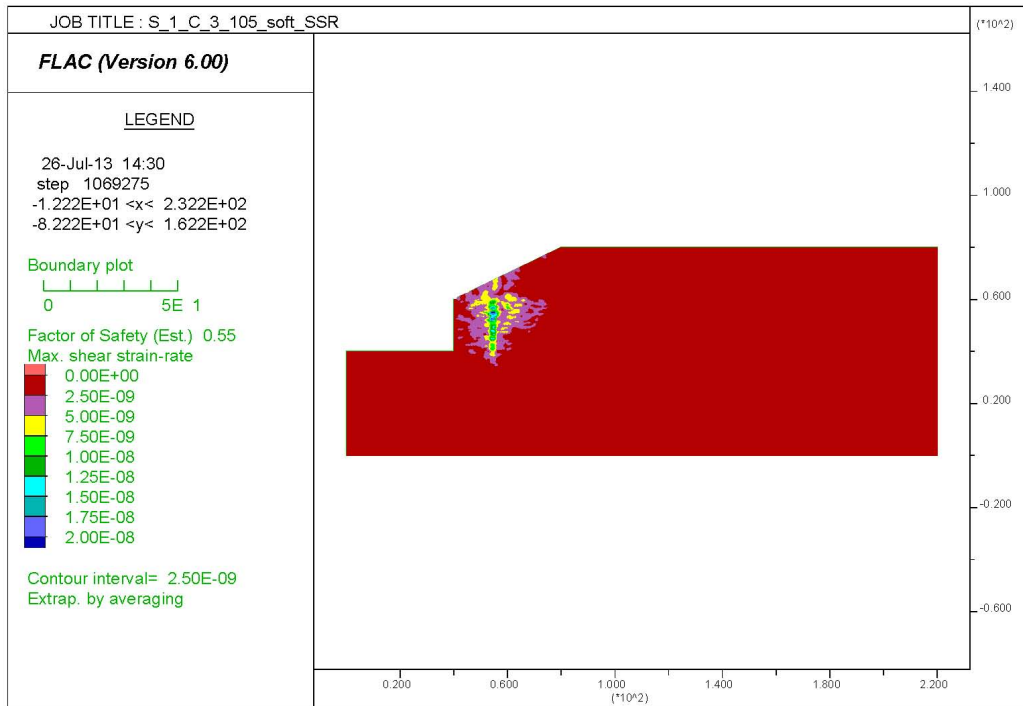


Figure C. 32. Series 1 Case 3 Foundation Angle  $\phi=30^\circ$ , Backfill Angle  $\phi=34^\circ$ , and  $\gamma=125$  pcf Maximum Shear Strain Rate.



**Figure C. 33. Series 1 Case 3 Foundation Angle  $\phi=35^\circ$ , Backfill Angle  $\phi=34^\circ$ , and  $\gamma=125$  pcf Maximum Shear Strain Rate.**



**Figure C. 34. Series 1 Case 3 Foundation  $c_u=500$  pcf, Backfill Angle  $\phi=34^\circ$ , and  $\gamma=105$  pcf Maximum Shear Strain Rate.**

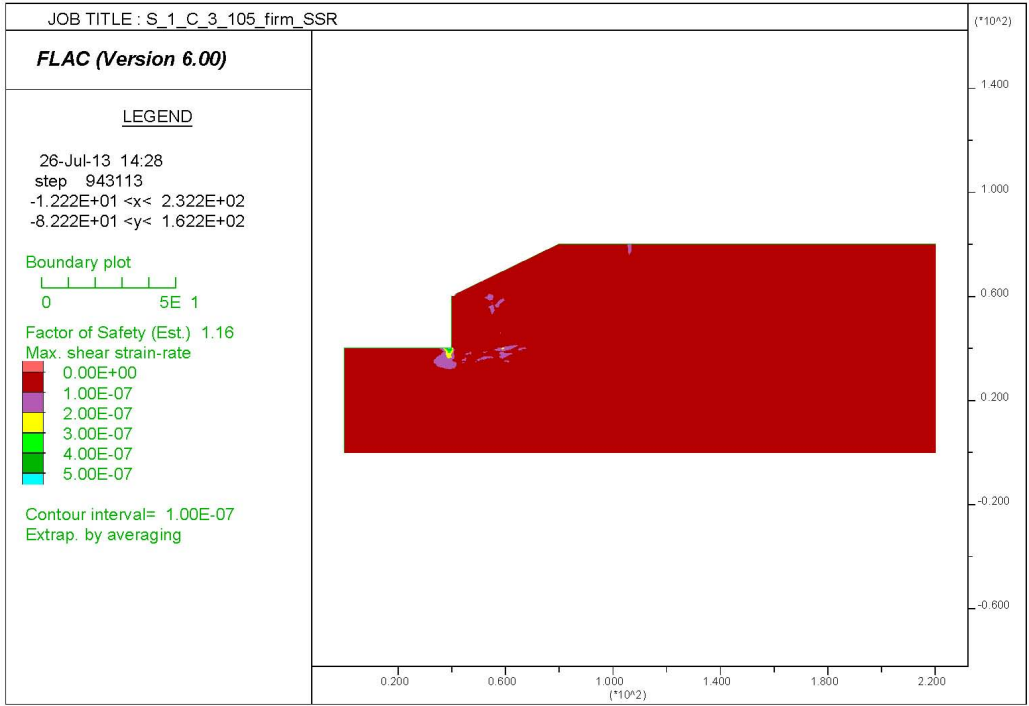


**Figure C. 35. Series 1 Case 3 Foundation  $c_u=1000$  psf, Backfill Angle  $\phi=34^\circ$ , and  $\gamma=105$  pcf Maximum Shear Strain Rate.**



**Figure C. 36. Series 1 Case 3 Foundation  $c_u=2000$  psf, Backfill Angle  $\phi=34^\circ$ , and  $\gamma=105$  pcf Maximum Shear Strain Rate.**

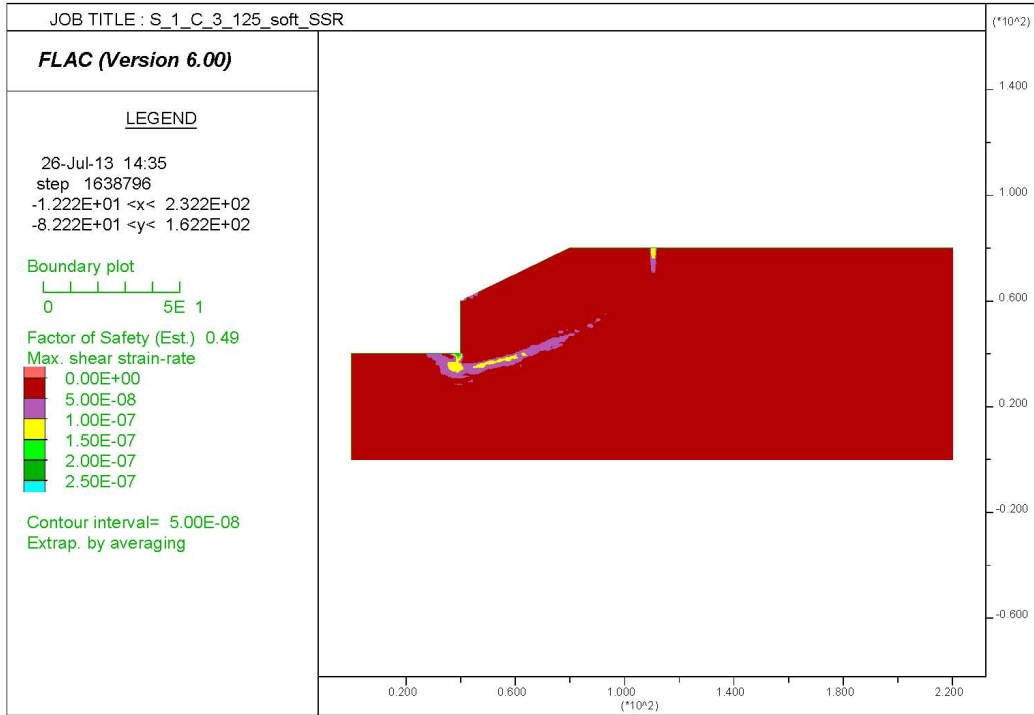


**Figure C. 37. Series 1 Case 3 Foundation  $c_u=500$  psf, Backfill Angle  $\phi=34^\circ$ , and  $\gamma=125$  pcf Maximum Shear Strain Rate.**

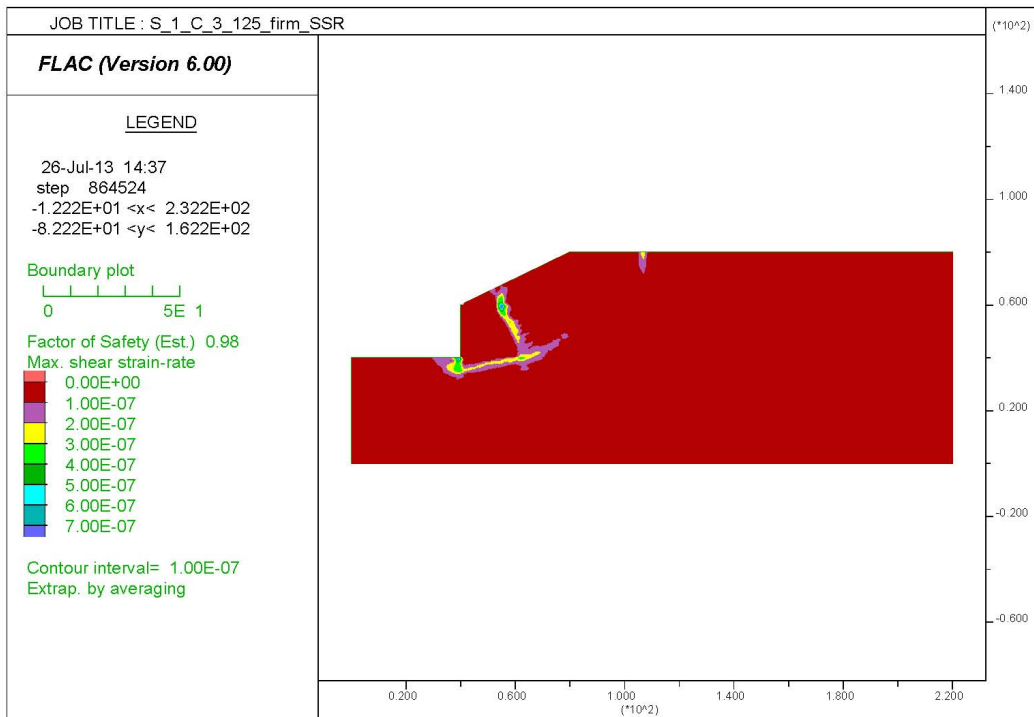


**Figure C. 38. Series 1 Case 3 Foundation  $c_u=1000$  psf, Backfill Angle  $\phi=34^\circ$ , and  $\gamma=125$  pcf Maximum Shear Strain Rate.**

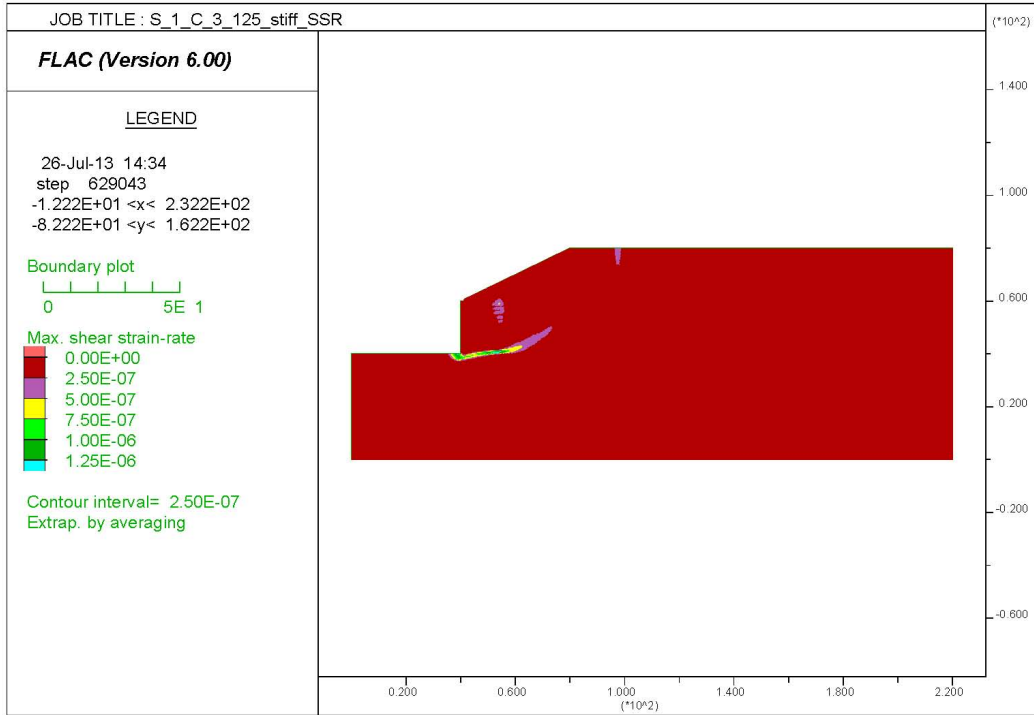


**Figure C. 39. Series 1 Case 3 Foundation  $c_u=2000$  psf, Backfill Angle  $\phi=34^\circ$ , and  $\gamma=125$  pcf Maximum Shear Strain Rate.**

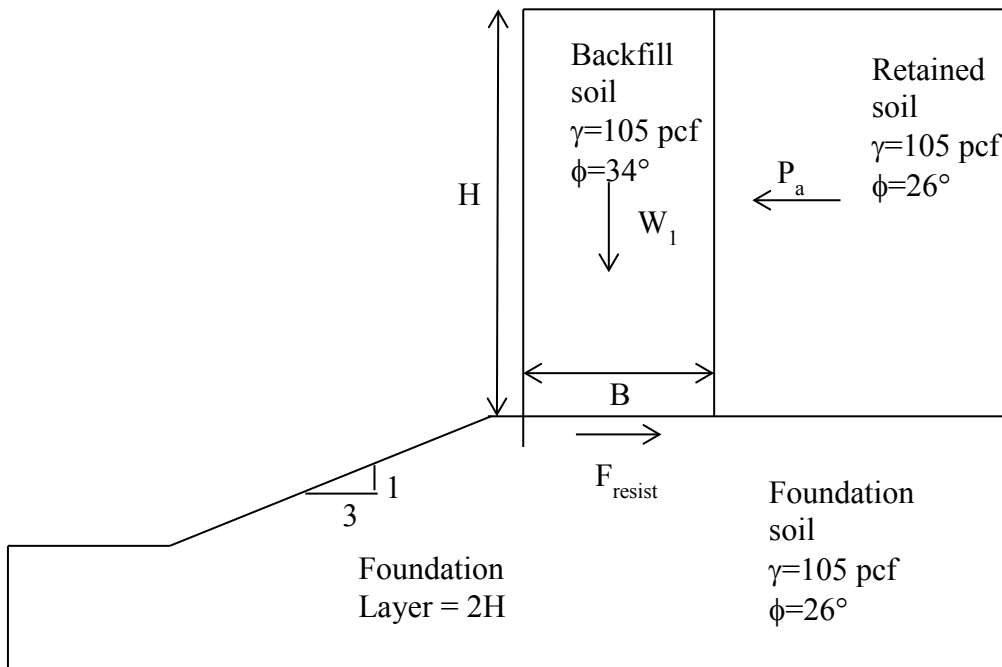


**Figure C. 40. Dimensions and Properties Used for Series 2 Case 2.**

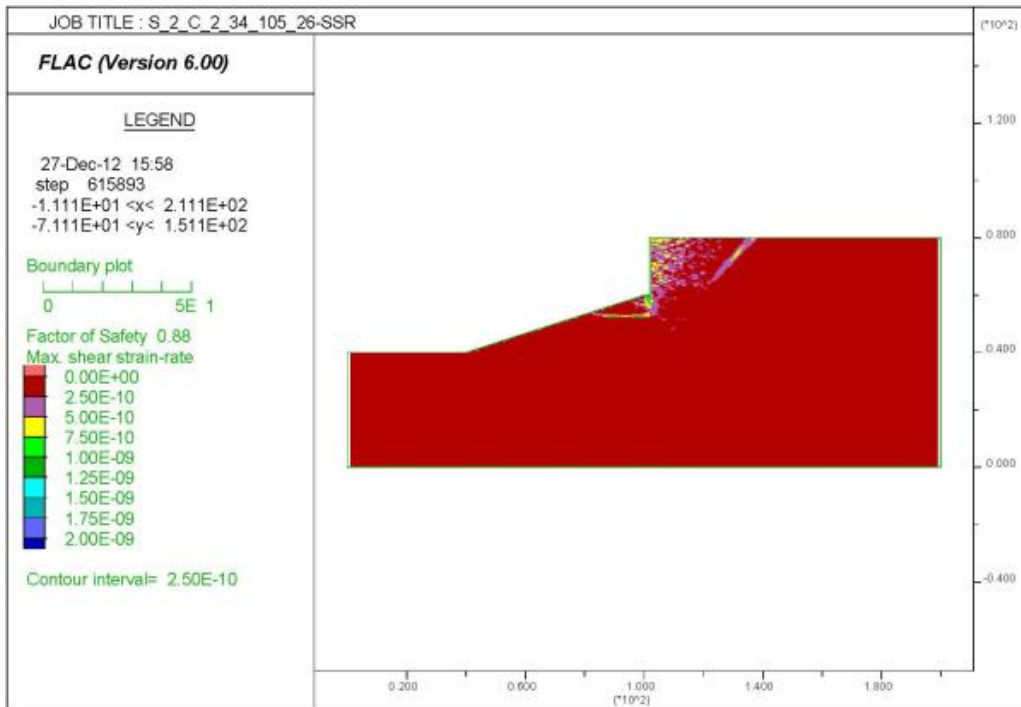


Figure C. 41. Series 2 Case 2 Foundation Angle  $\phi=26^\circ$ , Backfill Angle  $\phi=34^\circ$ , and  $\gamma=105$  pcf Maximum Shear Strain Rate.

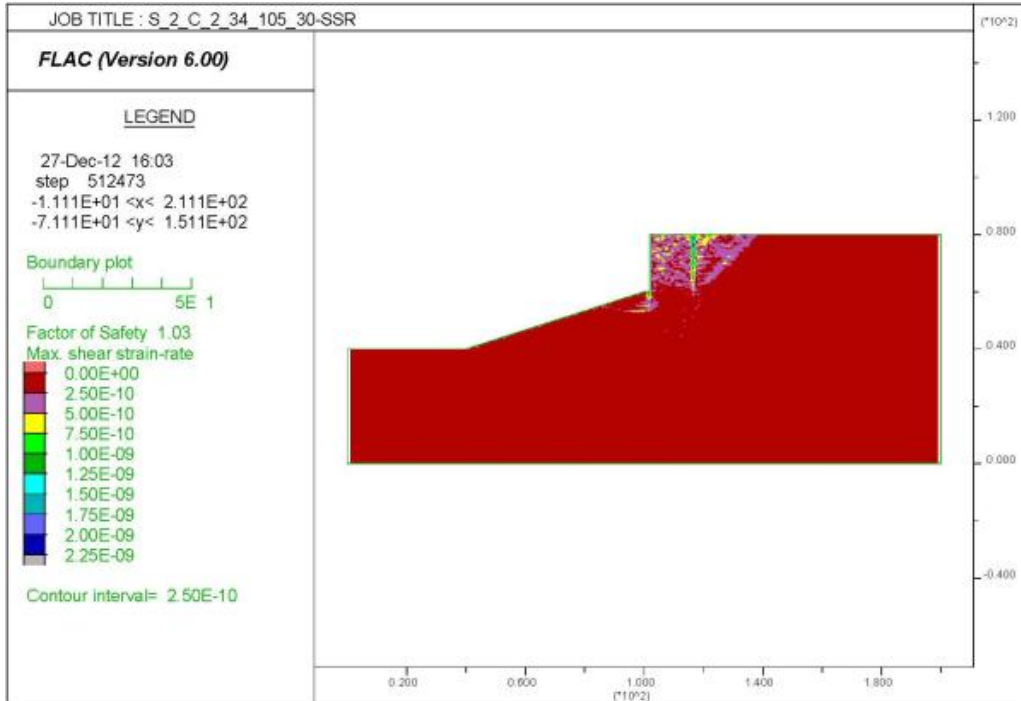
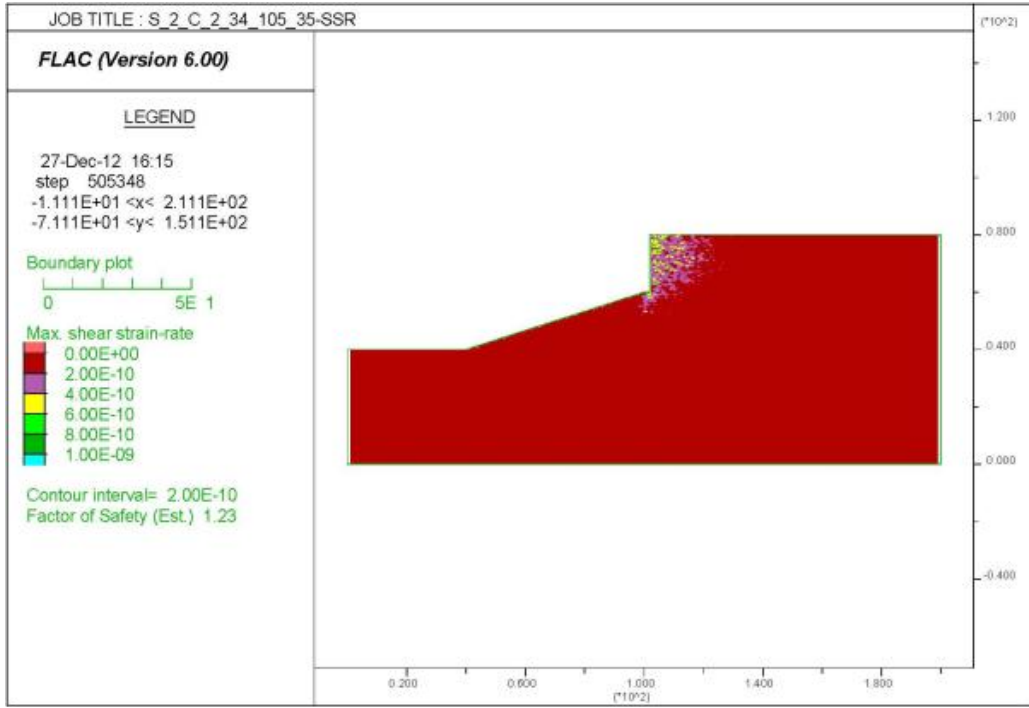
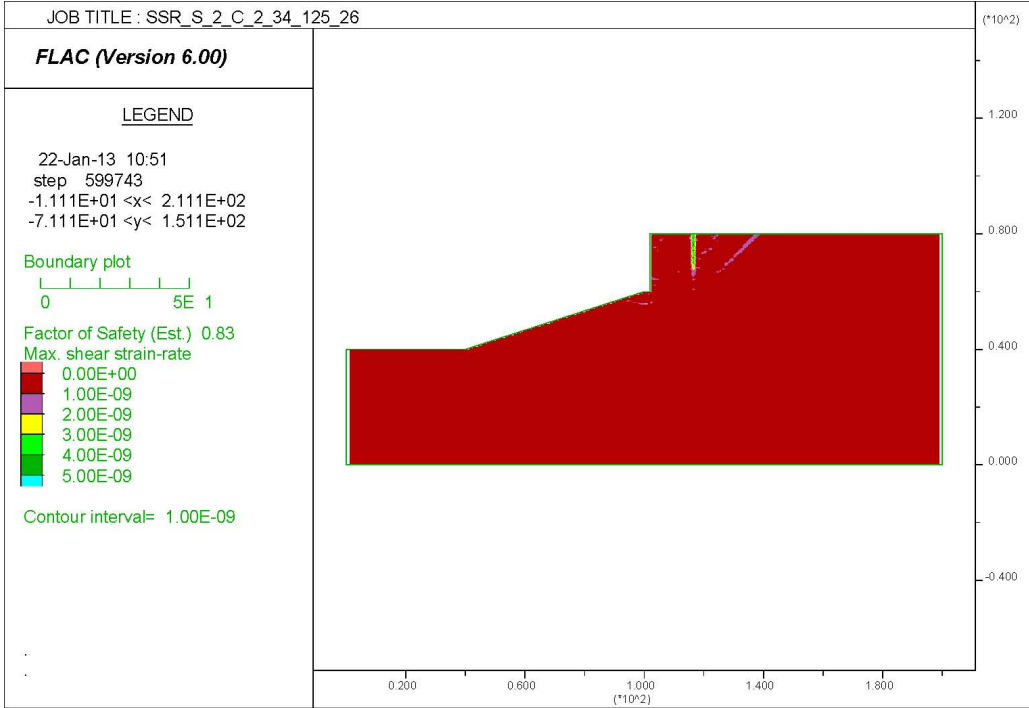


Figure C. 42. Series 2 Case 2 Foundation Angle  $\phi=30^\circ$ , Backfill Angle  $\phi=34^\circ$ , and  $\gamma=105$  pcf Maximum Shear Strain Rate.



**Figure C. 43. Series 2 Case 2 Foundation Angle  $\phi=35^\circ$ , Backfill Angle  $\phi=34^\circ$ , and  $\gamma=105$  pcf Maximum Shear Strain Rate.**



**Figure C. 44. Series 2 Case 2 Foundation Angle  $\phi=26^\circ$ , Backfill Angle  $\phi=34^\circ$ , and  $\gamma=125$  pcf Maximum Shear Strain Rate.**



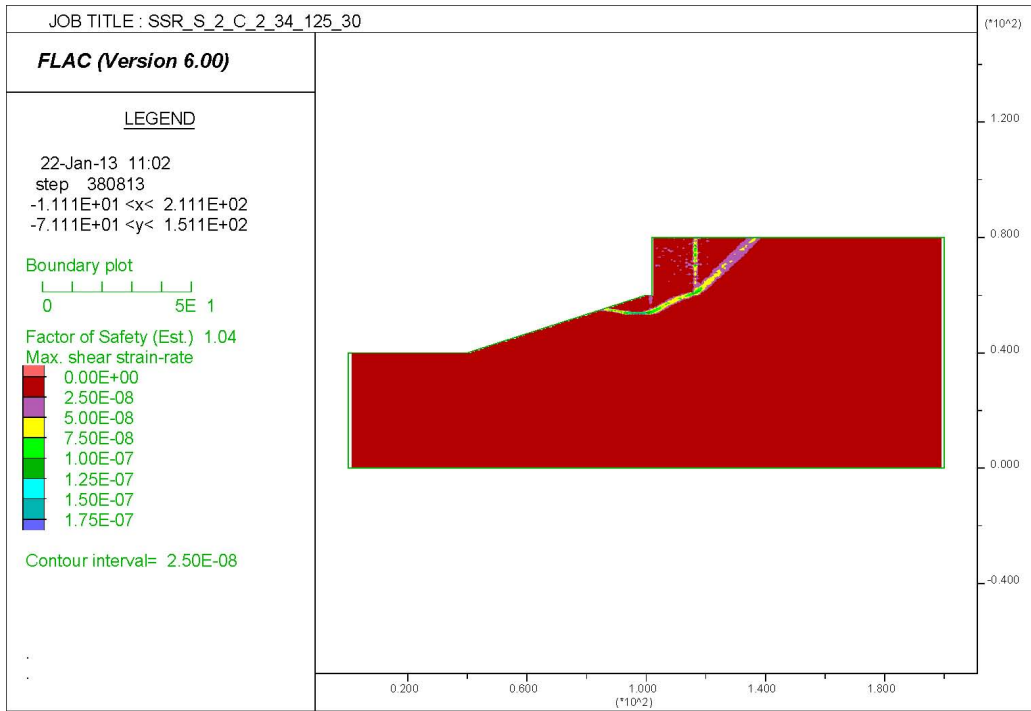


**Figure C. 45. Series 2 Case 2 Foundation Angle  $\phi=30^\circ$ , Backfill Angle  $\phi=34^\circ$ , and  $\gamma=125$ pcf Maximum Shear Strain Rate.**

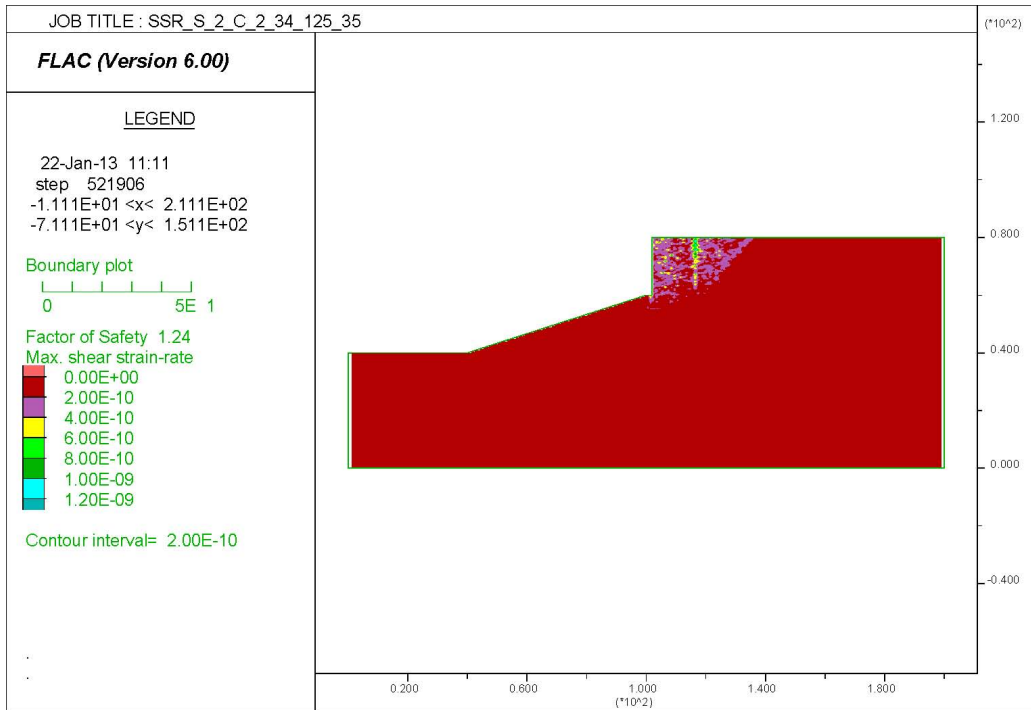


**Figure C. 46. Series 2 Case 2 Foundation Angle  $\phi=35^\circ$ , Backfill Angle  $\phi=34^\circ$ , and  $\gamma=125$ pcf Maximum Shear Strain Rate.**

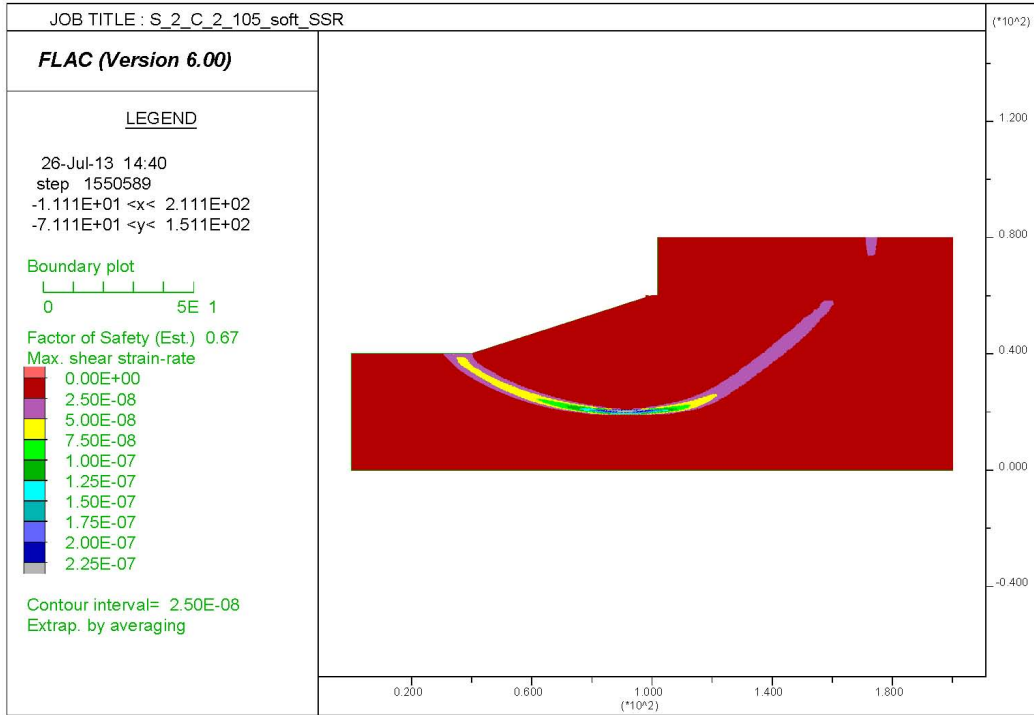


**Figure C. 47. Series 2 Case 2 Foundation  $c_u=500$  psf, Backfill Angle  $\phi=34^\circ$ , and  $\gamma=105$  pcf Maximum Shear Strain Rate.**

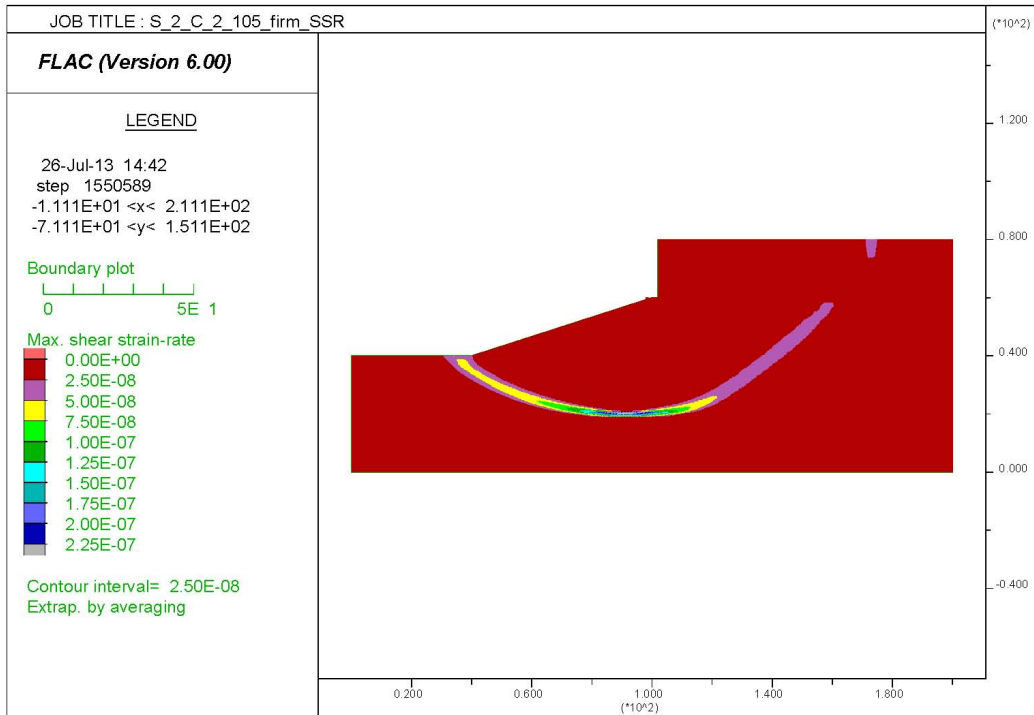


**Figure C. 48. Series 2 Case 2 Foundation  $c_u=1000$  psf, Backfill Angle  $\phi=34^\circ$ , and  $\gamma=105$  pcf Maximum Shear Strain Rate.**

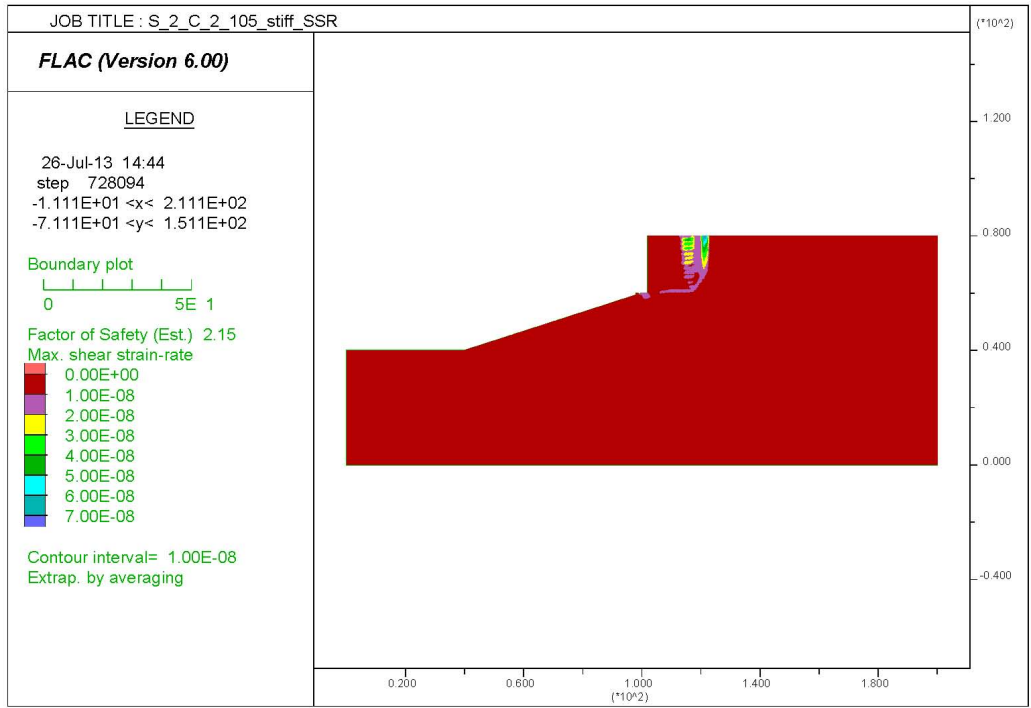


**Figure C. 49. Series 2 Case 2 Foundation  $c_u=2000$  psf, Backfill Angle  $\phi=34^\circ$ , and  $\gamma=105$  pcf Maximum Shear Strain Rate.**

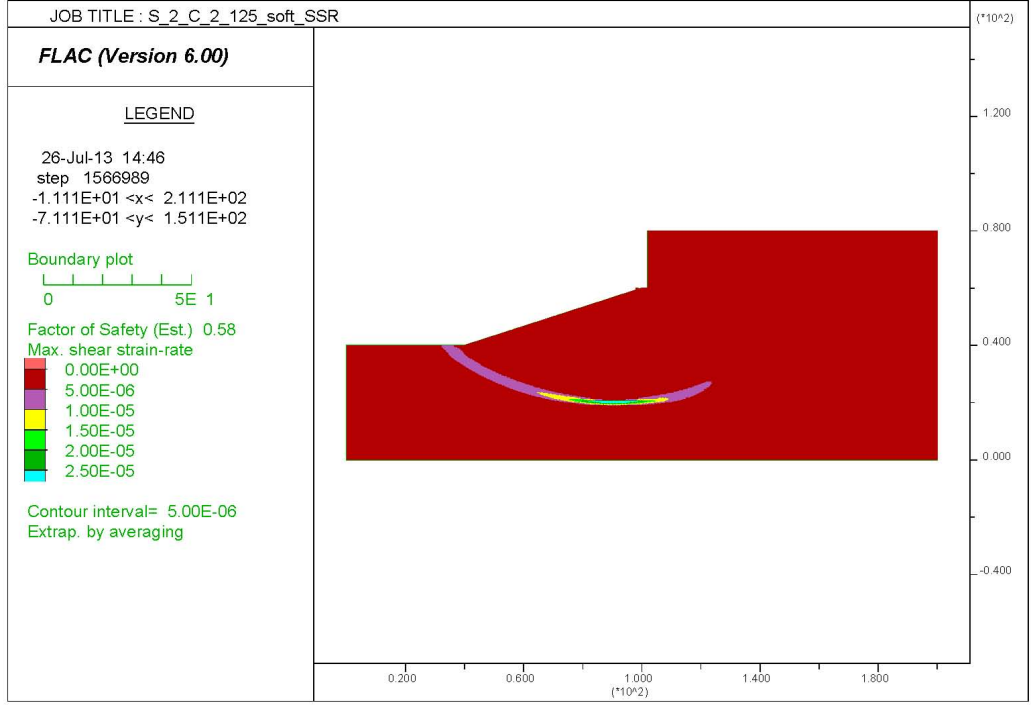


**Figure C. 50. Series 2 Case 2 Foundation  $c_u=500$  psf, Backfill Angle  $\phi=34^\circ$ , and  $\gamma=125$  pcf Maximum Shear Strain Rate.**

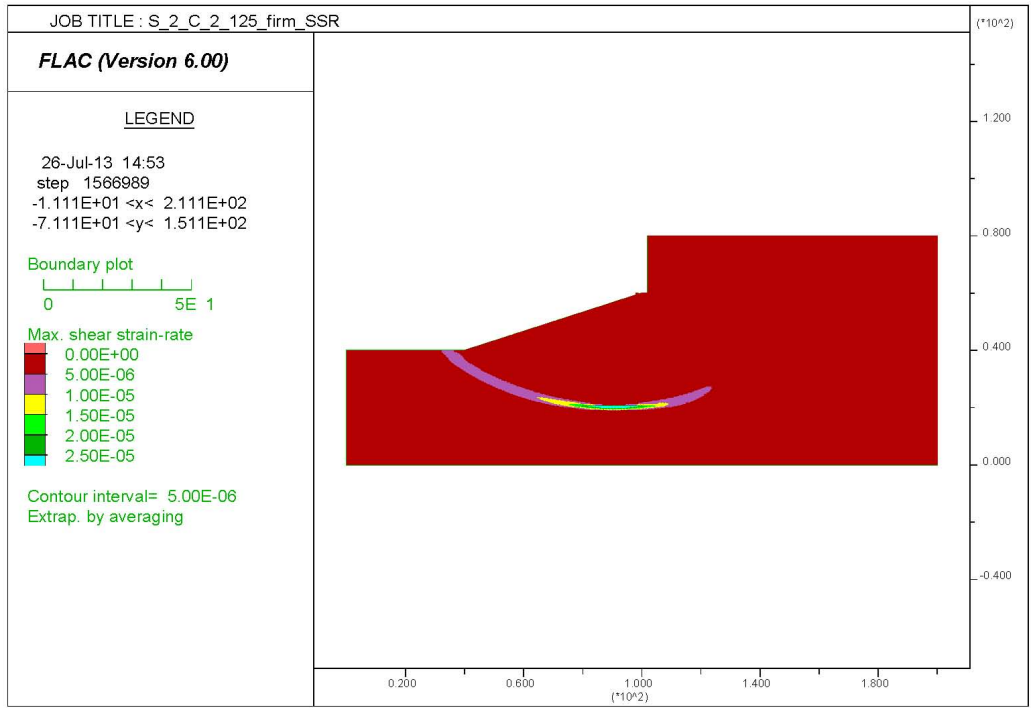


Figure C. 51. Series 2 Case 2 Foundation  $c_u=1000$  psf, Backfill Angle  $\phi=34^\circ$ , and  $\gamma=125$  pcf Maximum Shear Strain Rate.

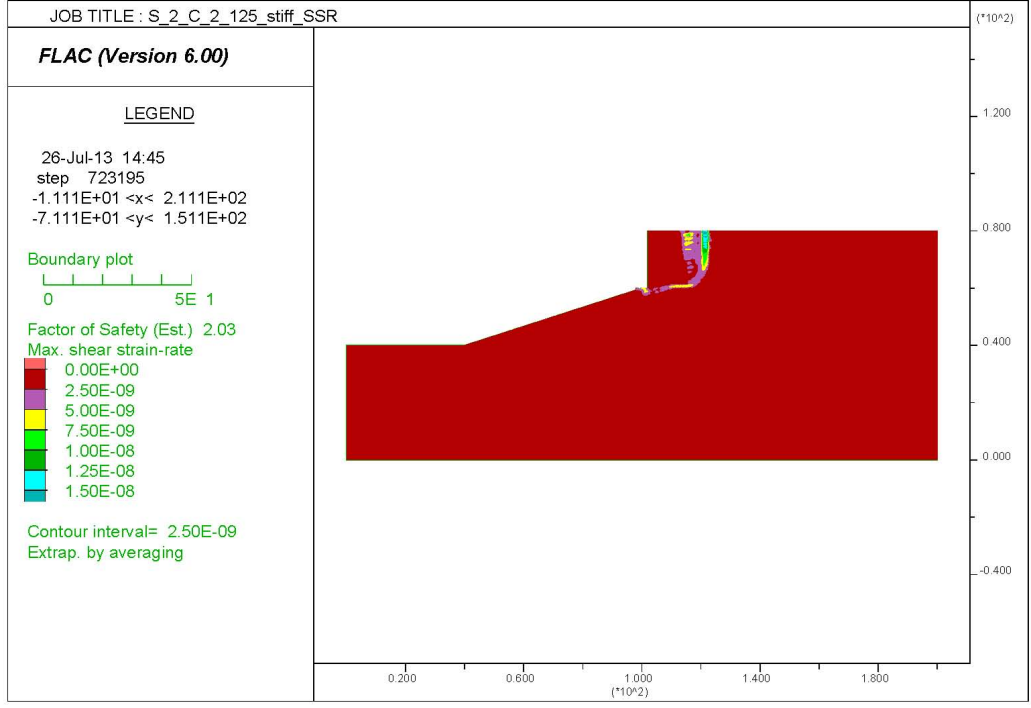


Figure C. 52. Series 2 Case 2 Foundation  $c_u=2000$  psf, Backfill Angle  $\phi=34^\circ$ , and  $\gamma=125$  pcf Maximum Shear Strain Rate.

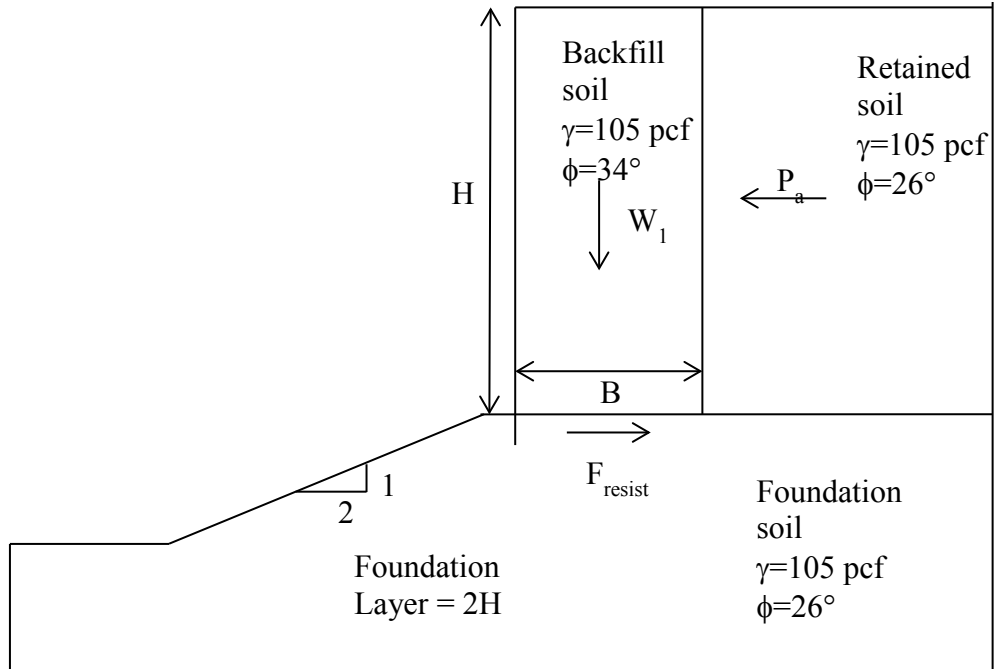


Figure C. 53. Dimensions and Properties Used for Series 2 Case 3.

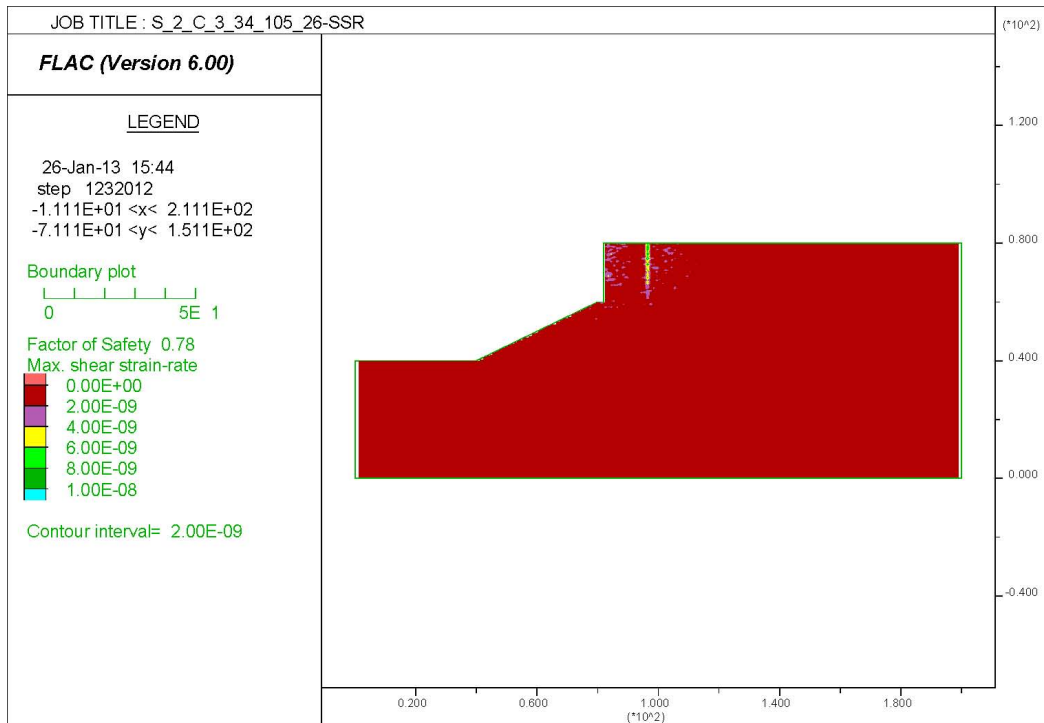
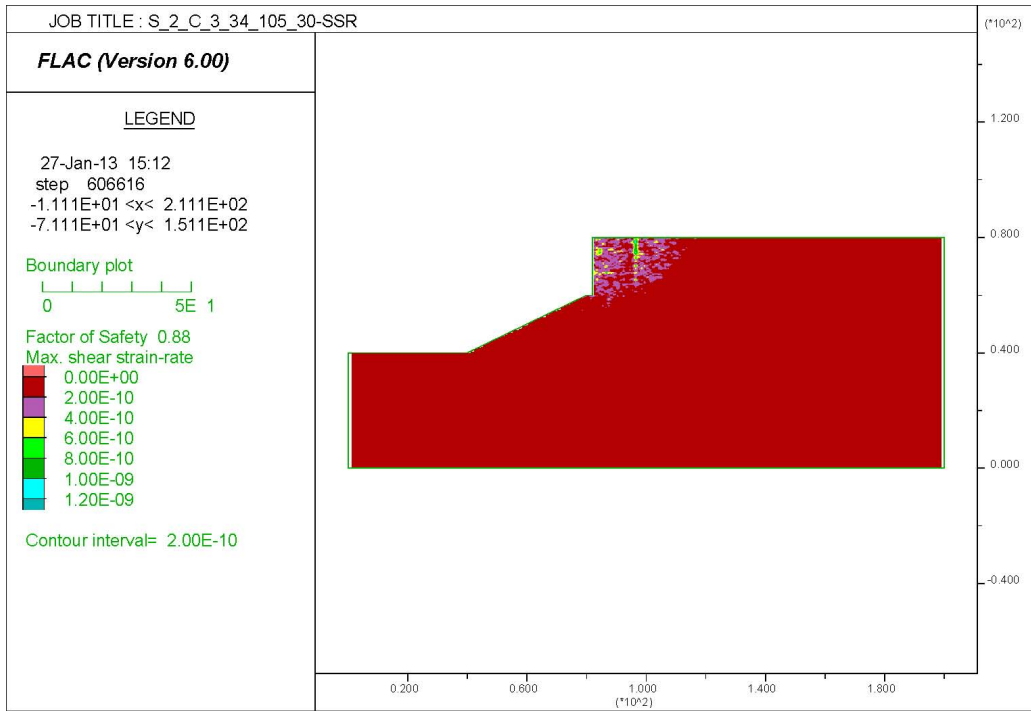
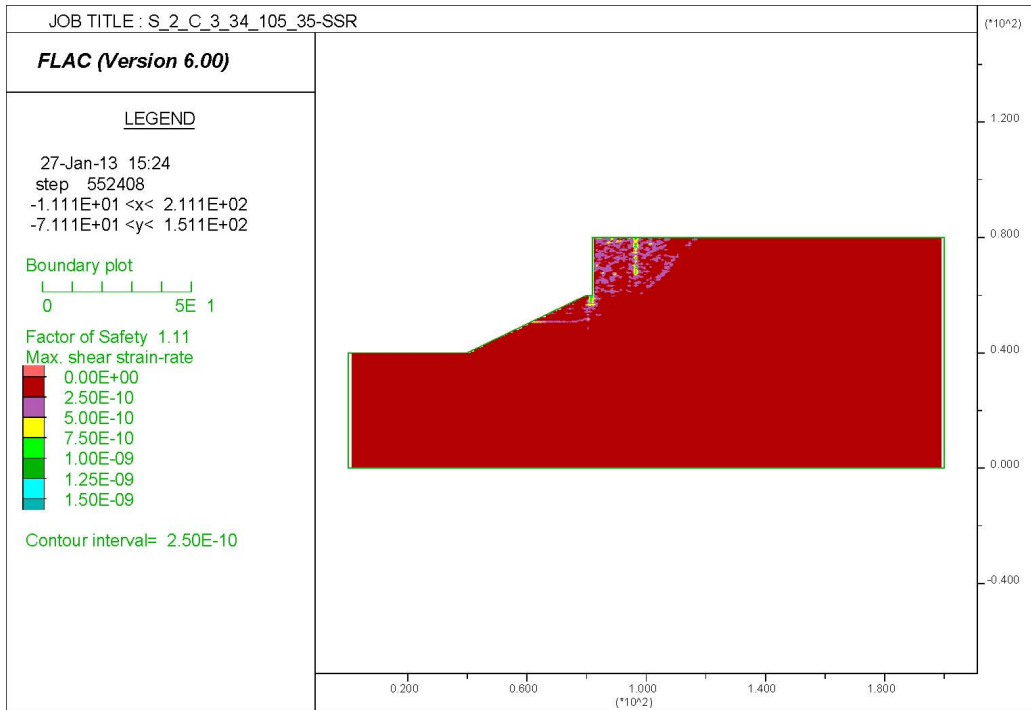


Figure C. 54. Series 2 Case 3 Foundation Angle  $\phi=26^\circ$ , Backfill Angle  $\phi=34^\circ$ , and  $\gamma=105$  pcf Maximum Shear Strain Rate.



**Figure C. 55. Series 2 Case 3 Foundation Angle  $\phi=30^\circ$ , Backfill Angle  $\phi=34^\circ$ , and  $\gamma=105$ pcf Maximum Shear Strain Rate.**



**Figure C. 56. Series 2 Case 3 Foundation Angle  $\phi=35^\circ$ , Backfill Angle  $\phi=34^\circ$ , and  $\gamma=105$ pcf Maximum Shear Strain Rate.**

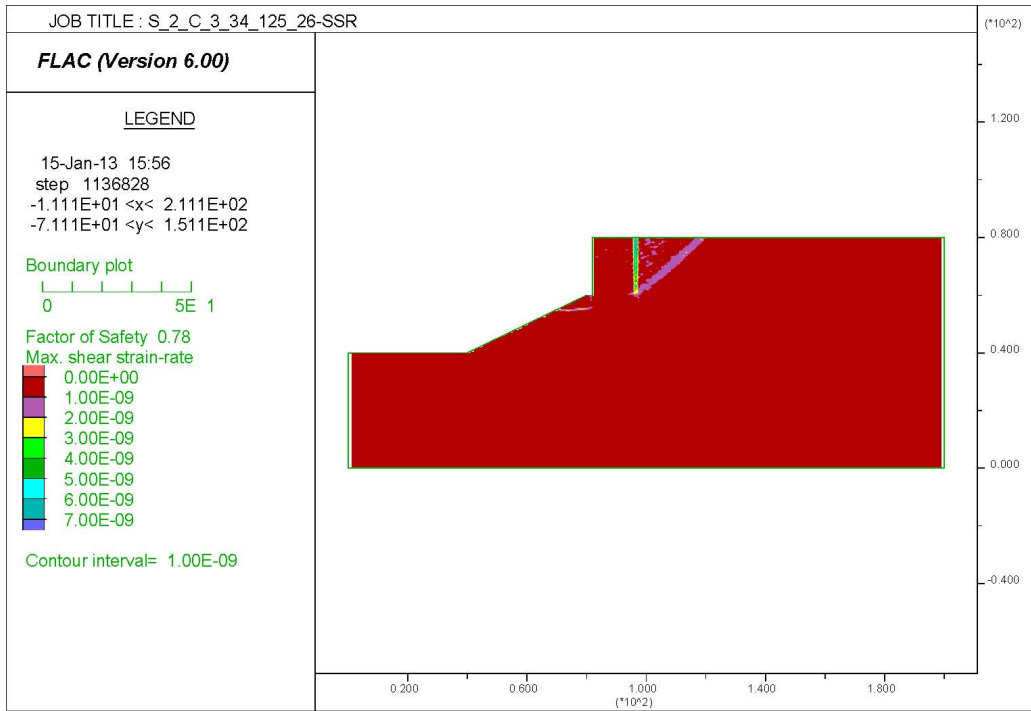


**Figure C. 57. Series 2 Case 3 Foundation Angle  $\phi=26^\circ$ , Backfill Angle  $\phi=34^\circ$ , and  $\gamma=125$  pcf Maximum Shear Strain Rate.**

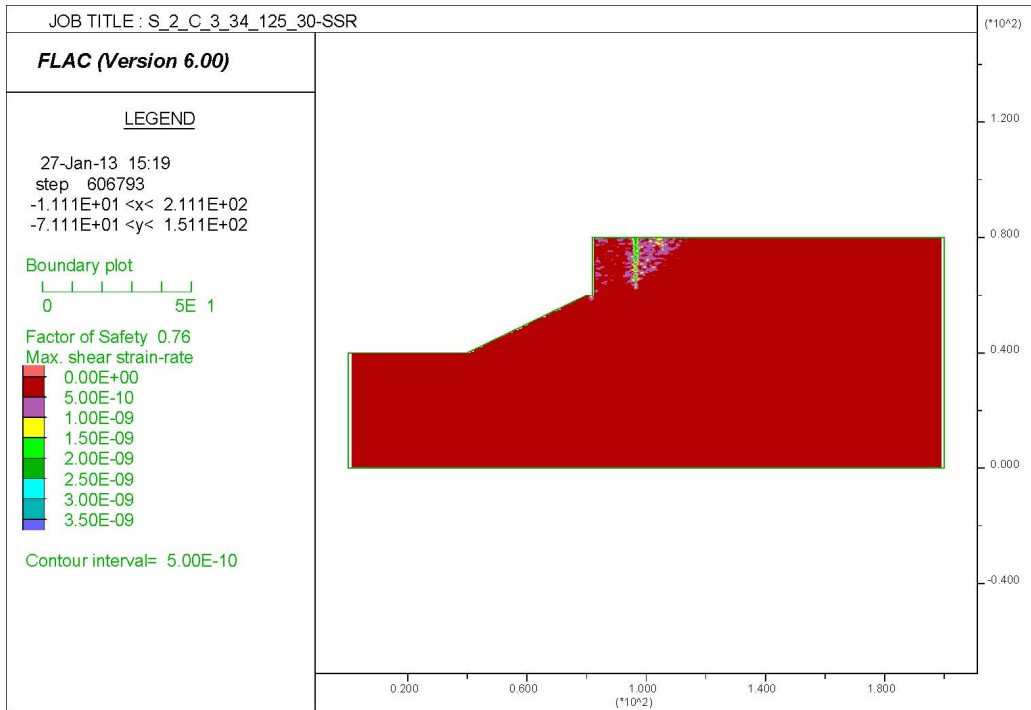


**Figure C. 58. Series 2 Case 3 Foundation Angle  $\phi=30^\circ$ , Backfill Angle  $\phi=34^\circ$ , and  $\gamma=125$  pcf Maximum Shear Strain Rate.**

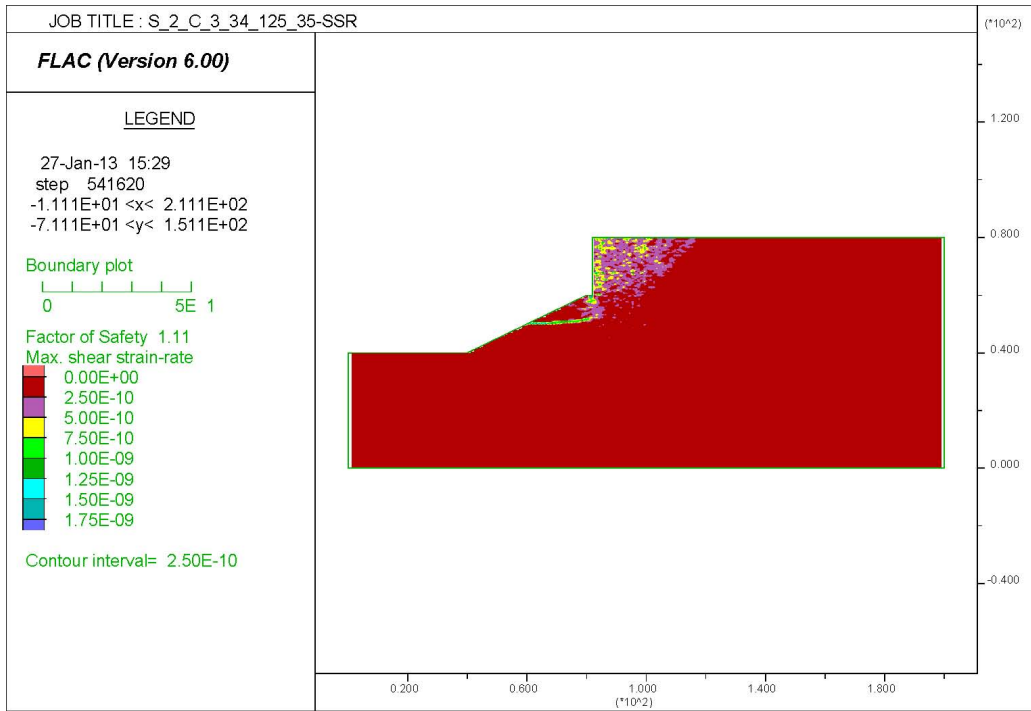


Figure C. 59. Series 2 Case 3 Foundation Angle  $\phi=35^\circ$ , Backfill Angle  $\phi=34^\circ$ , and  $\gamma=125$  pcf Maximum Shear Strain Rate.

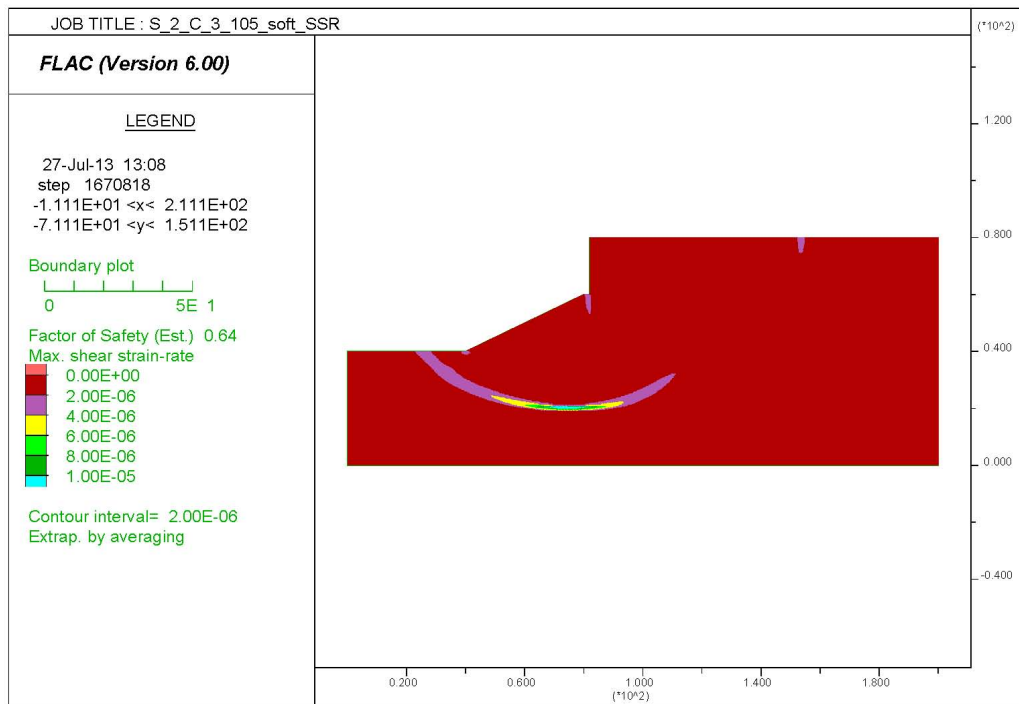
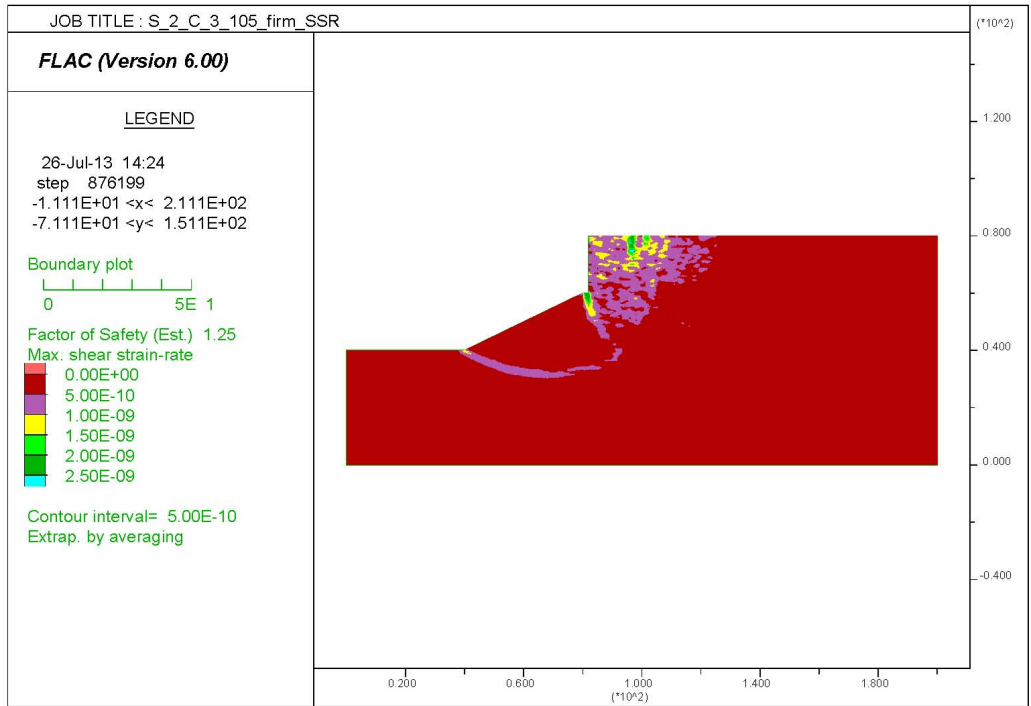
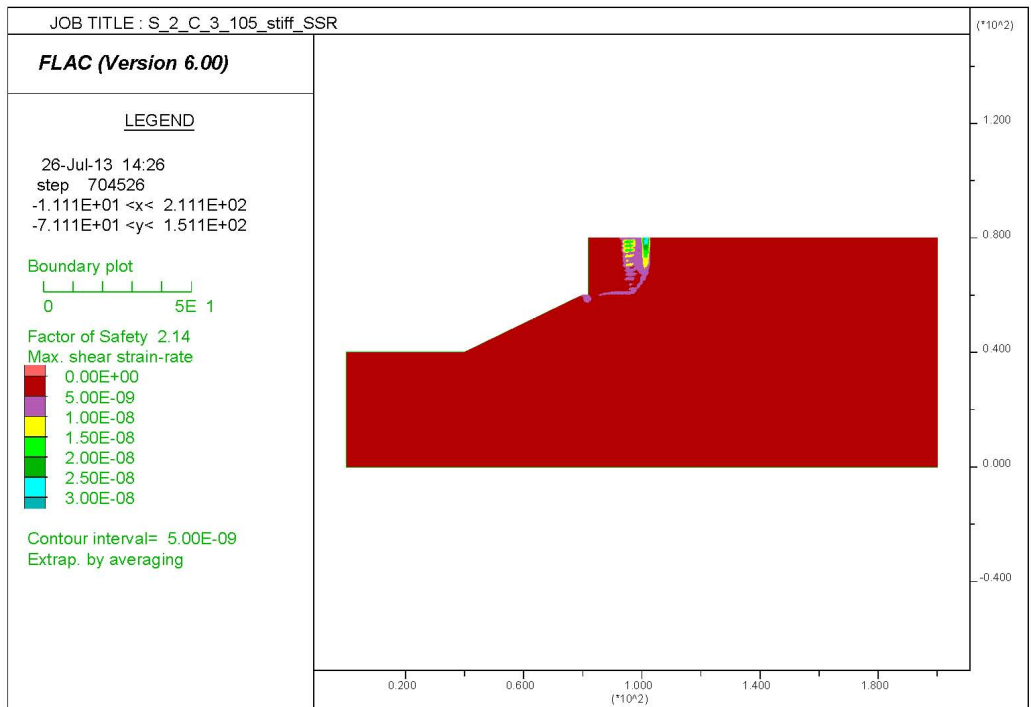


Figure C. 60. Series 2 Case 3 Foundation  $c_u=500$  pcf, Backfill Angle  $\phi=34^\circ$ , and  $\gamma=105$  pcf Maximum Shear Strain Rate.





**Figure C. 61. Series 2 Case 3 Foundation  $c_u=1000$  psf, Backfill Angle  $\phi=34^\circ$ , and  $\gamma=105$  pcf Maximum Shear Strain Rate.**



**Figure C. 62. Series 2 Case 3 Foundation  $c_u=2000$  psf, Backfill Angle  $\phi=34^\circ$ , and  $\gamma=105$  pcf Maximum Shear Strain Rate.**

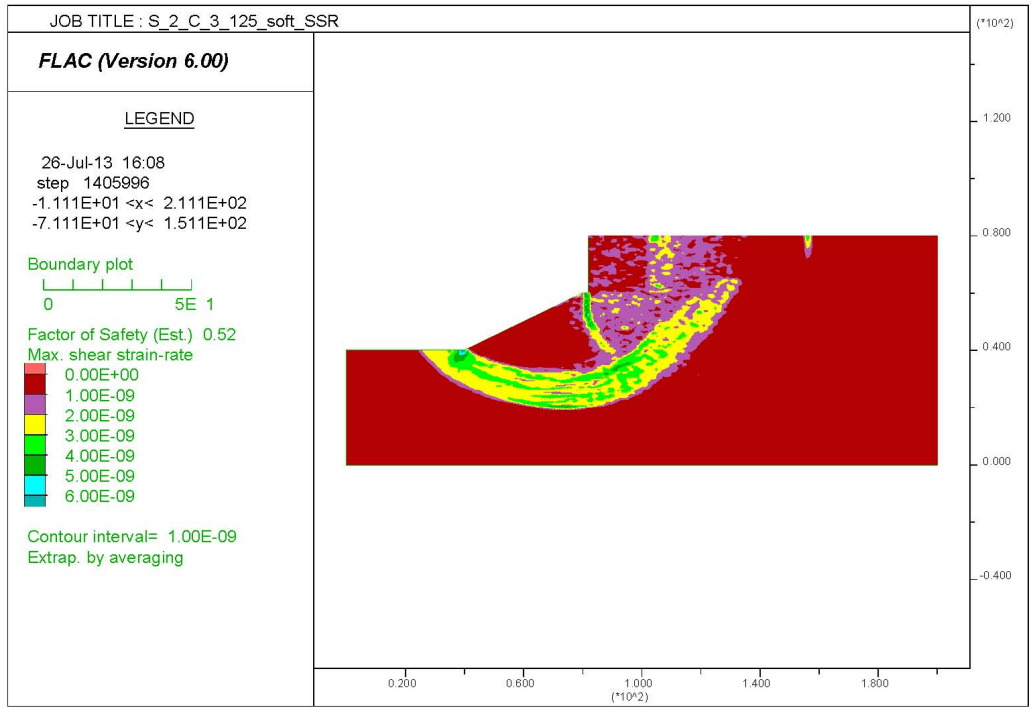


**Figure C. 63. Series 2 Case 3 Foundation  $c_u=500$  psf, Backfill Angle  $\phi=34^\circ$ , and  $\gamma=125$  pcf Maximum Shear Strain Rate.**

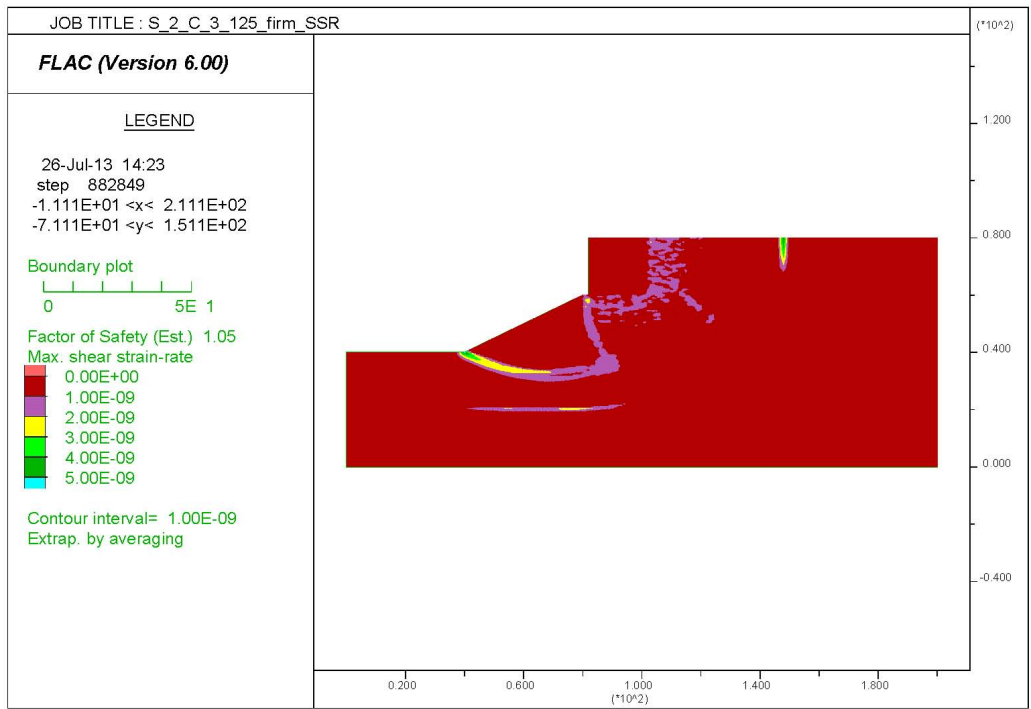


**Figure C. 64. Series 2 Case 3 Foundation  $c_u=1000$  psf, Backfill Angle  $\phi=34^\circ$ , and  $\gamma=125$  pcf Maximum Shear Strain Rate.**

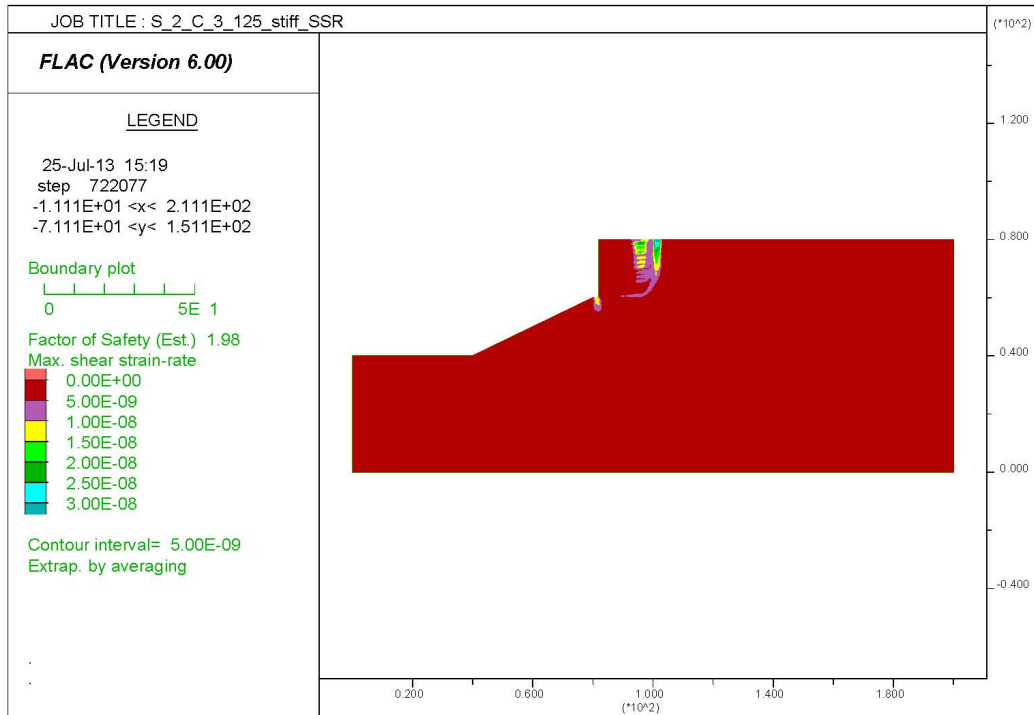


**Figure C. 65. Series 2 Case 3 Foundation  $c_u=2000$  psf, Backfill Angle  $\phi=34^\circ$ , and  $\gamma=125$  pcf Maximum Shear Strain Rate.**

